

The relationship between dental complexity and mandibular shape: implications for dietary inference in stem mammals

By

Wade Harris (1646023)

ORCID number: **0000-0002-6981-954**

A **dissertation** submitted to the Faculty of Science, University of the Witwatersrand, Johannesburg, in fulfilment of the requirements for the degree of **Master of Science** in **Palaeontology**.

Supervisor: Prof. Jonah N. Choiniere

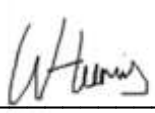
Co-supervisors: Prof. Roger Benson, Dr. Kathleen Dollman





1. DECLARATION

I declare that this dissertation is my own, unaided work. It is being submitted for the Degree of Master of Science at the University of the Witwatersrand, Johannesburg. It has not been submitted before for any degree or examination at any other University.



Wade Harris

Signed on the 10th day of June 2024 at the Evolutionary Studies Institute, University of the Witwatersrand, Johannesburg

2. ABSTRACT

Non-mammalian cynodonts exhibit some of the first major morphological innovations that contributed to the success of their descendent lineage, mammals. This includes features that are hypothesized to enable adaptation to a highly varied suite of diets such as specialized tooth crowns with complex occlusal surfaces and a jaw muscle configuration where two major muscles contribute to jaw closing. Surprisingly, inferences on cynodont diets so far have been based on qualitative evidence, and the quantification of these dietary adaptations could assist in testing these inferences. Here, I evaluate the relationships of mandibular shape, dental complexity and the combined data on body mass and relative mandible size, to known diets in living mammals, to assess the utility of these ecomorphological proxies for inferring the diets of extinct non-mammalian cynodonts. To assess relationships between diet and jaw shape, I collected 12 fixed landmarks (type 2) and four sliding landmarks (type 3) for six non-mammalian cynodonts, 51 marsupial mammals and 211 placental mammals. Dental complexity (OPCR) values were collected using the R package molaR, for a sample of 19 non-mammalian cynodonts, 47 marsupial mammals and 193 placental mammals. Procrustes-aligned shape coordinates, OPCR values, body mass estimates and relative mandible size data were then subjected to phylogenetic Procrustes ANOVA regressions and phylogenetic regressions. Neither mandible shape nor OPCR are strongly correlated to diet (carnivory, frugivory, granivory, herbivory, nectivory, invertivory), but the combination of these variables are a somewhat reliable predictor of diet, particularly mandible shape. Extinct non-mammalian cynodonts have mandible shapes that are comparable to those of mammals, however they occupy a narrow morphospace and their OPCR scores are generally much lower than those of mammals. Consequently, when these variables were entered into a predictive framework for diet, I observed limited inferential power since non-mammalian cynodonts do not strongly resemble mammals.

3. ACKNOWLEDGEMENTS

I’d like to thank everyone who played a role making this research successful. This endeavour would not have been possible without the mentorship of Prof. Jonah Choiniere, I have learned so much while working alongside you, thank you for all the guidance and encouragement.

I’m deeply indebted to my supervisors: Prof. Jonah Choiniere, Prof. Roger Benson and Dr. Kathleeen Dollman. Thank you all for being incredibly patient, and generously providing your expertise. Particularly Prof. Roger Benson, I’m amazed at the invaluable set of skills I’ve learnt from our interactions, thank you.

I’d like to thank Gideon Chinamatria for taking the time to CT-scan my specimens.

To my parents, my brother, my partner, and friends thank you for believing in me and encouraging me to keep moving forward. To my lab-members, thank you for all your support and advice, especially to Frederick Tolchard, for the many insightful conversations, and to Chandelé Montgomery whose contagious enthusiasm has never failed to brighten up my days.

This research would not have been possible without the support from Genus: DSI-NRF Centre of Excellence in Palaeoscience under Grant No. 86073.

4. CONTENTS

1. DECLARATION ii

2. ABSTRACT iii

3. ACKNOWLEDGEMENTS iv

4. CONTENTS v

5. LIST OF INSTITUTIONAL ABBREVIATIONS ix

6. LIST OF FIGURES xi

7. LIST OF TABLES xvii

8. LIST OF SYMBOLS xx

9. INTRODUCTION 1

9.1 The Karoo Basin 1

9.2 Cynodonts and their dietary adaptations 2

9.3 Dietary inferences in the fossil record 6

9.4 Dietary evaluation using craniodental anatomy 7

9.4.1 Dietary inferences using mandible shape 7

9.4.2 Dietary inferences using teeth 11

9.4.3 Size and its association with diet 14

10. RESEARCH RATIONALE 16

11. MATERIALS 18

11.1 Data samples 18

11.2 Phylogenetic data 18

11.3 Functional data 19

11.3.1 Diet 19

11.3.2 Body mass 19

12. METHODS 21

12.1 Specimen imaging 21

12.2 Tooth model development 21

12.3 Phylogeny 23
12.4 Diet categorization 24
12.5 Landmarking protocol 25
12.6 OPCR 28
12.7 Statistical analyses 29
12.7.1 Mandible shape variation 29
12.7.1.1 Phylogenetically-aligned principal component analysis (PCA) 29
12.7.1.2 Phylogenetic ANOVA regressions (procDpgls) 30
12.7.1.3 Phylogenetically informed discriminant analysis (pDFA) 31
12.7.2 Mandible size and its association with diet 32
12.7.2.1 Phylogenetic regressions (pgls) 32
12.7.2.2 Phylogenetically informed discriminant analysis (pDFA) 35
12.7.3 Dental complexity 36
12.7.3.1 Generation of box and whisker plots 36
12.7.3.2 Phylogenetic regressions (pgls) 36
12.7.3.3 Phylogenetically informed discriminant analysis (pDFA) 37
12.7.4 Dietary inferences using mandible shape and dental complexity 38
12.7.4.1 Phylogenetic ANOVA regressions 39
12.7.4.2 Phylogenetically informed discriminant function analysis (pDFA) 39
13. RESULTS 40
13.1 Mandible shape and its association to diet 40
13.1.1 PCA 40
13.1.2 Phylogenetic ANOVA regressions (procDgls) 47
13.1.3 pDFA: mandible shape 58
13.2 Mandible size and its association with diet 64
13.2.1 Phylogenetic regressions (pgls) 64
13.2.2 pDFA: mandible size 71

13.2.2.1 pDFA: considering only mandible size 71
13.2.2.2 pDFA: considering mandible size and shape 75
13.3 Dental complexity (OPCR) and its association with diet 79
13.3.1 Average dental complexity (OPCRavg): distribution and trends 79
13.3.1.1 OPCRavg: box and whisker plots 79
13.3.1.2 OPCRavg: phylogenetic regressions (pgls) 84
13.3.2 Summed dental complexity (OPCRsum): distribution and trends 88
13.3.2.1 OPCRsum: box and whisker plots 88
13.3.2.2 OPCRsum: phylogenetic regressions (pgls) 93
13.3.3 Dental complexity of the first molar (OPCRm1): distribution and trends 97
13.3.3.1 OPCRm1: box and whisker plots 97
13.3.3.2 OPCRm1: phylogenetic regressions (pgls) 102
13.3.4 Dental complexity of the second molar (OPCRm2): distribution and trends 106
13.3.4.1 OPCRm2: box and whisker plots 106
13.3.4.2 OPCRm2: phylogenetic regressions (pgls) 111
13.3.5 Dental complexity of the third molar (OPCRm3): distribution and trends 115
13.3.5.1 OPCRm3: box and whisker plots 115
13.3.5.2 OPCRm3: phylogenetic regressions (pgls) 120
13.3.6 pDFA: OPCR 125
13.3.6.1 pDFA: OPCRavg and OPCRsum 125
13.3.6.2 pDFA: OPCRm1-m3 133
13.3.6.3 pDFA: OPCRm1-m3 and $\log_{10}$ body mass 141
13.4 Dietary inferences using mandible shape and OPCR variables 146
13.4.1 Phylogenetic ANOVA regressions 146
13.4.2 pDFA: mandible shape and OPCR 150

14. DISCUSSION 157

14.1 Mandibular form and its correlation to dietary disparity in mammals 157

14.2 Dental complexity's correlation to dietary disparity in mammals 165

14.3 Implications for dietary inference in cynodonts 169

14.4 Implications for macroevolutionary evolution 176

15. CONCLUSION 181

16. APPENDICES 183

16.1 Appendix A 183

16.2 Appendix B 204

16.3 Appendix C 207

16.4 Appendix D 262

16.5 Appendix E 270

16.6 Appendix F 320

17. REFERENCES 345

5. LIST OF INSTITUTIONAL ABBREVIATIONS

AMNH	American Museum of Natural History, New York, New York, USA
BP	Evolutionary Studies Institute (formerly Bernard Price Institute for Palaeontological Research), University of the Witwatersrand, Johannesburg, South Africa
Du Baa	Duke University, Durham, North Carolina, USA
FLMNH	Field Museum of Natural History, Chicago, Illinois, USA
GWU	Center for Advanced Study of Human Palaeobiology, George Washington University, Washington, D.C, USA
JSM	University of Chicago, Chicago, Illinois, USA
MCP	Science Technology Museum, Porto Alegre, Brazil
MCN	Museu de Ciências Naturais da Fundação Zoobotânica do Rio Grande do Sul, Porto Alegre, Brazil
MCZ	Museum of Comparative Zoology, Harvard University, Cambridge, Massachusetts, USA
NHM-PV	Natural History Museum, London,England, UK
NHMUK	Natural History Museum, London, England, UK
NMQR	National Museum, Bloemfontein, South Africa
NMS	National Museum Scotland, Edinburgh, Scotland, UK
OUMNH	Oxford University Museum of Natural History, Oxford, England, UK
PVL	Instituto Miguel Lillo, San Miguel de Tucumán, Argentina
SAM-PK	Iziko, the South African Museum, Cape Town, South Africa
UF	Florida Museum of Natural History, Gainesville, Florida, USA
UFRGS	Universidade Federal do Rio Grande do Sul, Farroupilha, Brazil

UMMZ	University of Michigan Museum of Zoology, Ann Arbor, Michigan,USA
UMZC	University Museum of Zoology, Cambridge, UK
USNM	Smithsonian National Museum of Natural History, Washington, D.C, USA
UWBM	UW Burke Museum of Natural History and Culture, Seattle, Washington, USA
WLM	Wits Life Science Museum, University of the Witwatersrand, Johannesburg, South Africa
YPM	Yale Peabody Museum of Vertebrate Zoology, New Haven, Connecticut, USA

6. LIST OF FIGURES

Figure 1: Lithostratigraphy and vertebrate biozonation ranges of the Beaufort and Stormberg groups of South Africa's Karoo Supergroup showing the stratigraphic ranges of South Africa's cynodonts..... 2

Figure 2: Cynodont phylogeny alongside stratigraphic scale showing relationships and occurrences of members. 5

Figure 4: Postcanine tooth form variation in a carnivorous, herbivorous, and invertivorous mammal. 12

Figure 5: Differences in tooth complexity (OPCR) in the first molar of a carnivorous and herbivorous mammal. 14

Figure 6: Tooth model generation for an exemplar specimen (*Acinonyx jubatus*)..... 22

Figure 7: Landmarks placed on examplar specimen. 26

Figure 8: Scatterplot of $\log_{10}$ mandible centroid size and $\log_{10}$ body mass, illustrating an example of a significant interaction effect. 34

Figure 9: PC 1 and PC 2 axes associated with major mandible shape variation in fully landmarked mammal species. 40

Figure 10: Landmark configurations corresponding to the PC 1 and PC 2 extreme values of fully landmarked mammal species. 41

Figure 11: PC 1 and PC 2 axes associated with major mandible shape variation in partially landmarked mammal and non-mammalian cynodont species. 43

Figure 12: Landmark configurations corresponding to the PC 1 and PC 2 extreme values of partially landmarked mammal and cynodont species. 44

Figure 13: PC 1 and PC 2 axes of shape variation amongst partially landmarked mammal and non-mammalian cynodont species, partitioned according to major taxonomic groups. 46

Figure 14: Scatterplot of shape regression scores and $\log_{10}$ body mass, alongside the mandibular shape differences associated with the effect of increasing $\log_{10}$ body mass. 48

Figure 15: Scatterplot of shape regression scores and log_{10} mandible centroid size, alongside the mandibular shape differences associated with increasing log_{10} centroid size 49

Figure 16: Scatterplot of shape and the arcsine transformed carnivory values, alongside the mandibular shape differences associated with the partial effect of carnivory. 50

Figure 17: Landmark configurations in a small-bodied and large-bodied carnivore.. 51

Figure 18: Scatterplot of shape and the arcsine transformed nectivory values, alongside the mandible shape differences associated with the partial effect of nectivory. 52

Figure 19: Landmark configurations in a small-bodied and large-bodied nectivore.. 53

Figure 20: Scatterplot of shape and the arcsine transformed granivory values, alongside the mandible shape differences associated with the partial effect of granivory. 53

Figure 21: Landmark configurations in a small-bodied and large-bodied granivore.. 54

Figure 23: Landmark configurations in a small-bodied and large-bodied invertivore. 55

Figure 22: Scatterplot of shape and the arcsine transformed invertivory values, alongside the mandible shape differences associated with the partial effect of invertivory. 55

Figure 24: Scatterplot of shape and the arcsine transformed herbivory values, alongside the mandible shape differences associated with the main effect of herbivory. 56

Figure 25: Landmark configurations in a small-bodied and large-bodied herbivore.. 57

Figure 26: Landmark configurations in a small-bodied and large-bodied frugivore... 57

Figure 27: Landmark configurations representing mandible shape differences in a correctly classified herbivorous mammal and herbivorous mammals misclassified as a carnivore or invertivore. 59

Figure 28: Landmark configurations representing mandible shape differences in a correctly classified carnivorous mammal and carnivorous mammals misclassified as an invertivore or carnivore. 60

Figure 29: Landmark configurations representing mandible shape differences in a correctly classified invertivorous mammal and invertivorous mammals misclassified as a carnivore or herbivore. 62

Figure 30: Landmark configurations representing mandible shape of non-mammalian cynodonts estimated as carnivorous, herbivorous and invertivorous. 64

Figure 31: Scatterplot of $\log_{10}$ mandible centroid size and $\log_{10}$ body mass. 67

Figure 32: Scatterplot of $\log_{10}$ mandible centroid size and $\log_{10}$ body mass, illustrating the interaction that $\log_{10}$ body mass with frugivory, relative to non-frugivorous mammals. 68

Figure 33: Scatterplot of $\log_{10}$ mandible centroid size and $\log_{10}$ body mass, illustrating the interaction that $\log_{10}$ body mass has with granivory, relative to non-granivorous mammals. 69

Figure 34: Scatterplot of relative mandible size and $\log_{10}$ body mass amongst mammals and non-mammalian cynodonts. 70

Figure 35: Box and whisker plots showing the distribution of average OPCR scores (OPCRavg) amongst non-mammalian cynodonts within qualitatively inferred diet categories. 79

Figure 36: Box and whisker plots showing the distribution of average OPCR scores (OPCRavg) amongst major mammalian orders relative to non-mammalian cynodonts. 80

Figure 37: Box and whisker plots showing the distribution of average OPCR scores (OPCRavg) amongst mammal species within major diet categories. 83

Figure 38: Box and whisker plots showing the distribution of average OPCR scores (OPCRavg) amongst mammal species within finer diet categories. 84

Figure 39: Scatterplot of average OPCR scores (OPCRavg) and $\log_{10}$ body mass, illustrating the interaction that $\log_{10}$ body mass has with granivory, relative to non-granivorous mammals. 87

Figure 40: Box and whisker plots showing the distribution of summed OPCR scores (OPCRsum) amongst non-mammalian cynodonts within qualitatively inferred dietary categories. 89

Figure 41: Box and whisker plots showing the distribution of summed OPCR scores (OPCRsum) amongst major mammalian orders relative to non-mammalian cynodonts. 90

Figure 42: Box and whisker plots showing the distribution of summed OPCR scores (OPCRsum) amongst mammal species within major diet categories. 92

Figure 43: Box and whisker plots showing the distribution of summed OPCR scores (OPCRsum) amongst mammal species within finer diet categories. 93

Figure 44: Scatterplot of summed OPCR scores (OPCRsum) and $\log_{10}$ body mass, illustrating the interaction that $\log_{10}$ body mass has with granivory, relative to non-granivorous mammals. 96

Figure 45: Distribution of OPCR scores for the third-last postcanine tooth, or functionally analogous ‘first molar’ (OPCrm1), among non-mammalian cynodonts within qualitatively inferred dietary categories. 98

Figure 46: Box and whisker plots showing the distribution of OPCR scores for the first molar (OPCRm1) amongst major mammalian orders relative to non-mammalian cynodonts. 99

Figure 47: Box and whisker plots showing the distribution of OPCR scores for the first molar (OPCRm1) amongst mammal species within major diet categories. 101

Figure 48: Box and whisker plots showing the distribution of OPCR scores for the first molar (OPCRm1) scores amongst mammal species within finer diet categories.... 102

Figure 49: Scatterplot of OPCR scores for the first molar (OPCRm1) and $\log_{10}$ body mass, illustrating the interaction that $\log_{10}$ body mass has with granivory, relative to non-granivorous mammals. 105

Figure 50: Distribution of OPCR scores for the second-last postcanine tooth, or functionally analogous ‘second molar’ (OPCrm2), among non-mammalian cynodonts within qualitatively inferred dietary categories. 106

Figure 51: Box and whisker plots showing the distribution of OPCR scores for the second molar (OPCRm2) amongst major mammalian orders relative to non-mammalian cynodonts..... 107

Figure 52: Box and whisker plots showing the distribution of OPCR scores for the second molar (OPCRm2) amongst mammal species within major diet categories..110

Figure 53: Box and whisker plots showing the distribution of OPCR scores for the second molar (OPCRm2) amongst mammal species within finer diet categories.... 111

Figure 55: Distribution of OPCR scored for the posteriormost postcanine tooth, or functionally analogous ‘third molar’ (OPCRm3), among non-mammalian cynodonts within qualitatively inferred dietary categories. 116

Figure 56: Box and whisker plots showing the distribution of OPCR scores for the third molar (OPCRm3) amongst major mammalian orders relative to non-mammalian cynodonts. 117

Figure 57: Box and whisker plots showing the distribution of OPCR scores for the third molar (OPCRm3) amongst mammal species within major diet categories. 119

Figure 58: Box and whisker plots showing the distribution of OPCR scores for the third molar (OPCRm3) amongst mammal species within finer diet categories. 120

Figure 59: Scatterplot of OPCR scores for the third molar (OPCRm3) and $\log_{10}$ body mass, illustrating the interaction that $\log_{10}$ body mass has with granivory, relative to non-granivorous mammals. 123

Figure 60: Scatterplot of OPCR scores for the third molar (OPCRm3) and $\log_{10}$ body mass, illustrating the interaction that $\log_{10}$ body mass has with carnivory, relative to non-carnivorous mammals. 124

Figure 61: Occlusal views of OPCR 3D colours maps and associated OPCR scores (OPCRavg and OPCRsum) amongst a correctly classified invertivorous mammal and invertivorous mammals misclassified as a herbivore or carnivore. 126

Figure 62: Occlusal views of OPCR 3D colours maps and associated OPCR scores (OPCRavg and OPCRsum) amongst a correctly classified carnivorous mammal and carnivorous mammals misclassified as an invertivore or herbivore 128

Figure 63: Occlusal views of OPCR 3D colours maps and associated OPCR scores (OPCRavg and OPCRsum) amongst a correctly classified herbivore and herbivorous mammals misclassified as an invertivore or carnivore. 129

Figure 64: Occlusal views of OPCR 3D colour maps and associated OPCR scores (OPCRavg and OPCRsum) in cynodont species that pDFA iterations estimated as a carnivore, invertivore and herbivore. 131

Figure 65: Occlusal views of OPCR 3D colours maps and associated OPCR scores (OPCRm1-m3) amongst a correctly classified carnivorous mammal and carnivorous mammals misclassified as a herbivore or invertivore. 135

Figure 66: Occlusal views of OPCR 3D colours maps and associated OPCR scores (OPCRm1-m3) amongst a correctly classified herbivorous mammal and herbivorous mammals misclassified as an invertivore or carnivore. 136

Figure 67: Occlusal views of OPCR 3D colours maps and associated OPCR scores (OPCRm1-m3) amongst a correctly classified invertivorous mammal and invertivorous mammals misclassified as a herbivore or carnivore. 137

Figure 68: Occlusal views of OPCR 3D colour maps and associated OPCR scores in cynodont species estimated as a carnivore, invertivore and herbivore. 140

Figure 69: Scatterplot of shape regression scores and OPCRm1 scores, alongisde the mandibular shape differences associated with the effect of increasing OPCRm1 scores. 147

Figure 70: Scatterplot of shape regression scores and OPCRm3 scores, alongisde the mandibular shape differences associated with the effect of increasing OPCRm3 scores. 149

Figure 71: Landmark configurations alongside associated OPCR 3D colour maps and OPCRm1-m3 scores amongst a correctly classified herbivorous mammal and herbivorous mammals misclassified as a carnivore or invertivore. 151

Figure 72: Landmark configurations alongside associated OPCR 3D colour maps and OPCRm1-m3 scores amongst a correctly classified invertivorous mammal and invertivorous mammals misclassified as a carnivore or herbivore. 153

Figure 73: Landmark configurations alongside associated OPCR 3D colour maps and OPCRm1-m3 scores amongst a correctly classified carnivorous mammal and carnivorous mammals misclassified as an invertivore or carnivore. 154

Figure B1: Time-scaled phylogenetic tree of mammal species. 204

Figure B2: Time-scaled phylogenetic tree used for non-mammalian cynodont species. 205

Figure B3: Merged super-tree containing mammal and non-mammalian cynodont species. 206

Table 1: Majority consumed diet categories and descriptions. 25

Table 2: Traditional, or ‘major’ diet categories and descriptions 25

Table 3: Landmark number, count and description associated with the dermacation of the placement of each landmark. 27

Table 4: An example of a pgls model which assesses whether herbivores have a different pattern of mandible allometry than non-herbivores. 33

Table 5: Phylogenetic ANOVA regressions (procDgls) assessing the association between mandible shape (Shape) and log_{10} body mass (BM), log_{10} centroid size (Size) and dietary variables amongst mammal species. 47

Table 6: Confusion table for pDFAs which estimated diet using mandible shape. 58

Table 7: The estimated diets of non-mammalian cynodont species associated with pDFAs which made use of mandible shape. 63

Table 8: Phylogenetic regressions assessing log_{10} mandible centroid size's association with log_{10} body mass and dietary variables amongst mammal species. 65

Table 9: Confusion table for pDFAs which estimated diet using log_{10} mandible centroid size residuals and log_{10} body mass. 71

Table 10: The estimated diets of non-mammalian cynodont species associated with pDFAs that used log_{10} mandible centroid size residuals and log_{10} body mass. 74

Table 11: Confusion table for pDFAs which estimated diet using mandible shape, log_{10} mandible centroid size residuals and log_{10} body mass 75

Table 12: The estimated diets of non-mammalian cynodont species associated with the pDFAs that used mandible shape, log_{10} mandible centroid size residuals and log_{10} body mass. 78

Table 13: Phylogenetic regressions assessing the association that OPCRavg has with log_{10} body mass, log_{10} mandible centroid size and dietary variables amongst mammal species 85

Table 14: Phylogenetic regressions assessing the association that OPCRavg has with log_{10} body mass, log_{10} mandible centroid size and dietary variables amongst living taxa 94

Table 15: Phylogenetic regressions assessing the association that OPCRm1 has with log_{10} body mass, log_{10} mandible centroid size and dietary variables amongst living taxa. 103

Table 16: Phylogenetic regressions assessing the association that OPCRm2 has with log_{10} body mass, log_{10} mandible centroid size and dietary variables amongst living taxa. 112

Table 17: Phylogenetic regressions assessing the association that OPCRm3 has with log_{10} body mass, log_{10} mandible centroid size and dietary variables amongst living taxa. 121

Table 18: Confusion table for pDFAs which estimated the diet of mammal species using OPCRavg and OPCRsum scores. 126

Table 19: The estimated diets of cynodont species associated with the pDFAs which that used using OPCRavg and OPCRsum scores as training data. 132

Table 20: Confusion table for pDFAs which estimated diet using OPCRm1-m3 scores. 133

Table 21: The estimated diets of cynodont species associated with the pDFAs which that used using OPCRm1-m3 scores as training data. 139

Table 22: Confusion table for pDFAs which estimated diet using OPCRm1-m3 scores and log_{10} body mass. 141

Table 23: The estimated diets of cynodont species associated with the pDFAs which that used using OPCRm1-m3 scores and log_{10} body mass. 145

Table 24: Phylogenetic ANOVA regressions assessing mandibular shape's association with OPCR variables. 146

Table 25: Confusion table for pDFAs which estimated diet using mandible shape and OPCRm1-m3 scores. 151

Table 26: The estimated diets of cynodont species associated with pDFAs which made use of mandible shape (first seven PCA axes) and OPCRm1-m3 scores. ... 155

Table A1: List of mammal species sampled, together with their specimen numbers and taxonomic affiliations. 183

Table A2: List of cynodont species sampled, together with their specimen numbers and taxonomic affiliations. 201

Table A3: CT scanning parameters of specimens that were scanned at the Evolutionary Studies Institute (ESI). 203

Table C1: Diet data used for mammal species and the associated metadata. 207

Table C2: Expected diets of non-mammalian cynodont species inferred based off qualitative observations and the associated metadata. 261

Table D1: Body mass data for mammal species and associated metadata. 262

Table D2: Body mass approximations used for non-mammalian cynodont species and associated metadata..... 268

Table D3: Skull length (SL) measurements and the respective body mass estimates. 269

Table E1: OPCR scores used for the lower premolars (pm1-3) of mammal species. 270

Table E2: OPCR scores used for the lower premolars and molars (pm4; m1-m2) of mammal species..... 283

Table E3: OPCR scores used for the lower molars (m2-m4) of mammal species. . 295

Table E4: Postcanine teeth counts reported amongst non-mammalian cynodont species. 303

Table E5: OPCR scores used for the lower molars (m3-5) in non-mammalian cynodont species..... 304

Table E6: OPCR scores used for the lower postcanines (pc1-3) of non-mammalian cynodont species..... 306

Table E7: OPCR scores used for the lower postcanines (pc4-pc6) in non-mammalian cynodont species..... 308

Table E8: OPCR scores used for the lower postcanines (pc7-9) in non-mammalian cynodont species..... 310

Table E9: OPCR scores used for the lower postcanines (pc10-13) in non-mammalian cynodont species..... 312

Table E10: OPCRsum and OPCRavg scores used for mammal and non-mammalian cynodont species..... 314

7. LIST OF SYMBOLS

P5	5th percentile
P95	95th percentile
PP	Posterior probability

8. INTRODUCTION

8.1 The Karoo Basin

The sedimentary rock units of South Africa's Karoo Basin contain an abundant, almost-continuous plant and animal fossil record from the Late Carboniferous (300 Ma) to the Early Jurassic (190 Ma) (Smith et al., 2020). These fossils (particularly from the Beaufort and Stormberg groups) document the early evolutionary history of major extant vertebrate groups including fish, amphibians, reptiles, birds (via dinosaurs), and most importantly mammals via their cynodont ancestors (Smith, 1990, Smith et al., 2020).

Cynodonts are a key group of synapsids that includes all living mammals and their closest extinct relatives among Therapsida (Hopson and Kitching, 2001, Liu and Olsen, 2010). Within Cynodontia, several reciprocally monophyletic groups form a nested grade of successive sister-taxon relationships with Mammaliaformes, including tritylodontids, brasilidontids, trithelodontids and gomphodonts (Kemp, 1983, Rowe, 1988, Smith, 1990, Rowe, 1993, Liu and Olsen, 2010). These groups, which fall outside mammaliaforms, form a paraphyletic grade often referred to as "non-mammalian cynodonts".

Fossils of non-mammalian cynodonts are well represented in the Main Karoo Basin (MKB), with 24 recognized taxa (Figure 1) (Botha and Smith, 2020, Hancox et al., 2020, Rubidge and Day, 2020, Smith et al., 2020, Smith, 2020, Viglietti, 2020, Viglietti et al., 2020a, Viglietti et al., 2020b). Their first appearance in the MKB is documented in the *Endothiodon* Assemblage Zone of the Beaufort Group, which dates back the Early Late Permian (Wuchiapingian age) (Botha et al., 2007, Rubidge and Day, 2020), and their last appearance is in the Early Jurassic (Rhaetian age), as recorded in the *Massospondylus* Assemblage Zone (Crompton, 1964). Their temporal range, spanning approximately 58 Ma, documents the acquisition of mammalian characteristics (Luo, 2007, Lautenschlager et al., 2017). The cynodonts that emerged during this period often lived contemporaneously (Figure 1), and exhibited a wide range of size classes and feeding apparatuses (i.e., tooth forms and mandible forms) (Abdala et al., 2006, Kemp, 2016, Abdala and Gaetano, 2018, Hendrickx et al., 2019, Hendrickx et al., 2020).

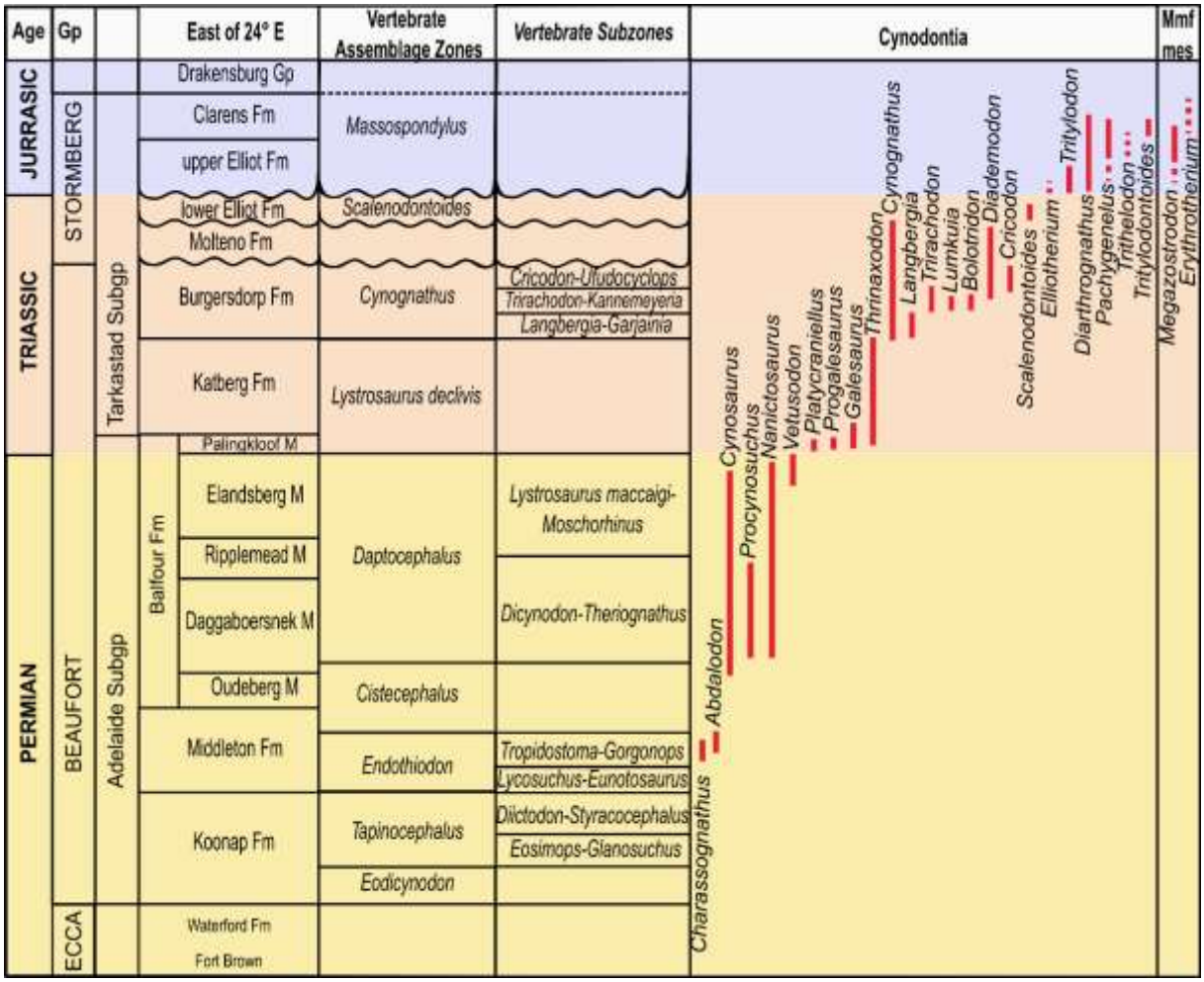


Figure 1: Lithostratigraphy and vertebrate biozonation ranges of the Beaufort and Stormberg groups of South Africa's Karoo Supergroup showing the stratigraphic ranges of South Africa's cynodonts. Solid lines indicate known ranges, dotted lines indicated suspected ranges that have not been confirmed. Figure modified from Smith et al. (2020).

8.2 Cynodonts and their dietary adaptations

Living mammal species are characterized by their primary jaw joint being between the dentary and squamosal, and the lower jaw consists of a single bone, the dentary (Crompton, 1963, Crompton et al., 1972). Non-mammalian cynodonts have postdentary bones (angular, articular, surangular and splenial), and in early members, the jaw joint is between the quadrate and the angular. During the course of cynodontian evolution, these postdentary bones eventually become reduced and the quadrate and articular bones migrate to form part of the middle ear (Luo, 2007). This transition coincided with changes in muscle orientation, mandible shape, and tooth form and occlusion (Gow, 1978, Lautenschlager et al.,

2017), which are often regarded as adaptations associated with the evolutionary success and ultimate radiation of mammals (Evans and Pineda-Munoz, 2018, Berkovitz and Shellis, 2018).

Early members of Cynodontia, such as *Procynosuchus*, had a prominent dentary bone with a high coronoid process, present but highly reduced post-dentary bones and heterodont dentition. The occlusal surfaces of the posterior postcanine tooth crowns are more “complex” than the anterior teeth because they bear cuspules and a fully expressed cingulum. The teeth did not precisely occlude at this stage. According to Kemp (1979), these features implied that *Procynosuchus* ate insects and was somewhat adapted to chewing them instead of swallowing them whole.

Cynodonts branching later than *Procynosuchus* and its close relatives like *Thrinaxodon* form the Eucynodontia (Figure 2). Even the earliest eucynodonts are distinguished from basal members by an even larger dentary, with postdentary bones that are reduced to a small rod. The coronoid process is tall, and there is a large angular process ventrally (Kemp, 2005). These features, together with a prominent fossa on the lateral surface of the coronoid process, indicate that these eucynodonts had already developed masseteric musculature (Crompton and Hotton III, 1967, Barghusen, 1968, Bramble, 1978, Lautenschlager et al., 2017). There was no mammal-like jaw joint, but the group possessed a secondary contact between the surangular and squamosal bones (Jenkins, 1971).

Gomphodontia are an early-branching diverse group of eucynodonts that lived from the Middle Late Triassic (Seeley, 1895, Crompton, 1972, Crompton et al., 1972, Hopson et al., 1991, Kemp, 2005). Gomphodonts are characterized by the presence of buccolingually expanded molariform postcanine teeth that occluded in a manner similar to mammals, although it was unlikely to have been precise (Crompton et al., 1972, Kemp, 1982, Sues and Hopson, 2010, Hendrickx et al., 2016). Gomphodont postcanines are broadened and contain accessory cusps, ridges and basins that increase the complexity of their occlusal surface (Seeley, 1895, Sues and Hopson, 2010, Abdala and Gaetano, 2018, Hendrickx et al., 2019). The diets of gomphodonts are broadly inferred as herbivorous or omnivorous based off the presence of these gomphodont postcanines (Reisz and

Sues, 2000, Abdala and Ribeiro, 2003, Abdala and Sa-Teixeira, 2004, Hopson and Sues, 2006, Sues and Hopson, 2010, Hendrickx et al., 2020).

Gomphodontia contains three main groups: Diademodontidae, Trirachodontidae and Traversodontidae (Figure 2) (Seeley, 1895, Liu and Abdala, 2014). Diademodontidae are the earliest-branching clade of gomphodonts and have a combination of gomphodont and sectorial teeth (Gow, 1978). Trirachodontidae branch after diademodontids, and are currently hypothesized to be a sister group to Traversodontids (Sidor and Hopson, 2017). Trirachodontids also have a combination of gomphodont and sectorial teeth, with fewer sectorial teeth than in diademodontids (Sidor and Hopson, 2017, Hendrickx et al., 2019). Traversodontidae are the most taxonomically diverse gomphodont group, and they formed a major component of the cynodont fauna in the Triassic of Gondwana. Traversodontid postcanines consist of mainly gomphodont teeth (Abdala and Ribeiro, 2003, Abdala et al., 2006, Sues and Hopson, 2010). They are the latest-surviving group amongst gomphodonts, with their last appearance dating back to the Late Triassic (Hopson, 1984, Sues and Olsen, 1990, Sues et al., 1992, Gow et al., 1993, Sues et al., 1999). The ~30 Ma that their lineage persisted records an increase in body sizes, concomitant with an increase in tooth complexity (i.e., qualitatively observed) (Martinelli and Soares, 2016), and these features are assumed to correspond to a change in food resources (Abdala and Ribeiro, 2010, Martinelli and Soares, 2016, Abdala and Gaetano, 2018).

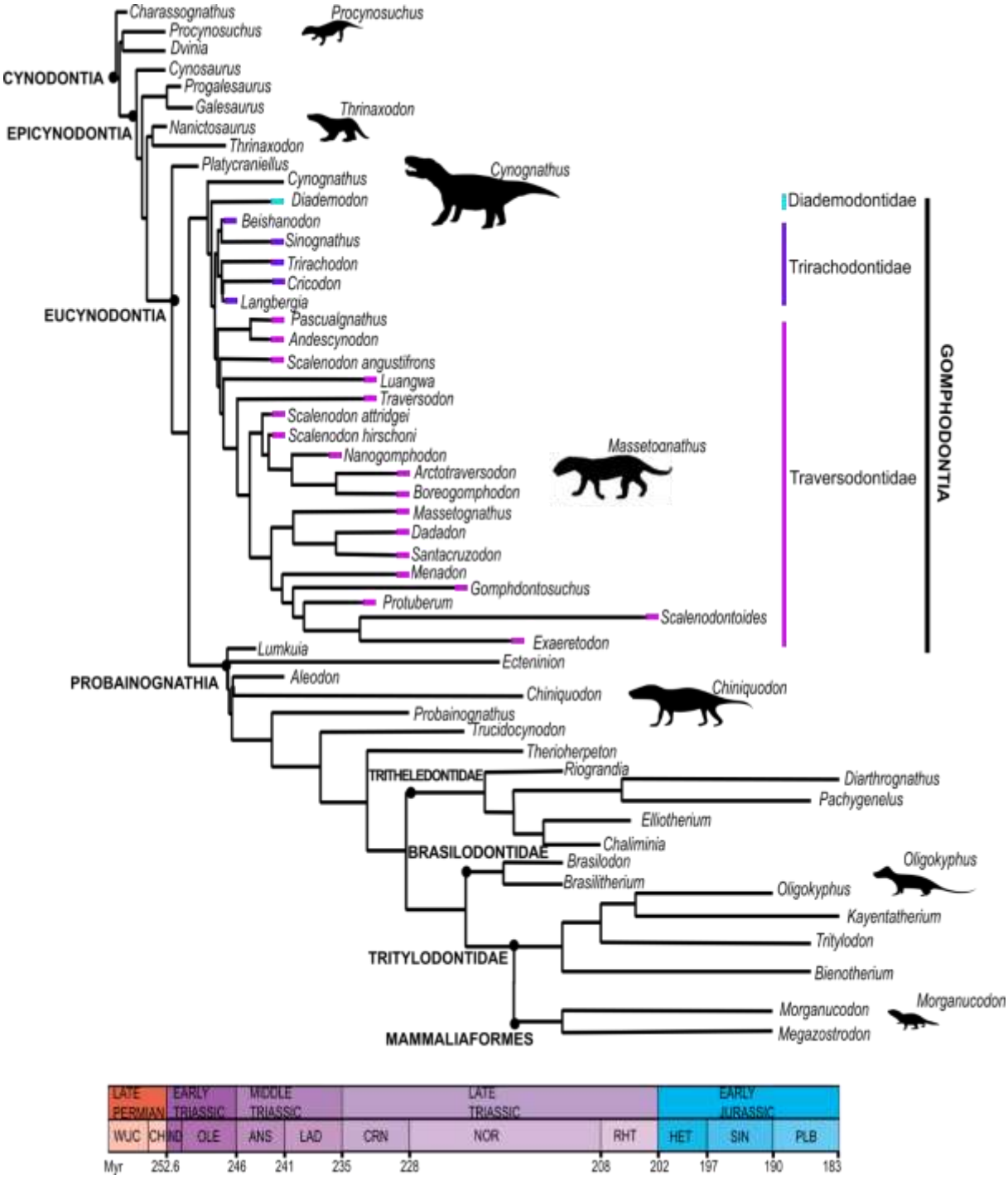


Figure 2: Cynodont phylogeny alongside stratigraphic scale showing relationships and occurrences of members. The relationships within families of Gomphodontia are annotated. Figure modified from Ruta et al. (2013).

8.3 Dietary inferences in the fossil record

Dietary inferences in the fossil record are made using a wide range of methods such as dental microwear, stable isotopes, and qualitative comparative studies (e.g., Goswami et al., 2005, Clementz, 2012, Pineda-Munoz et al., 2016, Evans and Pineda-Munoz, 2018, Melstrom and Irmis, 2019, Morales-García et al., 2021). However, inferring diet from the fossil record is difficult because direct evidence of paleoecology (i.e., fossilized stomach contents, coprolites) is relatively rare or understudied (Martill et al., 1994, Kriwet et al., 2008, Zipfel et al., 2023). Nevertheless, reconstructing the diets of fossils is important because diet is a fundamental aspect of biology which can influence a species' physiology and morphology (Carbone et al., 1999, Price and Hopkins, 2015). Additionally, reconstructing the diets of fossils is crucial for understanding past ecosystems. The importance of studying diet in deep time and its evolutionary history therefore calls for continued efforts to find osteomorphological traits that strongly correlate with dietary preferences (Grossnickle et al., 2019). Ecomorphological studies that are targeted at understanding the link between form and function are highly relevant to palaeobiology because our understanding of an extinct animal's ecology hinges on the relationship that morphological adaptations have with behaviour in living organisms (Price and Hopkins, 2015, Benevento et al., 2019, Morales-García et al., 2021).

Living mammal species have an incredibly diverse diet, and they encompass a wide range of dietary niches that evolved repeatedly among phylogenetically independent groups (Jones and Safi, 2011, Wang et al., 2020). This dietary variation is coupled with conspicuous differences in osteological components of the feeding apparatus, particularly the lower jaw and teeth (Hoshi, 1971, Ungar, 2010), making them an ideal natural testing ground for dietary ecomorphology. Non-mammalian cynodonts document the evolutionary origins of some of the major adaptations to which the adaptive success of Mammalia has been attributed. These adaptations include precise tooth occlusion and the squamosal-dentary jaw joint (Kardong, 2012, Bonnan, 2016). These changes enabled mammals to become the "champion chewers" that they are today, and the disparity of tooth forms, mandible shapes and sizes are widely regarded as morphological adaptations to the types of food eaten (Hoshi, 1971, Liem et al.,

2001, Bonnan, 2016). By comparing the breadth of dietary adaptations in extant mammal species to non-mammalian cynodonts we can learn more about the evolutionary sequence that led to the first true mammals (Botha et al., 2005).

Comparative ecomorphological studies often focus on craniodental features, particularly the mandible and teeth, because of the association that these features have with dietary adaptations (Frederich et al., 2008, Cassini, 2013, Hedrick and Dumont, 2018). Additionally, these elements are thought to be evolutionarily decoupled from adaptations of the sensory systems (Ross et al., 2012, Prevosti et al., 2012). Historically, studies of non-mammalian cynodont diets have used qualitative inference through anatomical comparisons of mandibular and dental morphology (e.g., Gow, 1978, Reisz and Sues, 2000, Fastovsky, 2001).

A growing number of recent studies have attempted to establish quantitative means of dietary inference (Morales-García et al., 2021, Huttenlocker et al., 2021). This allows more explicit testing of non-mammalian cynodont diets. However, these inferences are limited if they are not transparently benchmarked against the known diets of living taxa.

This thesis aims to evaluate the relationships between diet and the predictor variables of mandible shape, size (the combined information from body mass and relative mandible size), and dental complexity in extant mammals. My aims are: 1) to assess the strength of these associations in living mammal species, where diet is known; and 2) to assess the utility of these variables for inferring the diets of cynodont species.

8.4 Dietary evaluation using craniodental anatomy

8.4.1 Dietary inferences using mandible shape

Mandible shape provides key information about the biomechanics of the feeding apparatus (Marcé-Nogué et al., 2017). The well-developed theory of lever mechanics provides testable links between the shape changes of the mandible, orientation of the muscle action and aspects of feeding such as gape and bite (Fabre et al., 2018, Sella-Tunis et al., 2018).

Clear osteomorphological features have been hypothesized to have relevance to the functional adaptations of carnivorous and herbivorous diets (Radinsky, 1981a,

Liem et al., 2001, Cox et al., 2012, Barbero et al., 2023). For example, carnivorous mammals have a large temporalis muscle, which inserts on a large triangular shaped coronoid process (Figure 3) (Radinsky, 1981a, Hartstone-Rose et al., 2012). The orientation of the temporalis increases the mechanical advantage and maximizes the muscle's line of action, enabling a powerful bite force (Liem et al., 2001, Hartstone-Rose et al., 2012, Hartstone-Rose et al., 2019). Relative to carnivores, herbivorous animals have much large masseter and mandibular pterygoid muscles which inserts on an enlarged posterior mandible body (Figure 3) (Pérez-Barbería and Gordon, 1999, Crompton et al., 2010). The mandibular condyles of herbivores are elevated (Figure 3), and this together with the orientation of the masseter and pterygoid increases the mechanical advantage. This provides herbivores with the necessary force and freedom of movement (around the mandibular condyle) that is required for grinding plant material (Liem et al., 2001).

Morphometrics is the study of shape variation and its covariation with other variables. The association, causes and effects that variables have with shapes are assessed by applying multivariate statistical analyses to sets of morphological variables (Bookstein, 1991). Early research in morphometrics entailed quantifying shape through linear distance measurements, angles or ratios (Bouvier, 1986b, Takahashi and Pan, 1994), but using these metrics became challenging as there was no consensus amongst researchers on suitable size correction methods. Additionally, linear distances were not always defined by homologous points and these measurements did not capture the general shape of the object well. These challenges prompted researchers to explore alternative methods of quantifying shape, which eventually gave rise to modern geometric morphometrics (Kendall, 1984, Rohlf and Slice, 1990, Bookstein, 1991, Rohlf and Marcus, 1993, Adams et al., 2004). In geometric morphometrics, shape is quantified as a set of landmark-based coordinates or outlines that represent biologically defined points. This enables the retention of the general shape or geometry of an object, particularly the relative spatial positions of points (Slice, 2007).

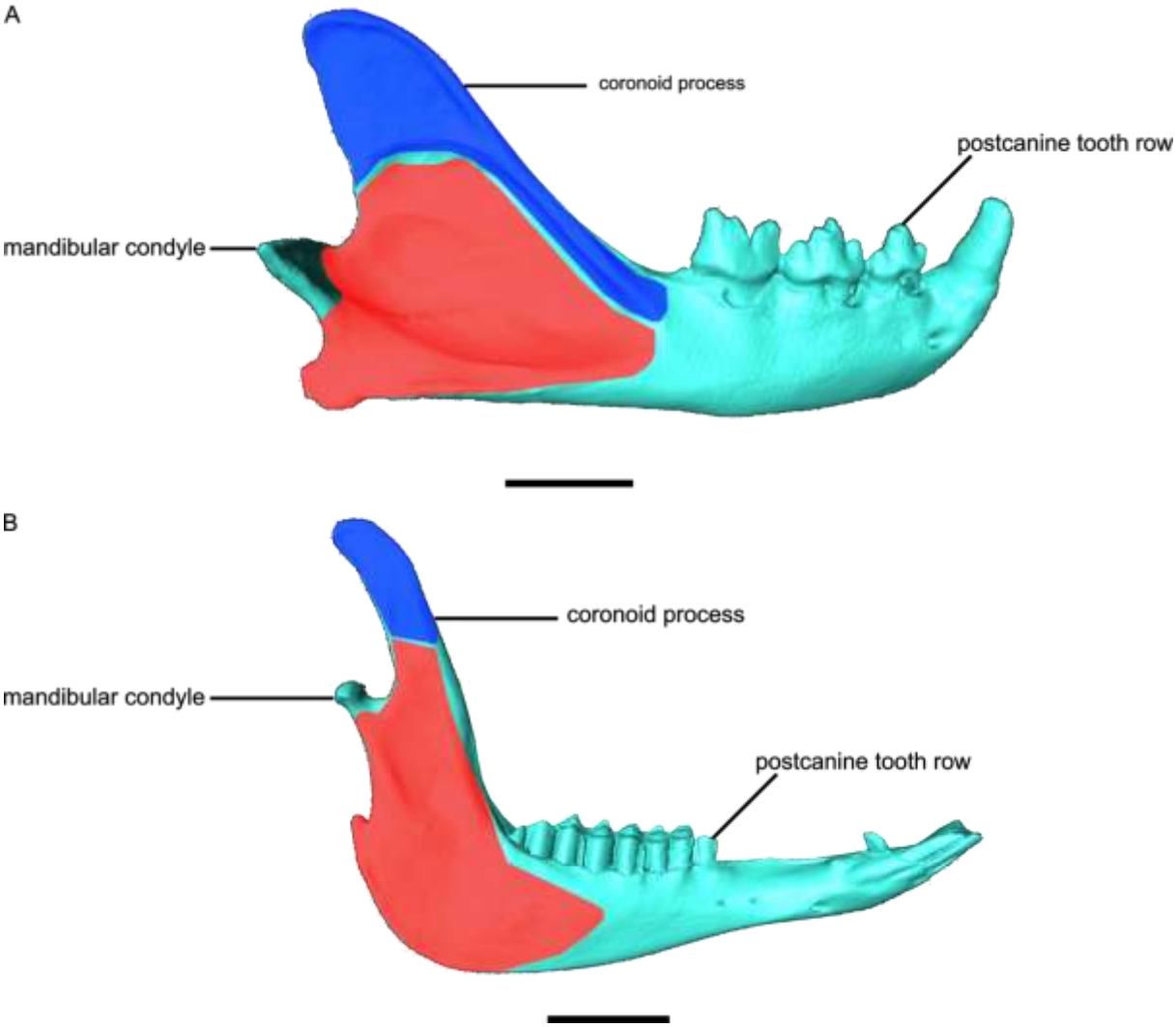


Figure 3: Representative variation in mandibular morphology in A: carnivorous mammal (a cheetah, *Acinonyx jubatus*; scale bar equals 39mm); B: herbivorous mammal (a vicuña, *Vicugna vicugna*; scale bar equals 54 mm). Mandibles shown in lateral view. Blue shading represents the temporal group's muscle attachment sites, and the red shading represents the masseter muscle group's attachment sites. Musculature based off Pérez-Barbería and Gordon (1999) and Hartstone-Rose et al. (2012).

There are three main categories of landmarks. Type 1 landmarks are discrete juxtapositions which are distinct objectively locatable points in space, these include foramina and the points at which three bones meet. Type 2 landmarks are maxima of curvatures or points of correspondence indicated by geometry, such as the tip of a process or the notch of a bone. Type 3 landmarks are extremal endpoints which are defined in relation to the positions of other structures

elsewhere on the bone, such as the anterior-most point of a bone and inter-landmark segments (Bookstein, 1991, Bookstein, 1985, Bookstein and Cutting, 1988, Cooke and Terhune, 2015, Palci and Lee, 2019). Generalized Procrustes Analysis (GPA) translates and rotates each specimen to minimize the squared summed distance between corresponding landmarks, and by doing this specimens are scaled to the same unit (centroid size). This brings the landmarks to a common coordinate system which enables differences in configuration (not orientation, scale or rotation) of shapes to be expressed (Bookstein, 1991, Rohlf, 1999, Slice, 2007).

Previous ecomorphological studies that made use of mandible shape (i.e., using geometric morphometric frameworks) generally found that diet explains little of the variation in mandible shape (Hautier et al., 2008, Prevosti et al., 2012, Wang et al., 2021). However, there is often no standardization in dietary categorization and the proxies (e.g., Procrustes coordinates, PCA coordinates, partial warps) used to represent mandible shape which makes it difficult to compare their results and understand which factors cause studies to arrive at different conclusions. Procrustes coordinates directly represent shape variation, and studies that made use of these found that diet explains approximately 8% of the mandible shape variation in rodents (MANOVA R^2=0.0082) and bovids (procDgls R^2=0.08). Hautier et al. (2008) partitioned diet as hypercarnivory, animal-dominated omnivory, plant-dominated omnivory, and herbivory whereas Wang et al. (2021) partitioned diet according to browsers, mixed-feeders and grazers.

Diet explained 42% (pgls using PCA coordinates of shape R^2=0.42) of the variation in the major aspects of mandible shape as described by principal axes (PC) in bats (Nogueira et al., 2009, Hedrick and Dumont, 2018). Nogueira et al. (2009) partitioned the diet of bats into insectivory, frugivory, nectivory, and carnivory. Hedrick and Dumont (2018) instead categorized diet by assigning one of five character states, informed by the mechanical properties of food, whereby one was indicative of a liquid diet and five was indicative of a very hard diet.

Prevosti et al. (2012) found that diet plays a key factor in mandibular shape of marsupial and placental carnivorous taxa using partial warps. Although no direct correlation statistic is reported, Prevosti et al. (2012) reports that there was still a

substantial amount of variation in mandible shape that phylogenetic patterns or diet could not explain. Diet was partitioned into hypercarnivores, meso-carnivores, insectivores, and herbivores.

Outside Mammalia, the disparity of mandible shape has been associated with the diet of aquatic snakes, birds, and some groups of fish (Burress et al., 2016, Fabre et al., 2016, Navalón et al., 2019, Orkney et al., 2021). Although dietary hypotheses have been tested using mandibular morphometrics in extinct mammals (Morales-García et al., 2021), the mandible shapes of cynodonts have not been studied using a morphometric framework.

8.4.2 Dietary inferences using teeth

Teeth operate as the main mechanical interface between food and an animal's body, and teeth are directly involved in both food acquisition and food processing in mammals. Dental form and function have been the subject of many studies due to this close relationship (e.g., Crompton and Hiiemae, 1969, Sheine and Kay, 1977, Popowics, 2003, Evans and Sanson, 2006). Postcanine teeth in mammals are made up of premolars and molars. The premolars puncture and crush food, and the molars grind, crush, or shred food. The postcanine teeth are mainly adapted for mechanical processing of food within the oral cavity, and have stronger dietary signals relative to incisors and canines (Evans and Pineda-Munoz, 2018).

For example, members of the Carnivora have specialized postcanine molars known as "carnassials" which bear a sharpened surface used to cut flesh (Figure 4) (Butler, 1946, Popowics, 2003). Insectivorous mammals generally have tribosphenic or dilambdodont molars, characterized by shearing crests and a deep crushing basin (Figure 4) (Strait, 1993, Butler, 1996). Herbivorous mammals have developed a suite of modifications enabling their plant-rich diet that aid in cellulose cell wall breakdown in many taxa, including hardened enamel lophs and crests and increased occlusal surface areas through the molarization of premolars and larger tooth size (Figure 4) (Janis and Fortelius, 1988).

Due to this qualitative association between tooth shape and diet, gross tooth morphology has historically been used to infer the diet of fossil species. The disadvantage of these qualitative observations is that they often rely on the presence of specific features, and the observations may be influenced by subjective interpretations, potentially leading to bias (Pineda-Munoz et al., 2016). The first attempts to quantify tooth morphology entailed using geographic information systems (GIS) approaches in a novel way to quantify tooth shape without relying on landmarks (Zuccotti et al., 1998, Jernvall and Selänne, 1999, Ungar and Williamson, 2000). Further development of GIS methods gave rise to dental topography analysis- which is broadly defined as making use of a method that quantifies 2D/3D tooth shapes using a single metric without the use of landmarks (Dennis et al., 2004, Winchester et al., 2014).

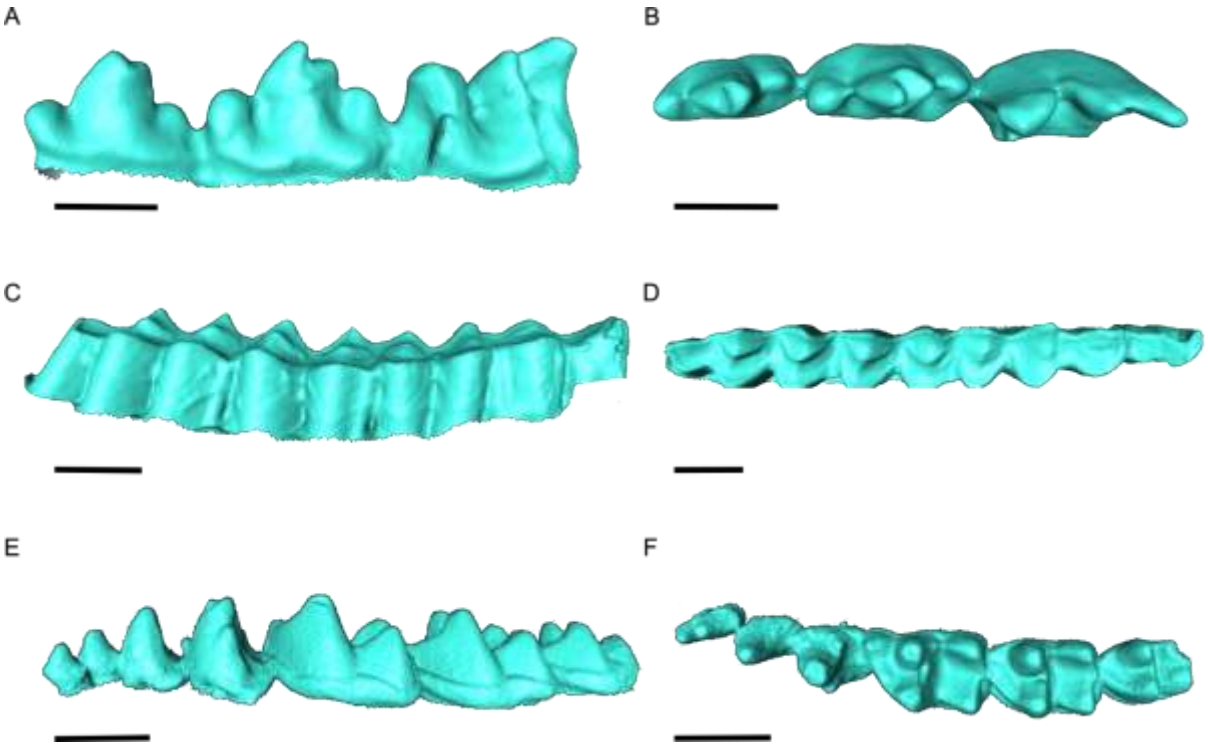


Figure 4: Postcanine tooth form variation in A, B; a carnivorous mammal (a cheetah, *Acinonyx jubatus*); C, D an herbivorous mammal (a sheep, *Ovis aries*); E, F an invertivorous mammal (moonrat, *Echinosorex gymnura*). Note differences in number of teeth and shape. Tooth rows shown in labial (A,C,E) and occlusal views (B,D,F). A,B,C scale bar equals 14mm. D scale bar equals 11mm. E,F scale bar equals 8mm.

There are many metrics that quantify various attributes of the tooth, such as relief index, Dirichlet normal energy and orientation patch count, or orientation patch count rotated (OPCR) (Berthaume et al., 2018). Amongst these metrics, OPCR is generally preferred for its broad applicability as a methodology, which enables inferences of diet in mammals (Evans et al., 2007, Santana et al., 2011) and reptiles (Melstrom and Wistort, 2021, Shipps et al., 2023).

Orientation patch count (OPC) is a univariate metric that quantifies the surface complexity of a 2D/3D mesh model of a tooth surface. Dental complexity is a measure of the number of additional features, or 'tools', on a tooth surface (Evans et al., 2007). Conceptually, this analysis is a proxy for the mechanical processing capacity of a tooth. Processing capability is hypothesized to improve when more 'tools', or features, are added to the tooth surface, as it increases the tooth's capability to divide food per mastication event. In other words, by adding more tools to the tooth, the tooth becomes more efficient at breaking food (Evans et al., 2007, Evans and Jernvall, 2009, Bunn et al., 2011). Hence, OPC can quantitatively reflect the differences in the mechanical processing capabilities between the teeth of grazers and carnivores. A grazer's tooth often has more "tools" to break down plant material because plant cell walls contain cellulose which is difficult to digest and requires breaking down physically through extensive mastication, and this results in higher OPC scores. This contrasts a carnivore's tooth, which generally have less "tools" as meat is readily digestible and requires minimal processing (mainly requires shearing), resulting in lower OPC scores (Figure 5) (Evans et al., 2007, Santana et al., 2011).

OPC summarizes the slope orientation and topographic elevation of the occlusal region of a tooth into distinct patches (Figure 5). Contiguous regions of the tooth that have the same slope orientation and topographic elevation are binned together (forming one patch) according to eight categories based on the intercardinal direction that the patch is orientated in. The dental complexity is the count of this topographic patch count (Evans et al., 2007). OPC is particularly sensitive to the initial orientation of the tooth. To reduce this sensitivity, Evans and Jernvall (2009) modified OPC to be more robust to orientation differences in the input surface. This was done by rotating an occlusally aligned tooth clockwise and calculating OPC at each new orientation for a specified number of iterations and

averaging all OPC values together. This modified method is called orientation patch count rotated (OPCR).

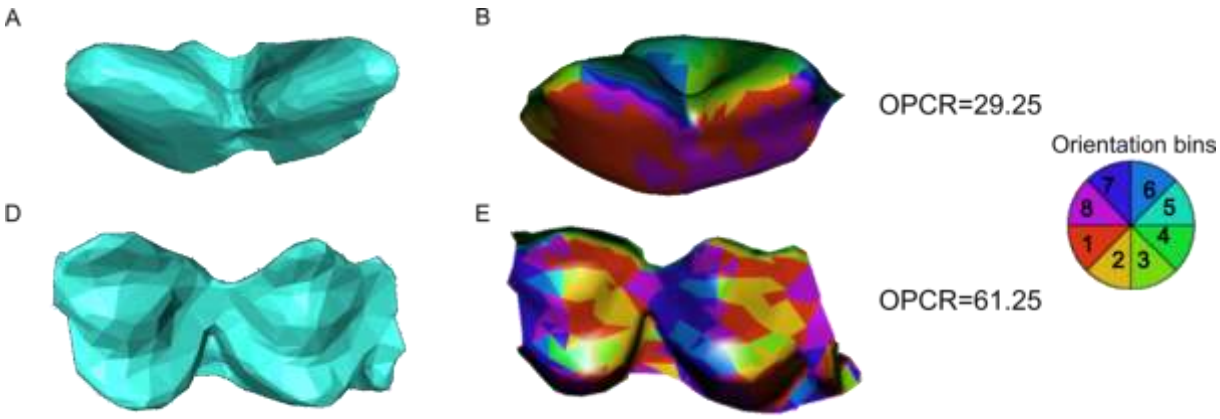


Figure 5: Differences in tooth complexity (OPCR) in the first molar of A, B: a carnivorous mammal (a cheetah, *Acinonyx jubatus*) and D, E: an herbivorous mammal (Vicuña, *Vicugna vicugna*).

Dental complexity has proved to be a useful tool, largely because it enables dietary inferences without relying on specific homologous features. Dental complexity has significant correlations with diet in rodents, mammals, marsupials, bats, and lemurs (Evans et al., 2007, Santana et al., 2011, Godfrey et al., 2012, Smits and Evans, 2012).The correlation between dental complexity and diet in such diverse groups is important, as it potentially allows inferences of diet in extinct groups that don't have close living relatives with similar ecological diversity. For example, this correlation has been used to infer diet in stem crocodylians and large-bodied diprotodontids (Melstrom and Irmis, 2019, White et al., 2021). It also facilitates evaluations of the dietary breadth of groups which have no modern analogues, such as multituberculates (Wilson et al., 2012). The dental complexity of cynodonts has only recently been evaluated, however these dental complexity values have never been compared to those of extant taxa with known dietary habits (Hendrickx et al., 2024).

8.4.3 Size and its association with diet

Allometry is broadly defined as the study of how biological variables (e.g., shape, length, physiology), change with size (Huxley, 1924, Huxley and Teissier, 1936, Thompson, 1942, Kleiber, 1947, Huxley, 1950). A fundamental observation is the

square-cube law (or surface law), whereby an organism's surface area and length should scale proportionally with mass (Huxley and Teissier, 1936, Thompson, 1942, Kleiber, 1947). The scaling relationships between mass other variables are powerfully influenced by this fundamental scaling principal. This can be explained arithmetically, as a cube with a length of 1cm, will have a surface area of $1cm^2$ and a volume of $1cm^3$. A cube that has double this length (2cm), will have a surface area of $4cm^2$ and a volume of $8cm^3$. Similarly, when an organism's volume increases proportionally to mass, or when its length increases with mass to the power 1/3 (2=cubed root of eight), we say that it scales isometrically (West and West, 2012). Deviations from this are referred to as allometric scaling (West et al., 1999).

Considering the effects of body mass is important because an animal's ecology and evolution are considerably influenced by diet and body mass (McNab, 1986, Price and Hopkins, 2015, Cooke et al., 2022, Reuter et al., 2023). For instance, terrestrial mammalian invertivores have a maximum mass of 52,350g (in myrmecophages, *Orycteropus afer*) or 900g (in other invertivores such as *Tenrec ecaudatus*), because the distribution, abundance and energy content associated with feeding on exclusively small protein rich invertebrates becomes energetically infeasible at larger body sizes (Carbone et al., 1999, Cooke et al., 2022).

Extant mammalian herbivores occupy a wide range of body sizes (13g—2,915,040g), and include species with large body sizes, unique to herbivores (not attained by mammalian carnivores and invertivores). This distribution has been linked to large-bodied mammalian herbivores strategy to prioritize food resource abundance over food resource quality (Clauss et al., 2013, Pineda-Munoz et al., 2016).

Mammalian carnivores occupy medium to large size classes (12,000g—30,000g), which has been linked to the energy constraints associated with predation as heavier carnivores are those that hunt large-bodied prey (Gittleman, 1985).

Although size, and body mass have not generally been used as a quantitative proxy for dietary inferences in fossil species (but see Clark et al., 2023), these measures have often been used to justify qualitative dietary inferences in older publications (e.g., Gow, 1978).

9. RESEARCH RATIONALE

Understanding diet in deep time is important for reconstructing past ecosystems, and exploring how dietary adaptations possibly played a role in the diversification and adaptive success of members from major amniote lineages, but inferring the diets of extinct species can be difficult. Traditionally, the ecology (i.e., diet, lifestyle) of extinct species would be inferred using qualitative approaches (Crompton and Jenkins, 1968, Jenkins and Parrington, 1976, Gow, 1978). However, in recent years there have been more studies that make use of quantitative approaches (White et al., 2021, Morales-García et al., 2021). This is largely because quantitative inferences are less subjective to human error and bias. However, this advancement in palaeobiology has been coupled with the development of more techniques that quantify aspects of morphology (Fortelius and Solounias, 2000, Evans et al., 2007, Boyer, 2008, Pineda-Munoz et al., 2017, Shan et al., 2019, Fulwood et al., 2021), and it's important to evaluate the strength of the correlations that these variables have with diet before drawing inferences about extinct species.

Understanding cynodonts' adaptations to different diets and the possible interplay that this had with body mass is important because derived cynodonts document many of the first major innovations to which the success of mammals has been attributed. These innovations include features related to improved masticatory ability such as tooth occlusion and the mammalian muscle configuration. Given that existing knowledge relied on qualitative approaches to infer the diet most cynodont species, predominantly though craniodental observations, this study will evaluate the applicability of geometric morphometrics and OPCR in inferring dietary preferences in cynodonts. While these methods are established for the crown group of mammals, cynodonts are located on the stem lineage and may not have developed the typical mammalian associations between diet, dental complexity, and mandibular shape. These relationships may still be useful in understanding cynodont's dietary adaptations.

This research has two primary aims: firstly, to understand the correlation that diet has with mandible shape, mandible size, body mass and dental complexity

(OPCR) in extant mammalian species; and secondly, to assess the utility of these variables for inferring the diets of extinct cynodonts.

10. MATERIALS

10.1 Data samples

To evaluate the relationships of mandible shape and dental complexity to diet and size, I compiled a database of three-dimensional (3D) models of the mandibles of 262 taxa across the major mammalian clades (Afrotheria, Euarchontoglires, Laurasiatheria, Marsupialia, Monotremes and Xenarthra). I selected mammals from these clades to capture as much variance in evolutionary history, size and dietary habits as possible (Table A1). These data were mostly obtained from previous scans available from the online 3D data repository, Morphosource (www.morphosource.org). Two of the mammal species were scanned at the ESI using a Nikon Metrology XTH 22/320 LC dual source micro-CT system (Table A3, Castor canadensis_WLM unnumbered, Dugong dugon_WLM unnumbered).

To determine the degree of confidence in dietary inferences made using mandible shape, size and OPCR for non-mammalian cynodonts, I broadly sampled members across fossils of extinct members of Cynodontia. This palaeontological dataset included early-diverging cynodonts such as *Procynosuchus* and *Cynognathus*, as well as more derived members such as gomphodont cynodonts and the mammaliaform, *Megazostrodon* (Table A2). Four of these specimens were CT scanned at the ESI (Table A3), and 3D models of *Procynosuchus* and *Trirachodon* were obtained from MorphoSource (Table A2). Photogrammetry models of the postcanine dentition from 14 gomphodont cynodonts were also included in the database (Table A2).

10.2 Phylogenetic data

A time-scaled phylogenetic tree of mammals (Figure B1) was obtained from VertLife (www.vertlife.org), a multi-institutional project that aims to study the biodiversity of terrestrial vertebrates (Gauthier, 2019). The phylogenetic tree was assembled from input phylogenies inferred from DNA data (Upham et al., 2019a, Upham et al., 2019b).

The topology of the phylogenetic tree that I constructed for extinct cynodonts (Figure B2) was based on Ruta et al. (2013) and Hendrickx et al. (2020). Ruta et al. (2013) made use of 150 discrete skeletal characters, and Hendrickx et al.

(2020) made use of mostly dental characters, but also included skeletal characters. The occurrences of cynodont species that were used to time scale the phylogenetic trees were obtained from the Palaeobiology Database (www.paleobiob.org).

10.3 Functional data

10.3.1 Diet

The diets of mammal species were collected from the Elton Traits Ecological Archives (E095-178-D1), which describes diet quantitatively using data sourced from existing literature (Wilman et al., 2014). The authors of the dataset partitioned diet into nine diet categories: invertivory, endothermic vertebrates, ectothermic vertebrates, unknown vertebrates, piscivory, scavenger, frugivory, nectivory, granivory and herbivorous. Under this classification scheme, the diet of an obligate grazer would be scored as “100 % herbivorous” and a taxon that has more omnivorous dietary habits could be scored, for example, as “20% herbivorous”, “50% endothermic vertebrates” and “30% nectivorous” (Table C1). This approximated the dietary breadth of each taxon. For comparability, I additionally collected verbal descriptions regarding the diet of living specimens from Nowak (1999).

The diet assigned to each extinct cynodont species was ascertained from the literature (Table C2). I refer to this as the “expected diet” throughout. These prior dietary inferences were often made using qualitative interpretations of tooth morphology, tooth wear and some authors considered body mass and the lever mechanics of the mandible (Jenkins and Parrington, 1976, Gow, 1978). The diets of many gomphodont cynodonts are broadly categorized as herbivorous based on their buccolingually expanded postcanine dentition, and amongst these the traversodontids are hypothesized to be the most specialized for herbivory (Kemp, 2005, Hendrickx et al., 2019).

10.3.2 Body mass

The body mass of living species was collected from the Elton Traits Ecological Archives (E095-178-D1) (Wilman et al., 2014) (Table D1).

When possible, body mass estimates for extinct cynodont species were collected from the literature (Table D2). However, there were some instances where body mass had not been reported, and I approximated body mass for five extinct taxa using skull length measurements reported in the literature (Table D3).

The skull is not a major weight-bearing bone and does not have the strongest relationship with body mass (Campione and Evans, 2012). However, the postcranial skeletons of cynodonts are generally understudied, and skull lengths were more frequently reported in the literature. I modified the methodology used to infer body mass from Pavanatto et al. (2019), and used two equations to estimate the body mass. The first equation ($BM_a = 2.7 \times (SL \div 10)^3$) used was developed by Quiroga, based on the relationship between skull length and body mass in therapsids (Quiroga, 1980, Quiroga, 1984). The second equation ($BM_b = (10^{3.13 \times \log(SL) - 5.59} \times 1000)$) was developed by Van Valkenburgh, based on the relationship between skull length and body mass in extant mammals (Van Valkenburgh, 1990). The average of these computations was used as the body mass for five extinct taxa (Table D3).

11. METHODS

11.1 Specimen imaging

180 mammal species and two cynodont specimens were already rendered as 3D models available for download from MorphoSource. I made 3D models of the mandibles of an additional 88 mammal species and four cynodonts in VG Studio Max version 3.2.3. These reconstructions and existing 3D models were subsequently used to landmark specimens and create 3D tooth models.

Photogrammetry images compiled by Christophe Hendrickx using a Dino-lite digital microscope were used to build photogrammetry models using Agisoft Photoscan Professional. These were exported as STL models and were subsequently used to create 3D tooth models.

11.2 Tooth model development

Postcanine tooth models were created in Avizo 3D version 2021.1. Teeth were cropped by approximately following the enamel cap of the tooth. Cropping often resulted in the mesial and distal portions of the tooth being removed, as these contacted the teeth in front and behind it. However, this had a negligible effect since these portions are not occlusal and do not play an active role in chewing. Each tooth model was smoothed using the “Smooth surface” tool, with the number of iterations set to 100 and lambda set to 0.6. The resolution varied after smoothing, ranging from 7,000 to 12,000 faces. To standardize the data to comparable resolutions, I used the “Simplification editor” tool to reduce the surface’s complexity to 1,000 faces as the literature has established that 1,000 faces is sufficient in retaining the occlusal topography without obscuring the model with artefacts of scanning (i.e., cracks) (Melstrom and Wistort, 2021).

The resultant number of faces and vertices present in each tooth model was recorded for screening purposes (Appendix E, Tables E1-E9). The quality of the tooth model was assessed based on the number of faces, number of vertices and whether the occlusal topography was retained in the model. The postcanine tooth models of 40 mammals had low-resolutions or had clearly lost a considerable amount of their occlusal topography after standardization and were disregarded in

further analyses (refer to specimens labelled “F” for OPCR calculated in Table A1).

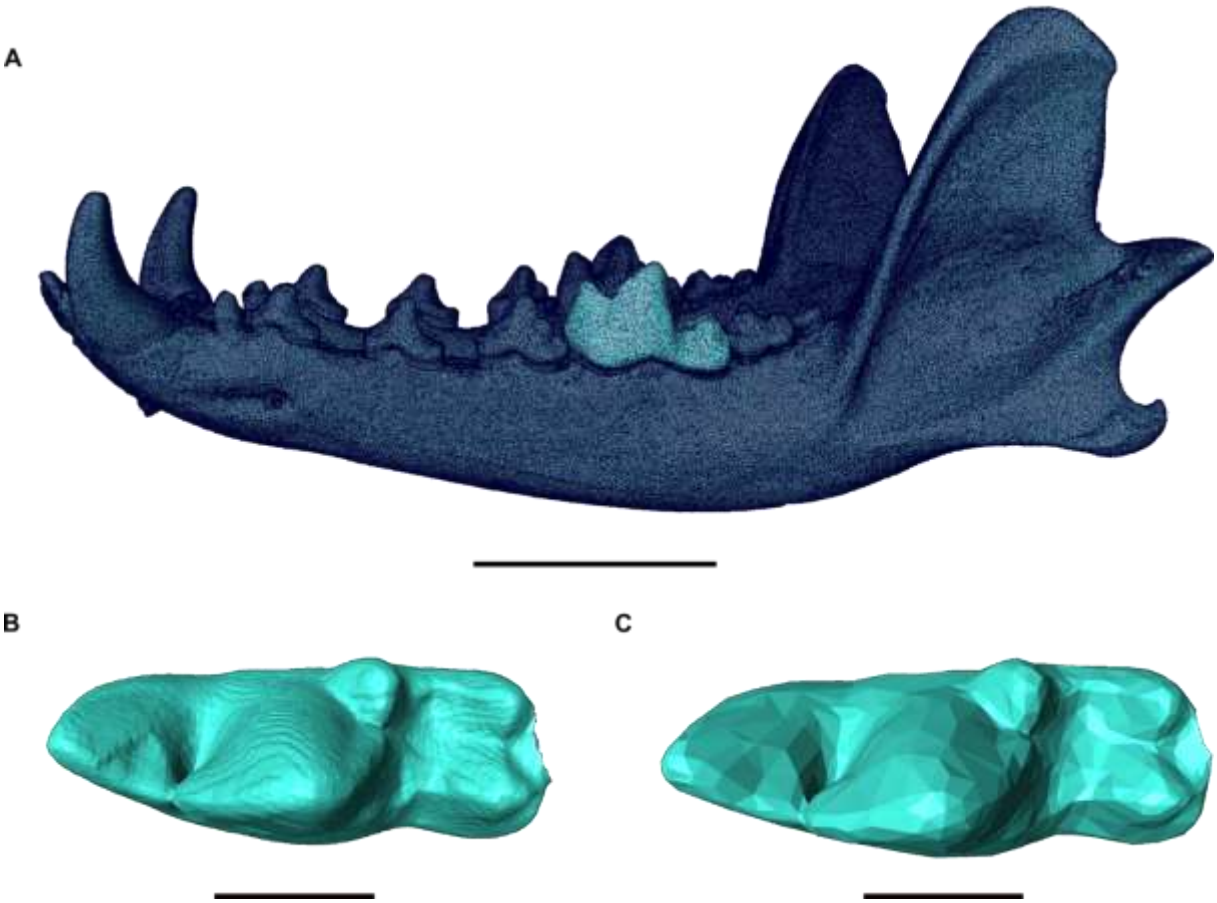


Figure 6: Tooth model generation for an exemplar specimen (*Acinonyx jubatus*). A: illustration of how tooth models were cropped from the mandible, shown in lateral view. Dark blue regions indicate areas to be cropped, while the lighter blue region highlights the resultant tooth model. Scale bar equals 40.61 mm. B: tooth model in occlusal view before smoothing and simplification. Scale bar equals 6.74 mm. C: tooth model in occlusal view after smoothing and simplification. Scale bar equals 6.88 mm.

The number of tooth models generated for each specimen were dependent on the dental formula. Tooth models were generated for the three posteriormost teeth. Amongst eutherian mammal species, these were often molars or a combination of molars and premolars. Metatherian mammal species have four molars, and tooth models were generated for all four molars.

The dental formula amongst the cynodonts sampled is highly variable and they could have up to 13 postcanine teeth (Martinelli et al., 2009). I generated tooth

models for the three most posterior postcanines along each specimen's tooth row. Extinct cynodonts would have used these most-posterior postcanines to do most of the food processing (Gow, 1978), making them functionally analogous to the posteriormost teeth that were sampled for most mammals.

Non-mammalian cynodonts exhibited a wide variation of tooth forms along their tooth row, however the three posteriormost postcanine teeth were often a combination of sectorial and gomphodont teeth. Some exhibited only gomphodont teeth in these positions, this included *Cricodon*, *Luangwa*, *Massetognathus*, and *Santacruzodon*. The posteriormost postcanines of *Trirachodon* sp. are only sectorial teeth.

11.3 Phylogeny

The phylogenetic tree for extinct species (Figure B2) was made using Mesquite version 3.70 (build 490) (Maddison, 2007). I scaled the branch lengths in the statistical computing language and environment R, version 2.3.4 (R Core Team, 2013). This was done using the DatePhylo command from the strap package, version 1.6-0 (Bell et al., 2022), and made use of occurrences from Palaeobiology Database (www.paleobiob.org).

The extant and extinct trees were merged to create a super-tree using the bind.tree command from the ape package, version 5.7-1 (Paradis and Schliep, 2019). The resultant composite tree was used during some statistical analyses (Figure B3).

The analyses that only contained mammal species made use of the scaled phylogenetic tree for mammal species sourced from VertLife (Figure B1). These analyses included: phylogenetically-aligned principal component analysis (Collyer and Adams, 2021) (see results section 13.1.1); phylogenetic Procrustes ANOVA regressions (Adams, 2014) (see results sections 13.1.2 and 13.4.1); and phylogenetic regressions (Grafen, 1989, Orme et al., 2023) (see results sections 13.2.1, 13.3.1.2, 13.3.2.2, 13.3.3.2, 13.3.4.2, and 13.3.5.2).

The analyses that contained a combination of cynodont and mammal species made use of the super-tree (Figure B3), this included: phylogenetically-aligned principal component analysis (Collyer and Adams, 2021) (see result section

13.1.1); and phylogenetically informed discriminant function analyses (Motani and Schmitz, 2011) (see result sections 13.1.3, 13.2.2, 13.3.6, and 13.4.2).

11.4 Diet categorization

The quantitative dietary data for mammal species was modified by creating an additional column that contains the sum of the values from the columns containing data on the consumption of vertebrates (endothermic vertebrates, ectothermic vertebrates, unknown vertebrates, piscivory, scavenger). This was done because ecomorphological studies that are relevant to palaeobiology do not make use of many subdivisions of carnivory (e.g., Melstrom and Irmis, 2019, Morales-García et al., 2021, White et al., 2021). Modifying this data resulted in a total of six dietary categories (invertivore, carnivore, frugivore, nectivore, granivore and herbivore), which were quantitatively encoded, representing the proportions at which mammal species consumed different food items. I converted the percentages to decimal form and arcsine transformed the quantitative dietary data to normalize the data for analyses. The individual effects of dietary variables were assessed separately in analyses to avoid multicollinearity.

The quantitative dietary data was converted into two sets of categorical variables, but this was used for visualization purposes only. Two dietary categories were assigned to each species using the quantitative data and the descriptions from Nowak (1999).

The first dietary category, majority consumed (Table 1), is based on the food type that each specimen ate most frequently and includes the same six categories as the quantitative dietary data.

Table 1: Majority consumed diet categories and descriptions.

Diet category	**Description**
Invertivore	Shrimp, krill, squid, crustaceans, molluscs, cephalopods, polychaetes, gastropods, orthoptera, ground insects, insect larvae, worms, orthopterans, flying insects, and other general invertebrates
Carnivore	Mammals, birds, reptiles, snakes, amphibians, salamanders, fish, scavenge, garbage, offal, carcasses, carrion, general unknown vertebrates
Frugivore	Fruit, drupes
Nectivore	Nectar, pollen, plant exudates, gums
Granivore	Seed, maize, nuts, spores, wheat, grains
Herbivore	Grass, ground vegetation, seedlings, weeds, lichen, moss, small plants, reeds, cultivated crops, forbs, vegetables, fungi, roots, tubers, legumes, bulbs, leaves, above-ground vegetation, twigs, bark, shrubs, herbs, shoots, aquatic vegetation, aquatic plants

The second dietary category (Table 2), which I often refer to as traditional, or major dietary categories, contains a total of three categories and partitions the diet into the three more broad categories that are commonly used.

Table 2: Traditional, or "major" diet categories and descriptions.

Dietary category	**Description**
Herbivore	Plant materials
Carnivore	Vertebrates
Invertivore	Hard and soft-bodied arthropods

11.5 Landmarking protocol

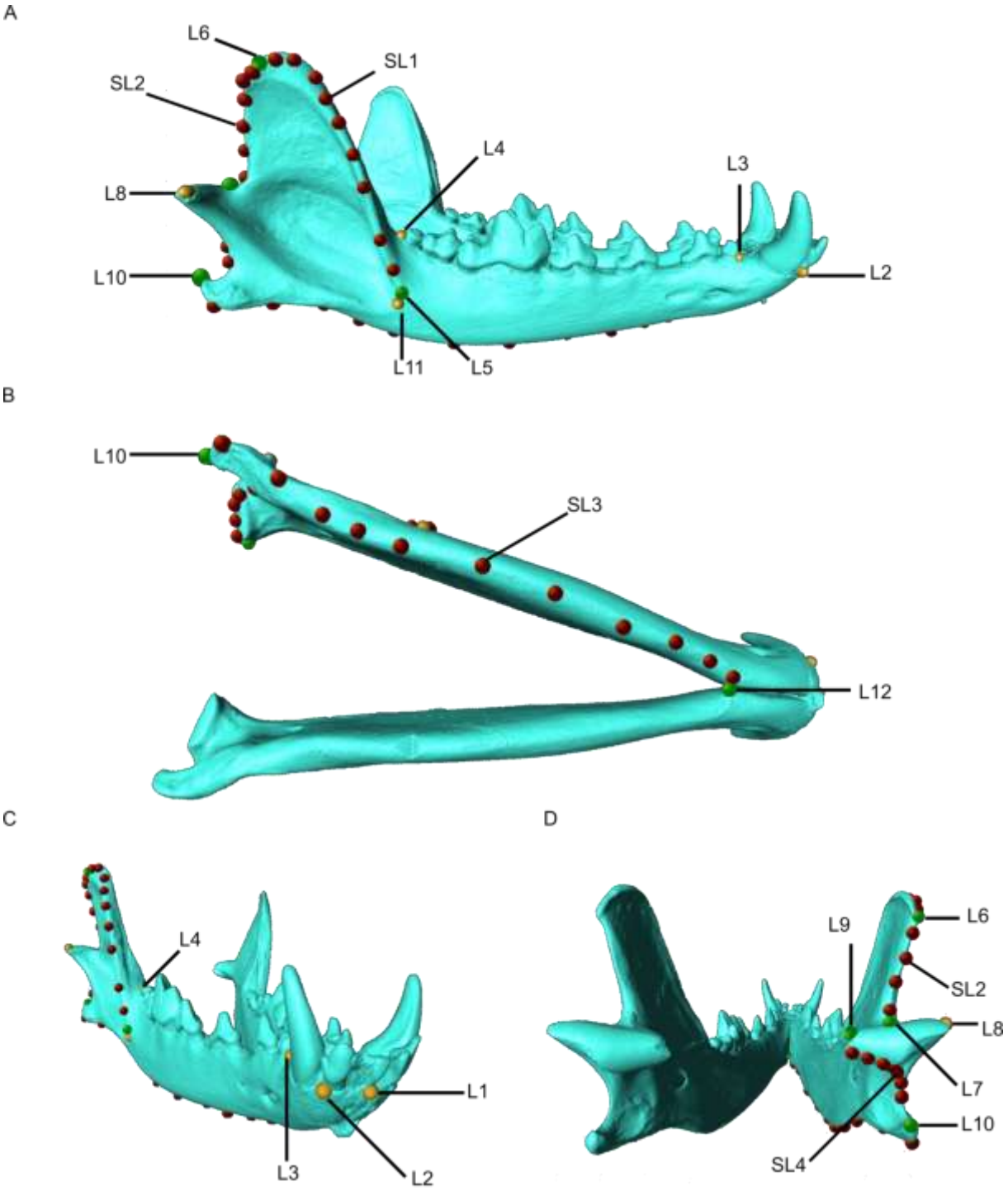


Figure 7: Landmarks placed on examplar specimen (a cheetah*, Acinonyx jubatus*), in A: right lateral; B: ventral; C: anterolateral and D: posterior views. The yellow circles represent fixed landmarks; green circles represent fixed landmarks which delineate stop/start points of curve semi-landmarks, and the red circles represent the curve semi-landmarks bound between the stop/start points.

A geometric morphometric landmark dataset was created that characterized the shape of the mandible. This was informed by the location of teeth, biomechanics,

and the overall shape of the mandible. The landmark dataset contained a total of 16 landmarks: 12 type 2 fixed homologous landmarks and four type 3 series of curve semi-landmarks that were treated as sliding semi-landmarks in my analysis (Figure 7, Table 3). The landmarks were placed on the lateral surface of all specimens using Avizo's landmarking tool (Figure 7). This recorded the landmarks as coordinates that encoded geometric information, such as distances and angles between landmarks (Slice, 2007). In this way, the coordinate system reflects the unique orientation and shape of each mandible.

Table 3: Landmark number, count and description associated with the dermacation of the placement of each landmark.

Landmark	Type	Count	Description
L1	Type 2 fixed homologous	1	Middle of incisors
L2	Type 2 fixed homologous	1	Most lateral point of incisors
L3	Type 2 fixed homologous	1	Most anterior point of tooth row after canine (If canine is present)
L4	Type 2 fixed homologous	1	Most posterior point of tooth row
L5	Type 2 fixed homologous	1	Beginning of anterior edge of coronoid process which marks the beginning of SL1
L6	Type 2 fixed homologous	1	Tip of coronoid process which marks the end of SL1 and start of SL2
L7	Type 2 fixed homologous	1	Middle anterior point of the condyle which marks the end of SL2
L8	Type 2 fixed homologous	1	Most lateral point of condyle
L9	Type 2 fixed homologous	1	Most medial point of the condyle, marks the end of SL4
L10	Type 2 fixed homologous	1	Tip of the angular process, marks the start of SL3 and SL4
L11	Type 2 fixed homologous	1	Most anterior point of masseteric fossa
L12	Type 2 fixed homologous	1	Ventral end of the mandibular symphysis, marks the end of SL3
SL1	Type 3 sliding	30	Anterior edge of the coronoid process
SL2	Type 3 sliding	22	Posterior edge of the coronoid process
SL3	Type 3 sliding	46	Ventral edge of the mandible
SL4	Type 3 sliding	32	Posterior edge of the mandible

A total of 268 specimens were landmarked, comprising a dataset of 262 mammal species and six non-mammalian cynodont species. Two extinct cynodont species were only partially landmarked and did not contain the anterior-most landmarks L1 and L2 (Table 1) due to the fragmentary nature of the specimens. However, the rest of the sample was fully landmarked. Of the landmarked specimens, 127 mammal species were previously landmarked by Alberto Martin-Serra and Catherine Johnson, and I landmarked the remaining 135 mammal species and the six cynodont species.

The landmarks were read into R using a script provided by Roger Benson (see Appendix F, R script for mandible shape analyses). The script reflected left-sided landmarks to ensure that the compiled landmark list only consisted of landmarks for the right mandible (or reflected left mandible). The script resampled the points along each curve semi-landmark series to equal counts.

I created two functional landmark lists, one called the fully-landmarked set, containing only mammal species that were fully landmarked. And another, called the partially-landmarked set, containing mammal and cynodont species which were partially landmarked and did not contain the anterior-most landmarks, L1 and L2 (Table 3). I used the earlier mentioned script provided by Roger Benson to drop L1 and L2 in specimens that were fully landmarked.

Following reading the landmarks into R, both sets (full-landmarked and partially-landmarked) of the landmark data were scaled, rotated and aligned to the mean shape by computing generalized Procrustes analysis (GPA). This was done in R by making using of the gpagen function from the geomorph package, version 4.0.5 (Adams and Otárola-Castillo, 2013). The outputs of GPA include (i) Procrustes coordinates, which are used as a shape variable in my analyses, and (ii) the centroid size of the mandible, which is used as a size variable in my analyses.

11.6 OPCR

Tooth complexity was calculated in R using the OPCr command from the molaR package, version 5.3 (Pampush et al., 2016b). The minimum face count threshold was set to three triangles per patch, this threshold is established to capture important morphological patterns (Melstrom and Wistort, 2021). Visualizations of

these scores were generated using the OPC3d function from the molaR package. This renders the mesh faces and assigns them to patches, these colour maps were inspected to identify and correct possible errors. This procedure was done for a total of 259 specimens, comprising 240 mammal species and 19 non-mammalian cynodont species (Appendix E, Tables E1-E9).

Average and summed OPCR scores were computed in R using the rowSums and rowMeans functions from native R. In metatherians, the first molar was excluded from the average and sum calculation. The posteriormost three teeth were selected because this is hypothesized to be analogous to the last three teeth in eutherian mammals (O'Leary et al., 2013, Williamson et al., 2014).

11.7 Statistical analyses

All statistical analyses were computed in R (Appendix F) and made use of the geomorph version 4.0.5 (Adams and Otárola-Castillo, 2013), caper version 1.0.2 (Orme et al., 2023), and the custom code available from Motani and Schmitz (2011).

11.7.1 Mandible shape variation

12.7.1.1 Phylogenetically-aligned principal component analysis (PCA)

I assessed the major axes of evolutionary variation in mandible shape amongst mammal species using a phylogenetically-aligned principal component analysis on the Procrustes shape coordinates from the fully-landmarked dataset of mammal species (n= 262). A phylogenetically-aligned PCA aligns the data to the axis of greatest phylogenetic signal, not the axis of greatest dispersion (Collyer and Adams, 2021). This was done using the gm.prcomp command from the geomorph package version 4.0.5 (Adams and Otárola-Castillo, 2013).

A separate phylogenetically aligned principal component analysis was computed to assess how the morphospace of cynodonts (n=6) compares to that of mammal species (n=262). This analysis made use of the use of the Procrustes shape coordinates associated with the partially-landmarked dataset.

I generated shape-difference plots using the plotRefToTarget command from the geomorph package. The mean shape of the Procrustes coordinates was calculated using the mshape command from the geomorph package (Adams and

Otárola-Castillo, 2013). The shape associated with the extreme ends (minimum and maximum) of the PC axes were compared to the mean shape. I used the adjectives “long” and “short” to describe anteroposterior variation and the adjectives “tall” and “low” to describe dorsoventral variation.

12.7.1.2 Phylogenetic ANOVA regressions (procDpgls)

I assessed the association that mandible shape variation had with dietary variables and body mass by computing Procrustes ANOVAs (procDpgls) using the procD.pgls function from the geomorph package. These tested statistical hypotheses and described patterns of shape variation and covariation within a set of Procrustes shape coordinates. These hypotheses were evaluated in a phylogenetic framework that made use of permutation processes (Adams and Otárola-Castillo, 2013, Adams, 2014, Adams and Collyer, 2015, Adams and Collyer, 2016, Adams and Collyer, 2018). Considering the shared evolutionary history amongst species is important because assuming independence of species traits causes an inflation of p values, potentially leading to false-positive inferences (Felsenstein, 1985, Grafen, 1989).

I evaluated the association between individual predictor variables and mandible shape (e.g., models of the form Shape ~ Herbivory). Since many studies have shown that skeletal elements show shape allometry, the partial (e.g., models of the form Shape ~ Body Mass + Herbivory) and interaction effects (e.g., models of the form Shape ~ Body Mass * Herbivory) of dietary variables were assessed. The model “Shape ~ BM + Herbivory” assesses whether herbivory influences mandible shape after accounting for the effects of body mass on shape variation. If the partial effect of herbivory is significant in this model, the answer to this question is yes (Grafen and Hails, 2002). If the model “Shape ~ BM * Herbivory” is significant it suggests that herbivores have a different pattern of shape allometry to non-herbivores (Grafen and Hails, 2002, Franzese and Kam, 2009).

I explored how predictor variables affected mandible morphology in models that were significant in explaining mandible shape variation by plotting the shape variation implied from the procDpgls models. The coefficients of a variable are interpreted as the effect that the predictor (e.g., diet) has on the response variable (i.e., shape) for every unit change. The effects of predictor variables were

visualized by generating shape deformation plots, where the mean shape was represented by model's intercept coefficients and "effect" of the predictor variable was characterized by scaling the coefficients of the respective predictor variable with an exaggeration factor.

The model "Shape ~ BM * Herbivory" assesses whether herbivores have different patterns of shape allometry than non-herbivores. There is no existing technique/method available that evaluates the shape deformations associated with significant interaction effects in a geometric morphometric framework. To understand the effects of body mass on shape within dietary variables I manually approximated the shape disparity associated with significant interaction effects. This was done by plotting the landmark configurations of the associated small-bodied and large-bodied species within the diet category. However, this only provides a broad approximation.

There is also no current method available to evaluate the Akaike information criterion (AIC) in a geometric morphometric framework, instead the R^2 values from procDpgls ANOVA tables were used to compare the goodness of fit amongst models.

12.7.1.3 Phylogenetically informed discriminant analysis (pDFA)

I evaluated how informative mandible shape is for estimating diet by computing a phylogenetically flexible discriminant function analysis (pDFA) using the custom code available from Motani and Schmitz (2011). I followed the methodology used in Morales-García et al. (2021) and used the coordinates of the first seven PCA axes as the input predictor variables, these coordinates summarized most of the total mandible shape variation (99.99%, see section 13.1.1). The pDFA analyzes the association that mandible shape (PC axes) has with dietary categories (herbivore, carnivore and invertivore) in mammal species and used the trends found from this association to estimate the diet of mammal and non-mammalian cynodont species based on the input predictor variables.

Each taxon is assigned a posterior probability (PP) that coincides with the chances/probability that the taxon belongs to the assigned diet based on the associations found between mandible shape and the dietary categories. The posterior probability of an assigned diet being high is indicative of a high

confidence that this taxon belongs in the diet; inversely a low probability is indicative of a lower confidence level. Posterior probabilities above 0.75 are considered “high”, and posterior probabilities less than 0.50 are considered “low” throughout this study.

My sample of mammal species contained an unequal number of herbivores (n=147), carnivores (n=43) and invertivores (n=72). Biased samples such as these, with unequal representation among classes can strongly affect posterior estimates and to correct for this I followed the methodology of Chapelle et al. (2020) and Hermanson et al. (2022) using iterative random sampling of an equal number of species from each dietary category.

I computed 400 iterations of a pDFA, and each pDFA iteration randomly sampled 30 carnivores, 30 herbivores and 30 invertivores from my larger sample of mammal species. This meant that each iteration had 90 mammal species, and under these parameters the random guess success rate is 33.33% (the probability of randomly guessing the correct class= 1/3; error rate of 66.67%).

I used the median, the 5th percentile (P5) and the 95th percentile (P95) of the percentage of correct classifications per iteration to evaluate the overall success. Mammals that were frequently misclassified, particularly those that were misclassified at high posterior probabilities, were reported, these edge cases provide interesting insights into understanding the possible limitations of using mandible shape to predict diet. The estimated diets of non-mammalian cynodont species and their posterior probabilities were also reported.

11.7.2 Mandible size and its association with diet

12.7.2.1 Phylogenetic regressions (pgls)

I assessed the correlation between mandible size and body mass by computing a phylogenetic regression using the pgls command from the caper package (Orme et al., 2023). This implemented a generalized least square (GLS) model while accounting for phylogeny (Grafen, 1989). The centroid size from the Procrustes analysis was used as a size variable. I transformed centroid size and body mass by base 10 logging both variables.

I assessed whether the residual variation in mandible size was explained by variation in diet using the pgls command from caper. These models assessed the partial effects that dietary variables had after accounting for the effects of body mass (e.g., Size ~ Body Mass + Herbivory).

I also assessed the interaction effects that diets have with body mass; for example, the model "Size ~ Body Mass * Herbivory" assesses whether herbivores have a different pattern of mandible allometry than non-herbivores. The effects of significant interactions were interpreted in detail by using simple slope tests, which are designed to interpret the effect of two continuous predictor variables (Bauer and Curran, 2005).

A statistical model can be written as a linear equation $(y = mx + c)$, where the slope (m) represents the coefficient of the predictor variable (x), and the intercept (c) represents the coefficient of the intercept variable. For instance, the linear equation that represents the model in Table 4 can be written as:

$$Size = 0.9 + 0.5 \times BM + 1.1 \times Herbivory - 0.43 \times BM \times Herbivory$$

Table 4: An example of a pgls model which assesses whether herbivores have a different pattern of mandible allometry than non-herbivores.

Model	p-value (model)	Variable	Coefficient	Pr(>|t|)
Size ~ BM * Herbivory	**<0.001**	Intercept	0.9	0.221
		BM	0.5	**<0.001**
		Herbivory	1.1	**0.005**
		BM:Herbivory	-0.43	**<0.001**

A significant interaction between a dietary variable, such as herbivory (Table 4), and $\log_{10}$ body mass means that the slope of the relationship between body mass and mandible size in herbivores is significantly different to that in non-herbivores.

To illustrate and interpret the interaction that diet and $\log_{10}$ body mass had, I derived two separate regression lines from the equation that described the original model by treating the dietary variable (e.g., Herbivory) as a binary variable (1/0).

Setting the value of $Herbivory$ to 0 produces an equation that explained the relationship that $\log_{10}$ body mass had with mandible size for mammals that were not herbivores:

$$Size_{Herbivory-0} = 0.9 + 0.5 \times BM$$

Likewise, setting the value of $Herbivory$ to 1 produces an equation that explained the relationship that $\log_{10}$ body mass had with mandible size for herbivorous mammals:

$$Size_{Herbivory-1} = 2 + 0.07 \times BM$$

According to the model Size ~BM * Herbivory (Table 4, Figure 8), a herbivore will have a $\log_{10}$ mandible size 1.1 times larger than non-herbivores (Figure 8, difference in $Herbivory - 1$ and $Herbivory - 0$ intercepts). With increasing body mass, herbivorous mammals $\log_{10}$ mandible centroid size increases 0.43 times slower than non-herbivores (Figure 8, difference in $Herbivory - 1$ and $Herbivory - 0$ gradients). So, at smaller body sizes (1g—500g) herbivorous mammals have larger relative mandible centroid sizes, and at larger body sizes (500g—1,000,000g) herbivorous mammals have smaller relative mandible sizes.

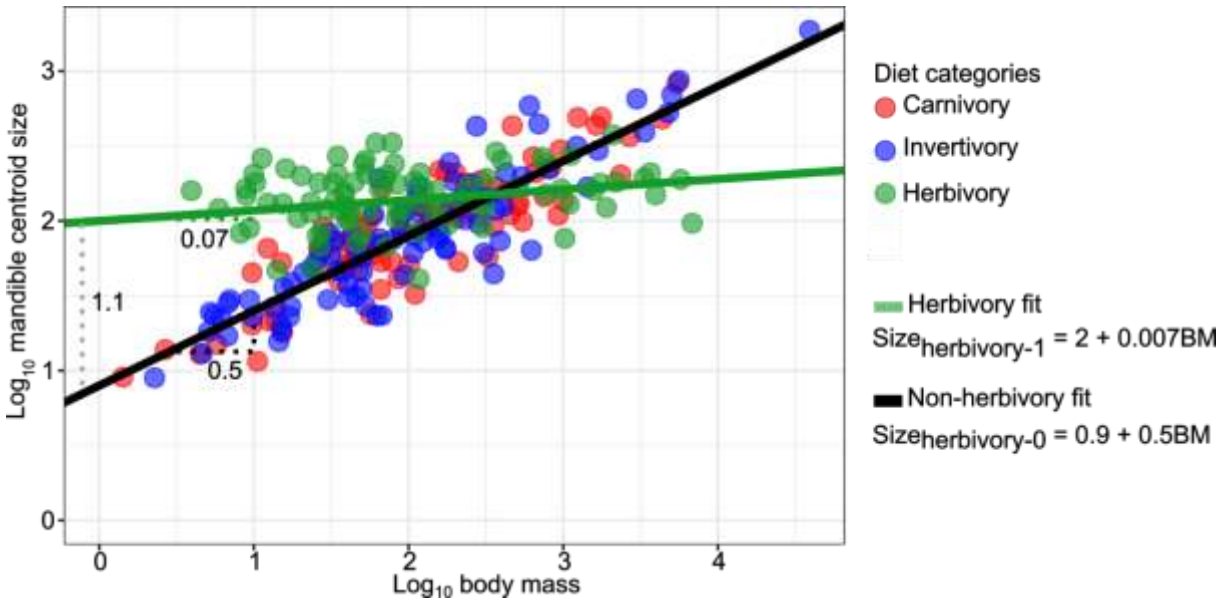


Figure 8: Scatterplot of $\log_{10}$ mandible centroid size (Size) and $\log_{10}$ body mass (BM), illustrating the example of a significant interaction effect (Table 4). Note differences in the intercepts (grey dotted line), and gradients describing the relationship between centroid size and body mass in herbivores (green dotted line) and non-herbivores (black dotted line).

Akaike information criterions (AIC) and Akaike information weights (AICw) were calculated to assess goodness of fit amongst pgls models. AIC and AICw were calculated in R making use of R's native AIC and akaike.weights commands.

12.7.2.2 Phylogenetically informed discriminant analysis (pDFA)

12.7.2.2.1 Size

I evaluated how informative size is for dietary estimates by computing a pDFA for 400 iterations which iteratively randomly sampled 30 carnivores, 30 herbivores and 30 invertivores (n=90). The probability of randomly guessing the correct class is 33.33%. I used $\log_{10}$ body mass and the residuals from the model that assessed $\log_{10}$ mandible centroid size's relationship with $\log_{10}$ body mass (Size ~ BM) as input predictor variables. These residuals represent the variation in $\log_{10}$ mandible centroid size not explained by $\log_{10}$ body mass.

I used the median, the 5th percentile (P5) and the 95th percentile (P95) of the percentage of correct classifications per iteration to evaluate the overall success. Mammals that were frequently misclassified, particularly those that were misclassified at high posterior probabilities, were reported. The estimated diets of non-mammalian cynodont species and their posterior probabilities were also reported.

12.7.2.2.2 Considering size and shape

I evaluated whether considering size together with shape would improve dietary estimates, relative to predictive analyses using only shape. I computed 400 iterations of a pDFA, and each pDFA iteratively randomly sampled 30 carnivores, 30 herbivores and 30 invertivores (n=90). I used the coordinates of the first seven PCA axes, $\log_{10}$ body mass and the residuals from the model that assessed $\log_{10}$ mandible centroid size's association with $\log_{10}$ body mass (Size ~ BM) as input predictor variables.

I used the median, the 5th percentile (P5) and the 95th percentile (P95) of the percentage of correct classifications per iteration to evaluate the overall success. Mammals that were frequently misclassified, particularly those that were misclassified at high posterior probabilities, were reported. The estimated diets of

non-mammalian cynodont species and their posterior probabilities were also reported.

11.7.3 Dental complexity

I assessed whether dietary preferences correlated to OPCR scores using five OPCR variables. The first OPCR variable is the average OPCR score (OPCRavg), which is the mean dental complexity of the three posteriormost teeth. It should be noted that this was dependent on the dental formula of the specimen and was not always the mean of three molars. The second OPCR variable is the summed OCPR score (OPCRsum), which is the summed dental complexity of the three posteriormost teeth- this was similarly dependent on the dental formula of specimens. The last three variables are the dental complexity scores of the molars, OPCRm1-m3. Cynodont species don't have molars, but the posteriormost teeth along the tooth row are functionally analogous to molars because of their presumed role in chewing activities (Bramble, 1978, Crompton, 1995).

12.7.3.1 Generation of box and whisker plots

I generated box and whisker plots to visually compare the OPCR scores of non-mammalian cynodonts within hypothesized dietary categories, these summarized the distribution of OPCR scores within major dietary categories. To visually compare the OPCR scores of non-mammalian cynodonts to those of mammals from major mammalian clades, I generated box and whisker plots summarizing the distribution of OPCR scores within major dietary categories.

I visualized the distribution of OPCR scores amongst only mammal species (which have known dietary habits), using box and whisker plots which summarized the distribution according to major and finer diet categories.

Box and whisker plots were generated for all five OPCR variables (OPCRavg, OPCRsum, OPCRm1, OPCRm2, OPCRm3), and the distributions of OPCR scores within each box and whisker plot were compared using the median, interquartile range, and range.

12.7.3.2 Phylogenetic regressions (pgls)

I assessed the association between diet variables and dental complexity by computing phylogenetic regressions using the pgls command from the caper

package. I also assessed the association that OPCR scores have with $\log_{10}$ body mass and $\log_{10}$ mandible centroid size.

To determine whether OPCR scores correlate to diet after accounting for the variation explained by body mass, I assessed the partial effects that dietary variables had on OPCR scores after the effects of body mass on OPCR scores have been considered (e.g., OPCR ~ Body Mass + Herbivory). I also assessed whether animals with different dietary habits showed different OPCR allometry patterns using a model containing an interaction term (e.g., OPCR ~ Body Mass * Herbivory). I interpreted models that contained significant interaction effects using simple slope tests, and I reported the differences in intercept and gradient terms to understand dietary variable's covariation with body mass.

Akaike information criterions (AIC) and Akaike information weights (AICw) were calculated to assess goodness of fit amongst pgls models. AIC and AICw were calculated in R making use of R's native AIC and akaike.weights commands.

The phylogenetic regressions were computed using only the OPCR scores of mammals (as they have known dietary habits); and this was replicated for all five OPCR variables (OPCRavg, OPCRsum, OPCRm1, OPCRm2, OPCRm3).

12.7.3.3 Phylogenetically informed discriminant analysis (pDFA)

12.7.3.3.1 OPCRavg and OPCRsum

I evaluated how informative average and summed dental complexity scores were in estimating diet by computing 400 iterations of a pDFA, iteratively randomly sampling 30 carnivores, 30 herbivores and 30 invertivores (n=90). The probability of randomly guessing the correct class is 33.33%. I used OPCRavg and OPCRsum as input predictor variables.

I used the median, the 5th percentile (P5) and the 95th percentile (P95) of the percentage of correct classifications per iteration to evaluate the overall success. Mammals that were frequently misclassified, particularly those that were misclassified at high posterior probabilities, were reported. The estimated diets of non-mammalian cynodont species and their posterior probabilities were also reported.

12.7.3.3.2 OPCRm1-m3

I evaluated how informative the dental complexity scores of the molars were in making dietary predictions by computing 400 iterations of a pDFA, iteratively randomly sampling 15 carnivores, 15 herbivores and 15 invertivores (n=45). I used OPCRm1, OPCRm2 and OPCRm3 scores as input predictor variables. This data frame is smaller because there are fewer mammal species that have all three molars, however the probability of randomly guessing the correct class is still 33.33% (probability of correct diet classification is still 1/3).

I used the median, the 5th percentile (P5) and the 95th percentile (P95) of the percentage of correct classifications per iteration to evaluate the overall success. Mammals that were frequently misclassified, particularly those that were misclassified at high posterior probabilities, were reported. The estimated diets of non-mammalian cynodont species and their posterior probabilities were also reported.

12.7.3.3.3 OPCRm1-m3 and size

I evaluated how informative considering dental complexity scores of the molars and body mass were in making dietary predictions by computing 400 iterations of a pDFA which randomly sampling 15 carnivores, 15 herbivores and 15 invertivores (n=45). I used OPCRm1, OPCRm2, OPCRm3 and $\log_{10}$ body mass as input predictor variables. The probability of randomly guessing the correct class is 33.33%.

This was only done using OPCRm1-m3 scores because preliminary data suggested that the dental complexity of the molars (OPCRm1-m3) has a stronger relationship with dietary preferences relative to summed and average dental complexity scores.

I used the median, the 5th percentile (P5) and the 95th percentile (P95) of the percentage of correct classifications per iteration to evaluate the overall success. Mammals that were frequently misclassified, particularly those that were misclassified at high posterior probabilities, were reported. The estimated diets of non-mammalian cynodont species and their posterior probabilities were also reported.

11.7.4 Dietary inferences using mandible shape and dental complexity

12.7.4.1 Phylogenetic ANOVA regressions

I assessed whether mandible shape variation correlates to OPCR variables (OPCRavg, OPCRsum, OPCRm1-m3) by computing Procrustes ANOVAs (procDpgls) using the procD.pgls command from the geomorph package.

I explored how OPCR variables affected mandible morphology in models that were significant in explaining mandible shape variation by plotting the shape variation implied from the procDpgls models. The coefficients of a variable are interpreted as the effect that the predictor (i.e., OPCR variable) has on the response variable (i.e., shape) for every unit change. The effects of predictor variables were visualized by generating shape deformation plots, where the mean shape was represented by model's intercept coefficients and "effect" of the predictor variable was characterized by scaling the coefficients of the respective predictor variable with an exaggeration factor.

12.7.4.2 Phylogenetically informed discriminant function analysis (pDFA)

I evaluated whether considering both mandible shape and OPCRm1-m3 scores improved dietary estimates by computing 400 iterations of a pDFA, iteratively randomly sampling 12 carnivores, 12 herbivores and 12 invertivores (n=36). The coordinates of the first seven PCA axes and OPCRm1-m3 scores were used as input predictor variables. The probability of randomly guessing the correct class is 33.33%. This dataset is small because not all landmarked mammals had OPCR scores calculated for them (Table A1), and even fewer had all three molars (varying dental formulae).

I used the median, the 5th percentile (P5) and the 95th percentile (P95) of the percentage of correct classifications per iteration to evaluate the overall success. Mammals that were frequently misclassified, particularly those that were misclassified at high posterior probabilities, were reported. The estimated diets of non-mammalian cynodont species and their posterior probabilities were also reported.

12. RESULTS

12.1 Mandible shape and its association to diet

12.1.1 PCA

The PCA amongst only extant taxa (Figure 9) contained 262 mammal species that were fully landmarked. The first seven PC axes contained 99.98% of the total shape variation, and approximately 97.02% was contained in the first two PC axes.

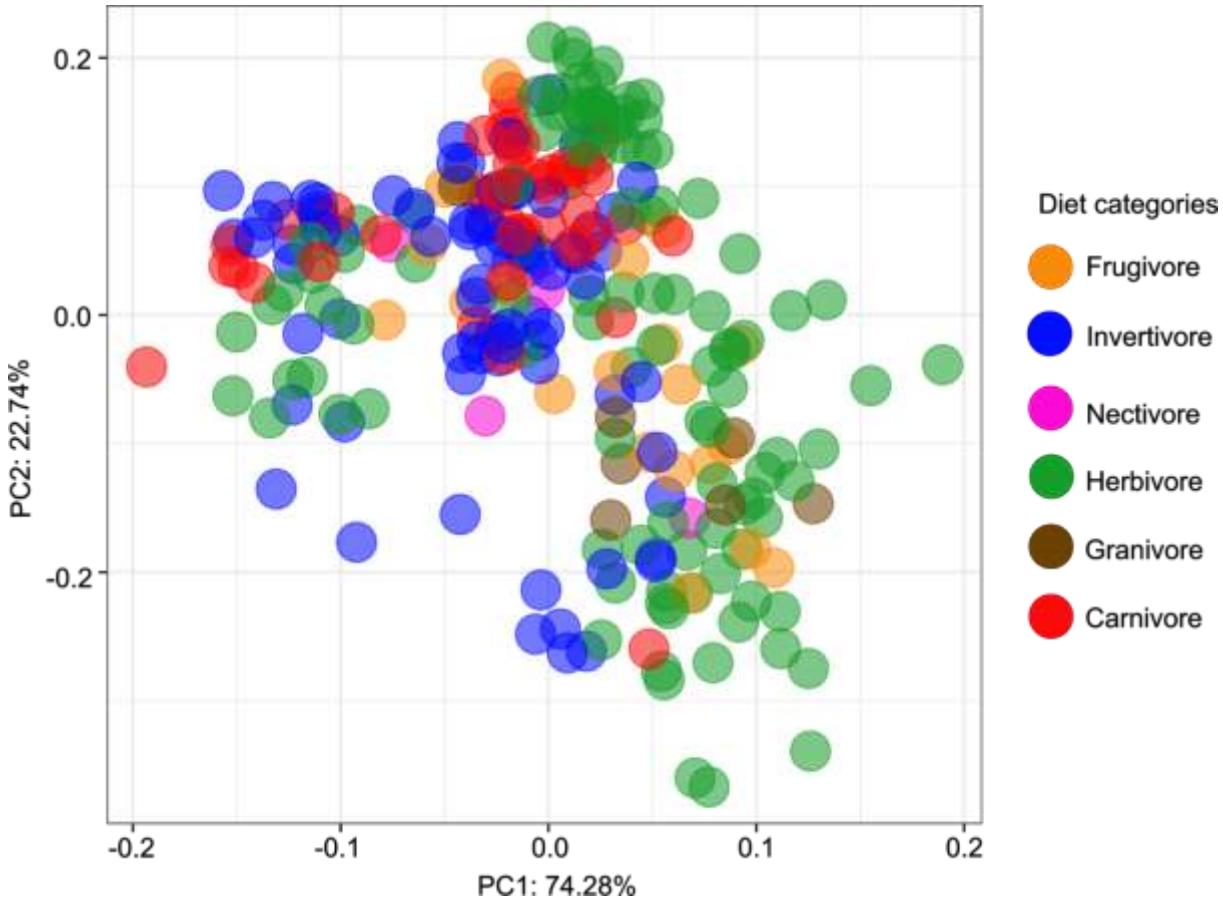


Figure 9: PC 1 and PC 2 axes associated with major mandible shape variation in fully landmarked mammal species (n=262). Numbers adjacent to the PC axes indicate the percentage of shape variation described by the corresponding axes.

The PC 1 axis accounted for approximately 74% of the shape variation (Figure 9). Mandibles with positive PC 1 scores are short, and both the anterior and posterior end of the mandible body are tall, the posterior end of the mandible body is expanded. The coronoid process is low, and the mandibular condyle is spherical, relative to the mean shape. The angular process is laterally inflected (Figure 10, positive PC 1). Mandibles with negative PC 1 scores are long, and the posterior end of the mandible body is tall. The anterior end of the mandible body is low relatively to the mean shape. The coronoid process is tall, and the mandibular condyle is ovoid. The angular process is prominent and is medially inflected (Figure 10, negative PC 1).

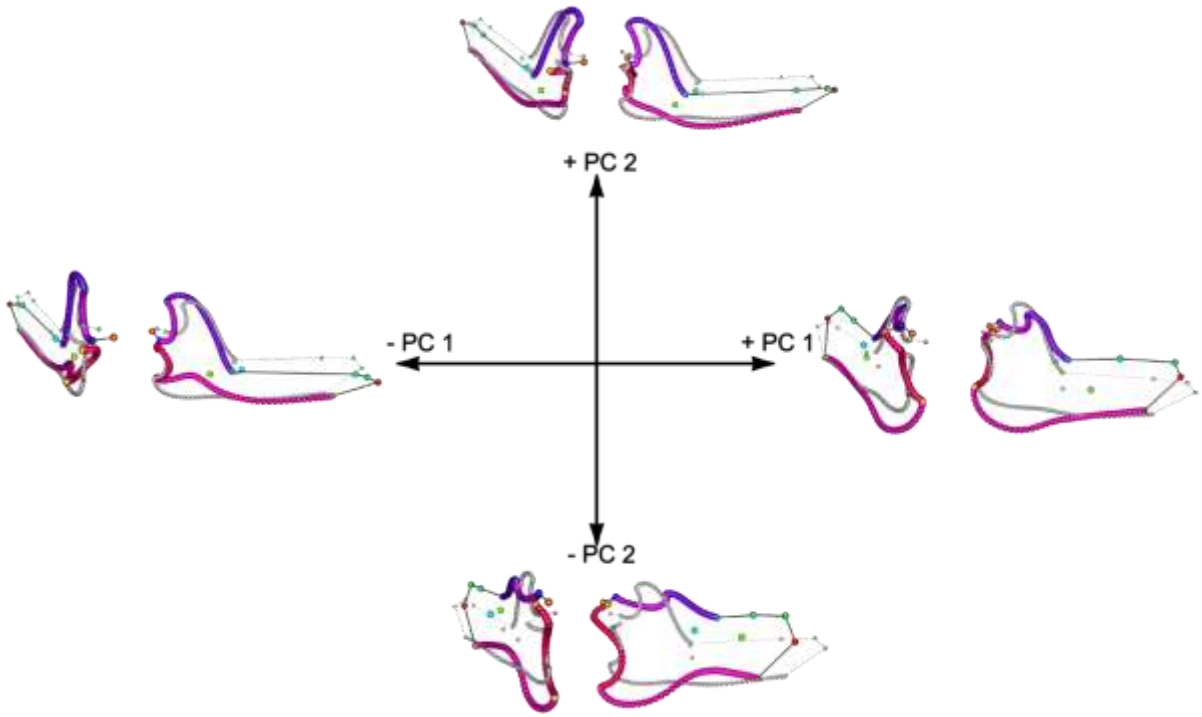


Figure 10: Landmark configurations corresponding to the PC 1 and PC 2 extreme values, which are shown in colour (corresponding to landmarks), relative to the mean shape (grey) of fully landmarked mammal species. Landmark configurations shown in lateroposterior (left) and lateral (right) views.

The PC 2 axis accounted for approximately 23% of the shape variation (Figure 9). Mandibles with positive PC 2 scores are long, the anterior end of the mandible body is low and posterior end of the mandible body is tall. The coronoid process is tall, and the mandibular condyle is ovoid. The angular process is rounded (Figure 10, positive PC 2). Mandibles with negative PC 2 scores are short, and the

anterior and posterior ends of the mandible body are tall. The coronoid process is low, and the mandibular condyle is spherical and notably smaller than that of the mean shape. The angular process projects posteriorly and is ventrally expanded (Figure 10, negative PC 2).

When the finer diet categories are used to visualize patterns in the morphospace (Figure 9)- the frugivorous, invertivorous, nectivorous, and herbivorous species have wide ranges of PC values. Granivores and carnivores occupy a narrow range of PC 1 and PC 2 scores, suggesting that granivorous and carnivorous species have a limited morphospace relative to other dietary categories. All granivores have a combination of positive PC 1 (0—0.15) and negative PC 2 values (-0.2—0), indicative of a short mandible with a relatively tall coronoid process and a ventrally expanded angular process that projects posteriorly. Although carnivores generally have a wide range of PC 1 scores between -0.15 and 0.5, they have a narrow range positive PC 2 scores (-0.15—0.5). However, the majority of the carnivorous species sampled have a relatively narrow range of PC 1 scores between -0.5 and 0.5. This range of PC 1 and PC 2 scores is indicative of a long mandible with an anteriorly low mandible body and a tall coronoid process.

The PCA that made use of the partially landmarked specimens contained six cynodont species and 262 mammal species (Figure 11). The first seven PC axes contained 99.99% of the total shape variation, and approximately 95.88% was contained in the first two PC axes.

PC 1 accounted for approximately 76% of the variation (Figure 11). Mandibles with positive PC 1 scores are short, the anterior end of the mandible body is tall, and the posterior end of the mandible body is tall and expanded. The coronoid process is low, and the mandibular condyle is spherical. The angular process is rounded and is laterally inflected (Figure 12, positive PC 1). Mandibles with negative PC 1 scores are long, the anterior end of the mandible body is low, and the posterior end of the mandible body is tall. The coronoid process is tall, and the mandibular condyle is ovoid. The angular process is prominent and medially inflected (Figure 12, negative PC 1)

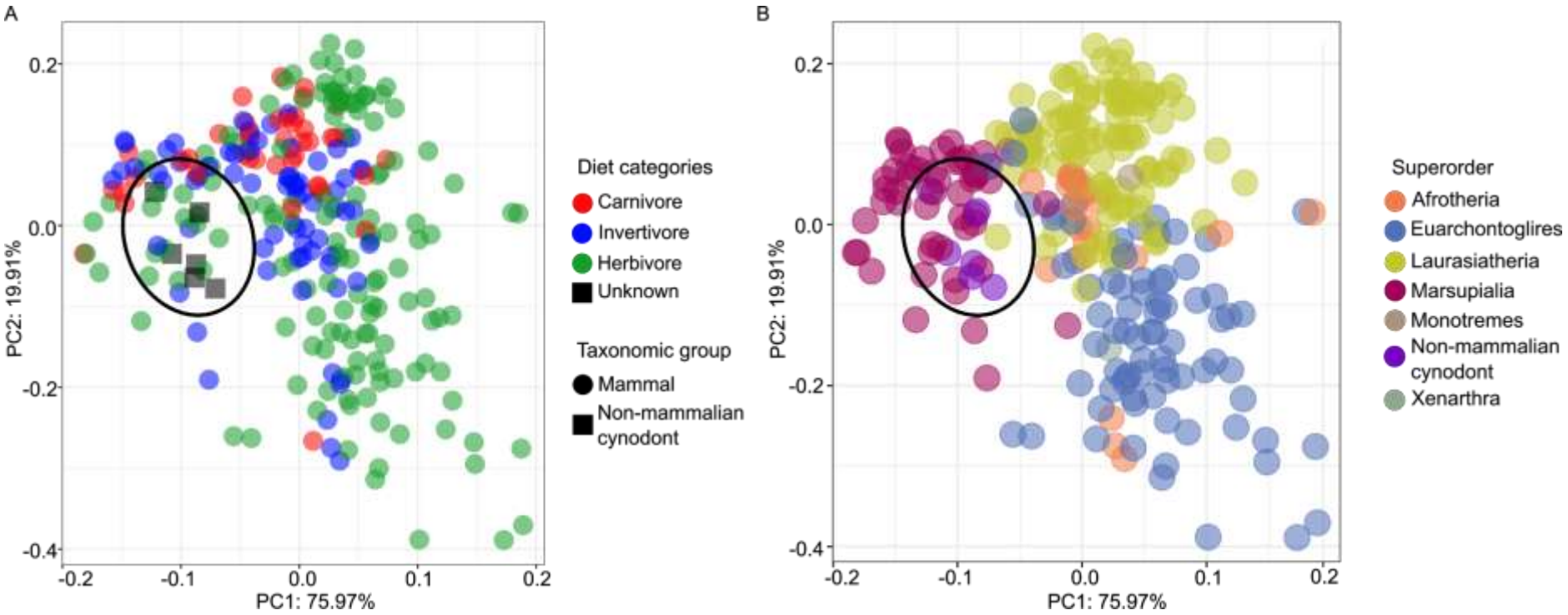


Figure 11: PC 1 and PC 2 axes associated with major mandible shape variation in partially landmarked mammal and non-mammalian cynodont species (n=268). Numbers adjacent to the PC axes indicate the percentage of shape variation described by the corresponding axes. Shows mandible shape variation within major dietary categories (A) and within major taxonomic groups (B). Circles demarcate the morphospace occupied by cynodonts.

PC 2 accounted for approximately 20% of the variation. Mandibles with positive PC 2 scores are long, the anterior end of the mandible body is low, and the posterior end is tall. The coronoid process is tall, and the mandibular condyle is ovoid. The angular process is rounded (Figure 12, positive PC 2). Mandibles with negative PC 2 scores are short, and the anterior and posterior ends of the mandible body are tall. The coronoid process is low, and the mandibular condyle is spherical and notably smaller than that of the mean shape. The angular process projects posteriorly and is ventrally expanded (Figure 12, negative PC 2).

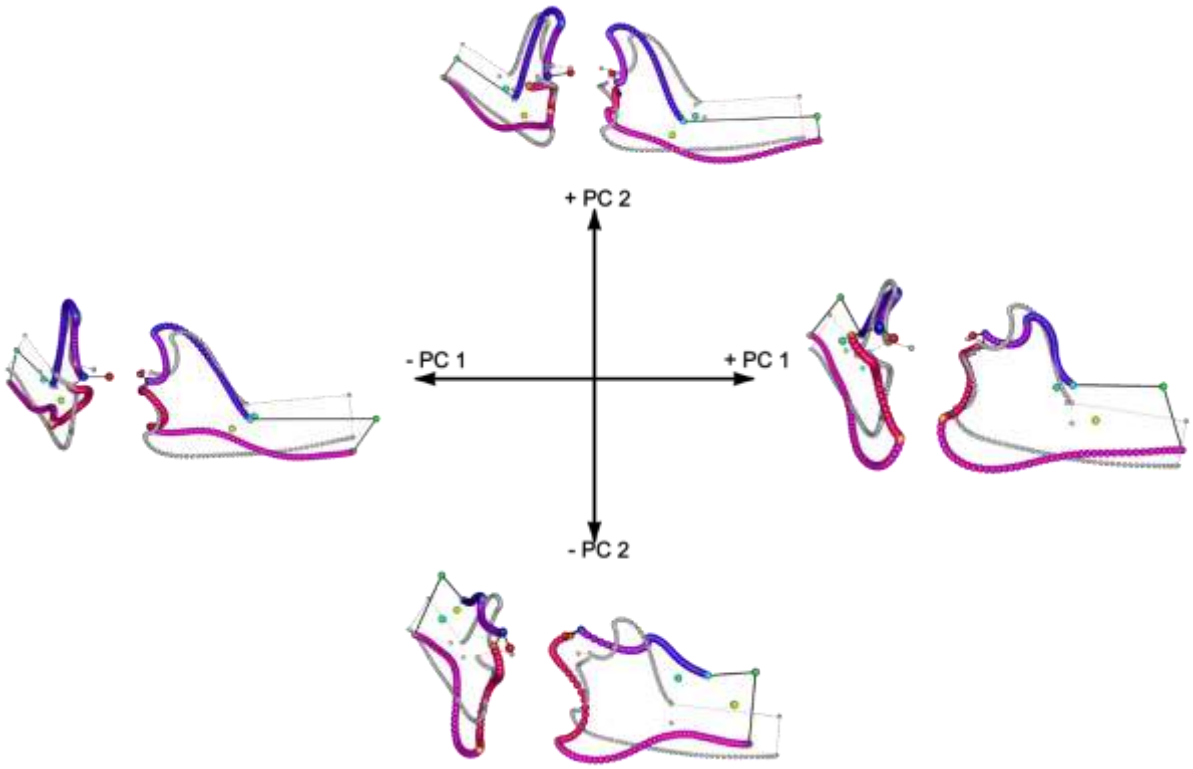


Figure 12: Landmark configurations corresponding to the PC 1 and PC 2 extreme values, which are shown in colour (corresponding to landmarks), relative to the mean shape (grey) of partially landmarked mammal and cynodont species. Landmark configurations shown in lateroposterior (left) and lateral (right) views.

The patterns in the morphospace within traditional dietary categories (Figure 11, A) are similar to those observed using the finer dietary categories (Figure 9). Phylogenetic affinities show clearer clustering of mandible shapes than diet categories (Figure 11). Herbivores and invertivores have a wider variety of mandible shapes relative to carnivores (Figure 11). Extinct taxa occupied a narrow

range of PC 1 and PC 2 scores. They do not have a unique morphospace as the distribution of taxa overlapped with mammal species.

Carnivores have a relatively wide range of PC 1 scores; however, carnivores generally occupy a narrow range of PC 2 scores (-0.15—0.5). Majority of the carnivorous species sampled have a narrow range of PC 1 scores (-0.5—0.5) and this range of PC 1 and PC 2 scores is indicative of a long mandible with an anteriorly low mandible body and a tall coronoid process. Although the mandible shapes of non-mammalian cynodonts are within the same morphospace as mammal species, they occupy a narrow range of PC 1 (-0.15— -0.05) and PC 2 scores (-0.1—0.1).

Species with the same diet have similar PC1 and PC2 scores within the same mammal group, however different mammalian groups have different ranges of PC1 and PC2 scores (Figure 11). This is most striking in herbivorous mammal species, which are distributed widely and occupy extreme values of negative PC1 and PC2 scores, and positive PC2 scores (Figure 11, Figure 13).

Herbivorous afrotherian taxa have positive PC 1 and negative PC 2 scores indicative of short mandibles with a low coronoid process and a rounded angular process. Herbivorous euarchontoglires also have positive PC 1 and negative PC 2 scores, however herbivorous euarchontoglires occupy a wider range of negative PC 2 scores that are more negative than those occupied by afrotherians. Herbivorous euarchontoglires have mandibles that are short with a low coronoid process and a prominent angular process that projects posteriorly. Herbivorous laurasiatherians have positive PC 1 and PC 2 scores and have mandibles that are long with a tall coronoid process and a rounded angular process. Most herbivorous marsupials have negative PC 1 and PC 2 scores indicative of long mandibles with a tall coronoid process and a prominent angular process that projects medially (Figure 11, Figure 12, Figure 13).

The PC 1 axis partitions marsupials from eutherian animals (placentals), since marsupials have a medially inflected angular process, and placental mammals lack this feature (Figure 11, Figure 12, Figure 13). Non-mammalian cynodonts have negative PC 1 scores and share a morphospace with metatherian animals, however, they are not on the extreme end of this (most negative PC 1 scores) which indicates that this feature may not be as exaggerated in extinct cynodonts. There’s no pattern of non-mammalian cynodonts gradually shifting towards a

particular morphospace and early forms like *Procynosuchus* have a morphospace most similar to that of later forms such as *Trirachodon berryi (*Figure 13*)*.

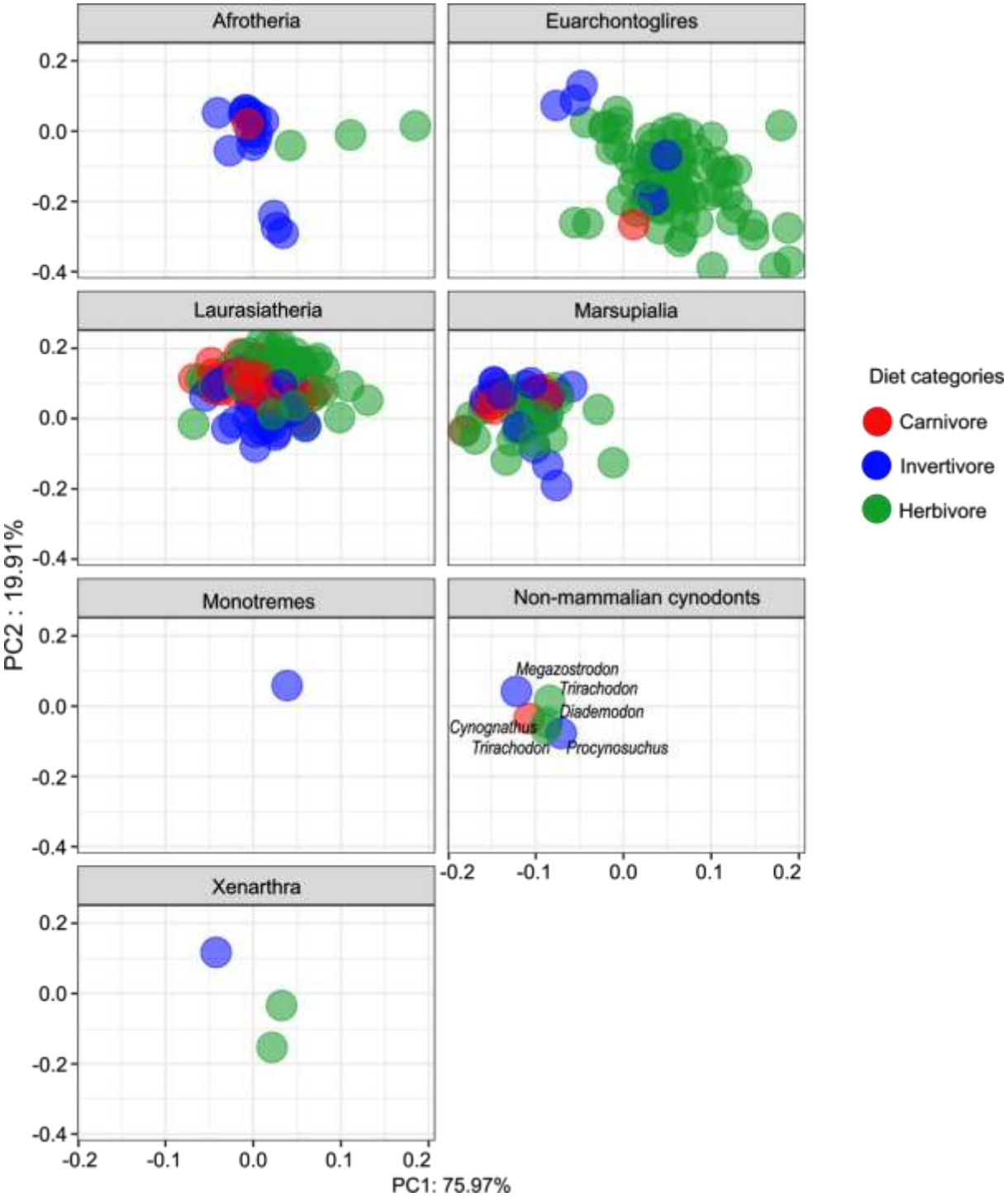


Figure 13: PC 1 and PC 2 axes of shape variation amongst partially landmarked mammal and non-mammalian cynodont species (n=268), partitioned according to major taxonomic groups.

12.1.2 Phylogenetic ANOVA regressions (procDgls)

Table 5: Phylogenetic ANOVA regressions (procDgls) assessing the association between mandible shape (Shape) and log_{10} body mass (BM), log_{10} centroid size (Size) and dietary variables amongst mammal species (n=262).

Model	n	R^2 model	Variable	R^2	Z	Pr(>F)
Shape ~ BM * Carnivory	262	0.049	BM	0.021	4.12	**0.0001**
			Carnivory	0.019	3.50	**0.0001**
			BM:Carnivory	0.010	2.21	**0.0139**
Shape ~ BM * Nectivory	262	0.046	BM	0.018	3.79	**0.0001**
			Nectivory	0.017	2.79	**0.0020**
			BM:Nectivory	0.012	2.26	**0.0134**
Shape ~ BM * Granivory	262	0.045	BM	0.021	4.14	**0.0001**
			Granivory	0.012	2.75	**0.0017**
			BM:Granivory	0.011	2.23	**0.0143**
Shape ~ BM * Invertivory	262	0.042	BM	0.015	3.46	**0.0001**
			Invertivory	0.017	3.24	**0.0003**
			BM:Invertivory	0.009	2.12	**0.0181**
Shape ~ BM + Carnivory	262	0.04	BM	0.021	4.11	**0.0001**
			Carnivory	0.019	3.49	**0.0001**
Shape ~ BM + Nectivory	262	0.034	BM	0.018	3.77	**0.0001**
			Nectivory	0.017	2.79	**0.0021**
Shape ~ BM + Frugivory	262	0.034	BM	0.021	4.11	**0.0001**
			Frugivory	0.005	0.81	0.2071
			BM:Frugivory	0.008	1.76	**0.0402**
Shape ~ BM + Granivory	262	0.034	BM	0.021	4.13	**0.0001**
			Granivory	0.012	2.74	**0.0018**
Shape ~ BM + Invertivory	262	0.033	BM	0.015	3.45	**0.0001**
			Invertivory	0.017	3.23	**0.0003**
Shape ~ BM * Herbivory	262	0.033	BM	0.018	3.70	**0.0002**
			Herbivory	0.006	1.43	0.0761
			BM:Herbivory	0.009	2.22	**0.0133**
Shape ~ BM + Frugivory	262	0.026	BM	0.021	4.10	**0.0001**
			Frugivory	0.005	0.80	0.2098
Shape ~ BM + Herbivory	262	0.024	BM	0.018	3.69	**0.0002**
			Herbivory	0.006	1.42	0.0776
Shape ~ Invertivory	262	0.022	Invertivory	0.022	3.67	**0.0001**
Shape~ Size	262	0.021	Size	0.021	3.99	**0.0001**
Shape ~ BM * Size	262	0.02	BM	0.007	1.43	0.0774
			Size	0.007	1.52	0.0649
			BM:Size	0.007	1.49	0.0703
Shape ~ BM	262	0.02	BM	0.020	4.03	**0.0001**
Shape ~ Carnivory	262	0.019	Carnivory	0.019	3.40	**0.0001**
Shape ~ Nectivory	262	0.019	Nectivory	0.019	2.97	**0.0008**
Shape ~ Granivory	262	0.012	Granivory	0.012	2.59	**0.0039**
Shape ~ Herbivory	262	0.009	Herbivory	0.009	2.17	**0.0142**
Shape ~ Frugivory	262	0.004	Frugivory	0.004	0.49	0.3109

All dietary variables have significant interaction effects with log_{10} body mass, this indicates that all dietary groups have different shape-allometry patterns. Amongst all relationships considered, the “best” model which explained the most variation is Shape ~ BM * Carnivory which explained 4.9% of the variation in mandible shape.

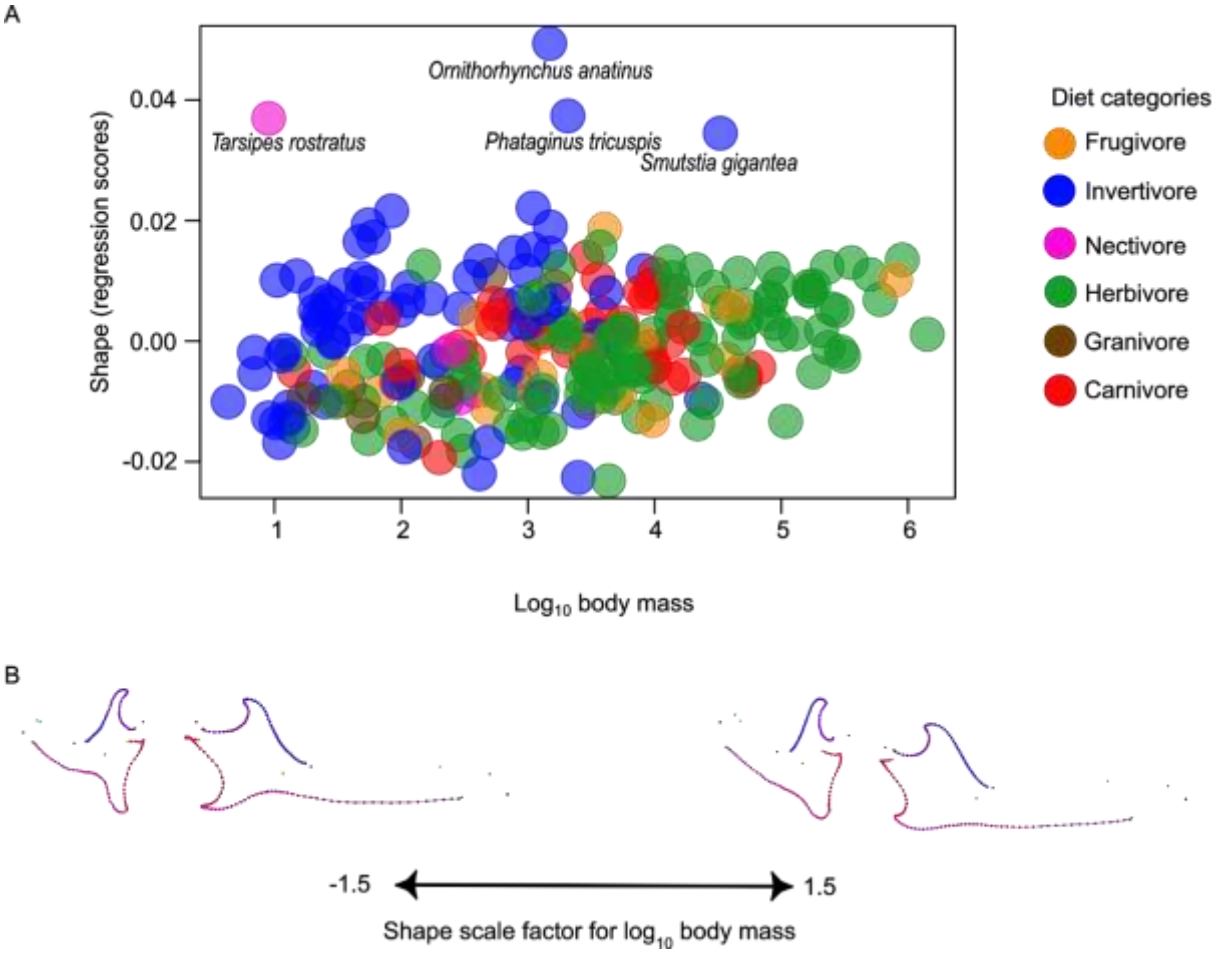


Figure 14: Scatterplot of shape regression scores and log_{10} body mass (A), alongside the mandibular shape differences associated with the effect of increasing log_{10} body mass (B). Landmark configurations shown in lateroposterior (left) and lateral (right) views.

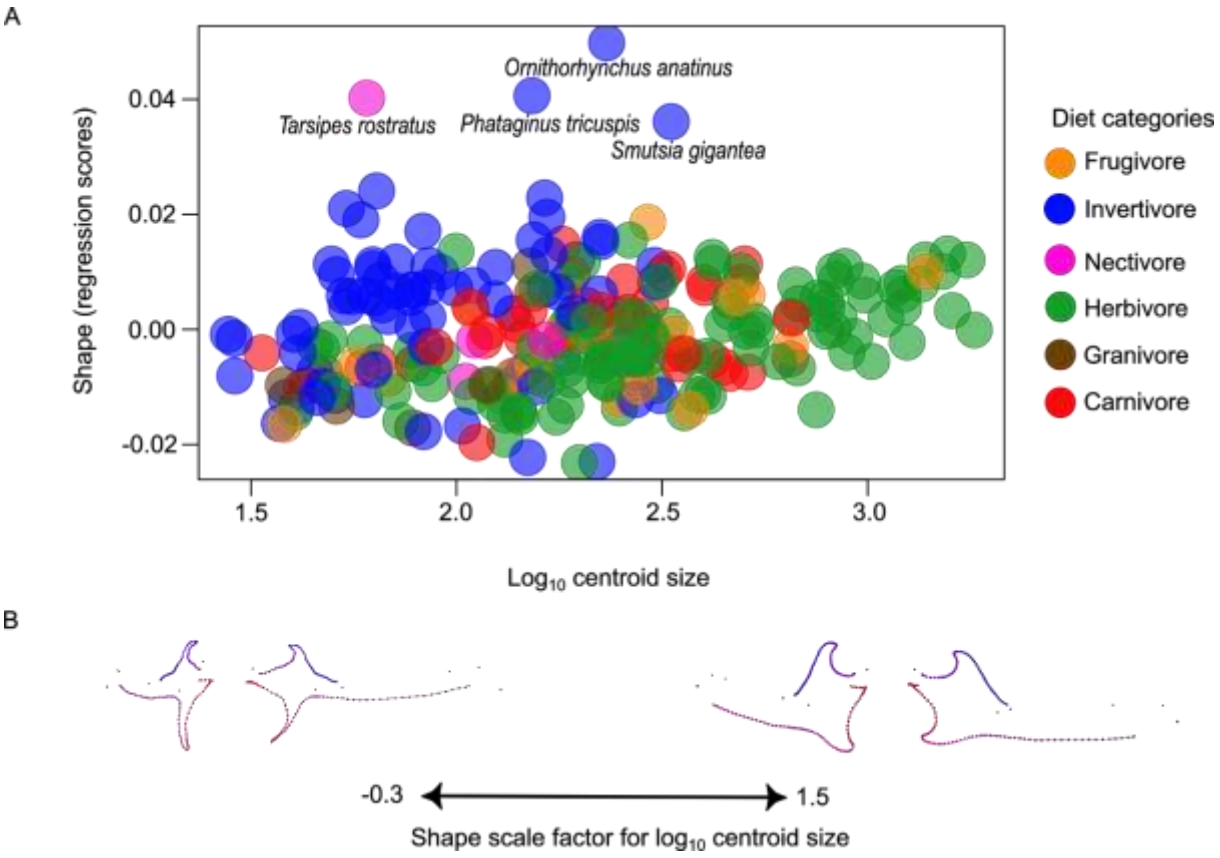


Figure 15: Scatterplot of shape regression scores and log_{10} mandible centroid size, alongside the mandibular shape differences associated with the effect of increasing log_{10} centroid size (B). Landmark configurations shown in lateroposterior (left) and lateral (right) views.

The relationship between log_{10} body mass and mandible shape was significant and explained 2% of the variation in mandible shape (Shape ~ BM, R^2; Table 5). Relative to small-bodied mammals, large-bodied mammals have an anteriorly taller mandible body, with a taller coronoid process and a less prominent angular process (Figure 14, B). Relative mandible size (log_{10} mandible centroid size) is also significant and explains 2.1% of the variation in mandible shape (Shape ~ Size; R^2; Table 5). Relative to mammals with a small centroid size, mammals with a larger centroid size have an anteriorly taller mandible body, with a taller coronoid process and a less prominent angular process (Figure 15, B). However, log_{10} body mass does not interact with relative mandible size in a way that influences mandible shapes (Shape ~ BM * Size; Table 5).

Carnivory has a significant influence on mandible shape when accounting for the effect of body mass (Shape ~ BM + Carnivory) or not (Shape ~ Carnivory). Both the main and partial effect of carnivory explain 1.9% of the variation in mandibular shape (Shape ~ Carnivory and Shape ~ BM + Carnivory, R^2; Table 5).

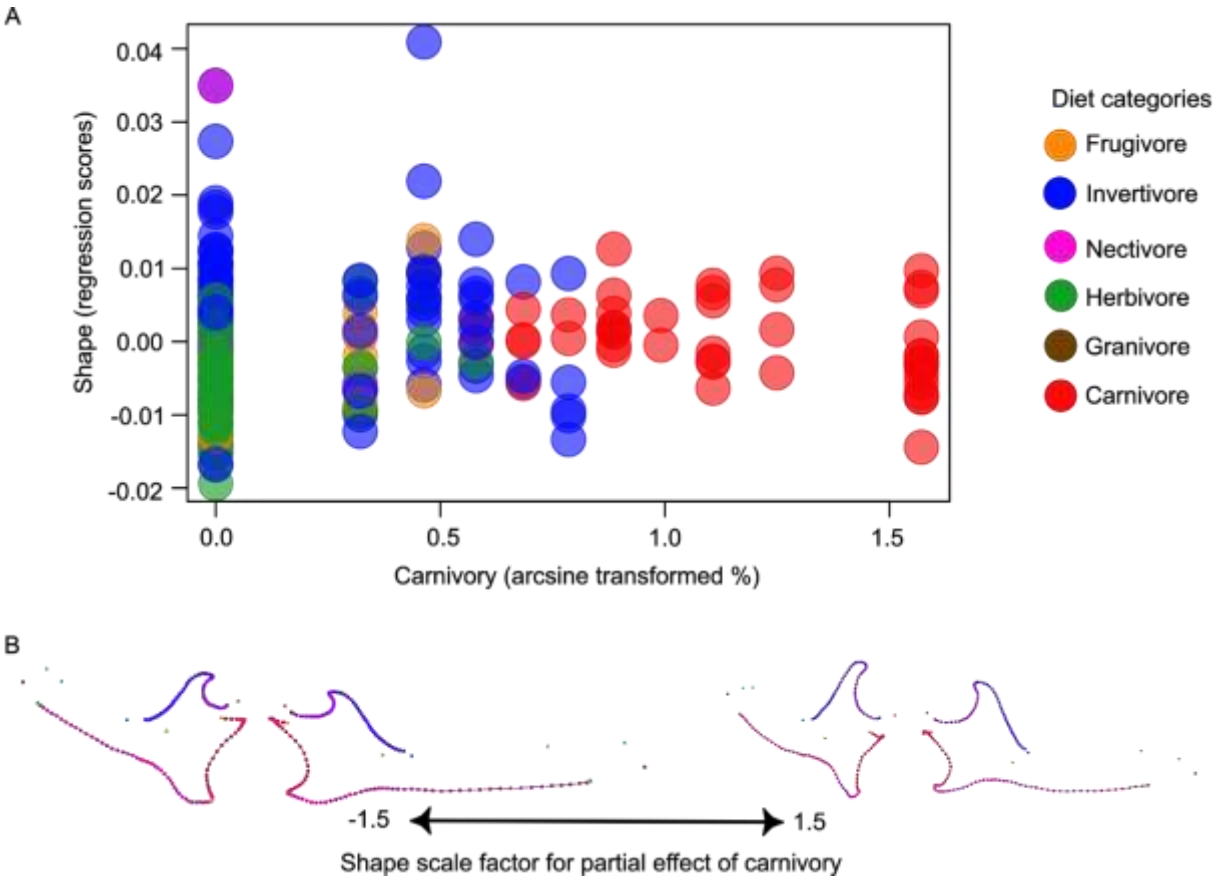


Figure 16: Scatterplot of shape (regression scores) and the arcsine transformed carnivory values (A), alongside the mandibular shape differences associated with the partial effect of carnivory (B). Landmark configurations shown in lateroposterior (left) and lateral (right) views.

Carnivores have different patterns of shape allometry than non-carnivores, this relationship explained 4.9% of the variation in mandible shapes (Shape ~ BM * Carnivory, R^2). Notably, this relationship describes the most variation in mandible shape relative to other relationships considered here. Highly carnivorous mammals have shorter mandibles relative to those of mammals with other diets. The anterior and posterior ends of the mandible body are taller, and the mandibular condyle is positioned lower relative to the horizontal plane. The angular process is less prominent relative to non-carnivorous mammals (Figure

16, B). Small-bodied and large-bodied carnivorous species both have a tall coronoid process (Figure 17). However, smaller carnivorous species generally have a more prominent angular process relative to large-bodied carnivorous species (Figure 17).



Figure 17: Landmark configurations in A: small-bodied carnivore (bicoloured musk shrew, *Crocidura fuscomurina*) and B: large-bodied carnivore (spotted hyaena, *Crocuta crocuta*). Landmark configurations shown in lateroposterior (left) and lateral (right) views.

Nectivory has a significant influence on mandible shape when accounting for the effect of body mass (Shape ~ BM + Nectivory) or not (Shape ~ Nectivory). The main effect of nectivory explains 1.9% of the variation in mandibular shape (Shape ~ Nectivory, R^2; Table 5). After accounting for the effect of body mass, nectivory explains 1.7% of the variation in mandible shape (Shape ~ BM + Nectivory, R^2; Table 5). Highly nectivorous mammals have longer and less robustly shaped mandibles than non-nectivores. The anterior end of the mandible body is lower, and the angular process is less prominent (Figure 18, B). Nectivores have different patterns of shape allometry than non-nectivores, this relationship explained 4.6% of the variation in mandible shapes (Shape ~ BM * Nectivory, R^2).

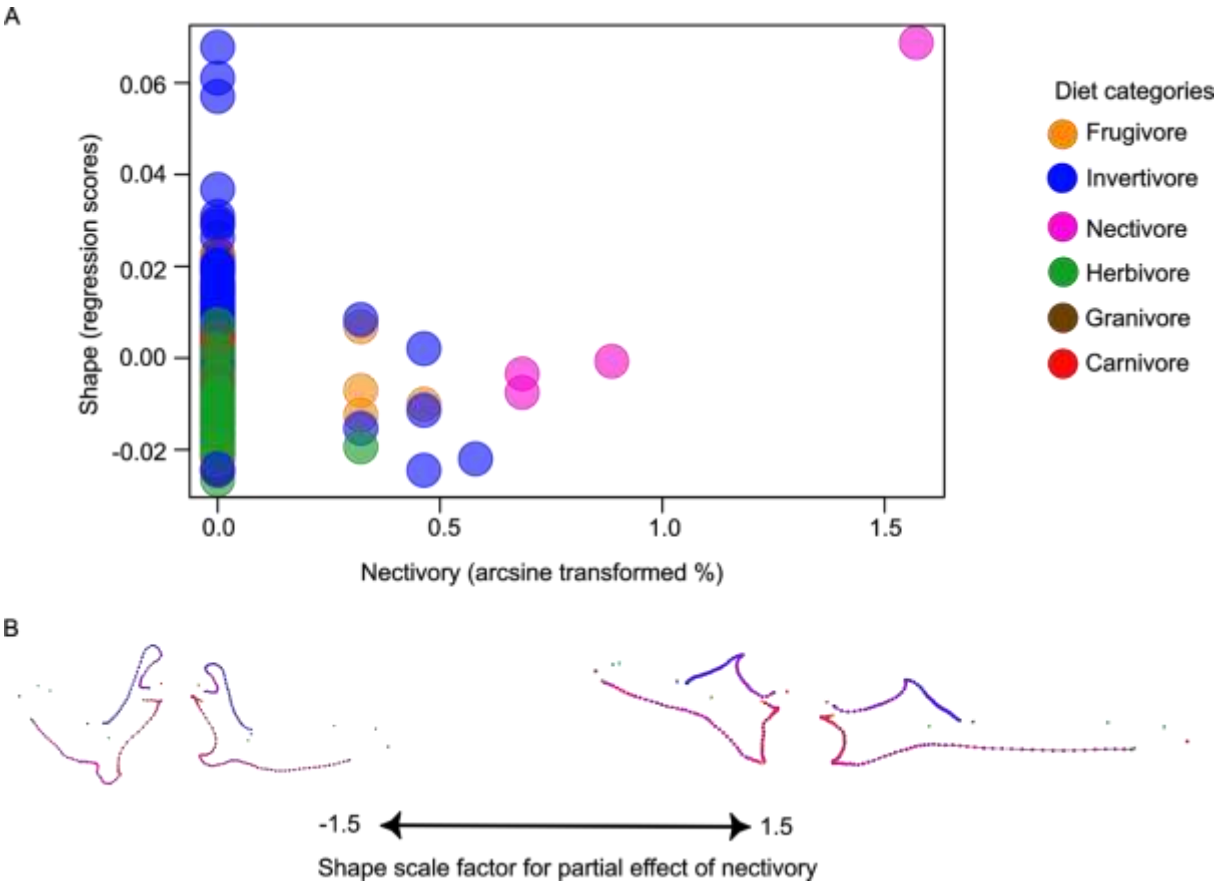


Figure 18: Scatterplot of shape (regression scores) and the arcsine transformed nectivory values (A), alongside the mandible shape differences associated with the partial effect of nectivory (B). Landmark configurations shown in lateroposterior (left) and lateral (right) views.

Nectivorous species sampled (n=4) are only small-bodied bodied (less than 300g). The smallest (less than 100g) amongst these is the honey possum (*Tarsipes rostratus,* a diprotodontid) which has a long mandible with a low anterior and posterior mandible body (Figure 19). The coronoid process is low, and the angular process is absent. Relatively larger (100g—300g) nectivorous species have mandible shapes that are characterized by a posteriorly tall mandible body with a relatively taller coronoid process (Figure 19).

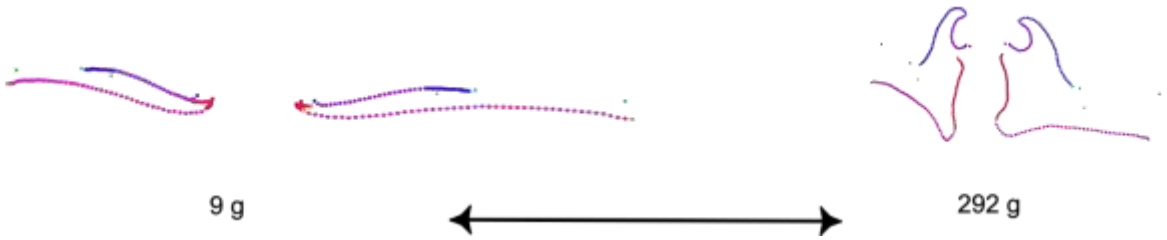


Figure 19: Landmark configurations in: A: small-bodied nectivore (honey possum, *Tarsipes rostratus*) and B: large-bodied nectivore (common marmoset, *Callithrix jacchus*). Landmark configurations shown in lateroposterior (left) and lateral (right) views.

Granivory has a significant influence on mandible shape when accounting for the effect of body mass (Shape ~ BM + Granivory) or not (Shape ~ Granivory). Both the main and partial effect of granivory explain 1.2% of the variation in mandible shape (Shape ~ Granivory and Shape ~ BM + Granivory, R2; Table 5).

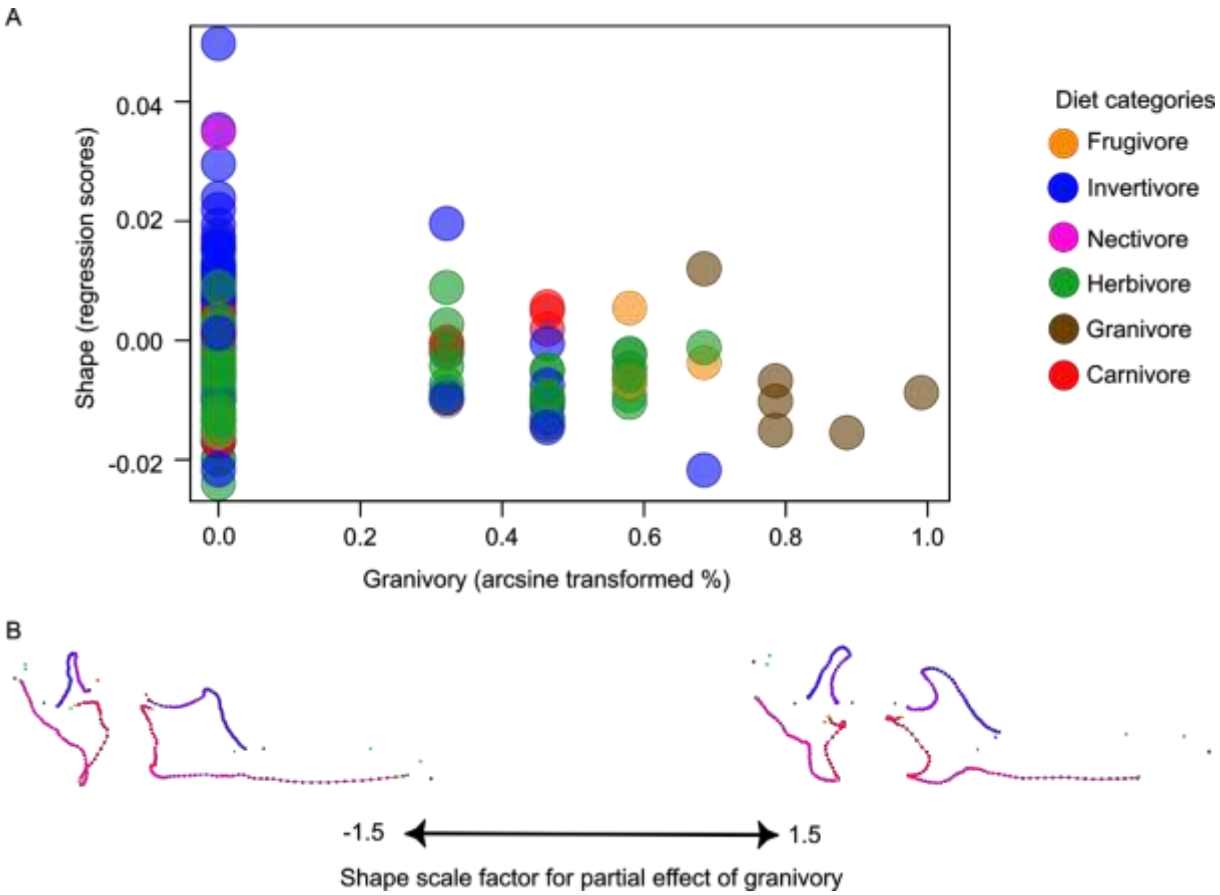


Figure 20: Scatterplot of shape (regression scores) and the arcsine transformed granivory values (A), alongside the mandible shape differences associated with the partial effect of granivory (B). Landmark configurations shown in lateroposterior (left) and lateral (right) views.

Relative to non-granivorous mammals, granivorous mammals have mandibles with an anteriorly taller mandible body, and a taller coronoid process. The mandibular condyle is smaller, the angular process is prominent and ventrally expanded relative to those of non-granivores. The ventral margin of the mandible is concave (Figure 20, B). Granivores have different patterns of shape allometry than non-granivores, this relationship explained 4.5% of the variation in mandible shapes (Shape ~ BM * Granivory, R^2). Small-bodied (less than 1,000g) granivorous species are characterized by a tall coronoid process and a prominent and expanded angular process (Figure 21). The ventral margin of the mandible is concave (Figure 21). Large bodied granivorous species lack a prominently expanded angular process and have an even taller coronoid process (Figure 21).



Figure 21: Landmark configurations in: A: small-bodied granivore (meadow jumping mouse, *Zapus hudsonicus*) and B: large-bodied granivore (white-lipped peccary, *Tayassu pecari*). Landmark configurations shown in lateroposterior (left) and lateral (right) views.

Invertivory has a significant influence on mandible shape when accounting for the effect of body mass (Shape ~ BM + Invertivory) or not (Shape ~ Invertivory). The main effect of invertivory explains 2.2% of the variation in mandible shape (Shape ~ Invertivory, R^2; Table 5). After accounting for the effect of body mass, invertivory explains 1.7% of the variation (Shape ~ BM+Invertivory, R^2; Table 5). Invertivores have different patterns of shape allometry than non-invertivores, this relationship explained 4.2% of the variation in mandible shapes (Shape ~ BM * Invertivory, R^2).

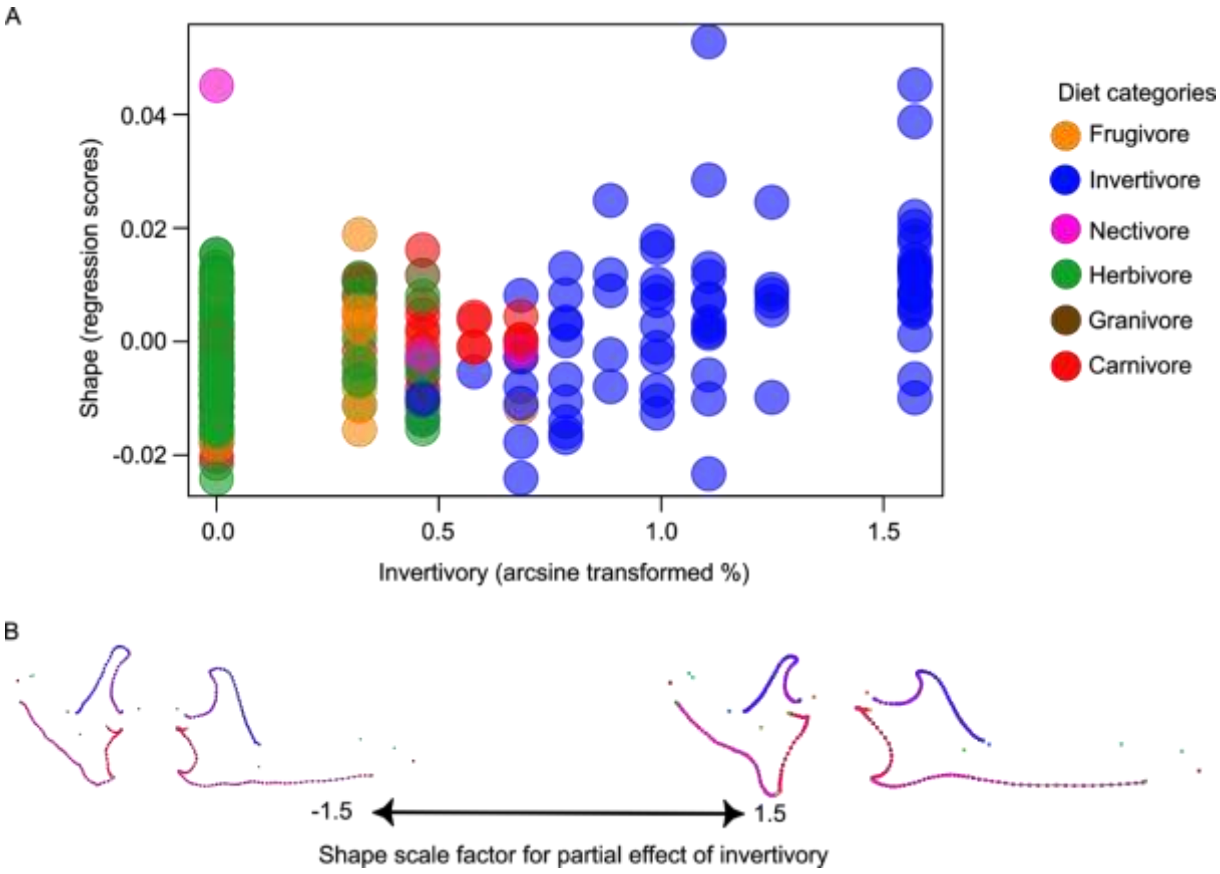


Figure 23: Scatterplot of shape (regression scores) and the arcsine transformed invertivory values (A), alongside the mandible shape differences associated with the partial effect of invertivory (B). Landmark configurations shown in lateroposterior (left) and lateral (right) views.

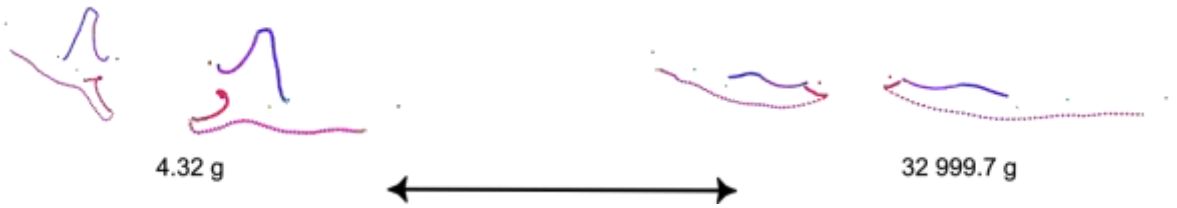


Figure 22: Landmark configurations in: A: small-bodied invertivore (Howell's forest shrew, *Sylivisorex howelli*) and B: large-bodied invertivore (giant pangolin, *Smutsia gigantea*). Landmark configurations shown in lateroposterior (left) and lateral (right) views.

Highly invertivorous mammals have longer mandibles relative to those of mammals with other diets. The coronoid process is lower, and the position of the mandibular condyle is higher relative to the horizontal plane. The angular process is more prominent relative to the mandibles of non-invertivorous mammals (Figure 22, B). Small-bodied invertivorous mammals have a long mandible, with a tall coronoid process and a prominent angular process. Large-bodied invertivorous mammal have a long mandible with a low coronoid process, and the angular process is absent (Figure 23).

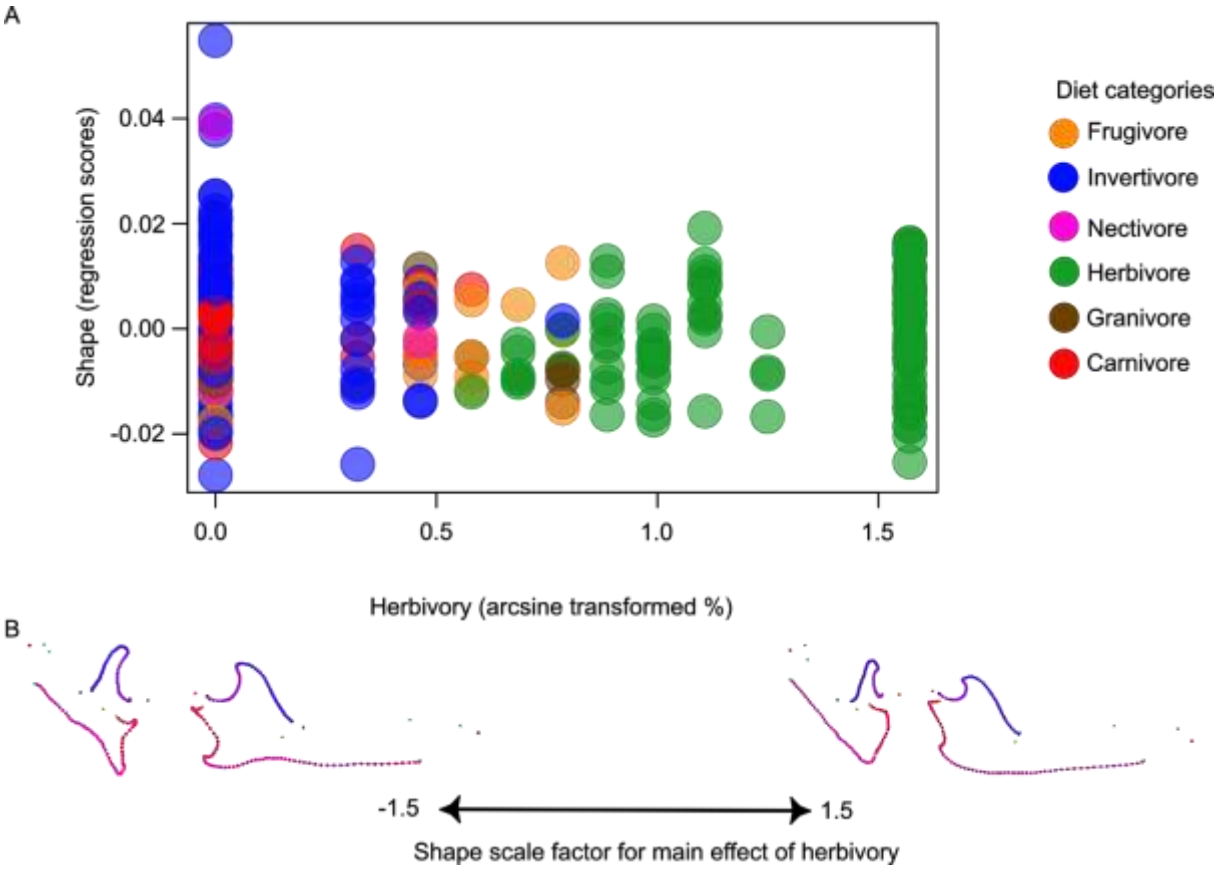


Figure 24: Scatterplot of shape (regression scores) and the arcsine transformed herbivory values (A), alongside the mandible shape differences associated with the main effect of herbivory (B). Landmark configurations shown in lateroposterior (left) and lateral (right) views.

Herbivory has a significant influence on mandible shape which explains 0.9% of the variation in mandible shape (Shape ~ Herbivory, R^2). However, herbivory has no significant influence on mandible shape after accounting for the effect of body mass (Shape ~ BM + Herbivory; Table 5). Highly herbivorous mammals have mandibles with a tall posterior mandible body and a low coronoid process. The mandibular condyle is high relative to the horizontal plane and the angular

process is rounded (Figure 24, B). Herbivores have different patterns of shape allometry than non-herbivores, this relationship explained 3.3% of the variation in mandible shapes (Shape ~ BM * Herbivory, R^2).



Figure 25: Landmark configurations in: A: small-bodied herbivore (gerbil mouse, *Malacothrix typica*) and B: large-bodied herbivore (giraffe, *Giraffa camelopardalis*). Landmark configurations shown in lateroposterior (left) and lateral (right) views.

Small-bodied and large-bodied herbivores both have a posteriorly tall mandible body (Figure 25). Small-bodied herbivorous species have mandibles that are short with a relatively short coronoid process and a prominent ventrally expanded angular process, whereas large-bodied herbivorous species have mandibles that are relatively long with a relatively taller coronoid process (Figure 25). Large-bodied herbivores have a highly reduced angular process.

Frugivory has no significant influence on mandible shape when accounting for body mass or not (Shape ~ BM + Frugivory, Shape ~ Frugivory; Table 5). Frugivores have different patterns of shape allometry than non-frugivores, this relationship explained 3.4% of the variation in mandible shapes (Shape ~ BM * Frugivory, R^2).



Figure 26: Landmark configurations in: A: small bodied frugivore (pygmy scaly-tailed flying squirrel, *Idiurus zenkeri*) and B: large-bodied frugivore (Sumatran rhinoceros, *Dicerorhinus sumatrensis*). Landmark configurations shown in lateroposterior (left) and lateral (right) views.

Small-bodied frugivorous species have mandibles that are short with a prominent angular process (expanded) and a shorter coronoid process, whereas large-bodied frugivorous species have mandibles that are relatively long with a relatively taller coronoid process (Figure 26). Large-bodied frugivores have a highly reduced (absent) angular process (Figure 26).

12.1.3 pDFA: mandible shape

The median success rate of predicting an animal's diet (herbivore, carnivore or invertivore) using the first seven PCA axes as a proxy for mandible shape is 75 % (P5=70%, P95=81.05%). This is approximately 62% better than randomly guessing the diet (relative to error rate of 66% under guesswork). Mandible shape is best at predicting the diet of herbivores; however, it is also good at predicting the diet of carnivores and invertivores (Table 6).

Mandible shape was best at predicting the diet of herbivores and an average of only 16.67% herbivorous mammals were misclassified as carnivores or invertivores (Table 6). Amongst herbivorous mammals correctly classified those associated with the highest posterior probabilities have mandible shapes characterized by a posteriorly tall mandible body with a low coronoid process (Figure 24, A; Figure 27, A). This included the dugong (*Dugong dugon*, $PP_{herbivore}$= 0.96), vicunã (*Vicugna vicugna,* $PP_{herbivore}$= 0.95) and the pygmy scaly-tailed flying squirrel (*Idiurus zenkeri,* $PP_{herbivore}$= 0.99).

Table 6: Confusion table for pDFAs which estimated diet using mandible shape (first seven PCA axes). Note differences in the median, 5th (P5) percentile and 95th (P95) percentile counts per dietary category.

Predicted diet (pDFA)	**True diet**		
	Carnivore	Herbivore	Invertivore
Carnivore	23 (P5=21, P95=26)	4 (P5=1, P95=6)	7 (P5=4, P95=9)
Median %	76.67%	13.34%	23.33%
Herbivore	1 (P5=0, P95=2)	25 (P5=22, P95=28)	3 (P5=1, P95=5)
Median %	3.33%	83.33%	10%
Invertivore	6 (P5=4, P95=8)	1 (P5=0, P95=4)	20 (P5=17, P95=23)
Median %	20%	3.33%	66.67%
Median % correct	76.67%	83.33%	66.67%

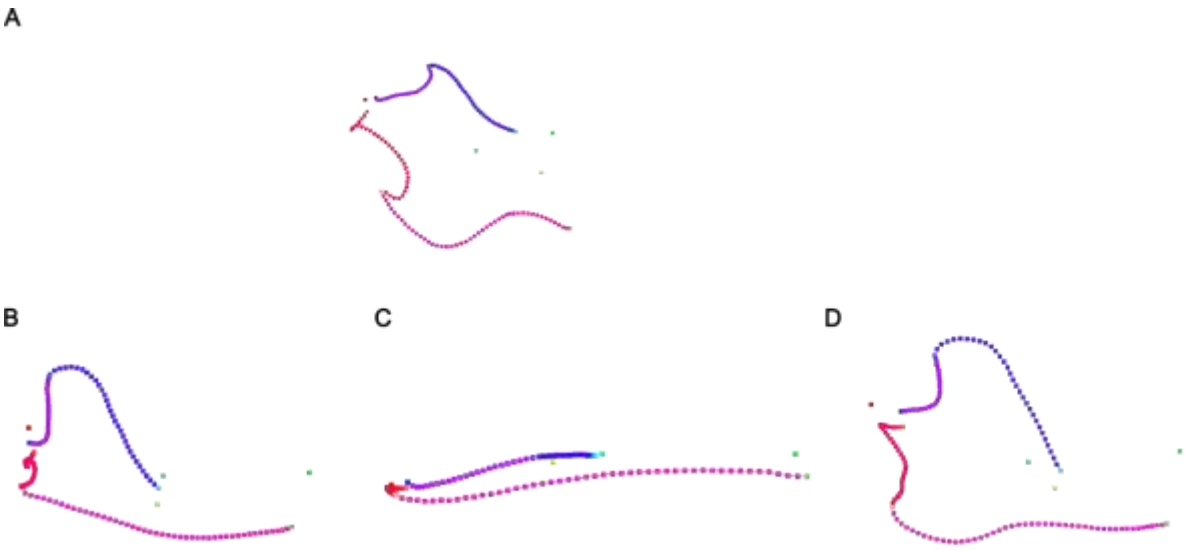


Figure 27: Landmark configurations representing mandible shape differences in A: a correctly classified herbivorous mammal (pygmy scaly-tailed flying squirrel); B: a herbivorous mammal misclassified as a carnivore (African palm civet) and C, D: herbivorous mammals misclassified as invertivores (C: honey possum, D: common brushtail possum). Landmark configurations shown in lateral views.

Herbivores were more frequently misclassified as carnivores (Table 6), and instances of this included many herbivorous members of Carnivora which have tall coronoid processes such as the giant panda (*Ailuropoda melanoleuca*, $PP_{carnivore}$= 0.62), African palm civet (*Nandinia binotata*, $PP_{carnivore}$= 0.82), and the central African oyan (*Poiana richardsonii*, $PP_{carnivore}$= 0.77). Herbivores misclassified as carnivores also included primates such as the aye-aye (*Daubentonia madagascariensis*, $PP_{carnivore}$= 0.49) and the black lemur (*Eulemur macaco*, $PP_{carnivore}$= 0.47); as well as marsupials such as the black-shouldered opossum (*Caluromysiops irrupta*, $PP_{carnivore}$= 0.49) and the sugar glider (*Petaurus breviceps*, $PP_{carnivore}$= 0.57). These primates and marsupials all have an expanded posterior mandible body and a tall coronoid process and are notably associated with low-to-medium posterior probabilities ($PP_{carnivore}$= 0.44—0.57). Amongst herbivores misclassified as carnivores, those associated with the highest posterior probabilities are herbivorous carnivorans ($PP_{carnivore}$= 0.62—0.82), such as the African palm civet ($PP_{carnivore}$= 0.82) which has a tall coronoid process (Figure 27, B).

Herbivores misclassified as invertivores included diprotodontids such as the common brushtail possum (*Trichosurus vulpecula*, $PP_{invertivore}$= 0.61) and the woylie (*Bettongia pencillata*, $PP_{invertivore}$= 0.48). The Baluchistan pygmy jerboa (*Salpingotulus michaelis*, $PP_{invertivore}$= 0.63), a rodent, was also misclassified as an invertivore. Amongst herbivores misclassified as invertivores, those associated with highest posterior probabilities, such as the honey possum (*Tarsipes rostratus,* $PP_{invertivore}$= 0.92) and the common brushtail possum ($PP_{invertivore}$= 0.61), have variable mandible shapes (Figure 27, C and D). The honey possum has a long mandible with a low coronoid process and the angular process is absent (Figure 27, C); whereas the common brushtail possum has an anteriorly low mandible body, with a tall coronoid process and a prominent angular process (Figure 27, D). Apart from the honey possum ($PP_{invertivore}$= 0.92), herbivores misclassified as invertivores generally have low-to-medium posterior probabilities ($PP_{invertivore}$= 0.48—0.63).

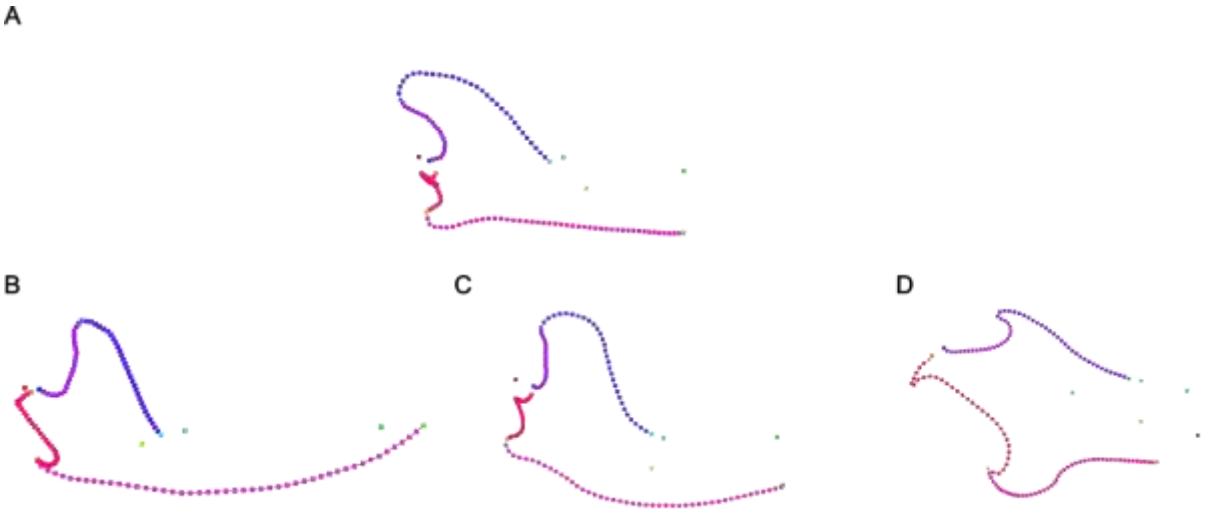


Figure 28: Landmark configurations representing mandible shape differences in A: correctly classified carnivorous mammal (leopard); B: a carnivorous mammal misclassified as an invertivore (eastern quoll); C: a carnivorous mammal misclassified as an herbivore (binturong) and D: the potentially carnivorous Cameroon scaly-tail. Landmark configurations shown in lateral views.

An average of 23.33% of carnivorous mammals sampled were misclassified as herbivores or invertivores using mandible shape. Amongst carnivores correctly classified, those associated with the highest posterior probabilities have mandible

shapes characterized by a tall coronoid process and a reduced angular process (Figure 16, B; Figure 28, A). This included the leopard (*Panthera pardus,* $PP_{carnivore}$=0.79) and the European badger (*Meles meles,* $PP_{carnivore}$= 0.76).

Carnivores were more frequently misclassified as invertivores (Table 6), and these included a variety of dasyuromorphs, soricids and carnivorans. This included the crest-tailed mulgara (*Dasycercus cristicauda*, $PP_{invertivore}$ = 0.89), eastern quoll (*Dasyurus viverrinus*, $PP_{invertivore}$ = 0.87), Eurasian water shrew (*Neomys fodiens*, $PP_{invertivore}$ = 0.82), Angolan genet (*Genetta genetta*, $PP_{invertivore}$ = 0.58) and the small Indian civet (*Viverricula indica*, $PP_{invertivore}$ = 0.61). Amongst carnivorous mammals misclassified as invertivores, carnivorans have medium posterior probabilities ($PP_{invertivore}$ =0.58—0.61), and those associated with the highest posterior probabilities are carnivorous marsupial and soricid species ($PP_{invertivore}$= 0.82—0.89) such as the eastern quoll ($PP_{invertivore}$ = 0.87) and the Eurasian water shrew ($PP_{invertivore}$ = 0.82). These species have mandibles with a relatively more prominent angular process (Figure 28, B).

Amongst carnivorous species misclassified as herbivores were Carnivora members which have a posteriorly tall and expanded mandible body as the binturong (*Arctictis binturong*, $PP_{herbivore}$ = 0.67), Asian palm civet (*Paradoxurus hermaphroditus*, $PP_{herbivore}$= 0.45) and the bush dog (*Speothos venaticus*, $PP_{herbivore}$ = 0.53). The potentially carnivorous Cameroon scaly-tail (*Zenkerella insignis*, $PP_{herbivore}$ = 0.91), a cryptic rodent, was classified as a herbivore in all iterations it was included in. This may be correct as not much is known about the Cameroon scaly-tail's ecology. The Cameroon scaly-tail has a short mandible with a low coronoid process and a ventrally expanded angular process (Figure 28, D). Apart from the Cameroon scaly-tail ($PP_{herbivore}$ = 0.91), most carnivores misclassified as herbivores have low-to-medium posterior probabilities ($PP_{herbivore}$= 0.45—0.67), and those associated with the relatively highest posterior probabilities, such as the binturong ($PP_{herbivore}$ = 0.67), have a posteriorly tall mandible body (Figure 28, C).

Mandible shape was relatively bad at predicting the diet of invertivorous mammals, and on average 33.33% of the invertivorous mammals sampled were misclassified as herbivores or carnivores (Table 6). Amongst invertivorous

mammals that were correctly classified, those associated with the highest posterior probabilities have long mandibles with an anteriorly low mandible body and a prominent angular process (Figure 22, B; Figure 29, A). This included the long-nosed echymipera (*Echymipera rufescens,* $PP_{invertivore}$= 0.82), the Cape golden mole (*Chrysochloris asiatica,* $PP_{invertivore}$= 0.81), and the Himalayan mole (*Euroscaptor micrura,* $PP_{invertivore}$=0.80).

Invertivorous mammals were more frequently misclassified as carnivores, these included mostly marsupial, soricid and Carnivora members that either have a anteriorly tall mandible such as the marsh mongoose (*Atilax paludinosus*, $PP_{carnivore}$= 0.53) or a mandible with a tall coronoid process such as the meerkat (*Suricata suricatta*, $PP_{carnivore}$= 0.82), Himalayan shrew (*Soriculus nigrescens*, $PP_{carnivore}$= 0.63) and the water opossum (*Chironectes minimus*, $PP_{carnivore}$= 0.47). Amongst invertivorous species misclassified as carnivores, those associated with the highest posterior probabilities, such as the meerkat ($PP_{carnivore}$= 0.82), have a tall and expanded coronoid process (Figure 29, B).

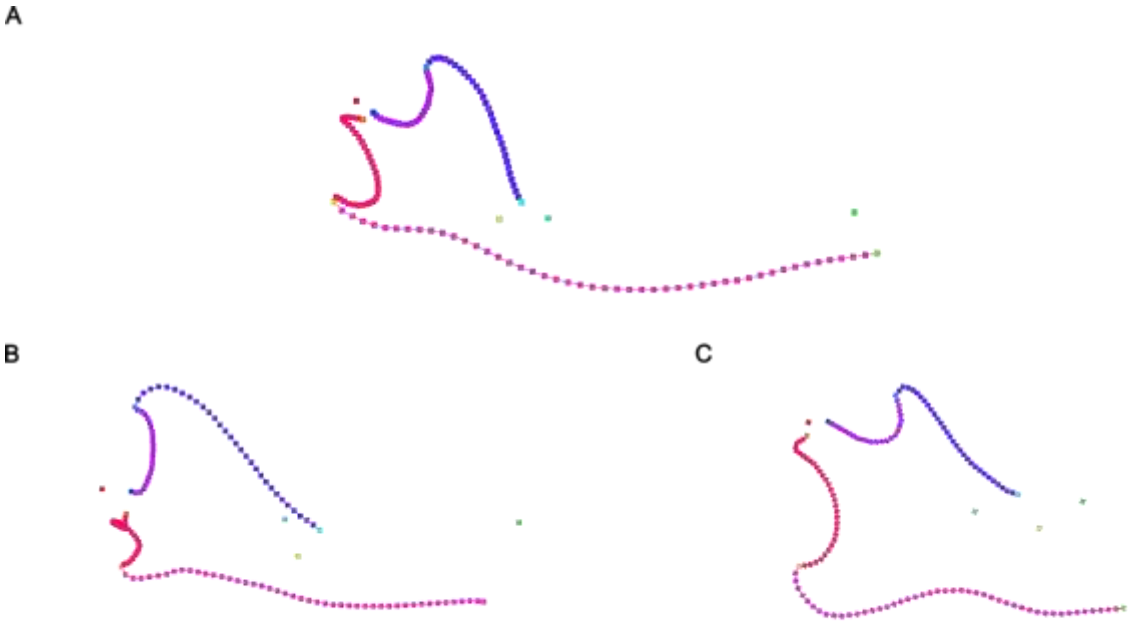


Figure 29: Landmark configurations representing mandible shape differences in A: a correctly classified invertivorous mammal (long-nosed echymipera); B: an invertivorous mammal misclassified as a carnivore (meerkat) and C: an invertivorous mammal misclassified as a herbivore (northern grasshopper mouse). Landmark configurations shown in lateral views.

Amongst invertivorous species misclassified as herbivores are macroscelids which have a relatively short mandible with a tall coronoid process, this included the round-eared elephant shrew (*Macroscelides proboscideus*, $PP_{herbivore}$= 0.62) and the black and rufous elephant shrew (*Rhynchocyon petersi*, $PP_{herbivore}$= 0.81). Species with a short and posteriorly tall mandible were also misclassified as herbivorous such as the northern grasshopper mouse (*Onychomys torridus*, $PP_{herbivore}$= 0.87), a rodent; and the slender loris (*Loris tardigradus*, $PP_{herbivore}$= 0.58), a primate. Amongst the invertivorous species misclassified as herbivores, those associated with the highest posterior probabilities, such as the northern grasshopper mouse ($PP_{herbivore}$= 0.87), have a posteriorly tall mandible (Figure 29, C).

Table 7: The estimated diets of non-mammalian cynodont species associated with pDFAs which made use of mandible shape (first seven PCA axes) as the input predictor variables. Note differences in median, 5th (P5) percentile and 95th percentile (P95) of posterior probabilities.

Taxon	Expected diet	Predicted diet	Posterior probability
Cynognathus crateronotus	Carnivore	Carnivore	**0.90** (P5=0.27, P95=**0.99**)
Diademodon tetragonus	Herbivore	Herbivore	0.46 (P5=0.009, P95=**0.99**)
Megazostrodon rudnerae	Invertivore	Invertivore	**0.92** (P5=0.43, P95=**0.99**)
Procynosuchus delaharpeae	Invertivore	Carnivore	**0.99** (P5=0.02, P95=**0.99**)
Trirachodon berryi	Herbivore	Carnivore	0.89 (P5=0.06, P95=**0.99**)
Trirachodon sp.	Herbivore	Carnivore	0.72 (P5=0.01, P95=**0.99**)

Cynognathus, Procynosuchus and Trirachodon are estimated as carnivorous when using mandible shape to predict diet (Table 7). These estimates do not coincide with the hypothesized diets of *Procynosuchus* and *Trirachodon*, which are based on morphological observations in the literature.

Although there are differences in the mandible shapes of *Cynognathus, Procynosuchus* and *Trirachodon,* all species have mandible shapes with a relatively large coronoid process, and the mandibular condyle is low relative to the horizontal plane (Figure 30, A).

Diademodon's mandible has a tall coronoid process, and the mandibular condyle is elevated relative to the horizontal plane (Figure 30, B). *Diademodon* is the only cynodont species classified as an herbivore using mandible shape (Table 7). Although this classification coincides with the expected diet, the associated posterior probability is low indicative of high uncertainty ($PP_{herbivore}$= 0.46, Table 7).

Megazostrodon, the only species estimated as an invertivore (Table 7) and has a long mandible with a low anterior and posterior mandible body and a low coronoid process (Figure 30, C). This estimate coincides with the expected diet and the associated posterior probability is high ($PP_{invertivore}$= 0.92, Table 7)



Figure 30: Landmark configurations representing mandible shape of A: *Cynognathus*, B: *Diademodon* and C: *Megazostrodon.* Landmark configurations shown in lateral views.

12.2 Mandible size and its association with diet

12.2.1 Phylogenetic regressions (pgls)

The relationship between log_{10} body mass and log_{10} mandible centroid size was highly significant and explained 80.13% of the variation in the model (Size ~ BM, R^2; Table 8); therefore, log_{10} body mass was included as a variable in all subsequent models. Including dietary variables only explained an additional 0.6% of the variation at most; and this indicates that log_{10} body mass explained a large portion of the log_{10} mandible centroid size variation (Table 8, Figure 31). This is solely because animals that have a large body mass inherently have larger body proportions.

Table 8: Phylogenetic regressions (pgls) assessing log_{10} mandible centroid size's (Size) association with log_{10} body mass (BM) and dietary variables amongst mammal species (n=262).

Model	n	AIC	AIC w	R^2	p-value (model)	Variable	Coefficient	Std err	Pr(>|t|)
Size ~ BM * Frugivory	262	-408.60	0.41	0.8093	**<0.0001**	(Intercept)	1.40	0.16	<0.0001
						BM	0.29	0.01	**<0.0001**
						Frugivory	-0.18	0.06	**0.005**
						BM:Frugivory	0.04	0.02	**0.032**
Size ~ BM + Carnivory	262	-407.77	0.27	0.8073	**<0.0001**	(Intercept)	1.38	0.16	<0.0001
						BM	0.29	0.01	**<0.0001**
						Carnivory	0.04	0.02	**0.005**
Size ~ BM * Carnivory	262	-406.32	0.13	0.8077	**<0.0001**	(Intercept)	1.39	0.16	<0.0001
						BM	0.29	0.01	**<0.0001**
						Carnivory	0.02	0.04	0.694
						BM:Carnivory	0.01	0.01	0.461
Size ~ BM + Frugivory	262	-405.93	0.11	0.8059	**<0.0001**	(Intercept)	1.38	0.16	<0.0001
						BM	0.30	0.01	**<0.0001**
						Frugivory	-0.05	0.02	**0.014**
Size ~ BM * Granivory	262	-403.57	0.03	0.8056	**<0.0001**	(Intercept)	1.36	0.16	<0.0001
						BM	0.30	0.01	**<0.0001**
						Granivory	0.17	0.08	**0.039**
						BM:Granivory	-0.06	0.03	**0.019**
Size ~ BM	262	-401.76	0.01	0.8013	**<0.0001**	(Intercept)	1.37	0.16	<0.0001
						BM	0.30	0.01	**<0.0001**
Size ~ BM + Invertivory	262	-400.47	0.01	0.8018	**<0.0001**	(Intercept)	1.39	0.16	<0.0001
						BM	0.29	0.01	**<0.0001**
						Invertivory	-0.02	0.02	0.404
Size ~ BM + nectivory	262	-400.41	0.01	0.8018	**<0.0001**	(Intercept)	1.37	0.16	<0.0001
						BM	0.30	0.01	**<0.0001**
						Nectivory	0.04	0.05	0.424
Size ~ BM * Invertivory	262	-400.29	0.01	0.8032	**<0.0001**	(Intercept)	1.37	0.16	<0.0001

						BM	0.30	0.01	**<0.0001**
						Invertivory	0.04	0.05	0.381
						BM:Invertivory	-0.02	0.01	0.181
Size ~ BM +Herbivory	262	-399.95	0.01	0.8014	**<0.0001**	(Intercept)	1.37	0.16	<0.0001
						BM	0.30	0.01	**<0.0001**
						Herbivory	-0.01	0.02	0.669
Size ~ BM + Granivory	262	-399.93	0.01	0.8014	**<0.0001**	(Intercept)	1.37	0.16	<0.0001
						BM	0.30	0.01	**<0.0001**
						Granivory	-0.01	0.03	0.682
Size ~ BM * Nectivory	262	-398.59	0.00	0.8019	**<0.0001**	(Intercept)	1.37	0.16	<0.0001
						BM	0.30	0.01	**<0.0001**
						Nectivory	0.09	0.13	0.479
						BM:Nectivory	-0.03	0.06	0.677
Size ~ BM * Herbivory	262	-398.11	0.00	0.8015	**<0.0001**	(Intercept)	1.37	0.16	<0.0001
						BM	0.30	0.01	**<0.0001**
						Herbivory	0.01	0.04	0.860
						BM:Herbivory	0.00	0.01	0.694

If $\log_{10}$ mandible centroid size had scaled isometrically, the $\log_{10}$ mandible centroid size coefficient would be 0.33 because all length-based properties change with mass to the power of a third (0.33). However, the coefficient is 0.3, indicative of slight negative allometry (Table 8). This means that $\log_{10}$ mandible centroid size increases slightly slower than $\log_{10}$ body mass.

The diets granivory, nectivory, invertivory and herbivory have no significant influence on $\log_{10}$ mandible centroid size after accounting for the effect of $\log_{10}$ body mass on $\log_{10}$ mandible centroid size (Table 8). This means the animals with these dietary preferences had mandible sizes that correspond to what was expected of an animal of its body mass (Figure 31).

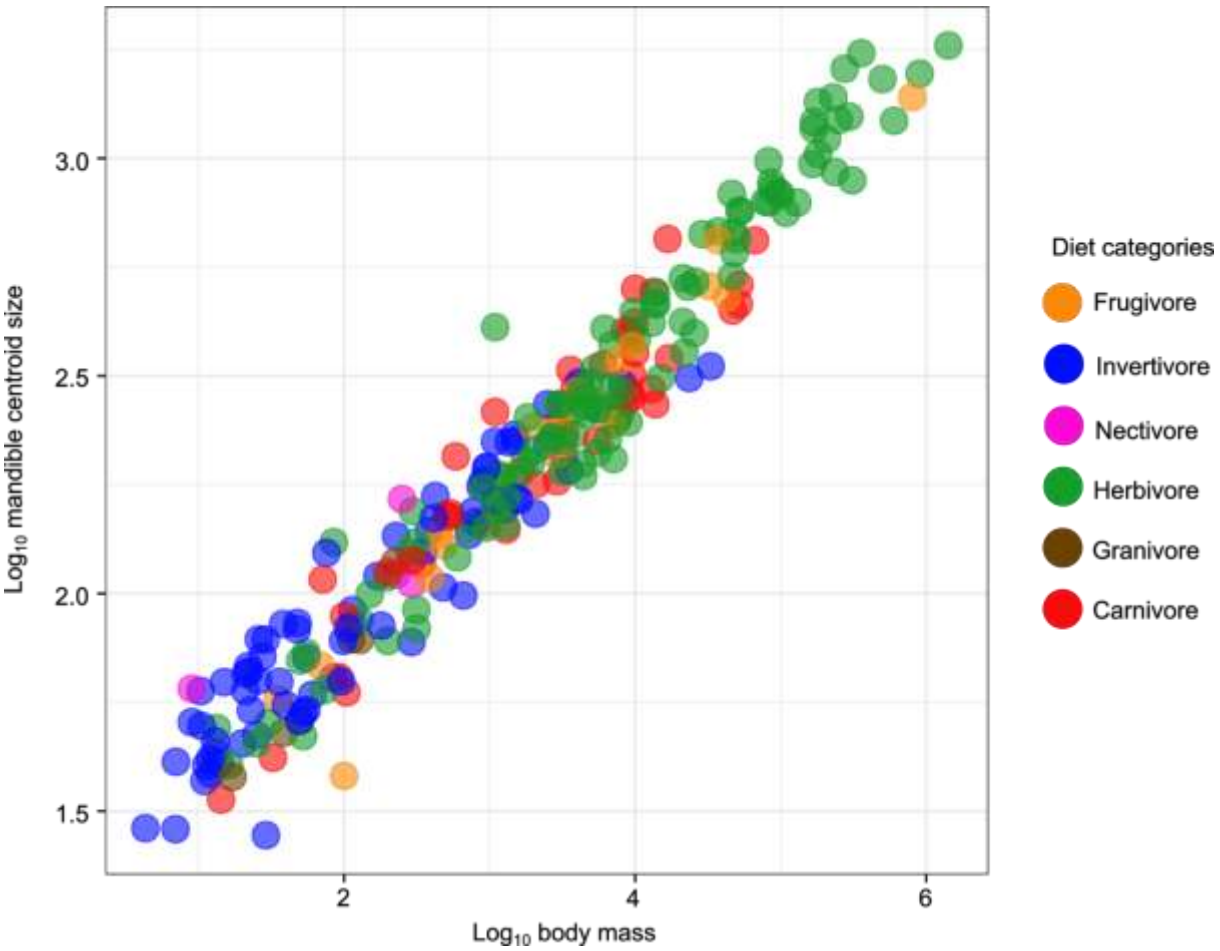


Figure 31: Scatterplot of $\log_{10}$ mandible centroid size and $\log_{10}$ body mass.

Frugivory and carnivory have significant partial effects on $\log_{10}$ mandible centroid size (Table 8). The model, Size ~ BM + Frugivory, explained 80.59% of the variation in $\log_{10}$ mandible centroid size and the coefficient (-0.05) indicates that frugivorous animals have smaller $\log_{10}$ mandible centroid sizes than what was expected given their $\log_{10}$ body mass (Size ~ BM + Frugivory, Table 8). This model has a cumulative model weight of 11% and ranks fourth-best amongst other relationships considered (Table 8).

The relationship that explained the most variation in $\log_{10}$ mandible centroid size assessed the interaction effect that $\log_{10}$ body mass has with frugivory (Size ~ BM * Frugivory). Frugivores have different $\log_{10}$ mandible centroid size allometry patterns relative to non-frugivores, and this relationship explained 80.93% of the variation in the model (Size ~ BM * Frugivory, R^2; Table 8). The associated AIC

and AIC weight values indicate that this is the best fitting model as it carries 41% of the cumulative model weight and has the lowest AIC score (Table 8).

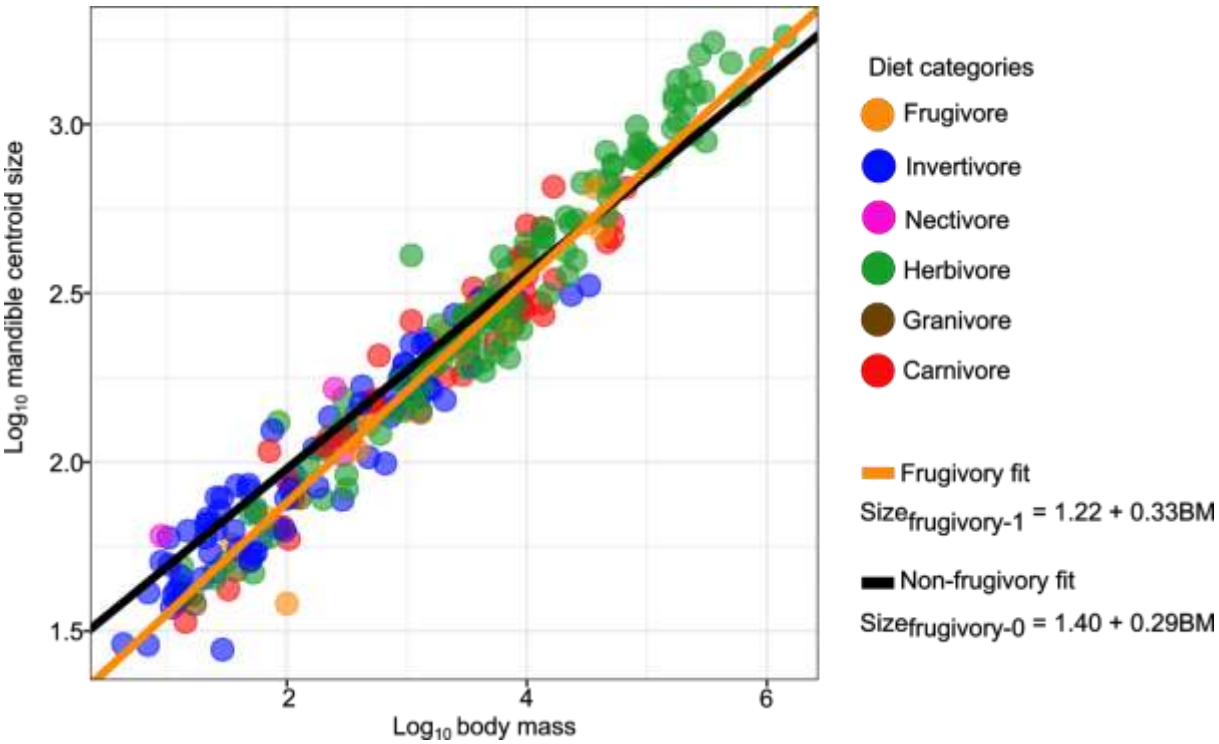


Figure 32: Scatterplot of $\log_{10}$ mandible centroid size and $\log_{10}$ body mass, illustrating the interaction that $\log_{10}$ body mass with frugivory (frugivory fit), relative to non-frugivorous mammals (non-frugivory fit).

According to the Size ~ BM * Frugivory model, at a body mass of 1g, a frugivore will have a $\log_{10}$ mandible centroid size 0.18 times smaller than that of a non-frugivore. However, with increasing body mass, a frugivore's $\log_{10}$ mandible centroid size will increase 0.04 times faster than non-frugivores. This means that at smaller body masses (less than 1,000g), frugivores tend to have relatively smaller mandible sizes and at larger body masses (more than 1,000g), frugivores tend to have mandible sizes that are relatively larger than non-frugivores (Figure 32).

The interaction that granivory has with $\log_{10}$ body mass significantly explains the variation in $\log_{10}$ mandible centroid sizes, and this accounts for 80.56% of the variation in mandible centroid sizes. This indicates that the $\log_{10}$ mandible centroid size allometry patterns amongst granivores are different from those of non-

granivores (Size ~ BM * Granivory, Table 8). This model has a cumulative model weight of 3% and ranks fifth-best amongst other relationships considered.

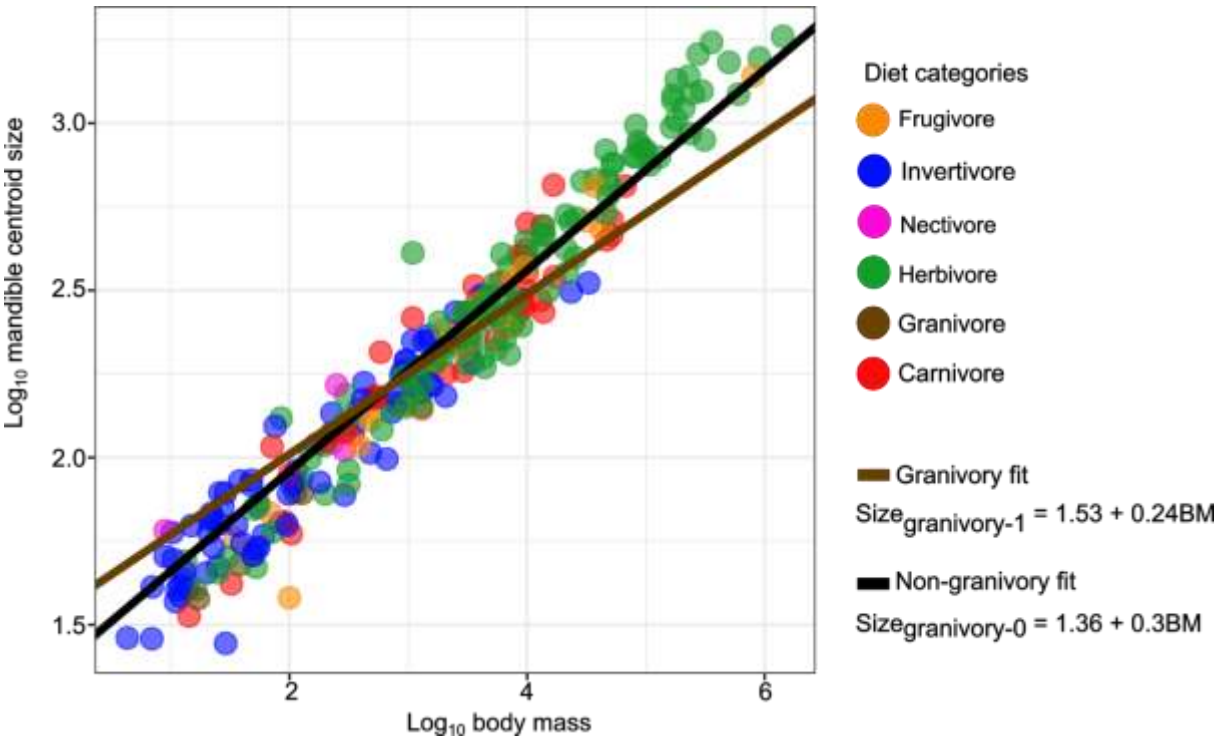


Figure 33: Scatterplot of log_{10} mandible centroid size and log_{10} body mass, illustrating the interaction that log_{10} body mass has with granivory (granivory fit), relative to non-granivorous mammals (non-granivory fit).

According to the Size ~ BM * Granivory model, at a body mass of 1g, a granivore will have a log_{10} mandible centroid size 0.17 times larger than a non-granivore. However, with increasing body mass, a granivore's log_{10} mandible centroid size will increase 0.06 times slower than non-granivores. This means that at smaller body masses (less than 1,000g), granivores tend to have relatively larger mandible sizes and at larger body masses (more than 1,000g), granivores tend to have mandible sizes that are relatively larger than non-granivores (Figure 33).

Carnivory, invertivory, nectivory, and herbivory all have non-significant interaction effects with body mass, this means animals within these dietary categories have $\log_{10}$ mandible centroid size allometry patterns which are congruent with what is expected given their body mass.

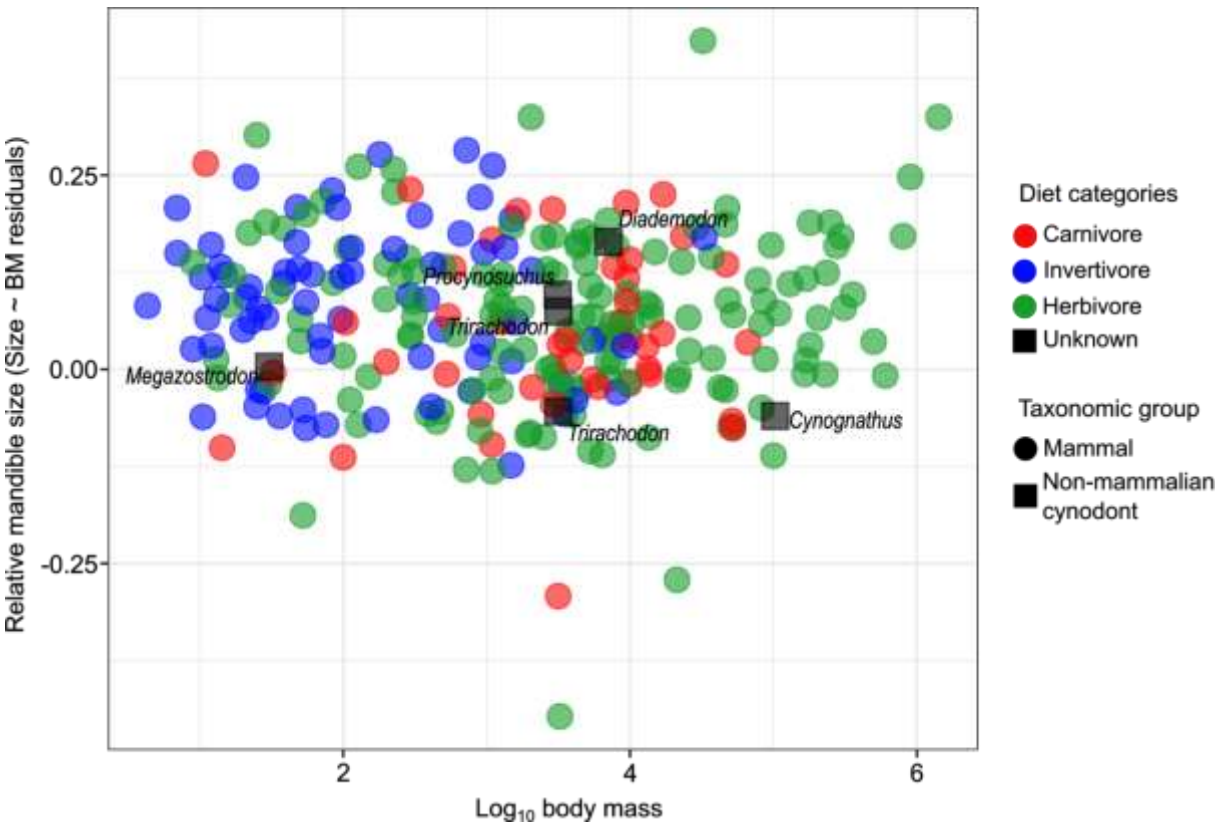


Figure 34: Scatterplot of relative mandible size (Size ~ BM residuals) and $\log_{10}$ body mass amongst mammals and non-mammalian cynodonts. Relative mandible size represents the variation in $\log_{10}$ mandible centroid size not explained by $\log_{10}$ body mass.

Amongst mammals within major dietary categories (Figure 34), invertivores have a relatively narrow range of $\log_{10}$ body masses and most invertivores are generally below 1,000g (Figure 34). Mammalian herbivores more frequently occupy size classes above 10,000g (Figure 34). Mammalian carnivores have an intermediate range of body masses ranging between 10g and 79,432g (Figure 34). Larger relative mandible sizes (positive residuals) are more common than smaller relative mandible sizes (negative residuals) amongst all dietary categories (Figure 34), and major dietary categories appear to be evenly distributed amongst relative mandible sizes (Figure 34).

12.2.2 pDFA: mandible size

13.2.2.1 pDFA: considering only mandible size

The median success rate of predicting an animal's diet (herbivore, carnivore or invertivore) using log_{10} body mass and the residual variation in mandible centroid size is 53% (P5=46, P95= 60). This is approximately 28.8% better than randomly guessing the diet (error rate of 66% under guesswork).

Table 9: Confusion table for pDFAs which estimated diet using log_{10} mandible centroid size residuals and log_{10} body mass. Note differences in the median, 5th (P5) percentile and 95th (P95) percentile counts per dietary category.

Predicted diet (pDFA)	**True diet**		
	Carnivore	Herbivore	Invertivore
Carnivore	6 (P5=1, P95=12)	3 (P5=0, P95=7)	3 (P5=0, P95=6)
Median %	20	10%	10%
Herbivore	16 (P5=12, P95=22)	19 (P5=13, P95=23)	4 (P5=1, P95=8)
Median %	53.33%	63.33%	13.33%
Invertivore	7 (P5=5, P95=10)	8 (P5=4, P95=12)	23 (P5=20, P95=25)
Median %	23.33%	26.67%	76.67%
Median % correct	20%	63.33%	76.67%

Amongst the major dietary categories, carnivores were misclassified the most, as an average 80% of the carnivorous mammals sampled were misclassified as invertivores or herbivores (Table 9). Amongst carnivorous mammals correctly classified those associated with the highest posterior probabilities have body masses under 10,000g, these included the Asian palm civet (*Paradoxurus hermaphroditus,* $PP_{carnivore}$= 0.50) and the bush dog (*Speothos venaticus,* $PP_{carnivore}$= 0.40). Although these associated posterior probabilities are the highest amongst those correctly classified, they are notably only low-to-medium values ($PP_{carnivore}$=0.40—0.50).

Carnivores were more frequently misclassified as herbivores (Table 9). This included medium to large sized carnivores (1,000g—66,000g) from Carnivora and Dasyuromorphia such as the Angolan genet (*Genetta angolensis*, $PP_{herbivore}$= 0.57), Tasmanian devil (*Sarcophilus harrisii*, $PP_{herbivore}$= 0.61), leopard *(Panthera*

pardus, $PP_{herbivore}$= 0.49), and the recently extinct thylacine (*Thylacinus cynocephalus*, $PP_{herbivore}$= 0.62). The carnivores misclassified as herbivores which are associated with the highest posterior probabilities are large-bodied species with larger relative mandible sizes such as the wolverine (*Gulo gulo*, $PP_{herbivore}$= 0.72), Tasmanian devil (*Sarcophilus harrissii*, $PP_{herbivore}$= 0.63) and the cheetah (*Acinonyx jubatus*, $PP_{herbivore}$= 0.62).

Small-bodied (10g—1,600g) carnivores from Didelphimorphia, Carnivora and Soricidae were misclassified as invertivorous, this included taxa such as the western quoll (*Dasyurus hallucatus*, $PP_{invertivore}$= 0.40), Eurasian water shrew (*Neomys fodiens*, $PP_{invertivore}$= 0.87), and the least weasel (*Mustela nivalis*, $PP_{invertivore}$= 0.66). The Cameroon scaly-tail (*Zenkerella insignis*, $PP_{invertivore}$= 0.54), a potentially carnivorous cryptic rodent, was also misclassified as an invertivore. Amongst carnivores misclassified as invertivores, those associated with the highest posterior probabilities all have body sizes below 100g, this included the crest-tailed mulgara (*Dasycercus cristicauda*, $PP_{invertivore}$= 0.70), piebald shrew (*Diplomesodon pulchellum*, $PP_{invertivore}$= 0.85) and the Eurasian water shrew (*Neomys fodiens*, $PP_{invertivore}$= 0.87).

On average, only 36.67% of the herbivorous mammals sampled were misclassified as carnivores or invertivores. Amongst herbivorous mammals correctly classified those associated with the highest posterior probabilities are large-bodied and have a body mass higher than 100,000g; this included species such as the hippopotamus (*Hippopotamus amphibius,* $PP_{herbivore}$= 0.89) and the horse (*Equus caballus,* $PP_{herbivore}$= 0.76).

Small-bodied (less than 300g) herbivores were more frequently misclassified as invertivores (Table 9), these were mostly rodents and some marsupials such as the agile gracile possum (*Gracilinanus agilis*, $PP_{invertivore}$=0.77), western pygmy possum (*Cercartetus concinnus*, $PP_{invertivore}$=0.75) and Derby's woolly opossum (*Caluromys derbianus*, $PP_{invertivore}$=0.43). Amongst herbivores misclassified as invertivores, those associated with the highest posterior probabilities were small-bodied rodents and marsupials with larger relative mandible sizes such as the fawn hopping mouse (*Notomys cervinus*, $PP_{invetivore}$=0.70), grey dwarf hamster (*Cricetulus migratorius*, $PP_{invertivore}$=0.73), western pygmy possum (*Cercartetus*

concinnus, $PP_{invertivore}$=0.75) and the agile gracile possum (*Gracilinanus agilis*, $PP_{invertivore}$=0.77).

The herbivores frequently misclassified as carnivores all have body masses between 500g and 50,000g, this included rodents, primates, marsupials, artiodactyls and carnivorans such as such as the African brush-tailed porcupine (*Aetherurus africanus*, $PP_{carnivore}$= 0.47), common ringtail possum (*Pseudocheirus peregrinus*, $PP_{carnivore}$= 0.43), southern pudu (*Pudu pudu*, $PP_{carnivore}$= 0.37) and the white-nosed coati (*Nasua narica*, $PP_{carnivore}$= 0.45). Amongst herbivores misclassified as carnivores, those associated with the highest posterior probabilities have smaller relative mandible sizes and medium to large body sizes such as the southern pudu (*Pudu pudu*, $PP_{carnivore}$= 0.50), Indian bandicoot rat (*Bandicota indica,* $PP_{carnivore}$= 0.51) and the fallow deer (*Dama dama,* $PP_{carnivore}$=0.57). Although these associated posterior probabilities are the highest amongst herbivores misclassified as carnivores, they are notably only medium values ($PP_{carnivore}$=0.50—0.57).

Invertivores were misclassified the least, and on average only 23.33% of the invertivorous mammals sampled were misclassified as carnivores or herbivores. Amongst invertivorous mammals correctly classified those associated with the highest posterior probabilities had body masses below 100g, this included the Abderdare mole shrew (*Surdisorex norae,* $PP_{invertivore}$= 0.82) and the large-eared tenrec (*Geogale aurita,* $PP_{invertivore}$= 0.80).

Invertivores were more frequently misclassified as carnivores (Table 9), these included relatively larger members of Carnivora such as the aardwolf (*Proteles cristata,* $PP_{carnivore}$=0.51) and the bat-eared fox (*Otocyon megalotis,* $PP_{carnivore}$= 0.44); as well as other large-bodied species that feed on aquatic invertebrates such as the Asian small-clawed otter (*Aonyx cinerea,* $PP_{carnivore}$= 0.45) and the platypus (*Ornithorhynchus anatinus*, $PP_{carnivore}$=0.47). Marsupials such as the water opossum (*Chironectes minimus,* $PP_{carnivore}$=0.38) and the striped possum (*Dactylopsila trivargata*, $PP_{carnivore}$= 0.42) were also misclassified as carnivores. Amongst invertivores misclassified as carnivores, those associated with the highest posterior probabilities are large-bodied and have smaller relative mandible sizes such as the platypus ($PP_{carnivore}$=0.47) and the aardwolf ($PP_{carnivore}$= 0.51).

Although these associated posterior probabilities are the highest amongst invertivore misclassified as carnivores, they are notably only low-to-medium values ($PP_{carnivore}$=0.47—0.51).

The invertivorous mammals that were misclassified as herbivores have body masses between 400g and 32,000g, and these included marsupials and Pholidota members such as the greater bilby (*Macrotis lagotis,* $PP_{herbivore}$=0.42) and the tree pangolin (*Phataginus tricuspis,* $PP_{herbivore}$=0.48). Afrotherian invertivores such as the golden-rumped elephant shrew (*Rhynchochyon petersi,* $PP_{herbivore}$=0.38) and the giant otter shrew (*Potamogale velox,* $PP_{herbivore}$= 0.37) were also misclassified as herbivores. Amongst invertivores misclassified as herbivores, those associated with the highest posterior probabilities are Pholidota members such as the tree pangolin ($PP_{herbivore}$=0.48) and the giant pangolin (*Smutstia gigantea,* $PP_{herbivore}$=0.62) which have relatively large body sizes and large relative mandible sizes. Apart from the giant pangolin (*Smutstia gigantea,* $PP_{herbivore}$=0.62), the posterior probabilities associated with the invertivores misclassified as herbivores are notably only low values ($PP_{herbivore}$=0.37—0.48).

Table 10: The estimated diets of non-mammalian cynodont species associated with pDFAs that used log_{10} mandible centroid size residuals and log_{10} body mass. Note differences in median, 5th (P5) percentile and 95th percentile (P95) of posterior probabilities.

Taxon	Expected diet	Predicted diet	Posterior probability
Cynognathus crateronotus	Carnivore	Herbivore	0.89 (P5=0.56, P95=**0.97**)
Diademodon tetragonus	Herbivore	Herbivore	0.76 (P5=0.56, P95=0.89)
Megazostrodon rudnerae	Invertivore	Invertivore	**0.90** (P5=0.79, P95=**0.93**)
Procynosuchus delaharpeae	Invertivore	Herbivore	0.89 (P5=0.68, P95=**0.97**)
Trirachodon berryi	Herbivore	Herbivore	0.68 (P5=0.53, P95=0.82)
Trirachodon sp.	Herbivore	Herbivore	0.63 (P5=0.33, P95=0.83)

Most non-mammalian cynodont species were estimated as herbivores when using relative mandible size (residuals) and body mass (Table 10), these species have approximated body masses ranging from 3,090g and 101,610g (Figure 34).

Cynognathus, Diademodon, Procynosuchus and Trirachodon are estimated as herbivorous when using residual mandible size and body mass (Table 10). The posterior probability associated with these estimates are medium-to-high values ($PP_{herbivore}$ = 0.63 —0.89). However, this only coincides with the hypothesized diet of *Diademodon (*$PP_{herbivore}$= 0.76*).*

Megazostrodon has an approximated body mass of 30g (Figure 34, Table D2) and was estimated as an invertivore; this coincides with the hypothesized diet and is associated with a high posterior probability ($PP_{invertivore}$=0.90).

13.2.2.2 pDFA: considering mandible size and shape

The median success rate of predicting an animal's diet using shape and size is 80% (P5=74, P95= 85). This is approximately 69.7% better than randomly guessing the diet (compared to an error rate of 66% under guesswork), and approximately 20% better than using just mandible shape (25% error rate using only mandibular shape). The proportion of correct classifications did not vary much amongst groups (Table 11).

Table 11: Confusion table for pDFAs which estimated diet using mandible shape (first seven PCA axes), log_{10} mandible centroid size residuals and log_{10} body mass. Note differences in the median, 5th (P5) percentile and 95th (P95) percentile counts per dietary category.

Predicted diet (pDFA)	**True diet**		
	Carnivore	Herbivore	Invertivore
Carnivore	23 (P5=21, P95=26)	4 (P5=1, P95=6)	4 (P5=2, P95=7)
Median %	76.67%	13.34%	13.33%
Herbivore	1 (P5=0, P95=2)	25 (P5=22, P95=28)	2 (P5=0, P95=4)
Median %	3.33%	83.33%	6.67%
Invertivore	6 (P5=4, P95=8)	1 (P5=0, P95=3)	24 (P5=21, P95=26)
Median %	20%	3.33%	80%
Median % correct	76.67%	83.33%	80%

Relative to using just mandible shape, also considering size improved the dietary predictions amongst invertivores by 40% (Table 6, Table 11). An average of only

20% of the invertivorous mammals sampled were misclassified as carnivores or herbivores (Table 11). Amongst invertivorous mammals correctly classified those associated with the highest posterior probabilities are small-bodied species such as the star-nosed mole (*Condylura cristata,* $PP_{invertivore}$= 0.98) and the southern marsupial mole (*Notoryctes typhlops,* $PP_{invertivore}$= 0.97), which have long mandibles with an anteriorly low mandible body and a prominent angular process (Figure 28, A).

Invertivores were misclassified as carnivores more frequently, these were mostly invertivores larger than 750g from Afrosoricida, Carnivora or Soricidae such as the giant otter shrew (*Potamogale velox* $PP_{carnivore}$= 0.71), common raccoon *(Procyon lotor,* $PP_{carnivore}$= 0.84), and the Hispaniolan solenodon (*Solenodon paradoxurus,* $PP_{carnivore}$= 0.43). The striped possum (*Dactylopsila trivirgata,* $PP_{carnivore}$= 0.78), a marsupial diprotodontid, was also misclassified as carnivore. Amongst invertivores misclassified as carnivores, those associated with the highest posterior probabilities are large-bodied species which have mandibles with a relatively reduced angular process such as the aardwolf (*Proteles cristata*, $PP_{carnivore}$= 0.77), northern glider ($PP_{carnivore}$= 0.78), raccoon ($PP_{carnivore}$= 0.84), and the Asian small-clawed otter (*Aonyx cinerea*, $PP_{carnivore}$= 0.95).

Invertivores misclassified as herbivores were only small-bodied (25g—479g) rodents, such as the rakali (*Hydromys chrysogaster*, $PP_{herbivore}$= 0.87) and the northern grasshopper mouse (*Onychomys torridus*, $PP_{herbivore}$= 0.55). These species have relatively short mandibles with a tall coronoid process and a ventrally expanded angular process.

Relative to using just mandible shape, also considering size did not improve or worsen the dietary predictions amongst herbivores (Table 6, Table 11). An average 16.67% of the herbivorous mammals sampled were misclassified as carnivores or invertivores (Table 11). Amongst herbivorous mammals correctly classified those associated with the highest posterior probabilities have a posteriorly tall mandible body and a low coronoid process (Figure 27, A) such as the capybara (*Hydrochoerus hydrochaerus,* $PP_{herbivore}$ =0.99*)* and the giraffe (*Giraffa camelopardalis,* $PP_{herbivore}$ =0.99*).* Notably, small bodied species such as the

gymnure (*Notomys cervinus,* $PP_{herbivore}$= 0.87) were also correctly classified with high confidence levels.

Herbivores were more frequently misclassified as carnivores, these were mostly large-bodied primates, diprotodontians and herbivorous Carnivora members such as the Hamadryas baboon (*Papio hamadryas*, $PP_{carnivore}$= 0.74), long-nosed potoroo (*Potorous tridactylus*, $PP_{carnivore}$= 0.77), and the red panda (*Ailurus fulgens*, $PP_{carnivore}$= 0.65). The black-shouldered opossum (*Caluromysiops irrupta*, $PP_{carnivore}$= 0.63), a Didelphimorphia member, was also misclassified as a carnivore. Amongst herbivores misclassified as carnivores, those associated with highest posterior probabilities have mandibles with a tall coronoid process, such as the brown bear (*Ursus arctos*, $PP_{carnivore}$= 0.81), Allen's olingo (*Bassaricyon alleni*, $PP_{carnivore}$= 0.77) and the long-nosed potoroo ($PP_{carnivore}$= 0.77).

Herbivores misclassified as invertivores included Derby's woolly opossum (*Caluromys derbianus*, $PP_{invertivore}$= 0.68), grey dwarf hamster (*Cricetulus migratorius*, $PP_{invertivore}$= 0.75), black lemur (*Eulemur macaco* $PP_{invertivore}$= 0.51) and the central African oyan (*Poiana richardsoni*, $PP_{invertivore}$= 0.49). Amongst these species, those associated with relatively higher posterior probabilities are small-bodied (32g—316g). This included the grey dwarf hamster ($PP_{invertivore}$= 0.75) and Derby's woolly opossum ($PP_{invertivore}$= 0.68).

Relative to using just mandible shape, also considering size did not improve or worsen the dietary predictions amongst carnivores (Table 6, Table 11). An average 23.33% of the carnivorous mammals sampled were misclassified as herbivores or invertivores (Table 11). Amongst carnivorous mammals correctly classified those associated with the highest posterior probabilities are species larger than 1,000g with mandibular shapes characterized by a tall coronoid process and a reduced angular process (Figure 27, A). This included the cheetah (*Acinonyx jubatus,* $PP_{carnivore}$= 0.97) and the leopard *(Panthera pardus,* $PP_{carnivore}$= 0.97).

Carnivores with relatively smaller body masses ranging from 11g to 2,884g were frequently misclassified as invertivores. This included many dasyuromorphs and soricid species such as the crest-tailed mulgara (*Dasycercus cristicauda*, $PP_{invertivore}$= 0.77), and the Eurasian water shrew (*Neomys fodiens*, $PP_{invertivore}$= 0.90). This also included Carnivora members such as the Angolan genet (*Genetta*

genetta, $PP_{invertivore}$= 0.67) and the small Indian civet (*Viverricula indica* $PP_{invertivore}$= 0.60), as well as the greater cane rat (*Setifer setosus*, $PP_{invertivore}$= 0.58), an afrosoricid. Amongst carnivores misclassified as invertivores, those associated with the highest posterior probabilities are dasyuromorphs and soricids such as the western quoll (*Dasyurus hallucatus*, $PP_{invertivore}$= 0.75), crest-tailed mulgara ($PP_{invertivore}$= 0.77), eastern quoll (*Dasyurus viverrinus*, $PP_{invertivore}$= 0.79), piebald shrew (*Diplomesodon pulchellum*, $PP_{invertivore}$= 0.78) and the Eurasian water shrew (*Neomys fodiens*, $PP_{invertivore}$= 0.90). These species all have a prominent angular process.

The Cameroon scaly-tail *(Zenkerella insignis,* $PP_{herbivore}$= 0.85), a potentially carnivorous cryptic rodent, was most frequently misclassified as an herbivore. The Cameroon scaly-tail is small-bodied (200g) and has a short jaw, with a prominent angular process (Figure 28, C).

Table 12: The estimated diets of non-mammalian cynodont species associated with the pDFAs that used mandible shape (first seven PC axes), log_{10} mandible centroid size residuals and log_{10} body mass. Note differences in median, 5th (P5) percentile and 95th percentile (P95) of posterior probabilities.

Taxon	Expected diet	Predicted diet	Posterior probability
Cynognathus crateronotus	Carnivore	Herbivore	**0.99** (P5=**0.99**, P95=**1.00**)
Diademodon tetragonus	Herbivore	Herbivore	0.84 (P5=0.01, P95=**0.99**)
Megazostrodon rudnerae	Invertivore	Invertivore	**0.99** (P5=0.84, P95=**0.99**)
Procynosuchus delaharpeae	Invertivore	Carnivore	**0.99** (P5=**0.96**, P95=**1.00**)
Trirachodon berryi	Herbivore	Carnivore	**0.99** (P5=0.71, P95=**0.99**)
Trirachodon sp.	Herbivore	Carnivore	**0.99** (P5=0.25, P95=**0.99**)

The dietary estimates made using both mandible shape and relative mandible size (Table 12) are similar to the dietary estimates obtained using only mandible shape (Table 10).

The estimates only differ for *Cynognathus*, which is now estimated as herbivorous. This does not coincide with the hypothesized diet. *Cynognathus* is

large-bodied (Figure 34, Table D2), and the associated posterior probability is high despite the mandibular shape most resembling carnivorous mammals (Table 10, Figure 30).

The posterior probabilities associated with estimates obtained using mandible shape together with size (PP= 0.84—0.99; Table 12) are generally much higher than those obtained when using only shape data (PP= 0.46—0.90; Table 7).

12.3 Dental complexity (OPCR) and its association with diet

12.3.1 Average dental complexity (OPCRavg): distribution and trends

13.3.1.1 OPCRavg: box and whisker plots

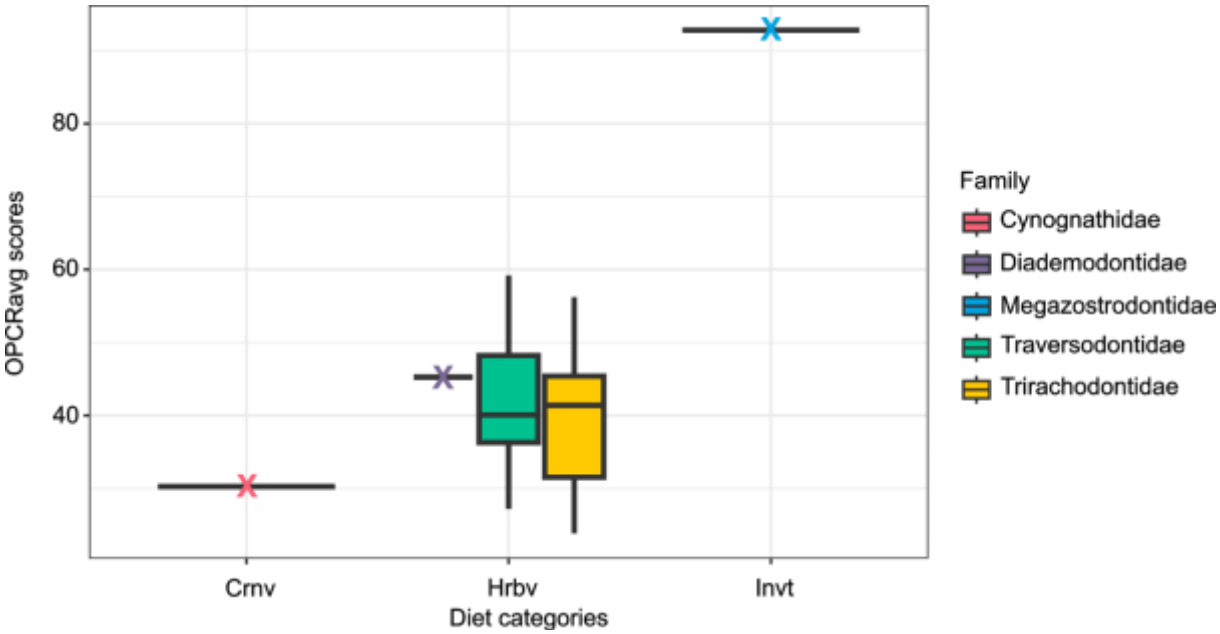


Figure 35: Box and whisker plots showing the distribution of average OCR scores (OPCRavg) amongst non-mammalian cynodonts within qualitatively inferred diet categories. Crnv= carnivore, Hrbv= herbivore, Invt= invertivore. 'X' marks on plot annotate the single estimates for Cyngonathidae (pink), Diademodontidae (purple), and Megazostrodontidae (blue).

The only hypothesized carnivorous non-mammalian cynodont sampled is *Cynognathus,* which has an OPCRavg score of 30.25, this is relatively lower than most other non-mammalian cynodonts sampled (Figure 35).

Amongst hypothesized herbivorous non-mammalian cynodonts sampled, *Diademodon* has an OCPRavg score of 45.35; traversodontids have a median OPCRavg score of 40.06 (interquartile range: 36.37—48.20, range: 27.12—59.18) and trirachodontids have a median OPCRavg score of 41.37 (interquartile range: 31.52—45.37, range: 23.81—56.25). Non-mammalian cynodonts qualitatively inferred as herbivorous generally have OPCRavg scores higher than those of *Cynognathus*, although there are some traversosdontids and trirachodontids with OPCRavg scores similar to those of *Cynognathus* (Figure 35).

The only hypothesized invertivorous non-mammalian cynodont sampled is *Megazostrodon,* which has an OCPRavg score 92.82, this is much higher than those of other non-mammalian cynodonts (Figure 35).

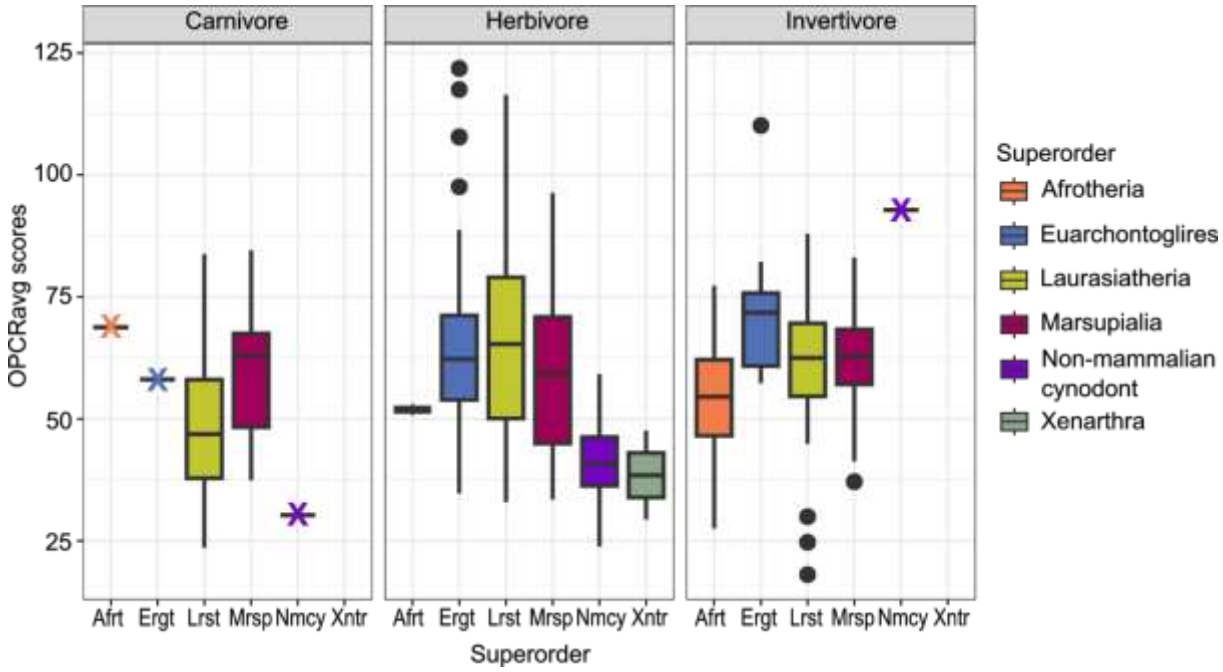


Figure 36: Box and whisker plots showing the distribution of average OPCR scores (OPCRavg) amongst major mammalian orders relative to non-mammalian cynodonts. Afrt= Afrotheria, Ergt= Euarchontoglires, Lrst= Laurasiatheria, Mrsp= Marsupialia, Nmcy= non-mammalian cynodonts, Xntr= Xenartha. 'X' marks on plot annotate the single estimates for Afrotheria (orange), Euarchontoglires (blue), and non-mammalian cynodonts (purple).

Amongst mammalian carnivores sampled (Figure 36), the only afrotherian carnivore sampled, the greater hedgehog tenrec (*Setifer setosus*), has an OPCRavg score of 68.76. The only Euarchtontoglire classified as a carnivore, the

potentially carnivorous Cameroon scaly-tail (*Zenkerella insignis*), has an OPCRavg score of 58.07. Laurasiatherian carnivores have a median OPCRavg score of 58 (interquartile range: 37.82—58.03, range: 23.57—83.76). Marsupial carnivores have a median OPCRavg score of 62.84 (interquartile range: 48.3—67.48, range: 37.37—84.57). Amongst mammalian carnivores, carnivorous laurasiatherians generally have much lower OPCRavg scores than species from other major mammalian groups (Figure 35). *Cynognathus,* the only hypothesized carnivorous non-mammalian cynodont, has an OPCRavg score of 30.25, which is in the lower range (bottom 50%) of OPCRavg scores for laurasiatherian carnivores. Notably, *Cynognathus* has an OPCRavg score much lower than those of carnivorous euarchontoglires, marsupials, and afrotherians.

Amongst mammalian herbivores (Figure 36), afrotherian herbivores have a median OPCRavg score of 51.87 (interquartile range: 51.25—52.50, range: 50.62—53.13). Herbivorous euarchontoglires have a median OPCRavg score of 62.26 (interquartile range: 53.88—71.19, range: 34.69—88.75). Laurasiatherian herbivores have a median OPCRavg score of 65.31 (50.06—79.01, range: 32.91—116.44). Marsupial herbivores have a median OPCRavg score of 59.37 (interquartile range: 44.94—70.87, range: 33.44—96.31). Xenarthran herbivores have a median OPCRavg score of 38.44 (interquartile range: 33.88—43, range: 29.32—47.57). Amongst mammalian herbivores, laurasiatherian herbivores have the widest range of OPCRavg scores, whereas other major mammalian groups have more limited distributions with lower maximum OPCRavg scores (Figure 36). Afrotherian and xenarthran herbivores generally have much lower OPCRavg scores. The distribution of OPCRavg scores amongst herbivorous euarchontoglires and marsupials are relatively similar to those of laurasiatherians, although these groups have relatively lower OPCRavg scores. Herbivorous non-mammalian cynodonts have median OPCRavg score of 40.81 (interquartile range: 36.25—46.25, range: 23.81—59.18), and this distribution is within the lower range (bottom 50%) of herbivorous euarchontoglires, laurasiatherian and marsupial OPCRavg scores. Herbivorous non-mammalian cynodonts have a wider range of OPCRavg scores than those of herbivorous afrotherians and xenarthrans.

Amongst mammalian invertivores (Figure 36), afrotherian invertivores have a median OPCRavg score of 54.50 (interquartile range: 46.53—62.13, range:

27.50—77.31). Invertivorous euarchontoglires have a median OPCRavg score of 71.72 (interquartile range: 60.81—75.76, range: 57.31—82.19). Laurasiatherian invertivores have a median OPCRavg score of 62.48 (interquartile range: 54.61—69.60, range: 44.87—87.94). Marsupial invertivores have a median OPCRavg score of 62.75 (interquartile range: 57.06—68.33, range: 41.25—83.07). Amongst mammalian invertivores, invertivorous afrotherians have the widest range of OPCRavg scores and these are relatively lower than those of other invertivorous mammals. Invertivorous euarchontoglires have relatively higher OPCRavg scores than those of other invertivorous mammals. The distribution of OPCRavg scores amongst laurasiatherian and marsupial invertivores are similar. The only invertivorous non-mammalian cynodont sampled, *Megazostrodon*, has an OPCRavg score of 92.82, and this is much higher on average than the OPCRavg scores of invertivorous mammals (Figure 36).

When the traditional diet categories were used to visualize average dental complexity scores amongst mammals (Figure 37), carnivorous mammal species generally have the lowest OPCRavg scores, with a median OPCRavg score of 51.31 (interquartile range: 39.26—63.81; range: 23.57—84.57). Herbivorous mammal species generally have higher OPCRavg scores, with a median OPCRavg score of 62.26 (interquartile range:50.88—73; range: 29.32—100.25). Invertivorous mammal species have a median OPCRavg score of 61 (interquartile range:54.24—69.69; range:35.44—87.94). The distributions of OPCRavg scores amongst herbivores and invertivores are highly similar and only notably differ in range (Figure 37).

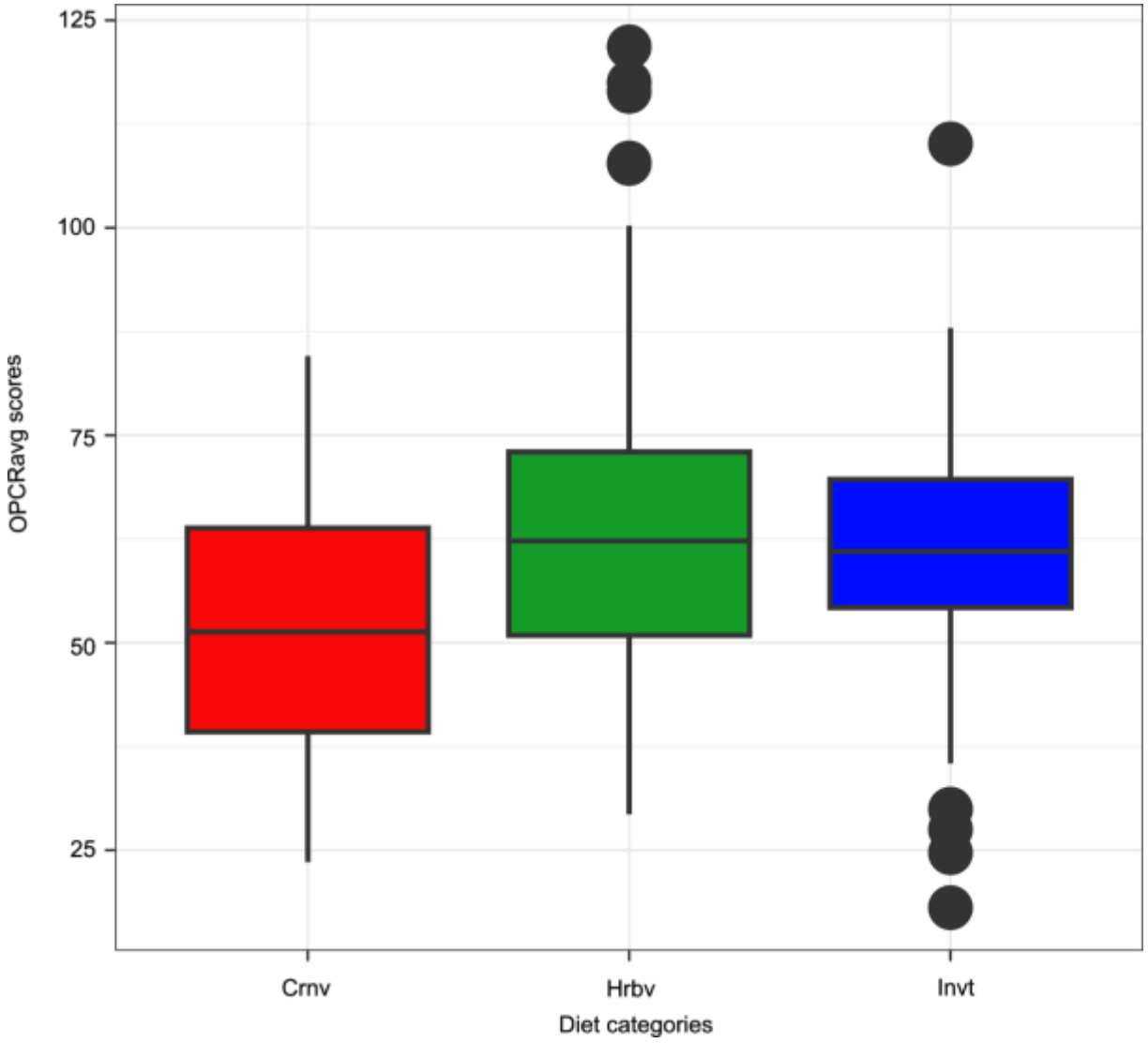


Figure 37: Box and whisker plots showing the distribution of average OPCR scores (OPCRavg) amongst mammal species within major diet categories. Crnv= carnivore, Hrbv= herbivore, Invt= invertivore.

When the finer diet categories (majority consumed) were used to visualize average dental complexity scores (Figure 38), frugivorous mammals have a median OPCRavg score of 61.5 (interquartile range: 51.56—67.1, range: 36.1—86.18). Invertivorous mammals have a median OPCRavg score of 61 (interquartile range: 53.44—69.5; range: 29.94—87.94). Nectivores have the most limited range of OPCRavg scores with a median OPCRavg score of 64.38 (interquartile range: 56.44—66.38; range: 48.5—68.38). Herbivores have the widest range of OPCRavg scores with a median OPCRavg score of 62.44

(interquartile range: 52.17 —75.49; range: 29.32—107.75). Granivores have a median OPCRavg score of 59.03 (interquartile range: 48.72—71.58; range: 42.41—82.68). Carnivores generally have the lowest OPCRavg scores, with a median OPCRavg score of 50 (interquartile range: 39.38—65.83; range:23.57—84.57). There are only minor differences in OPCRavg scores amongst different dietary groups and the interquartile ranges amongst dietary categories overlap (Figure 38).

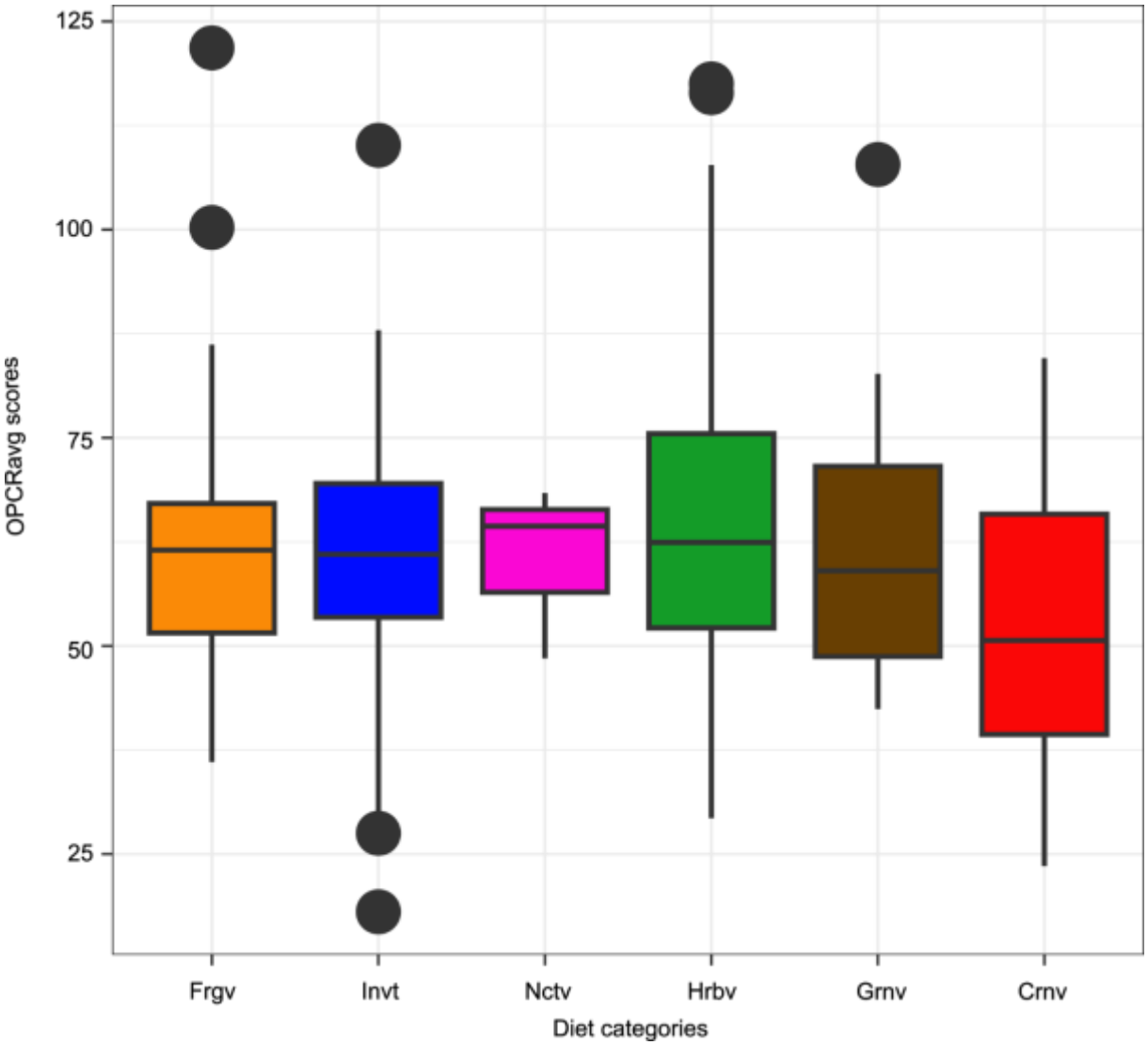


Figure 38: Box and whisker plots showing the distribution of average OPCR scores (OPCRavg) amongst mammal species within finer diet categories. Frgv= frugivore, Invt= invertivore, Nctv= nectivore, Hrbv= herbivore, Grnv= granivore, Crnv= carnivore.

13.3.1.2 OPCRavg: phylogenetic regressions (pgls)

Table 13: Phylogenetic regressions assessing the association that OPCRavg has with $\log_{10}$ body mass (BM), $\log_{10}$ mandible centroid size (Size) and dietary variables amongst mammal species (n=240).

Model	n	AIC	AIC w	R^2	p-value (model)	Variable	Coefficient	Std err	Pr(>|t|)
OPCRavg~BM*Granivory	240	2126.13	0.9950	0.082	**<0.001**	(Intercept)	66.10	25.68	0.011
						BM	-2.46	1.74	0.158
						Granivory	-50.28	14.68	**0.001**
						BM:Granivory	19.77	4.65	**<0.001**
OPCRavg~Granivory	240	2140.40	0.0008	0.010	0.128	(Intercept)	58.96	26.14	0.025
						Granivory	8.37	5.48	0.128
OPCRavg~Herbivory	240	2141.58	0.0004	0.005	0.284	(Intercept)	61.55	26.27	0.020
						Herbivory	-3.81	3.55	0.284
OPCRavg~Frugivory	240	2141.79	0.0004	0.004	0.331	(Intercept)	60.18	26.22	0.023
						Frugivory	-3.95	4.05	0.331
OPCRavg~BM+Granivory	240	2141.87	0.0004	0.012	0.242	(Intercept)	62.34	26.57	0.020
						BM	-1.29	1.78	0.467
						Granivory	7.89	5.53	0.155
OPCRavg~BM	240	2141.92	0.0004	0.003	0.367	(Intercept)	63.65	26.61	0.018
						BM	-1.60	1.77	0.367
OPCRavg~Carnivory	240	2141.94	0.0004	0.003	0.372	(Intercept)	58.99	26.22	0.025
						Carnivory	2.62	2.93	0.372
OPCRavg~Invertivory	240	2142.20	0.0003	0.002	0.462	(Intercept)	61.24	26.34	0.021
						Invertivory	-2.52	3.42	0.462
OPCRavg~Size	240	2142.49	0.0003	0.001	0.614	(Intercept)	65.25	28.59	0.023
						Size	-2.70	5.34	0.614
OPCRavg~BM+Carnivory	240	2142.68	0.0003	0.009	0.361	(Intercept)	64.08	26.60	0.017
						BM	-2.02	1.81	0.266
						Carnivory	3.31	2.99	0.269
OPCRavg~Nectivory	240	2142.74	0.0002	>0.001	0.959	(Intercept)	59.49	26.27	0.024
						Nectivory	0.63	12.23	0.959
OPCRavg~BM+Invertivory	240	2142.84	0.0002	0.008	0.391	(Intercept)	67.57	26.88	0.013

						BM	-2.14	1.84	0.248
						Invertivory	-3.69	3.57	0.302
OPCRavg~BM+Frugivory	240	2142.84	0.0002	0.008	0.391	(Intercept)	64.66	26.63	0.016
						BM	-1.71	1.77	0.335
						Frugivory	-4.19	4.05	0.302
OPCRavg~BM+Herbivory	240	2143.07	0.0002	0.007	0.437	(Intercept)	64.62	26.64	0.016
						BM	-1.29	1.80	0.476
						Herbivory	-3.32	3.62	0.359
OPCRavg~BM*Invertivory	240	2143.65	0.0002	0.013	0.384	(Intercept)	62.97	27.20	0.021
						BM	-1.17	2.05	0.567
						Invertivory	4.98	8.74	0.570
						BM:Invertivory	-2.87	2.65	0.279
OPCRavg~BM+Nectivory	240	2143.92	0.0001	0.003	0.665	(Intercept)	63.72	26.69	0.018
						BM	-1.61	1.79	0.368
						Nectivory	-0.81	12.34	0.947
OPCRavg~BM*Carnivory	240	2144.26	0.0001	0.010	0.486	(Intercept)	62.16	26.81	0.021
						BM	-1.37	2.07	0.509
						Carnivory	8.07	8.00	0.314
						BM:Carnivory	-1.42	2.21	0.522
OPCRavg~BM*Frugivory	240	2144.80	0.0001	0.008	0.591	(Intercept)	64.41	26.71	0.017
						BM	-1.63	1.82	0.371
						Frugivory	-1.99	12.12	0.870
						BM:Frugivory	-0.71	3.67	0.847
OPCRavg~BM*Herbivory	240	2145.01	0.0001	0.007	0.634	(Intercept)	63.75	26.93	0.019
						BM	-0.95	2.26	0.674
						Herbivory	-1.44	8.48	0.865
						BM:Herbivory	-0.55	2.24	0.806
OPCRavg~BM*Nectivory	240	2145.76	0.0001	0.004	0.808	(Intercept)	64.10	26.76	0.017
						BM	-1.73	1.81	0.341
						Nectivory	-22.80	56.64	0.688
						BM:Nectivory	9.63	24.20	0.691

The only relationship that significantly explained the variation in OPCRavg scores assessed the interaction effect that log_{10} body mass has with granivory (OPCRavg ~ BM * Granivory). Granivores have a different OPCRavg allometry pattern than non-granivores, and this relationship explained 8.2% of the variation in OPCRavg scores (OPCRavg ~ BM * Granivory, R^2). The associated AIC and AIC weight (AIC w) values indicate that the interaction effect between granivory and log_{10} body mass is the best-fitting model relative to the other evaluated relationships, as it carries 99.5% of the cumulative model weight and has the lowest AIC score (Table 13). However, the standard error associated with the granivory coefficient is particularly high (std err = 14.68) indicative of a high degree of uncertainty in the estimates of granivorous mammals (OPCRavg ~ BM * Granivory, Std err).

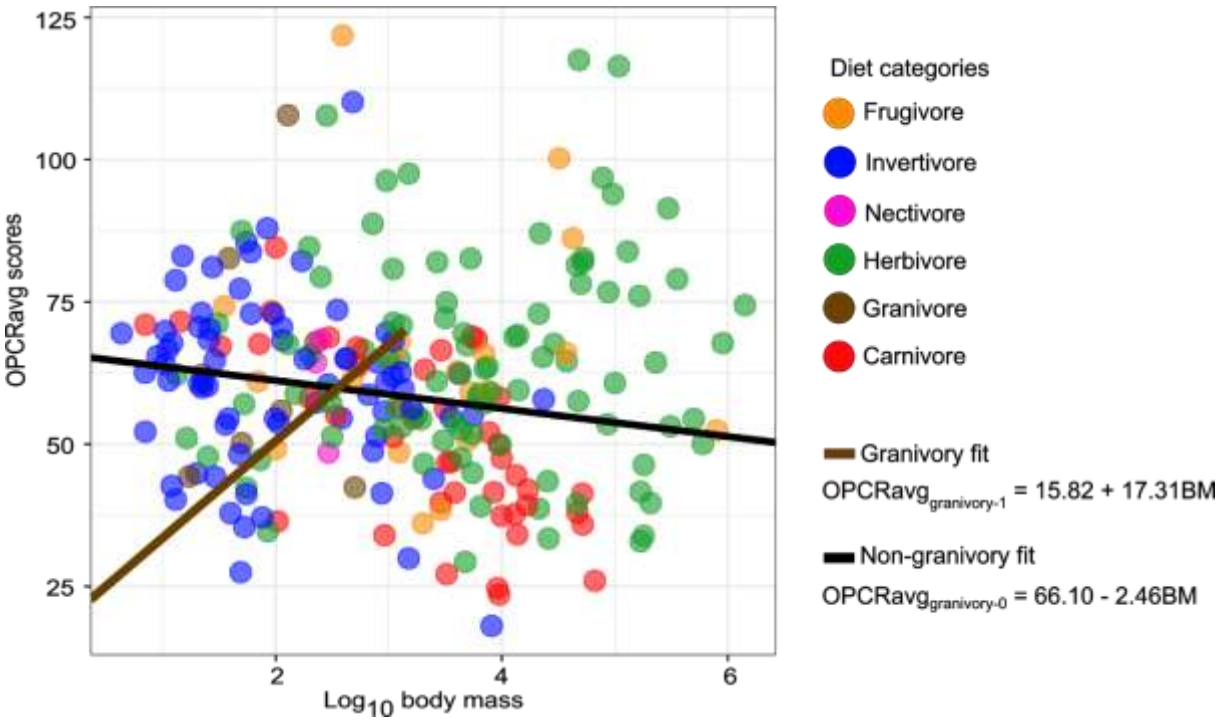


Figure 39: Scatterplot of average OPCR scores (OPCRavg) and log_{10} body mass, illustrating the interaction that log_{10} body mass has with granivory (granivory fit), relative to non-granivorous mammals (non-granivory fit). Note that granivorous mammals span a narrow range of body sizes, relative to non-granivorous mammals.

According to the OPCRavg ~ BM * Granivory model (Table 13), at a body mass of 1g, a granivore will have an OPCRavg score that is 50.28 times lower than non-granivores. However, with increasing body mass, a granivore's OPCRavg scores

increase 19.77 times faster than non-granivores. This means that at smaller body masses (less than 10,000g), granivores generally have less complex postcanine teeth (OPCRavg), and at larger body masses (more than 1,000g), granivores generally have more complex teeth relative to non-granivores (Figure 39).

The relationships that dietary variables, $\log_{10}$ body mass and $\log_{10}$ mandible centroid size have with OPCRavg are all non-significant (Table 13). Apart from granivory, dietary variables have non-significant interaction effects with $\log_{10}$ body mass.

12.3.2 Summed dental complexity (OPCRsum): distribution and trends

13.3.2.1 OPCRsum: box and whisker plots

The only hypothesized carnivorous non-mammalian cynodont sampled, *Cynognathus*, has an OPCRsum score of 60.5 (Figure 40). *Cynognathus* has a OPCRsum score that is relatively lower than most other non-mammalian cynodonts sampled (Figure 40).

Amongst hypothesized herbivorous non-mammalian cynodonts, *Diademodon* has an OPCRsum score of 90.5; traversodontids have a median OPCRsum score of 80.12 (interquartile range: 72.53—96.41, range: 40.75—118.36) and trirachodontids have a median OPCRsum score of 72.06 (interquartile range: 59.07—83.28, range: 47.62—92.49). Herbivorous non-mammalian cynodonts generally have OPCRsum scores higher than those of *Cynognathus*, however there are some traversosdontids and trirachodontids with OPCRsum scores similar to those of *Cynognathus* (Figure 40).

The only hypothesized invertivorous non-mammalian cynodont sampled, *Megazostrodon*, has an OPCRsum score 185.64. *Megazostrodon's* OPCRsum score is much higher than those of other non-mammalian cynodonts (Figure 40).

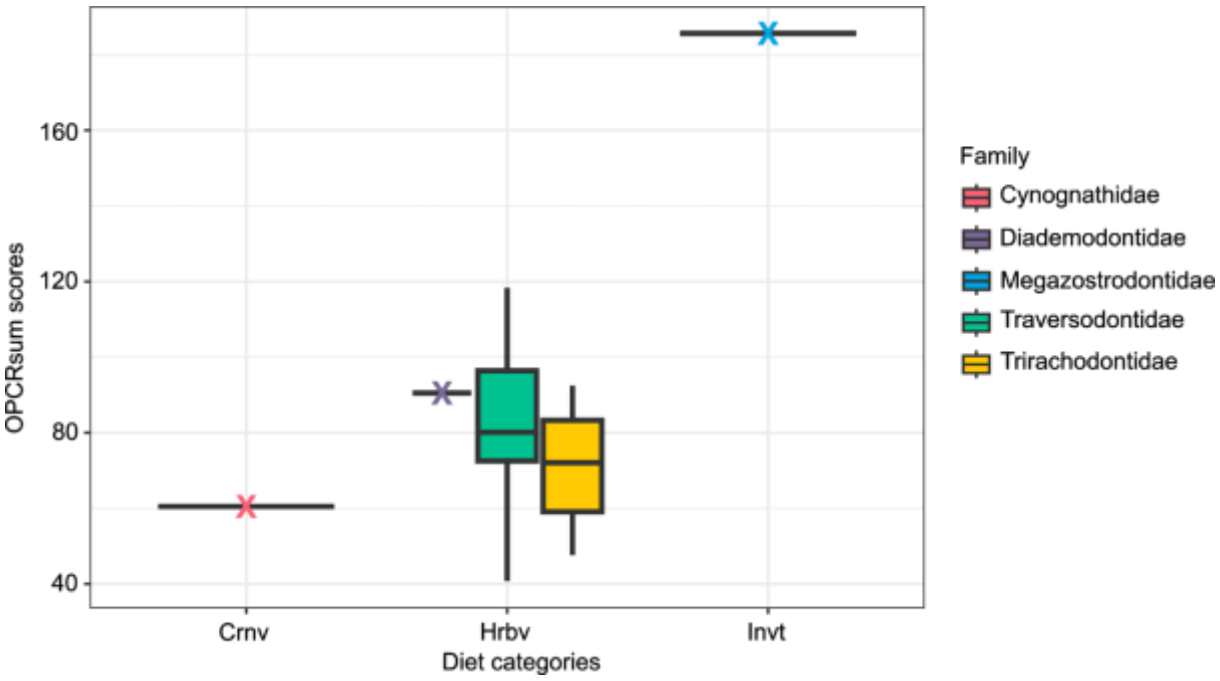


Figure 40: Box and whisker plots showing the distribution of summed OPCR scores (OPCRsum) amongst non-mammalian cynodonts within qualitatively inferred dietary categories. Crnv= carnivore, Hrbv= herbivore, Invt= invertivore. 'X' marks on plot annotate the single estimates for Cyngonathidae (pink), Diademodontidae (purple), and Megazostrodontidae (blue).

Amongst mammalian carnivores (Figure 41), the only afrotherian carnivore sampled, the greater hedgehog tenrec (*Setifer setosus*), has an OPCRsum score of 137.51. The only Euarchtontoglire classified as a carnivore, the potentially carnivorous Cameroon scaly-tail (*Zenkerella insignis*), has an OPCRsum score of 116.13. Laurasiatherian carnivores have a median OPCRsum score of 94.26 (interquartile range: 77.69—116.07, range: 26—167.51). Marsupial carnivores have a median OPCRsum score of 125.68 (interquartile range: 96.59—134.97, range: 74.74—169.13). Amongst mammalian carnivores, carnivorous laurasiatherians generally have much lower OPCRsum scores than species from other major mammalian groups. *Cynognathus* has an OPCRsum score of 60.5, this is in the lower range (bottom 50%) of OPCRsum scores for laurasiatherian carnivores. Notably, *Cynognathus* has an OPCRsum score much lower than those of carnivorous marsupials, afrotherians and euarchontoglires.

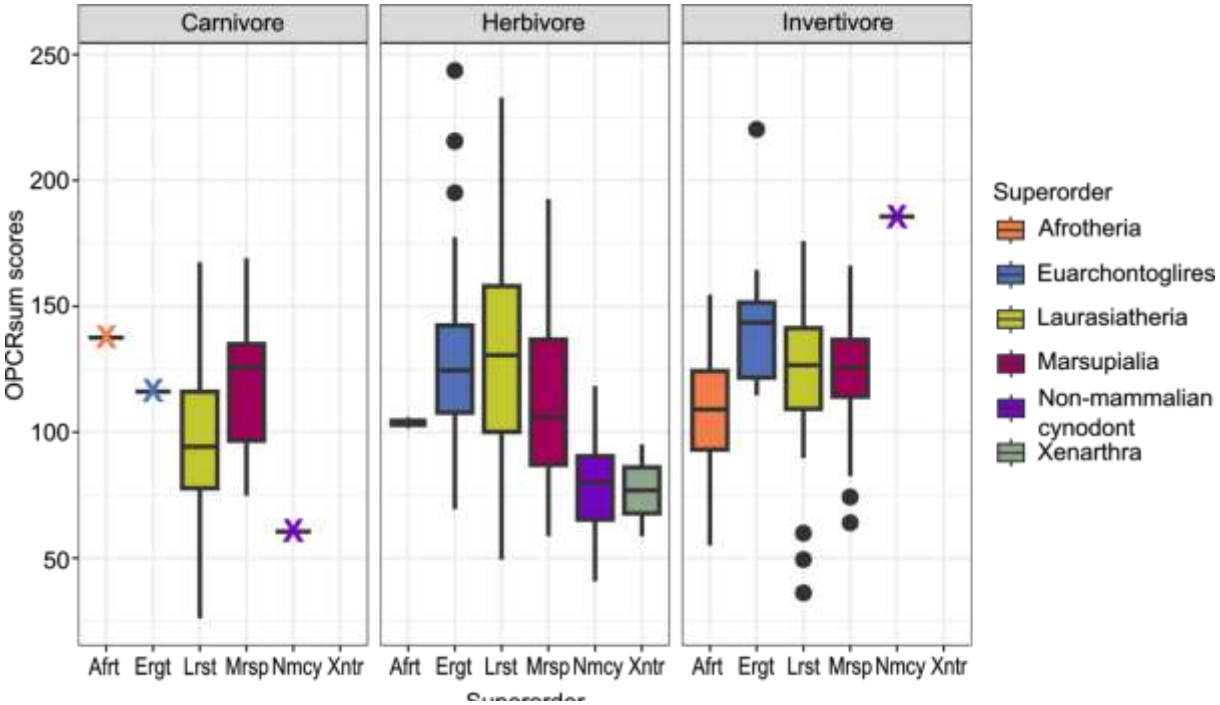


Figure 41: Box and whisker plots showing the distribution of summed OPCR scores (OPCRsum) amongst major mammalian orders relative to non-mammalian cynodonts. Afrt= Afrotheria, Ergt= Euarchontoglires, Lrst= Laurasiatheria, Mrsp= Marsupialia, Nmcy= non-mammalian cynodonts, Xntr= Xenartha. 'X' marks on plot annotate the single estimates for Afrotheria (orange), Euarchontoglires (blue), and non-mammalian cynodonts (purple).

Amongst mammalian herbivores (Figure 41), afrotherian herbivores have a median OPCRsum score of 103.75 (interquartile range: 102.49—105, range: 101.24—106.25). Herbivorous euarchontoglires have a median OPCRsum score of 124.51 (interquartile range:107.76—142.38, range: 69.37—177.50). Laurasiatherian herbivores have a median OPCRsum score of 130.62 (100.12—158.01, range: 49.37—232.88). Marsupial herbivores have a median OPCRsum score of 106 (interquartile range: 87—136.75, range: 58.62—192.62). Xenarthran herbivores have a median OPCRsum score of 76.88 (interquartile range: 67.76—86.01, range: 58.63—95.13). Laurasiatherian herbivores have a wide range of OPCRsum scores, whereas other major mammalian groups have more limited distributions with relatively lower maximum OPCRsum scores. Afrotherian and xenarthran herbivores generally have much lower OPCRsum scores. The distribution of OPCRsum scores amongst herbivorous euarchontoglires and marsupials are similar to those of laurasiatherians, although these groups have

relatively lower OPCRsum scores. Herbivorous non-mammalian cynodonts have a median OPCRsum score of 80 (interquartile range: 65.24—90.5, range: 40.75—118.36), and this distribution is within the lower range (bottom 50%) of herbivorous euarchontoglires, laurasiatherian and marsupial OPCRsum scores. Non-mammalian cynodonts have a wider range of OPCRsum scores than those of herbivorous afrotherians and xenarthrans

Amongst mammalian invertivores (Figure 41), afrotherian invertivores have a median OPCRsum score of 109.01 (interquartile range: 93.06—124.26, range: 55—154.62). Invertivorous euarchontoglires have a median OPCRsum score of 143.44 (interquartile range: 121.63—151.53, range: 114.62—164.38). Laurasiatherian invertivores have a median OPCRsum score of 126.62 (interquartile range: 109.22—141.31, range: 89.74—175.87). Marsupial invertivores have a median OPCRsum score of 125.50 (interquartile range: 114.12—136.66, range: 82.49—166.13). Invertivorous afrotherians have a wide range of OPCRsum scores and these are generally lower than those of other invertivorous mammals. Invertivorous euarchontoglires have relatively higher OPCRsum scores compared to those of other invertivorous mammals. The distribution of OPCRsum scores amongst laurasiatherian and marsupial invertivores are similar. The only invertivorous non-mammalian cynodont sampled, *Megazostrodon*, has an OPCRsum score of 185.64, and this is much higher on average than the OPCRsum scores of invertivorous mammals.

When the traditional diet categories were used to visualize summed dental complexity scores amongst all mammals (Figure 42), carnivorous mammal species have lower OPCRsum scores, with a median OPCRsum score of 102 (interquartile range: 79.5—127.62; range: 26—169.12). Herbivorous mammal species have the highest OPCRsum scores with a median OPCRsum score of 122.13 (interquartile range: 100.81—145.12; range:49.37—200.5). Herbivorous mammal species have a wide range of OPCRsum scores. Invertivorous mammal species have a median OPCRsum score of 122 (interquartile range: 108.47—139.91; range:64—175.87). The OPCRsum scores of herbivores and invertivores are highly similar, only notably differing in range as invertivores have a smaller range of OPCRsum scores (Figure 42).

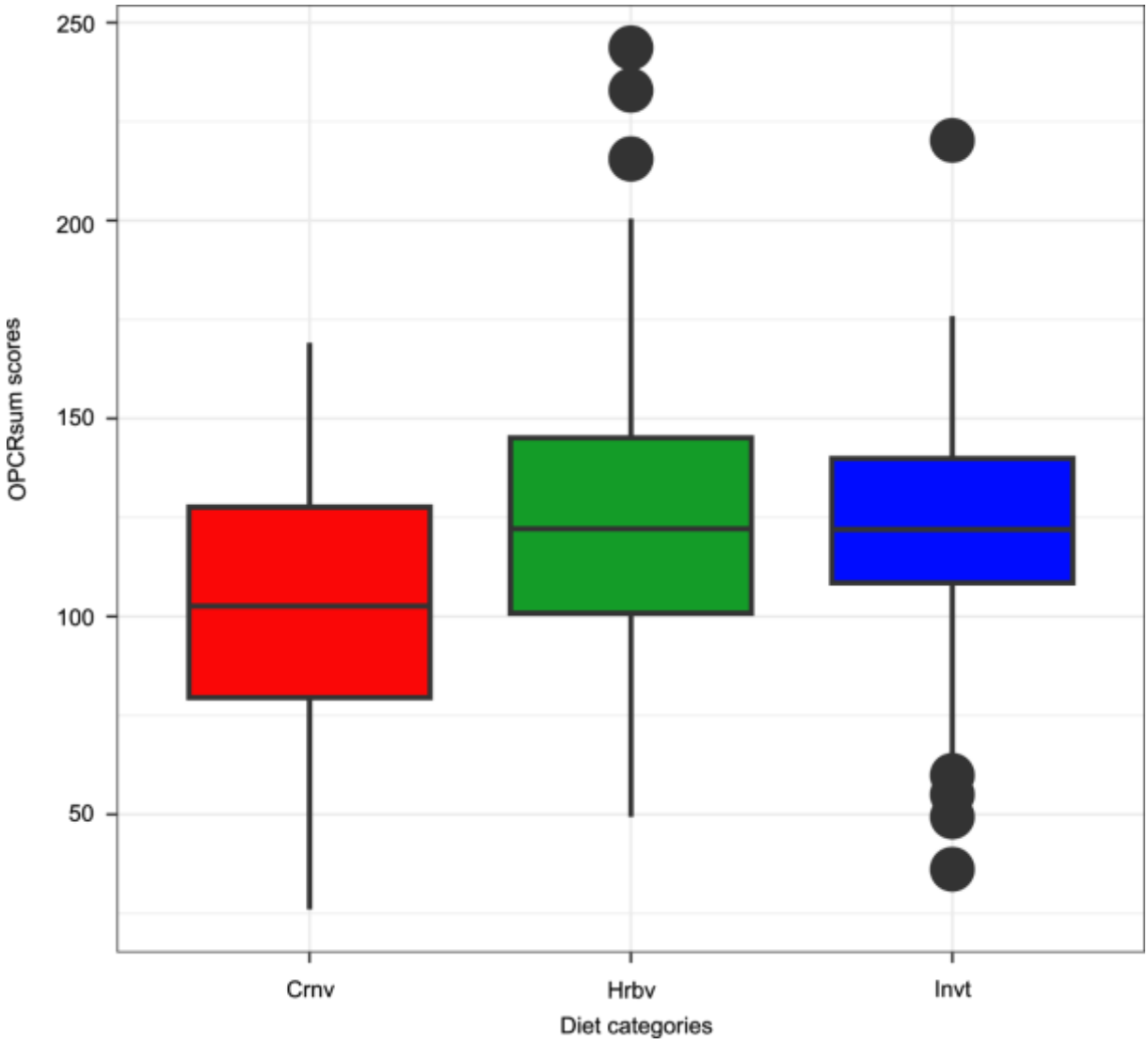


Figure 42: Box and whisker plots showing the distribution of summed OPCR scores (OPCRsum) amongst mammal species within major diet categories. Crnv= carnivore, Hrbv= herbivore, Invt= invertivore.

When the finer diet categories were used to visualise summed dental complexity scores (Figure 43), frugivorous mammal species have a median OPCRsum score of 123.01(interquartile range:103.13—134.19; range: 72.13—172.36). Invertivorous mammals have a median OPCRsum score of 122 (interquartile range: 106.88—139.26; range: 59.87—175.87). Nectivorous mammals have the most limited range of OPCRsum scores, with a median OPCRsum score of 64.38 (interquartile range: 56.44—66.38; range: 48.5—63.38). Herbivorous mammals

have the highest OPCRsum scores, with a median OPCRsum score of 121.5 (interquartile range:102.39—150.49; range: 49.37—215.5). Herbivorous mammals have the widest range of OCPRsum scores. Granivorous mammal species have a median OPCRsum score of 118.07 (interquartile range: 97.44—143.15; range: 63.62—165.36). Carnivores have a median OPCRsum score of 101.31 (interquartile range: 80.28—131.66; range:26—169.13).

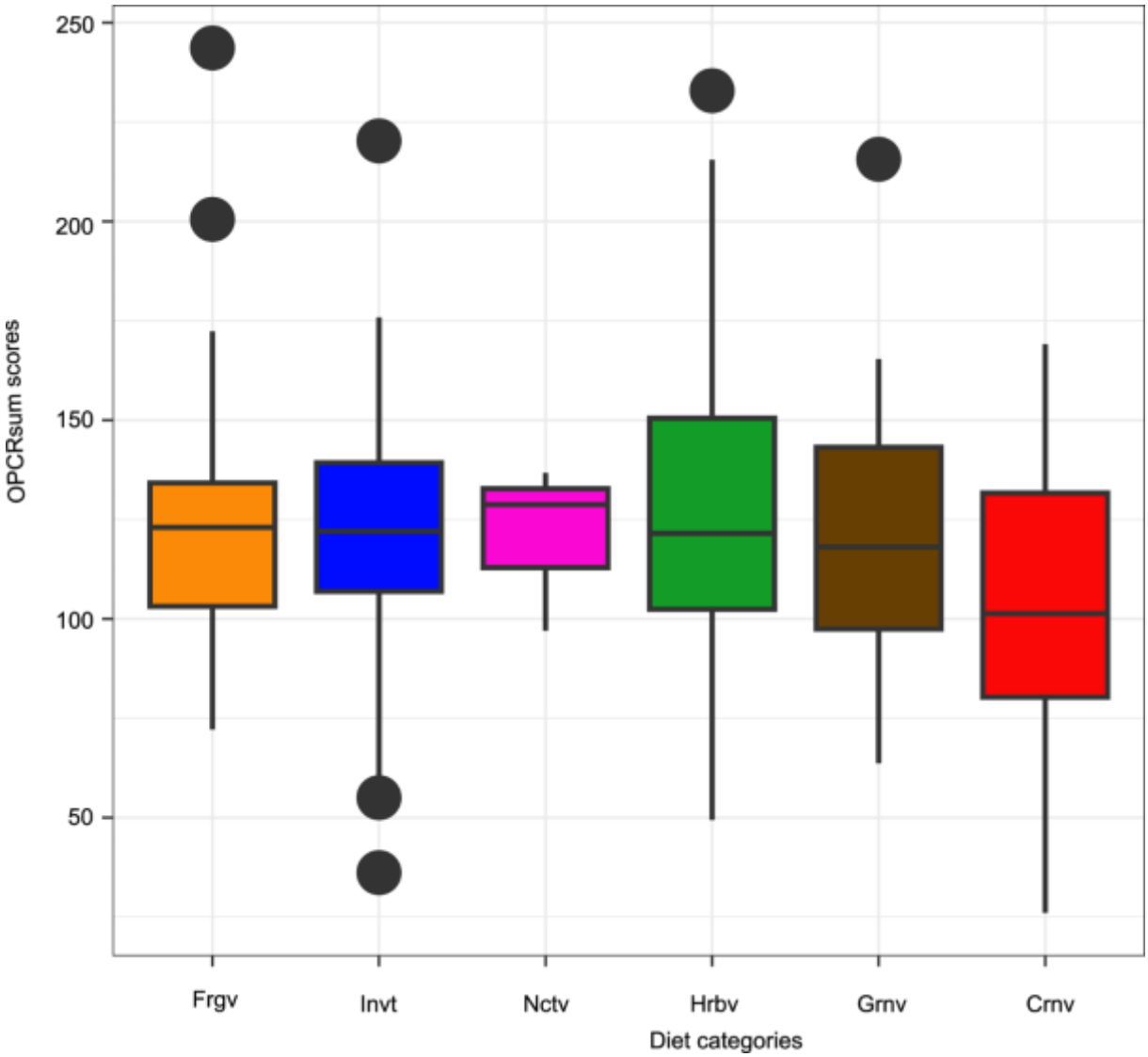


Figure 43: Box and whisker plots showing the distribution of summed OPCR scores (OPCRsum) amongst mammal species within finer diet categories. Frgv= frugivore, Invt= invertivore, Nctv= nectivore, Hrbv= herbivore, Grnv= granivore, Crnv= carnivore.

13.3.2.2 OPCRsum: phylogenetic regressions (pgls)

Table 14: Phylogenetic regressions (pgls) assessing the association that OPCRavg has with log_{10} body mass (BM), log_{10} mandible centroid size (Size) and dietary variables amongst living taxa (n=240).

Model	n	AIC	AIC w	R^2	p-value (model)	Variable	Coefficient	Std err	Pr(>|t|)
OPCRsum~BM*Granivory	240	2468.38	0.9950	0.081	**<0.001**	(Intercept)	132.96	52.38	0.012
						BM	-5.38	3.55	0.131
						Granivory	-108.70	29.95	**<0.001**
						BM:Granivory	40.95	9.48	**<0.001**
OPCRsum~Herbivory	240	2483.13	0.0006	0.006	0.218	(Intercept)	123.04	53.51	0.022
						Herbivory	-8.93	7.23	0.218
OPCRsum~Granivory	240	2483.32	0.0006	0.006	0.250	(Intercept)	117.41	53.40	0.029
						Granivory	12.93	11.20	0.250
OPCRsum~Frugivory	240	2483.33	0.0006	0.006	0.251	(Intercept)	119.88	53.41	0.026
						Frugivory	-9.48	8.24	0.251
OPCRsum~BM	240	2483.76	0.0005	0.004	0.344	(Intercept)	127.12	54.25	0.020
						BM	-3.42	3.61	0.344
OPCRsum~BM+Frugivory	240	2484.27	0.0004	0.010	0.307	(Intercept)	129.54	54.23	0.018
						BM	-3.69	3.61	0.307
						Frugivory	-10.01	8.26	0.226
OPCRsum~Size	240	2484.36	0.0003	0.001	0.587	(Intercept)	130.85	58.29	0.026
						Size	-5.93	10.90	0.587
OPCRsum~Carnivory	240	2484.38	0.0003	0.001	0.596	(Intercept)	117.64	53.52	0.029
						Carnivory	3.17	5.97	0.596
OPCRsum~BM+Herbivory	240	2484.59	0.0003	0.009	0.360	(Intercept)	129.44	54.27	0.018
						BM	-2.68	3.67	0.466
						Herbivory	-7.92	7.37	0.284
OPCRsum~Invertivory	240	2484.65	0.0003	>0.001	0.910	(Intercept)	117.72	53.75	0.029
						Invertivory	0.79	6.99	0.910
OPCRsum~BM+Granivory	240	2484.65	0.0003	0.008	0.370	(Intercept)	125.16	54.27	0.022
						BM	-2.96	3.63	0.415
						Granivory	11.83	11.29	0.296

OPCRsum~Nectivory	240	2484.66	0.0003	0.251	0.984	(Intercept)	118.29	53.55	0.028
						Nectivory	-0.52	24.94	0.984
OPCRsum~BM+Carnivory	240	2485.20	0.0002	0.006	0.485	(Intercept)	127.71	54.31	0.020
						BM	-3.99	3.69	0.280
						Carnivory	4.55	6.11	0.457
OPCRsum~BM+Invertivory	240	2485.73	0.0002	0.004	0.632	(Intercept)	128.36	54.91	0.020
						BM	-3.59	3.77	0.342
						Invertivory	-1.17	7.28	0.873
OPCRsum~BM+Nectivory	240	2485.74	0.0002	0.004	0.633	(Intercept)	127.44	54.40	0.020
						BM	-3.49	3.64	0.340
						Nectivory	-3.65	25.16	0.885
OPCRsum~BM*Carnivory	240	2486.14	0.0001	0.010	0.477	(Intercept)	121.46	54.64	0.027
						BM	-1.90	4.22	0.654
						Carnivory	20.01	16.32	0.221
						BM:Carnivory	-4.61	4.51	0.308
OPCRsum~BM*Frugivory	240	2486.14	0.0001	0.010	0.478	(Intercept)	128.59	54.40	0.019
						BM	-3.39	3.71	0.363
						Frugivory	-1.61	24.68	0.948
						BM:Frugivory	-2.70	7.47	0.718
OPCRsum~BM*Herbivory	240	2486.57	0.0001	0.009	0.559	(Intercept)	128.27	54.86	0.020
						BM	-2.23	4.61	0.629
						Herbivory	-5.39	17.27	0.755
						BM:Herbivory	-0.74	4.57	0.871
OPCRsum~BM*Nectivory	240	2487.29	0.0001	0.006	0.718	(Intercept)	128.72	54.50	0.019
						BM	-3.88	3.70	0.295
						Nectivory	-77.94	115.38	0.500
						BM:Nectivory	32.53	49.30	0.510
OPCRsum~BM*Invertivory	240	2487.62	0.0001	0.004	0.794	(Intercept)	125.42	55.69	0.025
						BM	-2.97	4.19	0.479
						Invertivory	4.37	17.90	0.808
						BM:Invertivory	-1.83	5.42	0.735

The only relationship that significantly explained the variation in OPCRsum scores assessed the interaction effect that log_{10} body mass has with granivory (OPCRsum ~ BM * Granivory). Granivores have a different OPCRsum allometry pattern than non-granivores, and this relationship explained 8.1% of the variation in the model (OPCRsum ~BM * Granivory, R^2). The associated AIC and AIC weight (AIC w) values indicate that the interaction effect between granivory and log_{10} body mass is the best-fitting model relative to the other evaluated relationships, it carries 99.5% of the cumulative model weight and has the lowest AIC score (Table 14). However, the standard error associated with the granivory coefficient is particularly high (std err = 29.95) indicative of low precision in the estimates of granivorous mammals (OPCRsum ~ BM * Granivory, Std err).

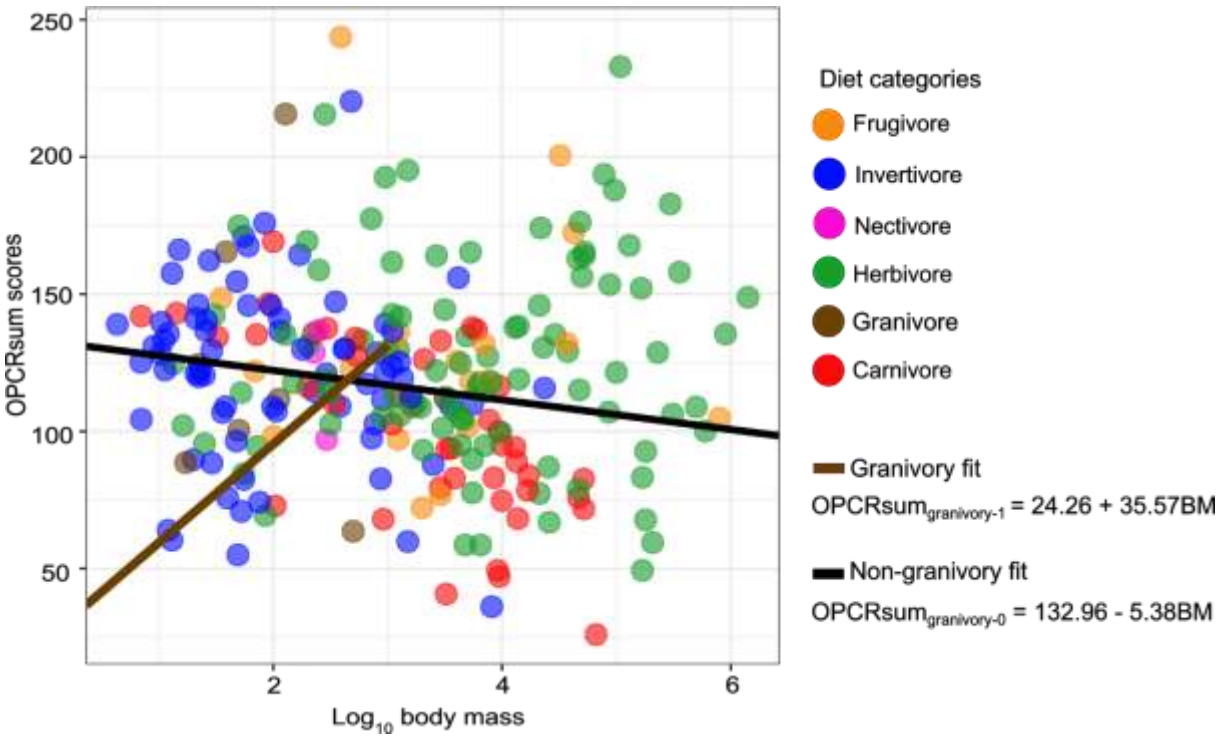


Figure 44: Scatterplot of summed OPCR scores (OPCRsum) and log_{10} body mass, illustrating the interaction that log_{10} body mass has with granivory (granivory fit), relative to non-granivorous mammals (non-granivory fit). Note that granivorous mammals span a narrow range of body size relative to non-granivores.

According to the OPCRsum ~ BM * Granivory model, at a body mass of 1g, a granivorous mammal has an OPCRsum score that is 108.7 times lower than non-

granivores. However, with increasing body mass, granivorous mammal's OPCR scores increase 40.95 times faster than non-granivores (Figure 44).

This indicates that at smaller body masses (less than 1,000g), granivorous mammal species have less complex tooth rows (OPCRsum), and at larger body masses (more than 1,000g), granivorous mammal species have more complex tooth rows relative than non-granivores (Figure 44).

The relationships that dietary variables, $\log_{10}$ body mass and $\log_{10}$ mandible centroid size have with OPCRsum are all non-significant (Table 14). Apart from granivory, dietary variables have non-significant interaction effects with $\log_{10}$ body mass.

12.3.3 Dental complexity of the first molar (OPCRm1): distribution and trends

13.3.3.1 OPCRm1: box and whisker plots

The only hypothesized carnivorous non-mammalian cynodont sampled, *Cynognathus,* has an OPCRm1 score 20.62 (Figure 45). Amongst hypothesized herbivorous non-mammalian cynodonts, *Diademodon* has an OPCRm1 score of 23; traversodontids have a median OPCRm1 score of 28.31 (interquartile range: 26.19—37.31, range: 22.88—40.62) and trirachodontids have a median OPCRm1 score of 24.56 (interquartile range: 23—35.97, range: 16.50—46.62) (Figure 45).

The OPCRm1 scores of *Cynognathus* and *Diademodon* are similar (Figure 45). Traversodontids and trirachodontids have relatively high OCPRm1 scores. Trirachodontids have a wider range of OPCRm1 scores relative to traversodontids (Figure 45).

The only hypothesized invertivorous non-mammalian cynodont sampled, *Megazostrodon*, has an OPCRm1 score 68.38. *Megazostrodon's* OPCRm1 score is much higher than those of other non-mammalian cynodonts (Figure 45).

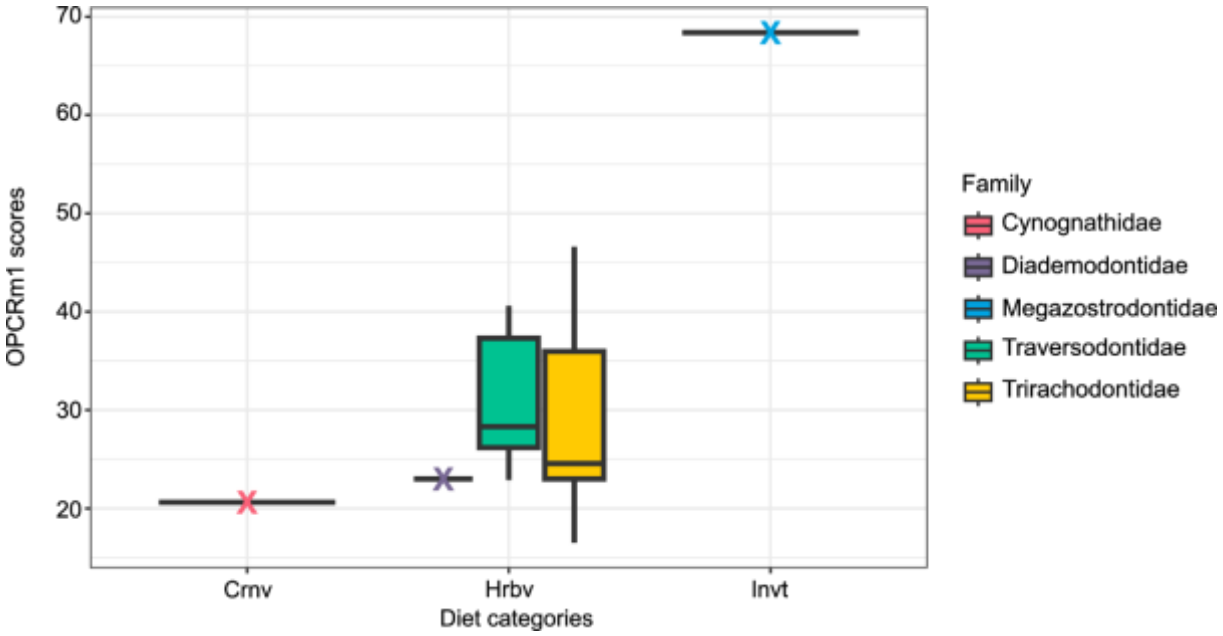


Figure 45: Distribution of OPCR scores for the third-last postcanine tooth, or functionally analogous “first molar” (OPCrm1), among non-mammalian cynodonts within qualitatively inferred dietary categories. Crnv= carnivore, Hrbv= herbivore, Invt= invertivore. ‘X’ marks on plot annotate the single estimates for Cyngonathidae (pink), Diademodontidae (purple), and Megazostrodontidae (blue).

Amongst mammalian carnivores (Figure 46), the only afrotherian carnivore sampled, the greater hedgehog tenrec (*Setifer setosus*), has an OPCRm1 score of 49.88. The only sampled Euarchtontoglire classified as a carnivore, the potentially carnivorous Cameroon scaly-tail (*Zenkerella insignis*), has an OPCRm1 score of 41. Laurasiatherian carnivores have a median OPCRm1 score of 38.63 (interquartile range: 31.16—47.76, range: 16—61.62). Marsupial carnivores have a median OPCRm1 score of 27.38 (interquartile range: 20.69—30.97, range: 14.62—38.62). Amongst mammalian carnivores, carnivorous marsupials generally have much lower OPCRm1 scores than species from other major mammalian groups. *Cynognathus* has an OPCRm1 score of 20.62, which is in the lower range (bottom 50%) of OPCRm1 scores for marsupial and laurasiatherian carnivores. Notably, *Cynognathus* has an OPCRm1 score much lower than those of the carnivorous afrotherian and euarchontoglires.

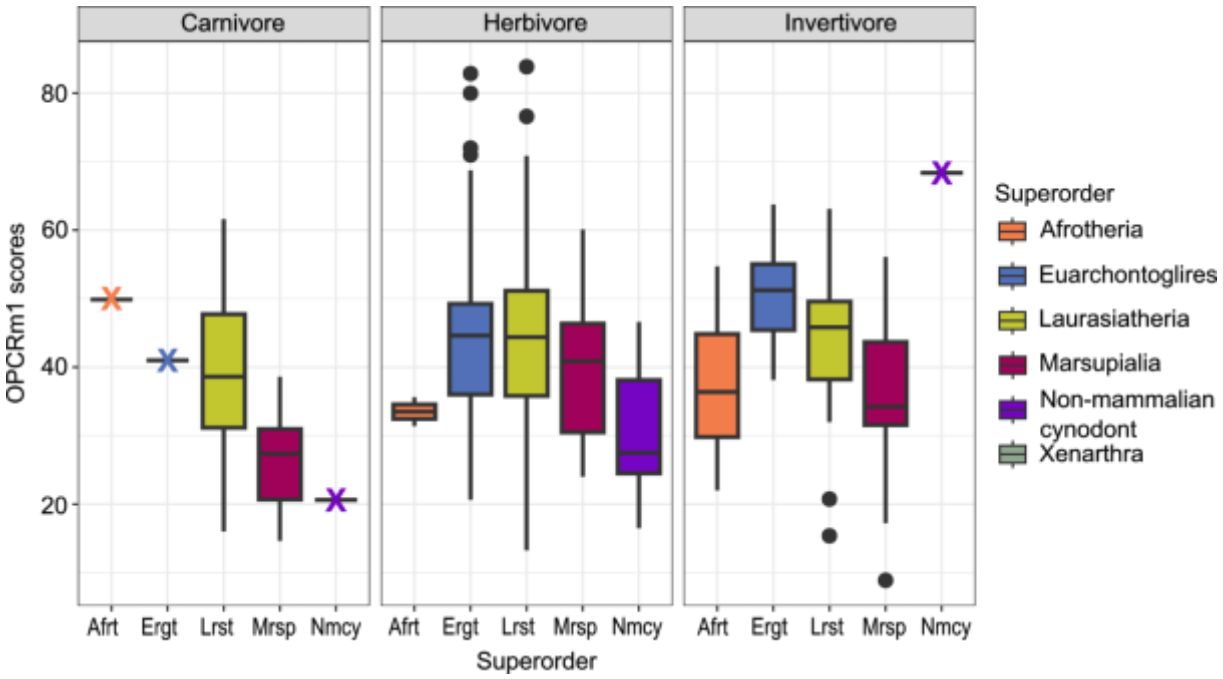


Figure 46: Box and whisker plots showing the distribution of OPCR scores for the first molar (OPCRm1) amongst major mammalian orders relative to non-mammalian cynodonts. Afrt= Afrotheria, Ergt= Euarchontoglires, Lrst= Laurasiatheria, Mrsp= Marsupialia, Nmcy= non-mammalian cynodonts, Xntr= Xenartha. 'X' marks on plot annotate the single estimates for Afrotheria (orange), Euarchontoglires (blue), and non-mammalian cynodonts (purple).

Amongst mammalian herbivores (Figure 46), afrotherian herbivores have a median OPCRm1 score of 33.5 (interquartile range: 32.44—34.56, range: 31.38—35.62). Herbivorous euarchontoglires have a median OPCRm1 score of 44.62 (interquartile range:36—49.25, range: 20.62—68.75). Laurasiatherian herbivores have a median OPCRm1 score of 44.38 (35.81—51.16, range: 13.25—70.88). Marsupial herbivores have a median OPCRm1 score of 40.88 (interquartile range: 30.50—46.38, range: 24—60.12). Amongst mammalian herbivores, laurasiatherian herbivores have the widest range of OPCRm1 scores. Although other major mammalian groups have more limited distributions, the distributions of herbivorous euarchontoglires and marsupials are similar and only differ in maximum values with laurasiatherians generally having higher OPCRm1 scores (Figure 46). Afrotherian herbivores generally have lower OPCRm1 scores. Herbivorous non-mammalian cynodonts have median OPCRm1 score of 27.50 (interquartile range: 24.50—38.12, range: 16.5—46.62), and this distribution is within the lower range (bottom 50%) of herbivorous euarchontoglires,

laurasiatherian and marsupial OPCRm1 scores. Non-mammalian cynodonts have a wider range of OPCRsum scores than those of herbivorous afrotherians.

Amongst mammalian invertivores (Figure 46), afrotherian invertivores have a median OPCRm1 score of 36.38 (interquartile range: 29.81—44.84, range: 22—54.75). Invertivorous euarchontoglires have a median OPCRm1 score of 51.25 (interquartile range: 45.41—55.06, range: 38.12—63.75). Laurasiatherian invertivores have a median OPCRm1 score of 45.82 (interquartile range: 38.22—49.59, range: 32—63.12). Marsupial invertivores have a median OPCRm1 score of 34.25 (interquartile range: 31.56—43.69, range: 17.23—56.12). Amongst mammalian invertivores, invertivorous euarchontoglires and afrotherians have the widest ranges of OPCRm1 scores. Laurasiatherians and euarchontoglires generally have higher OPCRm1 scores and their OPCRm1 scores and this falls within the top 50% of afrotherian and marsupials. The distribution of OPCRm1 scores amongst afrotherian and marsupial invertivores are similar. The only invertivorous non-mammalian cynodont sampled, *Megazostrodon*, has an OPCRm1 score of 68.38, and this is much higher on average than the OPCRm1 scores of invertivorous mammals.

When the traditional diet categories were used to visualize the dental complexity of the first molar amongst mammals (Figure 47), carnivores have the lowest OPCRm1 scores, with a median OPCRm1 score of 35.9 (interquartile range: 28.88—47; range: 14.62—61.62). Herbivores have the highest OPCRm1 scores with a median OPCRm1 score of 43.5 9 (interquartile range: 34.97—48.97; range: 17.50—68.75). Herbivores have the widest range of OPCRm1 scores. The OPCRm1 scores of invertivores have a median of 44.3 9 (interquartile range: 34—48.91; range: 15.38—63.75). The overall distribution of OPCRm1 scores are similar to those of OPCRavg and OPCRsum, and there at only minor differences in the distribution of OPCRm1 scores amongst herbivores and invertivores (Figure 47).

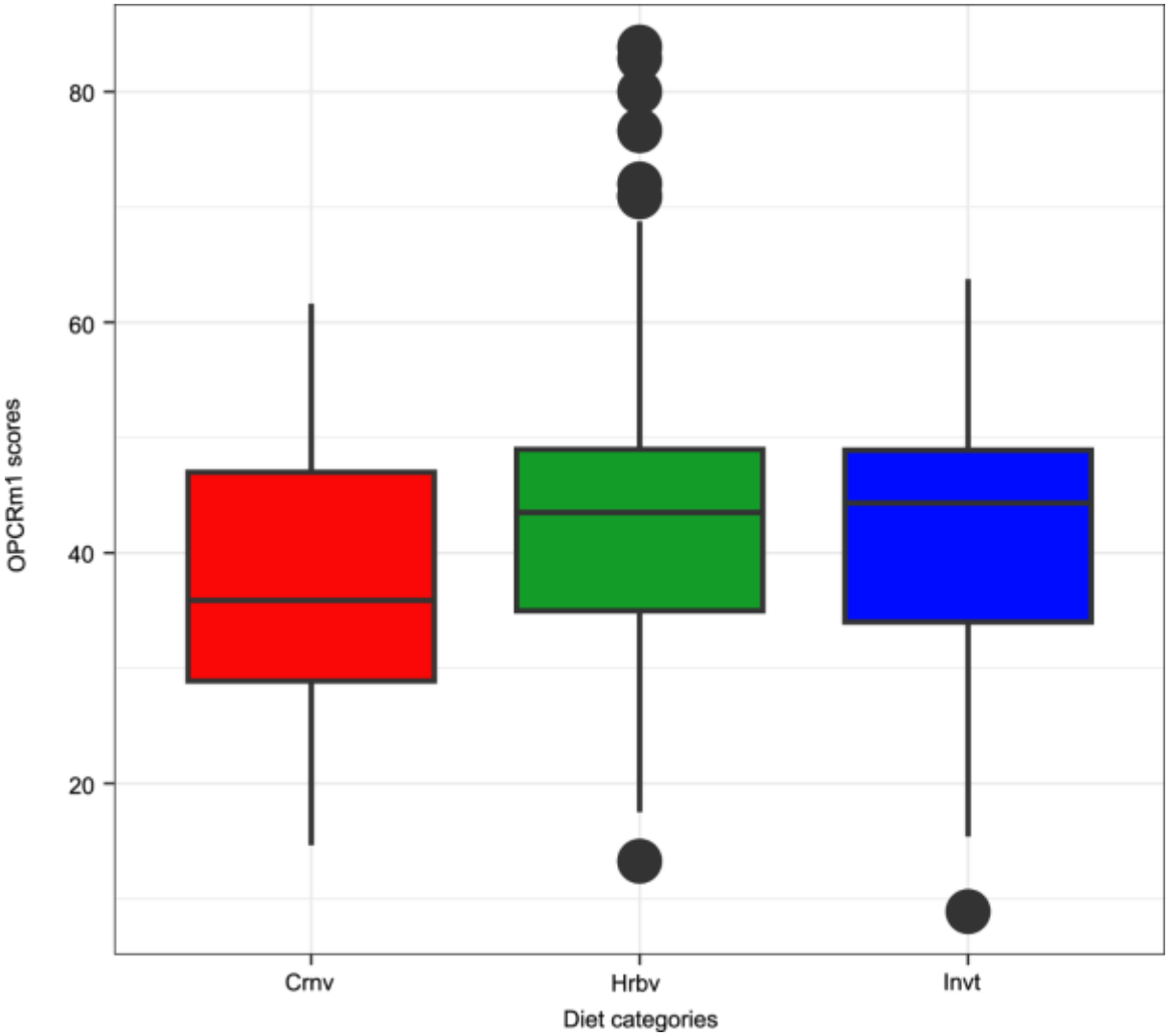


Figure 47: Box and whisker plots showing the distribution of OPCR scores for the first molar (OPCRm1) amongst mammal species within major diet categories. Crnv= carnivore, Hrbv= herbivore, Invt= invertivore.

When the finer diet categories (Figure 48) were used to visualize the dental complexity of the first molar, frugivores have a median OPCRm1 value of 44.48 (interquartile range:39.82—49.94; range: 30.5—58.62). Invertivores have a median OPCRm1 value of 43.75 (interquartile range: 32.75—48.88; range: 8.88—63.75). Nectivores have the most limited range of OPCRm1 scores with a median OPCRm1 of 43.75 (interquartile range: 37.63—48.44; 29.50—51.12). Herbivores have the highest OPCRm1 scores with a median OPCRm1 value of 45.75 (interquartile range: 35.5—48.65; range: 17.50—65.62). Herbivores have the widest range of OPCRm1 scores. Granivores have a median OPCRm1 score of

40.36 (interquartile range: 35.06—51.22; range: 32.62—68.75). Carnivores have the lowest OPCRm1 scores with a median OPCRm1 score of 36.75 (interquartile range: 29.03—46.88; range: 16—61.62).

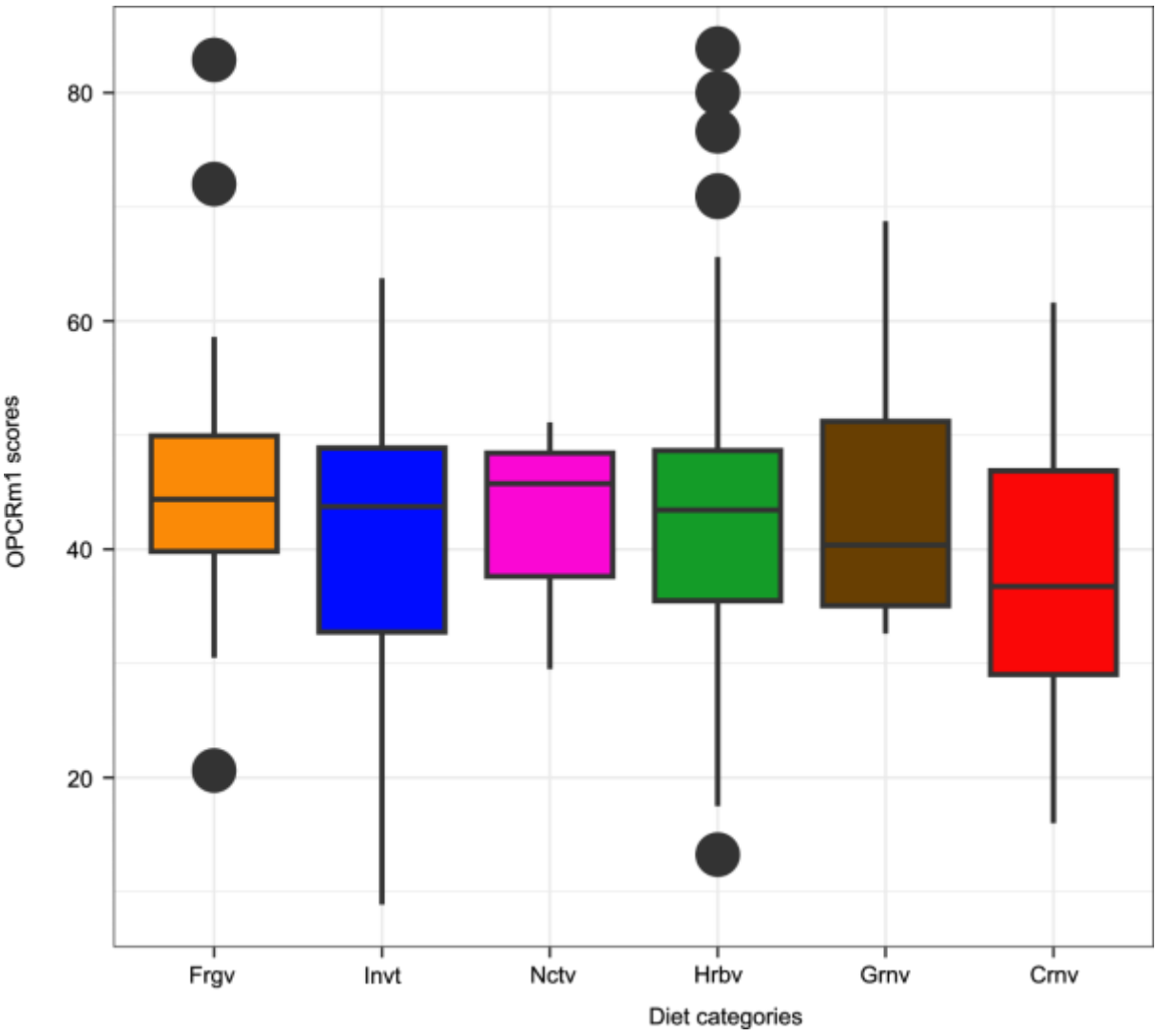


Figure 48: Box and whisker plots showing the distribution of OPCR scores for the first molar (OPCRm1) scores amongst mammal species within finer diet categories. Frgv= frugivore, Invt= invertivore, Nctv= nectivore, Hrbv= herbivore, Grnv= granivore, Crnv= carnivore.

13.3.3.2 OPCRm1: phylogenetic regressions (pgls)

Table 15: Phylogenetic regressions (pgls) assessing the association that OPCRm1 has with $\log_{10}$ body mass (BM), $\log_{10}$ mandible centroid size (Size) and dietary variables amongst living taxa (n=237).

Model	n	AIC	AIC w	R^2	p-value (model)	Variable	Coefficient	Std err	Pr(>|t|)
OPCRm1~BM*Granivory	237	2001.63	0.9950	0.0585	**0.003**	(Intercept)	44.58	21.02	0.035
						BM	-1.61	1.42	0.258
						Granivory	-30.48	11.98	**0.012**
						BM:Granivory	12.72	3.79	**0.001**
OPCRm1~Herbivory	237	2008.426	0.0006	0.0146	0.063	(Intercept)	43.10	21.13	0.042
						Herbivory	-5.34	2.86	0.063
OPCRm1~Carnivory	237	2008.765	0.0003	0.0132	0.078	(Intercept)	39.62	21.10	0.062
						Carnivory	4.16	2.35	0.078
OPCRm1~Frugivory	237	2008.765	0.0006	0.0004	0.766	(Intercept)	40.65	21.24	0.057
						Frugivory	-0.98	3.28	0.766
OPCRm1~Granivory	237	2009.182	0.0006	0.0115	0.100	(Intercept)	39.98	21.12	0.060
						Granivory	7.28	4.41	0.100
OPCRm1~BM+Carnivory	237	2009.331	0.0002	0.0191	0.104	(Intercept)	43.88	21.39	0.041
						BM	-1.73	1.45	0.235
						Carnivory	4.76	2.40	**0.048**
OPCRm1~BM+Herbivory	237	2010.218	0.0003	0.0155	0.162	(Intercept)	44.64	21.44	0.038
						BM	-0.66	1.45	0.651
						Herbivory	-5.09	2.92	0.082
OPCRm1~BM+Granivory	237	2010.819	0.0003	0.0130	0.217	(Intercept)	42.18	21.46	0.051
						BM	-0.86	1.43	0.550
						Granivory	6.96	4.45	0.119
OPCRm1~Invertivory	237	2010.951	0.0003	0.0040	0.330	(Intercept)	42.46	21.29	0.047
						Invertivory	-2.70	2.76	0.330
OPCRm1~BM*Carnivory	237	2011.233	0.0001	0.0195	0.203	(Intercept)	44.62	21.56	0.040
						BM	-1.98	1.66	0.235
						Carnivory	2.91	6.42	0.650
						BM:Carnivory	0.55	1.78	0.757

OPCRm1~BM	237	2011.283	0.0005	0.0026	0.431	(Intercept)	43.34	21.52	0.045
						BM	-1.13	1.43	0.431
OPCRm1~BM+Invertivory	237	2011.71	0.0002	0.0092	0.338	(Intercept)	47.28	21.72	0.031
						BM	-1.65	1.48	0.269
						Invertivory	-3.59	2.88	0.213
OPCRm1~Size	237	2011.847	0.0003	0.0003	0.803	(Intercept)	42.76	23.10	0.065
						Size	-1.08	4.31	0.803
OPCRm1~Nectivory	237	2011.904	0.0003	>0.0001	0.938	(Intercept)	40.46	21.24	0.058
						Nectivory	0.77	9.86	0.938
OPCRm1~BM*Herbivory	237	2012.05	0.0001	0.0162	0.284	(Intercept)	43.51	21.65	0.046
						BM	-0.21	1.82	0.908
						Herbivory	-2.59	6.81	0.704
						BM:Herbivory	-0.73	1.80	0.685
OPCRm1~BM*Invertivory	237	2012.456	0.0001	0.0145	0.334	(Intercept)	43.42	21.99	0.049
						BM	-0.85	1.65	0.606
						Invertivory	3.57	7.05	0.613
						BM:Invertivory	-2.37	2.13	0.267
OPCRm1~BM+Frugivory	237	2013.159	0.0004	0.0032	0.690	(Intercept)	43.61	21.57	0.044
						BM	-1.16	1.43	0.420
						Frugivory	-1.15	3.29	0.728
OPCRm1~BM+Nectivory	237	2013.282	0.0002	0.0026	0.733	(Intercept)	43.36	21.58	0.046
						BM	-1.13	1.44	0.434
						Nectivory	-0.25	9.95	0.980
OPCRm1~BM*Frugivory	237	2014.194	0.0001	0.0072	0.639	(Intercept)	42.59	21.60	0.050
						BM	-0.83	1.47	0.572
						Frugivory	7.84	9.78	0.424
						BM:Frugivory	-2.89	2.97	0.330
OPCRm1~BM*Nectivory	237	2015.25	0.0001	0.0028	0.885	(Intercept)	43.23	21.64	0.047
						BM	-1.09	1.46	0.458
						Nectivory	7.71	45.66	0.866
						BM:Nectivory	-3.48	19.51	0.858

The only relationship that significantly explained the variation in OPCRm1 scores assessed the interaction effect that log_{10} body mass has with granivory (OPCRm1 ~ BM*Granivory). Granivores have different a different OPCRm1 allometry pattern than non-granivores, and this relationship explained 5.85% of the variation in OPCRm1 scores (OPCRm1~BM*Granivory, R^2). The associated AIC and AIC weight (AIC w) values indicate that the interaction effect between granivory and log_{10} body mass is the best-fitting model relative to the other evaluated relationships, as it carries 99.5% of the cumulative weight and has the lowest AIC score (Table 15). However, the standard error associated with the granivory coefficient is particularly high (std err = 11.98) indicative of a high degree of uncertainty in the estimates of granivorous mammals (OPCRm1 ~BM*Granivory, Std err).

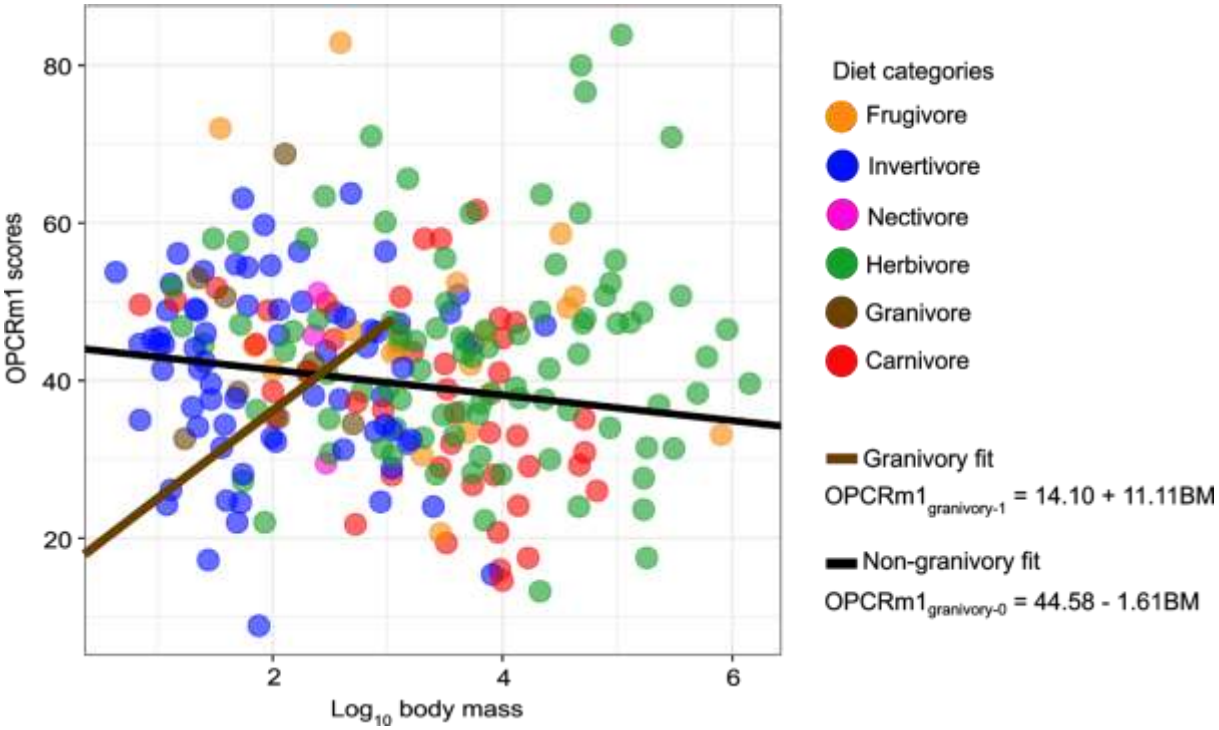


Figure 49: Scatterplot of OPCR scores for the first molar (OPCRm1) and log_{10} body mass, illustrating the interaction that log_{10} body mass has with granivory (granivory fit), relative to non-granivorous mammals (non-granivory fit). Note that granivorous mammals span a narrow range of body sizes relative to non-granivorous mammals.

According to the OPCRm1 ~ BM * Granivory model, at a body mass of 1g, a granivore will have an OPCRm1 score 30.48 times lower than those of non-granivores, However, with increasing body mass, granivore's OPCRm1 scores increase 12.72 times faster than non-granivores. This means that at smaller body masses (less than 1,000g), granivores tend to have less complex first molars (OPCRm1), and at larger body masses (more than 1,000g), granivores tend to have more complex first molars relative to non-granivores (Figure 49).

The relationships that dietary variables, $\log_{10}$ body mass and $\log_{10}$ mandible centroid size have with the dental complexity of the first molar (OPCRm1) are all non-significant (Table 15). Apart from granivory, dietary variables have non-significant interaction effects with $\log_{10}$ body mass.

12.3.4 Dental complexity of the second molar (OPCRm2): distribution and trends

13.3.4.1 OPCRm2: box and whisker plots

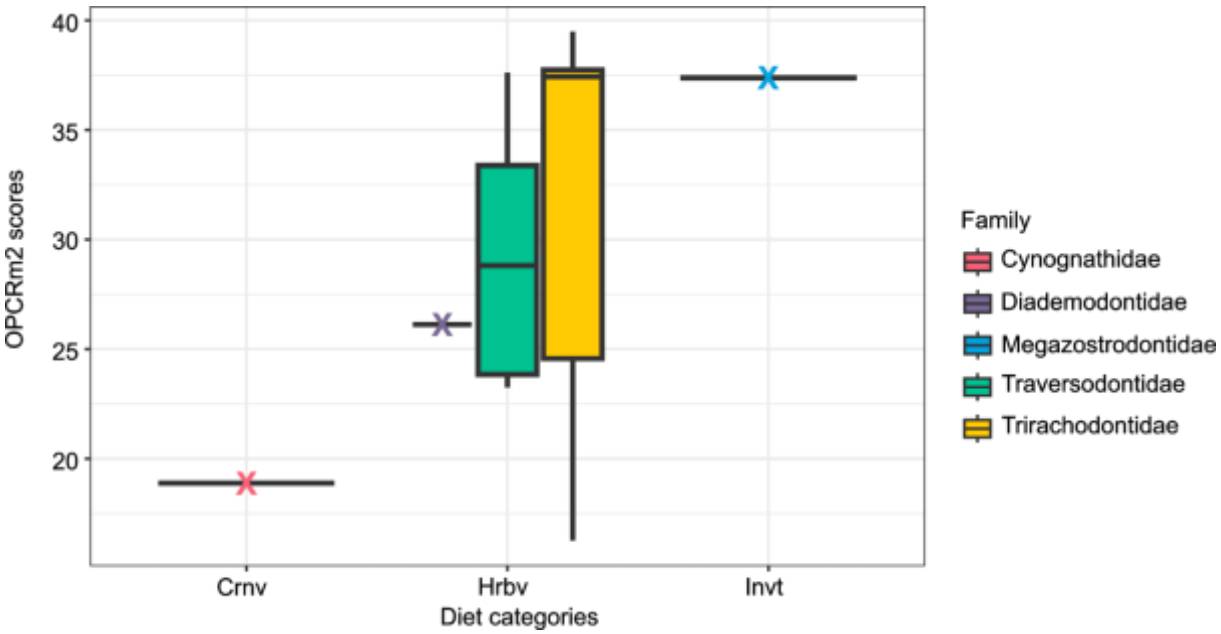


Figure 50: Distribution of OPCR scores for the second-last postcanine tooth, or functionally analogous "second molar" (OPCrm2), among non-mammalian cynodonts within qualitatively inferred dietary categories. Crnv=carnivore, Hrbv= herbivore, Invt= invertivore. 'X' marks on plot annotate the single estimates for Cyngonathidae (pink), Diademodontidae (purple), and Megazostrodontidae (blue).

The only hypothesized carnivorous non-mammalian cynodont sampled, *Cynognathus*, has an OPCRm2 score of 18.88 (Figure 50). Amongst

hypothesized herbivorous non-mammalian cynodonts, *Diademodon* has an OPCRm2 score of 26.12; traversodontids have a median OPCRm2 score of 28.82 (interquartile range: 23.84—33.38, range: 23.25—37.62) and trirachodontids have a median OPCRm2 score of 37.44 (interquartile range: 24.57—37.75, range: 16.25—39.50) (Figure 50).

The OPCRm2 scores of herbivorous non-mammalian cynodonts are generally higher than those of *Cynognathus* (Figure 50). Trirachodontids have the widest range of OPCRm2 scores, and traversodontids generally have higher OPCRm2 scores (Figure 50).

The only hypothesized invertivorous non-mammalian cynodont sampled, *Megazostrodon*, has an OPCRm2 score 37.38. *Megazostrodon's* OPCRm2 score falls within the higher range of OPCRm2 scores amongst herbivorous non-mammalian cynodonts (top 25%) (Figure 50).

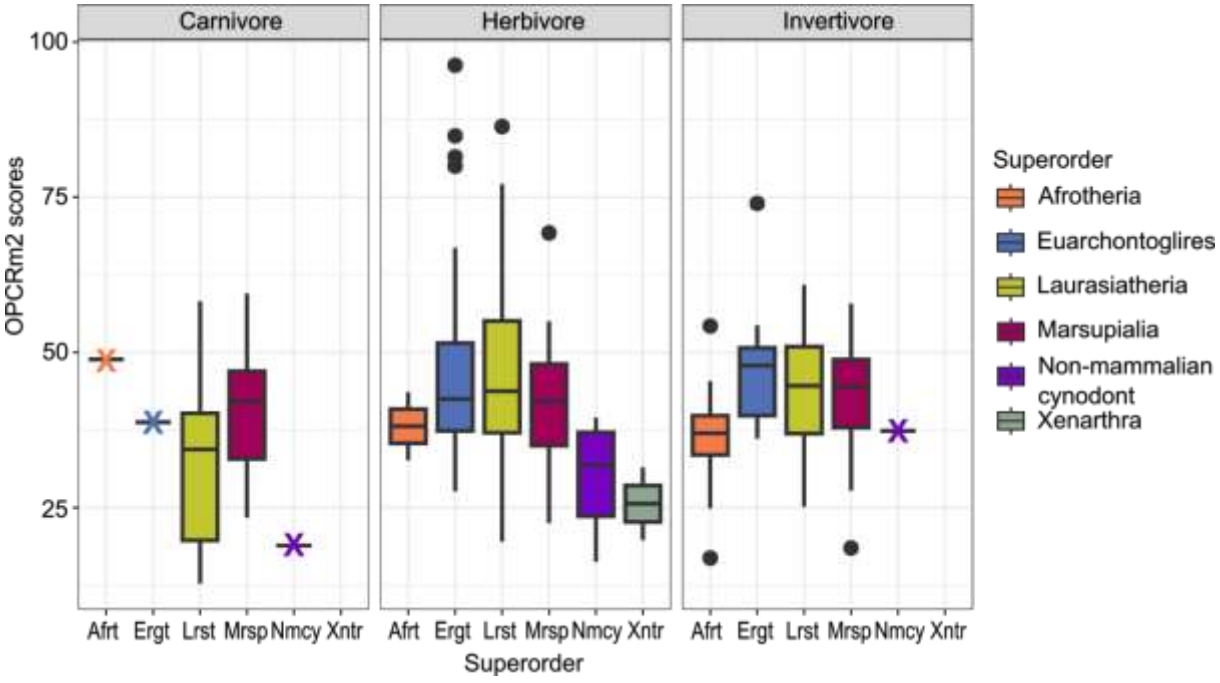


Figure 51: Box and whisker plots showing the distribution of OPCR scores for the second molar (OPCRm2) amongst major mammalian orders relative to non-mammalian cynodonts. Afrt= Afrotheria, Ergt= Euarchontoglires, Lrst= Laurasiatheria, Mrsp= Marsupialia, Nmcy= non-mammalian cynodonts, Xntr= Xenartha. 'X' marks on plot annotate the single estimates for Afrotheria (orange), Euarchontoglires (blue), and non-mammalian cynodonts (purple).

Amongst mammalian carnivores (Figure 51), the only afrotherian carnivore sampled, the greater hedgehog tenrec (*Setifer setosus*), has an OPCRm2 score of 48.88. The only sampled Euarchtontoglire classified as a carnivore, the cryptic Cameroon scaly-tail (*Zenkerella insignis*), has an OPCRm2 score of 38.75. Laurasiatherian carnivores have a median OPCRm2 score of 34.37 (interquartile range: 19.72—40.19, range: 12.75—58.25). Marsupial carnivores have a median OPCRm2 score of 42.06 (interquartile range: 32.84—46.97, range: 23.38—59.5). Amongst mammalian carnivores, carnivorous laurasiatherians generally have much lower OPCRm2 scores than species from other major mammalian groups. The only carnivorous non-mammalian cynodont sampled, *Cynognathus* has an OPCRm2 score of 18.88. This is in the lower range (bottom 25%) of OPCRm2 scores for laurasiatherian carnivores. Notably, *Cynognathus* has an OPCRm2 score much lower than those of species from major mammalian groups outside Laurasiatheria.

Amongst mammalian herbivores (Figure 51), afrotherian herbivores have a median OPCRm2 score of 38.12 (interquartile range: 35.37—40.87, range: 32.62—43.62). Herbivorous euarchontoglires have a median OPCRm2 score of 42.5 (interquartile range: 37.38—51.5, range: 27.62—66.88). Laurasiatherian herbivores have a median OPCRm2 score of 43.75 (37.07—55.06, range: 19.5—77.12). Marsupial herbivores have a median OPCRm2 score of 42.12 (interquartile range: 35—48.12, range: 22.5—55). Xenarthran herbivores have a median OPCRm2 score of 22.63 (interquartile range: 22.69—28.56, range: 19.75—31.5). Laurasiatherian herbivores have a wide range of OPCRm2 scores. Although the other major mammalian groups have more limited distributions relative to laurasiatherians, the distributions of herbivorous euarchontoglires and marsupials are similar and only differ in maximum values as laurasiatherians generally have much higher and lower OPCRm2 scores. Afrotherian and xenarthran herbivores generally have lower OPCRm2 scores. Herbivorous non-mammalian cynodonts have a median OPCRm2 score of 31.88 (interquartile range: 23.62—37.12, range: 16.25—39.5), and this distribution is within the lower range (bottom 50%) of herbivorous euarchontoglires, laurasiatherian and marsupial OPCRm2 scores. Non-mammalian cynodonts have a wider range of OPCRm2 scores than those of herbivorous afrotherians and xenarthrans.

Amongst mammalian invertivores (Figure 51), afrotherian invertivores have a median OPCRm2 score of 37 (interquartile range: 33.51—39.81, range: 24.88—45.38). Invertivorous euarchontoglires have a median OPCRm2 score of 47.88 (interquartile range: 39.82—50.72, range: 36.12—54.38). Laurasiatherian invertivores have a median OPCRm2 score of 44.62 (interquartile range: 36.94—50.94, range: 25.12—60.88). Marsupial invertivores have a median OPCRm2 score of 44.44 (interquartile range: 37.88—48.85, range: 27.75—57.88). Amongst mammalian invertivores, invertivorous laurasiatherians have the widest range of OPCRm2 scores and this is similar to the distribution of OPCRm2 scores amongst euarchontoglires and marsupials. However, invertivorous euarchontoglires generally have relatively higher OPCRm2 scores and afrotherians generally have lower OPCRm2 scores. The only invertivorous non-mammalian cynodont sampled, *Megazostrodon*, has an OPCRm2 score of 37.38, and this is within the lower 50% of OPCRm2 scores amongst laurasiatherian and marsupial mammals. *Megazostrodon's* OPCRm2 score is relatively lower than that of invertivorous euarchontoglires.

Using the traditional dietary categories (Figure 52), carnivorous mammals have the lowest OPCRm2 scores with a median OPCRm2 score of 35.35 (interquartile range: 24.25—42.9; range: 12.75—59.5). Herbivorous mammal species have relatively higher OPCRm2 scores with a median OPCRm2 score of 42.50 (interquartile range: 36—51.75; range: 19.5—69.38). Herbivorous mammals have the widest range of OPCRm2 scores. Invertivorous mammal species have a median OPCRm2 score of 43.50 (interquartile range: 36.5—49; range: 18.5—60.88). The interquartile ranges of OPCRm2 scores amongst diet categories overlap and there are only minor differences between them (Figure 52).

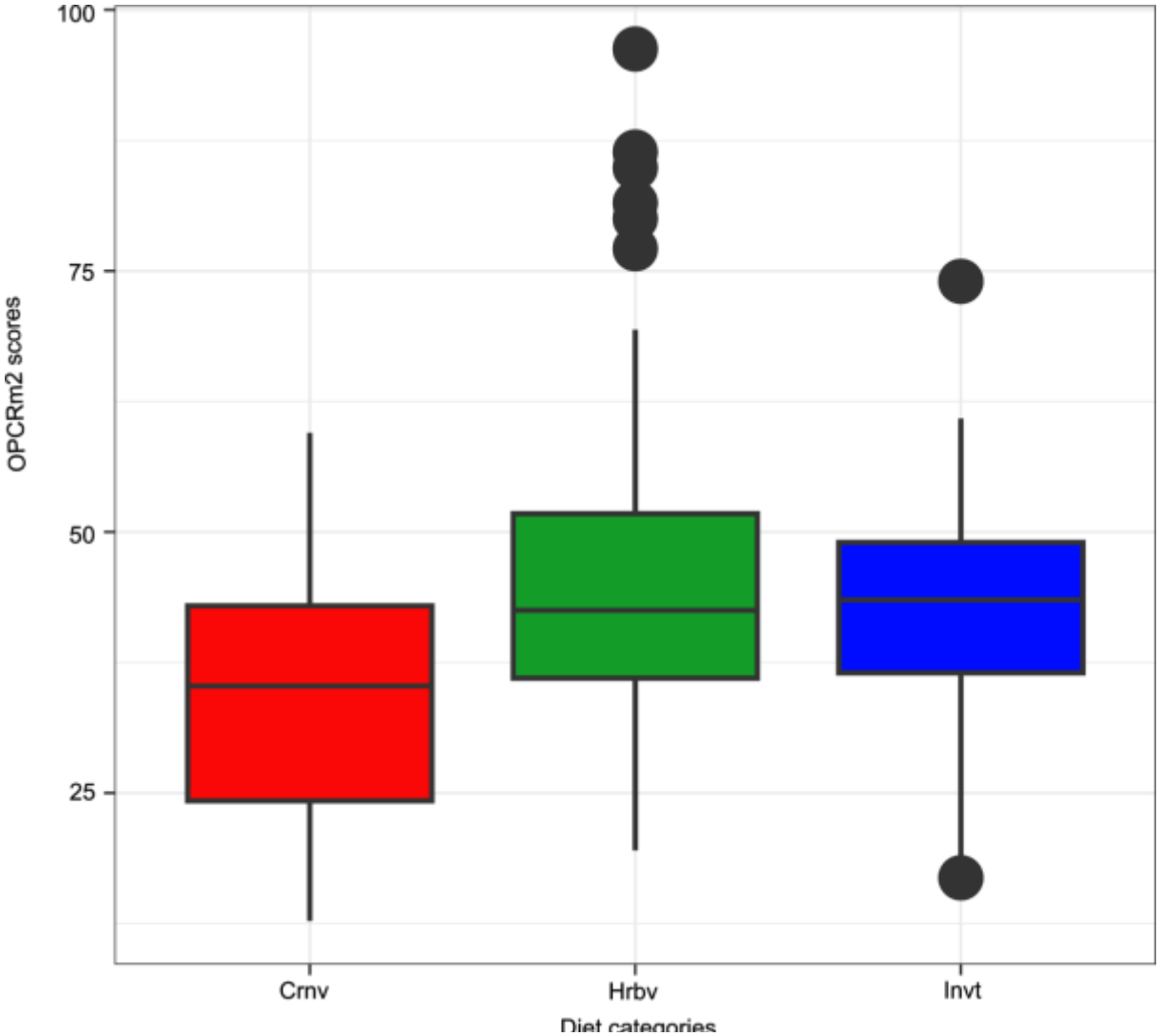


Figure 52: Box and whisker plots showing the distribution of OPCR scores for the second molar (OPCRm2) amongst mammal species within major diet categories. Crnv= carnivore, Hrbv= herbivore, Invt= invertivore.

Using the finer diet categories (Figure 53) to visualize differences in dental complexity, frugivorous mammal species have a median OPCRm2 score of 40.23 (interquartile range: 37.81—48.19; range: 27.62—54). Invertivorous mammal species have a median OPCRm2 score of 43.5 (interquartile range: 36.31—48.57; range: 18.5—60.88). Nectivorous mammal species have the most limited range of OPCRm2 scores with a median OPCRm2 score of 42.5 (interquartile range: 40.69—42.69; range: 38.88—42.88). Herbivorous mammal species have the highest OPCRm2 scores with a median OPCRm2 score of 42.5 (interquartile range: 35.63—52.38; range:19.5—77.12). Granivorous mammal species have a

median OPCRm2 score of 44.88 (interquartile range: 36.13—52.5; range: 33—56.12). Carnivorous mammal species have the lowest OPCRm2 scores with a median OPCRm2 score of 32.25 (interquartile range: 24.25—44.25; range: 12.75—59.5).

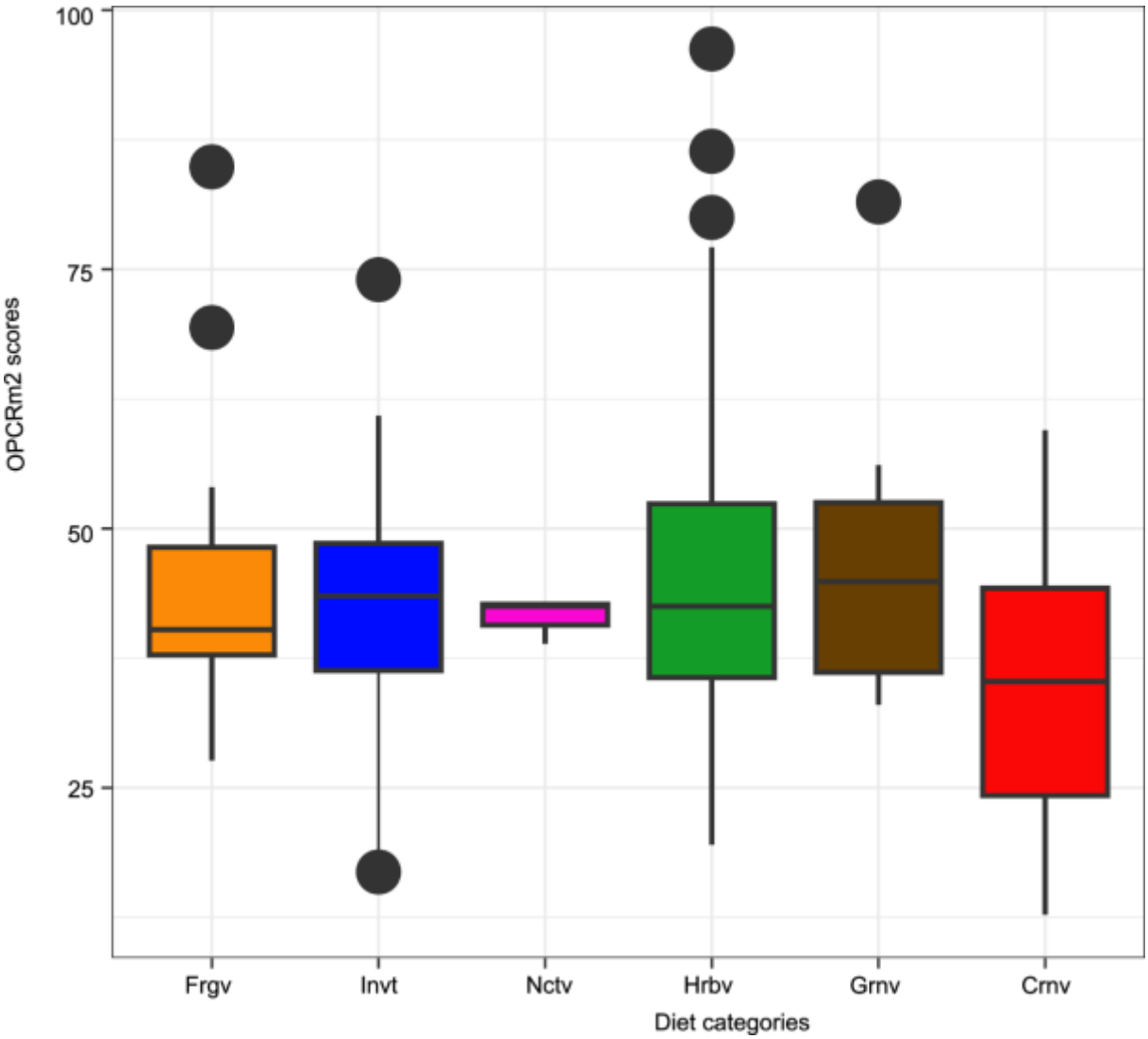


Figure 53: Box and whisker plots showing the distribution of OPCR scores for the second molar (OPCRm2) amongst mammal species within finer diet categories. Frgv= frugivore, Invt= invertivore, Nctv= nectivore, Hrbv= herbivore, Grnv= granivore, Crnv= carnivore.

13.3.4.2 OPCRm2: phylogenetic regressions (pgls)

Table 16: Phylogenetic regressions (pgls) assessing the association that OPCRm2 has with log_{10} body mass (BM), log_{10} mandible centroid size (Size) and dietary variables amongst living taxa (n=229).

Model	n	AIC	AIC w	R^2	p-value (model)	Variable	Coefficient	Std err	Pr(>|t|)
OPCRm2~BM*Granivory	229	1909.12	0.99400	0.0904	**<0.001**	(Intercept)	44.63	19.28	0.021
						BM	-1.20	1.37	0.379
						Granivory	-30.71	11.32	**0.007**
						BM:Granivory	13.95	3.50	**<0.001**
OPCRm2~Granivory	229	1920.81	0.00288	0.0259	**0.015**	(Intercept)	40.95	19.51	0.037
						Granivory	11.02	4.49	**0.015**
OPCRm2~BM+Granivory	229	1922.75	0.00109	0.0261	**0.050**	(Intercept)	41.84	19.89	0.037
						BM	-0.34	1.39	0.807
						Granivory	10.93	4.51	**0.016**
OPCRm2~Herbivory	229	1926.14	0.00020	0.0029	0.415	(Intercept)	42.87	19.79	0.031
						Herbivory	-2.22	2.72	0.415
OPCRm2~Frugivory	229	1926.32	0.00018	0.0021	0.486	(Intercept)	42.05	19.75	0.034
						Frugivory	-2.22	3.18	0.486
OPCRm2~BM	229	1926.62	0.00016	0.0009	0.659	(Intercept)	43.28	20.09	0.032
						BM	-0.62	1.40	0.659
OPCRm2~Nectivory	229	1926.72	0.00015	0.0004	0.762	(Intercept)	41.57	19.77	0.037
						Nectivory	2.79	9.21	0.762
OPCRm2~Size	229	1926.73	0.00015	0.0004	0.776	(Intercept)	44.22	21.68	0.043
						Size	-1.20	4.20	0.776
OPCRm2~Carnivory	229	1926.78	0.00015	0.0002	0.852	(Intercept)	41.58	19.77	0.037
						Carnivory	0.49	2.61	0.852
OPCRm2~Invertivory	229	1926.79	0.00014	0.0001	0.890	(Intercept)	41.97	19.88	0.036
						Invertivory	-0.43	3.09	0.890
OPCRm2~BM*Carnivory	229	1927.63	0.00010	0.0138	0.371	(Intercept)	39.68	20.16	0.050
						BM	0.58	1.59	0.715
						Carnivory	11.03	6.65	0.098
						BM:Carnivory	-3.46	2.03	0.090

OPCRm2~BM+Herbivory	229	1928.07	0.00008	0.0032	0.693	(Intercept)	43.77	20.12	0.031
						BM	-0.38	1.44	0.790
						Herbivory	-2.05	2.79	0.463
OPCRm2~BM+Frugivory	229	1928.10	0.00008	0.0031	0.705	(Intercept)	43.75	20.12	0.031
						BM	-0.65	1.40	0.643
						Frugivory	-2.26	3.19	0.478
OPCRm2~BM+Invertivory	229	1928.55	0.00006	0.0012	0.878	(Intercept)	44.10	20.38	0.032
						BM	-0.72	1.45	0.623
						Invertivory	-0.83	3.20	0.796
OPCRm2~BM+Nectivory	229	1928.55	0.00006	0.0011	0.881	(Intercept)	43.07	20.15	0.034
						BM	-0.57	1.42	0.687
						Nectivory	2.28	9.31	0.807
OPCRm2~BM+Carnivory	229	1928.56	0.00006	0.0011	0.882	(Intercept)	43.26	20.13	0.033
						BM	-0.66	1.42	0.642
						Carnivory	0.63	2.63	0.811
OPCRm2~BM*Invertivory	229	1929.59	0.00004	0.0053	0.752	(Intercept)	41.02	20.62	0.048
						BM	0.09	1.67	0.959
						Invertivory	5.14	6.92	0.459
						BM:Invertivory	-2.32	2.38	0.332
OPCRm2~BM*Frugivory	229	1929.73	0.00003	0.0047	0.785	(Intercept)	44.41	20.18	0.029
						BM	-0.87	1.45	0.549
						Frugivory	-7.50	9.17	0.414
						BM:Frugivory	1.70	2.79	0.543
OPCRm2~BM*Herbivory	229	1930.03	0.00003	0.0034	0.856	(Intercept)	44.37	20.38	0.031
						BM	-0.62	1.85	0.739
						Herbivory	-3.24	6.52	0.620
						BM:Herbivory	0.35	1.74	0.841
OPCRm2~BM*Nectivory	229	1930.55	0.00002	0.0011	0.968	(Intercept)	43.13	20.21	0.034
						BM	-0.59	1.44	0.683
						Nectivory	-0.76	42.78	0.986
						BM:Nectivory	1.33	18.27	0.942

The relationship that explained the most variation in OPCRm2 scores assessed the interaction effect that log_{10} body mass has with granivory (OPCRm2 ~ BM * Granivory). Granivores have a different OPCRm2 allometry patterns than non-granivores, and this relationship explained 9.04% of the variation in OPCRm2 scores (OPCRm2 ~ BM * Granivory). The associated AIC and AIC weight (AIC w) values indicate that this is the best-fitting model relative, as it carries 99.4% of the cumulative weight and has the lowest AIC score (Table 16). However, the standard error associated with the granivory coefficients is particularly high (std err = 14.68), this is indicative of a high degree of uncertainty (low precision) in the estimates of granivorous mammals (OPCRm2 ~BM * Granivory, Std err).

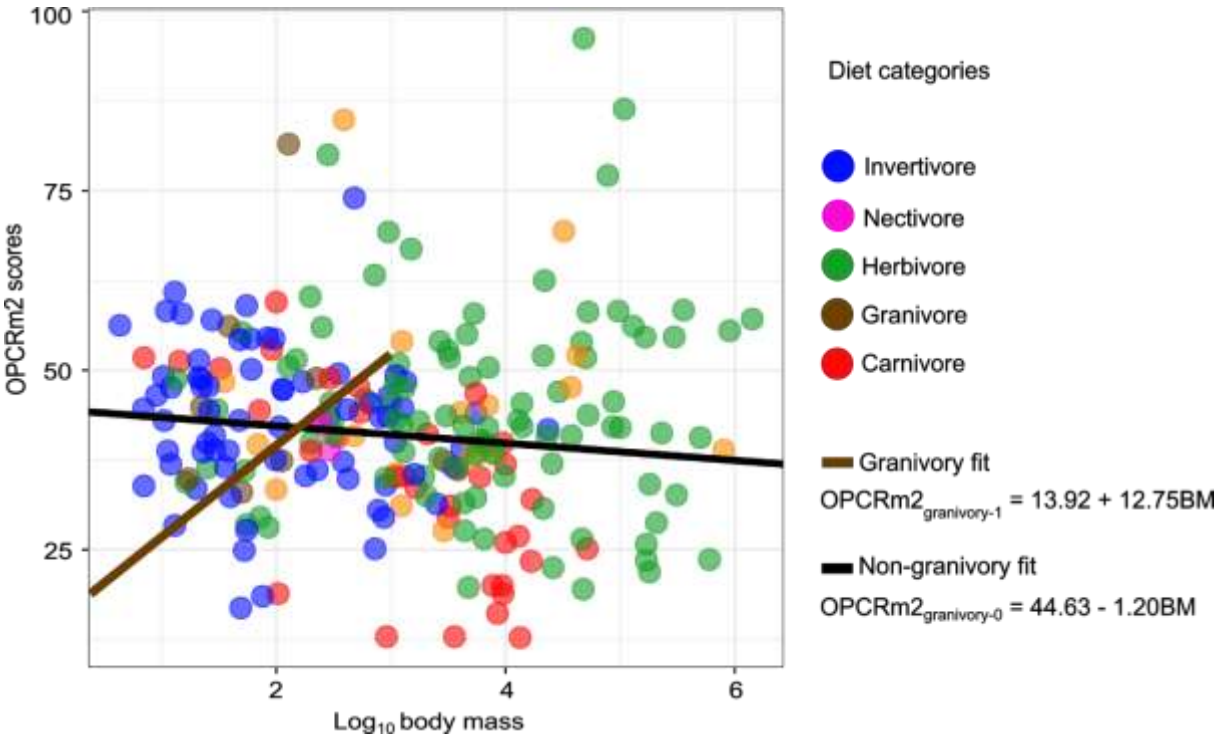


Figure 54: Scatterplot of OPCR scores for the second molar (OPCRm2) and log_{10} body mass, illustrating the interaction that log_{10} body mass has with granivory (granivory fit), relative to non-granivorous mammals (non-granivory fit). Note that granivorous mammals span a narrow range of body sizes relative to non-granivorous mammals.

According to the OPCRm2 ~ BM * Granivory model, at a body mass of 1g, a granivore will have an OPCR m2 score 30.71 times lower than non-granivores. However, with increasing body mass, granivore's OPCR sores increase 13.95 times faster than non-granivores. This means that at smaller body masses (less

than 1,000g), granivores have less complex second molars (OPCRm2), and at larger body masses (more than 1,000g), granivores have more complex second molars relative to non-granivores (Figure 54).

Granivory has a significant influence on OPCRm2 scores when accounting for the effect of body mass (OPCRm2 ~ BM + Granivory), or not (OPCRm2 ~ Granivory). The main effect of granivory explains 2.59% of the variation in OPCRm2 scores (OPCRm2~Granivory, R^2). The relationship between the main effect of granivory and OPCRm2 scores is the second-best amongst those considered, the associated AIC value is 11.69 AIC units higher and this model only carries 0.28% of the cumulative model weight (Table 16). According to this relationship, on average, highly granivorous mammals have OPCRm2 scores that are 11.02 times higher than non-granivorous mammals. The partial effect of granivory is significant and indicates that after accounting for the effects of body mass, granivory explained 2.61% of the variation in OPCRm2 scores (OPCRm2~ BM+Granivory, R^2). According to this model (OPCRm2 ~ BM + Granivory), highly granivorous mammals have OPCRm2 scores that are 10.93 times higher than non-granivorous mammals.

The relationships that the remaining dietary variables, $\log_{10}$ body mass and $\log_{10}$ mandible centroid size have with OPCRm2 are all non-significant. Apart from granivory, the interaction effects between dietary variables and $\log_{10}$ body mass are non-significant (Table 16).

12.3.5 Dental complexity of the third molar (OPCRm3): distribution and trends

13.3.5.1 OPCRm3: box and whisker plots

The only hypothesized carnivorous non-mammalian cynodont, *Cynognathus*, has an OPCRm3 score of 21 (Figure 55). Amongst hypothesized herbivorous non-mammalian cynodonts sampled, *Diademodon* has an OPCRm3 score of 41.38; traversodontids have a median OPCRm1 score of 30.44 (interquartile range: 16.90—40.28, range: 13.38—42.62) and trirachodontids have a median OPCRm3 score of 19.75 (interquartile range: 17.69—20.13, range: 15.62—20.50) (Figure 55).

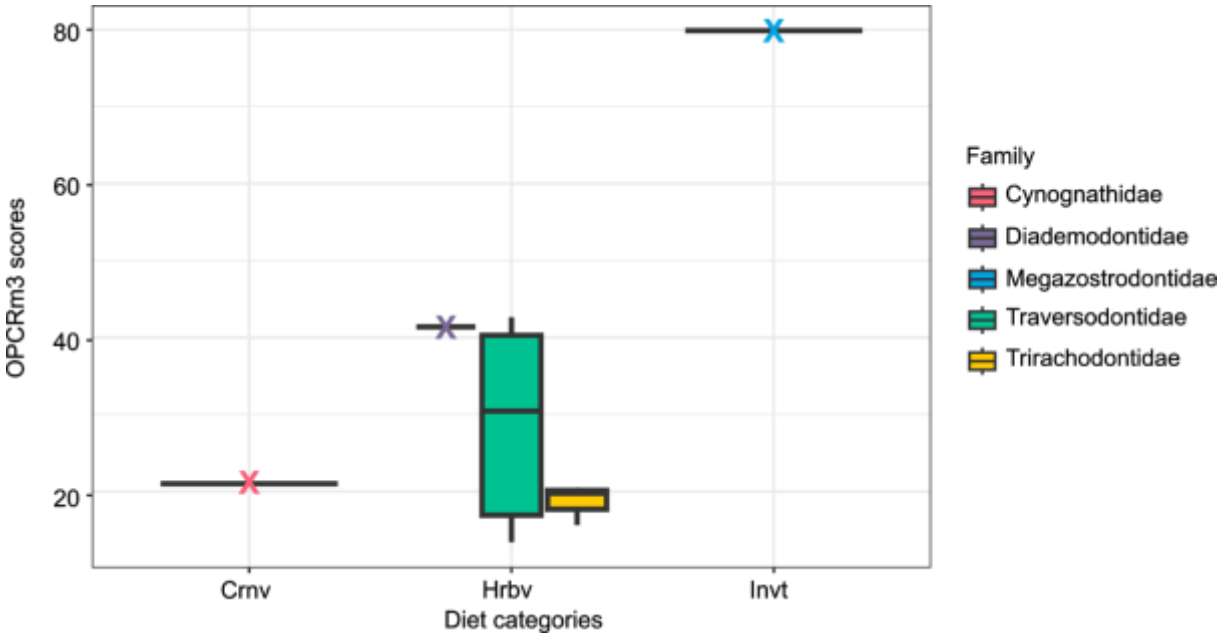


Figure 55: Distribution of OPCR scored for the posteriormost postcanine tooth, or functionally analogous “third molar” (OPCRm3), among non-mammalian cynodonts within qualitatively inferred dietary categories. Crnv= carnivore, Hrbv= herbivore, Invt= invertivore. ‘X’ marks on plot annotate the single estimates for Cyngonathidae (pink), Diademodontidae (purple), and Megazostrodontidae (blue).

Traversodontids have the widest range of OPCRm3 scores, and these are generally higher than those of trirachodontids. However, *Diademodon* has a OPCRm3 score higher on average than those of traversodontids as it falls within the top 25% of traversodontid OPCRm3 scores. Trirachodontids have a limited range of OPCRm3 scores, which are generally lower than those of other non-mammalian cynodonts. The OPCRm3 scores amongst some herbivorous non-mammalian cynodonts are notably lower than that of expected carnivore, *Cynognathus* (Figure 55).

The only hypothesized invertivorous non-mammalian cynodont sampled, *Megazostrodon*, has an OPCRm3 score 79.88. *Megazostrodon’s* OPCRm3 score is much higher than those of other non-mammalian cynodonts (Figure 55).

Amongst mammalian carnivores (Figure 56), the only afrotherian carnivore sampled, the greater hedgehog tenrec (*Setifer setosus*), has an OPCRm3 score of 38.75. The only sampled Euarchtontoglire classified as a carnivore, the cryptic Cameroon scaly-tail (*Zenkerella insignis*), has an OPCRm3 score of 36.38. Laurasiatherian carnivores have a median OPCRm3 score of 33.62 (interquartile

range: 32.38—41.75, range: 32.38—41.75). Marsupial carnivores have a median OPCRm3 score of 44.75 (interquartile range: 33.75—48.94, range: 25.38—54.88). Carnivorous marsupials have the widest range of OPCRm3 scores, and species from other major mammalian groups generally have much lower OPCRm3 scores. The only non-mammalian cynodont sampled hypothesized as carnivorous, *Cynognathus*, has an OPCRm3 score of 21, which is much lower than those of mammals on average.

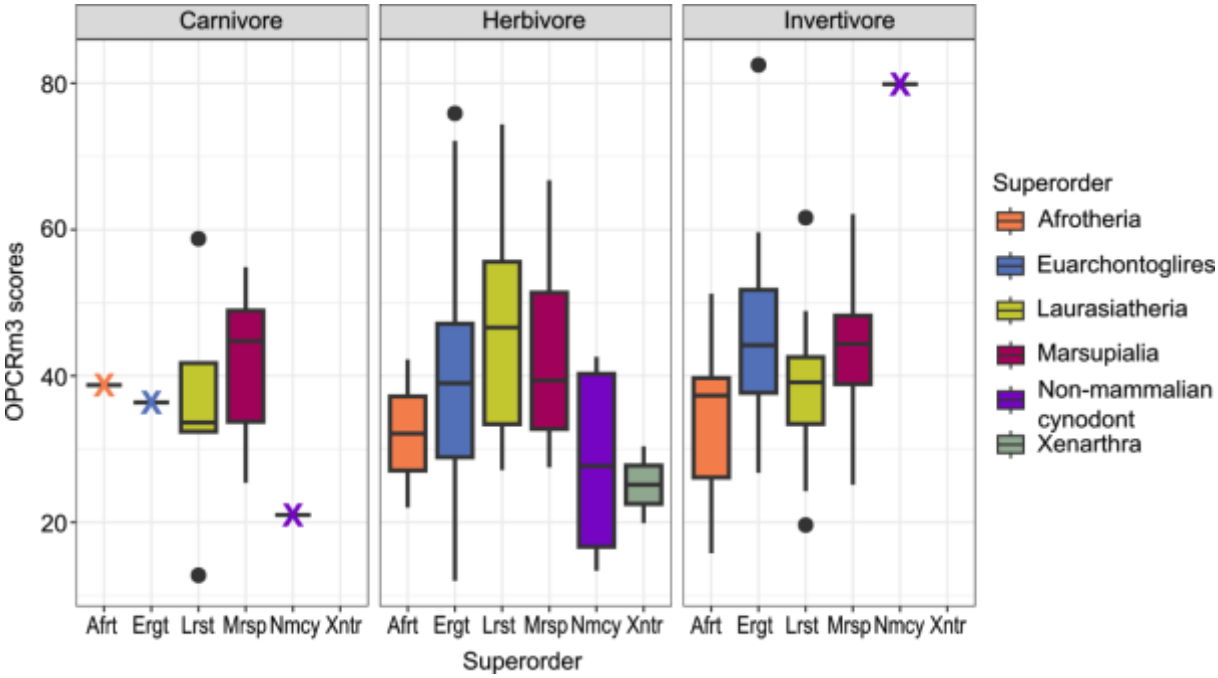


Figure 56: Box and whisker plots showing the distribution of OPCR scores for the third molar (OPCRm3) amongst major mammalian orders relative to non-mammalian cynodonts. Afrt= Afrotheria, Ergt= Euarchontoglires, Lrst= Laurasiatheria, Mrsp= Marsupialia, Nmcy= non-mammalian cynodonts, Xntr= Xenartha. 'X' marks on plot annotate the single estimates for Afrotheria (orange), Euarchontoglires (blue), and non-mammalian cynodonts (purple).

Amongst mammalian herbivores (Figure 56), afrotherian herbivores have a median OPCRm3 score of 32.12 (interquartile range: 27.06—37.19, range: 22—42.25). Herbivorous euarchontoglires have a median OPCRm3 score of 39 (interquartile range:28.88—47.12, range: 12—72.12). Laurasiatherian herbivores have a median OPCRm3 score of 46.62 (interquartile range: 33.41—55.59, range: 27.12—74.38). Marsupial herbivores have a median OPCRm3 score of 39.38 (interquartile range: 32.75—51.38, range: 27.5—66.75). Xenarthrans herbivores

have a median OPCRm3 score of 25.13 (interquartile range: 22.51—27.76, range: 19.88—30.38). Herbivorous euarchontoglires have the widest range of OPCRm3 scores. Laurasiatherian and marsupial herbivores have relatively higher OPCRm3 scores. Afrotherian and xenarthran herbivores have relatively lower OPCRm3 scores. Herbivorous non-mammalian cynodonts have median OPCRm3 score of 27.69 (interquartile range: 16.65—40.28, range: 13.38—42.62), and this distribution is within the lower range (bottom 50%) of herbivorous euarchontoglires, laurasiatherian and marsupial OPCRsum scores. Herbivorous non-mammalian cynodonts have a wider range of OPCRsum scores than those of herbivorous afrotherians and xenarthrans

Amongst mammalian invertivores (Figure 56), afrotherian invertivores have a median OPCRm3 score of 37.32 (interquartile range: 26.12—39.72, range: 15.75—51.25). Invertivorous euarchontoglires have a median OPCRm3 score of 44.19 (interquartile range: 37.69—51.75, range: 26.75—59.62). Laurasiatherian invertivores have a median OPCRm3 score of 39.12 (interquartile range: 33.44—42.56, range: 24.25—48.88). Marsupial invertivores have a median OPCRm3 score of 44.38 (interquartile range: 38.87—48.25, range: 25.12—62.12). Amongst mammalian invertivores, invertivorous marsupials have a wide range of OPCRsum scores and this is most similar to the distribution of invertivorous euarchontoglires. Laurasiatherian and afrotherian invertivores have relatively lower OPCRm3 scores. The only invertivorous non-mammalian cynodont sampled, *Megazostrodon*, has an OPCRm3 score of 79.88, and this is much higher on average than the OPCRm3 scores of invertivorous mammals.

Using the traditional or major dietary categories to visualize the differences in dental complexity amongst all mammals sampled (Figure 57), carnivorous mammal species have a median OPCRm3 score of 38.75 (interquartile range: 33—48.25; range: 12.75—58.75). Herbivorous mammal species have a median OPCRm3 score of 39.25 (interquartile range: 31.53—50.53; range: 12—75.88). Invertivorous mammal species have a median OPCRm3 score of 39.5 (interquartile range: 34.38—46; range: 18.62—62.12).

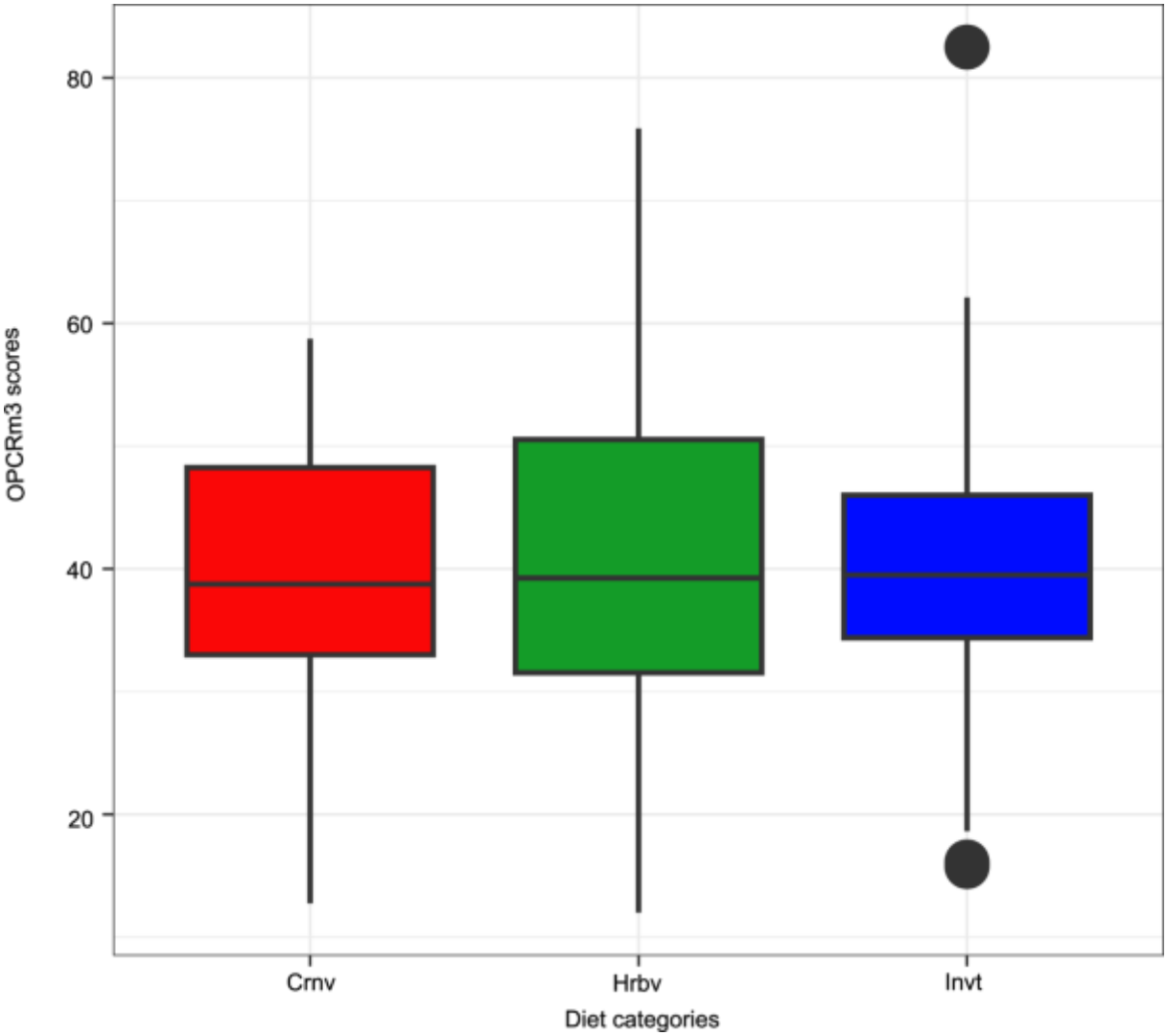


Figure 57: Box and whisker plots showing the distribution of OPCR scores for the third molar (OPCRm3) amongst mammal species within major diet categories. Crnv= carnivore, Hrbv= herbivore, Invt= invertivore.

Using the finer dietary categorization to visualize differences in dental complexity scores (Figure 58), frugivorous mammal species have a median OPCRm3 of 36.31 (interquartile range: 32.26 - 44.38; range: 23.5-51.88). Invertivorous mammal species have a median OPCRm3 score of 39 (interquartile range: 33.44 - 46.69; range: 15.75—62.12). Nectivorous mammal species have a median OPCRm3 score of 46.19 (interquartile range: 43.15—49.22; range: 40.12 — 52.25). Herbivorous mammal species have a median OPCRm3 score of 40.38 (interquartile range: 31.69—50.44; range: 14.5—74.38). Granivorous mammal

species have a median OPCRm3 of 39.12 (interquartile range: 27.69—51.62; range: 21.12—65.38). Carnivorous mammal species have a median OPCRm3 score of 40.62 (interquartile range: 34—44.69; range: 24.2—56.34).

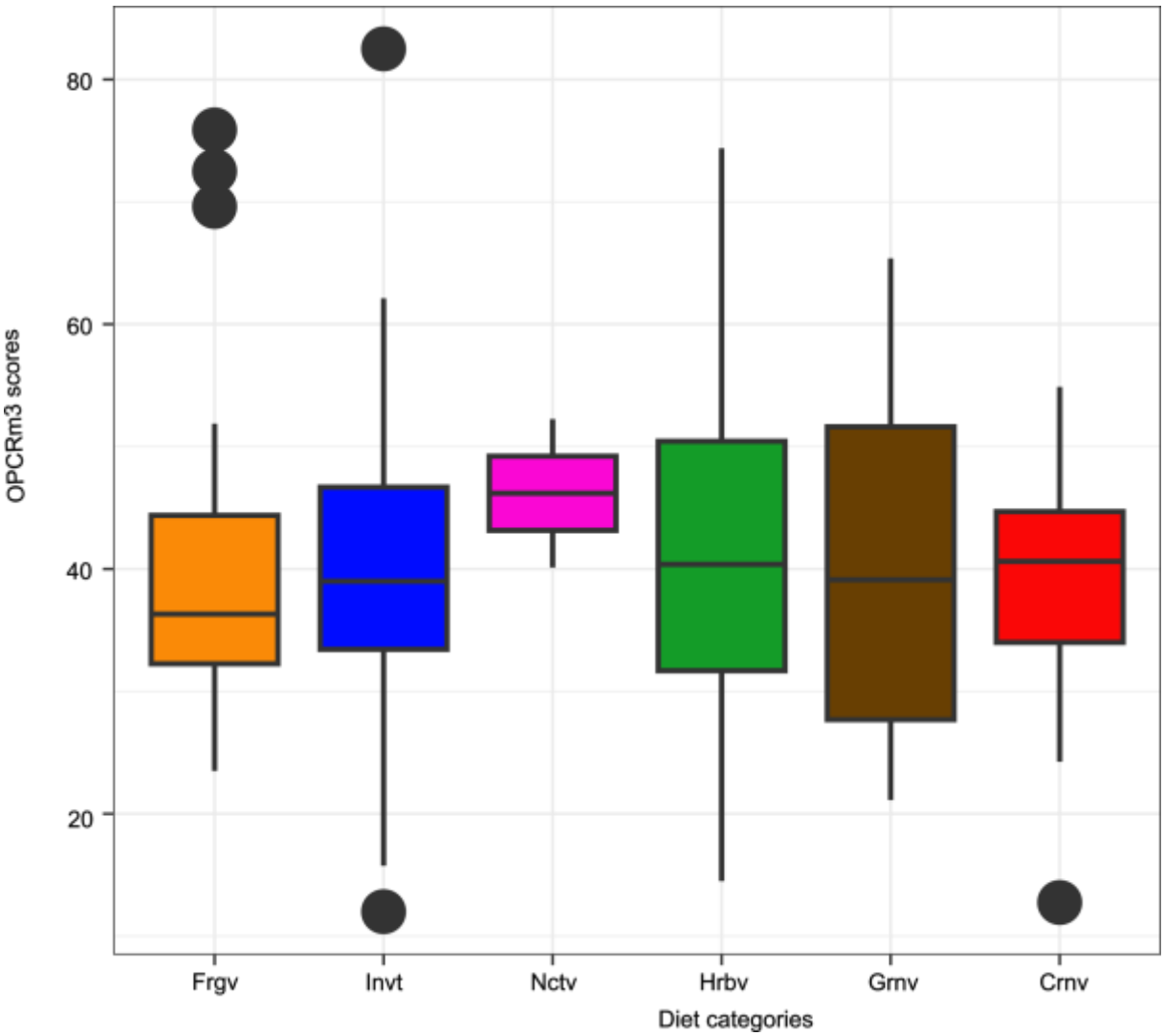


Figure 58: Box and whisker plots showing the distribution of OPCR scores for the third molar (OPCRm3) amongst mammal species within finer diet categories. Frgv= frugivore, Invt= invertivore, Nctv= nectivore, Hrbv= herbivore, Grnv= granivore, Crnv= carnivore.

13.3.5.2 OPCRm3: phylogenetic regressions (pgls)

Table 17: Phylogenetic regressions (pgls) assessing the association that OPCRm3 has with log_{10} body mass (BM), log_{10} mandible centroid size (Size) and dietary variables amongst living taxa (n=194).

Model	n	AIC	AIC w	R^2	p-value (model)	Variable	Coefficient	Std err	Pr(>|t|)
OPCRm3~BM*Granivory	194	1624.45	0.99800	0.124	**<0.001**	(Intercept)	45.43	18.65	0.016
						BM	-2.58	1.45	0.077
						Granivory	-33.56	10.96	**0.003**
						BM:Granivory	15.29	3.45	**<0.001**
OPCRm3~BM*Carnivory	194	1638.50	0.00089	0.058	**0.0099**	(Intercept)	38.21	19.39	0.050
						BM	0.21	1.62	0.898
						Carnivory	19.17	7.96	**0.017**
						BM:Carnivory	-7.61	2.51	**0.003**
OPCRm3~Granivory	194	1640.54	0.00032	0.028	**0.0195**	(Intercept)	38.18	19.13	0.047
						Granivory	11.11	4.71	**0.019**
OPCRm3~BM+Granivory	194	1641.50	0.00020	0.033	**0.0393**	(Intercept)	42.16	19.52	0.032
						BM	-1.53	1.50	0.311
						Granivory	10.63	4.74	**0.026**
OPCRm3~Size	194	1644.46	0.00005	0.008	0.2073	(Intercept)	51.31	21.66	0.019
						Size	-5.84	4.62	0.207
OPCRm3~BM	194	1644.55	0.00004	0.008	0.2196	(Intercept)	43.71	19.71	0.028
						BM	-1.86	1.51	0.220
OPCRm3~Carnivory	194	1644.78	0.00004	0.007	0.2591	(Intercept)	39.62	19.34	0.042
						Carnivory	-3.61	3.19	0.259
OPCRm3~Nectivory	194	1645.55	0.00003	0.003	0.4714	(Intercept)	38.61	19.37	0.048
						Nectivory	7.73	10.71	0.471
OPCRm3~Invertivory	194	1645.64	0.00003	0.002	0.5149	(Intercept)	37.45	19.50	0.056
						Invertivory	2.16	3.31	0.515
OPCRm3~Herbivory	194	1645.68	0.00002	0.002	0.5363	(Intercept)	39.95	19.45	0.041
						Herbivory	-1.90	3.06	0.536
OPCRm3~BM+Carnivory	194	1645.69	0.00002	0.012	0.3094	(Intercept)	43.63	19.72	0.028
						BM	-1.60	1.54	0.300

						Carnivory	-2.98	3.24	0.359
OPCRm3~Frugivory	194	1645.74	0.00002	0.002	0.5659	(Intercept)	39.23	19.39	0.044
						Frugivory	-2.00	3.49	0.566
OPCRm3~BM+Frugivory	194	1646.13	0.00002	0.010	0.3837	(Intercept)	44.22	19.76	0.026
						BM	-1.91	1.51	0.208
						Frugivory	-2.24	3.49	0.521
OPCRm3~BM+Nectivory	194	1646.22	0.00002	0.010	0.4015	(Intercept)	43.19	19.77	0.030
						BM	-1.75	1.53	0.253
						Nectivory	6.13	10.80	0.571
OPCRm3~BM+Herbivory	194	1646.45	0.00002	0.008	0.4502	(Intercept)	43.92	19.77	0.028
						BM	-1.73	1.57	0.271
						Herbivory	-0.97	3.18	0.760
OPCRm3~BM+Invertivory	194	1646.46	0.00002	0.008	0.4519	(Intercept)	42.66	20.08	0.035
						BM	-1.72	1.59	0.281
						Invertivory	1.02	3.48	0.770
OPCRm3~BM*Frugivory	194	1646.86	0.00001	0.016	0.3679	(Intercept)	45.37	19.77	0.023
						BM	-2.30	1.55	0.140
						Frugivory	-12.28	9.64	0.204
						BM:Frugivory	3.32	2.97	0.265
OPCRm3~BM*Nectivory	194	1647.26	0.00001	0.014	0.4295	(Intercept)	44.04	19.79	0.027
						BM	-2.03	1.55	0.192
						Nectivory	-33.40	42.11	0.429
						BM:Nectivory	17.90	18.42	0.333
OPCRm3~BM*Invertivory	194	1648.36	0.00001	0.009	0.6414	(Intercept)	43.67	20.39	0.034
						BM	-2.00	1.84	0.278
						Invertivory	-0.89	7.10	0.900
						BM:Invertivory	0.79	2.56	0.758
OPCRm3~BM*Herbivory	194	1648.45	0.00001	0.008	0.6612	(Intercept)	43.97	20.12	0.030
						BM	-1.75	2.14	0.413
						Herbivory	-1.06	6.69	0.875
						BM:Herbivory	0.03	1.85	0.988

The relationship that explained the most variation in OPCRm3 scores assessed the interaction effect that log_{10} body mass has with granivory (OPCRm3 ~ BM * Granivory). Granivores have a different OPCRm3 allometry pattern than non-granivores, and this relationship explained 12.4% of the variation in the model (OPCRm3 ~ BM * Granivory, R^2). The associated AIC and AIC weight (AIC w) values indicate that this is the best-fitting model, as it carries 99.8% of the cumulative model weight and has the lowest AIC score (Table 17). However, the standard error associated with the granivory coefficient is particularly high (std err = 10.96) indicative of a high degree of uncertainty (low precision) in the estimates of granivorous mammals (OPCRm3 ~ BM * Granivory, Std err).

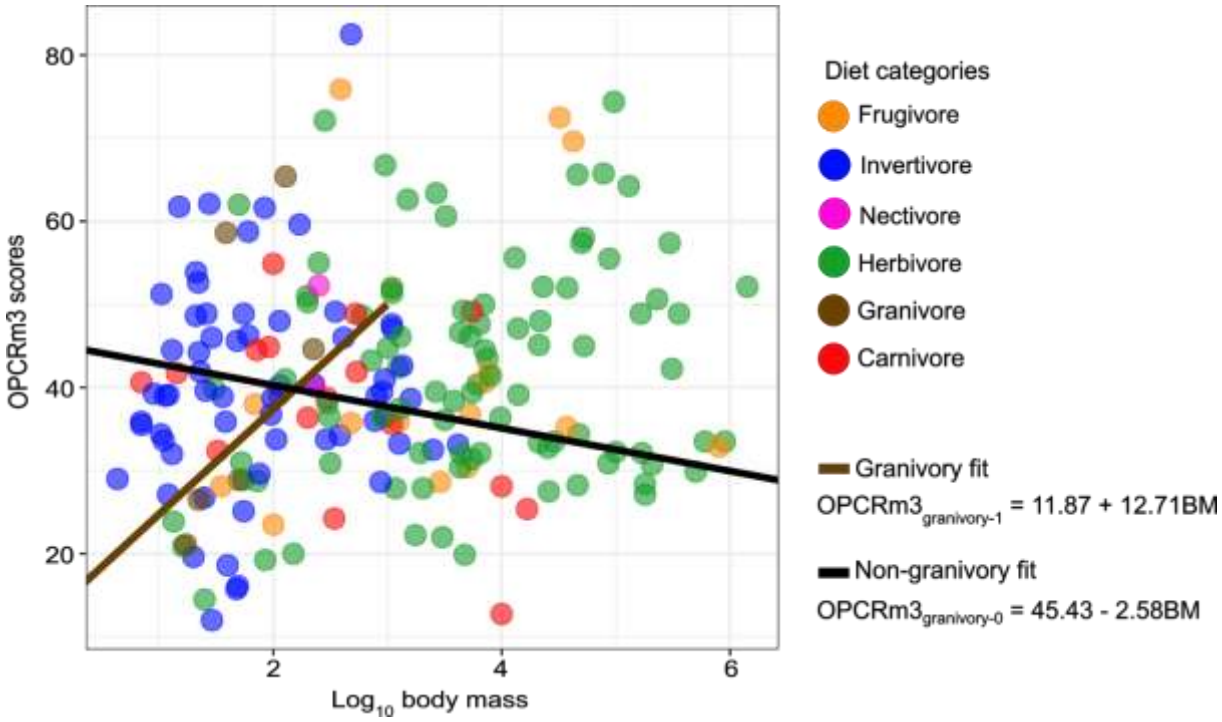


Figure 59: Scatterplot of OPCR scores for the third molar (OPCRm3) and log_{10} body mass, illustrating the interaction that log_{10} body mass has with granivory (granivory fit), relative to non-granivorous mammals (non-granivory fit). Note that granivorous mammals span a narrow range of body sizes relative to non-granivores.

According to the OPCRm3 ~ BM * Granivory model, at a body mass of 1g, a granivore will have an OPCRm3 score 33.56 times lower than non-granivores. However, with increasing body mass, a granivore's OPCRm3 sore increase 15.29 times faster than non-granivores. This means that at smaller body masses (less

than 1,000g), granivores have less complex third molars (OPCRm3), and at larger body masses (more than 1,000g), granivores have more complex third molars relative to non-granivores (Figure 59).

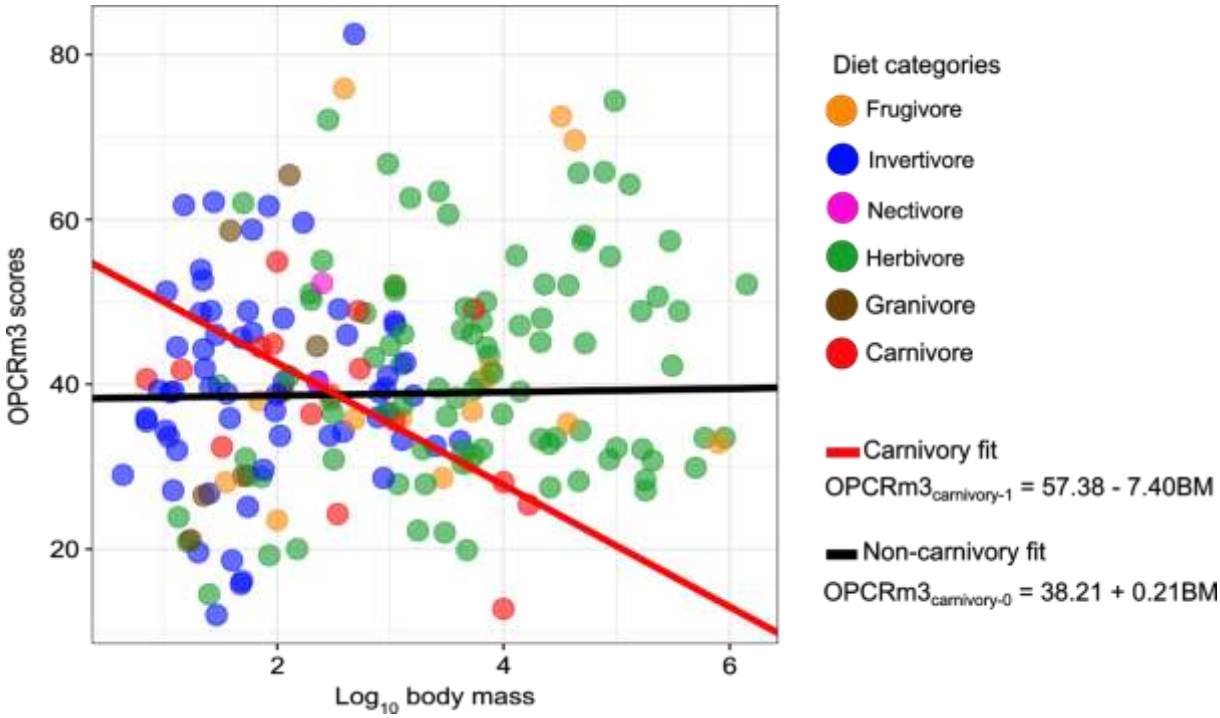


Figure 60: Scatterplot of OPCR scores for the third molar (OPCRm3) and $\log_{10}$ body mass, illustrating the interaction that $\log_{10}$ body mass has with carnivory (carnivory fit), relative to non-carnivorous mammals (non-carnivory fit).

The next-best model, OPCRm3 ~BM * Carnivory, evaluated the interaction effect between carnivory and $\log_{10}$ body mass. Carnivores' have a different OPCRm3 allometry pattern than non-carnivores, and this relationship explained 5.8% of the variation in OPCRm3 scores (OPCRm3 ~ BM * Carnivory, R^2). The associated AIC value is 14.05 units higher and carries 0.089% of the cumulative model weight (Table 17).

According to the OPCRm3 ~ BM * Carnivory model, at a body mass of 1g, a carnivore will have an OPCRm3 score 19.71 times higher than a non-carnivore. However, with increasing body mass, carnivore's OPCRm3 scores increase 7.61 times slower than non-carnivores. So, at smaller body masses (less than 1,000g), carnivores have more complex third molars (OPCRm3), and at larger body

masses (more than 1,000g), carnivores have less complex third molars relative to non-carnivores (Figure 60).

Granivory has a significant influence on OPCRm3 scores when accounting for the effect if body mass (OPCRm3 ~ BM + Granivory, R^2), or not (OPCRm3 ~ Granivory). The main effect of granivory explains 2.8% of the variation in the OPCRm3 scores (OPCRm3~Granivory, R^2). According to the OPCRm3 ~ Granivory model, on average, highly granivorous mammals have OPCRm3 scores that are 11.11 times higher than non-granivorous mammals. The partial effect of granivory explains 3.3% of the variation in OPCRm3 scores (OPCRm3~ BM + Granivory, R^2). According to this model (OPCRm3~BM+Granivory), highly granivorous mammals have OPCRm3 scores that are 10.63 times higher than non-granivorous mammals (Table 17). However, the relationship that explained the most variation in OPCRm3 scores assessed the interaction effect between granivory and $\log_{10}$ body mass (Table 17).

The relationships that the remaining dietary variables, $\log_{10}$ body mass and $\log_{10}$ mandible centroid size have with OPCRm3 were all non-significant. Apart from granivory and carnivory, the interaction effects between dietary variables and $\log_{10}$ body mass are non-significant (Table 17).

12.3.6 pDFA: OPCR

13.3.6.1 pDFA: OPCRavg and OPCRsum

The median success rate of predicting an animal's diet (herbivore, carnivore or invertivore) using OPCRavg and OPCRsum scores is 44% (P5=38, P95=51). This is approximately 15% better than randomly guessing the diet. The proportion of correct classifications varied amongst major dietary groups and using OCPRavg and OPCRsum is best at predicting the diets of invertivores (Table 18).

Table 18: Confusion table for pDFAs which estimated the diet of mammal species using OPCRavg and OPCRsum scores. Note differences in the median, 5th percentile (P5) and 95th percentile (P95) counts.

Predicted diet (pDFA)	**True diet**		
	Carnivore	Herbivore	Invertivore
Carnivore	13 (P5=2, P95=16)	6 (P5=0, P95=11)	5 (P5=1, P95=8)
Median %	43.33%	20%	16.67%
Herbivore	3 (P5=0, P95=9)	10 (P5=1, P95=16)	4 (P5=0, P95=11)
Median %	10%	33.33%	13.33%
Invertivore	14 (P5=9, P95=21)	14 (P5=9, P95=22)	21 (P5=12, P95=26)
Median %	46.67%	46.67%	70%
Median % correct	43.33%	33.33%	70%

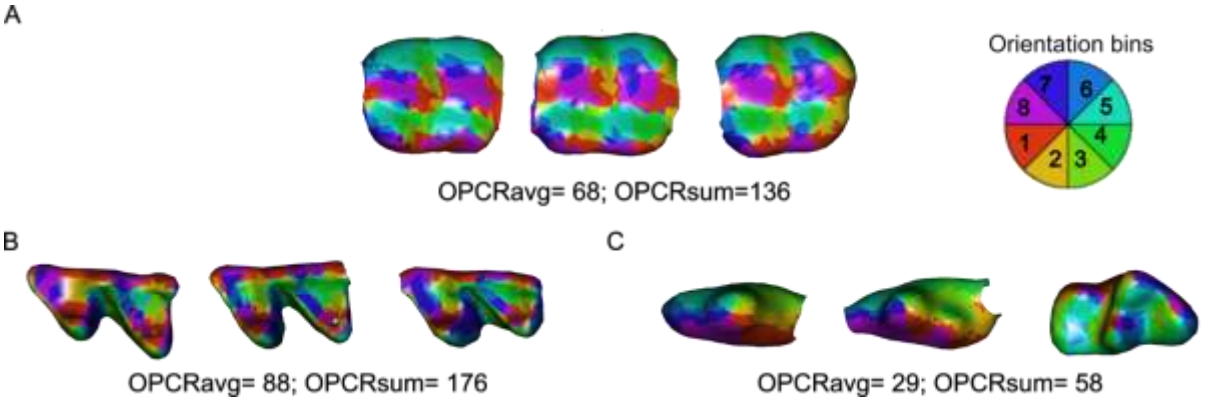


Figure 61: Occlusal views of OPCR 3D colours maps and associated OPCR scores (OPCRavg and OPCRsum) amongst A: a correctly classified invertivorous mammal (striped possum); B: an invertivorous mammal misclassified as an herbivore (star-nosed mole) and C: an invertivorous mammal misclassified as a carnivore (Malagasy civet).

An average of 30% of invertivorous mammals sampled were misclassified as carnivores or herbivores (Table 18). Invertivores were misclassified as carnivores and herbivores at similar frequencies (Table 18). Amongst invertivorous mammals correctly classified, those associated with the highest posterior probabilities had OPCRavg scores between 57 and 68; and OPCRsum scores between 114 and 136. This included the Hispaniolan solenodon (*Solenodon paradoxurus,* $PP_{invertivore}$= 0.35), northern brown bandicoot (*Isoodon obesulus,* $PP_{invertivore}$= 0.37) and the striped possum (*Dactylopsila trivirgata,* $PP_{invertivore}$= 0.37). Although these

associated posterior probabilities are the highest amongst invertivores correctly classified, they are notably only low values ($PP_{invertivore}$ =0.35—0.37). Additionally, the posterior probabilities associated invertivores misclassified as herbivores or carnivores are similarly only low values ($PP_{herbivore}$ =0.36—0.42; $PP_{carnivore}$= 0.35—0.50).

Amongst the invertivores misclassified as herbivores were afrosoricids, soricids and Macroscelididae members such as the star-nosed mole (*Condylura cristata*, $PP_{herbivore}$= 0.42), moonrat (*Echinosorex gymnure*, $PP_{herbivore}$= 0.36), and the North African elephant shrew (*Elephantulus rozeti*, $PP_{herbivore}$= 0.39). Invertivorous mammals misclassified as herbivores generally had OPCRavg scores between 69 and 120; and OPCRsum scores between 62 and 240, however, those associated with the highest posterior probabilities, such as the star-nosed mole ($PP_{herbivore}$= 0.42), have relatively high OPCR scores (Figure 61).

Invertivores misclassified as carnivores included mostly afrosoricids and members of Carnivora such as the Cape golden mole (*Chrysochloris asiatica*, $PP_{carnivore}$= 0.53), Stuhlmann's golden mole (*Chrysochloris stuhlmanni,* $PP_{carnivore}$= 0.41), Ruwenzori otter shrew (*Micropotamogale ruwenzorii*, $PP_{carnivore}$=0.35), marsh mongoose (*Atilax paludinosus*, $PP_{carnivore}$=0.36) and the meerkat (*Suricata suricatta*, $PP_{carnivore}$=0.37). Invertivorous mammals misclassified as carnivores generally had OPCRavg scores between 22 and 55, and OPCRsum scores between 44 and 109, and those associated with the highest posterior probabilities, such as the Malagasy civet (*Fossa fossana,* $PP_{carnivore}$= 0.50), have relatively low OPCR scores (Figure 61).

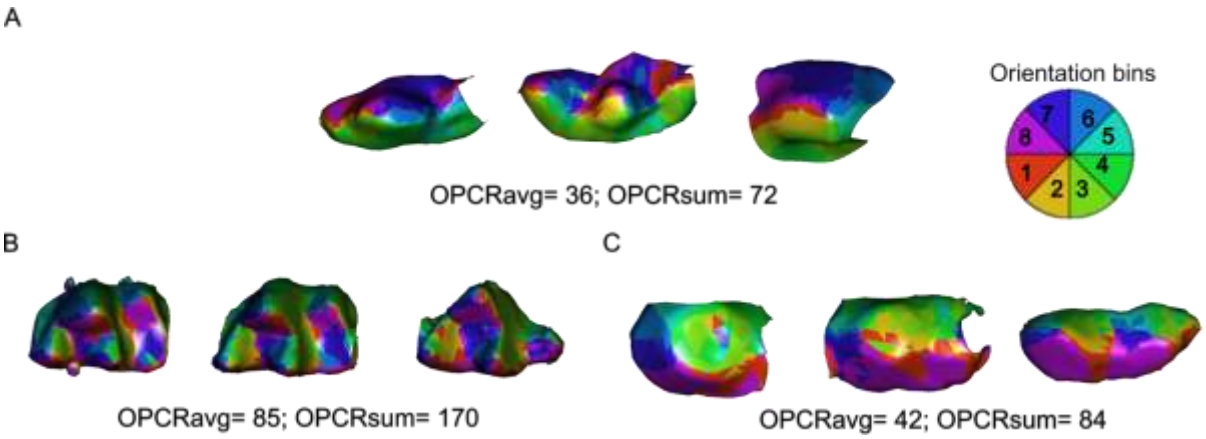


Figure 62: Occlusal views of OPCR 3D colours maps and associated OPCR scores (OPCRavg and OPCRsum) amongst A: a correctly classified carnivorous mammal (European polecat); B: a carnivorous mammal misclassified as an invertivore (crest-tailed mulgara) and C: a carnivorous mammal misclassified as an herbivore (spotted hyaena).

An average of 56.67% of the carnivorous mammals sampled were misclassified as invertivores or herbivores (Table 18). Amongst carnivorous mammals correctly classified, those associated with the highest posterior probabilities had OPCRavg scores between 36 and 44; and OPCRsum scores between 69 and 88. This included the European polecat (*Mustela putorius,* $PP_{carnivore}$= 0.41), caracal (*Caracal caracal,* $PP_{carnivore}$= 0.40) and the domestic cat (*Felis catus* $PP_{carnivore}$= 0.38). Although these associated posterior probabilities are the highest amongst carnivores correctly classified, they are notably only low values ($PP_{carnivore}$ =0.38—0.41). Additionally, the posterior probabilities associated with carnivores misclassified as invertivores or herbivores are similarly low values ($PP_{invertivore}$ =0.36—0.41; $PP_{herbivore}$= 0.40—0.43).

Carnivorous mammals were more frequently misclassified as invertivores (Table 18). These included many hypercarnivorous dasyuromorphs, soricids and Carnivora members, such as the Tasmanian devil (*Sarcophilus harrisii*, $PP_{invertivore}$= 0.37), eastern quoll (*Dasyurus viverrinus*, $PP_{invertivore}$= 0.37), coyote (*Canis latrans*, $PP_{invertivore}$ = 0.36), mountain lion (*Puma concolor*, $PP_{invertivore}$= 0.36), elegant water shrew (*Nectogale elegans*, $PP_{invertivore}$= 0.37) and the piebald shrew (*Diplomesodon pulchellum,* $PP_{invertivore}$= 0.36). Carnivorous mammals misclassified as invertivores generally had OPCRavg scores between 35 and 70;

and OPCRsum scores between 70 and 146; however, those associated with the highest posterior probabilities, such as the crest-tailed mulgara (*Dasycercus cristicauda,* $PP_{invertivore}$= 0.41), had relatively high OPCR scores (Figure 62).

Carnivorous mammals that were misclassified as herbivores mostly included members of Carnivora and soricids, such as the spotted hyena (*Crocuta crocuta*, $PP_{herbivore}$= 0.43), margay (*Leopardus wiedii*, $PP_{herbivore}$= 0.40) and the Pyrenean desman (*Galemys pyrenaicus*, $PP_{herbivore}$= 0.41) were also misclassified. These species had OPCRavg scores that ranged from 27 to 85, and OPCRsum scores that ranged from 41 to 171. The carnivorous mammals misclassified as herbivores generally had OPCRavg scores between 27 and 85; and OPCRsum scores between 41 and 171. Amongst carnivorous mammals misclassified as herbivores those associated with the highest posterior probabilities, such as the spotted hyena ($PP_{herbivore}$= 0.43), had relatively high OPCR scores (Figure 62).

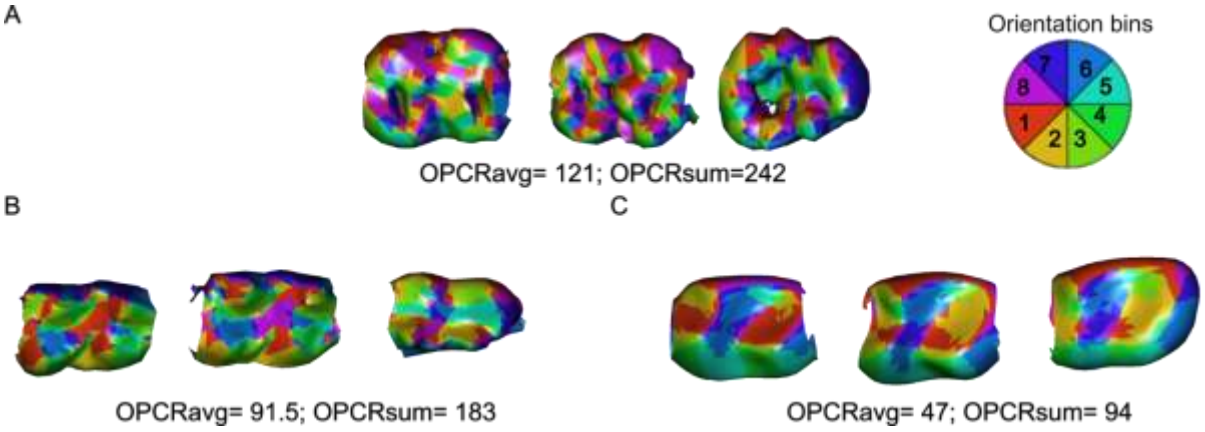


Figure 63: Occlusal views of OPCR 3D colours maps and associated OPCR scores (OPCRavg and OPCRsum) amongst A: a correctly classified herbivorous mammal (Beecrofti's flying squirrel); B: a herbivorous mammal misclassified as an invertivore (lemuroid ringtail possum) and C: a herbivorous mammal misclassified as a carnivore (black lemur).

Using OPCRavg and OPCRsum scores was worst at identifying herbivores, and on average 67% of the herbivorous mammals sampled were misclassified as invertivores or carnivores (Table 18). Amongst herbivorous mammals correctly classified, those associated with the highest posterior probabilities had OPCRavg scores between 72 and 121; and OPCRsum scores 108 and 242. This included the rufous rat kangaroo (*Aepyprymnus rufescens,* $PP_{herbivore}$= 0.78), Beecroft's

flying squirrel (*Anomalurus beecrofti,* $PP_{herbivore}$= 0.52) and the South American tapir (*Tapirus terrestris* $PP_{herbivore}$= 0.48). The posterior probabilities amongst herbivores correctly classified are highly variable ($PP_{herbivore}$ =0.48—0.78), however, they are notably not only low values. The posterior probabilities associated herbivores misclassified as invertivores or carnivores are notably only low values ($PP_{invertivore}$ =0.36—0.42; $PP_{carnivore}$= 0.37—0.41).

Amongst herbivores misclassified as invertivores were artiodactyls, rodents, primates, diprotodontians and herbivorous members of Carnivora. These included many grazers, such as the pronghorn (*Antilocapra americana*, $PP_{invertivore}$= 0.40), dorcas gazelle (*Gazella dorcas*, $PP_{invertivore}$= 0.37), sheep (*Ovis aries,* $PP_{invertivore}$=0.39), Vicuña (*Vicugna viguna*, $PP_{invertivore}$= 0.36), and the southern hairy-nosed wombat (*Lasiorhinus latifrons,* $PP_{invertivore}$= 0.38). Relatively more herbivorous Carnivora members were also misclassified, this included the red panda (*Ailurus fulgens*, $PP_{invertivore}$= 0.38) and the brown bear (*Ursus arctos*, $PP_{invertivore}$= 0.36). Rodents such as the lesser Egyptian gerbil (*Gerbillus gerbillus*, $PP_{invertivore}$= 0.37), arrow flying squirrel (*Petinomys sagitta,* $PP_{invertivore}$= 0.40), and the eastern chipmunk (*Tamias striatus*, $PP_{invertivore}$= 0.36). Herbivorous mammals misclassified as invertivores had OPCR average scores between 45 and 91; and OPCRsum scores between 91 and 183. However, those associated with the highest posterior probabalities, such as the lemuroid ringtail possum (*Hemibelideus lemuroides,* $PP_{invertivore}$= 0.42), had relatively high OPCR scores (Figure 63).

Herbivorous species that were misclassified as carnivores included mostly primates, rodents and Carnivora members such as the aye-aye (*Daubentonia madagascariensis*, $PP_{carnivore}$= 0.42), black lemur (*Eulemur macaco*, PPcarnivore = 0.41), southeastern pocket gopher (*Geomys pinetus*, $PP_{carnivore}$= 0.38), naked mole-rat (*Heterocephalus glaber*, $PP_{carnivore}$= 0.40), brown bear (*Ursus arctos*, $PP_{carnivore}$= 0.39) and the African palm civet (*Nandinia binotata*, $PP_{carnivore}$= 0.37). Herbivorous mammals misclassified as carnivores had OPCRavg scores between 35 and 54; and OPCRsum scores between 71 and 107. However, those associated with the highest posterior probabilities, such as the black lemur (*Eulemur macaco*, $PP_{carnivore}$ = 0.41) had relatively low OPCR scores (Figure 63).

When OPCRavg and OPCRsum scores were used to estimate the diet of cynodont species, most cynodont species were estimated as carnivores or invertivores (Table 19)

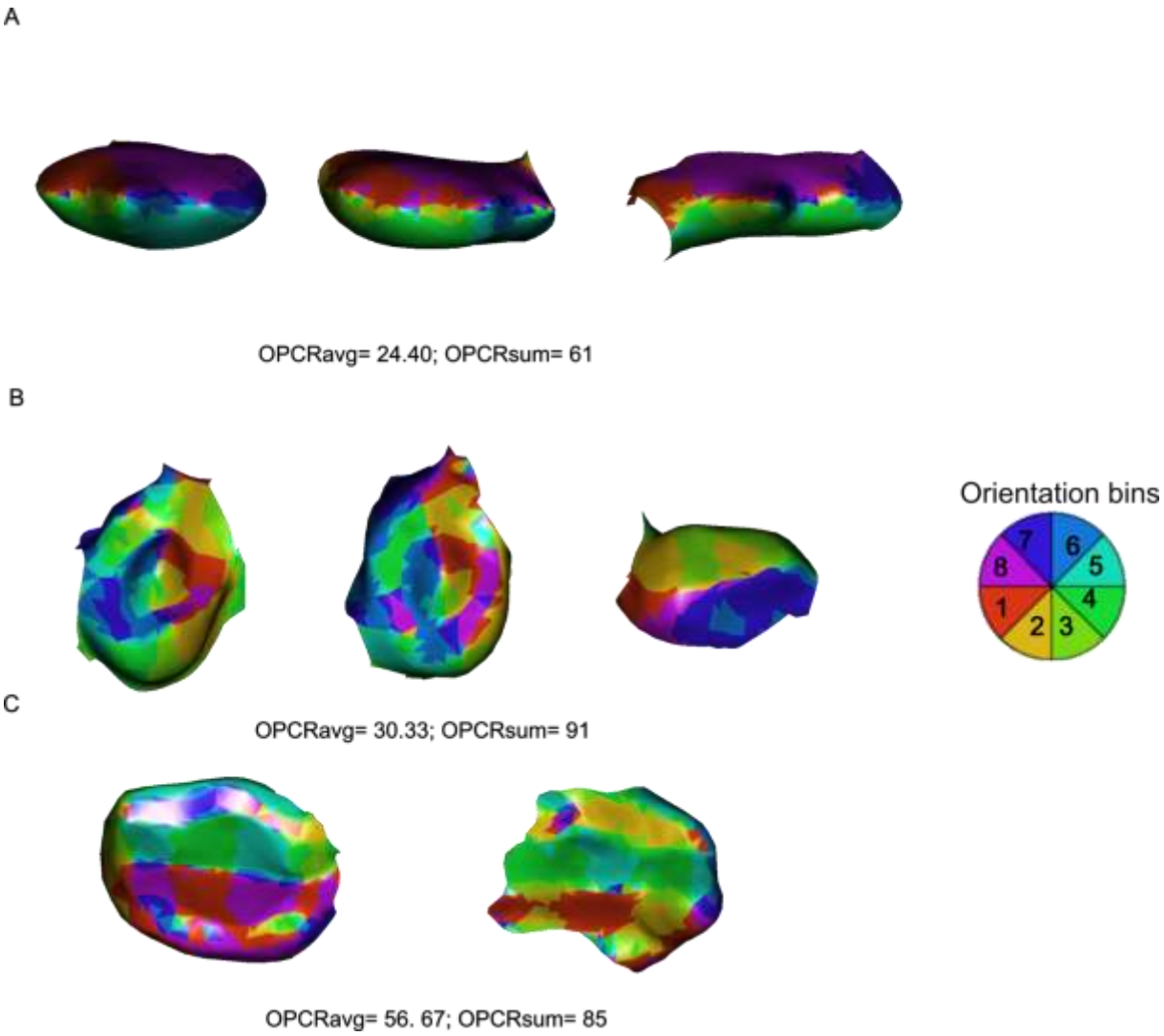


Figure 64: Occlusal views of OPCR 3D colour maps and associated OPCR scores (OPCRavg and OPCRsum) in cynodont species that pDFA iterations estimated as A: a carnivore (*Trirachodon sp.*); B: an invertivore (*Langbergia modisei*) and C: a herbivore (*Cricodon metabolus*). Note gradient of OPCRavg scores from carnivore to herbivore estimates.

Table 19: The estimated diets of cynodont species associated with the pDFAs which that used using OPCRavg and OPCRsum scores as input predictor variables. Note differences in median, 5th (P5) percentile and 95th percentile (P95) posterior probabilities.

Taxon	Expected diet	Predicted diet	Posterior probability
Andescynodon mendozensis	Herbivore	Insectivore	0.46 (P5=0.29, P95=0.61)
Andescynodon sp.	Herbivore	Insectivore	0.46 (P5=0.30, P95=0.61)
Cricodon metabolus	Herbivore	Herbivore	**0.95** (P5=0.36, P95=**0.99**)
Cricodon sp.	Herbivore	Insectivore	0.45 (P5=0.27, P95=0.64)
Cynognathus crateronotus	Carnivore	Carnivore	0.49 (P5=0.30, P95=0.73)
Diademodon tetragonus	Herbivore	Insectivore	0.46 (P5=0.32, P95=0.58)
Exaeretodon argentinus	Herbivore	Carnivore	0.43 (P5=0.25, P95=0.72)
Langbergia modisei	Herbivore	Insectivore	0.51 (P5=0.37, P95=0.65)
Luangwa sudamericana	Herbivore	Insectivore	0.49 (P5=0.42, P95=0.57)
Massetognathus pascuali	Herbivore	Invertivore	0.41 (P5=0.26, P95=0.54)
Megazostrodon rudnerae	Insectivore	Herbivore	0.48 (P5=0.25, P95=0.72)
Menadon besairiei	Herbivore	Carnivore	0.48 (P5=0.33, P95=0.67)
Pascualgnathus polanskii	Herbivore	Carnivore	0.42 (P5=0.29, P95=0.59)
Santacruzodon hopsoni	Herbivore	Insectivore	0.47 (P5=0.41, P95=0.54)
Traversodontid sp.	Herbivore	Carnivore	0.45 (P5=0.17, P95=0.74)
Trirachodon berryi	Herbivore	Carnivore	0.63 (P5=0.34, P95=0.89)
Trirachodon sp.	Herbivore	Carnivore	0.56 (P5=0.31, P95=0.81)
Trirachodontid sp.	Herbivore	Herbivore	0.82 (P5=0.14, P95=**0.99**)

Notably *Cynognathus* ($PP_{carnivore}$= 0.49) was estimated as a carnivore when using OPCRavg and OPCRsum scores. This coincides with the hypothesized diet, although the low posterior probability is indicative of a high level of uncertainty (Table 19).

Most gomphodont species, were estimated as carnivores and invertivores. These are all species which are expected to be herbivorous based off morphological observations. Amongst gomphodonts were many traversodontids such as *Massetognathus (*$PP_{invertivore}$= 0.41*)*, *Exaeretodon (*$PP_{carnivore}$= 0.43*)*, *Menadon (*$PP_{carnivore}$= 0.48*), and Pascualgnathus (*$PP_{carnivore}$= 0.42*)*. The posterior probabilities associated with this are low (less than 0.5), indicating a high level of uncertainty. Amongst gomphodont species included, only the trirachodontids, *Cricodon metabolus (*$PP_{herbivore}$= 0.95*)* and *Trirachodon sp (*$PP_{herbivore}$= 0.82*)* were estimated as herbivorous – the posterior probabilities associated with these classifications were high (greater than 0.75), indicative of high certainty.

Megazostrodon ($PP_{herbivore}$=0.48) was estimated as herbivore using OPCRavg and OPCRsum scores, although the posterior probability associated with this classification is low (less than 0.5), indicative of a high level of uncertainty (Table 19).

13.3.6.2 pDFA: OPCRm1-m3

Table 20: Confusion table for pDFAs which estimated diet using OPCRm1-m3 scores. Note differences in the median, 5th percentile (P5) and 95th percentile (P95) counts.

Predicted diet (pDFA)	**True diet**		
	Carnivore	Herbivore	Invertivore
Carnivore	9 (P5=6, P95=11)	4 (P5=2, P95=6)	4 (P5=2, P95=6)
Median %	60%	26.67%	26.67%
Herbivore	3 (P5=1, P95=5)	7 (P5=3, P95=10)	5 (P5=1, P95=7)
Median %	20%	46.67%	33.33%
Insectivore	3 (P5=1, P95=5)	4 (P5=2, P95=7)	6 (P5=3, P95=10)
Median %	20%	26.67%	40%
Median % correct	60%	46.67%	40%

The median success rate of predicting an animal's diet (herbivore, carnivore or invertivore) using the dental complexity of the molars (m1-m3) is 48% (P5=40, P95=57). This is approximately 21% better than randomly guessing the diet (33.33%). This is approximately 7% better than using OPCRavg and OPCRsum

scores (44%). The proportion of correct classifications varied amongst major dietary groups and using OPCRm1-m3 scores were best at predicting the diets of carnivores. It was relatively less useful in predicting the diets of herbivores and invertivores (Table 20).

An average of 40% carnivorous species sampled were misclassified as herbivores or invertivores. Amongst carnivorous mammals correctly classified, those associated with the highest posterior probabilities had OPCRm1-m3 values between 12 and 60. This included the western quoll (*Dasyurus hallucatus,* $PP_{carnivore}$= 0.65), Tasmanian devil (*Sarcophilus harrisii*, $PP_{carnivore}$= 0.55), and the piebald shrew (*Diplomesodon pulchellum,* $PP_{carnivore}$= 0.53). Notably, the highest posterior probabilities associated with correctly classified carnivores are only medium values ($PP_{carnivore}$= 0.53—0.65). Additionally, the posterior probabilities associated with carnivores misclassified as herbivores or invertivores are only low-to-medium values ($PP_{herbivore}$ =0.38—0.51; $PP_{invertivore}$= 0.35—0.46).

Carnivores were misclassified as invertivores or herbivores at similar frequencies (Table 20). Soricids, canids and afrosoricids were misclassified as herbivores, such as the Pyrenean desman (*Galemys pyrenaicus*, $PP_{herbivore}$= 0.49), Eurasian water shrew (*Neomys fodiens,* $PP_{herbivore}$= 0.39), greater cane rat (*Setifer setosus*, $PP_{herbivore}$= 0.41) and the Ethiopian wolf (*Canis simensis*, $PP_{herbivore=}$ 0.51). The Cameroon scaly-tail (*Zenkerella insignis*, $PP_{herbivore}$= 0.38), a cryptic rodent, was also classified as a herbivore. Carnivorous mammals misclassified as herbivores had OPCRm1-m3 scores between 13 and 56, and those associated with the highest posterior probabilities, such as the Ethiopian wolf (*Canis simensis*, $PP_{herbivore=}$ 0.51), had relatively high OPCR scores (Figure 65).

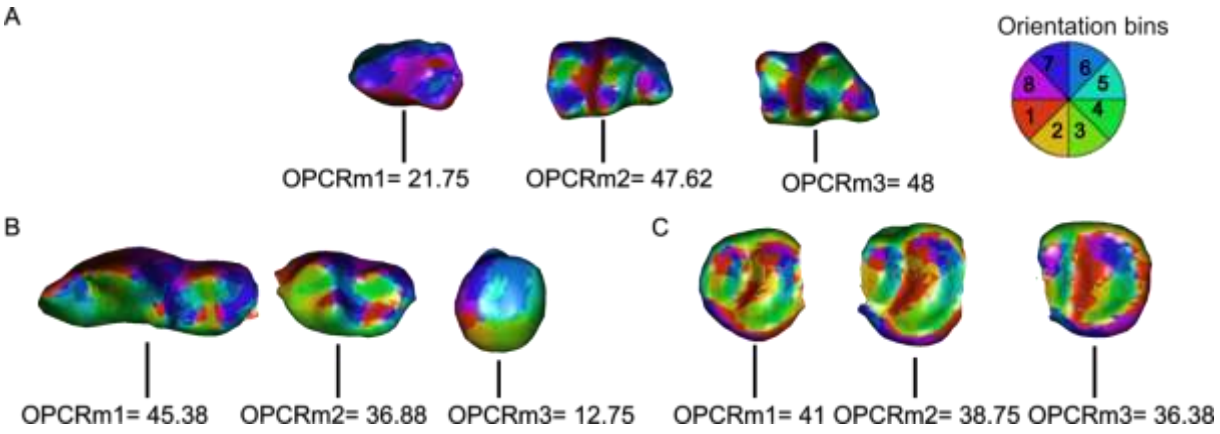


Figure 65: Occlusal views of OPCR 3D colours maps and associated OPCR scores (OPCRm1-m3) amongst A: a correctly classified carnivorous mammal (western quoll); B: a carnivorous mammal misclassified as an herbivore (Ethiopian wolf); and C: a carnivorous mammal misclassified as an invertivore (Cameroon scaly-tail).

The carnivorous species that had been misclassified as invertivores include the Eurasian water shrew (*Neomys fodiens*, $PP_{invertivore}$= 0.35), Pyrenean desman (*Galemys pyrenaicus,* $PP_{invertivore}$= 0.46), greater cane rat (*Setifer setosus*, $PP_{invertivore}$= 0.38) and the Cameroon scaly-tail (*Zenkerella insignis*, $PP_{invertivore}$= 0.41). Carnivorous mammal species misclassified as invertivores had OPCRm1-m3 between 31 and 59, and those associated with the highest posterior probabilities, such as the Cameroon scaly-tail (*Zenkerella insignis*, $PP_{invertivore}$= 0.41), had relatively lower OPCR scores (Figure 65).

An average of 53% of the herbivorous mammal species sampled were misclassified as carnivores or invertivores (Table 20). Herbivores were misclassified as carnivores and herbivores at similar frequencies (Table 20). Amongst herbivorous mammals correctly classified, those associated with the highest posterior probabilities had OPCRm1-m3 values between 42 and 80. This included the impala (*Aepyceros melampus,* $PP_{herbivore}$= 0.65), Malayan tapir (*Tapirus indicus*, $PP_{herbivore}$= 0.55), and the wild boar (*Sus scrofa,* $PP_{herbivore}$= 0.53). Notably, the highest posterior probabilities associated with correctly classified herbivores are only medium values ($PP_{herbivore}$= 0.53—0.65). Additionally, the posterior probabilities associated with herbivores misclassified as carnivores or

invertivores are only low-to-medium values ($PP_{carnivore}$ =0.39—0.64; $PP_{invertivore}$= 0.33—0.52).

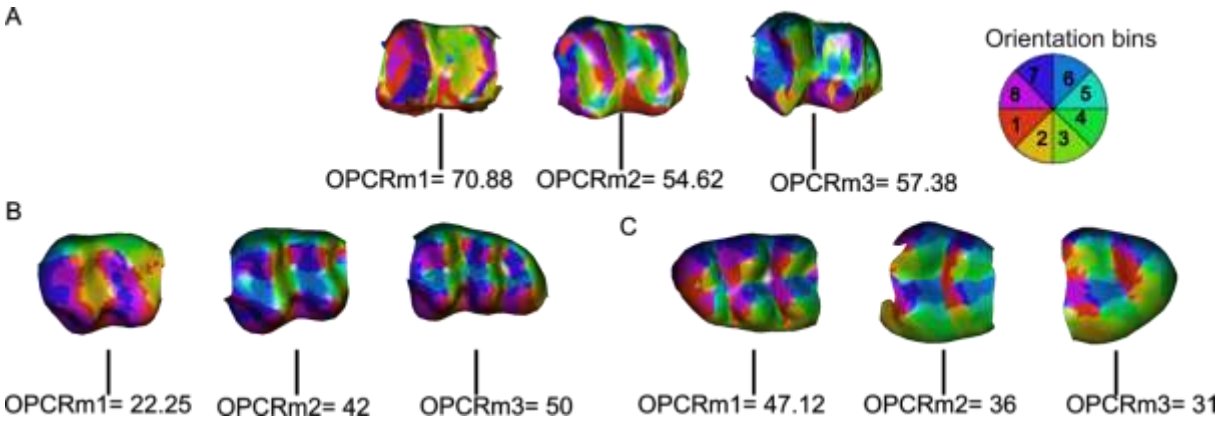


Figure 66: Occlusal views of OPCR 3D colours maps and associated OPCR scores (OPCRm1-m3) amongst A: a correctly classified herbivorous mammal (impala); B: a herbivorous mammal misclassified as an invertivore (Cairo spiny mouse); and C: a herbivorous mammal misclassified as an carnivore (Barbary macaque).

Herbivorous mammal species that were misclassified as carnivores included artiodactyls, rodents and diprotodontians such as the moose (*Alces alces*, $PP_{carnivore}$= 0.39), mountain beaver (*Aplodontia rufa*, $PP_{carnivore}$= 0.39), and the common brushtail possum (*Trichosurus vulpecula*, $PP_{carnivore}$=0,45). These species had OPCR scores between 26 and 60. Herbivorous mammals misclassified as carnivores had OPCRm1-m3 scores between 26 and 60, and those associated with the highest posterior probabilities, such as the Barbary macaque (*Macaca sylvanus,* $PP_{carnivore}$= 0.64), had relatively lower OPCR scores (Figure 66).

Herbivorous mammals that were misclassified as invertivores included mostly artiodactyls such as the saiga antelope (*Saiga tatarica*, $PP_{invertivore}$= 0.47), fallow deer (*Dama dama*, $PP_{invertivore}$=0.44), red deer (*Cervus elephus*, $PP_{invertivore}$= 0.38) and the hippopotamus (*Hippopotamus amphibius*, $PP_{invertivore}$= 0.39). However, this also included rodents such as Siberian zokor (*Myospalax myospalax*, $PP_{invertivore}$= 0.33), Patagonian mara (*Dolichotis patagonum*, $PP_{invertivore}$= 0.38); and primates such as the diademed sifaka (*Propithecus diadema*, $PP_{invertivore}$=0.44) and the sooty langur (*Presbytis femoralis*, $PP_{invertivore}$= 0.39). Herbivorous mammals misclassified as invertivores had OPCR scores between 23 and 56, and

those associated with the highest posterior probabilities, such as the Cairo spiny mouse (*Acomys cahirinus,* $PP_{invertivore}$= 0.52), had relatively low OPCR scores (Figure 66).

An average of 60% of the invertivorous mammals sampled were misclassified as carnivores or herbivores. Amongst invertivorous mammals correctly classified, those associated with the highest posterior probabilities had OPCRm1-m3 scores between 16 and 44. This included the Cape golden mole (*Chrysochloris asiatica,* $PP_{invertivore}$= 0.44), Hispaniolan solenodon (*Solenodon paradoxurus,* $PP_{invertivore}$= 0.39) and the gray mouse lemur (*Microcebus murinus,* $PP_{invertivore}$= 0.37). Notably, the highest posterior probabilities associated with correctly classified invertivores are only low values ($PP_{invertivore}$= 0.37—0.44). Additionally, the posterior probabilities associated with invertivores misclassified as herbivores or carnivores are only low-to-medium values ($PP_{herbivore}$ =0.38—0.64; $PP_{carnivore}$= 0.35—0.64).

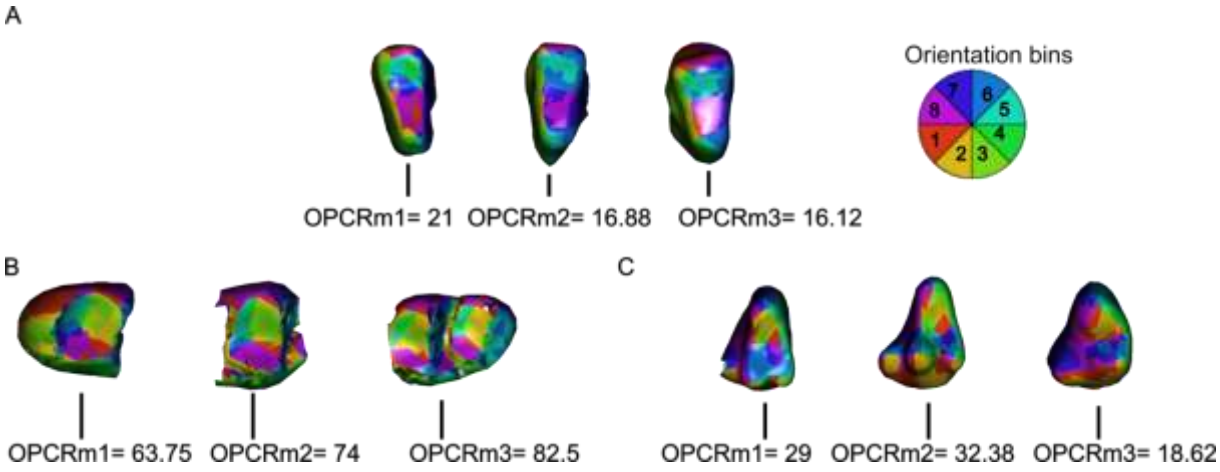


Figure 67: Occlusal views of OPCR 3D colours maps and associated OPCR scores (OPCRm1-m3) amongst A: a correctly classified invertivorous mammal (Cape golden mole); B: an invertivorous mammal misclassified as a herbivore (Rakali water rat); and C: an invertivorous mammal misclassified as a carnivore (Stuhlmann's golden mole).

Invertivores were more commonly misclassified as herbivores than carnivores. Invertivorous species that were commonly misclassified as herbivores included afrosoricids, dasyuromorphs and Paucituberculata members, such as Drouhard's shrew tenrec (*Microgale drouhardi*, $PP_{herbivore}$= 0.48), Stuhlmann's golden mole (*Chrysochloris stuhmanni*, $PP_{herbivore}$=0.64), Andean shrew opossum

(*Rhyncholestes raphanurus*, $PP_{herbivore}$= 0.38), Inca mouse (*Lestoros inca*, $PP_{herbivore}$= 0.44), and the fat-tailed dunnart (*Sminthopsis crassicaudata*, $PP_{herbivore}$= 52). Invertivorous mammals misclassified as herbivores had OPCRm1-m3 scores between 16 and 68; however, and those associated with the highest posterior probabilities, such as the Rakali water rat (*Hydromys chrysogaster,* $PP_{herbivore}$= 0.53), have relatively high OPCR scores (Figure 67).

Invertivorous species that were frequently misclassified as carnivores included afrosoricids, soricids, macroscelids and members from Peramelemorphia. This included Stuhlmann's golden mole (*Chrysochloris stuhmanni*, $PP_{carnivore}$= 0.64), tailless tenrec (*Tenrec ecaudatus*, $PP_{carnivore}$= 0.48), Howell's forest shrew (*Sylvisorex howelli*, $PP_{carnivore}$= 0.39), bicolored musk shrew (*Crocidura fuscomurina*, $PP_{carnivore}$= 0.41), greater bilby (*Macrotis lagotis*, $PP_{carnivore}$= 0.35), and the common echymipera (*Echymipera rufescens*, $PP_{carnivore}$= 0.50). Invertivorous mammals misclassified as carnivores had OPCRm1-m3 scores between 9 and 69, and those associated with the highest posterior probabilities, such as Stuhlmann's golden mole (*Chrysochloris stuhmanni*, $PP_{carnivore}$=0.64), have relatively low OPCR scores (Figure 67).

When OPCRm1-m3 scores were used to estimate the diet of cynodonts, most cynodont species were estimated as carnivores or invertivores. *Cynognathus* ($PP_{invertivore}$= 0.32), the only hypothesized carnivorous non-mammalian cynodont sampled, was estimated as an invertivore. However, the associated posterior probability is low, indicative of a high level of uncertainty (Table 21).

Table 21: The estimated diets of cynodont species associated with the pDFAs which that used using OPCRm1-m3 scores as the input predictor variables. Note differences in median, 5th percentile (P5) and 95th percentile (P95) posterior probabilities.

Taxon	Expected diet	Predicted diet	Posterior probability
Andescynodon mendozensis	Herbivore	Invertivore	0.35 (P5=0.05, P95=0.76)
Andescynodon sp.	Herbivore	Carnivore	0.73 (P5=0.20, P95=**0.96**)
Cricodon sp.	Herbivore	Carnivore	**0.97** (P5=0.77, P95=**0.99**)
Cynognathus crateronotus	Carnivore	Invertivore	0.32 (P5=0.04, P95=0.77)
Diademodon tetragonus	Herbivore	Herbivore	0.32 (P5=0.04, P95=0.78)
Exaeretodon argentinus	Herbivore	Carnivore	0.41 (P5=0.18, P95=0.75)
Langbergia modisei	Herbivore	Carnivore	0.51 (P5=0.11, P95=**0.91**)
Luangwa sudamericana	Herbivore	Herbivore	0.44 (P5=0.20, P95=0.72)
Massetognathus pascuali	Herbivore	Invertivore	0.37 (P5=0.06, P95=0.79)
Megazostrodon rudnerae	Insectivore	Herbivore	0.78 (P5=0.005, P95=**0.99**)
Menadon besairiei	Herbivore	Carnivore	0.39 (P5=0.10, P95=0.78)
Pascualgnathus polanskii	Herbivore	Carnivore	0.38 (P5=0.10, P95=0.78)
Santacruzodon hopsoni	Herbivore	Herbivore	0.53 (P5=0.13, P95=0.88)
Traversodontid sp.	Herbivore	Herbivore	0.51 (P5=0.15, P95=0.85)
Trirachodontid sp.	Herbivore	Carnivore	0.62 (P5=0.15, P95=**0.96**)

Most gomphodont species were estimated as carnivores or invertivores, amongst these were trirachodontids such as *Cricodon sp* ($PP_{carnivore}$= 0.97), *Langbergia* ($PP_{carnivore}$= 0.51) and *Trirachodon sp* ($PP_{carnivore}$= 0.61). The posterior probability associated with *Cricodon sp* is particularly high (greater than 0.75), indicative of a high certainty in this classification. However, the posterior probabilities associated with other trirachodontids such as *Langbergia* and *Trirachodon sp* have medium values, indicative of high uncertainty. Traversodontids such as *Andescynodon sp* ($PP_{carnivore}$= 0.73), *Exaeretodon* ($PP_{carnivore}$= 0.41), *Massetognathus* ($PP_{invertivore}$=

0.37) *and Pascualgnathus* ($PP_{carnivore}$= 0.38) were estimated as invertivores or carnivores- however apart from *Andescynodon sp*, the posterior probabilities associated with these classifications were mostly low values (less than 0.5) indicative of high uncertainty. Some gomphodonts were estimated as herbivores, such as *Diademodon* ($PP_{herbivore}$= 0.32), *Luangwa* ($PP_{herbivore}$= 0.44), *Santacruzodon* ($PP_{herbivore}$= 0.53) and *Traversodon sp* ($PP_{herbivore}$= 0.51). The posterior probabilities of these predictions were low to medium values (between 0.3 and 0.75), indicative of high uncertainty (Table 21).

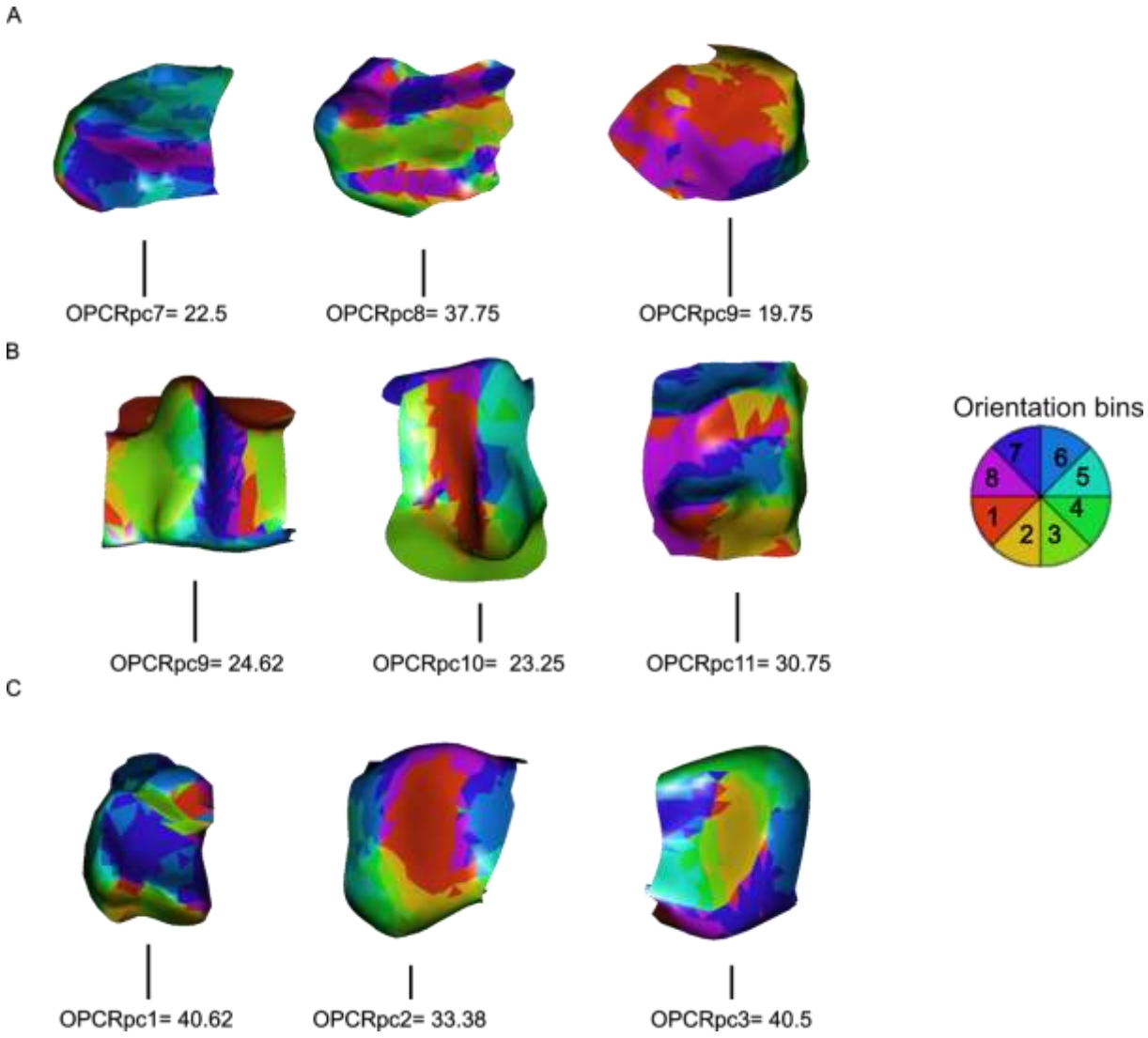


Figure 68: Occlusal views of OPCR 3D colour maps and associated OPCR scores in cynodont species estimated as A: a carnivore (*Cricodon sp.*); B: an invertivore (*Massetognathus*) and C: a herbivore (*Santacruzodon*).

Megazostrodon ($PP_{herbivore}$= 0.78*)*, a hypothesized invertivore, was estimated as an herbivore. The posterior probability associated with this classification is relatively high (greater than 0.75) indicative of high certainty (Table 21).

13.3.6.3 pDFA: OPCRm1-m3 and log_{10} body mass

The median success rate of predicting an animal's diet (herbivore, carnivore or invertivore) using the dental complexity scores of the molars (m1-m3) and log_{10} body mass is 66% (P5=55, P95=75). This is approximately 48% better than randomly guessing the diet, and 34% better than using only OPCRm1-m3 scores. Additionally, it is 28% better than using only size.

Table 22: Confusion table for pDFAs which estimated diet using OPCRm1-m3 scores and log_{10} body mass. Note differences in the median, 5th (P5) percentile and 95th percentile (P95) counts.

Predicted diet (pDFA)	**True diet**		
	Carnivore	Herbivore	Invertivore
Carnivore	9 (P5=7, P95=10)	3 (P5=1, P95=5)	3 (P5=1, P95=5)
Median %	60%	20%	20%
Herbivore	2 (P5=1, P95=4)	10 (P5=7, P95=12)	1 (P5=0, P95=3)
Median %	13.33%	66.67%	6.67%
Invertivore	4 (P5=1, P95=4)	2 (P5=1, P95=5)	11 (P5=9, P95=13)
Median %	26.67%	13.33%	73.33%
Median % correct	60%	66.67%	73.33%

An average of 27% of the invertivores sampled were misclassified as carnivores or herbivores (Table 22). Amongst invertivorous species correctly classified, those associated with the highest posterior probabilities are small-bodied (less than 200g), with OPCRm1-m3 scores between 39 and 59. This included Drouhard's shrew tenrec (*Microgale drohardi,* $PP_{invertivore}$= 0.72), common treeshrew (*Tupaia glis,* $PP_{invertivore}$= 0.60) and the elegant fat-tailed mouse opossum (*Thylamys elegans* $PP_{invertivore}$ =0.59). Notably, the highest posterior probabilities associated with correctly classified invertivores are only medium values ($PP_{invertivore}$= 0.59—0.72).

Invertivores were more frequently misclassified as carnivores than herbivores. Small to medium sized (48g—1,350g) macroscelids and marsupials with OPCR scores between 16 and 59 were misclassified as carnivores, such as the short-snouted elephant shrew (*Elephantulus brachyrhynchus*, $PP_{carnivore}$= 0.63), Ruwenzori otter shrew (*Micropotamogale ruwenzorii*, $PP_{carnivore}$= 0.44) and the greater bilby (*Macrotis lagotis*, $PP_{carnivore}$= 0.43). Amongst invertivorous species misclassified as carnivores, those associated with the relatively higher posterior probabilities, such as the short-snouted elephant shrew (*Elephantulus brachyrhynchus*, $PP_{carnivore}$= 0.63), are small-bodied species with relatively low OPCRm1-m3 (Table E2, Table E3). Notably, the highest posterior probabilities associated with invertivores misclassified as carnivores are low-to-medium values ($PP_{carnivore}$= 0.44—0.63).

Invertivorous species misclassified as herbivorous have relatively larger body sizes, and OPCRm1-m3 scores between 34 and 42. This included the bat-eared fox (*Otocyon megalotis*, $PP_{herbivore}$= 0.60) and the greater bilby (*Macrotis lagotis*, $PP_{herbivore}$= 0.47). The bat eared fox, which is associated with the highest posterior probability has a relatively larger body mass and lower OPCR scores, than those of the greater bilby (Table E2, Table E3).

An average of 40% of the carnivores sampled were misclassified as herbivores or invertivores. Amongst correctly classified carnivorous species, those associated with the highest posterior probabilities had a variable body mass (11g—1000g), and OPCR scores between 14 and 49. This included the northern quoll (*Dasyurus hallucatus,* $PP_{carnivore}$= 0.72), piebald shrew (*Diplomesodon pulchellum,* $PP_{carnivore}$= 0.65) and the Tasmanian devil (*Sarcophilus harrisii,* $PP_{carnivore}$ =0.61). Notably, the highest posterior probabilities associated with correctly classified carnivores are only medium values ($PP_{carnivore}$= 0.61—0.72).

Carnivores were more frequently misclassified as invertivores (Table 22). Carnivorous species that were misclassified as invertivores included many small-bodied (less than 300g) rodent and soricid species that have OPCR scores between 30 and 58. This included the Eurasian water shrew (*Neomys fodiens*, $PP_{invertivore}$= 0.54), elegant water shrew (*Nectogale elegans*, $PP_{invertivore}$= 0.48) and the cryptic Cameroon scaly-tail (*Zenkerella insignis*, $PP_{invertivore}$= 0.50). The

Pyrenean desman (*Galemys pyrenaicus,* $PP_{invertivore}$= 0.71), a talpid was also misclassified an invertivore. Amongst carnivorous species misclassified as invertivorous, those associated with the relatively higher posterior probabilities, such as the Pyrenean desman (*Galemys pyrenaicus,* $PP_{invertivore}$= 0.71), have relatively high dental complexity scores (Table E2, Table E3). Notably, the highest posterior probabilities associated with carnivores misclassified as invertivores are medium-to-high values ($PP_{invertivore}$= 0.48—0.71).

Carnivorous species that were misclassified as herbivores included medium and large sized (1,000g—10,000g) members of Carnivora and Dasyuromorphia with OPCR scores between 22 and 47- such as the Ethiopian wolf (*Canis simensis*, $PP_{herbivore}$= 0.45), Tasmanian devil (*Sarcophilus harrisii*, $PP_{herbivore}$= 0.48) and the eastern quoll (*Dasyurus viverrinus*, $PP_{herbivore}$= 0.35). Amongst carnivorous species misclassified as herbivores, those associated with the highest posterior probabilities, such as the Tasmanian devil (*Sarcophilus harrisii*, $PP_{herbivore}$= 0.48), have relatively high OPCR scores (Table E2, Table E3). Notably, the highest posterior probabilities associated with carnivores misclassified as herbivores are only low values ($PP_{herbivore}$= 0.35—0.48).

An average of 33% of the herbivorous species sampled were misclassified as carnivorous or invertivorous. Amongst herbivorous species correctly classified, those associated with the highest OCPR scores are large-bodied (greater than 20,000g), with OPCRm1-m3 scores between 35 and 74. This included the wild boar (*Sus scrofa,* $PP_{herbivore}$= 0.84), Bornean orangutan (*Pongo pygmaeus,* $PP_{herbivore}$= 0.77) and the sitatunga (*Tragelaphus spekii,* $PP_{herbivore}$= 0.76). The associated posterior probabilities amongst these are notably medium-to-high values ($PP_{herbivore}$=0.76—0.84).

Herbivorous species were more frequently misclassified as carnivores than invertivores (Table 22). Amongst herbivores misclassified as carnivores were the lesser Egyptian gerbil (*Gerbillus gerbillus* $PP_{carnivore}$= 0.63), long-nosed potoroo (*Potorous tridactylus* $PP_{carnivore}$= 0.45), lemuroid ringtail possum (*Hemibelideus leucodon*, $PP_{carnivore}$= 0.37) and the common brushtail possum (*Trichosurus vulpecula*, $PP_{carnivore}$= 0.43). These were mostly medium-sized (1,000—5,000g) rodents and diprotodontians with OPCR scores between 30 and 58. The rock

hyrax (*Procavia capensis,* $PP_{carnivore}$= 0.70), a Hyracoidea member, was also misclassified a carnivore. Amongst herbivorous species misclassified as carnivores, those associated with the highest posterior probabilities, such as the rock hyrax (*Procavia capensis,* PPcarnivore= 0.70), have relatively lower OPCR scores (Table E2, Table E3). Notably, the highest posterior probabilities associated with herbivores misclassified as carnivores are low-to-medium values ($PP_{carnivore}$= 0.43—0.70).

Herbivorous species misclassified as invertivores were small-bodied (30g—1,000g) rodents and diprotodontians with OPCR scores between 27 and 71, such as the fawn hopping mouse (*Notomys cervinus*, $PP_{invertivore}$= 0.44), house mouse (*Mus musculus*, $PP_{invertivore}$ =0.65), arrow flying squirrel (*Petinomys sagitta* , $PP_{invertivore}$= 0.53), western pygmy possum (*Cercartetus concinnus*, $PP_{invertivore}$= 0.54) and the common wombat (*Vombatus ursinus*, $PP_{invertivore}$= 0.44). Amongst herbivorous species misclassified as invertivores, those associated with the highest posterior probabilities, such as the arrow flying squirrel (*Mus musculus sagitta*, $PP_{invertivore}$= 0.65), have relatively higher OPCR scores (Table E2, Table E3). Notably, the highest posterior probabilities associated with herbivores misclassified as invertivores are low-to-medium values ($PP_{invertivore}$= 0.44—0.65).

When OCPRm1-m3 and log_{10} body mass were used to predict the diet of cynodont species, most cynodonts were estimated as herbivores (Table 23). *Cynognathus* ($PP_{herbivore}$=0.91) was classified as herbivore, the associated posterior probability is high (greater than 0.75), indicative of a high certainty in this classification (Table 23).

Table 23: The estimated diets of cynodont species associated with the pDFAs which that used using OPCRm1-m3 scores and log_{10} body mass as input predictor variables. Note differences in median, 5th percentile (P5) and 95th percentile (P95) posterior probabilities.

Taxon	Expected diet	Predicted diet	Posterior probability
Andescynodon mendozensis	Herbivore	Herbivore	0.39 (P5=0.05, P95=0.83)
Andescynodon sp.	Herbivore	Carnivore	0.57 (P5=0.05, P95=**0.96**)
Cricodon sp.	Herbivore	Carnivore	0.86 (P5=0.15, P95=**0.99**)
Cynognathus crateronotus	Carnivore	Herbivore	**0.91** (P5=0.35, P95=**0.99**)
Diademodon tetragonus	Herbivore	Herbivore	0.53 (P5=0.09, P95=**0.90**)
Exaeretodon argentinus	Herbivore	Carnivore	0.83 (P5=0.38, P95=**0.96**)
Langbergia modisei	Herbivore	Herbivore	0.69 (P5=0.05, P95=**0.99**)
Luangwa sudamericana	Herbivore	Herbivore	0.72 (P5=0.46, P95=0.87)
Massetognathus pascuali	Herbivore	Herbivore	0.89 (P5=0.47, P95=**0.98**)
Megazostrodon rudnerae	Insectivore	Insectivore	**0.98** (P5=0.17, P95=**0.99**)
Menadon besairiei	Herbivore	Herbivore	0.72 (P5=0.19, P95=**0.97**)
Pascualgnathus polanskii	Herbivore	Herbivore	0.46 (P5=0.05, P95=**0.90**)
Santacruzodon hopsoni	Herbivore	Herbivore	0.60 (P5=0.18, P95=0.88)
Traversodontid sp.	Herbivore	Herbivore	**0.95** (P5=0.81, P95=**0.99**)
Trirachodontid sp.	Herbivore	Carnivore	0.70 (P5=0.18, P95=**0.97**)

Most gomphodont species were classified as herbivores, such as *Diademodon* ($PP_{herbivore}$= 0.53), *Langbergia* ($PP_{herbivore}$= 0.69), *Massetognathus* ($PP_{herbivore}$= 0.89), *Pascualgnathus* ($PP_{herbivore}$=0.46) and *Santacruzodon* ($PP_{herbivore}$=0.60). The posterior probabilities associated with these estimates were low to medium values (between 0.3 and 0.75), indicative of high uncertainty in these classifications. Some gomphodont species were estimated as carnivores, such as *Andescynodon sp.* ($PP_{carnivore}$= 0.57), *Cricodon sp.* ($PP_{herbivore}$= 0.86), *Exaeretodon* ($PP_{herbivore}$=0.83*)*, and *Trirachodontid sp.* ($PP_{carnivore}$=0.70). Apart from

Andescynodon sp., most posterior probabilities associated with this classification were high (greater than 0.75), indicative of high certainty.

Megazostrodon ($PP_{invertivore}$=0.98) was estimated as an invertivore, the posterior probability associated with this classification is high (greater than 0.75) indicative of high certainty (Table 23).

12.4 Dietary inferences using mandible shape and OPCR variables

12.4.1 Phylogenetic ANOVA regressions

Table 24: Phylogenetic ANOVA regressions (procDgls) assessing mandibular shape's (Shape) association with OPCR variables. Note variable sample sizes amongst OPCR variables.

Model	n	R^2 (model)	Variable	R^2	Z	Pr(>F)
Shape ~ OPCRm1	231	0.011	OPCRm1	0.011	2.03	**0.022**
Shape ~ OPCRm3	188	0.01	OPCRm3	0.010	1.81	**0.034**
Shape ~ OPCRavg	234	0.007	OPCRavg	0.007	1.40	0.081
Shape ~ OPCRsum	234	0.007	OPCRsum	0.007	1.35	0.090
Shape ~ OPCRm2	233	0.006	OPCRm2	0.006	0.88	0.191

OPCRm1 and OPCRm3 are the only OPCR variables that are significantly correlation with mandible shape amongst the relationships considered (Table 24). The relationships that the remaining OPCR variables (OCPRavg, OPCRsum, OPCRm2) have with mandible shape are non-significant.

The relationship between OPCRm1 and mandible shape explains 1.1% of the variation in mandible shape and is the “best” model amongst those considered (Table 24). Mammals with low OPCRm1 scores have mandibles with a relatively shorter coronoid process and a more prominent angular process, relative to mammals with high OPCRm1 scores (Figure 69).

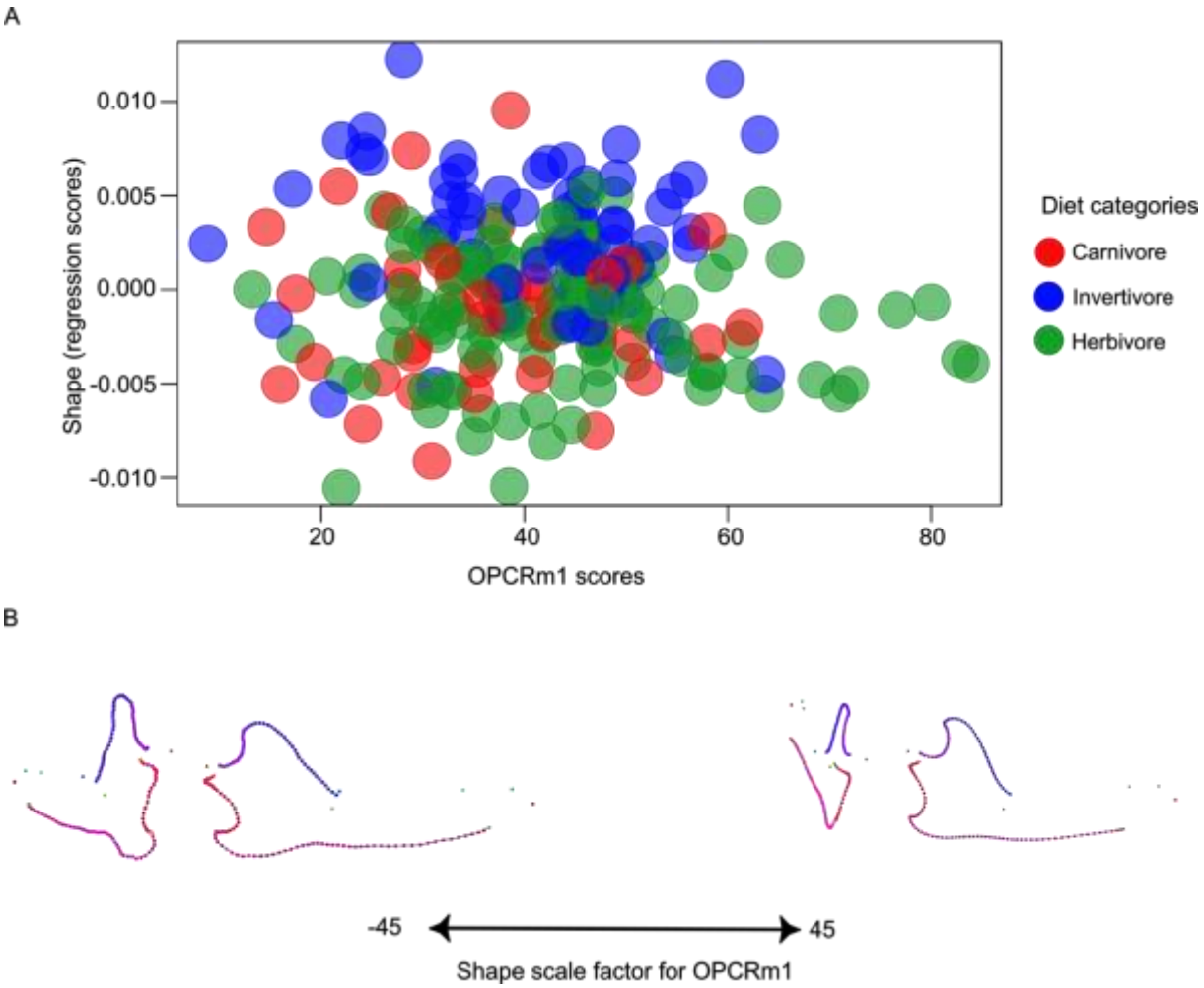


Figure 69: Scatterplot of shape regression scores and OPCRm1 scores (A), alongisde the mandibular shape differences associated with the effect of increasing OPCRm1 scores (B). Landmark configurations shown in lateroposterior (left) and lateral (right) views.

Amongst mammals sampled, those with particularly low OPCR scores (less than 20) included a variety of carnivorous, herbivorous, and invertivorous species (Figure 69, A). These included dasyuromorphs and carnivorans such as the Tasmanian devil (*Sarcophilus harrisii*), spotted hyaena (*Crocuta crocuta*) and the margay (*Leopardus wiedii*). Herbivorous mammals with low OPCRm1 scores included some artiodactyls such as collared peccary (*Pecari tajacu*) and the blue wildebeest (*Connochaetes taurinus*), as well as the ring-tailed lemur (*Lemur catta*), a primate. Invertivorous mammals with low OPCRm1 scores included marsupial species such as Lineaus's mouse opossum (*Marmosa murina*) and the brown antechinus (*Antechinus stuartii*), as well as the aardwolf (*Proteles cristata*),

a carnivoran. Notably, the invertivorous mouse opossum has the lowest OPCRm1 score amongst sampled mammals.

Most mammals with high OPCRm1 scores (greater than 50) are herbivorous artiodactyl and rodent species such as the Nile lechwe (*Kobus megaceros*), moose (*Alces alces*), wild boar (*Sus scrofa*), American beaver (*Castor canadensis*), the shiny guinea pig (*Cavia fulgida*), and the capybara (*Hydrochoerus hydrochaeris*). Other herbivorous species with high OPCRm1 scores included marsupials such as the black-shouldered opossum (*Caluromysiops irrupta*) and the lemuroid ringtail possum (*Hemibelideus lemuroides*); the Malayan tapir (*Tapirus indicus*), a perissodactyl; the common chimpanzee (*Pan troglodytes*), a primate; and carnivorans such as the white-nosed coati (*Nasua narica*) and the giant panda (*Ailuropoda melanoleuca*), which notably has the highest OPCRm1 score amongst herbivorous mammals sampled. Although few, there are also carnivorous and invertivorous species with high OPCRm1 scores (Figure 69, A), the carnivorous species include carnivorans such as the bush dog (*Speothos venaticus*), striped skunk (*Mephitis mephitis*) and the striped polecat (*Ictonyx striatus*); as well as the Eurasian water shrew, a soricid. Invertivorous species with high OPCRm1 scores included talpids such as the northern-broad footed mole (Scapanus latimanus) and star-nosed mole (*Condylura cristata*); rodents such as the rakali (*Hydromys chrysogaster*), the northern grasshopper mouse (*Oncyhomys torridus*); as the erinaceid Moonrat (*Echinosorex gymnure*); and the bat-eared fox (*Otocyon megalotis*).

The relationship between OPCRm3 and mandible shape explains 1% of the variation in mandible shape. Mammals with low OPCRm3 scores have mandibles with a shorter coronoid process and a less prominent angular process, relative to mammals with high OPCRm3 scores (Figure 70).

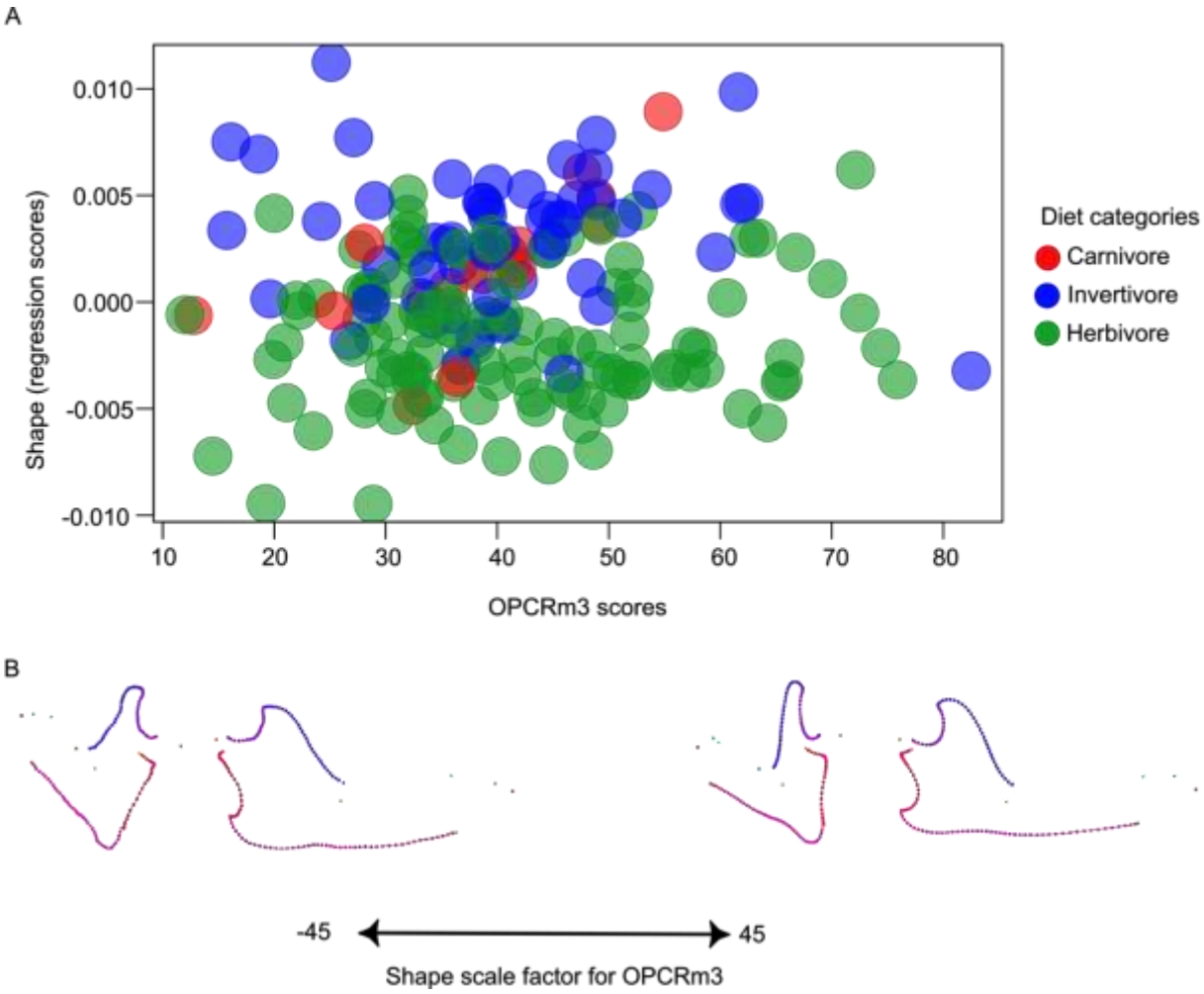


Figure 70: Scatterplot of shape regression scores and OPCRm3 scores (A), alongisde the mandibular shape differences associated with the effect of increasing OPCRm3 scores (B). Landmark configurations shown in lateroposterior (left) and lateral (right) views.

Amongst mammals sampled, those with particularly low OPCRm3 scores (less than 20) included mostly herbivorous rodents such as the Baluchistran pygmy jerboa (*Salpingotulus michaelis*), lesser Egyptian gerbilus (*Gerbillus gerbillus*), southeastern pocket gopher (*Geomys pinetus*) and the house mouse (*Mus musculus*); as well as Hoffman's two-toed sloth (*Choloepus hoffmani*). The baluchistran pygmy jerboa, a herbivore, notably has the lowest OPCRm3 score amongst mammal species sampled. Invertivorous species sampled with low OPCRm3 scores included afrosoricid species such as the Cape golden mole (*Chrysochloris asiatica*) and Stuhlmann's golden mole (*Chrysochloris stuhlmanni*); as well as the soricid Chinese mole (*Anousorex squamipes*), and the macroscelid,

short-snouted elephant shrew (*Elephantulus brachyrhynchus*). The only carnivorous mammal sampled with a OPCRm3 score below 20 is the Ethiopian wolf (*Canis simensis*).

Most mammals with high OPCRm3 scores (greater than 50) are mostly herbivorous artiodactyl and rodent species such as the siberian ibex (*Capra sibirica*), European edible dormouse (*Glis glis*), wild boar (*Sus scrofa*), and Beecroft's flying squirrel (*Anomalurus beecrofti*). Other herbivorous species with high OPCRm3 scores included diprotodont species such as the rufous rat kangaroo (*Aepyrmnus rufescens*) and the lemuroid ringtail possum (*Hemibelideus lemuroides*) as well as the common chimpanzee (*Pan troglodytes*), a primate. Invertivorous species with high OPCRm3 scores included marsupials such as the Incan caenolestid (*Lestoros inca*), fat-tailed dunnart (*Sminthopsis crassicaudata*) and the brown antechinus (*Antechinus stuartii*); as well as the common treeshrew (*Tupaia glis*), a Scandentia member; Drouhard's shrew tenrec (*Microgale drouhardi*), an afrosoricid; the talpid star-nosed mole (*Condylura cristata*) and the rakali (*Hydromys chrysogaster*). The rakali notably has the highest OPCRm3 score amongst mammals sampled.

12.4.2 pDFA: mandible shape and OPCR

The median success rate of predicting an animal's diet (herbivore, carnivore or invertivore) using both mandible shape (first 7 PC axes) and OPCRm1-m3 scores is 80% (P5=69, P95=90). This is approximately 70% better than randomly guessing diet (error rate of 66.67% when randomly guessing). Additionally, this is approximately 20% better than using only mandible shape (error rate of 25% when using only mandible shape), and 61.54% better than using only OPCRm1-m3 scores (error rate of 52% when using only OPCRm1-m3 scores.

Using mandible shape and OPCRm1-m3 scores was best at predicting the diet of herbivores, and an average of only 8.33% herbivorous mammals sampled were misclassified as carnivores or herbivores (Table 25). This is substantially lower than the error rates associated with using mandible shape (error rate of 16.67%) or OPCRm1-m3 (error rate of 53.3%) individually. Amongst herbivorous mammals correctly classified, those associated with the highest posterior probabilities, such as the American beaver (*Castor candensis,* $PP_{herbivore}$= 0.99), European edible

dormouse (*Glis glis,* $PP_{herbivore}$= 0.99), such as have short mandibles characterized by a posteriorly tall mandible body and relatively high OPCRm1-m3 scores (Figure 71, A).

Table 25: Confusion table for pDFAs which estimated diet using mandible shape (first seven PCA axes) and OPCRm1-m3 scores. Note differences in the median, 5th percentile (P5), and 95th percentile counts per dietary category.

Predicted diet (pDFA)	**True diet**		
	Carnivore	Herbivore	Invertivore
Carnivore	9 (P5=7, P95=11)	1 (P5=0, P95=2)	2 (P5=0, P95=4)
Median %	75%	8.33%	16.67%
Herbivore	1 (P5=0, P95=1)	11 (P5=9, P95=12)	1 (P5=0, P95=2)
Median %	8.33%	91.67%	8.33%
Invertivore	2 (P5=1, P95=4)	0 (P5=0, P95=2)	9 (P5=7, P95=11)
Median %	16.67	0%	75%
Median % correct	75%	91.67%	75%

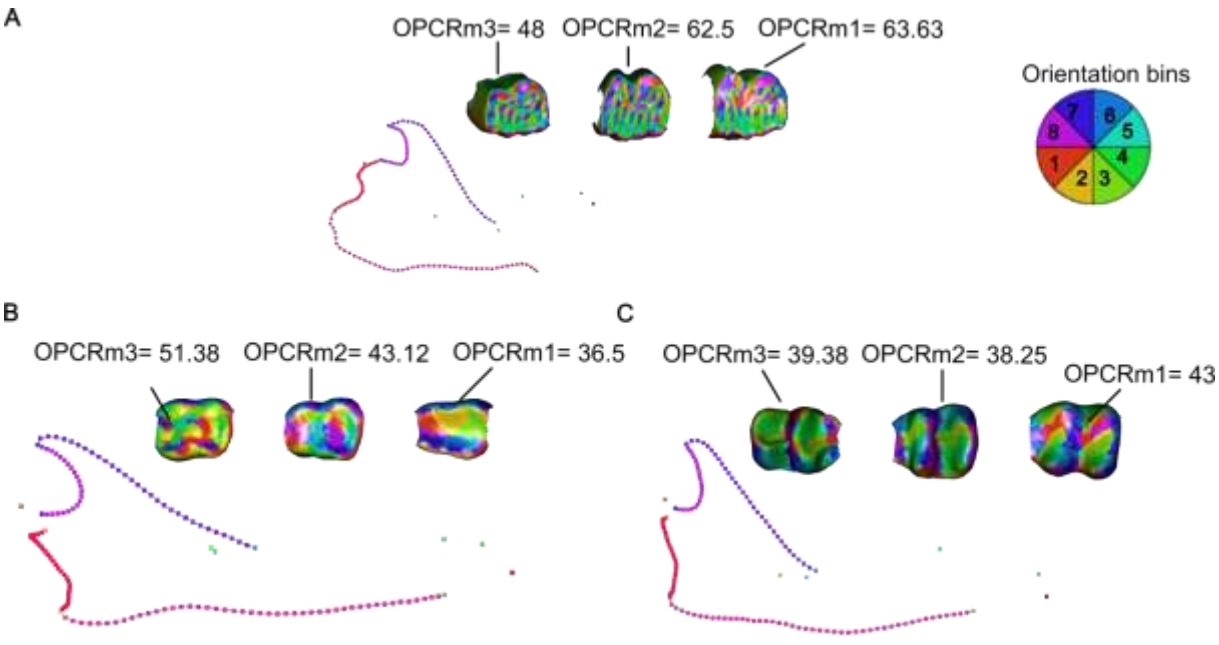


Figure 71: Landmark configurations alongside associated OPCR 3D colour maps and OPCRm1-m3 scores amongst A: correctly classified herbivorous mammal (American beaver); B: a herbivorous mammal misclassified as an carnivore (long-nosed potoroo); and C: a herbivorous mammal misclassified as invertivore (bridled nail-tail wallaby). Landmark configurations shown in lateral views.

Herbivores were misclassified as carnivores relatively more frequently (Table 25) and instances of this included diprotodontians such as the bridled nail-tail wallaby (*Onychogalea fraenata,* $PP_{carnivore}$= 0.40) and the long-nosed potoroo (*Potorous tridactylus,* $PP_{carnivore}$= 0.72), these species have relatively high OPCRm1-m3 scores (36—51). The aye-aye (*Daubentonia madagascariensis*, $PP_{carnivore}$=0.69) was also frequently misclassified as a herbivore, and notably has the lowest OPCRm1-m3 scores amongst species frequently misclassified (24—32.5). The long-nosed potoroo ($PP_{carnivore}$= 0.72) is associated with the highest posterior probability and has a long mandible with an anteriorly low mandible body and a tall coronoid process (Figure 71, B). Notably, the highest posterior probabilities associated with herbivores misclassified as carnivores are low-to-medium values ($PP_{carnivore}$= 0.40—0.72).

Although rare (Table 25), herbivores misclassified as invertivores included the bridled nail-tail wallaby ($PP_{invertivore}$= 0.50), a diprotodontid; as well as the Hamadryas baboon (*Papio hamadryas,* $PP_{invertivore}$=0.40), a primate. These species have similar OPCRm1-m3 scores (37—43). The bridled nail-tail wallaby ($PP_{invertivore}$= 0.50) is associated with a relatively higher posterior probability. The bridled nail-tail wallaby has a long mandible with an anteriorly low mandible body and a tall coronoid process (Figure 71, C). Notably, the posterior probabilities associated with herbivores misclassified as invertivores are only low values ($PPi_{nvertivore}$=0.40—0.50)

An average 25% of the invertivorous mammals were misclassified as carnivores or herbivores when using mandible shape OPCRm1-m3 scores (Table 25). This is substantially lower than the error rates associated with using mandible shape (error rate of 33.33%) or OPCRm1-m3 (error rate of 60%) individually. Amongst invertivorous mammals correctly classified those associated with the highest posterior probabilities, such as the cape golden mole (*Chrysochloris asiatica*, $PP_{invertivore}$=0.99) and the marsupial mole (*Notoryctes typhlops*, $PP_{invertivore}$=0.99), have relatively low OPCRm1-m3 scores (16—28) and long mandibles with a low coronoid process and a prominent angular process (Figure 72, A).

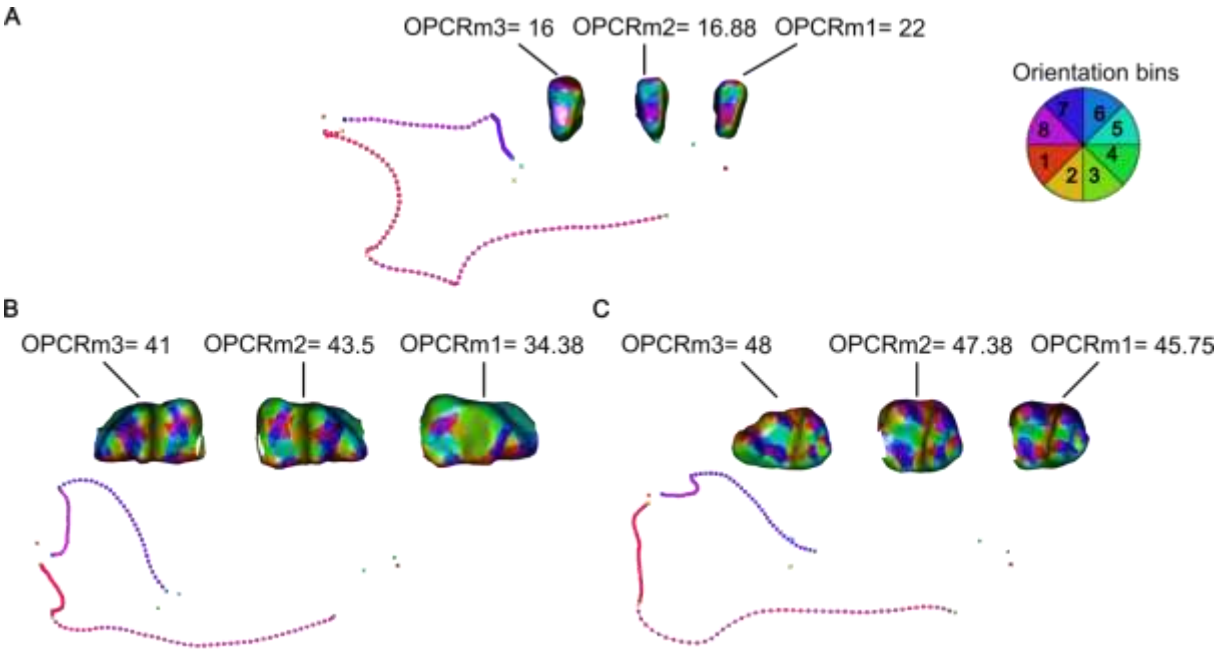


Figure 72: Landmark configurations alongside associated OPCR 3D colour maps and OPCRm1-m3 scores amongst A: correctly classified invertivorous mammal (Cape golden mole); B: a invertivorous mammal misclassified as an carnivore (water possum); and C: an invertivorous mammal misclassified as herbivore (Philippine tarsier). Landmark configurations shown in lateral views.

Invertivores were misclassified as carnivores more frequently (Table 25) and instances of this included marsupials such as the monito del monte (*Dromiciops gliroides,* $PP_{carnivore}$= 0.79), gray short-tailed opossum (*Monodelphis domestica*, $PP_{carnivore}$=0.54) and the feathertail glider (*Acrobates pygmaeus*, $PP_{carnivore}$= 0.61); as well as the water opossum (*Chironectes minimus*, $PP_{carnivore}$= 0.80), a soricid. Amongst invertivores misclassified as carnivores, those associated with the highest posterior probabilities, such as the monito del monte ($PP_{carnivore}$= 0.79) and the water opossum ($PP_{carnivore}$= 0.80), have relatively higher OPCRm1-m3 scores (24—47) and long mandibles with a tall coronoid process and a relatively reduced angular process (Figure 72, B). Notably, the highest posterior probabilities associated with invertivores misclassified as carnivores are medium-to-high values ($PP_{carnivore}$= 0.54—0.80).

Invertivores misclassified as herbivores included the Philippine tarsier (*Tarsius syrichta*, $PP_{herbivore}$=0.55) and the big-eared swamp rat (*Malacomys longipes*, $PP_{herbivore}$=0.42). These species are characterized by mandibles with a low

coronoid process and an expanded angular process. Although neither are associated with particularly high posterior probabilities, the Philippine tarsier ($PP_{herbivore}$=0.55) is associated with a relatively higher posterior probability and has relatively lower OPCRm1-m3 scores (Figure 72, C) compared to those of big-eared swamp rat (36—54). Notably, the posterior probabilities associated with invertivores misclassified as herbivores are only low-to-medium values ($PPi_{nvertivore}$=0.42—0.55).

An average of 25% carnivorous species sampled were misclassified as herbivorous or invertivorous when using mandible shape and OPCRm1-m3 scores. This is substantially lower than the error rate associated with using only OPCRm1-m3 (error rate of 40%), however, it is marginally worse than using only mandible shape (error rate of 23.33%). Amongst carnivorous mammals correctly classified, those associated with the highest posterior probabilities such as the piebald shrew (*Diplomesodon pulchellum*, $PP_{carnivore}$=0.99) and the northern quoll (*Dasyurus hallucatus*, $PP_{carnivore}$=0.97), have mandible shapes characterized by a tall coronoid process and a prominent angular process with OPCRm1-m3 scores between 21 and 58 (Figure 73, A).

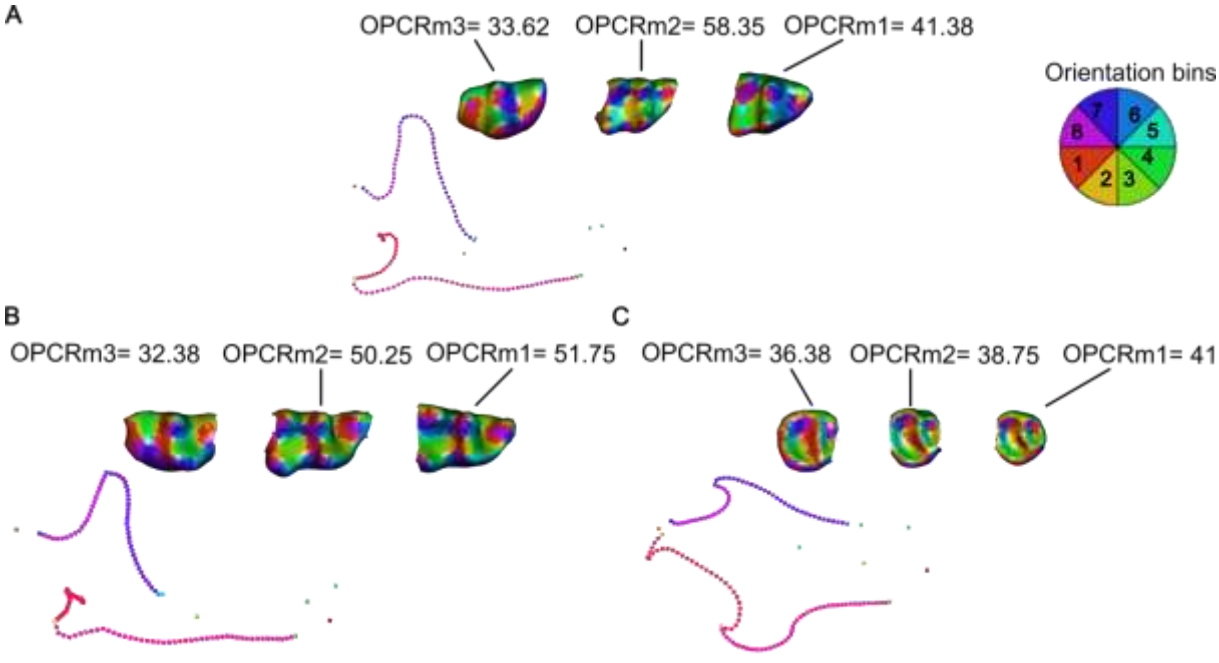


Figure 73: Landmark configurations alongside associated OPCR 3D colour maps and OPCRm1-m3 scores amongst A: correctly classified carnivorous mammal (piebald shrew); B: a carnivorous mammal misclassified as an invertivore (elegant water shrew); and C: a carnivorous mammal misclassified as herbivore (Cameroon scaly-tail). Landmark configurations shown in lateral views.

Carnivores were more frequently misclassified as herbivores (Table 25), and instances of this included marsupials such as the eastern quoll (*Dasyurus viverrinus*, $PP_{invertivore}$=0.56) and the crest-tailed mulgara (*Dasycercus cristicaudata*, $PP_{invertivore}$=0.52). Soricids such as the elegant water shrew (*Nectogale elegans*, $PPi_{nvertivore}$=0.87) and the Eurasian water shrew (*Neomys fodiens,* $PP_{invertivore}$=0.62) were also misclassified as invertivores. Amongst carnivores misclassified as herbivores, those associated with the highest posterior probabilities, such as the elegant water shrew ($PP_{invertivore}$=0.87) and the Eurasian water shrew ($PP_{invertivore}$=0.62), have long mandibles with a tall coronoid process and a prominent angular process. These species notably have OPCRm1-m3 scores generally comparable to those of correctly classified carnivores (Figure 73). Notably, the highest posterior probabilities associated with carnivores misclassified as invertivores are medium-to-high values ($PP_{invertivore}$= 0.52—0.87).

The cryptic Cameroon scaly-tail (*Zenkerella insignis*, $PP_{herbivore}$=0.97), is the only carnivorous species misclassified as a herbivore. The Cameroon scaly-tail has a short mandible with a low coronoid process and a prominent expanded angular process with OPCRm1-m3 scores between 36 and 41 (Figure 73, C).

Table 26: The estimated diets of cynodont species associated with pDFAs which made use of mandible shape (first seven PCA axes) and OPCRm1-m3 scores as input predictor variables. Note differences in median, 5th (P5) percentile and 95th percentile (P95) of posterior probabilities.

Taxon	Expected diet	Predicted diet	Posterior probability
Cynognathus crateronotus	Carnivore	Carnivore	**0.98** (P5=0.02, P95=**0.99**)
Diademodon tetragonus	Herbivore	Carnivore	**0.92** (P5=0.009, P95=**0.99**)
Megazostrodon rudnerae	Invertivore	Invertivore	**0.99** (P5=0.43, P95=**0.99**)
Trirachodon berryi	Herbivore	Carnivore	**0.99** (P5=0.01, P95=**0.99**)
Trirachodon sp	Herbivore	Carnivore	**0.99** (P5=0.01, P95=**0.99**)

Most non-mammalian cynodonts are estimated as carnivorous when using both mandible shape and OPCRm1-m3 scores to predict diet (Table 26) – this does not coincide with the hypothesized diets of *Diademodon* and *Trirachodon* which are

expected to be herbivorous. All carnivorous estimates are associated with high posterior probability values ($PP_{carnivore}$= 0.92—0.99).

Megazostrodon, the only hypothesized invertivore is estimated as invertivorous when using mandible shape and OPCRm1-m3 scores. This estimate is associated with a high posterior probability ($PP_{invertivore}$= 0.99).

13. DISCUSSION

13.1 Mandibular form and its correlation to dietary disparity in mammals

I found that mandibular shape variance amongst mammals is best explained by the shape-allometry patterns associated with different diets. Most dietary variables significantly explain some variation in mandible shape after accounting for the effect of body mass. Although the main effects of body mass, relative mandible size and most diets significantly correlate with mandible shape disparity, this explains relatively little mandible shape variation. Body mass and the dietary variables used in this study collectively explain 4.9% of the variation in mandible shape.

My results show that mandible size is significant in explaining some mandibular shape variation, and mandible size variation is best explained by body mass. The mandible scales with negative allometry with respect to body mass. Some of the residual variation in mandible size is explained by carnivory and frugivory. The mandible sizes of frugivores and granivores are characterized by different allometric relationships compared to those of mammals from other diets.

Mandibular shape is strongly partitioned by phylogenetic relationships, and mammals from the same lineage occupy relatively constrained portions of the mandibular shape morphospace (Figure 11, Figure 13). Although most diets significantly influence mandible shape (Table 5), mammals from different lineages with similar diet classes do not converge on the same mandible shape in the morphospace (Figure 9, Figure 11). A potential explanatory reason for this observed pattern is the ordinal-level morphofunctional features of the jaw, particularly the coronoid, angular, and mandibular condyle. These changes are documented to correspond to different muscle configurations and masticatory movements, which tend to be shared amongst mammals of the same order (Becht, 1953, Wolff-Exalto, 1951, Hemae, 1967, Hoshi, 1971, Herring and Herring, 1974, Herring, 1993). I find little evidence that ordinal-level disparity overprints these shape changes, such that adaptations of mandibular shape to similar diets generally occur within the shape framework characteristic of the respective clades.

This is most apparent in marsupials, laurasiatherians and euarchontoglires, which occupy the extreme ends of the morphospace despite having members with similar dietary habits (Figure 11, Figure 13). This is potentially because rodents, ungulates (artiodactyls and perissodactyls) and marsupials possess highly specialized muscle configurations (Sánchez-Villagra and Smith, 1997, Clauss et al., 2008, Druzinsky et al., 2011). Even though studies have found that these muscle configurations and associated masticatory movements correspond to diet within these groups (Warburton, 2009, Wang et al., 2021, Barbero et al., 2023), members from these taxonomic orders are specialized in their own right. In fact, these specializations explain the shape-allometry patterns in granivores, frugivores and herbivores, as these are primarily between small-bodied rodents relative to large-bodied ungulates (Figure 21, Figure 25, Figure 26). The body mass and mandibular shape differences amongst rodents are generally much smaller relative to those between rodents and ungulates. However, the mandibular shape differences between these groups are telling of the different approaches that these animals have evolved to similar diets. For example, the shiny guinea pig (*Cavia fulgida*) and the sheep (*Ovis aries*) are both herbivores and aside from the body mass differences, they are characterized by different mandibular shapes, masticatory muscle configurations and chewing patterns. The shiny guinea pig, a rodent, has a hystricomorph muscle orientation - and the enlarged masseter's configuration enhances the horizontal action of the masseter (Wood, 1965) and this accommodates its bilateral chewing cycles (Byrd, 1981). The shiny guinea pig's mandible is short and characterized by a ventrally expanded angular process and a low coronoid process. This differs substantially from the mandibular shape and the associated mandibular movement of an artiodactyl, such as a sheep (*Ovis aries*), which is long and characterized by a relatively taller coronoid process and a rounded angular process. The sheep chews in a single transverse movement of the mandible (Fortelius, 1985), and has a well-developed masseter and temporalis group (Ercoli et al., 2023).

Herbivores occupy a wide morphospace relative to those of invertivores and carnivores (Figure 9, Figure 11), suggesting that there are a wider range of morphological adaptations that accommodate herbivorous ecologies. Amongst herbivores sampled only herbivorous laurasiatherians, which include mostly large-

bodied ungulates, are limited in terms of morphospace (Figure 11, Figure 13). This explains why herbivory is non-significant after accounting for the effects of body mass (Table 5), as small-bodied herbivores have disparate mandible shapes. Small-bodied herbivores are predominantly rodents but also include some herbivorous marsupials and primates. The shape differences amongst these small-bodied herbivorous groups are underpinned by fundamentally different biomechanical systems, as each of these groups are characterized by different chewing patterns and muscle configurations (Crompton et al., 2008a, Crompton et al., 2008b, Cox et al., 2012, Potapova, 2020, Ercoli et al., 2023). However, there are also distinct differences in mandibular shapes, muscle configurations and associated chewing patterns within these groups. For instance, the tammar wallaby (*Macropus eugenii*) and the wombat (*Lasiorhinus latifrons*) are both marsupial grazers and even though there only minor differences in muscle configurations, they have different mandibular shapes and chewing patterns. The wombat has a much taller coronoid process and a more prominently inflected angular process relative to the wallaby. The ventral margin of the wombat's mandible is convex and the wombat's adductor muscles have a more lateral insertion point enabling greater torque around the jaw joint which enhances bite force at the molars. These adaptations allow the wombat's mandible to move transversely and linearly during molar occlusion, whereas the wallaby is characterized by a two-phase chewing pattern involving orthal and transverse movements (Crompton et al., 2008a, Crompton et al., 2008b).

Herbivorous euarchontoglires, which are predominantly rodents, occupy an even wider morphospace (Figure 11, Figure 13) because they have highly specialized masseter muscle configurations which are documented to correspond to gnawing proficiency or molar-chewing proficiency (Cox et al., 2012, Potapova, 2020). Rodents that are proficient in molar-chewing have the hystricomorph condition, and these include species such as the plains viscacha (*Lagostoma maximus*) and the earlier mentioned shiny guinea pig (*Cavia fulgida*). These species have short mandibles with a low coronoid process and a ventrally expanded angular process. Rodents that prioritize gnawing are often hard-food specialists and many were categorized as granivorous, these included the meadow jumping mouse (*Zapus hudsonius*) and the grey dwarf hamster (*Cricetulus migratorius*), which have a

short mandible with a tall coronoid process and a ventrally expanded angular process. These adaptations may explain why the mandibles of granivores are significantly different from those of other herbivores (Table 5). Functional studies corroborate that these morphofunctional characteristics are adaptations to generate enough force and handle the strain association with gnawing (Cox et al., 2012, Casanovas-Vilar and Van Dam, 2013, Ledogar et al., 2018, Maestri et al., 2016).

The narrow morphospace occupied by carnivores are a stark contrast to herbivory (Figure 11, Figure 13), and this suggests that hypercarnivory favours select morphofunctional characteristics. The mandibular musculature that characterizes hypercarnivorous members of Carnivora includes a highly developed temporalis muscle with a simplified masseter and pterygoideus muscle (Gorniak and Gans, 1980, Sacco and Van Valkenburgh, 2006). Carnivorous marsupials, such as the tiger quoll (*Dasyurus maculuatus*) and the common opossum (*Didelphis marsupialis*), are also characterized by this musculature (Thomas, 2023), even though their mandibular shapes differ from those of carnivorans as most have a prominent medially inflected angular process. This feature is reduced in carnivorans (Figure 16, Figure 17). Nonetheless, studies generally regard hypercarnivorous marsupials and carnivorans as functional equivalents based on this convergent masticatory apparatus (Ercoli et al., 2023, Thomas, 2023). This musculature maximizes the transverse movements that facilitate shearing (Ercoli et al., 2023, Liem et al., 2001, Radinsky, 1981b, Radinsky, 1981a). Amongst relationships considered here, the shape-allometry patterns in carnivores explains the most mandibular shape variation (Table 5). These shape-allometry differences are likely due to the mandible shape and body size disparity between small-bodied carnivorous soricids and large-bodied carnivorans (Figure 17). Although, the only conspicuous difference in mandibular shapes is in the prominence of the angular process (Figure 17). Carnivorous soricids may have unusual masticatory movements relative to hypercarnivorous marsupials and carnivorans because their angular process is pronounced even relative to those of carnivorous marsupials; however, I cannot ascertain a clear consensus on this because there are few studies on soricid chewing patterns. A plausible explanation for this shape-allometry pattern describing the most variation (Table 5, R^2= 0.049) may be

because carnivorans and soricids generally occupy a relatively narrow morphospace (Figure 9, Figure 11, Figure 13), this pattern is congruent with other studies which have documented a low craniodental morphological diversity amongst these groups (Churchfield and Sheftel, 1994, Huggins and Kennedy, 1989, Holliday and Steppan, 2004, Balisi and Van Valkenburgh, 2020).

Specialized mammals with unique adaptations drive the shape-allometry patterns in invertivores and nectivores (Table 5, Figure 19, Figure 21). The shape-allometry patterns in invertivores are due to the major shape differences between the large-bodied giant pangolin (*Smutsia gigantea*) relative to other small-bodied invertivores (Figure 21). Even though the invertivorous categorization used in this study included a wide variety of invertivorous foodstuffs with various physical properties, most small-bodied invertivores have similar mandible shapes. For instance, the round-eared elephant shrew (*Macroscelides proboscideus*) and southern marsupial mole (*Notoryctes typhlops*) consume hard-bodied ants and even though the Aberdare shrew (*Surdisorex norae*) eats soft-bodied worms, these species all have long mandibles with a tall coronoid process and a prominent angular process. Similarly, the star-nosed mole (*Condylura cristata*) has the same mandible shape despite consuming crustaceans and aquatic insects. Unlike other invertivores, pangolins have a long mandible with a low coronoid process and a reduced angular process. Pangolins are anomalous even amongst mammal species because they have evolved an entirely different way of using their mandible, characterized by unusual masticatory muscle configurations and mandibular movements (Naples, 1999). They are edentulous and have highly reduced masseter and temporalis muscles and unlike most mammals, pangolins swallow their food whole, only using their highly specialize tongue to transport food (Doran and Allbrook, 1973, Challender et al., 2019).

The shape-allometry patterns in nectivores are due to the major differences between the small-bodied honey possum (*Tarsipes rostratus*) relative to those of other mammals classified as nectivores in this study (Table 5, Figure 19). The broad categorization of nectivory implemented in this study included mammals that consume non-fibrous plant parts such as tree exudates (sap), gum and pollen together with those that consume nectar (Table 1). These included the sugar glider (*Petaurus breviceps*) and the common marmoset (*Caluromysiops irrupta*).

However, physical properties of these non-fibrous plant parts are not similar to nectar, and these species have substantially different mandible shapes characterized by a much taller mandible with a pronounced coronoid and angular process (Figure 19). Nectar-eating is rare in mammals and amongst species categorized as nectivorous, the honey possum is the only true obligate nectar-eater. Similar to pangolins, honey possums have a highly specialized feeding apparatus, characterized by a long mandible with a low coronoid process and a reduced angular process (Figure 19). Relative to other diprotodonts, honey possums have a more specialized muscle configuration, which includes a relatively larger pterygoid muscle and a reduced temporalis muscle (Rosenberg and Richardson, 1995). Chewing is not necessary for honey possums as they rely on a highly specialized tongue, which is covered by papillae that collects nectar or pollen (Richardson and Wooller, 1990).

The main effect of body mass explains a small amount of the variation (Table 5, R^2= 0.02) in mandibular shape and this correlation is likely due to body mass's underlying association with dietary variables. Invertivorous mammals predominantly occupy smaller body masses, whereas carnivorous and herbivorous mammals predominantly occupy larger body masses (Figure 14). These diets are characterized by distinct mandibular shapes and shape-allometry patterns, as already discussed.

Surprisingly, even though different diets are characterized by distinct shape differences (Table 5), approximately 95% of the variation in mandible shapes are not explained by diet or body mass. This may be because inherited muscle configurations limit the adaptive plasticity of the mandible. These constraints may be more stringent in groups such as Carnivora and Soricidae which have low craniodental morphological diversity. For instance, although the giant panda's bamboo feeding dates back to the Late Pleistocene (Jin et al., 2007), their mandible still strongly resembles those of their carnivorous relatives. This is likely because they still have the carnivoran muscle configuration characterized by a developed temporalis and reduced masseter and pterygoideus (Ercoli et al., 2023). My results also suggest that highly derived musculatures may be more challenging to escape and that the evolutionary trajectories of groups such as Carnivora, Rodentia and Artiodactyla may be limited by this. For instance, rodents

possessing the hystricomorph musculature exhibit similar jaw shapes and these adaptations are linked to proficient molar-chewing as observed in grazers like the shiny guinea pig (*Cavia fulgida*) and the plains viscacha (*Lagostomus maximus*). Close relatives such as the rakali (*Hydromys chrysogaster*) have diverged from this grazing habit but they still possess the same mandible shape and characteristics. Artiodactyls have not diverged from herbivory, but if such a divergence were to occur, they might encounter similar constraints because of their current specialized musculature configurations.

However, another reason to consider why diet explains a small portion of mandible shape variation may be because dietary variables have a complex relationship with mandible shape which does not take the form of a linear one-to-one relationship amenable to the forms of analysis used here. Diets such as herbivory accommodate a wide variety of chewing patterns whereas carnivory and granivory appear to have stricter functional requirements. Subsequently, it is possible that primarily herbivorous animals which are only partially granivorous or carnivorous, could develop mandible shapes reflecting adaptations associated with carnivorous or granivorous habits. Diets are often highly seasonal, and many mixed feeders may encounter these selective pressures. For example, the mandibular shapes of the round eared elephant shrew (*Macroscelides proboscideus*) and Beecroft's flying squirrel (*Anomalurus beecroft*) have mandibles with a ventrally concave margin and ventrally expanded angular process, as seen in highly granivorous species (Figure 21) – however, they are only partially granivorous and eat a wide variety of foodstuffs. Similarly, the mandibles of relatively more herbivorous, or omnivorous species such as the brown bear (*Ursus arctos*) and the western pygmy possum (*Cercetetus concinnus*) closely resemble those of carnivorous mammals.

Variation in mandible size is mostly explained by body mass (Table 8, R^2=0.80), an expected result given the size variation among mammals investigated here (Table D1). Mandible size only explains a small amount of the mandible shape variation (Table 5, R^2=0.021) and this correlation likely stems from the strong correlative relationship between mandible size and body mass (Table 8, R^2=0.80) since the residuals from this correlation reflect body mass's underlying association with dietary variables (Figure 15). This result is likely because animals with larger

body sizes inherently have larger body proportions. However, the proportional size of the mandible is affected by granivory, carnivory and frugivory (Table 8). A potential explanation for carnivorous species exhibiting disproportionately larger mandible sizes (Table 8, R^2= 0. 8073) could be that this is an adaptation for accommodating additional musculature without altering the muscle's configuration. This is likely a response to carnivory favouring a select configuration of muscles as imposed by functional requirements. A similar pattern has been found in felid skulls, where the selective pressure of uniform biting power amongst small-bodied felids selected a disproportionately larger braincase enabling small-bodied felids to maintain high bite forces through the accommodation of greater adductor musculature (Christiansen and Adolfssen, 2005). This strategy could also explain the mandible allometry patterns amongst granivores (Table 8, R^2=0.8056). Granivores are linked to specialized muscle configurations, and disproportionately altering mandible size may be an adaptation to enhance the mandible's ability to cope with strain without changing the underlying musculature. This adaptation favours relatively larger mandible sizes amongst small-bodied granivores and relatively smaller mandible sizes amongst large-bodied granivores (Figure 33).

Frugivory's main and partial effects have no significant influence on mandible shape (Table 5). However, the mandible allometry patterns amongst frugivores are different from those of non-frugivores, and this relationship explains the most variation in mandibular sizes (Table 8, R^2=0.8093). According to this allometric pattern, small-bodied frugivores have relatively smaller mandible sizes and large-bodied frugivores have relatively larger mandible sizes (Figure 32). These relative size differences are likely due to the mandible size disparity amongst small-bodied frugivorous rodents and relative to those of the large-bodied Sumatran rhinoceros (*Dicerorhinus sumatrensis*). The perissodactyl is the largest frugivorous animal sampled, however other large-bodied frugivorous animals include primates such as the Bornean orangutan (*Pongo pygmaeus*) and the chimpanzee (*Pan troglodytes*). Although untested, these size differences may correspond to the physical properties of the fruits that large-bodied and small-bodied frugivores prefer. This is corroborated by studies which found that large-bodied primates prefer tougher/harder diets, and these dietary preference correlate with large-

bodied species having disproportionately larger, more robust mandibles (Bouvier, 1986a, Ravosa, 1996, Ravosa, 2000).

13.2 Dental complexity's correlation to dietary disparity in mammals

I found that the distribution of dental complexity scores (OPCRavg, OPCRsum, OPCRm1, OPCRm2, OPCRm3) do not correspond closely to different diets in mammals. Of all the dietary variables considered here, granivory is the only dietary variable that significantly influenced the dental complexity of the second and third molar. Granivores also have different OPCR allometry patterns and these consistently describe the most variation in OPCR scores. Even so, these allometry patterns only describe up to 12.34% of the total variation in OPCR scores. Carnivores are characterized by different OPCRm3 allometry patterns. However, body mass, relative mandible size and most dietary variables are non-significant in explaining the variation in OPCR scores.

Tooth form, like most morphological attributes, is the product of both function and phylogeny and dentigerous animals that chew their food converge on similar diets through completely different means of tooth specializations (Ungar, 2010). This is primarily why dental complexity (OPCR) has been considered useful in palaeobiology as it enables the homology-free comparison of tooth forms by quantitatively demonstrating that distantly related taxa with similar diets converge on comparable dental complexity scores (Evans et al., 2007, Santana et al., 2011, Pineda-Munoz et al., 2016). I found a weak correlation between diet and OPCR across the seven marsupial orders and 17 placental orders sampled in this study (Tables 13—17). However, iterations of pDFA which made use of OPCR scores to estimate diet still generally associated relatively high OPCR scores with herbivory and low scores with carnivory (Figure 61, Figure 63, Figure 64, Figure 68), suggesting that OPCR's correlation to diet is present but weak.

Although OPCR scores do not closely correlate with dietary preferences (Tables 13—17), OPCRm1-m3 appear to be more closely related to diet as my results show that these scores have a relatively higher success in estimating the diet of mammals (Table 18, Table 20). The reason why OPCR scores are weakly correlated with diet is because members from some mammalian clades with similar dietary habits do not converge on similar OPCR scores (Figure 36, Figure

41, Figure 46, Figure 51, Figure 56). Subsequently, grouping mammals with dissimilar dental complexity patterns together resulted in highly similar distributions of dental complexities amongst major and finer dietary categories (Figure 37, Figure 42, Figure 47, Figure 52, Figure 57). Based on the differences in processing capabilities that OPCR scores are based on, herbivores were expected to have significantly higher OPCR scores relative to carnivores, and invertivores were expected to have intermediate OPCR scores (Evans et al., 2007). However, only laurasiatherian mammals appear to be somewhat characterized by this pattern (Figure 36, Figure 41, Figure 46, Figure 51, Figure 56). A possible reason why other mammalian clades may have different patterns of dental complexity could be because of the distinct differences in chewing patterns amongst groups, as discussed earlier. These variations in chewing behaviours may create diverse tooth wear patterns. This is especially apparent in euarchontoglires, as on average herbivorous euarchontoglires have relatively lower OPCR scores than their invertivorous counterparts (Figure 36, Figure 41, Figure 46, Figure 51, Figure 56). This could be because grazing rodents, which make up the largest component of euarchontoglires, show a remarkably high wear rate even relative to other grazers (Damuth and Janis, 2014). This wear may be the byproduct of the specialized chewing patterns observed in herbivorous rodents as they subject their jaws and teeth to high amounts of force during chewing (Cox et al., 2012).

Another possible reason why clades may have different patterns of dental complexity may be because different patterns of dental eruption potentially limit the teeth's adaptive plasticity. This may explain the generally homogenous distributions of dental complexity amongst herbivorous and invertivorous members from Afrotheria and Marsupialia (Figure 36, Figure 51, Figure 56). Even though this is only documented to affect adaptive plasticity in marsupials (Werdelin, 1987, Forasiepi and Sánchez-Villagra, 2014), which exclusively replace their last premolar; it is plausible that this may also affect afrotherians which are characterized by a delayed dental eruption (Asher and Lehmann, 2008). Carnivorous marsupials notably have OPCR scores that are generally much higher than those of carnivorous laurasiatherians and those of other marsupials (Figure 36, Figure 41, Figure 51, Figure 57). This is likely because carnivorous

marsupials do not have carnassial teeth. Although some large-bodied species, such as the Tasmanian devil (*Sarcophilus harrisii*), have teeth that show some carnassialization (Butler, 1946, Werdelin, 1987, Forasiepi and Sánchez-Villagra, 2014); most carnivorous marsupials generally do not have this feature and have lower molars characterized by complex occlusal surfaces, similar to those of invertivores, which result in high OPCR scores.

Another explanation for the poor correlation may be because dental complexity likely corresponds more closely to hardness indices or dietary categorizations that are more carefully partitioned with regards to material property differences amongst foodstuffs. This study aimed to broadly assess OPCR's affinity with dietary variables in tandem with determining its utility as a tool for dietary inference in non-mammalian cynodonts; as such the dietary categorization implemented in this study are broad since most palaeobiological studies partition diet into carnivory, herbivory and insectivory. The dietary categorization implemented for herbivory, invertivory and nectivory did not consider the fundamental differences in material properties (Table 1). The property differences amongst invertivorous and nectivorous foodstuffs have already been discussed. Similarly, the broad implementation of herbivory did not consider abrasiveness differences of foodstuffs such as grass, leaves, or herbs, which plays a significant role in influencing postcanine tooth morphology (Kay, 1978, Kubo and Yamada, 2014). Grazers and folivores likely have different distributions of OPCR scores; for example, the giraffe (*Giraffa camelopardalis*, OPCRavg=68.5; Table E10) predominantly browses and is associated with relatively lower OPCR scores than those of a grazer such as the sitatunga (*Tragelaphus spekii*, OPCRavg= 95; Table E10). This may also explain why herbivorous and invertivorous members are characterized by a wide range of highly similar OPCR scores (Figure 37, Figure 42, Figure 47, Figure 52, Figure 57).

Even though the dental complexity scores of the second and third molar are significantly influenced by granivory, these describe relatively less variation in OPCR scores than the OPCR allometry patterns (Table 16, Table 17). The OPCR allometry patterns in granivorous mammals consistently explain the most variation in dental complexity scores (Tables 13—17). Accordingly, these small-bodied granivorous mammals have less complex teeth than large-bodied granivorous

mammals (Figure 39, Figure 44, Figure 49, Figure 59). However, these relationships only explain up to 12.34% of the total variation in OPCR scores and are associated with high standard errors (Tables 13—17). This implies that the identified allometry patterns may be inaccurate, which is likely the case, given that none of the sampled granivorous species are obligate granivores, furthermore granivores were not extensively sampled (Table C1). However, a possible explanation for small-bodied granivores possessing less complex teeth compared to large-bodied granivores could be because small-bodied granivorous species have relatively blunter molars to enhance crack resistance. Although this is most prominent in granivorous primate species (see Rosenberger and Kinzey, 1976, Maier, 1984, Lucas et al., 1985, Yamashita, 1998), it's possible that small-bodied granivorous species have similar adaptations. Small-bodied granivorous species are mainly rodents such as the grey dwarf hamster, European edible dormouse (*Glis glis*) and the meadow jumping mouse (*Zapus husonius*), which have a suite of behavioural and physiological adaptations that enable them to be more dependent on seeds as a food source. This includes seed-hoarding, adaptative hypothermia (torpor), fat accumulation and communal huddling in nests. These adaptations, albeit non-morphoskeletal, allow small-bodied granivores to consume a larger proportion of seeds relative to large-bodied granivores. Large-bodied granivorous species, such as the white lipped-peccary (*Tayassu pecari*) and the central African oyan (*Poiana richardsonii*) are relatively less dependent on seeds and may require relatively more complex teeth to accommodate a wider variety of foodstuffs. The variation in tooth forms is notably similar among small-bodied and large-bodied granivorous mammals; as large-bodied and small-bodied granivorous species alike had either flattened (e.g., meadow jumping mouse and aye-aye), lophate (e.g., Desmarest's spiny pocket mouse and white-lipped peccary) or cuspidate (e.g., grey dwarf hamster and central African linsang) tooth forms.

The OPCRm3 allometry patterns amongst carnivores explained 5.8% of the variation in OPCRm3 scores (Table 17). According to this model the third molar of small-bodied carnivorous species have higher dental complexity scores, and large-bodied carnivorous species have third molars with lower dental complexity scores (Figure 60). This may be attributed to the fact that large-bodied

carnivorous species are obligate carnivores and these species may have simplified third molars reflective of their hypercarnivorous diet. Despite being predominantly carnivorous, small-bodied carnivorous species still incorporate some proportion of invertebrates in their diet. These include carnivorous soricids and didelphids such as the thick-tailed opossum (*Luterolina crassicaudata*) and the Eurasian water shrew (*Neomys fodiens*). These species typically possess tooth forms characterized by tall sharp cusps and deep crushing basins, commonly associated with an “insectivorous” tooth form, which could explain their relatively higher dental complexity. It is worth noting that this allometry pattern does not include most hypercarnivorous laurasiatherian species, such as felids and mustelids, as they lose their third molar to form a “slicing blade” (Balisi and Van Valkenburgh, 2020).

13.3 Implications for dietary inference in cynodonts

Even though mandible shape appears to be tightly constrained by inherited musculature, there are major shape differences amongst dietary categories and using mandible shape to predict the diet of mammals has a median success rate of 75%. Using body mass and relative mandible size to predict the diet of mammals has a median success rate of 53%, and considering these size variables together with mandible shape has a median success rate of 80%. My results show that dental complexity is poorly correlated with diet across different groups of mammals, and using OPCR scores to predict the diet of mammals has a median success rate of up to 48%. Using OPCR scores and body mass to predict the diet of mammals has a median success rate of 66%. Using both mandible shape and OPCR scores to predict diet has a median success rate of 80%. Mandible shape is influenced by OPCRm1 and OPCRm3 scores, although this only explains up to 1.1% of the variation in mandible shape.

Dietary inferences in non-mammalian cynodonts have been largely been based on tooth morphology (Jenkins and Parrington, 1976, Gow, 1978, Kemp, 1979, Reisz and Sues, 2000), however, my results show that mandible shape data is just as informative - as dietary estimates based on mandible shape data were more successful at predicting mammal’s diets compared to using only OPCR or size variables. Although the mandible seems to be highly constrained by an

animal's inherited musculature, there are major shape differences amongst dietary categories: herbivorous animals have a tall posterior mandible body (Figure 24); carnivorous animals have a tall coronoid process and reduced angular process (Figure 16); and invertivorous animals may have a tall coronoid process and a prominent angular process (Figure 22), or a long mandible with a low coronoid process and a reduced angular process (Figure 23, B). These shape differences facilitated reliable predictions of mammalian herbivores and invertivores at high confidence levels ($PP_{herbivore}$=0.96—0.99; $PP_{invertivore}$:0.80—0.82). While mammalian carnivores did not exhibit the highest misclassification rates using mandible shape (Table 6), these estimates were associated with relatively lower confidence levels ($PP_{carnivore}$=0.76—0.79). Herbivores are misclassified the least when using mandible shape (Table 6), this is likely because the dorsoventral expansion of the posterior mandible body makes them particularly conspicuous (Figure 24, Figure 27). Although herbivores have a wide morphospace (Figure 11, Figure 13), this dorsoventral expansion, which characterizes most mammalian herbivores, serves as an adaptation to maximize the attachment area for the masseter muscle groups. These muscles operate as the dominant jaw closing muscles in mammalian herbivorous groups (Turnbull, 1970, Pérez-Barbería and Gordon, 1999). Carnivores were often misclassified as invertivores, and vice versa (Table 6), likely because both exhibit a tall coronoid process (Figure 22, Figure 24, Figure 28, Figure 29). It is possible that these groups are characterized by different chewing mechanisms (Dötsch, 1986), however the tall coronoid process is documented as an adaptation to maximize the surface area for the temporalis muscle groups (Hartstone-Rose et al., 2019, Ito and Endo, 2019). This adaptation is essential for both carnivores and invertivores as they require high transverse movements during chewing (Dötsch, 1986, Greaves, 1991).

Since these shape differences broadly reflect the functional adaptations linked to different diets, the patterns of shape variation amongst diets still applied to non-mammalian cynodonts. Dietary estimates made using mandible shape data coincided with the expected diets documented in the literature to some degree (Table 7). Species characterized by a relatively tall coronoid process (Figure 30, A) were estimated as carnivores at high confidence levels ($PP_{carnivore}$= 0.72—0.99), this included *Cynognathus*, *Procynosuchus* and both *Trirachodon* species.

Cynognathus is considered as carnivorous in the existing literature (Gow, 1978). *Trirachodon* is generally considered omnivorous (Hendrickx et al., 2019, Reisz and Sues, 2000, Kemp, 2005), and was classified as “herbivorous” in this study, however their mandibles show no sign of adaptations to herbivory (Table 7). *Procynosuchus* is generally considered invertivorous based off the initial description done by Kemp (1979).

Diademodon was estimated as herbivorous, and this coincides with existing literature (Gow, 1978). *Diademodon’s* mandibular condyle is elevated relative to the horizontal plane (Figure 30, B), and this feature corresponds most to those of some mammalian herbivores (Figure 11, Figure 12). However, *Diademodon* still has a relatively large coronoid process which may explain why the associated confidence level is low ($PP_{herbivore}$= 0.42). *Megazostrodon* was estimated as invertivorous, and this dietary estimate also coincided with expected diet (Jenkins and Parrington, 1976, Debuysschere et al., 2015). *Megazostrodon’s* mandible is long with a highly reduced coronoid process (Figure 30, C) and angular process, these features are most associated with invertivory (Figure 23, B) which explains the high confidence level ($PP_{invertivore}$= 0.92).

Carnivory may be prone to overestimation given that non-mammalian cynodonts have the primitive jaw joint and that this is generally much lower than in mammals (Figure 30). This results in the appearance of a large coronoid process (due to placement of SL2) and may have contributed to the inflated confidence levels in carnivory estimates and low confidence levels in herbivory estimates. Future research may bypass this by employing alternate landmarking regimes. Considering that non-mammalian cynodonts underwent significant morphological changes during their evolution (Luo, 2007), it is possible that their mandibles display a greater adaptive plasticity to dietary adaptations than what is observed in present-day mammals. However, this requires further analysis as this study utilized a small sample of mandibles (Table A2). Notably, this sample did not include the mandibles of traversodontids which are acknowledged as being highly adapted to herbivory amongst gomphodonts (Crompton and Attridge, 1986, Abdala and Ribeiro, 2003).

Even though dietary inferences made using body mass and residual mandible size did not have the lowest success rate, these estimates are anticipated to provide less informative insights into diet. This is because body mass is only indirectly related to diet and relative mandible size only correlates to some dietary variables (Table 8, Figure 34). These size variables facilitated reliable predictions of mammalian herbivores and invertivores at high confidence levels ($PP_{herbivore}$= 0.76—0.89; $PP_{invertivore}$: 0.80—0.82), likely because mammals within these dietary groups occupy relatively distinct size classes (Figure 31). However, carnivores were prone to frequent misclassification (Table 9), and even when correctly estimated, these estimates were associated with low confidence levels ($PP_{carnivore}$=0.40—0.50). This is likely because carnivores have an intermediate distribution of body sizes (Figure 31). This underlying relationship that mammalian body mass has with diet (Figure 31, Figure 34), does not appear to strongly apply to non-mammalian cynodonts as most non-mammalian cynodonts were estimated as herbivores regardless of body size differences (Table 10). These herbivorous dietary estimates were associated with moderate to high confidence levels ($PP_{herbivore}$= 0.63—0.89), however the underlying pattern is unclear as non-mammalian cynodonts across a variety of size classes were estimated as herbivorous (Table 10, Table D2). The only exception to this was the small-bodied *Megazostrodon*, which was estimated as an invertivore at a high confidence level ($PP_{invertivore}$= 0.90).

Utilizing mandible shape and size estimates enhances the chances of predicting an animal's diet correctly, with an 80% median success rate. However, these estimates similarly are expected to provide less informative insights into diet. Relative to using only mandible shape, also considering size variables only significantly improved the reliability of predicting invertivores (Table 7, Table 11). This improvement is likely due to their generally limited distribution of body sizes (Figure 31, Figure 34). Using mandible shape in conjunction with size variables estimated *Procynosuchus* and *Trirachodon* species as carnivorous at high confidence levels ($PP_{carnivore}$=0.99). Relative to using only mandible shape, also considering size variables improved the confidence level associated with *Diademodon's* estimate as a herbivore ($PP_{herbivore}$=0.84). Even though using only mandible shape concluded that *Cynognathus* has a mandible shape most

resembles that of a carnivore (Table 7, $PP_{carnivore}$=0.90), its large-body mass led to a high confidence in its dietary estimation as a herbivore (Table 11, $PP_{herbivore}$=0.99). *Megazostrodon* is estimated as an invertivore at high confidence levels when using only mandible shape ($PP_{invertivore}$=0.92) or size variables ($PP_{invertivore}$=0.90) and considering these together also resulted in an even higher confidence level (Table 10, $PP_{invertivore}$=0.99).

My results show that OPCR scores are not appropriate to use on a macroevolutionary scale as using average and summed dental complexity scores (OPCRavg and OPCRsum) to estimate the diet of mammals has a median success rate of 44%, making it the worst proxy to use for dietary inferences amongst the variables evaluated here. Although the molar dental complexity scores (OPCRm1-m3) seem to have a relatively stronger correlation with diet, using these only marginally improved dietary estimates as they are associated with a median success rate of 48%. This is consistent with my previous findings (Tables 13—17), and the poor correlative relationships are likely because mammals are champion chewers, and they exhibit substantial variation in their chewing patterns across major mammalian clades. However, OPCR scores could still be useful within a more refined framework when addressing a targeted dietary inference question, with careful selection of appropriate comparative groups.

Iterations of pDFAs generally associated carnivory with low OPCR scores, however herbivory and invertivory were interchangeably associated with the highest OPCR scores (Figure 61, Figure 62, Figure 63, Figure 65, Figure 66, Figure 67). This may be because the distributions of OPCR scores amongst herbivores and invertivores were highly similar (Figure 37, Figure 42, Figure 47, Figure 52, Figure 57). Using OPCR variables for dietary predictions generally yields dietary estimates associated with much lower confidence levels compared to the other variables used in this study. However, the confidence levels associated with using OPCRm1-m3 scores were relatively higher than those of OPCRavg and OPCRsum scores. OPCRm1-m3 scores were best at predicting the diet of carnivores at moderate confidence levels ($PP_{carnivore}$=0.53—0.65). Herbivores and invertivores were frequently misclassified, and successful estimates are generally associated with low to intermediate confidence levels ($PP_{herbivore}$=0.53—0.64; $PP_{invertivore}$=0.33—0.52).

Since non-mammalian cynodonts generally have much lower OPCR scores than those of mammals (Figure 36, Figure 41, Figure 46, Figure 51, Figure 56), most non-mammalian cynodonts were estimated as carnivores when using dental complexity scores as a proxy for diet (Table 19, Table 21). This notably included many gomphodonts for which only tooth models were available (Table A2, Table 19, Table 21), these taxa bear bucco-lingually expanded postcanines which are regarded as an adaptation for their herbivorous ecology (Abdala and Gaetano, 2018, Hendrickx et al., 2019, Reisz and Sues, 2000). However, the only traversodontids that were estimated as herbivorous were *Cricodon*, *Luangwa* and *Traversodontid* sp (Table 19, Table 21). Other non-mammalian cynodonts estimated as herbivores included *Diademodon* and *Megazostrodon* (Table 19, Table 21). These taxa notably exhibited some of the highest OPCR scores amongst non-mammalian cynodonts (Figure 64, Figure 68).

Since there are distinct differences in the dental complexity scores amongst non-mammalian cynodonts of different hypothesized diets (Figure 35, Figure 40, Figure 45, Figure 50, Figure 56), dental complexity may still be a suitable proxy to use for dietary inferences. However, comparing these to an extant comparative group with similarly low distributions of OPCR scores may yield more palpable results. There is also a possibility that the differences in dental complexity scores reflect selective pressures favouring more complex teeth during the course of non-mammalian cynodont evolution (Gow, 1980, Crompton, 1995, Abdala and Gaetano, 2018). This may explain why the mammaliaforme, *Megazostrodon*, has a much higher dental complexity score than those of other non-mammalian cynodonts or mammalian invertivores (Figure 35, Figure 40, Figure 45, Figure 56). Another plausible explanation is that non-mammalian cynodonts may have different strategies to achieve dental complexity – in traversodontids this appears to be a large number of moderately complex teeth, whereas mammaliaformes have fewer teeth but these are highly complex (Figure 35, Figure 40, Figure 45, Figure 50, Figure 56). Additionally, considering that dental eruption patterns may have affected patterns of dental complexity in mammals, the same may be true for non-mammalian cynodonts which continuously replaced their teeth throughout their life (Greenwald, 1988, Luo et al., 2004).

Considering OPCRm1-m3 scores together with body mass improved dietary estimates in mammals by 34%. These estimates are regarded as less informative with regards to dietary adaptations, however, considering body mass and OPCRm1-m3 scores estimated most non-mammalian cynodonts as herbivorous (Table 21). These estimates seem to reflect body mass distributions more strongly than OPCR scores; since large-bodied taxa with low OPCRm1-m3 scores such as *Cynognathus* were estimated as herbivorous at a high confidence level ($PP_{herbivore}$= 0.91), and small-bodied taxa with high OPCRm1-m3 scores such as *Megzostrodon* were estimated as invertivorous at a high confidence level ($PP_{invertivore}$= 0.98). These estimates strongly contrast those of using only OPCRm1-m3.

Utilizing mandible shape in conjunction with either dental complexity scores or size variables provide the best chances of reliably predicting an animal's diet (Table 11, Table 25). Although these are generally similar in terms of average success, using mandible shape in conjunction with OPCR scores may offer more informative insights regarding dietary adaptations because animals that have constrained mandible shapes seem to show more adaptive plasticity in their teeth. For example, although the panda's mandible shape closely resembles those of other carnivorans, as previously discussed – the panda's first molar is extremely complex (see section 13.4.1). My results show that mandible shape and OPCR scores are generally weakly correlated, as only OPCRm1 and OPCRm3 scores significantly influence mandible shape (Table 24). Both relationships explain a small portion of total shape variation (R^2=0.010, R^2=0.011). These relationships may be due to the differences in mandible shape and OPCR scores between artiodactyls relative to soricids and dasyuromorphs (see section 13.4.1). However, their overall distribution shows that mandible shapes and OPCR scores are evenly distributed amongst diet categories (Figure 69, Figure 70). This may be because animals with limited plasticity in their teeth may have more adaptable mandible shapes, as seen in afrotherians which generally have homogenous OPCR scores (Figure 36, Figure 41, Figure 46, Figure 51, Figure 56) but occupy a wide morphospace in mandibular shapes (Figure 11, Figure 13). The inverse scenario may also be true, as exemplified by the earlier mentioned instance of the

panda. This highlights, once again, how animals generally have a wide range of alternative adaptations to the same diet.

Apart from *Megazostrodon*, all non-mammalian cynodonts were estimated as carnivorous when both mandible shape and OPCRm1-m3 scores were considered. These estimates were all associated with high confidence levels ($PP_{carnivore}$=0.92—0.98). This notably included *Diademodon* which was estimated as herbivorous when using only mandible shape to estimate diet. This result may be because non-mammalian cynodonts generally have much lower dental complexity scores. Additionally, the mandible adaptations that non-mammalian cynodonts may have for herbivory, as exhibited by *Diademodon* (Figure 30, B), are slight relative to the conspicuous adaptations to herbivory exhibited in herbivorous mammals (Figure 24).

While neither OPCR nor mandible shape exhibit strong correlations with diet, combining them may offer more robust dietary inferences, potentially enhancing our ability of detecting diet switching. However, this approach needs to be validated through additional testing within a single yet diverse mammalian order with well-known dietary habits, such as Rodentia, before extending its application to non-mammalian cynodonts.

13.4 Implications for macroevolution

A major outstanding question that this study prompts is: why does diet have such a poor quantitative relationship with masticatory features? Individual dietary variables that are statistically significant at most only account for a small amount of the variation in mandible shape (R^2=0.022; Table 5) or dental complexity (R^2=0.028; Table 17). This outcome contradicts my personal assumptions and the consensus in the existing literature which supports the idea that diet strongly influences the masticatory apparatus (e.g., Sheine and Kay, 1977, Liem et al., 2001, Popowics, 2003, Evans and Sanson, 2006, Nogueira et al., 2009, Figueirido and Soibelzon, 2010, Kardong, 2012, Casanovas-Vilar and Van Dam, 2013, Berkovitz and Shellis, 2018, Hedrick and Dumont, 2018). This discussion section is largely speculative and highlights some points to consider and areas of future research for macroevolutionary studies undertaking the investigation of diet's relationship with morphology.

My results suggest that diet generally has a weak selective pressure on masticatory features (Table 5, Table 13, Table 14, Table 16, Table 17) and a plausible explanation for this could be because frequent diet switching in mammalian lineages resulted in weak evidence of adaptation in existing lineages. Although evolutionary-scale information on dietary components is extremely limited and it is currently unknown whether the distribution of food types in living animals are similar to those of their extinct relatives, dietary specialization is a strategy seldomly employed amongst living mammals as dietary data shows that most taxa depend on a mixture of food types in their diets (Table D1). The reason why animals may opt for more flexible diets (mixed feeding) could be because being adapted to solely consume one food source increases the risk of extinction (e.g., Genovesi et al., 1996, Wiggins et al., 2006, Boyles and Storm, 2007, Shipley et al., 2009, Kahlke and Kaiser, 2011, Machado et al., 2023), especially in an ever-changing environment (Salamin et al., 2010, Rajak, 2021). These animals may rely on “generalist” or unspecialized mandible shapes and tooth morphologies which are readily adaptable. Dietary “specialists” which consume only one food source are generally more conspicuous in mandible shape and tooth complexity, as exemplified by grazing ungulates which exhibit highly specialized mandibular shapes (Figure 11, Figure 13) and higher dental complexity scores (Figure 36, Figure 41, Figure 46, Figure 51, Figure 56). Further analyses could attempt to quantify “specialization” to examine the effects that this has on mandible shape or OPCR scores relative to mixed feeders.

Another factor to consider is that diet may have a complex relationship with masticatory features which influences the masticatory apparatus in seemingly obscure ways. For instance, an animal’s fallback diet, which is only seasonally relied on when the preferred food source is scarce, may exert a stronger selective pressure on masticatory features than the preferred food source which an animal eats most of the time (Rosenberger, 2013). This has only been assessed in primates, and these studies show that fallback diets have a stronger selective pressure than the preferred diets, as these fallback diets strongly influence tooth topography and jaw robusticity (Lambert et al., 2004, Ungar, 2004, Taylor, 2006, Vogel et al., 2008, Marshall et al., 2009). My study overlooks the effect that these fallback diets have on masticatory features and future studies should utilize

secondary or tertiary categories of dietary classification to test whether mandible shape and dental complexity (OPCR) correspond more closely to these fallback diets as opposed to the foodstuff the animal mostly eats (i.e., preferred diet).

The dietary categorization utilized in this study is flawed as it does not properly account for the dissimilarities in material properties among different foodstuffs. Future research should carefully consider these aspects of diet during categorization, as they bear significant implications for the functional requirements associated with the consumption of different foodstuffs. However, it could be even more informative to assess how different material properties, such as Young's modulus (stiffness) and fracture toughness (energy required to propagate a crack), of various foodstuffs correlate with mandible shape or dental complexity (Strait, 1997). This would entail compiling a database containing different foodstuffs that animals reportedly eat and estimating these variables using a universal testing machine or a tensile testing machine. These material property variables will then be used instead of dietary categories. Studies that use material properties instead of traditional dietary categorization find that the mechanical variables correspond closely to masticatory features (i.e., tooth topography, mandibular robusticity) (Yamashita, 2008, Vogel et al., 2014). However, these studies are largely limited to primates and even though it's expected that these material property variables may explain a larger amount of the observed variation in masticatory features, it has not yet been assessed on a larger macroevolutionary scale.

Another observation that would be interesting to examine in greater detail is that there seems to be a trade-off relationship between mandible shape and dental complexity, whereby clades of mammals that have disparate mandible shapes show little variation in tooth complexity (e.g., Afrotheria; Figure 13, Figure 36, Figure 41, Figure 46, Figure 51, Figure 56) and vice versa (e.g., Laurasiatheria; Figure 13, Figure 36, Figure 41, Figure 46, Figure 51, Figure 56). However, most mammalian clades seem to have constrained mandible shapes and more diverse tooth complexities (Figure 11, Figure 13, Figure 36, Figure 41, Figure 46, Figure 51, Figure 56). This suggests that the evolutionary constraints on mandible shape (via constrained mandibular muscle configurations) are stronger than those on tooth morphology. Considering this point, while my results indicate that mandible

shape generally contains more information about diet than tooth complexity (Table 5, Table 13, Table 14, Table 16, Table 17), my results also show that diet has a weak selective pressure on mandibular shape since mammals of the same dietary preference generally do not converge on the same or highly similar mandible shapes (see section 14.1). This could be because deeply nested adaptations, such as muscle configurations, are under strong selective pressure, thus maintaining the shape of the jaw in descendent lineages and preventing them from evolving away from some constrained region of morphospace (see section 14.1). Future studies could examine this in greater detail by including extinct members from these major lineages, across a wide range of times and body sizes, to help understand whether this is a phenomenon of living clade endmembers, or whether it is present in deeper time.

Even though dietary adaptations take time to develop and naturally do not manifest immediately, my results suggest that teeth may be more plastic to dietary adaptations than mandible shape (see section 14.3). Therefore, future macroevolutionary dietary studies should focus on building on dental complexity by incorporating additional quantitative metrics. This is largely because dietary adaptations can take many forms in tooth morphologies. This could be through increased occlusal areas, modifying surface complexity (through cusps and lophs)(Janis and Fortelius, 1988), or through increasing the height of a tooth's crown (Janis, 2008). This study shows that there is still more to learn about diet's relationship with morphology, and that this relationship is evidently not as straightforward as one might intuitively assume. Consequently, although I found a poor correlative relationship between OPCR and the dietary variables used here, OPCR may covary with another variable in a way that captures dietary adaptations more clearly. A metric that may correspond to dietary adaptations and be suitable for use together with OPCR is the functional occlusal area which is broadly defined as the dental surface preferentially used during mastication. Studies report that occlusal area impacts chewing patterns (Bourdiol and Mioche, 2000), and that disproportionately larger occlusal areas (relative to body mass) are an adaptation to extensive food processing in ungulates (Janis and Fortelius, 1988, Vizcaíno et al., 2006, Janis, 2008, Heywood, 2010). However, its covariation with other dental morphological variables (e.g., dental complexity)

have never been investigated and it's unknown whether the variation in allometry-free occlusal area correlates to dietary preferences outside ungulates. Another viable approach is considering OPCR together with another quantitative metric commonly used in dental topography analysis, such as dental relief (RFI), which quantifies the relative height of a tooth (Boyer, 2008). Although studies have shown that RFI corresponds to dietary disparity in primates (M'kirera and Ungar, 2003, Boyer, 2008, Boyer et al., 2010, Allen et al., 2015), RFI's correlation to dietary disparity has not yet been assessed across Mammalia. Furthermore, studies that include both OPCR and RFI have not considered the combined explanatory power that these variables have on dietary preferences (Winchester et al., 2014, Pampush et al., 2016a). Either of these multifaceted approaches could potentially provide a more nuanced understanding of diet's relationship with tooth forms.

14. CONCLUSION

This study aimed to assess the viability of using mandible shape/size and dental complexity to infer the diet of non-mammalian cynodonts by evaluating the relationships between mandibular shape/size and dental complexity in mammals with known dietary habits. This is the first study to evaluate the correlative strength that these variables have with diet across Mammalia.

I found that relative mandible size closely corresponds to body mass in mammals (R^2= 0.8013), and most animals have mandible sizes that correspond to their body mass regardless of dietary preferences. Only carnivorous (R^2=0.8073) and frugivorous (R^2=0.8059) mammals have mandible sizes that are relatively disproportionate considering their body sizes. Even though body mass is only indirectly related to diet, using this and the relative mandible size residuals to predict diet has a median success rate of 55%. This is likely due to the underlying association that body mass has with diet in mammals.

Caution should be exercised when inferring diet solely based on mandible shape or dental complexity because both mandible shape (R^2= 0.049) and dental complexity (R^2=0.124) have relatively low explanatory power; this is likely because mammals are characterized by a wide range of masticatory musculatures and chewing patterns which enables mammals of the same diet to exhibit many equally optimal mandible shapes and OPCR scores. However, the mandible shape differences amongst major dietary categories were distinct enough to facilitate reliable dietary predictions, with a median success rate of 75%. Dental complexity was far less successful because the distributions of OPCR scores amongst major dietary categories were highly similar, subsequently using OPCRavg and OPCRsum scores had a median success rate of 44%, and OPCRm1-m3 scores had a median success rate of 48%. Nonetheless, this study shows that utilizing mandible shape in conjunction with either dental complexity scores or size variables provide the best chances of reliably predicting an animal's diet, as these both have a median success rate of 80%.

Non-mammalian cynodonts sampled have less disparate mandibular shapes and OPCR values, in some cases these are outside of or at the tail ends of the distribution of living mammals. This may reflect the relatively weak selective

pressures that diet has on mandible shape and OPCR, or alternatively reflect that these taxa had more varied diets. Alternatively, there may have been insufficient evolutionary time for these traits to evolve or there may have been stronger constraints involved with mandible and tooth shape evolution in non-mammalian cynodonts. Although the OPCR scores of non-mammalian cynodonts show differentiation amongst hypothesized dietary categories, this may correspond to cynodontian evolution selecting more complex teeth.

Future research should seek to understand the impact that fallback diets have on shaping masticatory features across Mammalia as this will improve our understanding of the constraints that diet may have on morphology. Future work should also explore alternative proxies for diet which may explain more of the observed variation in masticatory features.

16. APPENDICES

16.1 Appendix A

Table A1: List of mammal species sampled, together with their specimen numbers and taxonomic affiliations. Details on whether the mammal species had been landmarked or had OPCR scores calculated are provided by T or F, where T=True and F=False.

Taxon	Common name	Specimen number	Superorder	Data source	Landmarked	OPCR	Teeth used (OPCR=T)
Abrocoma cinerea	Ashy chinchilla rat	UMMZ 120621	Euarchontoglires	Morphosource	F	T	m1-3(L)
Acinonyx jubatus	Cheetah	AMNH 119657	Laurasiatheria	Morphosource	T	T	m1, pm1-2 (L)
Acomys cahirinus	Cairo spiny mouse	NHMUK 65.789-793	Euarchontoglires	Morphosource	T	T	m1-3(L)
Acrobates pygmaeus	Feathertail glider	NHMUK 82.7.29.23	Marsupialia	Morphosource	T	T	m1-3(L)
Aepyceros melampus	Impala	FMNH 127890	Laurasiatheria	Morphosource	T	T	m1-3(L)
Aepyprymnus rufescens	Rufous rat kangaroo	FMNH 124573	Marsupialia	Morphosource	T	T	m1-3(L)
Ailuropoda melanoleuca	Giant panda	FMNH 31128	Laurasiatheria	Morphosource	T	F	NA
Ailuropoda melanoleuca	Giant panda	IMNH C 302	Laurasiatheria	Morphosource	F	T	m1-2, pm4(R)
Ailurus fulgens	Red panda	NHMUK 1911.10.18.1	Laurasiatheria	Morphosource	T	T	m1-2, pm4(R)
Alces alces	Moose	NMS 1996.39	Laurasiatheria	Morphosource	T	T	m1-3(L)
Alouatta seniculus	Columbian red howler monkey	FMNH 18869	Euarchontoglires	Morphosource	T	T	m1-3(L)

Amblysomus hottentotus	Hottentot golden mole	UMZC 2010.15A	Afrotheria	Morphosource	T	T	m1-2, pm3(R)
Anomalurus beecrofti	Beecroft's flying squirrel	NHMUK 1989.174	Euarchontoglires	Morphosource	T	T	m1-3(R)
Anourosorex squamipes	Chinese mole	NHMUK 1933.4.1.165	Laurasiatheria	Morphosource	T	T	m1-3(L)
Antechinomys laniger	Kultarr bettong	NHMUK 32.2.11.23	Marsupialia	Morphosource	T	T	m1-4(R)
Antechinus stuartii	Brown antechinus	FMNH 129556	Marsupialia	Morphosource	T	T	m1-4(L)
Antilocapra americana	Pronghorn	FMNH 57215	Laurasiatheria	Morphosource	T	T	m1-3(R)
Antilope cervicapra	Blackbuck	NMS 2000.301.2	Laurasiatheria	Morphosource	T	T	m1-3(L)
Aonyx cinerea	Asian small-clawed otter	FMNH 62868	Laurasiatheria	Morphosource	T	T	m1-m2, pm3(L)
Aplodontia rufa	Mountain beaver	FMNH 60775	Euarchontoglires	Morphosource	F	T	m1-3(R)
Apodemus sylvaticus	Wood mouse	NHMUK unnumbered	Euarchontoglires	Morphosource	T	T	m1-3(L)
Arctictis binturong	Binturong	NMS 2015.164.1	Laurasiatheria	Morphosource	T	F	m1, Pm1 (R)
Ateles geoffroyi	Black-handed spider monkey	MCZ 10138	Euarchontoglires	Morphosource	T	T	m1-3(L)
Atelocynus microtis	Short-eared dog	FMNH 60674	Laurasiatheria	Morphosource	T	T	m1-m2, pm4(L)
Atherurus africanus	African brush-tailed porcupine	UMZC E.3489	Euarchontoglires	Morphosource	T	T	m1-3(L)
Atilax paludinosus	Marsh mongoose	NHMUK 1867.7.8.11	Laurasiatheria	Morphosource	T	T	m1-2, pm3(L)

Babyrousa babyrussa	Babirusa	NMS 2008.27	Laurasiatheria	Morphosource	T	T	m1-3(L)
Bandicota indica	Indian bandicoot rat	NHMUK 1978.896	Euarchontoglires	Morphosource	T	T	m1-3(L)
Bassaricyon alleni	Eastern lowland olingo	FMNH 104935	Laurasiatheria	Morphosource	T	T	m1-2, pm4(L)
Bettongia penicillata	Woylie	FMNH 129431	Marsupialia	Morphosource	T	T	m1-4(L)
Bison bonasus	European bison	NHMUK 194.9.6.29.1	Laurasiatheria	Morphosource	T	T	m1-3 (L)
Boselaphus tragocamelus	Nilgai	NHMUK 1974.411	Laurasiatheria	Morphosource	T	T	m1-2(L)
Bradypus variegatus	Brown-throated sloth	FMNH 69589	Xenarthra	Morphosource	T	T	m2-4(L)
Callimico goeldii	Goeldi's monkey	FMNH 58003	Euarchontoglires	Morphosource	T	T	m1-3(L)
Callithrix jacchus	Common marmoset	FMNH 231573	Euarchontoglires	Morphosource	T	T	m1-2, pm3(L)
Callosciurus notatus	Plantain squirrel	NHMUK 75.1337	Euarchontoglires	Morphosource	T	T	m1-3(R)
Caluromys derbianus	Derby's woolly opossum	UMMZ 114856	Marsupialia	Morphosource	T	T	m1-4(R)
Caluromysiops irrupta	Black-shouldered opossum	FMNH 60698	Marsupialia	Morphosource	T	T	m1-4(R)
Camelus dromedarius	Dromedary camel	OUMNH 144882	Laurasiatheria	Morphosource	T	T	m1-3(L)
Canis latrans	Coyote	UMZC K.3341	Laurasiatheria	Morphosource	T	T	m1-m2, pm4(L)
Canis mesomelas	Black-backed jackal	UMZC K3402	Laurasiatheria	Morphosource	T	T	m1-m2, pm4(L)
Canis simensis	Ethiopian wolf	AMNH 81001	Laurasiatheria	Morphosource	T	T	m1-3(R)

Capra sibirica	Siberian ibex	FMNH 134541	Laurasiatheria	Morphosource	T	T	m1-3(L)
Caracal caracal	Caracal	AMNH 113794	Laurasiatheria	Morphosource	T	T	m1, pm1-2(L)
Castor canadensis	American beaver	WLM unnumbered	Euarchontoglires	CT scanned (ESI)	T	T	m1-3(R)
Cavia fulgida	Shiny guinea pig	UMZC E3705	Euarchontoglires	Morphosource	T	T	m1-3(R)
Cephalophus nigrifrons	Black-fronted duiker	NHMUK 1936.10.28.33	Laurasiatheria	Morphosource	T	T	m1-3(R)
Cercartetus concinnus	Western pygmy possum	NHMUK 97.11.18.1	Marsupialia	Morphosource	T	T	m1-3(L)
Cervus elaphus	Red deer	NMS 1981.68	Laurasiatheria	Morphosource	T	T	m1-3(L)
Cheirogaleus major	Greater dwarf lemur	FMNH 85144	Euarchontoglires	Morphosource	T	F	m1-3(L)
Chironectes minimus	Water opossum	UMMZ 126289	Marsupialia	Morphosource	T	T	m1-4(R)
Chiropotes satanas	Black bearded saki	FMNH 95512	Euarchontoglires	Morphosource	T	F	m1-3(L)
Chlorocebus sabaeus	Green monkey	USNM 381445	Euarchontoglires	Morphosource	F	T	m1-3(L)
Choeropsis liberiensis	Pygmy hippopotamus	NMS Z.2005.3	Laurasiatheria	Morphosource	T	F	m1-m3(R)
Choloepus hoffmanni	Hoffmann's two-toed sloth	NHMUK 1973.824	Xenarthra	Morphosource	T	T	m2-4(L)
Chrysochloris asiatica	Cape golden mole	UMZC E.5472. F	Afrotheria	Morphosource	T	T	m1-3 (L)
Chrysochloris stuhlmanni	Stuhlmann's golden mole	NHMUK 1934.4.1.7.11	Afrotheria	Morphosource	T	T	m1-3 (L)
Coendou prehensilis	Brazilian porcupine	NHMUK 512.F	Euarchontoglires	Morphosource	T	T	m1-3(L)
Colobus satanas	Black colobus	NHMUK	Euarchontoglires	Morphosource	T	T	m1-3(L)

	monkey	1856.12.29.1					
Condylura cristata	Star-nosed mole	UMMZ 80270	Laurasiatheria	Morphosource	T	T	m1-3(L)
Connochaetes taurinus	Blue wildebeest	NHMUK 1935.12.14.3	Laurasiatheria	Morphosource	T	T	m1-3(R)
Cricetomys gambianus	Gambian pouched rat	NHMUK 1890.3.27.2	Euarchontoglires	Morphosource	T	T	m1-3(L)
Cricetulus migratorius	Grey dwarf hamster	UMZC E2322	Euarchontoglires	Morphosource	T	T	m1-3(L)
Crocidura fuscomurina	Bicoloured musk shrew	UMZC E 5251.G	Laurasiatheria	Morphosource	T	T	m1-3(L)
Crocuta crocuta	Spotted hyena	FMNH 127826	Laurasiatheria	Morphosource	T	T	m1, Pm1-2(L)
Cryptoprocta ferox	Fossa	NHMUK 1968.6.7.1	Laurasiatheria	Morphosource	T	T	m1-2, pm3(L)
Cryptotis mexicana	Mexican small-eared shrew	UMMZ 113138	Laurasiatheria	Morphosource	F	T	m1-3(L)
Cuniculus taczanowskii	Mountain paca	FMNH 70804	Euarchontoglires	Morphosource	T	F	NA
Cynocephalus volans	Philippine flying lemur	OUMNH 3404	Euarchontoglires	Morphosource	T	T	m1-3(L)
Dactylopsila trivirgata	Northern glider	NHMUK 1897.8.7.79	Marsupialia	Morphosource	T	T	m1-4(R)
Dama dama	European fallow deer	OUMNH 19343	Laurasiatheria	Morphosource	T	T	m1-3(L)
Dasycercus cristicauda	Crest-tailed mulgara	NHMUK 1897.11.3.4	Marsupialia	Morphosource	T	T	m1-4(R)
Dasyprocta punctata	Central American agouti	FMNH 21260	Euarchontoglires	Morphosource	T	T	m1-3(L)
Dasypus hybridus	Southern	AMNH M-	Xenarthra	Morphosource	T	F	Pm1-3(L)

	long-nosed armadillo	205706					
Dasyurus hallucatus	Northern quoll	FMNH 119804	Marsupialia	Morphosource	T	T	m2-4(L)
Dasyurus maculatus	Tiger quoll	UMZC A6.10-3	Marsupialia	Morphosource	T	T	m1-4(R)
Dasyurus viverrinus	Eastern quoll	SAMA M7222	Marsupialia	Morphosource	T	T	m1-4(R)
Daubentonia madagascariensis	Aye-aye	UMZC E.8021.A	Euarchontoglires	Morphosource	T	T	m1-3(L)
Dendrohyrax arboreus	Southern tree hyrax	FMNH 163770	Afrotheria	Morphosource	T	F	m1-3(L)
Dendrolagus dorianus	Doria's tree kangaroo	NMS 2006.38	Marsupialia	Morphosource	T	F	NA
Desmana moschata	Russian desman	UMMZ 124125	Laurasiatheria	Morphosource	T	T	m1-3(L)
Dicerorhinus sumatrensis	Sumatran rhinoceros	NMS 1994.131	Laurasiatheria	Morphosource	T	T	m1-3(L)
Didelphis marsupialis	Common opossum	NHMUK 1948.7.12.5	Marsupialia	Morphosource	T	T	m2-4(L)
Diplomesodon pulchellum	Piebald shrew	FMNH 137436	Laurasiatheria	Morphosource	T	T	m1-3(L)
Dolichotis patagonum	Patagonian mara	FMNH 49231	Euarchontoglires	Morphosource	T	T	m1-3(L)
Dorcopsis muelleri	Brown dorcopsis	NHMUK 1933.11.4.4	Marsupialia	Morphosource	T	T	m1-4(L)
Dromiciops gliroides	Monito del monte	UMMZ 156354	Marsupialia	Morphosource	T	T	m1-4(R)
Dugong dugon	Dugong	MVZ 101162	Afrotheria	Morphosource	T	F	NA
Dugong dugon	Dugong	WLM unnumbered	Afrotheria	CT scanned (ESI)	F	T	m1-3 (L)
Echinops telfairi	Lesser	NHMUK	Afrotheria	Morphosource	T	T	m1-2,

	hedgehog tenrec	1970.355					pm3(R)
Echinosorex gymnura	Moonrat	UMZC E.5111.C-E	Laurasiatheria	Morphosource	T	T	m1-3(L)
Echymipera rufescens	Long-nosed echymipera	FMNH 60525	Marsupialia	Morphosource	T	T	m1-4(L)
Elephantulus brachyrhynchus	Short-snouted elephant shrew	NHMUK 1963.1004	Afrotheria	Morphosource	T	T	m1-3(RI)
Elephantulus rozeti	North-African elephant shrew	NHMUK 1891.10.15.11	Afrotheria	Morphosource	T	T	m1-3(L)
Enhydra lutris	Sea otter	NHMUK 80.879	Laurasiatheria	Morphosource	T	T	m1-2, pm3(R)
Episoriculus caudatus	Hodgson's brown-toothed shrew	FMNH 114227	Laurasiatheria	Morphosource	T	T	m1-3(L)
Equus caballus	Horse	OUMNH 19193	Laurasiatheria	Morphosource	T	F	M3, pm2-3
Equus kiang	Kiang	NMS 2016.43	Laurasiatheria	Morphosource	T	F	m1-3(L)
Eulemur macaco	Black lemur	UMZC E8093A	Euarchontoglires	Morphosource	T	T	m1-3(L)
Euroscaptor micrura	Himalayan mole	NHMUK 99.10.25.1	Laurasiatheria	Morphosource	T	T	m1-3(L)
Felis catus	Cat	UMZC K.6182	Laurasiatheria	Morphosource	T	T	m1, pm2, Pm1 (L)
Fossa fossana	Malagasy civet	FMNH 85196	Laurasiatheria	Morphosource	T	T	m1, pm3-4(L)
Funambulus pennantii	Northern palm squirrel	UMMZ 62569	Euarchontoglires	Morphosource	T	T	m1-3(L)
Galago senegalensis	Senegal bushbaby	FMNH 123783	Euarchontoglires	Morphosource	T	T	m1-3(L)
Galemys	Pyrenean	OUMNH 9427	Laurasiatheria	Morphosource	F	T	m1-3(R)

pyrenaicus	desman						
Gazella dorcas	Dorcas gazelle	NMS 2004.46.5	Laurasiatheria	Morphosource	T	T	m1-3(R)
Genetta angolensis	Angolan genet	FMNH 163777	Laurasiatheria	Morphosource	T	T	m1-2, pm4(L)
Geocapromys brownii	Jamaican coney	AMNH 45156	Euarchontoglires	Morphosource	T	T	m1-3(R)
Geogale aurita	Large-eared tenrec	UMMZ 172217	Afrotheria	Morphosource	T	T	m1-3(R)
Geomys pinetis	Southeastern pocket gopher	UMMZ 164642	Euarchontoglires	Morphosource	T	T	m1-3(L)
Gerbillus gerbillus	Lesser Egyptian gerbil	NHMUK 1978.1062	Euarchontoglires	Morphosource	T	T	m1-3(L)
Giraffa camelopardalis	Giraffe	FMNH 34424	Laurasiatheria	Morphosource	T	T	m1-3(L)
Glis glis	European edible dormouse	NHMUK 1996.325	Euarchontoglires	Morphosource	T	T	m1-3(L)
Gracilinanus agilis	Agile gracile opossum	UMMZ 134557	Marsupialia	Morphosource	T	T	m1-4(R)
Gulo gulo	Wolverine	USNM 157327	Laurasiatheria	Morphosource	T	T	pm4, m1-m2
Hemibelideus lemuroides	Lemuroid ringtail possum	FMNH 60926	Marsupialia	Morphosource	T	T	m1-4(R)
Hemiechinus auritus	Long-eared hedgehog	UMMZ 156626	Laurasiatheria	Morphosource	T	T	m1-3(R)
Heterocephalus glaber	Naked mole-rat	NHMUK 91.235	Euarchontoglires	Morphosource	T	T	m1-3(L)
Heteromys desmarestianus	Desmarest's spiny pocket	NHMUK unregistered	Euarchontoglires	Morphosource	T	T	m1-3(L)

	mouse						
Hippopotamus amphibius	Hippopotamus	NMS Z.2008.35	Laurasiatheria	Morphosource	T	T	m1-M3(L)
Hydrochoerus hydrochaeris	Capybara	AMNH M-206440	Euarchontoglires	Morphosource	T	T	m1-2(L)
Hydromys chrysogaster	Rakali	NHMUK 1998.134	Euarchontoglires	Morphosource	T	T	M-3(L)
Hydropotes inermis	Water deer	NMS unnumbered	Laurasiatheria	Morphosource	T	T	m1-3(R)
Hypogeomys antimena	Malagasy giant rat	FMNH 151994	Euarchontoglires	Morphosource	T	T	m1-3(L)
Hystrix africaeaustralis	Cape porcupine	FMNH 60453	Euarchontoglires	Morphosource	T	F	NA
Ictonyx striatus	Striped polecat	UMZC K1874	Laurasiatheria	Morphosource	T	T	m1-2, pm3(L)
Idiurus zenkeri	Pygmy scaly-tailed flying squirrel	UMZC E1421	Euarchontoglires	Morphosource	T	T	m1-3(L)
Isoodon macrourus	Northern brown bandicoot	FMNH 120560	Marsupialia	Morphosource	T	T	m1-4(R)
Isoodon obesulus	Southern brown bandicoot	UMZC A7.4-5	Marsupialia	Morphosource	T	T	m1-4(L)
Kobus megaceros	Nile lechwe	NMS 2001.149.15	Laurasiatheria	Morphosource	T	T	m1-3(R)
Lagostomus maximus	Plains viscacha	NHMUK ZD 1991.174	Euarchontoglires	Morphosource	T	F	m1-3(L)
Lasiorhinus latifrons	Southern hairy-nosed wombat	NMS 1868.31	Marsupialia	Morphosource	T	T	m1-4(L)
Lemur catta	Ring-tailed	FMNH 157993	Euarchontoglires	Morphosource	T	T	m1-3(L)

	lemur						
Leopardus wiedii	Margay	NMS Z.2016.12.1	Laurasiatheria	Morphosource	T	T	m1, pm2 (L)
Lestoros inca	Incan caenolestid	UMMZ 160733	Marsupialia	Morphosource	T	T	m1-4(R)
Liomys irroratus	Mexican spiny pocket mouse	UMMZ 120788	Euarchontoglires	Morphosource	T	T	m1-3(R)
Lophocebus albigena	Grey-cheeked mangabey	NHMUK 1936.10.28.1	Euarchontoglires	Morphosource	T	T	m1-3(L)
Loris tardigradus	Red slender loris	UMZC E.8261.E	Euarchontoglires	Morphosource	T	T	m1-3(L)
Lutreolina crassicaudata	Big lutrine opossum	UMMZ 163450	Marsupialia	Morphosource	T	T	m1-4(R)
Lynx canadensis	Canada lynx	UMZC K.6682	Laurasiatheria	Morphosource	T	T	m1, pm1-2(L)
Macaca sylvanus	Barbary macaque	NHMUK 1858.4.5.1	Euarchontoglires	Morphosource	T	T	m1-3(L)
Macropus eugenii	Tammar wallaby	NHMUK 1948.7.12.3	Marsupialia	Morphosource	T	T	m1-3(R)
Macropus giganteus	Eastern grey kangaroo	NHMUK 72.4498	Marsupialia	Morphosource	T	T	m1-4(R)
Macropus rufus	Red kangaroo	NMS PH26.12	Marsupialia	Morphosource	T	T	m1-4(L)
Macroscelides proboscideus	Round eared elephant shrew	FMNH 137045	Afrotheria	Morphosource	T	T	m1-3(L)
Macrotis lagotis	Greater bilby	NHMUK 73.6.21.4	Marsupialia	Morphosource	T	T	m1-4(L)
Madoqua kirkii	Kirk's dik-dik	NMS POZ8.99	Laurasiatheria	Morphosource	T	T	m1-3(L)
Malacomys longipes	Big-eared swamp rat	UMZC E2265	Euarchontoglires	Morphosource	T	T	m1-3(R)
Malacothrix typica	Gerbil mouse	UMMZ 117815	Euarchontoglires	Morphosource	T	T	m1-3(R)
Marmosa	Woolly mouse	UMMZ 134562	Marsupialia	Morphosource	T	T	m1-4(L)

demerarae	opossum						
Marmosa murina	Linnaeus's mouse opossum	NHMUK 1881.11.1	Marsupialia	Morphosource	T	T	m1-4(R)
Marmota monax	Groundhog	AMNH M-67882	Euarchontoglires	Morphosource	T	T	m1-3(L)
Meles meles	European badger	NHMUK 2002.476	Laurasiatheria	Morphosource	T	T	m1-2, pm4(L)
Mellivora capensis	Honey badger	UMZC K1821	Laurasiatheria	Morphosource	T	F	NA
Mephitis mephitis	Striped skunk	FMNH 129327	Laurasiatheria	Morphosource	T	T	m1-2, pm3
Microcebus murinus	Gray mouse lemur	AMNH M-174537	Euarchontoglires	Morphosource	T	T	m1-3(L)
Microgale brevicaudata	Short-tailed shrew tenrec	UMMZ 174757	Afrotheria	Morphosource	T	T	m1-3(R)
Microgale drouhardi	Drouhard's shrew tenrec	UMMZ 168477	Afrotheria	Morphosource	T	T	m1-3(R)
Microgale thomasi	Thomas's shrew tenrec	UMMZ 172202	Afrotheria	Morphosource	T	T	m1-3(R)
Micropotamogale ruwenzorii	Ruwenzori otter shrew	NHMUK 67.213	Afrotheria	Morphosource	T	T	m1-3 (L)
Monodelphis domestica	Gray short-tailed opossum	UMMZ 165514	Marsupialia	Morphosource	T	T	m1-4(R)
Moschus moschiferus	Siberian musk deer	NHMUK 676.d.45.1.12.44	Laurasiatheria	Morphosource	T	T	m1-3(L)
Muntiacus reevesi	Reeves's muntjac	NMS 1996.142.8	Laurasiatheria	Morphosource	T	F	m1-3(R)
Mus musculus	House mouse	UMZC E.2202	Euarchontoglires	Morphosource	T	T	m1-3(L)
Mustela nivalis	Least weasel	FMNH 207033	Laurasiatheria	Morphosource	T	T	m1-2, pm3(L)
Mustela putorius	European	UMZC K.2361	Laurasiatheria	Morphosource	T	T	m1-2,

	polecat						pm4(L)
Myocastor coypus	Nutria	AMNH 206456	Euarchontoglires	Morphosource	T	F	NA
Myosorex kihaulei	Kihaule's mouse shrew	FMNH 209072	Laurasiatheria	Morphosource	T	T	m1-3(L)
Myospalax myospalax	Siberian zokor	UMMZ 110401	Euarchontoglires	Morphosource	T	T	m1-3(L)
Nandinia binotata	African palm civet	UMZC K.4492	Laurasiatheria	Morphosource	T	T	m1, pm2-3
Napaeozapus insignis	Woodland jumping mouse	UMMZ 126314	Euarchontoglires	Morphosource	F	T	m1-3(L)
Nasua narica	White-nosed coati	UMZC unnumbered	Laurasiatheria	Morphosource	T	T	m1-2, pm4(R)
Nectogale elegans	Elegant water shrew	AMNH M-115571	Laurasiatheria	Morphosource	T	T	m1-3(L)
Neomys fodiens	Eurasian water shrew	NHMUK 1973.917	Laurasiatheria	Morphosource	T	T	m1-3(L)
Neotetracus sinensis	Shrew gymnure	NHMUK ZD 1933.4.1.134	Laurasiatheria	Morphosource	T	T	m1-3(R)
Notomys cervinus	Fawn hopping mouse	NHMUK ZD 1936.12.8.17-8	Euarchontoglires	Morphosource	T	T	m1-3(R)
Notoryctes typhlops	Southern marsupial mole	UMZC A5.11	Marsupialia	Morphosource	T	T	m1-4(L)
Nycticebus coucang	Sunda slow loris	Du Baa 0002	Euarchontoglires	Morphosource	T	T	m1-3(L)
Ochotona alpina	Alpine pika	UMMZ 123059	Euarchontoglires	Morphosource	T	T	m1-3(L)
Okapia johnstoni	Okapi	NHMUK 1971/1738	Laurasiatheria	Morphosource	T	T	m1-M3(L)
Onychogalea fraenata	Bridled nail-tail wallaby	UMZC A12.59.3	Marsupialia	Morphosource	T	T	m1-3(L)
Onychomys	Northern	UWBM 37628	Euarchontoglires	Morphosource	T	T	m1-3(R)

torridus	grasshopper mouse						
Ornithorhynchus anatinus	Platypus	UMZC A2.2.10	Monotremes	Morphosource	T	F	NA
Oryctolagus cuniculus	European rabbit	NHMUK 1849.6.20.9	Euarchontoglires	Morphosource	T	F	NA
Oryx gazella	Gemsbok (Oryx)	NHMUK ZD 1963.10.21.1	Laurasiatheria	Morphosource	T	T	m1-3 (L)
Oryzorictes tetradactylus	Four-toed elephant shrew	UMZC E.5453.C	Afrotheria	Morphosource	T	T	m1-3 (L)
Otocyon megalotis	Bat-eared fox	USMN 49129	Laurasiatheria	Morphosource	T	T	m1-4(L)
Ovis aries	Sheep	OUMNH ZC 14858	Laurasiatheria	Morphosource	T	T	m1-3(L)
Pan troglodytes	Common chimpanzee	RMCA 77032m25	Euarchontoglires	Morphosource	T	T	m1-3(L)
Panthera pardus	Leopard	IMNH 2372	Laurasiatheria	Morphosource	T	T	m1-Pm1-2(R)
Papio hamadryas	Hamadryas baboon	UMZC E.7543.B	Euarchontoglires	Morphosource	T	T	m1-3(L)
Paracrocidura schoutedeni	Lesser large-headed shrew	FMNH 227382	Laurasiatheria	Morphosource	T	T	m1-3(R)
Paradoxurus hermaphroditus	Asian palm civet	FMNH 62837	Laurasiatheria	Morphosource	T	T	m1-2, pm4(L)
Pecari tajacu	Collared peccary	NMS 2002.164.2	Laurasiatheria	Morphosource	T	T	m1-3(L)
Pedetes capensis	South African springhare	FMNH 152053	Euarchontoglires	Morphosource	T	T	m1-3(L)
Perodicticus potto	Potto	USNM 465898	Euarchontoglires	Morphosource	T	T	m1-3(L)
Petauroides volans	Greater glider	NHMUK 1926.3.11.225	Marsupialia	Morphosource	T	T	m1-4(R)

Petaurus breviceps	Sugar glider	FMNH 129430	Marsupialia	Morphosource	T	T	m2-4(L)
Petinomys sagitta	Arrow flying squirrel	UMZC E1499	Euarchontoglires	Morphosource	T	T	m1-3(L)
Petrogale penicillata	Brush-tailed rock-wallaby	FMNH 64435	Marsupialia	Morphosource	T	T	m1-4(L)
Phacochoerus aethiopicus	Desert warthog	UF 31016	Laurasiatheria	Morphosource	T	F	NA
Phacochoerus africanus	Common warthog	OUMNH ZC 3617	Laurasiatheria	Morphosource	T	F	NA
Phascolarctos cinereus	Koala	NHMUK 75.1828	Marsupialia	Morphosource	T	F	m2-4(R)
Phataginus tricuspis	Tree pangolin	NHMUK 34.62.2.94	Laurasiatheria	Morphosource	T	F	NA
Philander opossum	Gray four-eyed opossum	UMMZ 114855	Marsupialia	Morphosource	T	F	NA
Podogymnura truei	Mindanao gymnure	FMNH 149591	Laurasiatheria	Morphosource	T	T	m1-3(L)
Poiana richardsonii	Central African oyan	Ypm VZ MAM 014715	Laurasiatheria	Morphosource	T	T	m1, pm4(L)
Pongo pygmaeus	Bornean orangutan	NHMUK 1986.1097	Euarchontoglires	Morphosource	T	T	m1-3(L)
Potamogale velox	Giant otter shrew	UMZC E5425F	Afrotheria	Morphosource	T	T	m2-3(R)
Potorous tridactylus	Long-nosed potoroo	FMNH 57805	Marsupialia	Morphosource	T	T	m2-4(L)
Presbytis femoralis	Raffles' banded langur	UMZC E.7226.C	Euarchontoglires	Morphosource	T	T	m1-3(L)
Prionailurus viverrinus	Fishing cat	NHMUK 1860.7.22.22	Laurasiatheria	Morphosource	T	T	m1, pm1-2
Procavia	Rock hyrax	FMNH 147999	Afrotheria	Morphosource	T	T	m1-3(L)

capensis							
Procyon lotor	Common raccoon	FMNH 1755311	Laurasiatheria	Morphosource	T	T	m1-2, pm4(L)
Proechimys guyannensis	Guyenne spiny rat	NHMUK 79.322	Euarchontoglires	Morphosource	T	F	NA
Pronolagus rupestris	Smith's red rock rabbit	FMNH 177246	Euarchontoglires	Morphosource	T	F	m1-3(L)
Propithecus diadema	Diademed sifaka	USNM 63350	Euarchontoglires	Morphosource	F	T	m1-3(L)
Propithecus diadema	Diademed sifaka	UMZC E8041A	Euarchontoglires	Morphosource	T	F	NA
Proteles cristata	Aardwolf	NMS unnumbered	Laurasiatheria	Morphosource	T	T	m1, pm2-3(L)
Pseudocheirus peregrinus	Common ringtail possum	UMZC A9.2.6.3	Marsupialia	Morphosource	T	T	m2-4(L)
Pudu puda	Southern pudu	NMS 2011.141.1	Laurasiatheria	Morphosource	T	T	m1-3(L)
Puma concolor	Mountain lion/ cougar	UMZC K5745	Laurasiatheria	Morphosource	T	T	m1, pm1-2(L)
Rangifer tarandus	Reindeer	OUMNH 19504	Laurasiatheria	Morphosource	T	T	m1-3(L)
Rhynchocyon petersi	Black and rufous elephant shrew	NHMUK 1886.9.21.1	Afrotheria	Morphosource	T	T	m1-2, pm4 (L)
Rhyncholestes raphanurus	Long-nosed caenolestid	NMS 1981.72	Marsupialia	Morphosource	T	T	m1-4(R)
Saiga tatarica	Saiga antelope	NMS 1981.72	Laurasiatheria	Morphosource	T	T	m1-3 (L)
Salpingotulus michaelis	Baluchistran pygmy jerboa	UMMZ 120132	Euarchontoglires	Morphosource	T	T	m1-3(L)
Sapajus apella	Tufted	FMNH 70621	Euarchontoglires	Morphosource	T	F	m1-3(L)

	capuchin						
Sarcophilus harrisii	Tasmanian devil	NHMUK 2003.331	Marsupialia	Morphosource	T	T	m2-4(R)
Scapanus latimanus	Northern broad-footed mole	UMMZ 74584	Laurasiatheria	Morphosource	T	T	m1-3(R)
Scutisorex somereni	Hero shrew	FMNH 160182	Laurasiatheria	Morphosource	T	T	m1-3(L)
Setifer setosus	Greater hedgehog tenrec	UMZC 2011.3.1	Afrotheria	Morphosource	T	T	m1-3(L)
Sminthopsis crassicaudata	Fat-tailed dunnart	FMNH 72923	Marsupialia	Morphosource	T	T	m1-4(L)
Smutsia gigantea	Giant pangolin	AMNH M-53847	Laurasiatheria	Morphosource	T	F	NA
Solenodon paradoxus	Hispaniolan solenodon	FMNH 51068	Laurasiatheria	Morphosource	T	T	m1-3(L)
Soriculus nigrescens	Himalayan shrew	UMMZ 122888	Laurasiatheria	Morphosource	T	F	NA
Spalacopus cyanus	Coruro	FMNH 49943	Euarchontoglires	Morphosource	T	T	m1-3(L)
Spalax microphthalmus	Greater blind mole-rat	FMNH 79299	Euarchontoglires	Morphosource	T	T	m1-3(L)
Speothos venaticus	Bush dog	NMS 2015.96.3	Laurasiatheria	Morphosource	T	T	m1-m2, pm4(L)
Spermophilopsis leptodactylus	Long-clawed ground squirrel	UMMZ 119250	Euarchontoglires	Morphosource	T	T	m1-3(L)
Surdisorex norae	Aberdare shrew	FMNH 190260	Laurasiatheria	Morphosource	T	T	m1-3(L)
Suricata suricatta	Meerkat	FMNH 101744	Laurasiatheria	Morphosource	T	T	m1-2, pm3(L)
Sus scrofa	Wild boar	GWU cashp	Laurasiatheria	Morphosource	T	T	m1-3(L)

		PT001					
Sylvilagus floridanus	Eastern cottontail	AMNH M-254438	Euarchontoglires	Morphosource	T	T	m1-3(L)
Sylvisorex howelli	Howell's forest shrew	FMNH 198205 198206	Laurasiatheria	Morphosource	T	T	m1-3(L)
Tachyoryctes splendens	Mount Elgon mole-rat	FMNH 173826 173827	Euarchontoglires	Morphosource	T	T	m1-3(L)
Tamias striatus	Northeast African mole-rat	UMZC E.1696	Euarchontoglires	Morphosource	T	T	m1-3(L)
Tapirus indicus	Malayan tapir	UF 31027	Laurasiatheria	Morphosource	T	T	m1-3(L)
Tapirus terrestris	South American tapir	NMS 2001.77.3	Laurasiatheria	Morphosource	T	T	m2-3(L)
Tarsipes rostratus	Honey possum	UMMZ 122547	Marsupialia	Morphosource	T	F	NA
Tarsius syrichta	Philippine tarsier	FMNH 142007	Euarchontoglires	Morphosource	T	T	m1-3(L)
Tayassu pecari	White-lipped peccary	IMNH R 228	Laurasiatheria	Morphosource	T	T	m1-3(L)
Tenrec ecaudatus	Tailless tenrec	UMMZ 138441	Afrotheria	Morphosource	T	T	m1-3 (L)
Thylacinus cynocephalus	Tasmanian tiger (Thylacine)	NHMUK 1963.8.3.0.1	Marsupialia	Morphosource	T	T	m1-3(L)
Thylamys elegans	Elegant fat-tailed mouse opossum	UMMZ 156033	Marsupialia	Morphosource	T	T	m1-4(L)
Thylogale stigmatica	Red-legged pademelon	UMZC A12.44-1	Marsupialia	Morphosource	T	T	m1-3(L)
Trachypithecus obscurus	Dusky leaf monkey	NHMUK 71.709	Euarchontoglires	Morphosource	T	T	m1-3(L)
Tragelaphus spekii	Sitatunga	NMS 2011.162.1	Laurasiatheria	Morphosource	T	T	m1-3(L)

Tragulus kanchil	Lesser mouse-deer	FMNH 68767	Laurasiatheria	Morphosource	T	F	NA
Trichosurus vulpecula	Common brushtail possum	UMZC A9.16-7	Marsupialia	Morphosource	T	T	m1-4(L)
Tupaia glis	Common treeshrew	UMZC E.4057.E	Euarchontoglires	Morphosource	T	T	m1-3(L)
Urocyon cinereoargenteus	Gray fox	NHMUK 1850.11.22.62	Laurasiatheria	Morphosource	T	T	m1-m2, pm4(L)
Urogale everetti	Mindanao treeshrew	FMNH 166482	Euarchontoglires	Morphosource	T	T	m1-3(L)
Ursus arctos	Brown bear	NHMUK 1963.11.7.1	Laurasiatheria	Morphosource	T	T	m1-3(L)
Vicugna vicugna	Vicuña	FMNH 36047	Laurasiatheria	Morphosource	T	T	m1-3(L)
Viverra zibetha	Large Indian civet	FMNH 104395	Laurasiatheria	Morphosource	T	T	m1-2, pm3(L)
Viverricula indica	Small Indian civet	UMZC K.4323	Laurasiatheria	Morphosource	T	T	m1-2, pm4(L)
Vombatus ursinus	Common wombat	UMZC A10.10.2	Marsupialia	Morphosource	T	T	m2-4(L)
Vulpes lagopus	Arctic fox	UMZC K3669	Laurasiatheria	Morphosource	T	T	m1-2, pm4(L)
Zapus hudsonius	Meadow jumping mouse	UMMZ 157417	Euarchontoglires	Morphosource	T	T	m1-3(L)
Zenkerella insignis	Cameroon scaly-tail	NHMUK 5.5.23.27	Euarchontoglires	Morphosource	T	T	m1-3(L)

Table A2: List of cynodont species sampled, together with their specimen numbers and taxonomic affiliations. Details on whether the cynodont species had been landmarked or had OPCR scores calculated are provided by T or F where T= True and F= False.

Taxon	**Specimen number**	**Order**	**Family**	**Data source**	**Landmarked**	**OPCR**
Andescynodon mendozensis	PVL 4069	Cynodontia	Traversodontidae	Photogrammetry	F	T
Andescynodon sp.	PVL 4907	Cynodontia	Traversodontidae	Photogrammetry	F	T
Cricodon metabolus	UMZC T905	Cynodontia	Trirachodontidae	Photogrammetry	F	T
Cricodon sp.	NHM PV R36800	Cynodontia	Trirachodontidae	Photogrammetry	F	T
Cynognathus crateronotus	BP 5208	Cynodontia	Cynognathidae	CT scanned (ESI)	T	T
Diademodon tetragonus	BP 3756	Cynodontia	Diademodontidae	CT scanned (ESI)	T	F
Diademodon tetragonus	SAM-PK 571	Cynodontia	Diademodontidae	Photogrammetry	F	T
Exaeretodon argentinus	PVL 2467	Cynodontia	Traversodontidae	Photogrammetry	F	T
Exaeretodon riograndensis	UFRGS PV 0715T	Cynodontia	Traversodontidae	Photogrammetry	F	T
Langbergia modisei	NMQR 3251	Cynodontia	Trirachodontidae	Photogrammetry	F	T
Luangwa sudamericana	MCP PV 3167	Cynodontia	Traversodontidae	Photogrammetry	F	T
Massetognathus pascuali	BP 4245	Cynodontia	Traversodontidae	Photogrammetry	F	T
Megazostrodon rudnerae	BP 4983	Morganucodonta	Megazostrodontidae	CT scanned (ESI)	T	T
Menadon besairiei	UFRGS PV 0891	Cynodontia	Traversodontidae	Photogrammetry	F	T
Pascualgnathus polanskii	PVL 4416	Cynodontia	Traversodontidae	Photogrammetry	F	T
Procynosuchus delaharpeae	BP 226	Cynodontia	Procynosuchidae	MorphoSource	T	F

Santacruzodon hopsoni	MCN 2752	Cynodontia	Traversodontidae	Photogrammetry	F	T
Traversodontid sp.	MCP PV 4053	Cynodontia	Traversodontidae	Photogrammetry	F	T
Trirachodon berryi	BP 4658	Cynodontia	Trirachodontidae	Photogrammetry	T	T
Trirachodon sp.	BP 4534	Cynodontia	Trirachodontidae	CT scanned (ESI)	T	T
Trirachodontid sp.	JSM 100	Cynodontia	Trirachodontidae	Photogrammetry	F	T

Table A3: CT scanning parameters of specimens that were scanned at the Evolutionary Studies Institute (ESI). Specimens were scanned using a Nikon Metrology XTH 22/320 LC dual source micro-CT system.

Taxon	Beam energy (kV)	Current (uA)	Frame Rate (fps)	Frame averaging	Filters	Isotropic Voxel Size (um)
Castor canadensis_WLM unnumbered	125	120	2	2	0mm Cu	77.5977
Cynognathus crateronotus_BP 5208	210	175	2	2	1.2mm Cu	40.0957
Diademodon tetragonus_BP 3756	219	185	1.4	2	3mm Cu	123.1713
Dugong dugon_WLM unnumbered	210	180	2	2	1.2 Cu	129.704
Megazostrodon rudnerae_BP4983	120	50	1	4	0mm Cu	18.09763
Trirachodon sp_BP 4534	210	185	2	2	1.2mm Cu	74.01754

16.2 Appendix B



Figure B1: Time-scaled phylogenetic tree of mammal species. Data obtained from VertLife (www.vertlife.org).

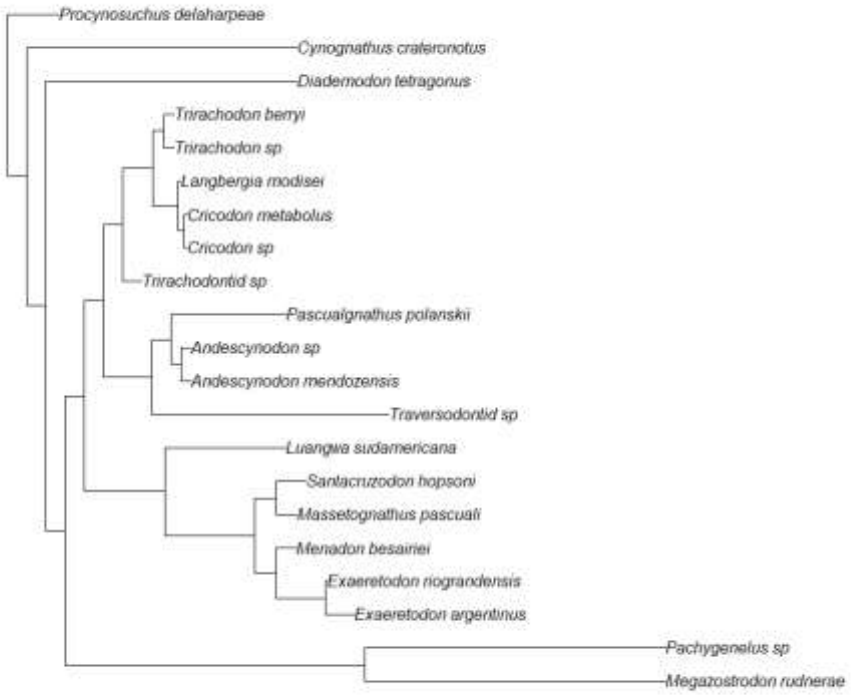


Figure B2: Time-scaled phylogenetic tree used for non-mammalian cynodont species. Topology of the phylogenetic tree is based on Ruta et al. (2013) and Hendrickx et al. (2020), and time-scale is based off occurrences obtained from the Palaeobiology Database.

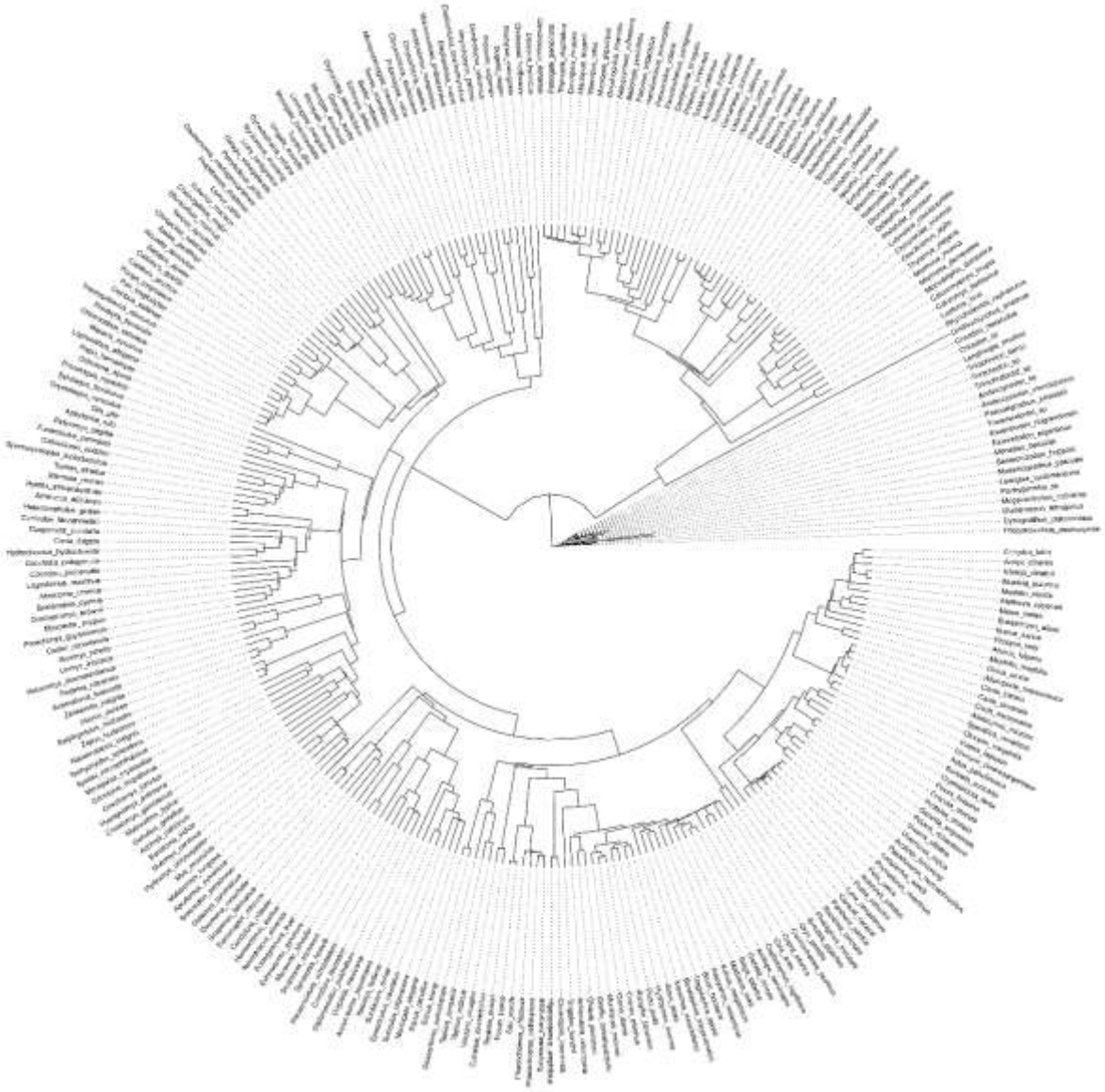


Figure B3: Merged super-tree containing mammal and non-mammalian cynodont species.

16.3 Appendix C

Table C1: Diet data used for mammal species and the associated metadata. References for diet data from: RF: Nowak (1999); RF2: Sunquist et al. (2009); RF3: Woods et al. (2003); RF4: Yom-Tov et al. (1995); RF5: Garbutt (2007); RF6: Albignac (1972). Diet_invert, Diet_invertebrates; Diet_vend, Diet_endothermic vertebrates; Diet_vect, Diet_ectothermic vertebrates; Diet_Vunk, Diet_unknown vertebrates; Diet_scav, Diet_scavenge; Diet_fruit, Diet_fruit; Diet_nect, Diet_nectar; Diet_plant, Diet_plant; Diet_Vtotal, Diet_total vertebrates; Diet_ref#, Diet_references.

Taxon	**Diet_invert**	**Diet_vend**	**Diet_vect**	**Diet_fish**	**Diet_Vunk**	**Diet_scav**	**Diet_fruit**	**Diet_nect**	**Diet_seed**	**Diet_plant**	**Diet_Vtotal**	**Diet_ref#**	**Diet_Notes (Walker's Mammals of the world)**
Abrocoma cinerea_UMMZ 120621	0	0	0	0	0	0	0	0	0	100	0	RF1	Various plant material
Acinonyx jubatus_AMNH 119657	0	100	0	0	0	0	0	0	0	0	100	RF1	Gazelles, impalas, medium-sized ungulates
Acomys cahirinus_NHMUK 65.789-793	0	0	0	0	30	0	0	0	0	70	30	RF1	Omnivorous; feeds mostly on plant material-especially grains and grasses; opportunistically feeds on

													arthropods
Acrobates pygmaeus_NHMUK 82.7.29.23	80	0	0	0	0	0	0	10	0	10	0	RF1	Insects and larvae; also consume nectar and other plant products
Aepyceros melampus_FMNH 127890	0	0	0	0	0	0	0	0	0	100	0	RF1	Grazer and browser of leaves of bushes and trees
Aepyprymnus rufescens_FMNH 124573	0	0	0	0	0	0	0	0	0	100	0	RF1	Mostly grasses
Ailuropoda melanoleuca_FMNH 31128	0	10	0	0	0	0	0	0	0	90	10	RF1	Bamboo shoots and roots
Ailurus fulgens_NHMUK 1911.10.18.1	10	10	0	0	0	0	10	0	10	60	10	RF1	Bamboo sprouts, grasses, fruits, acorns; opportunistically insectivorous and carnivorous
Alces alces_NMS 1996.39	0	0	0	0	0	0	0	0	0	100	0	RF1	Browser of shrubs and trees; feeds on water

													vegetation
Alouatta seniculus_FMNH 18869	0	0	0	0	0	0	40	0	0	60	0	RF1	Mainly leaves, also eats fruit and other vegetable matter
Amblysomus hottentotus_UMZC 2010.15A	100	0	0	0	0	0	0	0	0	0	0	RF1	Worms, larvae, pupae, and insects; also eats lizards
Anomalurus beecrofti_NHMUK 1989.174	10	0	0	0	0	0	40	10	0	40	0	RF1	Mainly bark and fruit; also eats flowers, leaves, nuts, and insects
Anourosorex squamipes_NHMUK 1933.4.1.165	100	0	0	0	0	0	0	0	0	0	0	RF1	Insects, their larvae, earthworms
Antechinomys laniger_NHMUK 32.2.11.23	80	10	10	0	0	0	0	0	0	0	20	RF1	Insects, and other small invertebrates; opportunistically carnivorous
Antechinus stuartii_FMNH	90	10	0	0	0	0	0	0	0	0	10	RF1	Insectivorous;

129556													opportunistically carnivorous
Antilocapra americana_FMNH 57215	0	0	0	0	0	0	0	0	0	100	0	RF1	Browses and grazes on wide variety of shrubs, forbs, cacti, other plants
Antilope cervicapra_NMS 2000.301.2	0	0	0	0	0	0	0	0	0	100	0	RF1	Obligate grazer
Aonyx cinerea_FMNH 62868	80	0	10	10	0	0	0	0	0	0	20	RF2	Crabs, mollusks, crustaceans, frogs
Aplodontia rufa_FMNH 60775	0	0	0	0	0	0	0	0	0	100	0	RF1	Any plant material, eats barks and small twigs seasonally
Apodemus sylvaticus_NHMUK unnumbered	20	0	0	0	0	0	20	0	20	40	0	RF1	Seeds, fruit, roots, grains, seeds, berries nut and insects
Arctictis binturong_NMS 2015.164.1	0	10	0	30	0	10	30	0	0	20	40	RF1	Fish, birds, carrion, leaves, fruit,

													shoots
Ateles geoffroyi_MCZ 10138	10	0	0	0	10	0	60	0	10	10	10	RF1	Mainly fruits, supplemented by leaves, seeds, insects
Atelocynus microtis_FMNH 60674	0	80	0	0	0	0	0	0	0	20	80	RF1	Small to medium-sized rodents
Atherurus africanus_UMCZ E.3489	0	0	0	0	0	0	0	0	0	80	0	RF1	Green vegetation, bark, roots, tubers, fruits, cultivated crops, insects, carrion
Atilax paludinosus_NHM UK 1867.7.8.11	40	30	20	10	0	0	0	0	0	0	60	RF2	Anything that it can kill, this includes insects, mussels, crabs, fish, frogs, snakes, eggs, small rodents,

													fruit
Babyrousa babyrussa_NMS 2008.27	0	0	0	0	0	0	40	0	0	60	0	RF1	Foliage and fruit
Bandicota indica_NHMUK 1978.896	20	0	0	0	0	0	0	0	0	80	0	RF1	Omnivorous, predominantly feeds on plant material
Bassaricyon alleni_FMNH 104935	20	10	0	0	0	0	70	0	0	0	10	RF1	Mainly frugivorous, also eats insects and small animals
Bettongia penicillata_FMNH 129431	0	0	0	0	0	0	0	0	30	70	0	RF1	Primarily herbivorous - consumes roots, tubers, seeds, and legumes; reports of eating marine refuse, carrion and meat; possibly also consumes

													large amounts of fungi
Bison bonasus_NHMUK 194.9.6.29.1	0	0	0	0	0	0	0	0	0	100	0	RF1	Leaves, twigs, bark of trees
Boselaphus tragocamelus_NHMUK_1974.411	0	0	0	0	0	0	20	0	0	80	0	RF1	Browser and grazer, fond of fruit and sugarcane
Bradypus variegatus_FMNH 69589	0	0	0	0	0	0	0	0	0	100	0	RF1	Young leaves, the tender twigs and buds of Cecropia
Callimico goeldii_FMNH 58003	40	0	0	0	10	0	50	0	0	0	10	RF1	Fruits, insects, some vertebrates
Callithrix jacchus_FMNH 231573	20	0	0	0	10	0	30	40	0	0	10	RF1	Insects, spiders, small vertebrates, birds' eggs, fruits, and tree exudates
Callosciurus notatus_NHMUK 75.1337	20	0	0	0	10	0	20	0	20	30	10	RF1	Fruits, nuts, seeds, buds, flowers,

													vegetable matter, insects, birds' eggs
Caluromys derbianus_UMMZ 114856	20	0	0	0	10	0	20	0	10	40	10	RF1	Omnivorous ; eats fruits, seeds, leaves, soft vegetables, insects, small vertebrates
Caluromysiops irrupta_FMNH 60698	20	0	0	0	0	0	20	40	0	20	0	RF1	Nectar, rodents and fruits
Camelus dromedarius_OUMNH 14882	0	0	0	0	0	0	0	0	0	100	0	RF1	Practically any vegetation, will also eat carrion if hungry
Canis latrans_UMZCK.3341	0	60	0	10	0	30	0	0	0	0	100	RF1	Mammalian flesh, such as jackrabbits, lagomorphs , and rodents; carrion is also consumed
Canis	10	30	0	0	0	30	0	0	0	30	60	RF1	Rodents,

mesomelas_UMZC K3402													antelopes, plant material, insects, carrion
Canis simensis_AMNH 81001	0	100	0	0	0	0	0	0	0	0	100	RF1	Rodents
Capra sibirica_FMNH 134541	0	0	0	0	0	0	0	0	0	100	0	RF1	Grasses, other plants
Caracal caracal_AMNH 113794	0	100	0	0	0	0	0	0	0	0	100	RF1	Birds, rodents, small antelopes
Castor canadensis_WLM unnumbered	0	0	0	0	0	0	0	0	0	100	0	RF1	Bark, cambium, twigs, leaves, roots of deciduous trees and shrubs
Cavia fulgida_UMZC E3705	0	0	0	0	0	0	0	0	0	100	0	RF1	Many kinds of vegetation
Cephalophus nigrifrons_NHMUK _1936.10.28.33	0	10	0	0	0	0	30	0	0	60	10	RF1	Grass, leaves, fruit
Cercartetus concinnus_NHMU K 97.11.18.1	20	0	10	0	0	0	20	20	10	20	10	RF1	Omnivorous ; eats leaves,

													nectar, fruits, nuts, insects, larvae, spiders, scorpions, small lizards
Cervus elaphus_NMS 1981.68	0	0	0	0	0	0	0	0	0	100	0	RF1	Grazing, browsing; eats grass seasonally, eats woody plants seasonally
Cheirogaleus major_FMNH 85144	20	0	0	0	0	0	30	20	0	30	0	RF1	Fruits, flowers, nectar, insects
Chironectes minimus_UMMZ 126289	50	0	0	30	0	0	0	0	0	20	30	RF1	Carnivorous - feeds on aquatic life like crayfish, shrimp, fish
Chiropotes satanas_FMNH 95512	10	0	0	0	0	0	40	0	20	30	0	RF1	Fruits, nuts, flowers, leaves, apparently insects and small vertebrates

Chlorocebus sabaeus_USNM 381445	20	0	0	0	20	0	40	0	0	20	20	RF1	Generalist omnivore, diet ranges between fruits, leaves, seeds, gum, insects, birds' eggs, crabs
Choeropsis liberiensis_NMSZ.2005.3	0	0	0	0	0	0	10	0	0	90	0	RF1	Water plants, grasses, tender shoots, leaves and fallen fruit
Choloepus hoffmanni_NHMUK 1973.824	0	0	0	0	0	0	30	0	0	70	0	RF1	Leaves, tender twigs, fruits
Chrysochloris asiatica_UMCZE.5472.F	100	0	0	0	0	0	0	0	0	0	0	RF1	Invertebrates such as beetles, grubs and worms
Chrysochloris stuhlmanni_NHMUK 1934.4.1.7.11	100	0	0	0	0	0	0	0	0	0	0	RF1	Invertebrates such as beetles, grubs and worms
Coendou prehensilis_NHMU	0	0	0	0	0	0	30	0	0	70	0	RF1	Leaves, tender

K 512.F													stems, fruits, blossoms, roots and seeds
Colobus satanas_NHMUK 1856.12.29.1	0	0	0	0	0	0	30	0	0	70	0	RF1	Mostly leaves, also eats fruits and flowers, and seeds
Condylura cristata_UMMZ 80270	80	0	0	20	0	0	0	0	0	0	20	RF1	Aquatic insects, crustaceans, small fish, and earthworms
Connochaetes taurinus_NHMUK 1935.12.14.3	0	0	0	0	0	0	0	0	0	100	0	RF1	Primarily grazes, also feeds on succulent plants
Cricetomys gambianus_NHMUK 1890.3.27.2	40	0	0	0	0	0	30	0	20	10	0	RF1	Mainly palm fruits and kernels, also eat vegetables, insects, and crabs; are opportunistic and will eat whatever is

													available
Cricetulus migratorius_UMZC E2322	0	0	0	0	0	0	0	0	50	50	0	RF1	Young shoots, roots, and seeds
Crocidura fuscomurina_UMZ C E 5251.G	50	0	10	0	0	40	0	0	0	0	50	RF1	Invertebrate s, opportunisti cally carnivorous
Crocuta crocuta_FMNH 127826	0	100	0	0	0	0	0	0	0	0	100	RF1	Medium-sized ungulates, mostly very young or old animals
Cryptoprocta ferox_NHMUK 1968.6.7.1	10	70	20	0	0	0	0	0	0	0	90	RF6	Small mammals, birds, reptiles, frogs, insects
Cryptotis mexicana_UMMZ 113138	40	0	30	0	0	30	0	0	0	0	60	RF2	Invertebrate s, small lizards, frogs, carrion, plant material; diet is affected by seasonality

Cuniculus taczanowskii_FMNH 70804	0	0	0	0	0	0	20	0	30	50	0	RF1	Leaves, stems, roots, seeds, fallen fruit
Cynocephalus volans_OUMNH 3404	0	0	0	0	0	0	0	0	0	100	0	RF1	Preference for young leaves; will eat fruit but predominant leaves
Dactylopsila trivirgata_NHMUK 1897.8.7.79	80	0	0	0	0	0	10	0	0	10	0	RF1	Mainly insects: like ants and other social insects, also eats fruits and leaves
Dama dama_OUMNH 19343	0	0	0	0	0	0	0	0	0	100	0	RF1	Predominantly a grazer also browses trees and shrubs
Dasycercus cristicauda_NHMUK 1897.11.3.4	30	70	0	0	0	0	0	0	0	0	70	RF1	Carnivorous and insectivorous; depend on the availability of food

Dasyprocta punctata_FMNH 21260	10	0	0	0	0	0	40	0	0	50	0	RF1	Fruits, vegetables, various succulent plants, and some animal matter; diet depends on seasonality
Dasypus hybridus_AMNH M-205706	100	0	0	0	0	0	0	0	0	0	0	RF1	Insects such as beetles and ants
Dasyurus hallucatus_FMNH 119804	40	30	20	0	0	0	10	0	0	0	50	RF1	Arthropods, fruits, small vertebrates (ie. bandicoots & fish)
Dasyurus maculatus_UMZC A6.10-3	30	60	10	0	0	0	0	0	0	0	70	RF1	Exclusively carnivorous
Dasyurus viverrinus_SAMA M7222	70	20	0	0	0	10	0	0	0	0	30	RF1	Small vertebrates, insects, and soft fruits
Daubentonia madagascariensis_ UMZC E.8021.A	40	0	0	0	0	0	0	20	40	0	0	RF1	Seeds, nectar, larvae
Dendrohyrax arboreus_FMNH	0	0	0	0	0	0	30	0	0	70	0	RF1	Strictly herbivorous

163770													; eats leaves, fruits, twigs, barks.
Dendrolagus dorianus_NMS 2006.38	0	0	0	0	0	0	50	0	0	50	0	RF1	Mainly leaves, fruits and flowers
Desmana moschata_UMMZ 124125	60	0	20	20	0	0	0	0	0	0	40	RF1	Insects, crustaceans, molluscs, fish, amphibians (captured in water), also eats plants
Dicerorhinus sumatrensis_NMS 1994.131	0	0	0	0	0	0	50	0	0	50	0	RF1	Favours fruits, and bamboo; also eats leaves, twigs, barks, and young saplings
Didelphis marsupialis_NHMUK 1948.7.12.5	20	0	0	0	30	30	0	0	0	20	60	RF1	Small vertebrates, carrion, invertebrates, vegetables
Diplomesodon	50	0	50	0	0	0	0	0	0	0	50	RF1	Lizards and

pulchellum_FMNH 137436													insects
Dolichotis patagonum_FMNH 49231	0	0	0	0	0	0	0	0	0	100	0	RF1	Any available vegetation
Dorcopsis muelleri_NHMUK 1933.11.4.4	0	0	0	0	0	0	20	0	0	80	0	RF1	Roots, leaves, grasses, and fruits
Dromiciops gliroides_UMMZ 156354	100	0	0	0	0	0	0	0	0	0	0	RF1	Largely insectivorous
Dugong dugon_MVZ 101162	0	0	0	0	0	0	0	0	0	100	0	RF3	Mostly sea grasses, also algae, crabs
Echinops telfairi_NHMUK 1970.355	60	0	0	0	0	0	40	0	0	0	0	RF5	Insects
Echinosorex gymnura_UMZC E.5111.C-E	50	0	30	20	0	0	0	0	0	0	50	RF1	Largely insectivorous, also consumes aquatic vertebrates, frogs, fish, crustaceans
Echymipera rufescens_FMNH 60525	60	0	0	0	0	0	40	0	0	0	0	RF1	Omnivorous; feeds on fruit, insects like earthworms

													and grubs
Elephantulus brachyrhynchus_NHMUK 1963.1004	100	0	0	0	0	0	0	0	0	0	0	RF1	Insects, especially ants and termites
Elephantulus rozeti_NHMUK 1891.10.15.11	100	0	0	0	0	0	0	0	0	0	0	RF1	Insects, especially ants and termites
Enhydra lutris_NHMUK 80.879	50	0	0	50	0	0	0	0	0	0	50	RF1	Slow-moving fish, and marine invertebrates like sea urchins, crabs, molluscs
Episoriculus caudatus_FMNH 114227	70	0	0	0	0	30	0	0	0	0	30	RF1	Earthworms, insects, invertebrates, is opportunistically carnivorous but mostly omnivorous
Equus caballus_OUMNH 19193	0	0	0	0	0	0	0	0	0	100	0	RF1	Primarily grazes, eats mainly grasses and low forage plants

Equus kiang_NMS 2016.43	0	0	0	0	0	0	0	0	0	100	0	RF1	Grass and low plants
Eulemur macaco_UMZC E8093A	0	0	0	0	0	0	30	0	0	70	0	RF1	Flowers, fruits, and leaves; is also largely frugivorous
Euroscaptor micrura_NHMUK 99.10.25.1	100	0	0	0	0	0	0	0	0	0	0	RF1	Insects and other small prey
Felis catus_UMZC K.6182	0	100	0	0	0	0	0	0	0	0	100	RF3	Rabbits, mice, birds, carrion
Fossa fossana_FMNH 85196	70	10	10	0	0	0	10	0	0	0	20	RF1	Crustaceans, worms, small eels and frogs; also consumes insects; diet is highly seasonal
Funambulus pennantii_UMMZ 62569	20	0	0	0	0	0	0	0	20	60	0	RF1	Seeds, nuts, stems, young bark, buds, leaves, flowers, insects, grubs
Galago senegalensis_FMN	40	0	0	0	0	0	0	60	0	0	0	RF1	Gums (of Acacia tree)

H 123783													and insects, eggs
Galemys pyrenaicus_OUMNH 9427	90	0	0	10	0	0	0	0	0	0	10	RF1	Small fish, crustaceans, insects, worms (brings prey to land)
Gazella dorcas_NMS 2004.46.5	0	0	0	0	0	0	20	0	0	80	0	RF4	Mainly a browser, but seasonally grazes
Genetta angolensis_FMNH 163777	10	70	20	0	0	0	0	0	0	0	90	RF1	Any small animals, including rodents, birds, reptiles and insects
Geocapromys brownii_AMNH 45156	0	0	0	0	0	0	30	0	0	70	0	RF3	Mainly bark, small twigs, and leaves
Geogale aurita_UMMZ 172217	70	30	0	0	0	0	0	0	0	0	30	RF1	Invertebrates, prefers termites
Geomys pinetis_UMMZ 164642	0	0	0	0	0	0	0	0	0	100	0	RF2	Underground roots, rhizomes, bulbs, sometimes succulent vegetation

Gerbillus gerbillus_NHMUK 1978.1062	20	0	0	0	0	0	0	0	30	50	0	RF1	Seeds, roots, nuts, grasses, insects
Giraffa camelopardalis_FMNH 34424	0	0	0	0	0	0	0	0	0	100	0	RF1	Obligate browser
Glis glis_NHMUK 1996.325	0	0	0	0	0	0	40	0	60	0	0	RF1	Seeds, nuts, acorns, berries, soft fruits
Gracilinanus agilis_UMMZ 134557	50	0	0	0	0	0	30	20	0	0	0	RF1	Fruits, plant exudates, insects, small invertebrates (insectivore-omnivore)
Gulo gulo_USNM 157327	0	20	0	0	20	40	20	0	0	0	80	RF1	Consumes carrion, eggs, lemmings, and berries
Hemibelideus lemuroides_FMNH 60926	0	0	0	0	0	0	0	0	0	100	0	RF1	Mostly leaves
Hemiechinus auritus_UMMZ 156626	30	0	0	0	30	20	10	0	10	0	50	RF1	Insects, other invertebrates, small

													vertebrates, eggs, carrion, fruits, and seeds
Heterocephalus glaber_NHMUK 91.235	0	0	0	0	0	0	0	0	0	100	0	RF1	Tubers, roots, corms
Heteromys desmarestianus_NHMUK unregistered xyz002	0	0	0	0	0	0	0	0	30	70	0	RF1	Seeds, green leaves, twigs, succulent plants
Hippopotamus amphibius_NMSZ.2008.35	0	0	0	0	0	0	0	0	0	100	0	RF1	Mostly grass and vegetation
Hydrochoerus hydrochaeris_AMNH M-206440	0	0	0	0	0	0	10	0	0	90	0	RF1	Mainly grasses, also eats aquatic plants, grains, melons, squashes
Hydromys chrysogaster_NHMUK 1998.134	50	10	10	30	0	0	0	0	0	0	50	RF1	Large aquatic insects mostly, also eats spiders, crustaceans

													, mussels, frogs, turtles, birds, bats
Hydropotes inermis_NMS unnumbered	0	0	0	0	0	0	0	0	0	100	0	RF1	Grasses, other vegetation, vegetables
Hypogeomys antimena_FMNH 151994	0	0	0	0	0	0	100	0	0	0	0	RF1	Fallen fruit in the wild and vegetation
Hystrix africaeaustralis_FMNH 60453	0	0	0	0	0	0	20	0	0	80	0	RF1	Barks, roots, tubers, rhizomes, bulbs, fallen fruits and cultivated crops; insects and small vertebrates occasionally consumed
Ictonyx striatus_UMZC K1874	40	40	10	0	10	0	0	0	0	0	60	RF1	Small rodents, large insects, also eats eggs, snakes, and

													other kinds of animals
Idiurus zenkeri_UMZC E1421	0	0	0	0	0	0	100	0	0	0	0	RF1	Pulp of oil palm fruits, is cryptic not much is known actually
Isoodon macrourus_FMNH 120560	100	0	0	0	0	0	0	0	0	0	0	RF1	Insects and worms
Isoodon obesulus_UMZC A7.4-5	100	0	0	0	0	0	0	0	0	0	0	RF1	Insects and worms, also plant roots and ferns (somewhat insectivorous-omnivorous)
Kobus megaceros_NMS 2001.149.15	0	0	0	0	0	0	0	0	0	100	0	RF1	Grazer
Lagostomus maximus_NHMUK ZD 1991.174	0	0	0	0	0	0	0	0	40	60	0	RF1	Mostly grass and seeds, nearly any kind of vegetation
Lasiorhinus latifrons_NMS 1868.31	0	0	0	0	0	0	0	0	0	100	0	RF1	Grass

Lemur catta_FMNH 157993	0	0	0	0	0	0	80	0	0	20	0	RF1	Mostly fruits, some leaves, other plants; rarely eats insects but is opportunistically carnivorous
Leopardus wiedii_NMSZ.2016.12.1	0	80	0	0	0	0	20	0	0	0	80	RF1	Squirrels, arboreal mammals, birds, terrestrial rodents, fruit
Lestoros inca_UMMZ 160733	70	0	0	0	10	0	10	0	0	10	10	RF1	Insects, worms, small vertebrates, largely insectivorous
Liomys irroratus_UMMZ 120788	0	0	0	0	0	0	0	0	50	50	0	RF1	Seeds and tender herbaceous plants
Lophocebus albigena_NHMUK 1936.10.28.1	0	0	0	0	0	0	50	0	0	50	0	RF1	Mainly fruits, nuts, and flowers

Loris tardigradus_UMZC E.8261.E	70	0	0	0	10	0	10	0	0	10	10	RF1	Mainly insectivorous, also eats shoots, leaves, birds' eggs and small vertebrates
Lutreolina crassicaudata_UM MZ 163450	20	40	20	20	0	0	0	0	0	0	80	RF1	Small mammals, birds, reptiles, fish, insects
Lynx canadensis_UMZC K.6682	0	80	0	20	0	0	0	0	0	0	100	RF1	Rabbits, deer, ungulates, rodents, birds and fish
Macaca sylvanus_NHMUK 1858.4.5.1	10	0	0	0	0	0	30	0	20	40	0	RF1	Plants, insects, small invertebrates, opportunistically carnivorous
Macropus eugenii_NHMUK 1948.7.12.3	0	0	0	0	0	0	0	0	0	100	0	RF1	Herbivorous, eats mainly grass
Macropus	0	0	0	0	0	0	0	0	0	100	0	RF1	Herbivorous

giganteus_NHMUK 72.4498													, eats mainly grass
Macropus rufus_NMS PH26.12	0	0	0	0	0	0	0	0	0	100	0	RF1	Herbivorous, eats mainly grass
Macroscelides proboscideus_FMNH 137045	80	0	0	0	0	0	10	0	0	10	0	RF1	Insects, particularly ants and termites; also eats tender shoots, roots, and berries
Macrotis lagotis_NHMUK 73.6.21.4	70	0	0	0	20	0	0	0	0	10	20	RF1	Feeds on mainly insects, also eats small vertebrates and plant material
Madoqua kirkii_NMS POZ8.99	0	0	0	0	0	0	0	0	0	100	0	RF1	Shrubs like Acacia and grasses
Malacomys longipes_UMZC E2265	50	0	0	0	0	0	20	0	20	10	0	RF1	Largely omnivorous, eats mostly insects, also eats

													animal and vegetable materials
Malacothrix typica_UMMZ 117815	0	0	0	0	0	0	0	0	0	100	0	RF1	Green vegetable matter, seeds and insects
Marmosa demerarae_UMMZ 134562	90	0	0	0	0	0	10	0	0	0	0	RF1	Insects, fruit, and nectar
Marmosa murina_NHMUK 1881.11.1	40	10	10	0	10	0	30	0	0	0	30	RF1	Mainly insects and fruits; also eats small rodents, lizards and birds' eggs
Marmota monax_AMNH M-67882	0	0	0	0	0	0	30	0	30	40	0	RF1	Green vegetation, especially grasses and forbs; also eats fruits, some legumes, and insects
Meles meles_NHMUK 2002.476	20	20	20	0	0	0	20	0	10	10	40	RF1	Omnivorous diet; eats any available food such

													as small mammals, birds, reptiles, frogs, molluscs, insects, larvae of bees and wasps, carrion, nuts, berries, acorns, fruits, seeds, tubers, rhizomes, and mushrooms
Mellivora capensis_UMZC K1821	20	40	20	0	0	10	0	0	0	10	60	RF1	Small mammals; the young of large mammals, birds, reptiles, arthropods, carrion, and vegetation
Mephitis mephitis_FMNH	20	30	0	0	0	0	20	0	10	20	30	RF1	Omnivorous; eats

129327													rodents and other small vertebrates, insects, fruit, grains, and green vegetation
Microcebus murinus_AMNH M-174537	20	0	20	0	0	0	30	10	0	20	20	RF1	Insects, spiders, fruits, flowers, nectars, gums, insect secretions, leaves; opportunistically carnivorous
Microgale brevicaudata_UMMZ 174757	100	0	0	0	0	0	0	0	0	0	0	RF1	Insects
Microgale drouhardi_UMMZ 168477	100	0	0	0	0	0	0	0	0	0	0	RF1	Insects
Microgale thomasi_UMMZ 172202	100	0	0	0	0	0	0	0	0	0	0	RF1	Insects
Micropotamogale ruwenzorii_NHMUK 67.213	60	0	20	20	0	0	0	0	0	0	40	RF1	Worms, insects, larvae, crabs, fish

													and small frogs
Monodelphis domestica_UMMZ 165514	20	20	0	0	0	20	20	0	20	0	40	RF1	Mainly feeds on insects; also eats small rodents, insects, carrion, seeds, fruit; opportunistically carnivorous
Moschus moschiferus_NHMUK 676.d.45.1.12.448	0	0	0	0	0	0	0	0	0	100	0	RF1	Variety of vegetation, such as grass, moss, tender shoots; in winter, twigs, buds, lichen
Muntiacus reevesi_NMS 1996.142.8	0	0	0	0	0	0	20	0	0	80	0	RF1	Grasses, low-growing leaves and tender shoots
Mus musculus_UMZC E.2202	20	0	0	0	0	0	0	0	20	60	0	RF1	Vegetable matter, seeds,

													fleshy roots, leaves, stems; opportunistically insectivorous and carnivorous
Mustela nivalis_FMNH 207033	0	100	0	0	0	0	0	0	0	0	100	RF1	Small rodents
Mustela putorius_UMZC K.2361	10	50	20	20	0	0	0	0	0	0	90	RF1	Small mammals, birds, frogs, fish and invertebrates
Myocastor coypus_AMNH 206456	0	0	0	0	0	0	0	0	0	100	0	RF1	Strictly vegetarian
Myosorex kihaulei_FMNH 209072	80	20	0	0	0	0	0	0	0	0	20	RF2	Insects, opportunistically carnivorous
Myospalax myospalax_UMMZ 110401	0	0	0	0	0	0	0	0	50	50	0	RF1	Roots and grains
Nandinia binotata_UMZC K.4492	10	10	0	0	0	0	80	0	0	0	10	RF1	Fruits, also eats rodents, birds' eggs, large

													beetles, and caterpillars
Napaeozapus insignis_UMMZ 126314	20	0	0	0	0	0	10	0	40	30	0	RF1	Mainly seeds, fungi and insects; also eats fruits, nuts and other vegetation (insectivorous-herbivorous)
Nasua narica_UMZC unnumbered	10	20	0	0	0	0	70	0	0	0	20	RF1	Mainly frugivorous, also consumes invertebrates, and large rodents
Nectogale elegans_AMNH M-115571	20	0	0	80	0	0	0	0	0	0	80	RF1	Fish and aquatic life
Neomys fodiens_NHMUK 1973.917	40	0	30	30	0	0	0	0	0	0	60	RF1	Various vertebrate and invertebrate prey, ranging from larvae to fish, and frogs

Neotetracus sinensis_NHMUK ZD1933.4.1.134	100	0	0	0	0	0	0	0	0	0	0	RF1	Earthworms, vegetable materiable (diet is largely unknown though)
Notomys cervinus_NHMUK ZD 1936.12.8.17-18	0	0	0	0	0	0	40	0	30	30	0	RF1	Predominantly eats seeds, also eats berries, leaves, seeds, other available vegetation
Notoryctes typhlops_UMZC A5.11	90	0	0	0	0	0	0	0	10	0	0	RF1	Mostly eats colonial insects such as ants, termites – also eats the larvae and eggs of beetles and seeds
Nycticebus coucang_Du Baa 0002	40	30	10	0	0	0	20	0	0	0	40	RF1	Floral nectar and nectar producing

													parts (sap, fruits, gum)
Ochotona alpina_UMMZ 123059	0	0	0	0	0	0	0	0	0	100	0	RF1	Variety of vegetable matter; in summer it eats grasses, sedges, weeds, flowering and woody plants and in winter: hay
Okapia johnstoni_NHMUK 1971.1738	0	0	0	0	0	0	0	0	0	100	0	RF1	Browser, eats leaves and other parts of plants, including fruits and seeds
Onychogalea fraenata_UMZC A12.59.3	0	0	0	0	0	0	0	0	0	100	0	RF1	Mainly roots of grasses and herbaceous vegetation
Onychomys torridus_UWBM 37628	90	0	0	0	0	0	0	0	0	10	0	RF1	Insectivorous, said to prey extensively

													on scorpions, small vertebrates, grasshoppers and other insects are also eaten
Ornithorhynchus anatinus_UMZC A2.2.10	80	0	0	20	0	0	0	0	0	0	20	RF1	Crayfish, shrimp, larvae, water insects, snails, tadpoles, worms, and small fish
Oryctolagus cuniculus_NHMUK 1849.6.20.9	0	0	0	0	0	0	0	0	0	100	0	RF1	Grasses, other herbaceaous plants
Oryx gazella_NHMUK ZD 1963.10.21.1	0	0	0	0	0	0	0	0	0	100	0	RF1	Grasses and shrubs
Oryzorictes tetradactylus_UMZC E.5453.C	100	0	0	0	0	0	0	0	0	0	0	RF1	Insects, other invertebrates like molluscs
Otocyon megalotis_USNM 49129	50	20	0	0	10	0	0	0	0	20	30	RF1	Predominantly insects (termites),

													also eats other arthropods, small rodents, eggs of birds, vegetable matter
Ovis aries_OUMNH ZC14858	0	0	0	0	0	0	0	0	0	100	0	RF1	Largely grasses, sedges and forbs
Pan troglodytes_RMCA 77032M25	10	0	0	0	0	0	60	0	0	30	0	RF1	Fruits, vegetation, animal matter
Panthera pardus_IMNH 2372	0	100	0	0	0	0	0	0	0	0	100	RF1	Small and medium sized ungulates, domestic livestock
Papio hamadryas_UMZC E.7543.B	10	0	0	0	10	0	0	0	0	80	10	RF1	Omnivorous, eats mainly fruit or vegetable material but mostly eats whatever is seasonally

													available
Paracrocidura schoutedeni_FMNH 227382	70	0	10	0	0	20	0	0	0	0	30	RF3	Presumably insectivorous, no explicit diet reported
Paradoxurus hermaphroditus_FMNH 62837	20	0	0	0	40	0	20	0	20	0	40	RF1	Largely herbivorous, also eats insects, fruit, seeds, and small vertebrates.
Pecari tajacu_NMS 2002.164.2	10	0	20	0	0	0	10	0	0	60	20	RF1	Mainly vegetarian, feeds on cactus fruits, berries, tubers, bulbs, rhizomes
Pedetes capensis_FMNH 152053	0	0	0	0	0	0	0	0	10	90	0	RF1	Maize, groundnuts, wheat, barley, oats
Perodicticus potto_USNM 465898	10	0	0	0	0	0	80	10	0	0	0	RF1	Mainly frugivorous, also consumes gums and insects

Petauroides volans_NHMUK 1926.3.11.225	0	0	0	0	0	0	0	0	0	100	0	RF1	Specialized; eats leaves, bark and bud debris of certain species of Eucalyptus
Petaurus breviceps_FMNH 129430	40	0	0	0	10	0	0	30	20	0	10	RF1	Feeds on sap, blossoms, nectar, insects, larvae, arachnoids
Petinomys sagitta_UMZC E1499	0	0	0	0	0	0	30	0	30	40	0	RF1	Nuts, fruits, young twigs, tender shoots, leaves; possibly also eats bark and insects
Petrogale penicillata_FMNH 64435	0	0	0	0	0	0	20	0	10	70	0	RF1	Mainly grasses, seasonally bark of different trees
Phacochoerus aethiopicus_UF	0	0	0	0	0	10	10	0	0	80	0	RF1	Omnivorous ; grass

31016													roots, berries, bark and carrion
Phacochoerus africanus_OUMNHZC3617	0	0	0	0	0	10	10	0	0	80	0	RF1	Omnivorous; grass roots, berries, bark and carrion
Phascolarctos cinereus_NHMUK 75.1828	0	0	0	0	0	0	0	0	0	100	0	RF1	*Euacalyptus leaves*
Phataginus tricuspis_NHMUK 34.6.2.94	100	0	0	0	0	0	0	0	0	0	0	RF1	Mainly ants and termites, sometimes other soft-bodied insects and larvae
Philander opossum_UMMZ 114855	30	30	20	0	10	0	10	0	0	0	60	RF1	Small mammals, birds' eggs, reptiles, amphibians, insects, freshwater crustaceans, snails, earthworms, fruits,

													carrion
Podogymnura truei_FMNH 146591	80	20	0	0	0	0	0	0	0	0	20	RF1	Insects, worms; opportunisti cally carnivorous
Poiana richardsonii_YPM VZ MAM 014715	20	20	0	0	0	0	0	0	40	20	20	RF1	Cola nuts and other plant materials, also eats insects and young birds.
Pongo pygmaeus_NHMU K 1986.1097	10	0	0	0	10	0	80	0	0	0	10	RF1	Fruit, really loves figs; also leaves, bark, nuts, seeds, insects, honey
Potamogale velox_UMZC E5425F	70	0	10	20	0	0	0	0	0	0	30	RF1	Insectivorou s, also (equally) eats crabs, fish, and amphibians
Potorous tridactylus_FMNH 57805	20	0	0	0	0	0	0	0	0	80	0	RF1	Mainly plants, seasonally fungi, also consumes grasses,

													roots and other vegetation, small vertebrates
Presbytis femoralis_UMZC E.7226.C	0	0	0	0	0	0	40	0	40	20	0	RF1	Mostly fruits, and their seeds but also foliage.
Prionailurus viverrinus_NHMUK 1860.7.22.22	20	20	20	40	0	0	0	0	0	0	80	RF1	Crustaceans, molluscs, frogs, snakes, birds, and small mammals
Procavia capensis_FMNH 147999	0	0	0	0	0	0	0	0	0	100	0	RF1	Browser, grazer, eats any plants
Procyon lotor_FMNH 175311	40	0	20	0	0	0	20	0	20	0	20	RF1	Omnivorous; eats mainly crayfish, crabs, arthropods, frogs, fish, nuts, seeds, acorns, berries
Proechimys guyannensis_NHM	0	0	0	0	0	0	20	0	10	70	0	RF1	Fruits, corn, coconuts,

UK 79.322													cereals, potatoes, cabbages
Pronolagus rupestris_FMNH 177246	0	0	0	0	0	0	0	0	0	100	0	RF1	Grass
Propithecus diadema_UMZC E8041A	0	0	0	0	0	0	30	0	0	70	0	RF1	Leaves, flowers, bark and fruits; highly variable diet largely dependent largely on season
Proteles cristata_NMS unnumbered	100	0	0	0	0	0	0	0	0	0	0	RF1	Termites, insect larvae
Pseudocheirus peregrinus_UMZC A9.2.6.3	0	0	0	0	0	0	20	10	0	70	0	RF1	Herbivorous; feeds on leaves, fruits, flowers, bark and sap
Pudu puda_NMS 2011.141.1	0	0	0	0	0	0	10	0	10	80	0	RF1	Mainly a browser, also eats barks, twigs, buds, blossoms, fruits,

													berries, acorns, and cultivated acorns
Puma concolor_UMZC K5745	0	100	0	0	0	0	0	0	0	0	100	RF1	Deer, other ungulates, beavers, porcupine, hares
Rangifer tarandus_OUMNH 19504	0	0	0	0	0	0	0	0	0	100	0	RF1	Wide variety of plant leaves, lichens, twigs
Rhynchocyon petersi_NHMUK 1886.9.21.1	100	0	0	0	0	0	0	0	0	0	0	RF1	Insectivorous, also eats mammals, birds' eggs, molluscs
Rhyncholestes raphanurus_FMNH 27476	80	0	0	0	0	0	0	0	0	20	0	RF1	Insectivorous, also eats worms and plant matter
Saiga tatarica_NMS 1981.72	0	0	0	0	0	0	0	0	0	100	0	RF1	Mainly grasses, also various herbs and shrubs
Salpingotulus michaelis_UMMZ 120132	50	0	0	0	0	0	0	0	0	50	0	RF1	Grass seeds, stems, and

													vegetation
Sapajus apella_FMNH 70621	20	0	0	0	10	0	20	10	20	20	10	RF1	Fruits, nuts, berries, seeds, flowers, buds, shoots, gums, insects, arachnids, eggs, small vertebrates and even some forms of marine life (noted as most varied diet of all New World Monkeys)
Sarcophilus harrisii_NHMUK 2003.331	100	0	0	0	0	100	0	0	0	0	100	RF1	Carnivorous; also known to consume plants and invertebrates
Scapanus latimanus_UMMZ 74584	100	0	0	0	0	0	0	0	0	0	0	RF1	Earthworms, insect larvae, and other small

													invertebrates
Scutisorex somereni_FMNH 160182	0	0	0	0	100	0	0	0	0	0	100	RF1	Small animals, some plants, insects, caterpillars
Setifer setosus_UMZC 2011.3.1	40	0	0	0	0	60	0	0	0	0	60	RF1	Naturally carrion and garbage, captives eat earthworms, grasshoppers, carcasses, is incapable of killing (prey)
Sminthopsis crassicaudata_FMNH 72923	80	10	10	0	0	0	0	0	0	0	20	RF1	Insectivorous, opportunistically carnivorous
Smutsia gigantea_AMNH M-53847	100	0	0	0	0	0	0	0	0	0	0	RF1	Mainly ants and termites, and sometimes other soft-bodied

													insects and larvae
Solenodon paradoxus_FMNH 51068	30	10	20	0	0	0	20	0	0	20	30	RF1	Various invertebrates, reptiles, fruits, vegetables, occasionally poultry
Soriculus nigrescens_UMMZ 122888	70	0	0	0	0	30	0	0	0	0	0	RF1	Earthworms, insects, invertebrates, opportunistically carnivorous
Spalacopus cyanus_FMNH 49943	0	0	0	0	0	0	0	0	0	100	0	RF1	Tubers, underground stems of lily Leucoryne ixiodes.
Spalax microphthalmus_FMNH 79299	0	0	0	0	0	0	0	0	0	100	0	RF1	Roots, bulbs, tubers, underground parts of plants
Speothos venaticus_NMS 2015.96.3	0	100	0	0	0	0	0	0	0	0	100	RF1	Large rodents
Spermophilopsis	20	0	0	0	0	0	20	0	20	40	0	RF1	Fruits,

leptodactylus_UMMZ 119250													seeds, bulbs, green vegetation, and insects
Surdisorex norae_FMNH 190260	100	0	0	0	0	0	0	0	0	0	0	RF1	Primarily earthworms
Suricata suricatta_FMNH 101744	70	0	0	0	20	0	0	0	0	10	20	RF1	Primarily insectivorous, also includes small vertebrates, eggs and vegetable matters
Sus scrofa_GWU cashp PT001	10	0	0	0	10	10	0	0	10	60	20	RF1	Fungi, tubers, bulbs, greens, vegetaion, grains, nuts, cultivated crops, invertebrates small vertebrates, carrion
Sylvilagus floridanus_AMNHM 254438	0	0	0	0	0	0	0	0	0	100	0	RF1	Woody vegetation, wide variety

													of plants
Sylvisorex howelli_FMNH 198205 198206	80	0	0	0	10	10	0	0	0	0	20	RF1	Presumably insectivorous; no explicit diet recorded
Tachyoryctes splendens_FMNH 173826 173827	0	0	0	0	0	0	0	0	0	100	0	RF1	Grass roots
Tamias striatus_UMZC E.1696	20	0	0	0	0	0	20	0	30	30	0	RF1	Nuts, acorns, seeds, mushrooms, fruits, berries corn
Tapirus indicus_UF 31027	0	0	0	0	0	0	0	0	0	100	0	RF1	Mainly shoots of most common browsing plants, also eats leaves, buds, twigs and fruits of low-growing terrestrial plants
Tapirus terrestris_NMS 2001.77.3	0	0	0	0	0	0	0	0	0	100	0	RF1	Mainly shoots of most common browsing

													plants, also eats leaves, buds, twigs and fruits of low-growing terrestrial plants
Tarsipes rostratus_UMMZ 122547	0	0	0	0	0	0	0	100	0	0	0	RF1	Exclusively nectar and pollen
Tarsius syrichta_FMNH 142007	100	0	0	0	0	0	0	0	0	0	0	RF1	Mainly insects, also small lizards, and crustaceans
Tayassu sp_IMNH R 228	10	0	0	0	10	0	30	0	30	20	10	RF1	Mostly fruits seeds, roots; opportunistically carnivorous
Tenrec ecaudatus_UMMZ 138441	90	0	0	0	0	0	0	0	0	10	0	RF1	Variety of invertebrates, some vegetable matter; opportunistically carnivorous
Thylacinus cynocephalus_NHMUK 1963.8.3.0.1	0	60	0	10	0	30	0	0	0	0	100	RF1	Carnivorous

Thylamys elegans_UMMZ 156033	80	0	0	0	10	0	10	0	0	0	10	RF1	Mostly Insects and fruit, also eats small vertebrates
Thylogale stigmatica_UMZC A12.44-1	0	0	0	0	0	0	0	0	0	100	0	RF1	Grasses
Trachypithecus obscurus_NHMUK 71.709	0	0	0	0	0	0	30	0	0	70	0	RF1	Mainly leaves, also some flowers and fruits
Tragelaphus spekii_NMS 2011.162.1	0	0	0	0	0	0	0	0	0	100	0	RF1	Mainly a grazer, feeding on reeds, sedges and grasses
Tragulus kanchil_FMNH 68767	0	0	0	0	0	0	20	0	0	80	0	RF2	Grass, leaves, fallen jungle fruit and berries
Trichosurus vulpecula_UMZC A9.16-7	0	0	0	0	0	0	20	0	20	60	0	RF1	Young shoots, leaves, flowers, fruits and seeds
Tupaia glis_UMZC E.4057.E	90	0	0	0	0	0	0	0	0	10	0	RF1	Insects, fruits,

													seeds, leaves
Urocyon cinereoargenteus_ NHMUK 1850.11.22.62	10	0	0	0	30	0	20	0	20	20	30	RF1	highly omnivorous; small vertebrates, insects, vegetable matter; eats more plantstuffs than other foxes
Urogale everetti_FMNH 166482	60	0	0	0	20	0	10	0	0	10	20	RF1	Omnivorous ; meat, insects, fruits, vegetables, lizards, earthworms
Ursus arctos_NHMUK 1963.11.7.1	10	10	0	0	0	0	20	0	0	60	10	RF1	Mainly vegetation but is highly omnivorous; seasonal diet changes; eats grasses, forbs, bulbs, tubers, insects,

													fungi, roots, small mammals
Vicugna vicugna_FMNH 36047	0	0	0	0	0	0	0	0	0	100	0	RF1	Grazer, eats low perennial grasses
Viverra zibetha_FMNH 104395	10	20	20	30	10	0	10	0	0	0	80	RF1	Mostly small mammals, birds, snakes, frogs, insects; also eats items like eggs, fruits, and some roots occasionally
Viverricula indica_UMZC K.4323	20	40	0	0	0	20	10	0	0	10	60	RF1	Small vertebrates, carrion, insects, their grubs
Vombatus ursinus_UMZC A10.10.2	0	0	0	0	0	0	0	0	0	100	0	RF1	Grass, roots, fungi
Vulpes lagopus_UMZC K3669	10	70	0	10	0	10	0	0	0	0	90	RF1	Lemmings, other small mammals like ground-

													nesting birds, stranded marine animals, carrion
Zapus hudsonius_UMMZ 157417	20	0	0	0	0	0	10	0	70	0	0	RF1	Mostly seeds, also fungus, nuts, berries, fruits, insects
Zenkerella insignis_NHMUK 5.5.23.27	0	0	0	0	100	0	0	0	0	0	100	RF1	Is cryptic, not much is known about it; diet is assumed to be vegetarians; but is assigned carnivorous based off % data

Table C2: Expected diets of non-mammalian cynodont species inferred based off qualitative observations and the associated metadata.

Taxon	Diet	Diet_ref
Andescynodon mendozensis_PVL 4069	Herbivore	Benton (2014),Reisz and Sues (2000),Hendrickx et al. (2019)
Andescynodon sp_PVL 4907	Herbivore	Benton (2014), Reisz and Sues (2000),Hendrickx et al. (2019)
Cricodon metabolus_UMZC T905	Herbivore	Benton (2014),Reisz and Sues (2000),Hendrickx et al. (2019)
Cricodon sp_NHM PV R36800	Herbivore	Benton (2014),Reisz and Sues (2000),Hendrickx et al. (2019)
Cynognathus crateronotus_BP 5208	Carnivore	Gow (1978)
Diademodon tetragonus_BP 3756	Herbivore	Gow (1978)
Diademodon tetragonus_SAM PK 571	Herbivore	Gow (1978)
Exaeretodon argentinus_PVL 2467	Herbivore	Benton (2014),Reisz and Sues (2000),Hendrickx et al. (2019)
Exaeretodon riograndensis_UFRGS PV 0715T	Herbivore	Benton (2014),Reisz and Sues (2000),Hendrickx et al. (2019)
Langbergia modisei_NMQR 3251	Herbivore	Benton (2014),Reisz and Sues (2000),Hendrickx et al. (2019)
Luangwa sudamericana_MCP PV 3267	Herbivore	Benton (2014),Reisz and Sues (2000),Hendrickx et al. (2019)
Massetognathus pascuali_BP 4245	Herbivore	Gow (1978),Benton (2014),Reisz and Sues (2000),Hendrickx et al. (2019)
Megazostrodon rudnerae_BP 4983	Insectivore	Jenkins and Parrington (1976),Debuysschere et al. (2015)
Menadon besairiei_UFRGS PV 0891	Herbivore	Benton (2014),Reisz and Sues (2000),Hendrickx et al. (2019) Hopson paper discussing tooth
Pascualgnathus polanskii_PVL 4416	Herbivore	Benton (2014),Reisz and Sues (2000),Hendrickx et al. (2019)
Procynosuchus delaharpwae_BP 226	Insectivore/carnivore	Benton (2014), Kemp (1979)
Sanatacruzodon hopsoni_MCN 2752	Herbivore	Benton (2014),Reisz and Sues (2000),Hendrickx et al. (2019)
Traversodontid sp_MCP PV 4053	Herbivore	Benton (2014),Reisz and Sues (2000),Hendrickx et al. (2019)
Trirachodon berryi_BP 4658	Herbivore/Omnivore	Benton (2014),Reisz and Sues (2000),Hendrickx et al. (2019)
Trirachodon sp_BP 4534	Herbivore/Omnivore	Benton (2014),Reisz and Sues (2000),Hendrickx et al. (2019)
Trirachodontid sp_JSM 100	Herbivore/Omnivore	Benton (2014),Reisz and Sues (2000),Hendrickx et al. (2019)

16.4 Appendix D

Table D1: Body mass data for mammal species and associated metadata. Body mass data obtained from: RF7: Smith et al. (2003), RF8: Jetz and Freckleton (2015); RF9: Genus average; RF10: Family average; RF11: Jones et al. (2009).

Taxon	Body mass (g)	Reference
Abrocoma cinerea_UMMZ 120621	250	RF7
Acinonyx jubatus_AMNH 119657	46700	RF7
Acomys cahirinus_NHMUK 65.789-793	52.45	RF7
Acrobates pygmaeus_NHMUK 82.7.29.23	12	RF7
Aepyceros melampus_FMNH 127890	52500.08	RF7
Aepyprymnus rufescens_FMNH 124573	3250	RF7
Ailuropoda melanoleuca_FMNH 31128	108400	RF7
Ailurus fulgens_NHMUK 1911.10.18.1	4900	RF7
Alces alces_NMS 1996.39	356998.2	RF7
Alouatta seniculus_FMNH 18869	6145.54	RF7
Amblysomus hottentotus_UMZC 2010.15A	52.6	RF7
Anomalurus beecrofti_NHMUK 1989.174	389	RF7
Anourosorex squamipes_NHMUK 1933.4.1.165	20	RF7
Antechinomys laniger_NHMUK 32.2.11.23	25.57	RF11
Antechinus stuartii_FMNH 129556	27.5	RF7
Antilocapra americana_FMNH 57215	46082.92	RF7
Antilope cervicapra_NMS 2000.301.2	37500	RF7
Aonyx cinerea_FMNH 62868	3527.59	RF11
Aplodontia rufa_FMNH 60775	1003.99	RF7
Apodemus sylvaticus_NHMUK unnumbered	30.45	RF7
Arctictis binturong_NMS 2015.164.1	9875	RF7
Ateles geoffroyi_MCZ 10138	5284.94	RF7
Atelocynus microtis_FMNH 60674	7749.97	RF7
Atherurus africanus_UMCZ E.3489	1934	RF7
Atilax paludinosus_NHMUK 1867.7.8.11	3299.97	RF7
Babyrousa babyrussa_NMS 2008.27	100000	RF7
Bandicota indica_NHMUK 1978.896	719.96	RF7
Bassaricyon alleni_FMNH 104935	1235.01	RF7
Bettongia penicillata_FMNH 129431	1300	RF7
Bison bonasus_NHMUK 194.9.6.29.1	500000	RF7
Boselaphus tragocamelus_NHMUK_1974.411	169000	RF7
Bradypus variegatus_FMNH 69589	4335.01	RF7
Callimico goeldii_FMNH 58003	480	RF7
Callithrix jacchus_FMNH 231573	292	RF7
Callosciurus notatus_NHMUK 75.1337	197.5	RF7
Caluromys derbianus_UMMZ 114856	297	RF7
Caluromysiops irrupta_FMNH 60698	250	RF7
Camelus dromedarius_OUMNH 14882	601000	RF7
Canis latrans_UMZC K.3341	13406.33	RF7
Canis mesomelas_UMZC K3402	8500.02	RF7

Canis simensis_AMNH 81001	10000	RF7
Capra sibirica_FMNH 134541	130000	RF7
Caracal caracal_AMNH 113794	13749.91	RF7
Castor canadensis_WLM unnumbered	21820	RF7
Cavia fulgida_UMZC E3705	282.5	RF7
Cephalophus nigrifrons_NHMUK_1936.10.28.33	13899.85	RF7
Cercartetus concinnus_NHMUK 97.11.18.1	13	RF7
Cervus elaphus_NMS 1981.68	165015.9	RF7
Cheirogaleus major_FMNH 85144	450	RF7
Chironectes minimus_UMMZ 126289	946	RF7
Chiropotes satanas_FMNH 95512	2999.99	RF7
Chlorocebus sabaeus_USNM 381445	4993	RF9, RF10
Choeropsis liberiensis_NMS Z.2005.3	235001.2	RF7
Choloepus hoffmanni_NHMUK 1973.824	4750.01	RF7
Chrysochloris asiatica_UMCZ E.5472.F	49	RF7
Chrysochloris stuhlmanni_NHMUK 1934.4.1.7.11	39.8	RF7
Coendou prehensilis_NHMUK 512.F	4399.97	RF7
Colobus satanas_NHMUK 1856.12.29.1	4319.96	RF7
Condylura cristata_UMMZ 80270	84	RF7
Connochaetes taurinus_NHMUK 1935.12.14.3	179999	RF7
Cricetomys gambianus_NHMUK 1890.3.27.2	1271	RF7
Cricetulus migratorius_UMZC E2322	38.5	RF7
Crocidura fuscomurina_UMZC E 5251.G	10.35	RF8
Crocuta crocuta_FMNH 127826	66492.06	RF7
Cryptoprocta ferox_NHMUK 1968.6.7.1	9500	RF7
Cryptotis mexicana_UMMZ 113138	7	RF7
Cuniculus taczanowskii_FMNH 70804	8999.95	RF11
Cynocephalus volans_OUMNH 3404	1250	RF7
Dactylopsila trivirgata_NHMUK 1897.8.7.79	413.53	RF7
Dama dama_OUMNH 19343	52375	RF7
Dasycercus cristicauda_NHMUK 1897.11.3.4	100	RF7
Dasyprocta punctata_FMNH 21260	2674.98	RF7
Dasypus hybridus_AMNH M-205706	1500	RF7
Dasyurus hallucatus_FMNH 119804	525	RF7
Dasyurus maculatus_UMZC A6.10-3	5500	RF7
Dasyurus viverrinus_SAMA M7222	1090	RF7
Daubentonia madagascariensis_UMZC E.8021.A	2500	RF7
Dendrohyrax arboreus_FMNH 163770	2949.99	RF7
Dendrolagus dorianus_NMS 2006.38	9581	RF7
Desmana moschata_UMMZ 124125	383	RF7
Dicerorhinus sumatrensis_NMS 1994.131	800000	RF7
Didelphis marsupialis_NHMUK 1948.7.12.5	1091.16	RF7
Diplomesodon pulchellum_FMNH 137436	11	RF7
Dolichotis patagonum_FMNH 49231	8000	RF7
Dorcopsis muelleri_NHMUK 1933.11.4.4	5500	RF7

Dromiciops gliroides_UMMZ 156354	22.3	RF7
Dugong dugon_MVZ 101162	310000	RF7
Echinops telfairi_NHMUK 1970.355	180	RF7
Echinosorex gymnura_UMZC E.5111.C-E	957	RF7
Echymipera rufescens_FMNH 60525	1100	RF7
Elephantulus brachyrhynchus_NHMUK 1963.1004	47.5	RF7
Elephantulus rozeti_NHMUK 1891.10.15.11	48	RF7
Enhydra lutris_NHMUK 80.879	23500	RF7
Episoriculus caudatus_FMNH 114227	6.95	RF9, RF10
Equus caballus_OUMNH 19193	250000	RF7
Equus kiang_NMS 2016.43	275000	RF7
Eulemur macaco_UMZC E8093A	2040	RF7
Euroscaptor micrura_NHMUK 99.10.25.1	60.47	RF7
Felis catus_UMZC K.6182	2884.8	RF11
Fossa fossana_FMNH 85196	1500	RF7
Funambulus pennantii_UMMZ 62569	200	RF7
Galago senegalensis_FMNH 123783	227.67	RF7
Galemys pyrenaicus_OUMNH 9427	60.17	RF7
Gazella dorcas_NMS 2004.46.5	23000.11	RF7
Genetta angolensis_FMNH 163777	1649.99	RF7
Geocapromys brownii_AMNH 45156	1500	RF7
Geogale aurita_UMMZ 172217	7	RF7
Geomys pinetis_UMMZ 164642	85	RF7
Gerbillus gerbillus_NHMUK 1978.1062	25.04	RF7
Giraffa camelopardalis_FMNH 34424	899994.8	RF7
Glis glis_NHMUK 1996.325	128.09	RF11
Gracilinanus agilis_UMMZ 134557	22	RF7
Gulo gulo_USNM 157327	17012.56	RF7
Hemibelideus lemuroides_FMNH 60926	952.5	RF7
Hemiechinus auritus_UMMZ 156626	342	RF7
Heterocephalus glaber_NHMUK 91.235	55	RF7
Heteromys desmarestianus_NHMUK unregistered xyz002	72.5	RF7
Hippopotamus amphibius_NMS Z.2008.35	1417490	RF7
Hydrochoerus hydrochaeris_AMNH M-206440	48144.91	RF11
Hydromys chrysogaster_NHMUK 1998.134	479.75	RF7
Hydropotes inermis_NMS unnumbered	14000	RF7
Hypogeomys antimena_FMNH 151994	1250	RF7
Hystrix africaeaustralis_FMNH 60453	14936.02	RF7
Ictonyx striatus_UMZC K1874	1299.99	RF7
Idiurus zenkeri_UMZC E1421	100	RF7
Isoodon macrourus_FMNH 120560	1600	RF7
Isoodon obesulus_UMZC A7.4-5	775	RF7
Kobus megaceros_NMS 2001.149.15	87500.39	RF7
Lagostomus maximus_NHMUK ZD 1991.174	4647.51	RF7
Lasiorhinus latifrons_NMS 1868.31	25500	RF7
Lemur catta_FMNH 157993	2900	RF7

Leopardus wiedii_NMS Z.2016.12.1	3249.97	RF7
Lestoros inca_UMMZ 160733	21.1	RF7
Liomys irroratus_UMMZ 120788	50	RF7
Lophocebus albigena_NHMUK 1936.10.28.1	7690.06	RF7
Loris tardigradus_UMZC E.8261.E	227.67	RF7
Lutreolina crassicaudata_UMMZ 163450	537.3	RF7
Lynx canadensis_UMZC K.6682	9373.25	RF7
Macaca sylvanus_NHMUK 1858.4.5.1	7000.03	RF7
Macropus eugenii_NHMUK 1948.7.12.3	6500	RF7
Macropus giganteus_NHMUK 72.4498	25875	RF7
Macropus rufus_NMS PH26.12	46250	RF7
Macroscelides proboscideus_FMNH 137045	38.2	RF7
Macrotis lagotis_NHMUK 73.6.21.4	1350	RF7
Madoqua kirkii_NMS POZ8.99	5300.05	RF7
Malacomys longipes_UMZC E2265	95.6	RF7
Malacothrix typica_UMMZ 117815	13.4	RF7
Marmosa demerarae_UMMZ 134562	75.75	RF7
Marmosa murina_NHMUK 1881.11.1	26	RF7
Marmota monax_AMNH M-67882	3801.72	RF7
Meles meles_NHMUK 2002.476	13000	RF7
Mellivora capensis_UMZC K1821	8500	RF7
Mephitis mephitis_FMNH 129327	2085.02	RF7
Microcebus murinus_AMNH M-174537	69	RF7
Microgale brevicaudata_UMMZ 174757	11.3	RF7
Microgale drouhardi_UMMZ 168477	10.5	RF7
Microgale thomasi_UMMZ 172202	22.9	RF7
Micropotamogale ruwenzorii_NHMUK 67.213	98.5	RF7
Monodelphis domestica_UMMZ 165514	71.4	RF7
Moschus moschiferus_NHMUK 676.d.45.1.12.448	13000	RF7
Muntiacus reevesi_NMS 1996.142.8	13500	RF7
Mus musculus_UMZC E.2202	16.25	RF7
Mustela nivalis_FMNH 207033	103.88	RF7
Mustela putorius_UMZC K.2361	915.37	RF7
Myocastor coypus_AMNH 206456	6937.45	RF7
Myosorex kihaulei_FMNH 209072	12.1	RF9, RF10
Myospalax myospalax_UMMZ 110401	225	RF7
Nandinia binotata_UMZC K.4492	2000	RF7
Napaeozapus insignis_UMMZ 126314	22.3	RF7
Nasua narica_UMZC unumbered	4030.05	RF7
Nectogale elegans_AMNH M-115571	32.5	RF7
Neomys fodiens_NHMUK 1973.917	14.3	RF7
Neotetracus sinensis_NHMUK ZD1933.4.1.134	290.15	RF9, RF10
Notomys cervinus_NHMUK ZD 1936.12.8.17-18	35	RF7
Notoryctes typhlops_UMZC A5.11	55	RF7
Nycticebus coucang_Du Baa 0002	803.5	RF7
Ochotona alpina_UMMZ 123059	150	RF7

Okapia johnstoni_NHMUK 1971.1738	230001.2	RF7
Onychogalea fraenata_UMZC A12.59.3	5500	RF7
Onychomys torridus_UWBM 37628	24.97	RF7
Ornithorhynchus anatinus_UMZC A2.2.10	1484.25	RF7
Oryctolagus cuniculus_NHMUK 1849.6.20.9	1832.22	RF7
Oryx gazella_NHMUK ZD 1963.10.21.1	169001.3	RF7
Oryzorictes tetradactylus_UMZC E.5453.C	36	RF7
Otocyon megalotis_USNM 49129	4150.02	RF7
Ovis aries_OUMNH ZC14858	50000	RF7
Pan troglodytes_RMCA 77032M25	42500	RF7
Panthera pardus_IMNH 2372	52038.22	RF7
Papio hamadryas_UMZC E.7543.B	21250.05	RF7
Paracrocidura schoutedeni_FMNH 227382	13	RF7
Paradoxurus hermaphroditus_FMNH 62837	3156.66	RF7
Pecari tajacu_NMS 2002.164.2	21266.69	RF7
Pedetes capensis_FMNH 152053	3155	RF7
Perodicticus potto_USNM 465898	1099.99	RF7
Petauroides volans_NHMUK 1926.3.11.225	1300	RF7
Petaurus breviceps_FMNH 129430	106.28	RF7
Petinomys sagitta_UMZC E1499	50	RF7
Petrogale penicillata_FMNH 64435	7100	RF7
Phacochoerus aethiopicus_UF 31016	82500	RF7
Phacochoerus africanus_OUMNH ZC3617	82500	RF7
Phascolarctos cinereus_NHMUK 75.1828	10250	RF7
Phataginus tricuspis_NHMUK 34.6.2.94	2066.67	RF7
Philander opossum_UMMZ 114855	585.5	RF7
Podogymnura truei_FMNH 146591	114	RF7
Poiana richardsonii_YPM VZ MAM 014715	500	RF7
Pongo pygmaeus_NHMUK 1986.1097	37000	RF7
Potamogale velox_UMZC E5425F	659.99	RF7
Potorous tridactylus_FMNH 57805	1100	RF7
Presbytis femoralis_UMZC E.7226.C	7000	RF7
Prionailurus viverrinus_NHMUK 1860.7.22.22	9140.33	RF7
Procavia capensis_FMNH 147999	3029.98	RF7
Procyon lotor_FMNH 175311	5524.97	RF7
Proechimys guyannensis_NHMUK 79.322	314.03	RF11
Pronolagus rupestris_FMNH 177246	1754	RF7
Propithecus diadema_UMZC E8041A	7500	RF7
Proteles cristata_NMS unnumbered	8139.39	RF11
Pseudocheirus peregrinus_UMZC A9.2.6.3	900	RF7
Pudu puda_NMS 2011.141.1	9749.9	RF7
Puma concolor_UMZC K5745	51600.04	RF7
Rangifer tarandus_OUMNH 19504	86033.98	RF7
Rhynchocyon petersi_NHMUK 1886.9.21.1	424	RF7
Rhyncholestes raphanurus_FMNH 27476	21	RF7
Saiga tatarica_NMS 1981.72	29000	RF7
Salpingotulus michaelis_UMMZ 120132	29.05	RF9, RF10

Sapajus apella_FMNH 70621	2500	RF7
Sarcophilus harrisii_NHMUK 2003.331	10000	RF7
Scapanus latimanus_UMMZ 74584	55	RF7
Scutisorex somereni_FMNH 160182	91.5	RF7
Setifer setosus_UMZC 2011.3.1	294	RF7
Sminthopsis crassicaudata_FMNH 72923	15	RF7
Smutsia gigantea_AMNH M-53847	32999.7	RF7
Solenodon paradoxus_FMNH 51068	900	RF7
Soriculus nigrescens_UMMZ 122888	14	RF7
Spalacopus cyanus_FMNH 49943	127.5	RF7
Spalax microphthalmus_FMNH 79299	316.04	RF8
Speothos venaticus_NMS 2015.96.3	5999.98	RF7
Spermophilopsis leptodactylus_UMMZ 119250	600	RF7
Surdisorex norae_FMNH 190260	9	RF7
Suricata suricatta_FMNH 101744	725.5	RF7
Sus scrofa_GWU cashp PT001	96118.09	RF7
Sylvilagus floridanus_AMNH M 254438	1172.79	RF7
Sylvisorex howelli_FMNH 198205 198206	4.32	RF7
Tachyoryctes splendens_FMNH 173826 173827	309.95	RF9, RF10
Tamias striatus_UMZC E.1696	111.91	RF7
Tapirus indicus_UF 31027	296250	RF7
Tapirus terrestris_NMS 2001.77.3	207500.9	RF7
Tarsipes rostratus_UMMZ 122547	9	RF7
Tarsius syrichta_FMNH 142007	113.5	RF7
Tayassu sp_IMNH R 228	32233.69	RF7
Tenrec ecaudatus_UMMZ 138441	868	RF7
Thylacinus cynocephalus_NHMUK 1963.8.3.0.1	16700	RF7
Thylamys elegans_UMMZ 156033	28.9	RF7
Thylogale stigmatica_UMZC A12.44-1	4600	RF7
Trachypithecus obscurus_NHMUK 71.709	6420	RF7
Tragelaphus spekii_NMS 2011.162.1	77999.17	RF7
Tragulus kanchil_FMNH 68767	3706.24	RF9, RF10
Trichosurus vulpecula_UMZC A9.16-7	2650	RF7
Tupaia glis_UMZC E.4057.E	169.83	RF7
Urocyon cinereoargenteus_NHMUK 1850.11.22.62	3833.72	RF7
Urogale everetti_FMNH 166482	350	RF7
Ursus arctos_NHMUK 1963.11.7.1	180520.4	RF7
Vicugna vicugna_FMNH 36047	47499.61	RF7
Viverra zibetha_FMNH 104395	9500	RF7
Viverricula indica_UMZC K.4323	2908.43	RF7
Vombatus ursinus_UMZC A10.10.2	1091.16	RF7
Vulpes lagopus_UMZC K3669	3584.37	RF11
Zapus hudsonius_UMMZ 157417	17.12	RF7
Zenkerella insignis_NHMUK 5.5.23.27	200	RF7

Table D2: Body mass approximations used for non-mammalian cynodont species and associated metadata.

Taxon	Body mass (g)	Body mass ref
Andescynodon mendozensis_PVL 4069	2700	Filippini et al. (2022)
Andescynodon sp_PVL 4907	2700	Filippini et al. (2022)
Cricodon metabolus_UMZC T905	22595.41	Calculated, see Table D3
Cricodon sp_NHM PV R36800	13928.3	Approximated, see Table D3
Cynognathus crateronotus_BP 5208	101610	Filippini et al. (2022)
Diademodon tetragonus_BP 3756	7000	Pavanatto et al. (2019)
Diademodon tetragonus_SAM PK 571	7000	Pavanatto et al. (2019)
Exaeretodon argentinus_PVL 2467	69496	Pavanatto et al. (2019)
Exaeretodon riograndensis_UFRGS PV 0715T	36436	Pavanatto et al. (2019)
Langbergia modisei_NMQR 3251	3576.16	Approximated, see Table D3
Luangwa sudamericana_MCP PV 3267	3048.19	Approximated, see Table D3
Massetognathus pascuali_BP 4245	40000	Filippini et al. (2022)
Megazostrodon rudnerae_BP 4983	30	Jenkins and Parrington (1976)
Menadon besairiei_UFRGS PV 0891	15114.46	Approximated, see Table D3
Pascualgnathus polanskii_PVL 4416	3700	Filippini et al. (2022)
Procynosuchus delaharpwae_BP 226	3090	Cavanaugh (2021)
Sanatacruzodon hopsoni_MCN 2752	1854.37	Approximated, see Table D3
Traversodontid sp_MCP PV 4053	26952.94	Approximated from the average of traversodontids in this sample
Trirachodon berryi_BP 4658	3125	Pavanatto et al. (2019)
Trirachodon sp_BP 4534	3125	Pavanatto et al. (2019)
Trirachodontid sp_JSM 100	6450.56	Approximated from the average of traversodontids in this sample

Table D3: Skull length (SL) measurements and the respective body mass estimates. Body mass calculations were modelled after methodology used in Pavanatto et al. (2019). BMa equation ($2.7 \times (SL \div 10)^3$) is derived based off the relationship between skull length and body mass estimates in therapsids (Quiroga, 1984, Quiroga, 1980). BMb equation ($10^{3.13 \times log(SL) - 5.59} \times 1000$) is based off the relationship between skull length and body mass in extant mammals (Van Valkenburgh, 1990). The average of these two calculations were used as a body mass measurement.

Taxon	**SL (mm)**	**SL_ref**	**BMa (g)**	**BMb (g)**	**Average (g)**
Cricodon metabolus	180	Sidor and Hopson (2017)	15746.4	29444.42	22595.41
Langbergia modisei	99	Abdala et al. (2006)	2619.81	4532.50	3576.16
Luangwa Sudamericana	94	Abdala and Sa-Teixeira (2004)	2242.58	3853.81	3048.19
Menadon besairirei	158	Flynn et al. (2000)	10649.64	19579.28	15114.46
Santacruzodon hopsoni	80	Abdala and Ribeiro (2003)	1382.4	2326.33	1854.37

16.5 Appendix E

Table E1: OPCR scores used for the lower premolars (pm1-3) of mammal species. States: 0=absent; 1= unerupted; 2= bad quality; 3= good quality; 4= great quality.

Taxon	pm1 OPCR	pm1 Faces	pm1 Vertices	pm1 State	pm2 OPCR	pm2 Faces	pm2 Vertices	pm2 State	pm3 OPCR	pm3 Faces	pm3 Vertices	pm3 State
Abrocoma cinerea_UMMZ 120621				0				0				0
Acinonyx jubatus_AMNH 119657	21.75	999	532	4	24.88	999	536	4				0
Acomys cahirinus_NHMUK 65.789-793				0				0				0
Acrobates pygmaeus_NHMUK 82.7.29.23				0				0				0
Aepyceros melampus_FMNH 127890				0				0				0
Aepyprymnus rufescens_FMNH 124573				0				0				0
Ailuropoda melanoleuca_IMNH C 302				0				0				0
Ailurus fulgens_NHMUK 1911.10.18.1				0				0				0
Alces alces_NMS 1996.39				0				0				0
Alouatta seniculus_FMNH 18869				0				0				0
Amblysomus hottentotus_UMZC 2010.15A				0				0	21.5	1000	518	4
Anomalurus beecrofti_NHMUK 1989.174				0				0				0
Anourosorex squamipes_NHMUK 1933.4.1.165				0				0				0
Antechinomys laniger_NHMUK 32.2.11.23				0				0				0
Antechinus stuartii_FMNH				0				0				0

129556												
Antilocapra americana_FMNH 57215				0				0				0
Antilope cervicapra_NMS 2000.301.2				0				0				0
Aonyx cinerea_FMNH 62868				0				0	24.38	999	539	4
Aplodontia rufa_FMNH 60775				0				0				0
Apodemus sylvaticus_NHMUK unnumbered				0				0				0
Ateles geoffroyi_MCZ 10138				0				0				0
Atelocynus microtis_FMNH 60674				0				0				0
Atherurus africanus_UMCZ E.3489				0				0				0
Atilax paludinosus_NHMUK 1867.7.8.11				0				0	23.62	999	535	4
Babyrousa babyrussa_NMS 2008.27				0				0				0
Bandicota indica_NHMUK 1978.896				0				0				0
Bassaricyon alleni_FMNH 104935				0				0				0
Bettongia penicillata_FMNH 129431				0				0				0
Bison bonasus_NHMUK 194.9.6.29.1				0				0				0
Boselaphus tragocamelus_NHMUK_1974.411				0				0				0
Bradypus variegatus_FMNH 69589				0				0				0
Callimico goeldii_FMNH 58003				0				0				0
Callithrix jacchus_FMNH 231573				0				0	28.62	1000	540	4
Callosciurus notatus_NHMUK 75.1337				0				0				0

Caluromys derbianus_UMMZ 114856				0				0				0
Caluromysiops irrupta_FMNH 60698				0				0				0
Camelus dromedarius_OUMNH 14882				0				0				0
Canis latrans_UMZC K.3341				0				0				0
Canis mesomelas_UMZC K3402				0				0				0
Canis simensis_AMNH 81001				0				0				0
Capra sibirica_FMNH 134541				0				0				0
Caracal caracal_AMNH 113794	14	1000	531	4	30.12	1000	535	4				0
Castor canadensis_WLM unnumbered				0				0				0
Cavia fulgida_UMZC E3705				0				0				0
Cephalophus nigrifrons_NHMUK_1936.10.28.33				0				0				0
Cercartetus concinnus_NHMUK 97.11.18.1				0				0				0
Cervus elaphus_NMS 1981.68				0				0				0
Chironectes minimus_UMMZ 126289				0				0				0
Chlorocebus sabaeus_USNM 381445				0				0				0
Choloepus hoffmanni_NHMUK 1973.824				0				0				0
Chrysochloris asiatica_UMCZ E.5472.F				0				0				0
Chrysochloris stuhlmanni_NHMUK 1934.4.1.7.11				0				0				0
Coendou prehensilis_NHMUK 512.F				0				0				0
Colobus satanas_NHMUK				0				0				0

1856.12.29.1												
Condylura cristata_UMMZ 80270				0				0				0
Connochaetes taurinus_NHMUK 1935.12.14.3				0				0				0
Cricetomys gambianus_NHMUK 1890.3.27.2				0				0				0
Cricetulus migratorius_UMZC E2322				0				0				0
Crocidura fuscomurina_UMZC E 5251.G				0				0				0
Crocuta crocuta_FMNH 127826				0	26.62	999	544	3	37.25	996	541	3
Cryptoprocta ferox_NHMUK 1968.6.7.1				0				0	12.25	999	533	4
Cryptotis mexicana_UMMZ 113138				0				0				0
Cynocephalus volans_OUMNH 3404				0				0				0
Dactylopsila trivirgata_NHMUK 1897.8.7.79				0				0				0
Dama dama_OUMNH 19343				0				0				0
Dasycercus cristicauda_NHMUK 1897.11.3.4				0				0				0
Dasyprocta punctata_FMNH 21260				0				0				0
Dasyurus hallucatus_FMNH 119804				0				0				0
Dasyurus maculatus_UMZC A6.10-3				0				0				0
Dasyurus viverrinus_SAMA M7222				0				0				0
Daubentonia madagascariensis_UMZC E.8021.A				0				0				0
Desmana moschata_UMMZ				0				0				0

124125												
Dicerorhinus sumatrensis_NMS 1994.131				0				0				0
Didelphis marsupialis_NHMUK 1948.7.12.5				0				0				0
Diplomesodon pulchellum_FMNH 137436				0				0				0
Dolichotis patagonum_FMNH 49231				0				0				0
Dorcopsis muelleri_NHMUK 1933.11.4.4				0				0				0
Dromiciops gliroides_UMMZ 156354				0				0				0
Dugong dugon_MVZ 101162				0				0				0
Echinops telfairi_NHMUK 1970.355				0				0	44.62	999	554	4
Echinosorex gymnura_UMZC E.5111.C-E				0				0				0
Echymipera rufescens_FMNH 60525				0				0				0
Elephantulus brachyrhynchus_NHMUK 1963.1004				0				0				0
Elephantulus rozeti_NHMUK 1891.10.15.11				0				0				0
Enhydra lutris_NHMUK 80.879				0				0	27	1000	544	4
Episoriculus caudatus_FMNH 114227				0				0				0
Eulemur macaco_UMZC E8093A				0				0				0
Euroscaptor micrura_NHMUK 99.10.25.1				0				0				0
Felis catus_UMZC K.6182	16	992	538	4	34.5	997	538	4				0
Fossa fossana_FMNH 85196				0				0	10.25	999	529	4
Funambulus pennantii_UMMZ				0				0				0

62569												
Galago senegalensis_FMNH 123783				0				0				0
Galemys pyrenaicus_OUMNH 9427				0				0				0
Gazella dorcas_NMS 2004.46.5				0				0				0
Genetta angolensis_FMNH 163777				0				0				0
Geocapromys brownii_AMNH 45156				0				0				0
Geogale aurita_UMMZ 172217				0				0				0
Geomys pinetis_UMMZ 164642				0				0				0
Gerbillus gerbillus_NHMUK 1978.1062				0				0				0
Giraffa camelopardalis_FMNH 34424				0				0				0
Glis glis_NHMUK 1996.325				0				0				0
Gracilinanus agilis_UMMZ 134557				0				0				0
Gulo gulo_USNM 157327				0				0				0
Hemibelideus lemuroides_FMNH 60926				0				0				0
Hemiechinus auritus_UMMZ 156626				0				0				0
Heterocephalus glaber_NHMUK 91.235				0				0				0
Heteromys desmarestianus_NHMUK unregistered xyz002				0				0				0
Hippopotamus amphibius_NMS Z.2008.35				0				0				0
Hydrochoerus hydrochaeris_AMNH M-206440				0				0				0
Hydromys chrysogaster_NHMUK				0				0				0

1998.134												
Hydropotes inermis_NMS unnumbered				0				0				0
Hypogeomys antimena_FMNH 151994				0				0				0
Ictonyx striatus_UMZC K1874				0				0	26.88	999	543	4
Idiurus zenkeri_UMZC E1421				0				0				0
Isoodon macrourus_FMNH 120560				0				0				0
Isoodon obesulus_UMZC A7.4-5				0				0				0
Kobus megaceros_NMS 2001.149.15				0				0				0
Lasiorhinus latifrons_NMS 1868.31				0				0				0
Lemur catta_FMNH 157993				0				0				0
Leopardus wiedii_NMS Z.2016.12.1				0	21.38	999	532	4				0
Lestoros inca_UMMZ 160733				0				0				0
Liomys irroratus_UMMZ 120788				0				0				0
Lophocebus albigena_NHMUK 1936.10.28.1				0				0				0
Loris tardigradus_UMZC E.8261.E				0				0				0
Lutreolina crassicaudata_UMMZ 163450				0				0				0
Lynx canadensis_UMZC K.6682	39	999	534	4				0				0
Macaca sylvanus_NHMUK 1858.4.5.1				0				0				0
Macropus eugenii_NHMUK 1948.7.12.3				0				0				0
Macropus giganteus_NHMUK 72.4498				0				0				0
Macropus rufus_NMS PH26.12				0				0				0
Macroscelides				0				0				0

proboscideus_FMNH 137045												
Macrotis lagotis_NHMUK 73.6.21.4				0				0				0
Madoqua kirkii_NMS POZ8.99				0				0				0
Malacomys longipes_UMZC E2265				0				0				0
Malacothrix typica_UMMZ 117815				0				0				0
Marmosa demerarae_UMMZ 134562				0				0				0
Marmosa murina_NHMUK 1881.11.1				0				0				0
Marmota monax_AMNH M-67882				0				0				0
Meles meles_NHMUK 2002.476				0				0	10	999	532	4
Mephitis mephitis_FMNH 129327				0				0	27.12	999	537	4
Microcebus murinus_AMNH M-174537				0				0				0
Microgale brevicaudata_UMMZ 174757				0				0				0
Microgale drouhardi_UMMZ 168477				0				0				0
Microgale thomasi_UMMZ 172202				0				0				0
Micropotamogale ruwenzorii_NHMUK 67.213				0				0				0
Monodelphis domestica_UMMZ 165514				0				0				0
Moschus moschiferus_NHMUK 676.d.45.1.12.448				0				0				0
Mus musculus_UMZC E.2202				0				0				0
Mustela nivalis_FMNH 207033				0				0	18.62	1000	530	4
Mustela putorius_UMZC K.2361				0				0	18.88	1000	525	4
Myosorex kihaulei_FMNH 209072				0				0				0

Myospalax myospalax_UMMZ 110401				0				0				0
Nandinia binotata_UMZC K.4492				0	18.38	1000	527	4	23.25	1000	522	4
Napaeozapus insignis_UMMZ 126314				0				0				0
Nasua narica_UMZC unumbered				0				0				0
Nectogale elegans_AMNH M-115571				0				0				0
Neomys fodiens_NHMUK 1973.917				0				0				0
Neotetracus sinensis_NHMUK ZD1933.4.1.134				0				0				0
Notomys cervinus_NHMUK ZD 1936.12.8.17-18				0				0				0
Notoryctes typhlops_UMZC A5.11				0				0				0
Nycticebus coucang_Du Baa 0002				0				0				0
Ochotona alpina_UMMZ 123059				0				0				0
Okapia johnstoni_NHMUK 1971.1738				0				0				0
Onychogalea fraenata_UMZC A12.59.3				0				0				0
Onychomys torridus_UWBM 37628				0				0				0
Oryx gazella_NHMUK ZD 1963.10.21.1				0				0				0
Oryzorictes tetradactylus_UMZC E.5453.C				0				0				0
Otocyon megalotis_USNM 49129				0				0				0
Ovis aries_OUMNH ZC14858				0				0				0
Pan troglodytes_RMCA 77032M25				0				0				0
Panthera pardus_IMNH 2372	14.75	1000	530	4	26.12	1000	525	4				0
Papio hamadryas_UMZC				0				0				0

E.7543.B												
Paracrocidura schoutedeni_FMNH 227382				0				0				0
Paradoxurus hermaphroditus_FMNH 62837				0				0				0
Pecari tajacu_NMS 2002.164.2				0				0				0
Pedetes capensis_FMNH 152053				0				0				0
Perodicticus potto_USNM 465898				0				0				0
Petauroides volans_NHMUK 1926.3.11.225				0				0				0
Petaurus breviceps_FMNH 129430				0				0				0
Petinomys sagitta_UMZC E1499				0				0				0
Petrogale penicillata_FMNH 64435				0				0				0
Podogymnura truei_FMNH 146591				0				0				0
Poiana richardsonii_YPM VZ MAM 014715				0				0				0
Pongo pygmaeus_NHMUK 1986.1097				0				0				0
Potamogale velox_UMZC E5425F				0				0	27.75	1000	534	4
Potorous tridactylus_FMNH 57805				0				0				0
Presbytis femoralis_UMZC E.7226.C				0				0				0
Prionailurus viverrinus_NHMUK 1860.7.22.22	10.38	999	525	4	18.25	1000	537	4				0
Procavia capensis_FMNH 147999				0				0				0
Procyon lotor_FMNH 175311				0				0				0
Pronolagus rupestris_FMNH				0				0				0

177246												
Propithecus diadema_USNM 63350				0				0				0
Proteles cristata_NMS unnumbered	11.38	999	522	4	9.38	1000	525	4				0
Pseudocheirus peregrinus_UMZC A9.2.6.3				0				0				0
Pudu puda_NMS 2011.141.1				0				0				0
Puma concolor_UMZC K5745				0	22.38	999	544	4				0
Rangifer tarandus_OUMNH 19504				0				0				0
Rhynchocyon petersi_NHMUK 1886.9.21.1				0	47.38	999	537	4				0
Rhyncholestes raphanurus_FMNH 27476				0				0				0
Saiga tatarica_NMS 1981.72				0				0				0
Salpingotulus michaelis_UMMZ 120132				0				0				0
Sarcophilus harrisii_NHMUK 2003.331				0				0				0
Scapanus latimanus_UMMZ 74584				0				0				0
Scutisorex somereni_FMNH 160182				0				0				0
Setifer setosus_UMZC 2011.3.1				0				0				0
Sminthopsis crassicaudata_FMNH 72923				0				0				0
Solenodon paradoxus_FMNH 51068				0				0				0
Spalacopus cyanus_FMNH 49943				0				0				0
Spalax microphthalmus_FMNH 79299				0				0				0
Speothos venaticus_NMS				0				0				0

2015.96.3												
Spermophilopsis leptodactylus_UMMZ 119250				0				0				0
Surdisorex norae_FMNH 190260				0				0				0
Suricata suricatta_FMNH 101744				0				0	26	1000	543	4
Sus scrofa_GWU cashp PT001				0				0				0
Sylvilagus floridanus_AMNH M 254438				0				0				0
Sylvisorex howelli_FMNH 198205 198206				0				0				0
Tachyoryctes splendens_FMNH 173826 173827				0				0				0
Tamias striatus_UMZC E.1696				0				0				0
Tapirus indicus_UF 31027				0				0				0
Tapirus terrestris_NMS 2001.77.3				0				0				0
Tarsius syrichta_FMNH 142007				0				0				0
Tayassu sp_IMNH R 228				0				0				0
Tenrec ecaudatus_UMMZ 138441				0				0				0
Thylacinus cynocephalus_NHMUK 1963.8.3.0.1				0				0				0
Thylamys elegans_UMMZ 156033	3			0				0				0
Thylogale stigmatica_UMZC A12.44-1				0				0				0
Trachypithecus obscurus_NHMUK 71.709				0				0				0
Tragelaphus spekii_NMS 2011.162.1				0				0				0
Trichosurus vulpecula_UMZC A9.16-7				0				0				0
Tupaia glis_UMZC E.4057.E				0				0				0
Urocyon				0				0				0

cinereoargenteus_NHMUK 1850.11.22.62												
Urogale everetti_FMNH 166482				0				0				0
Ursus arctos_NHMUK 1963.11.7.1				0				0				0
Vicugna vicugna_FMNH 36047				0				0				0
Viverra zibetha_FMNH 104395				0				0	28.62	1000	537	4
Viverricula indica_UMZC K.4323				0				0				0
Vombatus ursinus_UMZC A10.10.2				0				0				0
Vulpes lagopus_UMZC K3669				0				0				0
Zapus hudsonius_UMMZ 157417				0				0				0
Zenkerella insignis_NHMUK 5.5.23.27				0				0				0

Table E2: OPCR scores used for the lower premolars and molars (pm4; m1-m2) of mammal species. States: 0=absent; 1= unerupted; 2= bad quality; 3= good quality; 4= great quality.

Taxon	pm4 OPCR	pm4 Face	pm4 Vertices	pm4 State	m1 OPCR	m1 Face	m1 Vertices	m1 State	m2 OPCR	m2 Face	m2 Vertices	m2 State
Abrocoma cinerea_UMMZ 120621				0	47.75	1000	547	4	56	1000	557	4
Acinonyx jubatus_AMNH 119657				0	29.25	999	532	4				0
Acomys cahirinus_NHMUK 65.789-793				0	47.12	999	530	4	36	1000	549	4
Acrobates pygmaeus_NHMUK 82.7.29.23				0	24.25	985	533	4	36.88	999	536	4
Aepyceros melampus_FMNH 127890				0	76.62	1000	568	4	43.75	1000	547	4
Aepyprymnus rufescens_FMNH 124573				0	49.88	999	538	3	51.75	998	546	3
Ailuropoda melanoleuca_IMNH C 302	62.62	998	523	4	83.88	1000	534	4	86.38	1000	530	4
Ailurus fulgens_NHMUK 1911.10.18.1	40.75	999	539	4	45	999	539	4	49	1000	531	4
Alces alces_NMS 1996.39				0	50.75	1000	551	4	58.38	999	551	4
Alouatta seniculus_FMNH 18869				0	35.75	1000	545	4	40.25	1000	536	4
Amblysomus hottentotus_UMZC 2010.15A				0	24.5	996	519	4	24.88	999	521	4
Anomalurus beecrofti_NHMUK 1989.174				0	82.88	990	537	3	84.88	998	539	3
Anourosorex squamipes_NHMUK 1933.4.1.165				0	36.62	999	544	4	33.5	999	543	4
Antechinomys laniger_NHMUK 32.2.11.23				0	42.38	1000	532	4	47.75	999	538	4
Antechinus stuartii_FMNH 129556				0	17.23	999	528	4	57	1000	544	3
Antilocapra americana_FMNH 57215				0	43.38	1000	542	4	53.88	999	537	4
Antilope cervicapra_NMS 2000.301.2				0	36.25	999	560	4	40.88	999	555	4

Aonyx cinerea_FMNH 62868				0	48.62	1000	534	4	36.5	1000	529	4
Aplodontia rufa_FMNH 60775				0	38.88	1000	550	3	45.5	999	551	3
Apodemus sylvaticus_NHMUK unnumbered				0	58	999	540	4	44.5	996	549	4
Ateles geoffroyi_MCZ 10138				0	42	999	537	4	39.5	1000	534	4
Atelocynus microtis_FMNH 60674	50.75	1000	546	4	33.38	999	539	4	20	999	524	4
Atherurus africanus_UMCZ E.3489				0	41.38	999	556	4	35.25	1000	548	4
Atilax paludinosus_NHMUK 1867.7.8.11				0	38.88	999	531	4	31.12	1000	530	4
Babyrousa babyrussa_NMS 2008.27				0	47.25	1000	547	4	42	999	553	4
Bandicota indica_NHMUK 1978.896				0	71	934	500	3	63.25	970	528	3
Bassaricyon alleni_FMNH 104935	22.25	1000	544	4	43.75	1000	543	4	31.12	1000	544	4
Bettongia penicillata_FMNH 129431				0	37.62	999	552	4	38.62	1000	551	4
Bison bonasus_NHMUK 194.9.6.29.1				0	38.38	1000	537	4	40.62	999	544	4
Boselaphus tragocamelus_NHMUK_1974.411				0	23.62	999	544	4	25.75	1000	540	4
Bradypus variegatus_FMNH 69589				0				0	31.5	999	530	4
Callimico goeldii_FMNH 58003				0	46.38	998	550	4	40.88	1000	537	4
Callithrix jacchus_FMNH 231573				0	29.5	999	539	4	38.88	1000	535	4
Callosciurus notatus_NHMUK 75.1337				0	58	992	538	4	60.25	996	549	3
Caluromys derbianus_UMMZ 114856				0	40.88	999	542	4	45.5	999	559	4
Caluromysiops irrupta_FMNH 60698				0	51.12	999	535	4	42.5	999	536	4
Camelus dromedarius_OUMNH 14882				0	43	1000	547	3	23.62	1000	548	3
Canis latrans_UMZC K.3341	43.25	999	527	4	33	1000	537	4	12.75	1000	544	4
Canis mesomelas_UMZC K3402	39	1000	529	4	28	1000	531	4	16.12	1000	548	4

Canis simensis_AMNH 81001				0	45.38	1000	532	4	36.88	1000	526	4
Capra sibirica_FMNH 134541				0	47.38	999	553	4	56.12	999	548	4
Caracal caracal_AMNH 113794				0	24.12	999	525	4				0
Castor canadensis_WLM unnumbered				0	63.62	1000	530	4	62.5	1000	553	4
Cavia fulgida_UMZC E3705				0	63.38	1000	548	4	80	998	536	4
Cephalophus nigrifrons_NHMUK_1936.10.28.33				0	45.88	1000	546	4	45.38	999	543	4
Cercartetus concinnus_NHMUK 97.11.18.1				0	26.12	991	531	4	28.38	1000	564	4
Cervus elaphus_NMS 1981.68				0	48.62	990	530	3	54.62	990	325	3
Chironectes minimus_UMMZ 126289				0	34.38	1000	550	4	43.5	1000	546	4
Chlorocebus sabaeus_USNM 381445				0	33.38	1000	543	4	37.62	1000	562	4
Choloepus hoffmanni_NHMUK 1973.824				0				0	19.75	1000	524	4
Chrysochloris asiatica_UMCZ E.5472.F				0	22	1000	529	4	16.88	991	513	4
Chrysochloris stuhlmanni_NHMUK 1934.4.1.7.11				0	24.75	1000	525	4	32.38	999	528	4
Coendou prehensilis_NHMUK 512.F				0	45.5	1000	556	3	27.62	1000	555	3
Colobus satanas_NHMUK 1856.12.29.1				0	36	1000	533	4	42.25	999	536	4
Condylura cristata_UMMZ 80270				0	59.75	999	524	4	54.5	999	539	4
Connochaetes taurinus_NHMUK 1935.12.14.3				0	17.5	999	543	3	21.88	999	540	3
Cricetomys gambianus_NHMUK 1890.3.27.2				0	47.25	1000	542	4	44.75	1000	557	4
Cricetulus migratorius_UMZC E2322				0	50.62	1000	536	4	56.12	1000	543	4
Crocidura fuscomurina_UMZC E 5251.G				0	44.62	999	529	4	49.12	1000	531	4

Crocuta crocuta_FMNH 127826				0	26	999	538	3				0
Cryptoprocta ferox_NHMUK 1968.6.7.1				0	16	1000	533	3	18.88	1000	539	4
Cryptotis mexicana_UMMZ 113138				0	49.62	999	546	4	51.75	1000	543	4
Cynocephalus volans_OUMNH 3404				0	45	996	535	4	42.5	999	529	4
Dactylopsila trivirgata_NHMUK 1897.8.7.79				0	31.25	1000	541	4	44.5	1000	549	4
Dama dama_OUMNH 19343				0	47.88	997	533	3	58.12	999	551	4
Dasycercus cristicauda_NHMUK 1897.11.3.4				0	38.62	999	541	4	59.5	995	533	4
Dasyprocta punctata_FMNH 21260				0	46.62	999	557	4	54	998	546	4
Dasyurus hallucatus_FMNH 119804				0	21.75	1000	532	4	47.62	1000	537	4
Dasyurus maculatus_UMZC A6.10-3				0	26.75	999	537	4	46.75	1000	544	4
Dasyurus viverrinus_SAMA M7222				0	28.88	999	531	4	40	1000	541	4
Daubentonia madagascariensis_UMZC E.8021.A				0	24	999	536	4	31.38	1000	550	4
Desmana moschata_UMMZ 124125				0	37.62	1000	530	4	37.25	1000	528	4
Dicerorhinus sumatrensis_NMS 1994.131				0	33.12	999	543	4	38.88	999	548	4
Didelphis marsupialis_NHMUK 1948.7.12.5				0	28	999	534	4	35.12	999	541	4
Diplomesodon pulchellum_FMNH 137436				0	41.38	1000	535	4	58.25	1000	545	4
Dolichotis patagonum_FMNH 49231				0	38.38	999	543	4	38.38	1000	542	4
Dorcopsis muelleri_NHMUK 1933.11.4.4				0	28.25	999	540	4	32.25	1000	534	4

Dromiciops gliroides_UMMZ 156354				0	34.12	1000	532	4	47.75	1000	539	4
Dugong dugon_MVZ 101162				0	31.38	1000	532	4	32.62	1000	537	4
Echinops telfairi_NHMUK 1970.355				0	50	997	555	4	35.3	1000	538	4
Echinosorex gymnura_UMZC E.5111.C-E				0	56.38	999	539	4	46.38	1000	538	4
Echymipera rufescens_FMNH 60525				0	33.62	999	544	4	49.25	1000	542	4
Elephantulus brachyrhynchus_NHMUK 1963.1004				0	37.75	999	536	4	43	1000	541	4
Elephantulus rozeti_NHMUK 1891.10.15.11				0	54.75	999	543	4	54.25	996	541	4
Enhydra lutris_NHMUK 80.879				0	47	1000	544	4	41.75	997	532	4
Episoriculus caudatus_FMNH 114227				0	44.62	999	542	4	44.62	999	534	4
Eulemur macaco_UMZC E8093A				0	32.75	999	544	4	32.5	999	545	4
Euroscaptor micrura_NHMUK 99.10.25.1				0	49.5	999	535	4	50.12	999	538	4
Felis catus_UMZC K.6182				0	29	999	540	4				0
Fossa fossana_FMNH 85196	17.62	1000	531	4	32	999	524	4				0
Funambulus pennantii_UMMZ 62569				0	41.25	1000	547	4	39.88	999	553	4
Galago senegalensis_FMNH 123783				0	45.75	992	536	4	42.88	987	532	4
Galemys pyrenaicus_OUMNH 9427				0	54.38	1000	530	4	54.38	999	532	4
Gazella dorcas_NMS 2004.46.5				0	37.62	1000	556	4	40.88	1000	555	4
Genetta angolensis_FMNH 163777	31.75	1000	541	4	43.62	999	536	4	33.62	999	536	4
Geocapromys brownii_AMNH 45156				0	65.62	999	545	3	66.88	1000	524	3
Geogale aurita_UMMZ 172217				0	35	1000	549	4	33.88	999	540	4

Geomys pinetis_UMMZ 164642				0	22	1000	557	4	28.12	1000	550	4
Gerbillus gerbillus_NHMUK 1978.1062				0	44.62	1000	537	4	36.38	1000	560	4
Giraffa camelopardalis_FMNH 34424				0	46.5	999	546	4	55.5	999	542	4
Glis glis_NHMUK 1996.325				0	68.75	992	548	4	81.5	986	582	3
Gracilinanus agilis_UMMZ 134557				0	48.88	1000	541	4	48.75	1000	549	4
Gulo gulo_USNM 157327	22.88	1000	548	4	29.12	999	539	4	32	1000	541	4
Hemibelideus lemuroides_FMNH 60926				0	60.12	995	544	4	69.25	989	532	4
Hemiechinus auritus_UMMZ 156626				0	45.25	1000	541	4	40.62	999	540	4
Heterocephalus glaber_NHMUK 91.235				0	27.25	754	412	3	28.5	693	395	3
Heteromys desmarestianus_NHMUK unregistered xyz002				0	36.25	1000	556	3	29.5	1000	554	3
Hippopotamus amphibius_NMS Z.2008.35				0	39.62	1000	550	4	57.12	1000	547	4
Hydrochoerus hydrochaeris_AMNH M-206440				0	80	1000	548	3	96.25	1000	548	4
Hydromys chrysogaster_NHMUK 1998.134				0	63.75	943	479	4	74	904	434	4
Hydropotes inermis_NMS unnumbered				0	37.75	1000	553	3	42.12	1000	539	3
Hypogeomys antimena_FMNH 151994				0	46.38	992	532	4	54	997	551	4
Ictonyx striatus_UMZC K1874				0	50.62	1000	542	4	35.25	999	538	4
Idiurus zenkeri_UMZC E1421				0	41.38	999	545	4	33.38	999	542	4
Isoodon macrourus_FMNH 120560				0	32.5	999	543	4	35.5	999	554	4
Isoodon obesulus_UMZC A7.4-5				0	33.5	1000	533	4	30.5	1000	528	4
Kobus megaceros_NMS 2001.149.15				0	52.38	999	540	4	45.62	999	545	4

Lasiorhinus latifrons_NMS 1868.31				0	41.5	1000	539	3	37	999	537	3
Lemur catta_FMNH 157993				0	20.62	1000	539	4	27.62	1000	541	4
Leopardus wiedii_NMS Z.2016.12.1				0	19.38	1000	532	4				0
Lestoros inca_UMMZ 160733				0	49.12	1000	554	4	51.38	999	551	4
Liomys irroratus_UMMZ 120788				0	38.5	1000	555	4	33	999	572	4
Lophocebus albigena_NHMUK 1936.10.28.1				0	38.25	1000	545	4	38.38	1000	544	4
Loris tardigradus_UMZC E.8261.E				0	38.12	999	539	4	36.12	993	538	4
Lutreolina crassicaudata_UMMZ 163450				0	37.25	1000	547	4	44.12	997	555	4
Lynx canadensis_UMZC K.6682				0	41	1000	544	4	20	1000	537	4
Macaca sylvanus_NHMUK 1858.4.5.1				0	22.25	1000	538	4	42	999	537	4
Macropus eugenii_NHMUK 1948.7.12.3				0	37.12	999	545	4	26.5	999	536	4
Macropus giganteus_NHMUK 72.4498				0	30	999	542	4	22.5	999	548	4
Macropus rufus_NMS PH26.12				0	24	641	364	2	26.5	788	445	3
Macroscelides proboscideus_FMNH 137045				0	34.38	989	542	4	38.75	992	544	4
Macrotis lagotis_NHMUK 73.6.21.4				0	41.62	995	541	4	48.38	1000	543	4
Madoqua kirkii_NMS POZ8.99				0	61.25	992	534	4	57.88	996	537	4
Malacomys longipes_UMZC E2265				0	54.62	999	534	4	54.38	997	558	3
Malacothrix typica_UMMZ 117815				0	51.88	1000	542	4	48.75	1000	546	4
Marmosa demerarae_UMMZ 134562				0	8.88	410	233	2	18.5	778	429	3
Marmosa murina_NHMUK 1881.11.1				0	46	1000	536	4	44.38	999	549	4
Marmota monax_AMNH M-67882				0	33	999	544	4	36.38	999	542	4
Meles meles_NHMUK 2002.476	10	1000	524	4	47.38	1000	538	4	26.88	999	531	4

Mephitis mephitis_FMNH 129327				0	58	999	540	4	41.12	997	533	4
Microcebus murinus_AMNH M-174537				0	44.38	1000	541	4	39.62	999	547	4
Microgale brevicaudata_UMMZ 174757				0	44.62	999	541	4	38.75	999	536	4
Microgale drouhardi_UMMZ 168477				0	45.5	999	536	4	43	999	560	4
Microgale thomasi_UMMZ 172202				0	41.5	1000	562	4	38.62	999	555	4
Micropotamogale ruwenzorii_NHMUK 67.213				0	32.75	1000	537	4	37.5	1000	536	4
Monodelphis domestica_UMMZ 165514				0	44.62	999	541	4	44.38	999	552	4
Moschus moschiferus_NHMUK 676.d.45.1.12.448				0	39.12	1000	537	4	43	999	536	4
Mus musculus_UMZC E.2202				0	46.88	1000	533	4	34.38	999	561	4
Mustela nivalis_FMNH 207033				0	35.38	1000	550	4	18.88	1000	529	4
Mustela putorius_UMZC K.2361				0	36.25	1000	524	4	12.88	999	325	4
Myosorex kihaulei_FMNH 209072				0	48.88	1000	531	4	47.62	1000	539	4
Myospalax myospalax_UMMZ 110401				0	42.25	997	561	3	48.88	1000	561	3
Nandinia binotata_UMZC K.4492				0	30.5	999	526	4				0
Napaeozapus insignis_UMMZ 126314				0	53	990	533	4	44.88	1000	548	4
Nasua narica_UMZC unumbered	29.12	1000	539	4	52.38	1000	539	4	44.12	999	534	4
Nectogale elegans_AMNH M-115571				0	51.75	991	530	4	50.25	993	531	4
Neomys fodiens_NHMUK 1973.917				0	50.12	998	531	4	51.25	993	531	4
Neotetracus sinensis_NHMUK ZD1933.4.1.134				0	43.75	1000	538	4	43.5	997	546	4
Notomys cervinus_NHMUK ZD 1936.12.8.17-18				0	72	1000	535	4	48.38	999	533	4
Notoryctes typhlops_UMZC A5.11				0	28.12	999	523	4	27.75	1000	521	4
Nycticebus coucang_Du Baa 0002				0	46.12	999	542	4	43.5	999	540	4

Ochotona alpina_UMMZ 123059				0	46.25	1000	552	4	51.5	999	554	4
Okapia johnstoni_NHMUK 1971.1738				0	36.88	999	542	4	41.25	1000	542	4
Onychogalea fraenata_UMZC A12.59.3				0	43	999	536	4	38.25	1000	532	4
Onychomys torridus_UWBM 37628				0	53.88	982	501	4	39.88	1000	551	4
Oryx gazella_NHMUK ZD 1963.10.21.1				0	27.62	1000	538	4	23.5	1000	542	4
Oryzorictes tetradactylus_UMZC E.5453.C				0	31.5	999	543	4	36.5	999	534	4
Otocyon megalotis_USNM 49129				0	50.88	1000	546	4	39.12	1000	541	4
Ovis aries_OUMNH ZC14858				0	47.25	1000	551	4	51.75	1000	547	4
Pan troglodytes_RMCA 77032M25				0	50.62	999	542	4	52.12	1000	539	4
Panthera pardus_IMNH 2372				0	30.88	1000	521	4				0
Papio hamadryas_UMZC E.7543.B				0	48.75	998	538	4	52	1000	555	4
Paracrocidura schoutedeni_FMNH 227382				0	52.25	1000	539	4	60.88	999	541	4
Paradoxurus hermaphroditus_FMNH 62837	40.62	1000	545	4	42.12	995	547	4	29.5	999	542	4
Pecari tajacu_NMS 2002.164.2				0	13.25	501	284	3	30.75	681	383	3
Pedetes capensis_FMNH 152053				0	55.5	999	547	3	52.75	999	538	3
Perodicticus potto_USNM 465898				0	43.5	990	525	3	35.62	990	525	3
Petauroides volans_NHMUK 1926.3.11.225				0	45.75	999	539	4	47.5	999	538	4
Petaurus breviceps_FMNH 129430				0	32.25	999	534	4	42.12	999	549	4
Petinomys sagitta_UMZC E1499				0	57.62	998	543	4	55.25	995	542	3
Petrogale penicillata_FMNH 64435				0	46.38	1000	537	4	50.38	997	547	4
Podogymnura truei_FMNH 146591				0	49	999	533	4	47.25	999	542	4
Poiana richardsonii_YPM VZ MAM 014715	29.12	1000	534	4	34.5	996	524	4				0

Pongo pygmaeus_NHMUK 1986.1097				0	49.25	1000	554	4	47.62	999	549	4
Potamogale velox_UMZC E5425F				0	44.25	999	540	4	45.38	999	528	4
Potorous tridactylus_FMNH 57805				0	30.5	999	544	4	43.12	1000	546	4
Presbytis femoralis_UMZC E.7226.C				0	46	1000	562	4	45.12	999	562	4
Prionailurus viverrinus_NHMUK 1860.7.22.22				0	20.75	1000	529	4				0
Procavia capensis_FMNH 147999				0	35.62	999	547	4	43.62	999	538	4
Procyon lotor_FMNH 175311	21.25	999	538	4	44.62	1000	543	4	44	999	534	4
Pronolagus rupestris_FMNH 177246				0	45	1000	542	4	42.88	999	552	4
Propithecus diadema_USNM 63350				0	44.25	1000	555	4	39.5	999	552	4
Proteles cristata_NMS unnumbered				0	15.38	999	526	4				0
Pseudocheirus peregrinus_UMZC A9.2.6.3				0	31.38	999	534	4	35	999	535	4
Pudu puda_NMS 2011.141.1				0	28.12	1000	540	4	35.25	1000	541	4
Puma concolor_UMZC K5745				0	35.12	1000	557	4	25.12	997	545	4
Rangifer tarandus_OUMNH 19504				0	34	1000	549	4	42.12	1000	547	4
Rhynchocyon petersi_NHMUK 1886.9.21.1				0	48	999	545	4	34.88	999	538	4
Rhyncholestes raphanurus_FMNH 27476				0	44.12	1000	544	4	49	999	538	4
Saiga tatarica_NMS 1981.72				0	54.75	997	535	4	47	999	546	4
Salpingotulus michaelis_UMMZ 120132				0	37.62	999	538	4	38.88	999	545	4
Sarcophilus harrisii_NHMUK 2003.331				0	14.62	999	541	4	26	1000	538	4
Scapanus latimanus_UMMZ 74584				0	63.12	998	523	4	59	999	531	4
Scutisorex somereni_FMNH 160182				0	48.88	999	540	4	52.88	990	530	4

Setifer setosus_UMZC 2011.3.1				0	49.88	1000	561	4	48.88	999	535	4
Sminthopsis crassicaudata_FMNH 72923				0	56.12	999	535	4	57.88	999	535	4
Solenodon paradoxus_FMNH 51068				0	38	999	562	4	34	1000	546	4
Spalacopus cyanus_FMNH 49943				0	43.75	999	549	4	50.5	997	559	4
Spalax microphthalmus_FMNH 79299				0	30.75	999	535	4	41	999	558	4
Speothos venaticus_NMS 2015.96.3	40.12	999	531	4	61.62	997	521	4	35.12	1000	529	4
Spermophilopsis leptodactylus_UMMZ 119250				0	38.62	1000	548	3	45.88	1000	574	3
Surdisorex norae_FMNH 190260				0	45.25	999	543	4	46.5	999	539	4
Suricata suricatta_FMNH 101744				0	46.38	997	539	4	25.12	999	513	4
Sus scrofa_GWU cashp PT001				0	55.25	999	546	4	58.25	999	542	4
Sylvilagus floridanus_AMNH M 254438				0	34	998	549	4	50.88	999	553	4
Sylvisorex howelli_FMNH 198205 198206				0	53.75	997	542	4	56.25	995	537	4
Tachyoryctes splendens_FMNH 173826 173827				0	35.12	1000	533	4	42.5	1000	552	4
Tamias striatus_UMZC E.1696				0	35.25	998	543	3	37.38	999	547	3
Tapirus indicus_UF 31027				0	70.88	999	543	4	54.62	999	537	4
Tapirus terrestris_NMS 2001.77.3				0				0	28.75	999	529	4
Tarsius syrichta_FMNH 142007				0	45.75	989	998	4	47.38	999	999	4
Tayassu sp_IMNH R 228				0	58.62	999	545	4	69.38	1000	541	4
Tenrec ecaudatus_UMMZ 138441				0	24.62	999	534	4	29.5	1000	541	4
Thylacinus cynocephalus_NHMUK 1963.8.3.0.1				0	17.5	1000	534	4	23.38	1000	538	4
Thylamys elegans_UMMZ 156033				0	39.62	999	534	3	40.88	1000	536	3
Thylogale stigmatica_UMZC A12.44-1				0	43.5	995	572	4	55	999	550	4
Trachypithecus obscurus_NHMUK				0	30.38	999	538	4	39.75	999	536	4

71.709												
Tragelaphus spekii_NMS 2011.162.1				0	50.75	999	550	4	77.12	991	554	4
Trichosurus vulpecula_UMZC A9.16-7				0	28.12	1000	544	4	37.75	999	540	4
Tupaia glis_UMZC E.4057.E				0	56.38	999	545	4	48.38	1000	541	4
Urocyon cinereoargenteus_NHMUK 1850.11.22.62	11	1000	535	4	35.88	1000	535	4	36.12	1000	531	4
Urogale everetti_FMNH 166482				0	48.62	998	525	4	49.5	999	532	4
Ursus arctos_NHMUK 1963.11.7.1				0	31.5	1000	540	4	34.12	999	536	4
Vicugna vicugna_FMNH 36047				0	61.25	999	540	4	19.5	999	556	4
Viverra zibetha_FMNH 104395				0	47.88	1000	534	4	39.88	999	531	4
Viverricula indica_UMZC K.4323	37.62	999	539	4	58	997	534	4	37.38	1000	528	4
Vombatus ursinus_UMZC A10.10.2				0	47.5	999	541	4	48.12	997	540	4
Vulpes lagopus_UMZC K3669	48.88	1000	540	4	32	1000	535	4	12.88	926	490	4
Zapus hudsonius_UMMZ 157417				0	32.62	1000	539	3	34.88	999	551	3
Zenkerella insignis_NHMUK 5.5.23.27				0	41	1000	532	4	38.75	997	535	4

Table E3: OPCR scores used for the lower molars (m2-m4) of mammal species. States: 0=absent; 1= unerupted; 2= bad quality; 3= good quality; 4= great quality.

Taxon	m3 OPCR	m3 Faces	m3 Vertices	m3 State	m4 OPCR	m4 Faces	m4 Vertices	m4 State
Abrocoma cinerea_UMMZ 120621	55	998	541	4				0
Acinonyx jubatus_AMNH 119657				0				0
Acomys cahirinus_NHMUK 65.789-793	31	999	538	4				0
Acrobates pygmaeus_NHMUK 82.7.29.23	27.12	999	533	4				0
Aepyceros melampus_FMNH 127890	45	999	539	4				0
Aepyprymnus rufescens_FMNH 124573	60.62	997	541	3				1
Ailuropoda melanoleuca_IMNH C 302				0				0
Ailurus fulgens_NHMUK 1911.10.18.1				0				0
Alces alces_NMS 1996.39	48.88	999	535	4				0
Alouatta seniculus_FMNH 18869	40.38	999	532	4				0
Amblysomus hottentotus_UMZC 2010.15A				0				0
Anomalurus beecrofti_NHMUK 1989.174	75.88	987	525	3				0
Anourosorex squamipes_NHMUK 1933.4.1.165	19.62	1000	539	4				0
Antechinomys laniger_NHMUK 32.2.11.23	39.62	1000	533	4	49.38	999	529	4
Antechinus stuartii_FMNH 129556	62.12	1000	553	4	43.12	999	532	4
Antilocapra americana_FMNH 57215	65.62	999	535	4				0
Antilope cervicapra_NMS 2000.301.2	52	999	544	4				0
Aonyx cinerea_FMNH 62868				0				0
Aplodontia rufa_FMNH 60775	44.75	1000	540	3				0
Apodemus sylvaticus_NHMUK unnumbered	39.88	999	535	4				0
Ateles geoffroyi_MCZ 10138	36.75	999	540	4				0
Atelocynus microtis_FMNH 60674				0				0
Atherurus africanus_UMCZ E.3489	32.12	999	539	4				0
Atilax paludinosus_NHMUK 1867.7.8.11				0				0
Babyrousa babyrussa_NMS 2008.27	32.25	1000	534	4				0
Bandicota indica_NHMUK 1978.896	43.25	993	551	3				0
Bassaricyon alleni_FMNH 104935				0				0

Bettongia penicillata_FMNH 129431	37.5	999	545	4	29.88	1000	535	4
Bison bonasus_NHMUK 194.9.6.29.1	29.88	1000	536	4				0
Boselaphus tragocamelus_NHMUK_1974.411				0				0
Bradypus variegatus_FMNH 69589	30.38	999	531	4	33.25	999	531	4
Callimico goeldii_FMNH 58003	35.75	1000	531	4				0
Callithrix jacchus_FMNH 231573				0				0
Callosciurus notatus_NHMUK 75.1337	51	995	538	4				0
Caluromys derbianus_UMMZ 114856	38.12	1000	554	4	35.12	999	539	4
Caluromysiops irrupta_FMNH 60698	52.25	999	535	4	42	1000	533	4
Camelus dromedarius_OUMNH 14882	33.5	999	541	3				0
Canis latrans_UMZC K.3341				0				0
Canis mesomelas_UMZC K3402				0				0
Canis simensis_AMNH 81001	12.75	999	524	4				0
Capra sibirica_FMNH 134541	64.25	999	539	4				0
Caracal caracal_AMNH 113794				0				0
Castor canadensis_WLM unnumbered	48	999	533	4				0
Cavia fulgida_UMZC E3705	72.12	1000	549	4				0
Cephalophus nigrifrons_NHMUK_1936.10.28.33	47.12	1000	538	4				0
Cercartetus concinnus_NHMUK 97.11.18.1	32	997	539	4				0
Cervus elaphus_NMS 1981.68	48.88			3				0
Chironectes minimus_UMMZ 126289	41	999	539	4	37	999	539	4
Chlorocebus sabaeus_USNM 381445	30.38	999	541	4				0
Choloepus hoffmanni_NHMUK 1973.824	19.88	995	518	4	19	999	528	4
Chrysochloris asiatica_UMCZ E.5472.F	16.12	997	524	4				0
Chrysochloris stuhlmanni_NHMUK 1934.4.1.7.11	18.62	1000	517	4				0
Coendou prehensilis_NHMUK 512.F	32	997	538	3				0
Colobus satanas_NHMUK 1856.12.29.1	46.62	999	524	4				0
Condylura cristata_UMMZ 80270	61.62	1000	531	4				0
Connochaetes taurinus_NHMUK 1935.12.14.3	28.38	1000	534	3				0
Cricetomys gambianus_NHMUK 1890.3.27.2	33.25	999	541	4				0
Cricetulus migratorius_UMZC E2322	58.62	999	535	4				0
Crocidura fuscomurina_UMZC E 5251.G	34.38	1000	526	4				

Crocuta crocuta_FMNH 127826				0				0
Cryptoprocta ferox_NHMUK 1968.6.7.1				0				0
Cryptotis mexicana_UMMZ 113138	40.62	999	543	4				0
Cynocephalus volans_OUMNH 3404	42.38	1000	528	4				0
Dactylopsila trivirgata_NHMUK 1897.8.7.79	46	1000	544	4	39.5	1000	535	4
Dama dama_OUMNH 19343	58	1000	540	4				0
Dasycercus cristicauda_NHMUK 1897.11.3.4	54.88	1000	544	4	54.75	997	535	4
Dasyprocta punctata_FMNH 21260	63.38	1000	540	4				0
Dasyurus hallucatus_FMNH 119804	48.88	999	532	4	37.5	999	526	4
Dasyurus maculatus_UMZC A6.10-3	49.12	999	546	4	42	999	539	4
Dasyurus viverrinus_SAMA M7222	47.62	999	532	4	36.12	1000	528	4
Daubentonia madagascariensis_UMZC E.8021.A	32.5	999	532	4				0
Desmana moschata_UMMZ 124125	34.25	1000	527	4				0
Dicerorhinus sumatrensis_NMS 1994.131	32.88	999	530	4				0
Didelphis marsupialis_NHMUK 1948.7.12.5	35.62	999	537	4	31.88	1000	532	4
Diplomesodon pulchellum_FMNH 137436	33.62	999	532	4				0
Dolichotis patagonum_FMNH 49231	41.38	999	532	4				0
Dorcopsis muelleri_NHMUK 1933.11.4.4	31.38	1000	532	4	26.25	1000	528	4
Dromiciops gliroides_UMMZ 156354	44.25	1000	540	4	27.88	1000	531	4
Dugong dugon_MVZ 101162	42.25	1000	542	4				0
Echinops telfairi_NHMUK 1970.355				0				0
Echinosorex gymnura_UMZC E.5111.C-E	36.5	999	532	4				0
Echymipera rufescens_FMNH 60525	47.12	999	542	4	40	999	529	4
Elephantulus brachyrhynchus_NHMUK 1963.1004	15.75	1000	532	4				0
Elephantulus rozeti_NHMUK 1891.10.15.11	45.62	996	532	4				0
Enhydra lutris_NHMUK 80.879				0				0
Episoriculus caudatus_FMNH 114227	35.88	999	535	4				0
Eulemur macaco_UMZC E8093A	27.88	886	486	4				0
Euroscaptor micrura_NHMUK 99.10.25.1	46.25	1000	524	4				0
Felis catus_UMZC K.6182				0				0
Fossa fossana_FMNH 85196				0				0
Funambulus pennantii_UMMZ 62569	50.25	999	533	3				0

Galago senegalensis_FMNH 123783	40.12	1000	527	4				0
Galemys pyrenaicus_OUMNH 9427	58.75	1000	536	4				0
Gazella dorcas_NMS 2004.46.5	52.12	1000	540	4				0
Genetta angolensis_FMNH 163777				0				0
Geocapromys brownii_AMNH 45156	62.62	1000	541	3				0
Geogale aurita_UMMZ 172217	35.5	999	537	4				0
Geomys pinetis_UMMZ 164642	19.25	999	550	4				0
Gerbillus gerbillus_NHMUK 1978.1062	14.5	999	539	4				0
Giraffa camelopardalis_FMNH 34424	33.5	999	539	4				0
Glis glis_NHMUK 1996.325	65.38	988	536	4				0
Gracilinanus agilis_UMMZ 134557	52.62	999	547	4	44.75	1000	533	4
Gulo gulo_USNM 157327				0				0
Hemibelideus lemuroides_FMNH 60926	66.75	997	542	4	56.62	999	544	4
Hemiechinus auritus_UMMZ 156626	24.25	999	534	4				0
Heterocephalus glaber_NHMUK 91.235	28.88	696	382	3				0
Heteromys desmarestianus_NHMUK unregistered xyz002	28.75	1000	541	3				0
Hippopotamus amphibius_NMS Z.2008.35	52.12	1000	540	4				0
Hydrochoerus hydrochaeris_AMNH M-206440				0				0
Hydromys chrysogaster_NHMUK 1998.134	82.5	938	422	3				0
Hydropotes inermis_NMS unnumbered	39.12	1000	536	3				0
Hypogeomys antimena_FMNH 151994	35.88	999	543	4				0
Ictonyx striatus_UMZC K1874				0				0
Idiurus zenkeri_UMZC E1421	23.5	1000	531	4				0
Isoodon macrourus_FMNH 120560	38.62	1000	550	4	38.25	1000	536	4
Isoodon obesulus_UMZC A7.4-5	36	1000	534	4	36.25	1000	536	4
Kobus megaceros_NMS 2001.149.15	55.5	999	540	4				0
Lasiorhinus latifrons_NMS 1868.31	32.75	1000	543	3	17.25	767	415	3
Lemur catta_FMNH 157993	28.62	992	538	4				0
Leopardus wiedii_NMS Z.2016.12.1				0				0
Lestoros inca_UMMZ 160733	53.88	998	554	4	35.88	1000	536	4
Liomys irroratus_UMMZ 120788	28.88	1000	553	4				0

Lophocebus albigena_NHMUK 1936.10.28.1	41.88	1000	534	4				0
Loris tardigradus_UMZC E.8261.E	40.38	994	536	4				0
Lutreolina crassicaudata_UMMZ 163450	41.88	999	547	4	41.62	999	532	4
Lynx canadensis_UMZC K.6682				0				0
Macaca sylvanus_NHMUK 1858.4.5.1	50	1000	531	4				0
Macropus eugenii_NHMUK 1948.7.12.3	32.12	1000	536	4				1
Macropus giganteus_NHMUK 72.4498	27.5	999	540	4	16.88	999	533	4
Macropus rufus_NMS PH26.12	28.25	881	493	3	24.25	970	527	3
Macroscelides proboscideus_FMNH 137045	35.88	999	544	4				0
Macrotis lagotis_NHMUK 73.6.21.4	42.62	993	541	4	28.38	997	540	4
Madoqua kirkii_NMS POZ8.99	46.12	999	537	4				0
Malacomys longipes_UMZC E2265	36.75	1000	534	4				0
Malacothrix typica_UMMZ 117815	23.88	999	543	4				0
Marmosa demerarae_UMMZ 134562	29.62	1000	547	4	26.12	1000	535	4
Marmosa murina_NHMUK 1881.11.1	48.88	1000	544	4	47.12	999	534	4
Marmota monax_AMNH M-67882	38.38	1000	535	4				0
Meles meles_NHMUK 2002.476				0				0
Mephitis mephitis_FMNH 129327				0				0
Microcebus murinus_AMNH M-174537	38	999	532	4				0
Microgale brevicaudata_UMMZ 174757	39	1000	536	4				0
Microgale drouhardi_UMMZ 168477	51.25	1000	537	4				0
Microgale thomasi_UMMZ 172202	41.88	999	542	4				0
Micropotamogale ruwenzorii_NHMUK 67.213	38.75	1000	533	4				0
Monodelphis domestica_UMMZ 165514	44.5	999	546	4	46.38	999	533	4
Moschus moschiferus_NHMUK 676.d.45.1.12.448	55.62	999	537	4				0
Mus musculus_UMZC E.2202	20.88	1000	542	4				0
Mustela nivalis_FMNH 207033				0				0
Mustela putorius_UMZC K.2361				0				0
Myosorex kihaulei_FMNH 209072	39.12	999	531	4				0
Myospalax myospalax_UMMZ 110401	44.62	1000	560	3				0
Nandinia binotata_UMZC K.4492				0				0
Napaeozapus insignis_UMMZ 126314	26.5	1000	538	4				0

Nasua narica_UMZC unumbered				0				0
Nectogale elegans_AMNH M-115571	32.38	1000	532	4				0
Neomys fodiens_NHMUK 1973.917	41.75	998	531	4				0
Neotetracus sinensis_NHMUK ZD1933.4.1.134	33.75	999	529	4				0
Notomys cervinus_NHMUK ZD 1936.12.8.17-18	28.12	1000	543	4				0
Notoryctes typhlops_UMZC A5.11	25.12	1000	521	4	29.62	1000	521	4
Nycticebus coucang_Du Baa 0002	39	1000	536	4				0
Ochotona alpina_UMMZ 123059	20	1000	538	4				0
Okapia johnstoni_NHMUK 1971.1738	50.62	999	537	4				0
Onychogalea fraenata_UMZC A12.59.3	39.38	999	529	4				1
Onychomys torridus_UWBM 37628	26.75	997	535	4				0
Oryx gazella_NHMUK ZD 1963.10.21.1	32.12	1000	534	4				0
Oryzorictes tetradactylus_UMZC E.5453.C	38.88	1000	519	4				0
Otocyon megalotis_USNM 49129	33.12	999	527	4	32.88	1000	527	4
Ovis aries_OUMNH ZC14858	57.38	1000	544	4				0
Pan troglodytes_RMCA 77032M25	69.62	1000	534	4				0
Panthera pardus_IMNH 2372				0				0
Papio hamadryas_UMZC E.7543.B	45.12	1000	536	4				0
Paracrocidura schoutedeni_FMNH 227382	44.5	999	530	4				0
Paradoxurus hermaphroditus_FMNH 62837				0				0
Pecari tajacu_NMS 2002.164.2	33.38	990	534	3				0
Pedetes capensis_FMNH 152053	36.12	999	529	3				0
Perodicticus potto_USNM 465898	51.88			3				0
Petauroides volans_NHMUK 1926.3.11.225	46.12	1000	535	4	48.12	1000	540	4
Petaurus breviceps_FMNH 129430	33.75	999	539	4	31.5	1000	530	4
Petinomys sagitta_UMZC E1499	62	996	539	4				0
Petrogale penicillata_FMNH 64435	44.5	991	537	4				0
Podogymnura truei_FMNH 146591	40.25	1000	539	4				0
Poiana richardsonii_YPM VZ MAM 014715				0				0
Pongo pygmaeus_NHMUK 1986.1097	35.25	1000	538	4				0
Potamogale velox_UMZC E5425F				0				0
Potorous tridactylus_FMNH 57805	51.38	1000	538	4	48.12	1000	538	4

Presbytis femoralis_UMZC E.7226.C	40.62	1000	554	4			532	0
Prionailurus viverrinus_NHMUK 1860.7.22.22				0				0
Procavia capensis_FMNH 147999	22	999	529	4				0
Procyon lotor_FMNH 175311				0				0
Pronolagus rupestris_FMNH 177246	22.25	1000	538	4				0
Propithecus diadema_USNM 63350	43.5	999	537	4				0
Proteles cristata_NMS unnumbered				0				0
Pseudocheirus peregrinus_UMZC A9.2.6.3	36.5	1000	539	4	33.88	1000	530	4
Pudu puda_NMS 2011.141.1	36.38	999	529	4				0
Puma concolor_UMZC K5745				0				0
Rangifer tarandus_OUMNH 19504	30.88	999	534	4				0
Rhynchocyon petersi_NHMUK 1886.9.21.1				0				0
Rhyncholestes raphanurus_FMNH 27476	48.62	999	542	4	23.5	999	536	4
Saiga tatarica_NMS 1981.72	33.5	1000	543	4				0
Salpingotulus michaelis_UMMZ 120132	12	923	497	4				0
Sarcophilus harrisii_NHMUK 2003.331	28.12	1000	535	4	20.62	1000	534	4
Scapanus latimanus_UMMZ 74584	48.88	999	521	4				0
Scutisorex somereni_FMNH 160182	44.88	980	528	4				0
Setifer setosus_UMZC 2011.3.1	38.75	999	534	4				0
Sminthopsis crassicaudata_FMNH 72923	61.75	999	537	4	46.5	1000	533	4
Solenodon paradoxus_FMNH 51068	39.5	1000	529	4				0
Spalacopus cyanus_FMNH 49943	41	993	542	4				0
Spalax microphthalmus_FMNH 79299	30.88	996	537	4				0
Speothos venaticus_NMS 2015.96.3				0				0
Spermophilopsis leptodactylus_UMMZ 119250	48.62	1000	543	3				0
Surdisorex norae_FMNH 190260	39.25	1000	530	4				0
Suricata suricatta_FMNH 101744				0				0
Sus scrofa_GWU cashp PT001	74.38	999	540	4				0
Sylvilagus floridanus_AMNH M 254438	27.88	1000	539	4				0
Sylvisorex howelli_FMNH 198205 198206	29	999	530	4				0
Tachyoryctes splendens_FMNH 173826 173827	36.5	1000	535	4				0
Tamias striatus_UMZC E.1696	39.12	999	534	3				0

Tapirus indicus_UF 31027	57.38	1000	533	4				0
Tapirus terrestris_NMS 2001.77.3	30.75	999	523	4				0
Tarsius syrichta_FMNH 142007	48	999	529	4				0
Tayassu sp_IMNH R 228	72.5	1000	536	4				0
Tenrec ecaudatus_UMMZ 138441	28.62	1000	530	4				0
Thylacinus cynocephalus_NHMUK 1963.8.3.0.1	25.38	999	534	4	29.75	999	526	4
Thylamys elegans_UMMZ 156033	46	1000	535	3	42.62	999	528	4
Thylogale stigmatica_UMZC A12.44-1	49.25	999	538	4				0
Trachypithecus obscurus_NHMUK 71.709	47.62	1000	526	4				0
Tragelaphus spekii_NMS 2011.162.1	65.75	998	543	4				0
Trichosurus vulpecula_UMZC A9.16-7	39.5	1000	543	4	44.88	1000	539	4
Tupaia glis_UMZC E.4057.E	59.62	998	548	4				0
Urocyon cinereoargenteus_NHMUK 1850.11.22.62				0				0
Urogale everetti_FMNH 166482	49.12	999	526	4				0
Ursus arctos_NHMUK 1963.11.7.1	27.12	1000	534	4				0
Vicugna vicugna_FMNH 36047	34.38	999	547	4				0
Viverra zibetha_FMNH 104395				0				0
Viverricula indica_UMZC K.4323				0				0
Vombatus ursinus_UMZC A10.10.2	52	999	549	4	61.5	999	542	4
Vulpes lagopus_UMZC K3669				0				0
Zapus hudsonius_UMMZ 157417	21.12	998	536	3				0
Zenkerella insignis_NHMUK 5.5.23.27	36.38	997	536	4				0

Table E4: Postcanine teeth counts reported amongst non-mammalian cynodont species. Note variable number of postcanine teeth and teeth used to calculate OPCR scores.

Taxon	**Number of pc's reported**	Reference	**Teeth used**
Andescynodon sp_PVL 4907	7-10 pcs; last pc=7	Liu and Powell (2009)	pc5-7
Andescynodon mendozensis_PVL 4069	7-10 pcs; last pc=7	Liu and Powell (2009)	pc5-7
Cricodon metabolus_UMZC T905	9-10pcs; last pc=9	Sidor and Hopson (2017)	pc8-9
Cricodon sp_NHM PV R36800	9-10pcs; last pc=9	Sidor and Hopson (2017)	pc8-9
Cynognathus crateronotus_BP 5208	pc8	Hendrickx et al. (2019)	pc6-8
Diademodon tetragonus_BP 3756	13 pcs	Martinelli et al. (2009)	pc11-13
Exaeretodon argentinus_PVL 2467	6 pcs	Liparini et al. (2013)	pc4-pc6
Exaeretodon riograndensis_UFRGS PV 0715T	6 pcs	Liparini et al. (2013)	pc4-pc6
Langbergia modisei_NMQR 3251	7-8 pcs; last pc=7	Abdala et al. (2006)	pc5-7
Luangwa sudamericana_MCP PV 3167	8-9 pcs; last pc=8	Abdala and Sa-Teixeira (2004)	pc6-8
Massteognathus pascuali_BP 4245	12-14 pcs; last pc=12	Jun et al. (2008)	pc9-11
Megazostrodon rudnerae_BP 4983*	m1-5; last pc=5	Gow (1978)	m3-m5
Menadon besairiei_UFRGS PV 0891	6 pcs	Melo et al. (2015)	pc4-6
Pascualgnathus polanskii_PVL 4416	11-13 pcs; last pc=11	Martinelli et al. (2009)	pc9-11
Santacruzodon hopsoni_MCN 2752	9-10 pcs; last pc=9	Abdala and Ribeiro (2003)	pc7-9
Traversodontid sp_MCP PV 4053	indet, labeled as pc 1 -3		pc1-3
Trirachodon berryi_BP 4658	8-9 pcs; last pc=8	Hendrickx et al. (2019)	pc6-8
Trirachodon sp_BP 4534	8-9 pcs; last pc=8	Hendrickx et al. (2019)	pc6-8
Trirachondontid sp_JSM 100	8-9 pcs; last pc=8	Hendrickx et al. (2019)	pc6-8

Table E5: OPCR scores used for the lower molars (m3-5) in non-mammalian cynodont species. States: 0=absent; 1= unerupted; 2= bad quality; 3= good quality; 4= great quality.

Taxon	m3 OPCR	m3 Faces	m3 Vertices	m3 State	m4 OPCR	m4 Faces	m4 Vertices	m4 State	m5 OPCR	m5 Faces	m5 Vertices	m5 State
Andescynodon sp_PVL 4907				0		0		0				0
Andescynodon mendozensis_PVL 4069				0		0		0				0
Cricodon metabolus_UMZC T905				0		0		0				0
Cricodon sp_NHM PV R36800				0		0		0				0
Cynognathus crateronotus_BP 5208				0		0		0				0
Diademodon tetragonus_BP 3756				0		0		0				0
Exaeretodon argentinus_PVL 2467				0		0		0				0
Exaeretodon riograndensis_UFRGS PV 0715T				0		0		0				0
Langbergia modisei_NMQR 3251				0		0		0				0
Luangwa sudamericana_MCP PV 3167				0		0		0				0
Massteognathus pascuali_BP 4245				0		0		0				0
Megazostrodon rudnerae_BP 4983	68.38	991	528	4	37.38	1000	529	4	79.88	997	513	3
Menadon besairiei_UFRGS PV 0891				0		0		0				0
Pascualgnathus				0		0		0				0

polanskii_PVL 4416												
Santacruzodon hopsoni_MCN 2752				0		0		0				0
Traversodontid sp_MCP PV 4053				0		0		0				0
Trirachodon berryi_BP 4658				0		0		0				0
Trirachodon sp_BP 4534				0		0		0				0
Trirachondontid sp_JSM 100				0		0		0				0

Table E6: OPCR scores used for the lower postcanines (pc1-3) of non-mammalian cynodont species. States: 0=absent; 1= unerupted; 2= bad quality; 3= good quality; 4= great quality.

Taxon	pc1 OPCR	pc1 Faces	pc1 Vertices	pc1 State	pc2 OPCR	pc2 Faces	pc2 Vertices	pc2 State	pc3 OPCR	pc3 Faces	pc3 Vertices	pc3 State
Andescynodon sp_PVL 4907				0				0				0
Andescynodon mendozensis_PVL 4069				0				0				0
Cricodon metabolus_UMZC T905				0				0				0
Cricodon sp_NHM PV R36800				0				0				0
Cynognathus crateronotus_BP 5208				0				0				0
Diademodon tetragonus_BP 3756				0				0				0
Exaeretodon argentinus_PVL 2467				0				0				0
Exaeretodon riograndensis_UFRGS PV 0715T				0				0				0
Langbergia modisei_NMQR 3251				0				0				0
Luangwa sudamericana_MCP PV 3167				0				0				0
Massteognathus pascuali_BP 4245				0				0				0
Megazostrodon rudnerae_BP 4983				0				0				0
Menadon besairiei_UFRGS PV 0891				0				0				0
Pascualgnathus				0				0				0

polanskii_PVL 4416												
Santacruzodon hopsoni_MCN 2752				0				0				0
Traversodontid sp_MCP PV 4053	24.5	964	523	4	16.25	705	396	3	16.5	552	314	2
Trirachodon berryi_BP 4658				0				0				0
Trirachodon sp_BP 4534				0				0				0
Trirachondontid sp_JSM 100				0				0				0

Table E7: OPCR scores used for the lower postcanines (pc4-pc6) in non-mammalian cynodont species. States: 0=absent; 1= unerupted; 2= bad quality; 3= good quality; 4= great quality.

Taxon	pc4 OPCR	pc4 Faces	pc4 Vertices	pc4 State	pc5 OPCR	pc5 Faces	pc5 Vertices	pc5 State	pc6 OPCR	pc6 Faces	pc6 Vertices	pc6 State
Andescynodon sp_PVL 4907				0	34.88	999	528	4	35.5	1000	540	4
Andescynodon mendozensis_PVL 4069				0	25.75	999	541	4	25.75	999	537	4
Cricodon metabolus_UMZC T905				0				0				0
Cricodon sp_NHM PV R36800				0				0				
Cynognathus crateronotus_BP 5208				0				0	20.62	999	531	4
Diademodon tetragonus_BP 3756				0				0				0
Exaeretodon argentinus_PVL 2467	22.88	999	534	4	24.5	999	533	4	25.25	1000	531	4
Exaeretodon riograndensis_UFRGS PV 0715T	29.12	999	537	4	31.88	999	531	4	39.62	1000	543	4
Langbergia modisei_NMQR 3251				0	39.75	1000	542	4	37.12	1000	539	4
Luangwa sudamericana_MCP PV 3167				0				0	38.12	999	550	4
Massteognathus pascuali_BP 4245				0				0				0
Megazostrodon rudnerae_BP 4983				0				0				0
Menadon besairiei_UFRGS PV 0891	27.5	1000	539	4	23.62	999	535	4	14.12	644	349	3
Pascualgnathus				0				0				0

polanskii_PVL 4416												
Santacruzodon hopsoni_MCN 2752				0				0				0
Traversodontid sp_MCP PV 4053				0				0				0
Trirachodon berryi_BP 4658				0				0	21	999	544	4
Trirachodon sp_BP 4534				0				0	16.5	791	424	4
Trirachondontid sp_JSM 100				0				0				0

Table E8: OPCR scores used for the lower postcanines (pc7-9) in non-mammalian cynodont species. States: 0=absent; 1= unerupted; 2= bad quality; 3= good quality; 4= great quality.

Taxon	pc7 OPCR	pc7 Faces	pc7 Vertices	pc7 State	pc8 OPCR	pc8 Faces	pc8 Vertices	pc8 State	pc9 OPCR	pc9 Faces	pc9 Vertices	pc9 State
Andescynodon sp_PVL 4907	13.38	1000	518	4				0				0
Andescynodon mendozensis_PVL 4069	30.12	999	530	4				0				0
Cricodon metabolus_UMZC T905				0	46.62	1000	544	4	37.75	999	533	4
Cricodon sp_NHM PV R36800	22.5	999	535	4	37.75	999	533	4	19.75	1000	543	4
Cynognathus crateronotus_BP 5208	18.88	999	540	4	21	1000	537	4				0
Diademodon tetragonus_BP 3756				0				0				0
Exaeretodon argentinus_PVL 2467				0				0				0
Exaeretodon riograndensis_UFRGS PV 0715T				0				0				0
Langbergia modisei_NMQR 3251	15.62	1000	541	4				0				0
Luangwa sudamericana_MCP PV 3167	37.62	999	545	4	42.62	999	538	4				0
Massteognathus pascuali_BP 4245				0				0	24.62	999	535	4
Megazostrodon rudnerae_BP 4983				0				0				0
Menadon besairiei_UFRGS PV 0891				0				0				0
Pascualgnathus				0				0	31	999	542	4

polanskii_PVL 4416												
Santacruzodon hopsoni_MCN 2752	40.62	1000	544	4	33.38	999	543	4	40.5	1000	534	4
Traversodontid sp_MCP PV 4053				0				0				0
Trirachodon berryi_BP 4658	11.12	999	537	4	15.5	758	416	3				0
Trirachodon sp_BP 4534	20.38	922	494	4	20.5	671	380	3				0
Trirachondontid sp_JSM 100	24.62	999	544	4	39.5	1000	552	4				0

Table E9: OPCR scores used for the lower postcanines (pc10-13) in non-mammalian cynodont species. States: 0=absent; 1= unerupted; 2= bad quality; 3= good quality; 4= great quality.

Taxon	pc10 OPCR	pc10 Faces	pc10 Vertices	pc10 State	pc11 OPCR	pc11 Face #	pc11 Vertices	pc11 State	pc12 OPCR	pc12 Faces	pc12 Vertices	pc12 State	pc13 OPCR	pc13 Faces	pc13 Vertices	pc13 State
Andescynodon sp_PVL 4907				0				0				0				0
Andescynodon mendozensis_PVL 4069				0				0				0				0
Cricodon metabolus_UMZCT905				0				0				0				0
Cricodon sp_NHM PV R36800				0				0				0				0
Cynognathus crateronotus_BP 5208				0				0				0				0
Diademodon tetragonus_BP 3756				0	23	999	544	4	26.12	999	546	4	41.38	999	533	4
Exaeretodon argentinus_PVL 2467				0				0				0				0
Exaeretodon riograndensis_UFRGS PV 0715T				0				0				0				0
Langbergia modisei_NMQR 3251				0				0				0				0
Luangwa sudamericana_M				0				0				0				0

CP PV 3167																
Massteognathus pascuali_BP 4245	23.25	1000	541	4	30.75	999	537	4				0				0
Megazostrodon rudnerae_BP 4983				0				0				0				0
Menadon besairiei_UFRGS PV 0891				0				0				0				0
Pascualgnathus polanskii_PVL 4416	26.75	999	533	4	14.75	1000	536	4				0				0
Santacruzodon hopsoni_MCN 2752				0				0				0				0
Traversodontid sp_MCP PV 4053				0				0				0				0
Trirachodon berryi_BP 4658				0				0				0				0
Trirachodon sp_BP 4534				0				0				0				0
Trirachondontid sp_JSM 100				0				0				0				0

Table E10: OPCRsum and OPCRavg scores used for mammal and non-mammalian cynodont species.

Taxon	OPCRsum	OPCRavg
Abrocoma cinerea_UMMZ 120621	161	80.5
Acinonyx jubatus_AMNH 119657	75	37.5
Acomys cahirinus_NHMUK 65.789-793	108	54
Acrobates pygmaeus_NHMUK 82.7.29.23	62	41.33333
Aepyceros melampus_FMNH 127890	165	82.5
Aepyprymnus rufescens_FMNH 124573	108	72
Ailuropoda melanoleuca_FMNH 31128	237	118.5
Ailurus fulgens_NHMUK 1911.10.18.1	133	66.5
Alces alces_NMS 1996.39	162	81
Alouatta seniculus_FMNH 18869	122	61
Amblysomus hottentotus_UMZC 2010.15A	72	36
Andescynodon sp_PVL 4907	80	40
Andescynodon mendozensis_PVL 4069	84	42
Anomalurus beecrofti_NHMUK 1989.174	242	121
Anourosorex squamipes_NHMUK 1933.4.1.165	88	44
Antechinomys laniger_NHMUK 32.2.11.23	131	65.5
Antechinus stuartii_FMNH 129556	158	79
Antilocapra americana_FMNH 57215	164	82
Antilope cervicapra_NMS 2000.301.2	132	66
Aonyx cinerea_FMNH 62868	115	57.5
Aplodontia rufa_FMNH 60775	128	64
Apodemus sylvaticus_NHMUK unnumbered	143	71.5
Ateles geoffroyi_MCZ 10138	121	60.5
Atelocynus microtis_FMNH 60674	109	54.5
Atherurus africanus_UMCZ E.3489	108	54
Atilax paludinosus_NHMUK 1867.7.8.11	100	50
Babyrousa babyrussa_NMS 2008.27	129	64.5
Bandicota indica_NHMUK 1978.896	175	87.5
Bassaricyon alleni_FMNH 104935	97	48.5
Bettongia penicillata_FMNH 129431	105	52.5
Bison bonasus_NHMUK 194.9.6.29.1	108	54
Boselaphus tragocamelus_NHMUK_1974.411	45	30
Bradypus variegatus_FMNH 69589	94	47
Callimico goeldii_FMNH 58003	126	63
Callithrix jacchus_FMNH 231573	102	51
Callosciurus notatus_NHMUK 75.1337	180	90
Caluromys derbianus_UMMZ 114856	114	57
Caluromysiops irrupta_FMNH 60698	146	73
Camelus dromedarius_OUMNH 14882	99	49.5
Canis latrans_UMZC K.3341	82	41
Canis mesomelas_UMZC K3402	88	44
Canis simensis_AMNH 81001	93	46.5
Capra sibirica_FMNH 134541	167	83.5
Caracal caracal_AMNH 113794	69	34.5
Castor canadensis_WLM unnumbered	180	90

Cavia fulgida_UMZC E3705	218	109
Cephalophus nigrifrons_NHMUK_1936.10.28.33	137	68.5
Cercartetus concinnus_NHMUK 97.11.18.1	66	44
Cervus elaphus_NMS 1981.68	156	78
Chironectes minimus_UMMZ 126289	120	60
Chlorocebus sabaeus_USNM 381445	105	52.5
Choloepus hoffmanni_NHMUK 1973.824	57	28.5
Chrysochloris asiatica_UMCZ E.5472.F	50	25
Chrysochloris stuhlmanni_NHMUK 1934.4.1.7.11	77	38.5
Coendou prehensilis_NHMUK 512.F	104	52
Colobus satanas_NHMUK 1856.12.29.1	133	66.5
Condylura cristata_UMMZ 80270	176	88
Connochaetes taurinus_NHMUK 1935.12.14.3	62	31
Cricetomys gambianus_NHMUK 1890.3.27.2	124	62
Cricetulus migratorius_UMZC E2322	165	82.5
Cricodon metabolus_UMZC T905	85	56.66667
Cricodon sp_NHM PV R36800	78	39
Crocidura fuscomurina_UMZC E 5251.G	128	64
Crocuta crocuta_FMNH 127826	84	42
Cryptoprocta ferox_NHMUK 1968.6.7.1	50	25
Cryptotis mexicana_UMMZ 113138	139	69.5
Cynocephalus volans_OUMNH 3404	131	65.5
Cynognathus crateronotus_BP 5208	59	23.6
Dactylopsila trivirgata_NHMUK 1897.8.7.79	136	68
Dama dama_OUMNH 19343	155	77.5
Dasycercus cristicauda_NHMUK 1897.11.3.4	170	85
Dasyprocta punctata_FMNH 21260	166	83
Dasyurus hallucatus_FMNH 119804	130	65
Dasyurus maculatus_UMZC A6.10-3	146	73
Dasyurus viverrinus_SAMA M7222	115	57.5
Daubentonia madagascariensis_UMZC E.8021.A	92	46
Desmana moschata_UMMZ 124125	113	56.5
Diademodon tetragonus_BP 3756	117	46.8
Dicerorhinus sumatrensis_NMS 1994.131	112	56
Didelphis marsupialis_NHMUK 1948.7.12.5	102	51
Diplomesodon pulchellum_FMNH 137436	141	70.5
Dolichotis patagonum_FMNH 49231	121	60.5
Dorcopsis muelleri_NHMUK 1933.11.4.4	95	47.5
Dromiciops gliroides_UMMZ 156354	116	58
Dugong dugon_MVZ 101162	103	51.5
Echinops telfairi_NHMUK 1970.355	135	67.5
Echinosorex gymnura_UMZC E.5111.C-E	138	69
Echymipera rufescens_FMNH 60525	142	71
Elephantulus brachyrhynchus_NHMUK 1963.1004	92	46
Elephantulus rozeti_NHMUK 1891.10.15.11	168	84
Enhydra lutris_NHMUK 80.879	123	61.5

Episoriculus caudatus_FMNH 114227	123	61.5
Eulemur macaco_UMZC E8093A	94	47
Euroscaptor micrura_NHMUK 99.10.25.1	136	68
Exaeretodon argentinus_PVL 2467	73	36.5
Exaeretodon riograndensis_UFRGS PV 0715T	96	48
Felis catus_UMZC K.6182	88	44
Fossa fossana_FMNH 85196	58	29
Funambulus pennantii_UMMZ 62569	143	71.5
Galago senegalensis_FMNH 123783	126	63
Galemys pyrenaicus_OUMNH 9427	171	85.5
Gazella dorcas_NMS 2004.46.5	130	65
Genetta angolensis_FMNH 163777	105	52.5
Geocapromys brownii_AMNH 45156	193	96.5
Geogale aurita_UMMZ 172217	96	48
Geomys pinetis_UMMZ 164642	69	34.5
Gerbillus gerbillus_NHMUK 1978.1062	95	47.5
Giraffa camelopardalis_FMNH 34424	137	68.5
Glis glis_NHMUK 1996.325	194	97
Gracilinanus agilis_UMMZ 134557	143	71.5
Gulo gulo_USNM 157327	88	44
Hemibelideus lemuroides_FMNH 60926	183	91.5
Hemiechinus auritus_UMMZ 156626	100	50
Heterocephalus glaber_NHMUK 91.235	90	45
Heteromys desmarestianus_NHMUK unregistered xyz002	94	47
Hippopotamus amphibius_NMS Z.2008.35	148	74
Hydrochoerus hydrochaeris_AMNH M-206440	175	116.6667
Hydromys chrysogaster_NHMUK 1998.134	240	120
Hydropotes inermis_NMS unnumbered	134	67
Hypogeomys antimena_FMNH 151994	140	70
Ictonyx striatus_UMZC K1874	110	55
Idiurus zenkeri_UMZC E1421	96	48
Isoodon macrourus_FMNH 120560	121	60.5
Isoodon obesulus_UMZC A7.4-5	97	48.5
Kobus megaceros_NMS 2001.149.15	152	76
Langbergia modisei_NMQR 3251	91	30.33333
Lasiorhinus latifrons_NMS 1868.31	91	45.5
Lemur catta_FMNH 157993	77	38.5
Leopardus wiedii_NMS Z.2016.12.1	41	27.33333
Lestoros inca_UMMZ 160733	143	71.5
Liomys irroratus_UMMZ 120788	102	51
Lophocebus albigena_NHMUK 1936.10.28.1	118	59
Loris tardigradus_UMZC E.8261.E	116	58
Luangwa sudamericana_MCP PV 3167	124	62
Lutreolina crassicaudata_UMMZ 163450	141	70.5
Lynx canadensis_UMZC K.6682	91	45.5
Macaca sylvanus_NHMUK 1858.4.5.1	118	59
Macropus eugenii_NHMUK 1948.7.12.3	54	36

Macropus giganteus_NHMUK 72.4498	69	34.5
Macropus rufus_NMS PH26.12	72	36
Macroscelides proboscideus_FMNH 137045	111	55.5
Macrotis lagotis_NHMUK 73.6.21.4	127	63.5
Madoqua kirkii_NMS POZ8.99	176	88
Malacomys longipes_UMZC E2265	150	75
Malacothrix typica_UMMZ 117815	124	62
Marmosa demerarae_UMMZ 134562	75	37.5
Marmosa murina_NHMUK 1881.11.1	144	72
Marmota monax_AMNH M-67882	104	52
Massteognathus pascuali_BP 4245	85	42.5
Megazostrodon rudnerae_BP 4983	202	67.33333
Meles meles_NHMUK 2002.476	79	39.5
Menadon besairiei_UFRGS PV 0891	63	25.2
Mephitis mephitis_FMNH 129327	139	69.5
Microcebus murinus_AMNH M-174537	113	56.5
Microgale brevicaudata_UMMZ 174757	110	55
Microgale drouhardi_UMMZ 168477	147	73.5
Microgale thomasi_UMMZ 172202	132	66
Micropotamogale ruwenzorii_NHMUK 67.213	109	54.5
Monodelphis domestica_UMMZ 165514	132	66
Moschus moschiferus_NHMUK 676.d.45.1.12.448	141	70.5
Mus musculus_UMZC E.2202	106	53
Mustela nivalis_FMNH 207033	69	34.5
Mustela putorius_UMZC K.2361	72	36
Myosorex kihaulei_FMNH 209072	135	67.5
Myospalax myospalax_UMMZ 110401	135	67.5
Nandinia binotata_UMZC K.4492	71	35.5
Napaeozapus insignis_UMMZ 126314	124	62
Nasua narica_UMZC unumbered	133	66.5
Nectogale elegans_AMNH M-115571	134	67
Neomys fodiens_NHMUK 1973.917	151	75.5
Neotetracus sinensis_NHMUK ZD1933.4.1.134	123	61.5
Notomys cervinus_NHMUK ZD 1936.12.8.17-18	142	71
Notoryctes typhlops_UMZC A5.11	82	41
Nycticebus coucang_Du Baa 0002	132	66
Ochotona alpina_UMMZ 123059	117	58.5
Okapia johnstoni_NHMUK 1971.1738	126	63
Onychogalea fraenata_UMZC A12.59.3	74	49.33333
Onychomys torridus_UWBM 37628	110	55
Oryx gazella_NHMUK ZD 1963.10.21.1	90	45
Oryzorictes tetradactylus_UMZC E.5453.C	109	54.5
Otocyon megalotis_USNM 49129	163	65.2
Ovis aries_OUMNH ZC14858	156	78
Pan troglodytes_RMCA 77032M25	162	81
Panthera pardus_IMNH 2372	69	34.5
Papio hamadryas_UMZC E.7543.B	155	77.5

Paracrocidura schoutedeni_FMNH 227382	174	87
Paradoxurus hermaphroditus_FMNH 62837	109	54.5
Pascualgnathus polanskii_PVL 4416	70	35
Pecari tajacu_NMS 2002.164.2	79	39.5
Pedetes capensis_FMNH 152053	148	74
Perodicticus potto_USNM 465898	125	62.5
Petauroides volans_NHMUK 1926.3.11.225	145	72.5
Petaurus breviceps_FMNH 129430	105	52.5
Petinomys sagitta_UMZC E1499	171	85.5
Petrogale penicillata_FMNH 64435	99	66
Podogymnura truei_FMNH 146591	121	60.5
Poiana richardsonii_YPM VZ MAM 014715	61	40.66667
Pongo pygmaeus_NHMUK 1986.1097	131	65.5
Potamogale velox_UMZC E5425F	116	58
Potorous tridactylus_FMNH 57805	149	74.5
Presbytis femoralis_UMZC E.7226.C	131	65.5
Prionailurus viverrinus_NHMUK 1860.7.22.22	44	22
Procavia capensis_FMNH 147999	107	53.5
Procyon lotor_FMNH 175311	107	53.5
Pronolagus rupestris_FMNH 177246	105	52.5
Propithecus diadema_UMZC E8041A	133	66.5
Proteles cristata_NMS unnumbered	34	17
Pseudocheirus peregrinus_UMZC A9.2.6.3	107	53.5
Pudu puda_NMS 2011.141.1	103	51.5
Puma concolor_UMZC K5745	70	35
Rangifer tarandus_OUMNH 19504	106	53
Rhynchocyon petersi_NHMUK 1886.9.21.1	134	67
Rhyncholestes raphanurus_FMNH 27476	127	63.5
Saiga tatarica_NMS 1981.72	128	64
Salpingotulus michaelis_UMMZ 120132	85	42.5
Santacruzodon hopsoni_MCN 2752	112	56
Sarcophilus harrisii_NHMUK 2003.331	75	37.5
Scapanus latimanus_UMMZ 74584	174	87
Scutisorex somereni_FMNH 160182	146	73
Setifer setosus_UMZC 2011.3.1	138	69
Sminthopsis crassicaudata_FMNH 72923	165	82.5
Solenodon paradoxus_FMNH 51068	114	57
Spalacopus cyanus_FMNH 49943	142	71
Spalax microphthalmus_FMNH 79299	106	53
Speothos venaticus_NMS 2015.96.3	137	68.5
Spermophilopsis leptodactylus_UMMZ 119250	130	65
Surdisorex norae_FMNH 190260	125	62.5
Suricata suricatta_FMNH 101744	96	48
Sus scrofa_GWU cashp PT001	179	89.5
Sylvilagus floridanus_AMNH M 254438	103	51.5
Sylvisorex howelli_FMNH 198205 198206	145	72.5
Tachyoryctes splendens_FMNH 173826 173827	110	55
Tamias striatus_UMZC E.1696	116	58

Tapirus indicus_UF 31027	189	94.5
Tapirus terrestris_NMS 2001.77.3	57	38
Tarsius syrichta_FMNH 142007	133	66.5
Tayassu sp_IMNH R 228	196	98
Tenrec ecaudatus_UMMZ 138441	89	44.5
Thylacinus cynocephalus_NHMUK 1963.8.3.0.1	78	39
Thylamys elegans_UMMZ 156033	129	64.5
Thylogale stigmatica_UMZC A12.44-1	104	69.33333
Trachypithecus obscurus_NHMUK 71.709	114	57
Tragelaphus spekii_NMS 2011.162.1	190	95
Traversodontid sp_MCP PV 4053	57	28.5
Trichosurus vulpecula_UMZC A9.16-7	127	63.5
Trirachodon berryi_BP 4658	49	16.33333
Trirachodon sp_BP 4534	61	24.4
Trirachondontid sp_JSM 100	70	46.66667
Tupaia glis_UMZC E.4057.E	166	83
Urocyon cinereoargenteus_NHMUK 1850.11.22.62	79	39.5
Urogale everetti_FMNH 166482	146	73
Ursus arctos_NHMUK 1963.11.7.1	100	50
Vicugna vicugna_FMNH 36047	112	56
Viverra zibetha_FMNH 104395	116	58
Viverricula indica_UMZC K.4323	129	64.5
Vombatus ursinus_UMZC A10.10.2	164	82
Vulpes lagopus_UMZC K3669	92	46
Zapus hudsonius_UMMZ 157417	87	43.5
Zenkerella insignis_NHMUK 5.5.23.27	116	58

16.6 Appendix F

R script for mandible shape analyses:

```
#Loading libraries

#reading in packages
require( geomorph )
require( stringdist )
require( rgl )
require(tibble)
require(dplyr)
require(ggplot2)
require(rstatix)
require(ape)
require(phytools)
require(geiger)
require(nlme)
require(mvMORPH)
require(svglite)
require(caper)
require(rr2)

#Set working directory
setwd("C:/Users/wadey/Documents/Masters
Thesis/Data/ExtinctANDLivingSpecimens_25July")

#Read custom functions; written by Roger Benson
source('C:/Users/wadey/Documents/Masters
Thesis/Data/ExtinctANDLivingSpecimens_25July/getAvisoData _ updated 03
February 2023.R', chdir = TRUE)

#Load landmarks
load("Corrected landmarks 15Dec2023.RData")
#Deleting taxa that were not landmarked correctly and impaired analysis
names(landmark.list)

FaultyTaxa= c("Aplodontia rufa_FMNH 60775",
              "Chlorocebus sabaeus_USNM 38144",
              "Cryptotis mexicana_UMMZ 113138"  ,
              "Napaeozapus insignis_UMMZ 126314"  )

for(i in 1:length( landmark.list)){
  if(names(landmark.list)[i] %in% FaultyTaxa){
    landmark.list[[i]]=NULL
  }
}

names(landmark.list)

##This section coerces coordinates read into objects that can be
analysed using
#geomorph function; this section was mostly written by and relies on the
custom
```

```r
#code from Roger Benson
#Set identifiers for landmarks
landmark.info = read.table( "Elements landmark info.txt" , header = T )
landmark.info = landmark.info[ grepl( "Mandible" , rownames(
landmark.info ) ) , ]
#Creating subset of landmarks with only mammals
livingLandmarklist=landmark.list
Fossiltaxastr=c("Cynogntahus crateronotus_ BP 5208" ,
                "Diademodon tetragonus_BP 3756" ,
                "Megazostrodon rudnerae_ BP 4983 ramus",
                "Procynosuchus delaharpeae_BP 226 ",
                "Trirachodon berryi_BP 4658",
                "Trirachodon sp_ BP 4534"  )
names(landmark.list)
for(i in 1:length( livingLandmarklist)){
  if(names(livingLandmarklist)[i] %in% Fossiltaxastr){
    livingLandmarklist[[i]]=NULL
  }
}
names(livingLandmarklist)
length(livingLandmarklist)

if(length(livingLandmarklist)==263){
  livingLandmarklist[[252]]=NULL
}
#livinglandmarklist= only mammal subset
names(livingLandmarklist)
#landmark.list= full dataset containing extinct specimen
names(landmark.list)
#This summarizes the data; is used as checkpoint
#and objects are used as input to transform reflect landmark data
#during landmark compilation later
#Data summary for mixed sample (living+extinct)
lm.dimensions = landmarkListDimensions( landmark.list )
lm.data = getElementLandmarks( lm.dimensions , Element )
#Data summary for only mammals
lm.dimensions2=landmarkListDimensions(livingLandmarklist)
lm.data2=getElementLandmarks(lm.dimensions2,Element)
#Landmarks to be dropped in the mixed sample
drop.landmarks_1 = c( "Mandible__L1_middle_of_incisors",
                      "Mandible__L2_most_lateral_point_of_incisors",
                      "Mandible__L3_most_anterior_point_of_canine" ,
                      "Mandible__L4_most_posterior_point_of_canine",
                      "Mandible__SL5_anterior_edge_of_the_mandible")
#Landmarks to be dropped in mammals only sample
drop.landmarks_2 = c("Mandible__L3_most_anterior_point_of_canine" ,
                     "Mandible__L4_most_posterior_point_of_canine",
                     "Mandible__SL5_anterior_edge_of_the_mandible")
#This compiles landmarks into a landmark list object
#which can be analysed by geomorph functions
#the compilation relies on the custom functions written by Roger Benson
#mixed landmark list
compiled.element.landmarks_1 = compileLandmarkMatrix( landmark.list ,
                                                      landmark.info ,
```

```
                                                        element = Element
,

semilandmark.counts = c( "min"   , "mean" ) ,
                                                        reflect.sides = T
,
                                                        prefer.right = T ,
                                                        use.element = T ,
                                                        drop.missing = F,
                                                        drop.landmarks =
drop.landmarks_1 ,
                                                        side.missing = c(
"majority"  ),
                                                        median.term =
"middle" ,
                                                        majority.assign =
T )
#living landmark list
compiled.element.landmarks_3 = compileLandmarkMatrix( livingLandmarklist
,
                                                        landmark.info ,
                                                        element = Element
,

semilandmark.counts = c( "min"   , "mean" ) ,
                                                        reflect.sides = T
,
                                                        prefer.right = T ,
                                                        use.element = T ,
                                                        drop.missing = F,
                                                        drop.landmarks =
drop.landmarks_2 ,
                                                        side.missing = c(
"majority"  ),
                                                        median.term =
"middle" ,
                                                        majority.assign =
T )


#Flagging potential left/right errors
#Another custom function
Check.side.lms( compiled.element.landmarks_1[["min"]][[1]] )
Check.side.lms( compiled.element.landmarks_3[["min"]][[1]] )

#run Procustes superposition
#GPA.fit_Megazostrodon= mixed; GPA.fit_Living= Mammals only
lm.count = "mean"
GPA.fit_Megazostrodon =
  gpagen( compiled.element.landmarks_1[[ lm.count ]][[
"output.landmarks.array" ]] ,
          curves = compiled.element.landmarks_1[[ lm.count ]][[
"sliders" ]] , approxBE = T )
GPA.fit_Living=
```

```
  gpagen( compiled.element.landmarks_3[[ lm.count ]][[
"output.landmarks.array" ]] ,
          curves = compiled.element.landmarks_3[[ lm.count ]][[
"sliders" ]] , approxBE = T )
#Plot the mean shape; screening landmarks one last time before use
plot3d( GPA.fit_Megazostrodon$consensus , size = 6 ,
        col = compiled.element.landmarks_1[[ lm.count ]][[ "colours" ]]
,
        asp = "iso" )
plot.semilandmark.lines( GPA.fit_Megazostrodon$consensus ,
                         curves = compiled.element.landmarks_1[[
lm.count ]][[ "sliders" ]] )
plot3d( GPA.fit_Living$consensus ,
        size = 6 , col = compiled.element.landmarks_3[[ lm.count ]][[
"colours" ]] ,
        asp = "iso" )
plot.semilandmark.lines( GPA.fit_Living$consensus ,
                         curves = compiled.element.landmarks_3[[
lm.count ]][[ "sliders" ]] )
##At this point the landmarks have been read in and General
##Procrustes alignment has been performed on them
#Reading additional data in from csv
Mammal_data_full = read.csv("C:/Users/wadey/Documents/Masters
Thesis/Data/ExtinctANDLivingSpecimens_25July/Mammal_specimens_2023.csv")
#Del ref col and redundant diet % cols
#These are the Vertebrate endothermic, Vertebrate ectothermic etc.. vars
and
#Columns tracking references for diet and body mass (BM) data
dudCols=c("Diet_ref.",
          "BM_ref")
Mammal_data_full=Mammal_data_full[,!(colnames(Mammal_data_full) %in%
dudCols)]
# Mammal_data_full=Mammal_data_full %>% select(-contains("ref"))
str(Mammal_data_full)
Mammal_data_full=Mammal_data_full[,-16:-20]
##Creating dataframe containing Living mammals which have been
landmarked;
#Creating tree name
SuperData=Mammal_data_full[Mammal_data_full$Landmarking=="TRUE",]
SuperData$Tree_name=paste(SuperData$Genus,SuperData$Species, sep="_")
SuperData_Extant=SuperData
SuperData_Extant=SuperData[SuperData$Living.Extinct!="Extinct",]
#Changing the names in GPA.fit obj to correspond to phylo tree
dimnames(GPA.fit_Megazostrodon$coords)[[3]]=paste(SuperData$Tree_name)
dimnames(GPA.fit_Living$coords)[[3]]=paste(SuperData_Extant$Tree_name)
#two.d.array() produces a nxpxk matrix; cor to GPA.fit obj
GPAMeg_coords=two.d.array(GPA.fit_Megazostrodon$coords)
GPALiving_coords=two.d.array(GPA.fit_Living$coords)
#for phylo match
row.names(GPAMeg_coords)=SuperData$Tree_name
row.names(GPALiving_coords)=SuperData_Extant$Tree_name
#Loading tree (full)
Full_Tree=read.newick("SuperTree_10thNov.phy")
#creating obj containing data not in tree and in tree
```

```
Not_inTree1=name.check(Full_Tree, GPALiving_coords)
Not_inTree2=name.check(Full_Tree,GPAMeg_coords)
#create list of specimens not in tree
Drop_tips1=Not_inTree1$tree_not_data
Drop_tips2=Not_inTree2$tree_not_data
#creating new tree-Mammal_tree; contains only specimens in GPA.fit
SuperTree_Meg=drop.tip(Full_Tree,Drop_tips2)
SuperTree_Living=drop.tip(Full_Tree,Drop_tips1)
#should be "OK"
name.check(SuperTree_Living,GPALiving_coords)
name.check(SuperTree_Meg,GPAMeg_coords)
#checking trees
plot(SuperTree_Living)
plot(SuperTree_Meg)
#Creating MajConsumed category; for basic visualizations in plots
Diet_PercentageOnly_Meg=SuperData[14:19]
row.names(Diet_PercentageOnly_Meg)=SuperData$Tree_name
#Creating empty vector
Diet_class_2=vector(mode="character",
length=nrow(Diet_PercentageOnly_Meg))
for(i in 1:nrow(Diet_PercentageOnly_Meg)){
  maxRow=0
  newRow=0
  print(i)
  for (j in 1:length(Diet_PercentageOnly_Meg)){
    newRow=Diet_PercentageOnly_Meg[i,j]
    if (newRow>maxRow & is.na(newRow)==FALSE){
      maxRow=newRow
      print(maxRow)
      print(colnames(Diet_PercentageOnly_Meg[j]))
      Diet_class_2[i]= colnames(Diet_PercentageOnly_Meg[j])

    }
    if (is.na(newRow)==TRUE | maxRow==0){
      Diet_class_2[i]="Unknown"
    }

  }
}
#Creating index match for matching for smaller (living) subset
Living_index=match(SuperData_Extant$Tree_name,SuperData$Tree_name)
SuperData$MajorityConsumed=Diet_class_2
Diet_class=SuperData$MajorityConsumed[Living_index]
SuperData_Extant$MajorityConsumed=Diet_class
#Performing PCAx2
PaPCA_Extant=gm.prcomp(GPA.fit_Living$coords, phy=SuperTree_Living,
                       align.to.phy = T)
#Look at the proportion of variance tied to each comp
summary(PaPCA_Extant)
PaPCA_Meg=gm.prcomp(GPA.fit_Megazostrodon$coords,phy=SuperTree_Meg,
                    align.to.phy = T)
summary(PaPCA_Meg)
#Fixing scaling issues
SuperData$BM_g=as.numeric(SuperData$BM_g)
```

```
SuperData_Extant$BM_g=as.numeric(SuperData_Extant$BM_g)
PaPCALiving_df=cbind(SuperData_Extant,PaPCA_Extant$x,row.names=SuperData
_Extant$Tree_name)
PaPCALiving_df$Csize=GPA.fit_Living$Csize
smol_issues= c("Solenodon_paradoxus",
               "Podogymnura_truei" )
big_issues=c("Sus_scrofa")
matching_smol=row.names(PaPCALiving_df) %in% smol_issues
matching_big=row.names(PaPCALiving_df) %in% big_issues
PaPCALiving_df$Csize[matching_smol]=PaPCALiving_df$Csize[matching_smol]/
1000
PaPCALiving_df$Csize[matching_big]=PaPCALiving_df$Csize[matching_big]*10
00
PaPCAMeg_df=cbind(SuperData,PaPCA_Meg$x,row.names=SuperData$Tree_name)
PaPCAMeg_df$Csize=GPA.fit_Megazostrodon$Csize
matching_smol=row.names(PaPCAMeg_df) %in% smol_issues
matching_big=row.names(PaPCAMeg_df) %in% big_issues
PaPCAMeg_df$Csize[matching_smol]
PaPCAMeg_df$Csize[matching_smol]=PaPCAMeg_df$Csize[matching_smol]/1000
PaPCAMeg_df$Csize[matching_big]
PaPCAMeg_df$Csize[matching_big]=PaPCAMeg_df$Csize[matching_big]*1000
#Custom colour palettes
MajRulesCol=c("#fa8a0a","#000FFF","#fa0ad6",
              "#159e29","#6b4204","#fa0a0a", "#000000")
DietSimpleCol=c("#fa0a0a","#159e29","#000FFF","#000000")
#These are some basic division functions for later
div_100=function(x){
  result=x/100
  return(result)
}
div_20=function(x){
  result=x/20
  return(result)
}
div_12=function(x){
  result=x/12
  return(result)
}
div_30=function(x){
  result=x/30
  return(result)
}

#This function is from Hermansen et al 2022;
#it extracts the R2 from the AOV tables;
get.R2 <- function(X) {
  table.temp <- X$aov.table
  round(sum(table.temp[1:(nrow(table.temp)-2),'Rsq']),3)}

#now applying to arcsin transformation; standardizing % data for
analyses use
PaPCALiving_df$transDietFruit=asin(sqrt(div_100(PaPCALiving_df$Diet_frui
t)))
PaPCALiving_df$transDietNect=asin(sqrt(div_100(PaPCALiving_df$Diet_nect)
```

```
))
PaPCALiving_df$transDietPlant=asin(sqrt(div_100(PaPCALiving_df$Diet_plan
t)))
PaPCALiving_df$transDietSeed=asin(sqrt(div_100(PaPCALiving_df$Diet_seed)
))
PaPCALiving_df$transDietVtotal=asin(sqrt(div_100(PaPCALiving_df$Diet_Vto
tal)))
PaPCALiving_df$transDietInvert=asin(sqrt(div_100(PaPCALiving_df$Diet_inv
ert)))
#Reorganizing GPA coordinates to match order of tree
PCALiving_re=PaPCALiving_df[SuperTree_Living$tip.label,]
head(PCALiving_re)
GPALiving_coords_re=GPALiving_coords[SuperTree_Living$tip.label,]
head(GPALiving_coords_re)
#Creating mandible shape geomorph environment
Mandshape_env=geomorph.data.frame(MandibleShape=GPALiving_coords_re,
                                  phy=SuperTree_Living,
                                  BodySize=log10(PCALiving_re$BM_g),

CentroidSize=log10(GPA.fit_Living$Csize),
                                  DeadOrNot=PCALiving_re$Living.Extinct,

DietPerc_Fruit=PCALiving_re$transDietFruit,

DietPerc_Nect=PCALiving_re$transDietNect,

DietPerc_Seed=PCALiving_re$transDietSeed,

DietPerc_Plant=PCALiving_re$transDietPlant,

DietPerc_Vtotal=PCALiving_re$transDietVtotal,

DietPerc_Invert=PCALiving_re$transDietInvert,

MajRules=PCALiving_re$MajorityConsumed,
                                  SimpleDiet=PCALiving_re$Diet_Simple,
                                  VerdeDiet=PCALiving_re$Diet_Verde,

Verde_Adapted=PCALiving_re$Diet_Verde_Adapted,

BinarySplit=PCALiving_re$Diet_BinSplit,

SimpleStrict=PCALiving_re$Diet_SimpleStrict,

SimpleLoose=PCALiving_re$Diet_SimpleLoose,
                                  Habitat=PCALiving_re$Habitat.category,
                                  Burrow=PCALiving_re$Burrows)
#Creating the custom colour palettes for native plot function
SimpleDiet_pointcols=DietSimpleCol[Mandshape_env$SimpleDiet]
Majrules_pointcols=MajRulesCol[Mandshape_env$MajRules]
Habitat_pointcols=HabitatCol[Mandshape_env$Habitat]

#Creating a list of models to assess using procDgls
LM_VarList1=c("BodySize",
```

```
              "CentroidSize","BodySize * CentroidSize",

"DietPerc_Fruit","BodySize*DietPerc_Fruit","BodySize+DietPerc_Fruit",
              "DietPerc_Nect",
"BodySize*DietPerc_Nect","BodySize+DietPerc_Nect",

"DietPerc_Seed","BodySize*DietPerc_Seed","BodySize+DietPerc_Seed",

"DietPerc_Plant","BodySize*DietPerc_Plant","BodySize+DietPerc_Plant",

"DietPerc_Vtotal","BodySize*DietPerc_Vtotal","BodySize+DietPerc_Vtotal",
              "DietPerc_Invert",
"BodySize*DietPerc_Invert","BodySize+DietPerc_Invert")

LMList1=paste("MandibleShape~",LM_VarList1)
LMList1=lapply(LMList1,as.formula)
#Creating empty list to store output
glm_List1=list()
i=1
for( i in 1:length(LM_VarList1)){
  Fit=procD.pgls(LMList1[[i]],
                 phy=phy,data=Mandshape_env,SS.type = "II",iter=10000)
  glm_List1[[i]]=Fit
}
#Export as .txt file
sink("glm_list1_summary.txt")
lapply(glm_List1,summary)
lapply(glm_List1,get.R2)
sink()
#Slider variable to use for plotting
slider_living=compiled.element.landmarks_3[["mean"]][["sliders"]]
#This is a reshaping matrix which rearranges coordinates to
#the right format later for plotting (x; y; z coords)
#This function is written by chat GPT
reshape_matrix <- function(input_vector, num_rows, num_cols) {
  # Check if the length of the input vector is compatible with the
specified dimensions
  if (length(input_vector) != num_rows * num_cols) {
    stop("Input vector length is not compatible with the specified
dimensions.")
  }

  # Reshape the vector into a matrix
  reshaped_matrix <- matrix(input_vector, nrow = num_rows, ncol =
num_cols, byrow = TRUE)
  # Set dimnames
  dimnames(reshaped_matrix) <- list(1:num_rows, c("X", "Y", "Z"))

  return(reshaped_matrix)
}

exaggeration_factor=1.5
##This is for visualizing shape deformation;
#Code provided by Roger Benson
```

```
#The mean shape is the intercept
#Adjust by changing the number; in this instance it's 14
mean_shape=glm_List1[[14]][["pgls.coefficients"]]["(Intercept)",]
mean_shape_test=reshape_matrix(mean_shape,150,3)
#Check mean shape
plot3d( mean_shape_test , size = 10 , col =
compiled.element.landmarks_1[[ lm.count ]][[ "colours" ]]
,box="no",asp="iso" )

plot.semilandmark.lines( mean_shape_test ,
                         Living_sliders , col = "lightgrey")

#Visualize shape deformation associated with predictor vars
#check var list to put in index
attributes(glm_List1[[14]][["pgls.coefficients"]])

shape_pos=mean_shape+
  exaggeration_factor*glm_List1[[14]][["pgls.coefficients"]][
"BodySize:DietPerc_Plant",]
shape_pos=reshape_matrix(shape_pos,150,3)
shape_neg=mean_shape-
  exaggeration_factor*glm_List1[[14]][["pgls.coefficients"]][
"BodySize:DietPerc_Plant",]
shape_neg=reshape_matrix(shape_neg,150,3)
```

R script for template pDFA:

```
##Performing pDFA template; modifying direct source script provided by
Motani and Schmitz (2011)
#Template analyses jaw shape but since other variables followed this
same general format
#and they will not be included here to avoid repetitiveness
source("phylo.fda.v0.2.R")
ddA <- PaPCAMeg_df[,257:264]
head(ddA)
ddA= cbind(ddA,PaPCAMeg_df$Diet_DFA)
ddA=cbind(ddA,PaPCAMeg_df$Living.Extinct)
colnames(ddA)[9]="DietSimple"
colnames(ddA)[10]="DeadOrAlive"
head(ddA)
scores.all=as.matrix(ddA)
diet_categories=c("Herbivore","Carnivore","Insectivore")
head(scores.all)

#Used for visualization of unequal amount of
herbivore/carnivore/invertivore
#This for loop written by Chat gpt
for (category in diet_categories) {
  # Create a subset for the current category
  subset_df <- ddA[ddA$DietSimple == category, ]

  # Store the subset in the list
  subset_list[[category]] <- subset_df
}

set.seed(123)
# reps = 1000 #number of iterations
reps=400

#Bunch of empty lists to store results
pfda_shape_obj=list()
pfda_shape_priors=list()
pfda_test_priors=list()
Test_preds= vector("numeric",length=6)
pfda_err=list()
pfda_successrate=list()
pfda_carnivore_suc=list()
pfda_herbivores_suc=list()
pfda_insectivore_suc=list()
pfda_carn_carn=list()
pfda_carn_herb=list()
pfda_carn_ins=list()
pfda_herb_carn=list()
pfda_herb_herb=list()
pfda_herb_ins=list()
pfda_ins_carn=list()
pfda_ins_herb=list()
pfda_ins_ins=list()
subset_list=list()
```

```
bootstrap_samples=list()

#Loops over pDFA for 400 iterations
for (i in 1:reps){
  #This controls the parameters for bootstrapping
  #Adjusting size of "n_rows" will adjust size of bootstrapped sample
size
  #Adjusting size of "n_cols" will adjust the input predictor variables
  #I wrote bits of this code but Chat GPT helped me debug it
  for (category in diet_categories) {
    # Create a subset for the current category
    subset_df <- ddA[ddA$DietSimple == category, ]
    print(subset_df)
    n_rows=30
    n_cols=7

bootstrap_sample=subset_df[sample(nrow(subset_df[,1:7]),size=n_rows,repl
ace=F),1:n_cols]
    print(bootstrap_sample)
    bootstrap_samples[[category]]=bootstrap_sample
  }
  #concatenating the bootstrapped samples to a df
  temp_ddA=rbind(bootstrap_samples[[1]],
                 bootstrap_samples[[2]],
                 bootstrap_samples[[3]])

  #temp_ddA is the living taxa only here
  fossil_ddA=ddA[ddA$DeadOrAlive=="Extinct",]
  #then select the vars that are in temp_ddA
  #for this iteration it is the 1st 7 PC scores
  fossil_ddA=fossil_ddA[,1:7]
  ##
  #combine this to the temp ddA
  temp_ddA=rbind(temp_ddA,fossil_ddA)
  #now add the dietary categories
  temp_names=row.names(temp_ddA)
  match_index=match(temp_names,row.names(ddA))
  diet_sub=ddA$DietSimple[match_index]
  temp_ddA$DietSimple=diet_sub
  ##
  NotIt=name.check(SuperTree_Meg,temp_ddA)
  DropNames=NotIt$tree_not_data
  TempTree=drop.tip(SuperTree_Meg,DropNames)
  name.check(TempTree, temp_ddA)
  # Resolve polytomies if present
  if (!is.binary(TempTree)) TempTree <- multi2di(TempTree, random =
TRUE)
  temp_ddA = temp_ddA[match(TempTree$tip.label, rownames(temp_ddA)),]  #
Match data rows with tree tip labels

##########################################################################
########################
  # 2 Analysis
  # Define groups and taxa
```

```
  gA <- temp_ddA$DietSimple  # Extract group information
  taxaA <- row.names(temp_ddA)  # Extract species names
  rownames(temp_ddA) <- taxaA  # Assign species names as row names to
the data frame
  # Prepare data for analysis
  XA <- temp_ddA[, 1:7]  # Select specific variables from the dataset
  str(XA)
  dim(XA)
  # XA <- log10(XA)  # Apply log10 transformation to the selected
variables
  # XA <- signif(XA, 4)  # Round the transformed data
  testtaxa <- rownames(temp_ddA[gA == "Unknown",])  # Identify taxa with
unknown group (e.g., fossils)
  testtaxan <- row(temp_ddA)[gA == "Unknown", 1]  # Get the indices of
fossil species
  trainingtaxa <- rownames(temp_ddA[-testtaxan,])  # Create a dataframe
with taxa of known group affiliation
  X <- XA[-testtaxan,]  # Extract data for training (excluding fossils)
  dd <- temp_ddA[-testtaxan,]  # Extract the full data for training
(excluding fossils)
  g <- gA[-testtaxan]  # Extract group information for training
(excluding fossils)
  tre <- drop.tip(TempTree, testtaxa)  # Create a new phylogenetic tree
without fossil taxa
  # Identify the optimal lambda value
  filename_stem <- "default"  # Stem for saving plots (as a character
string)
  ol1 <- optLambda(X, g, tre, idc = filename_stem)  # Find the optimal
lambda value
  ol1$optlambda  # Display the optimal lambda value
  # Perform discriminant analysis
  pri <- c(0.05, 0.05, 0.05,0.05)  # Define prior probabilities for
groups
  optl <- ol1$optlambda[1,1]  # Replace with the optimal lambda value
from above
  current_pfda <- phylo.fda.pred(XA, gA, taxaA, TempTree, testtaxan, val
= optl, priin = pri)  # Perform phylogenetic flexible discriminant
analysis
  ##########
  #storing results
  pfda_shape_obj[[i]]=current_pfda #storing entire pfda objs in list
  training.class <- as.character(predict(current_pfda,
current_pfda$DATA, type = "class"))
  training.variates <- predict(current_pfda, current_pfda$DATA, type =
"variates")  # Discriminant scores
  training.prob <- predict(current_pfda, current_pfda$DATA,
type="posterior")
  training.results <- cbind(as.character(g), training.class,
training.prob, training.variates)
  colnames(training.results) <- c("true class", "predicted class",
"P(1)", "P(2)", "P(3)", "DA1", "DA2")
  rownames(training.results) <- trainingtaxa

  test.class <- as.character(predict(current_pfda,
```

```
current_pfda$DATAtest, type = "class"))  # Predicted group/class
  test.variates <- predict(current_pfda, current_pfda$DATAtest, type =
"variates")  # Discriminant scores
  test.prob <- predict(current_pfda, current_pfda$DATAtest, type =
"posterior")  # Posterior probabilities of group affiliations
  # Combine predictions for fossil taxa into one data frame
  test.results <- cbind(test.class, test.prob, test.variates)
  colnames(test.results) <- c("predicted class", "P(1)", "P(2)", "P(3)",
"DA1", "DA2")
  rownames(test.results) <- testtaxa  # Assign species names to the
results
  test.results
  #Store results
  pfda_shape_priors[[i]]=training.results
  pfda_test_priors[[i]]=test.results

Test_preds=rbind(as.vector(as.vector(pfda_shape_obj[[i]][["testpredictio
n_numeral"]])))
  table=current_pfda$confusion
  err_val=attr(table,'error')
  pfda_err[[i]]=err_val
  err_val=1-err_val
  err_val=err_val*100
  err_val=round(err_val,2)
  pfda_successrate[[i]]=err_val
  #Storing data for confusion table; carnivore data
  pfda_carn_carn[[i]]=table[1,1]
  pfda_carn_herb[[i]]=table[2,1]
  pfda_carn_ins[[i]]=table[3,1]
  carn_suc=div_30(table[1,1])
  carn_suc=carn_suc*100
  carn_suc=round(carn_suc,2)
  #storing data for confusion table; herbivore data
  pfda_herb_carn[[i]]=table[1,2]
  pfda_herb_herb[[i]]=table[2,2]
  pfda_herb_ins[[i]]=table[3,2]
  herb_suc=div_30(table[2,2])
  herb_suc=herb_suc*100
  herb_suc=round(herb_suc,2)
  #storing data for confusion table; invertivore data
  pfda_ins_carn[[i]]=table[1,3]
  pfda_ins_herb[[i]]=table[2,3]
  pfda_ins_ins[[i]]=table[3,3]
  ins_suc=div_30(table[3,3])
  ins_suc=ins_suc*100
  ins_suc=round(ins_suc,2)
  ##
  pfda_carnivore_suc[[i]]=carn_suc
  pfda_herbivores_suc[[i]]=herb_suc
  pfda_insectivore_suc[[i]]=ins_suc

}
##This is the basic format for how I reviewed the pDFA results:
#Example of creating obj to avg success rate
```

```
combined_successmatrix_shape=cbind(pfda_successrate,pfda_carnivore_suc,p
fda_herbivores_suc,pfda_insectivore_suc)
combined_successmatrix_shape=as.data.frame(combined_successmatrix_shape)
colnames(combined_successmatrix_shape)
colnames(combined_successmatrix_shape)=c("OverallSuccess","CarnivoreSucc
ess",

"HerbivoreSuccess","InsectivoreSuccess")
head(combined_successmatrix_shape)
median(as.integer(combined_successmatrix_shape$OverallSuccess))
quantile(as.integer(combined_successmatrix_shape$OverallSuccess),c(0.05,
0.95))
#Confusion table carnivore
carni_cols=cbind(pfda_carn_carn,pfda_carn_herb,pfda_carn_ins)
carni_cols=as.data.frame(carni_cols)
head(carni_cols)
median(as.integer(carni_cols$pfda_carn_ins))
quantile(as.integer(carni_cols$pfda_carn_ins),c(0.05,0.95))
herbicols=cbind(pfda_herb_carn,pfda_herb_herb,pfda_herb_ins)
herbicols=as.data.frame(herbicols)
median(as.integer(herbicols$pfda_herb_ins))
quantile(as.integer(herbicols$pfda_herb_ins),c(0.05,0.95))
insicol=cbind(pfda_ins_carn,pfda_ins_herb,pfda_ins_ins)
insicol=as.data.frame(insicol)
median(as.integer(insicol$pfda_ins_ins))
quantile(as.integer(insicol$pfda_ins_ins),c(0.05,0.95))
#Storing main results
sink("Combined_success.txt")
print(combined_successmatrix_shape)
sink()
#Posterior probabiltiies
setwd("C:/Users/wadey/Documents/Masters
Thesis/Data/ExtinctANDLivingSpecimens_25July/Phylo pfda_Shape data")
for(i in 1:reps){
  prob_n=pfda_shape_priors[[i]]
  # print(prob_n)
  output_filename=paste("TESTINGProb_n_ iteration",i,".csv")
  # print(output_filename)
  write.csv(prob_n,file=output_filename)
}
```

R script for analyses done for mandible size:

```
#Creating size dataframe; mandible centroid size was already stored as
variable
#in existing dataframe
SizeDF=PaPCALiving_df[c(256,21,27,257,519:525)]
#Checking
head(SizeDF)
#Logging variables
SizeDF$LogBM=log10(SizeDF$BM_g)
SizeDF$LogCsize=log10(SizeDF$Csize)
name.check(SuperTree_Living, SizeDF)
#Rearranging in the same order as the tree
SizeDF=SizeDF[SuperTree_Living$tip.label,]
#Creating comparative data frame as per pgls
Living_Comp=comparative.data(SuperTree_Living,SizeDF,Tree_name)
#Creating list of models
VariableList=c("LogBM",
               "LogBM*transDietVtotal",
               "LogBM * transDietPlant",
               "LogBM*transDietInvert",
               "LogBM*
transDietFruit","LogBM*transDietNect","LogBM*transDietSeed",
               "LogBM+
transDietVtotal","LogBM+transDietPlant","LogBM+transDietInvert",

"LogBM+transDietFruit","LogBM+transDietNect","LogBM+transDietSeed")

LiveGls_2=paste("LogCsize~",VariableList)
LiveGls_2=lapply(LiveGls_2,as.formula)
#Creating empty list to store variables
ComboAllometry_GLS=list()
i=1

for (i in seq_along(LiveGls_2)){
  ComboAllometry_GLS[[i]]=pgls(LiveGls_2[[i]],data = Living_Comp)
}
#looking at distribution of residuals etc.
lapply(ComboAllometry_GLS, plot)
lapply(ComboAllometry_GLS, summary)
values=unlist(lapply(ComboAllometry_GLS,AIC))
#Storing data
sink(file="SizeStats_21stDec.txt")
lapply(ComboAllometry_GLS, summary)
lapply(ComboAllometry_GLS,AIC)
lapply(values,aic.w)
akaike.weights(values)
sink()
```

R script for OPCR analyses:

```
#Subsetting only OPCR
OPCR_df=Mammal_data_full[Mammal_data_full$OPCr=="TRUE",]
#Redoing the MajorityConsumed dietary category; which is used
#only for visualization purposes
OPC_Percentages=OPCR_df[14:19]
OPC_DietClass= vector(mode="character",
length=nrow(OPC_Percentages))#Creating empty vector
#Creating treename for later phylo match
OPCR_df$Tree_name=paste(OPCR_df$Genus,OPCR_df$Species, sep="_")
row.names(OPCR_df)=OPCR_df$Tree_name
#MajorityConsumed
for(i in 1:nrow(OPC_Percentages)){
  maxRow=0
  newRow=0
  print(i)
  for (j in 1:length(OPC_Percentages)){
    newRow=OPC_Percentages[i,j]
    if (newRow>maxRow & is.na(newRow)==FALSE){
      maxRow=newRow
      print(maxRow)
      print(colnames(OPC_Percentages[j]))
      OPC_DietClass[i]= colnames(OPC_Percentages[j])
    }
    if (is.na(newRow)==TRUE | maxRow==0){
      OPC_DietClass[i]="Unknown"
    }
  }
}
#storing as variable
OPCR_df$MajorityConsumed=OPC_DietClass
#Isolating M1-m4 so that only M2-m4 can be used in marsupials for
#which 4 molars were collected to accurately reflect "last 3 teeth"
#in OPCRavg and OPCRsum assessments
M1_stat=OPCR_df[,c(34,36,37,40)]
M2_stat=OPCR_df[,c(42,44,45,48)]
M3_stat=OPCR_df[,c(50,52,53,56)]
M4_stat=OPCR_df[,c(58,60,61,64)]
#Index match for later use
Marsindex=which(OPCR_df$Superorder=="Marsupialia")
#Paritioning OPCRvals out and associated states
OPCR_avDF = OPCR_df[, grepl("OPCR_ave", colnames(OPCR_df))]
OPCR_states=OPCR_df[,grepl("_State",colnames(OPCR_df))]
OPCR_avDF=cbind(OPCR_avDF,OPCR_states)
##
#There's probably a better way to do this but alas,
#I just need the vals that i've marked as faulty via states
#to not be included in my sum and average
#so i'm replacing them with NAs at the actual vals here based off states
OPCR_avDF$M1_OPCR_ave[OPCR_avDF$M1_State %in% c(0,1,2,5)]=NA
OPCR_avDF$M2_OPCR_ave[OPCR_avDF$M2_State %in% c(0,1,2,5)]=NA
OPCR_avDF$M3_OPCR_ave[OPCR_avDF$M3_State %in% c(0,1,2,5)]=NA
OPCR_avDF$M4_OPCR_ave[OPCR_avDF$M4_State %in% c(0,1,2,5)]=NA
```

```
OPCR_avDF$M5_OPCR_ave[OPCR_avDF$M5_State %in% c(0,1,2,5)]=NA
OPCR_avDF$M6_OPCR_ave[OPCR_avDF$M6_State %in% c(0,1,2,5)]=NA
OPCR_avDF$M7_OPCR_ave[OPCR_avDF$M7_State %in% c(0,1,2,5)]=NA
OPCR_avDF$PM1_OPCR_ave[OPCR_avDF$PM1_State %in% c(0,1,2,5)]=NA
OPCR_avDF$PM2_OPCR_ave[OPCR_avDF$PM2_State %in% c(0,1,2,5)]=NA
OPCR_avDF$PM3_OPCR_ave[OPCR_avDF$PM3_State %in% c(0,1,2,5)]=NA
OPCR_avDF$PM4_OPCR_ave[OPCR_avDF$PM4_State %in% c(0,1,2,5)]=NA
OPCR_avDF$PM6_OPCR_ave[OPCR_avDF$PM6_State %in% c(0,1,2,5)]=NA
OPCR_avDF$PM7_OPCR_ave[OPCR_avDF$PM7_State %in% c(0,1,2,5)]=NA
OPCR_avDF$PC1_OPCR_ave[OPCR_avDF$PC1_State %in% c(0,1,2,5)]=NA
OPCR_avDF$PC2_OPCR_ave[OPCR_avDF$PC2_State %in% c(0,1,2,5)]=NA
OPCR_avDF$PC3_OPCR_ave[OPCR_avDF$PC3_State %in% c(0,1,2,5)]=NA
OPCR_avDF$PC4_OPCR_ave[OPCR_avDF$PC4_State %in% c(0,1,2,5)]=NA
OPCR_avDF$PC5_OPCR_ave[OPCR_avDF$PC5_State %in% c(0,1,2,5)]=NA
OPCR_avDF$PC6_OPCR_ave[OPCR_avDF$PC6_State %in% c(0,1,2,5)]=NA
OPCR_avDF$PC7_OPCR_ave[OPCR_avDF$PC7_State %in% c(0,1,2,5)]=NA
OPCR_avDF$PC8_OPCR_ave[OPCR_avDF$PC8_State %in% c(0,1,2,5)]=NA
OPCR_avDF$PC9_OPCR_ave[OPCR_avDF$PC9_State %in% c(0,1,2,5)]=NA
OPCR_avDF$PC10_OPCR_ave[OPCR_avDF$PC10_State %in% c(0,1,2,5)]=NA
OPCR_avDF$PC11_OPCR_ave[OPCR_avDF$PC11_State %in% c(0,1,2,5)]=NA
OPCR_avDF$PC12_OPCR_ave[OPCR_avDF$PC12_State %in% c(0,1,2,5)]=NA
OPCR_avDF$PC13_OPCR_ave[OPCR_avDF$PC13_State %in% c(0,1,2,5)]=NA
##
#deleting character states as these metrics would wrongfully be included
in the
#OPCRavg and OPCRsum metric
OPCR_avDF=OPCR_avDF[,-28:-54]
#Calculating OPCRavg and OPCRsum
#Replacing marsupials with proper OPCRavg and OPCRsum at the end to
#accurately reflect the last 3 PC's
OPCRavsub=OPCR_avDF[Marsindex,][2:4]
OPCR_avDF$Sum=rowSums(OPCR_avDF,na.rm = T)
OPCR_avDF$Mean=rowMeans(OPCR_avDF,na.rm=T)
OPCRavsub$Sum=rowSums(OPCRavsub,na.rm=T)
OPCRavsub$Mean=rowMeans(OPCRavsub,na.rm = T)
OPCR_avDF$Sum[Marsindex]=OPCRavsub$Sum
OPCR_avDF$Mean[Marsindex]=OPCRavsub$Mean
#Adding these to the larger dataframe
OPCR_df$OPCR_avSum=OPCR_avDF$Sum
OPCR_df$OPCR_avMean=OPCR_avDF$Mean
#For plotting and analyses purposes
GoodTeeth=c(3,4)
#Creating tree
NotOPC=name.check(Full_Tree,OPCR_df) #creating obj containing data not
in tree and in tree
DropOPC=NotOPC$tree_not_data #create list of specimens not in tree
OPCTree=drop.tip(Full_Tree,DropOPC) #creating new tree-Mammal_tree;
contains only specimens in GPA.fit
name.check(OPCTree,OPCR_df) #should be "OK"
#Rearranging dataframe according to order of phylogenetic tree
OPCdf_temp=OPCR_df[OPCTree$tip.label,]
#Arcsine transforming % diet data
OPCdf_temp$transDietFruit=asin(sqrt(div_100(OPCdf_temp$Diet_fruit)))
OPCdf_temp$transDietNect=asin(sqrt(div_100(OPCdf_temp$Diet_nect)))
```

```
OPCdf_temp$transDietPlant=asin(sqrt(div_100(OPCdf_temp$Diet_plant)))
OPCdf_temp$transDietSeed=asin(sqrt(div_100(OPCdf_temp$Diet_seed)))
OPCdf_temp$transDietVtotal=asin(sqrt(div_100(OPCdf_temp$Diet_Vtotal)))
OPCdf_temp$transDietInvert=asin(sqrt(div_100(OPCdf_temp$Diet_invert)))
#logging BM
OPCdf_temp$LogBM=log10(OPCdf_temp$BM_g)
#Subsetting df to include only living mammals
row.names(OPCdf_temp[1:19,])
OPCdf_temp_2=OPCdf_temp[-c(1:19),]
OPC_sub1=OPCdf_temp[c(27,256:270)]
OPC_sub2=OPC_sub1[-c(1:19),]
head(OPC_sub2)
#Creating extant mammal tree (OPCR=T)
NotOPC=name.check(Full_Tree,OPC_sub2) #creating obj containing data not
in tree and in tree
DropOPC=NotOPC$tree_not_data #create list of specimens not in tree
OPC_extant=drop.tip(Full_Tree,DropOPC) #creating new tree-Mammal_tree;
contains only specimens in GPA.fit
name.check(OPCTree,OPCR_df) #should be "OK"
#rearranging according to phylogenetic tree
OPCdf_temp=OPCdf_temp[OPCTree$tip.label,]
#Creating two model lists
#One for OPCRavg; One for OPCRsum
VarList= c("LogBM",
           "transDietFruit","transDietNect","transDietPlant",
           "transDietSeed","transDietVtotal","transDietInvert",
           "LogBM*transDietFruit"," LogBM*transDietNect","LogBM
*transDietPlant",
           "LogBM * transDietSeed "," LogBM * transDietVtotal","LogBM *
transDietInvert",
           "LogBM + transDietFruit","LogBM + transDietNect ","LogBM +
transDietPlant",
           "LogBM + transDietSeed"," LogBM + transDietVtotal "," LogBM+
transDietInvert ")
##
gls1=paste("OPCR_avMean~",VarList)
gls1=lapply(gls1,as.formula)
gls2=paste("OPCR_avSum ~",VarList)
gls2=lapply(gls2,as.formula)
name.check(OPC_sub2,OPC_extant)
OPC_LMdf=comparative.data(OPC_extant,OPC_sub2,Tree_name)
#Merging data frame for centroid size model;
#evaluated separately
OPC_sub2_size=merge(OPC_sub2,SizeDF,by="Tree_name",sort=F)
name.check(OPC_sub2_size,OPC_extant)
OPC_sub2_size=comparative.data(OPC_extant,OPC_sub2_size,Tree_name)
#empty lists to store results
OPC_glm_List1=list()
OPC_glm_List2=list()
#Running analyses
i=1
for (i in seq_along(gls1)){
  OPC_glm_List1[[i]]=pgls(gls1[[i]],data = OPC_LMdf)
}
```

```
OPC_glm_List1[[20]]=pgls(OPCR_avMean~LogCsize,data=OPC_sub2_size)
OPC_glm_List2=list()
i=1
for (i in seq_along(gls2)){
  OPC_glm_List2[[i]]=pgls(gls2[[i]],data = OPC_LMdf)
}
OPC_glm_List2[[20]]=pgls(OPCR_avSum~LogCsize,data=OPC_sub2_size)
##Looking at and storing results
lapply(OPC_glm_List1,summary.pgls)
lapply(OPC_glm_List1,AIC)
values=unlist(lapply(OPC_glm_List1,AIC))
sink(file="OPCR_AVERAGE_STATS_LATEST_Withsize.txt")
lapply(OPC_glm_List1, summary)
lapply(OPC_glm_List1,AIC)
akaike.weights(values)
sink()
lapply(OPC_glm_List2,summary.pgls)
lapply(OPC_glm_List2,AIC)
values=unlist(lapply(OPC_glm_List2,AIC))
sink(file="OPCR_SUM_STATS_LATEST_WithSize.txt")
lapply(OPC_glm_List2,summary.pgls)
lapply(OPC_glm_List2,AIC)
akaike.weights(values)
sink()
##Individual Teeth
#This portion of code creates dataframes for m1-m3 only
#and runs pgls on each Df; it had to be done this way because
#species have variable dental formulae
M1_state=as.numeric(OPCdf_temp_2$M1_State)
M2_state=as.numeric(OPCdf_temp_2$M2_State)
M3_state=as.numeric(OPCdf_temp_2$M3_State)
M1_OPCR_ave=OPCdf_temp_2$M1_OPCR_ave
M2_OPCR_ave=OPCdf_temp_2$M2_OPCR_ave
M3_OPCR_ave=OPCdf_temp_2$M3_OPCR_ave
#Creating M1 dataframe and tree
M1_df=cbind(OPC_sub2,M1_state,M1_OPCR_ave)
M1_df=M1_df[M1_df$M1_state %in% GoodTeeth,]
NotM1=name.check(OPC_extant,M1_df) #creating obj containing data not in
tree and in tree
DropM1=NotM1$tree_not_data #create list of specimens not in tree
M1Tree=drop.tip(OPC_extant,DropM1) #creating new tree-Mammal_tree;
contains only specimens in GPA.fit
name.check(M1Tree,M1_df) #should be "OK"
##M2 dataframe and M2 tree
M2_df=cbind(OPC_sub2,M2_state,M2_OPCR_ave)
M2_df=M2_df[M2_df$M2_state %in% GoodTeeth,]
Not_OPC=name.check(OPC_extant, M2_df) #creating obj containing data not
in tree and in tree
Drop_tips=Not_OPC$tree_not_data #create list of specimens not in tree
M2Tree=drop.tip(OPC_extant,Drop_tips) #creating new tree-Mammal_tree;
contains only specimens in GPA.fit
name.check(M2Tree,M2_df) #should be "OK"
##M3 dataframe and M3 tree
```

```
M3_df=cbind(OPC_sub2,M3_state,M3_OPCR_ave)
M3_df=M3_df[M3_df$M3_state %in% GoodTeeth,]
Not_OPC=name.check(OPC_extant, M3_df) #creating obj containing data not
in tree and in tree
Drop_tips=Not_OPC$tree_not_data #create list of specimens not in tree
M3Tree=drop.tip(OPC_extant,Drop_tips) #creating new tree-Mammal_tree;
contains only specimens in GPA.fit
name.check(M3Tree,M3_df) #should be "OK"
#Creating seperate comparative df's
OPC_M1df=comparative.data(M1Tree,M1_df,Tree_name)
OPC_M2df=comparative.data(M2Tree,M2_df,Tree_name)
OPC_M3df=comparative.data(M3Tree,M3_df,Tree_name)
#M1 centroid size variable (evaluated seperately as before)
M1_Csize=merge(M1_df,SizeDF,by="Tree_name",sort = F)
name.check(M1_Csize,M1Tree)
OPC_M1_size=comparative.data(M1Tree,M1_Csize,Tree_name)
#M2 Centroid size variable (evaluated seperately as before)
M2_Csize=merge(M2_df,SizeDF,by="Tree_name",sort=F)
name.check(M2_Csize,M2Tree)
OPC_M2_size=comparative.data(M2Tree,M2_Csize,Tree_name)
OPC_M2_size$data$M2_OPCR_ave
OPC_M2_size$data$LogCsize
#M3 size variable (evaluated seperataley as before)
M3_Csize=merge(M3_df,SizeDF,by="Tree_name",sort=F)
name.check(M3_Csize,M3Tree)
OPC_M3_size=comparative.data(M3Tree,M3_Csize,Tree_name)
#Creating variable lists for models
gls_M1=paste("M1_OPCR_ave~",VarList)
gls_M2=paste("M2_OPCR_ave~",VarList)
gls_M3=paste("M3_OPCR_ave~",VarList)
gls_M1=lapply(gls_M1,as.formula)
gls_M2=lapply(gls_M2,as.formula)
gls_M3=lapply(gls_M3,as.formula)
#M1 empty list to store data
OPC_M1_List=list()
#Evaluating M1 stats
i=1
for (i in seq_along(gls_M1)){
  OPC_M1_List[[i]]=pgls(gls_M1[[i]],data = OPC_M1df)

}
OPC_M1_List[[20]]=pgls(M1_OPCR_ave~LogCsize,data=OPC_M1_size)
lapply(OPC_M1_List,summary)
values=unlist(lapply(OPC_M1_List,AIC))
#Storing results
sink(file="OPCR_M1_stats_WITHSIZE.txt")
lapply(OPC_M1_List,summary.pgls)
lapply(OPC_M1_List,AIC)
akaike.weights(values)
sink()
#Creating empty var; evaluating m2 stats
OPC_M2_List=list()
i=1
for (i in seq_along(gls_M2)){
```

```
  OPC_M2_List[[i]]=pgls(gls_M2[[i]],data = OPC_M2df)
}
OPC_M2_size$data$M2_OPCR_ave
OPC_M2_size$data$LogCsize
OPC_M2_List[[20]]=pgls(M2_OPCR_ave~LogCsize,data=OPC_M2_size)
#storing stats for m2
values=unlist(lapply(OPC_M2_List,AIC))
sink(file="OPCR_M2_stats_WITHSIZE.txt")
lapply(OPC_M2_List,summary.pgls)
lapply(OPC_M2_List,AIC)
akaike.weights(values)
sink()
#Empty list and analysis for OPCRm3
OPC_M3_List=list()
i=1
for (i in seq_along(gls_M3)){
  OPC_M3_List[[i]]=pgls(gls_M3[[i]],data = OPC_M3df)

  # names(OPCRSum_pgls[[i]])=as.character(OPCR_Models[i])
}
OPC_M3_size$data$M3_OPCR_ave
OPC_M3_size$data$LogCsize
OPC_M3_List[[20]]=pgls(M3_OPCR_ave~LogCsize,data=OPC_M3_size)
lapply(OPC_M3_List,summary)
values=unlist(lapply(OPC_M3_List,AIC))
#Storing m3 results
sink(file="OPCR_M3_STATS_WITHSIZE.txt")
lapply(OPC_M3_List,summary.pgls)
lapply(OPC_M3_List,AIC)
akaike.weights(values)
sink()
```

R script for mandible shape and OPCR:

```
#Creating df
head(PaPCALiving_df)
Intersection_Living=PaPCALiving_df[PaPCALiving_df$OPCr=="TRUE",]
#Evaluatingavg and sum stats for the smaller subset
Int_OPCR_sub=Intersection_Living[,grepl("OPCR_ave",colnames(Intersection
_Living))]
Int_states=Intersection_Living[,grepl("_State",colnames(Intersection_Liv
ing))]
Int_sub_df=cbind(Int_OPCR_sub,Int_states)
Marsindex=which(Intersection_Living$Superorder=="Marsupialia")
#Replacing possible faulty OCPR scores with NAs
#To ascertain that they're excluded from analyss
Int_sub_df$M1_OPCR_ave[Int_sub_df$M1_State %in% c(0,1,2,5)]=NA
Int_sub_df$M2_OPCR_ave[Int_sub_df$M2_State %in% c(0,1,2,5)]=NA
Int_sub_df$M3_OPCR_ave[Int_sub_df$M3_State %in% c(0,1,2,5)]=NA
Int_sub_df$M4_OPCR_ave[Int_sub_df$M4_State %in% c(0,1,2,5)]=NA
Int_sub_df$M5_OPCR_ave[Int_sub_df$M5_State %in% c(0,1,2,5)]=NA
Int_sub_df$M6_OPCR_ave[Int_sub_df$M6_State %in% c(0,1,2,5)]=NA
Int_sub_df$M7_OPCR_ave[Int_sub_df$M7_State %in% c(0,1,2,5)]=NA
Int_sub_df$PM1_OPCR_ave[Int_sub_df$PM1_State %in% c(0,1,2,5)]=NA
Int_sub_df$PM2_OPCR_ave[Int_sub_df$PM2_State %in% c(0,1,2,5)]=NA
Int_sub_df$PM3_OPCR_ave[Int_sub_df$PM3_State %in% c(0,1,2,5)]=NA
Int_sub_df$PM4_OPCR_ave[Int_sub_df$PM4_State %in% c(0,1,2,5)]=NA
Int_sub_df$PM6_OPCR_ave[Int_sub_df$PM6_State %in% c(0,1,2,5)]=NA
Int_sub_df$PM7_OPCR_ave[Int_sub_df$PM7_State %in% c(0,1,2,5)]=NA
Int_sub_df$PC1_OPCR_ave[Int_sub_df$PC1_State %in% c(0,1,2,5)]=NA
Int_sub_df$PC2_OPCR_ave[Int_sub_df$PC2_State %in% c(0,1,2,5)]=NA
Int_sub_df$PC3_OPCR_ave[Int_sub_df$PC3_State %in% c(0,1,2,5)]=NA
Int_sub_df$PC4_OPCR_ave[Int_sub_df$PC4_State %in% c(0,1,2,5)]=NA
Int_sub_df$PC5_OPCR_ave[Int_sub_df$PC5_State %in% c(0,1,2,5)]=NA
Int_sub_df$PC6_OPCR_ave[Int_sub_df$PC6_State %in% c(0,1,2,5)]=NA
Int_sub_df$PC7_OPCR_ave[Int_sub_df$PC7_State %in% c(0,1,2,5)]=NA
Int_sub_df$PC8_OPCR_ave[Int_sub_df$PC8_State %in% c(0,1,2,5)]=NA
Int_sub_df$PC9_OPCR_ave[Int_sub_df$PC9_State %in% c(0,1,2,5)]=NA
Int_sub_df$PC10_OPCR_ave[Int_sub_df$PC10_State %in% c(0,1,2,5)]=NA
Int_sub_df$PC11_OPCR_ave[Int_sub_df$PC11_State %in% c(0,1,2,5)]=NA
Int_sub_df$PC12_OPCR_ave[Int_sub_df$PC12_State %in% c(0,1,2,5)]=NA
Int_sub_df$PC13_OPCR_ave[Int_sub_df$PC13_State %in% c(0,1,2,5)]=NA
#Deleting states so that they are not included in avg and sum score
Int_sub_df=Int_sub_df[,-28:-54]
#Marsupial index for OPCRavg and OPCRsum readjustment
Int_mars=Int_sub_df[Marsindex,][2:4]
#Calculating avg and sum scores
Int_sub_df$Sum=rowSums(Int_sub_df,na.rm = T)
Int_sub_df$Mean=rowMeans(Int_sub_df,na.rm=T)
Int_mars$Sum=rowSums(Int_mars,na.rm=T)
Int_mars$Mean=rowMeans(Int_mars,na.rm = T)
#Replacing marsupial OPCRavg and OPCRsum
Int_sub_df$Sum[Marsindex]=Int_mars$Sum
Int_sub_df$Mean[Marsindex]=Int_mars$Mean
#Subsetting GPA coordinates
GPALiving_coords_re
```

```
row.names(GPALiving_coords_re)
matched_rows_int=match(row.names(Int_OPCR_sub),row.names(GPALiving_coord
s_re))
GPA_living_coords_INT= GPALiving_coords_re[matched_rows_int,
,drop=FALSE]
nrow(GPA_living_coords_INT)
nrow(Int_sub_df)
#Making phylo tree
NotIt=name.check(Full_Tree,Int_sub_df)
DropIt=NotIt$tree_not_data
IntTree=drop.tip(Full_Tree,DropIt)
name.check(IntTree,Int_sub_df)
name.check(IntTree,GPA_living_coords_INT)
#Creating geomorph enviroment
OPCRavgandsumdf=geomorph.data.frame(
MandibleShape=GPA_living_coords_INT,
                                    phy=IntTree,
                                    OPCRavg=Int_sub_df$Mean,
                                    OPCRsum=Int_sub_df$Sum

)
nrow(Int_sub_df)
Intersection_List=list()
#Evaluating OPCRavg and OPCRsum scores
Int_Fit1=procD.pgls(MandibleShape~OPCRavg,
                    phy=phy,data=OPCRavgandsumdf,
                    SS.type = "II",iter=10000)
Intersection_List[[1]]=Int_Fit1
Int_Fit2=procD.pgls(MandibleShape~OPCRsum,
                    phy=phy,data=OPCRavgandsumdf,
                    SS.type = "II",iter=10000)
Intersection_List[[2]]=Int_Fit2
#m1-m3 subsets
M1_INTdf=Intersection_Living[Intersection_Living$M1_State %in%
GoodTeeth,]
M2_INTdf=Intersection_Living[Intersection_Living$M2_State %in%
GoodTeeth,]
M3_INTdf=Intersection_Living[Intersection_Living$M3_State %in%
GoodTeeth,]
#Creating m1 tree
matched_rows_int=match(row.names(M1_INTdf),row.names(GPALiving_coords_re
))
GPA_living_coords_M1_INT= GPALiving_coords_re[matched_rows_int,
,drop=FALSE]
NotIt=name.check(Full_Tree,M1_INTdf)
DropIt=NotIt$tree_not_data
M1_IntTree=drop.tip(Full_Tree,DropIt)
name.check(M1_IntTree,M1_INTdf)
name.check(M1_IntTree,GPA_living_coords_M1_INT)
#creating geomorph env
M1_int_env =geomorph.data.frame( MandibleShape=GPA_living_coords_M1_INT,
                                    phy=M1_IntTree,
                                     OPCRm1=M1_INTdf$M1_OPCR_ave,
                                SimpleDiet=M1_INTdf$Diet_Simple,
```

```
                                MajorityCons=M1_INTdf$MajorityConsumed)
nrow(M1_INTdf)
#M1 analyses
Int_Fit3=procD.pgls(MandibleShape~OPCRm1,
                    phy=phy,data=M1_int_env,
                    SS.type = "II",iter=10000)
Intersection_List[[3]]=Int_Fit3
summary(Int_Fit3)
##
m1_Dietsimple_pointcols=DietSimpleCol[M1_int_env$SimpleDiet]
#Creating m2 tree
matched_rows_int=match(row.names(M2_INTdf),row.names(GPALiving_coords_re
))
GPA_living_coords_M2_INT= GPALiving_coords_re[matched_rows_int,
,drop=FALSE]
NotIt=name.check(Full_Tree,M2_INTdf)
DropIt=NotIt$tree_not_data
M2_IntTree=drop.tip(Full_Tree,DropIt)
name.check(M2_IntTree,M2_INTdf)
name.check(M2_IntTree,GPA_living_coords_M2_INT)
#creating m2 geomorph environment
M2_int_env =geomorph.data.frame( MandibleShape=GPA_living_coords_M2_INT,
                                phy=M2_IntTree,
                                OPCRm2=M2_INTdf$M2_OPCR_ave)
nrow(M2_INTdf)
#analysis
Int_Fit4=procD.pgls(MandibleShape~OPCRm2,
                    phy=phy,data=M2_int_env,
                    SS.type = "II",iter=10000)
Intersection_List[[4]]=Int_Fit4
summary(Int_Fit4)
#creating m3 df
matched_rows_int=match(row.names(M3_INTdf),row.names(GPALiving_coords_re
))
GPA_living_coords_M3_INT= GPALiving_coords_re[matched_rows_int,
,drop=FALSE]
NotIt=name.check(Full_Tree,M3_INTdf)
DropIt=NotIt$tree_not_data
M3_IntTree=drop.tip(Full_Tree,DropIt)
name.check(M3_IntTree,M3_INTdf)
name.check(M3_IntTree,GPA_living_coords_M3_INT)
#creating m3 geomorph df
M3_int_env =geomorph.data.frame( MandibleShape=GPA_living_coords_M3_INT,
                                phy=M3_IntTree,
                                OPCRm3=M3_INTdf$M3_OPCR_ave,
                                SimpleDiet=M3_INTdf$Diet_Simple,
                                MajorityCons=M3_INTdf$MajorityConsumed)
nrow(M3_INTdf)
#m3 analyses
Int_Fit5=procD.pgls(MandibleShape~OPCRm3,
                    phy=phy,data=M3_int_env,
                    SS.type = "II",iter=10000)
Intersection_List[[5]]=Int_Fit5
summary(Int_Fit5)
```

```
m3_Dietsimple_pointcols=DietSimpleCol[M3_int_env$SimpleDiet]
#review stats
models_int_R2=unlist(lapply(Intersection_List,get.R2))
#save results
sink("Intersection.txt")
lapply(Intersection_List, summary)
print(models_int_R2)
sink()
```

17. REFERENCES

ABDALA, F. & GAETANO, L. C. 2018. The Late Triassic record of cynodonts: time of innovations in the mammalian lineage. *The Late Triassic World: Earth in a Time of Transition*, 407-445.

ABDALA, F., NEVELING, J. & WELMAN, J. 2006. A new trirachodontid cynodont from the lower levels of the Burgersdorp Formation (Lower Triassic) of the Beaufort Group, South Africa and the cladistic relationships of Gondwanan gomphodonts. *Zoological Journal of the Linnean Society,* 147, 383-413.

ABDALA, F. & RIBEIRO, A. M. 2003. A new traversodontid cynodont from the Santa Maria Formation (Ladinian-Carnian) of southern Brazil, with a phylogenetic analysis of Gondwanan traversodontids. *Zoological Journal of the Linnean Society,* 139, 529-545.

ABDALA, F. & RIBEIRO, A. M. 2010. Distribution and diversity patterns of Triassic cynodonts (Therapsida, Cynodontia) in Gondwana. *Palaeogeography, Palaeoclimatology, Palaeoecology,* 286, 202-217.

ABDALA, F. & SA-TEIXEIRA, A. 2004. A traversodontid cynodont of African affinity in the South American Triassic. *Palaeontologia africana,* 40, 11-22.

ADAMS, D. C. 2014. A method for assessing phylogenetic least squares models for shape and other high-dimensional multivariate data. *Evolution,* 68, 2675-2688.

ADAMS, D. C. & COLLYER, M. L. 2015. Permutation tests for phylogenetic comparative analyses of high-dimensional shape data: what you shuffle matters. *Evolution,* 69, 823-829.

ADAMS, D. C. & COLLYER, M. L. 2016. On the comparison of the strength of morphological integration across morphometric datasets. *Evolution,* 70, 2623-2631.

ADAMS, D. C. & COLLYER, M. L. 2018. Multivariate phylogenetic comparative methods: evaluations, comparisons, and recommendations. *Systematic biology,* 67, 14-31.

ADAMS, D. C. & OTÁROLA-CASTILLO, E. 2013. geomorph: an R package for the collection and analysis of geometric morphometric shape data. *Methods in ecology and evolution,* 4, 393-399.

ADAMS, D. C., ROHLF, F. J. & SLICE, D. E. 2004. Geometric morphometrics: ten years of progress following the 'revolution'. *Italian journal of zoology,* 71, 5-16.

ALBIGNAC, R. 1972. The carnivora of Madagascar. *Biogeography and ecology in Madagascar.* Springer Dordrecht.

ALLEN, K. L., COOKE, S. B., GONZALES, L. A. & KAY, R. F. 2015. Dietary inference from upper and lower molar morphology in platyrrhine primates. *PloS one,* 10, e0118732.

ASHER, R. J. & LEHMANN, T. 2008. Dental eruption in afrotherian mammals. *BMC biology,* 6, 1-11.

BALISI, M. A. & VAN VALKENBURGH, B. 2020. Iterative evolution of large-bodied hypercarnivory in canids benefits species but not clades. *Communications biolology,* 3, 461.

BARBERO, S., TETA, P. & CASSINI, G. H. 2023. An ecomorphological approach to the relationship between craniomandibular morphology and diet in sigmodontine rodents from central-eastern Argentina. *Zoology,* 156, 1-12.

BARGHUSEN, H. R. 1968. The lower jaw of cynodonts (Reptilia, Therapsida) and the evolutionary origin of mammal-like adductor jaw musculature. *Postilla,* 116, 1-49.

BAUER, D. J. & CURRAN, P. J. 2005. Probing interactions in fixed and multilevel regression: Inferential and graphical techniques. *Multivariate behavioral research,* 40, 373-400.

BECHT, G. 1953. Comparative biologic-anatomical researches on mastication in some mammals. . *Konink Nederl Akad Wetensch Ser C.,* 56, 508-527.

BELL, M. A., LLOYD, G. T. & BELL, M. M. A. 2022. Package 'strap'.

BENEVENTO, G. L., BENSON, R. B. J. & FRIEDMAN, M. 2019. Patterns of mammalian jaw ecomorphological disparity during the Mesozoic/Cenozoic transition. *Proceedings of the Royal Society B: Biological Sciences,* 286, 20190347.

BENTON, M. J. 2014. *Vertebrate palaeontology*, John Wiley & Sons.

BERKOVITZ, B. & SHELLIS, P. 2018. *The teeth of mammalian vertebrates*, Academic Press.

BERTHAUME, M. A., DELEZENE, L. K. & KUPCZIK, K. 2018. Dental topography and the diet of Homo naledi. *Journal of human evolution,* 118, 14-26.

BONNAN, M. F. 2016. *The bare bones: an unconventional evolutionary history of the skeleton*, Indiana University Press.
BOOKSTEIN, F. 1991. *Morphometric tools for landmark data* New York, Cambridge University Press.
BOOKSTEIN, F. L. 1985. *Morphometrics in evolutionary biology: the geometry of size and shape change, with examples from fishes*, Academy of Natural Sciences of Philadelphia.
BOOKSTEIN, F. L. & CUTTING, C. 1988. A proposal for the apprehension of curving craniofacial form in three dimensions. *Cranofacial Morphogenesis and Dysmorphogenesis*, 127-140.
BOTHA, J., ABDALA, F. & SMITH, R. 2007. The oldest cynodont: new clues on the origin and early diversification of the Cynodontia. *Zoological Journal of the Linnean Society,* 149, 477-492.
BOTHA, J., LEE-THORP, J. & CHINSAMY, A. 2005. The palaeoecology of the non-mammalian cynodonts Diademodon and Cynognathus from the Karoo Basin of South Africa, using stable light isotope analysis. *Palaeogeography, Palaeoclimatology, Palaeoecology,* 223, 303-316.
BOTHA, J. & SMITH, R. 2020. Biostratigraphy of the Lystrosaurus declivis Assemblage Zone (Beaufort Group, Karoo Supergroup), South Africa. *South African Journal of Geology,* 123, 207-216.
BOURDIOL, P. & MIOCHE, L. 2000. Correlations between functional and occlusal tooth-surface areas and food texture during natural chewing sequences in humans. *Archives of Oral Biology,* 45, 691-699.
BOUVIER, M. 1986a. A biomechanical analysis of mandibular scaling in Old World monkeys. *American Journal of Physical Anthropology,* 69, 473-482.
BOUVIER, M. 1986b. Biomechanical scaling of mandibular dimensions in New World monkeys. *International Journal of Primatology,* 7, 551-567.
BOYER, D. M. 2008. Relief index of second mandibular molars is a correlate of diet among prosimian primates and other euarchontan mammals. *Journal of human evolution,* 55, 1118-1137.
BOYER, D. M., EVANS, A. R. & JERNVALL, J. 2010. Evidence of dietary differentiation among late Paleocene–early Eocene plesiadapids (Mammalia, Primates). *American Journal of Physical Anthropology,* 142, 194-210.
BOYLES, J. G. & STORM, J. J. 2007. The perils of picky eating: dietary breadth is related to extinction risk in insectivorous bats. *PLoS One,* 2, e672.
BRAMBLE, D. M. 1978. Origin of the mammalian feeding complex: models and mechanisms. *Paleobiology,* 4, 271-301.
BUNN, J. M., BOYER, D. M., LIPMAN, Y., ST CLAIR, E. M., JERNVALL, J. & DAUBECHIES, I. 2011. Comparing Dirichlet normal surface energy of tooth crowns, a new technique of molar shape quantification for dietary inference, with previous methods in isolation and in combination. *American journal of physical anthropology,* 145, 247-61.
BURRESS, E. D., DUARTE, A., SERRA, W. S. & LOUREIRO, M. 2016. Rates of piscivory predict pharyngeal jaw morphology in a piscivorous lineage of cichlid fishes. *Ecology of Freshwater Fish,* 25, 590-598.
BUTLER, P. 1946. The evolution of carnassial dentitions in the Mammalia. *Proceedings of the Zoological Society of London,* 116, 198-220.
BUTLER, P. M. 1996. Dilambodont Molars: a functional interpretation of their evolution. *Palaeovertebrata,* 25, 205-213.
BYRD, K. E. 1981. Mandibular movement and muscle activity during mastication in the guinea pig (Cavia porcellus). *Journal of Morphology,* 170, 147-169.
CAMPIONE, N. E. & EVANS, D. C. 2012. A universal scaling relationship between body mass and proximal limb bone dimensions in quadrupedal terrestrial tetrapods. *BMC biology,* 10, 1-22.
CARBONE, C., MACE, G. M., ROBERTS, S. C. & MACDONALD, D. W. 1999. Energetic constraints on the diet of terrestrial carnivores. *Nature,* 402, 286-288.
CASANOVAS-VILAR, I. & VAN DAM, J. 2013. Conservatism and adaptability during squirrel radiation: what is mandible shape telling us? *PLoS One,* 8, e61298.
CASSINI, G. H. 2013. Skull geometric morphometrics and paleoecology of Santacrucian (late early Miocene; Patagonia) native ungulates (Astrapotheria, Litopterna, and Notoungulata). *Ameghiniana,* 50, 193-216.

CAVANAUGH, T. 2021. *Reconstructing body size and center of mass in synapsids.* Doctoral dissertation, Harvard University.
CHALLENDER, D. W., NASH, H. C. & WATERMAN, C. 2019. *Pangolins: science, society and conservation*, Academic Press.
CHAPELLE, K. E., BENSON, R. B., STIEGLER, J., OTERO, A., ZHAO, Q. & CHOINIERE, J. N. 2020. A quantitative method for inferring locomotory shifts in amniotes during ontogeny, its application to dinosaurs and its bearing on the evolution of posture. *Palaeontology,* 63**,** 229-242.
CHRISTIANSEN, P. & ADOLFSSEN, J. S. 2005. Bite forces, canine strength and skull allometry in carnivores (Mammalia, Carnivora). *Journal of Zoology,* 266**,** 133-151.
CHURCHFIELD, S. & SHEFTEL, B. 1994. Food niche overlap and ecological separation in a multi-species community of shrews in the Siberian taiga. *Journal of Zoology,* 234**,** 105-124.
CLARK, A. D., HU, H., BENSON, R. B. & O'CONNOR, J. K. 2023. Reconstructing the dietary habits and trophic positions of the Longipterygidae (Aves: Enantiornithes) using neontological and comparative morphological methods. *PeerJ,* 11**,** e15139.
CLAUSS, M., HOFMANN, R. R., STREICH, W. J., FICKEL, J. & HUMMEL, J. 2008. Higher masseter muscle mass in grazing than in browsing ruminants. *Oecologia,* 157**,** 377-385.
CLAUSS, M., STEUER, P., MÜLLER, D. W., CODRON, D. & HUMMEL, J. 2013. Herbivory and body size: allometries of diet quality and gastrointestinal physiology, and implications for herbivore ecology and dinosaur gigantism. *PloS one,* 8**,** e68714.
CLEMENTZ, M. T. 2012. New insight from old bones: stable isotope analysis of fossil mammals. *Journal of Mammalogy,* 93**,** 368-380.
COLLYER, M. L. & ADAMS, D. C. 2021. Phylogenetically aligned component analysis. *Methods in Ecology and Evolution,* 12**,** 359-372.
COOKE, R., GEARTY, W., CHAPMAN, A. S., DUNIC, J., EDGAR, G. J., LEFCHECK, J. S., RILOV, G., MCCLAIN, C. R., STUART-SMITH, R. D. & KATHLEEN LYONS, S. 2022. Anthropogenic disruptions to longstanding patterns of trophic-size structure in vertebrates. *Nature Ecology & Evolution,* 6**,** 684-692.
COOKE, S. B. & TERHUNE, C. E. 2015. Form, function, and geometric morphometrics. *The Anatomical Record,* 298**,** 5-28.
COX, P. G., RAYFIELD, E. J., FAGAN, M. J., HERREL, A., PATAKY, T. C. & JEFFERY, N. 2012. Functional evolution of the feeding system in rodents. *PLoS One,* 7**,** e36299.
CROMPTON, A. 1963. The evolution of the mammalian jaw. *Evolution***,** 431-439.
CROMPTON, A. 1964. A preliminary description of a new mammal from the Upper Triassic of South Africa. *Proceedings of the Zoological Society of London,* 142**,** 441-452.
CROMPTON, A. 1995. Masticatory function in nonmammalian cynodonts and early mammals. *Functional morphology in Vertebrate Paleontology.* Cambridge University Press.
CROMPTON, A. & ATTRIDGE, J. 1986. Masticatory apparatus of the larger herbivores during Late Triassic and Early Jurassic times. *The Beginning of the Age of the Dinosaurs.* Cambridge University Press.
CROMPTON, A. & HIIEMAE, K. 1969. How mammalian molar teeth work. *Discovery,* 5**,** 23-34.
CROMPTON, A. & JENKINS, F. A. 1968. Molar occlusion in Late Triassic mammals. *Biological Reviews,* 43**,** 427-458.
CROMPTON, A., JOYSEY, K. & KEMP, T. 1972. The evolution of the jaw articulation of cynodonts. *Studies in vertebrate evolution,* 17**,** 231-251.
CROMPTON, A. W. 1972. Postcanine occlusion in cynodonts and tritylodontids. *Bulletin of the British Museum (Natural History) (Geology),* 21**,** 29-71.
CROMPTON, A. W., BARNET, J., LIEBERMAN, D. E., OWERKOWICZ, T., SKINNER, J. & BAUDINETTE, R. V. 2008a. Control of jaw movements in two species of macropodines (Macropus eugenii and Macropus rufus). *Comparative Biochemistry and Physiology Part A: Molecular & Integrative Physiology,* 150**,** 109-123.

CROMPTON, A. W. & HOTTON III, N. 1967. Functional morphology of the masticatory apparatus of two dicynodonts (Reptilia, Therapsida). *Postilla,* 109**,** 1-51.
CROMPTON, A. W., LIEBERMAN, D. E., OWERKOWICZ, T., BAUDINETTE, R. V. & SKINNER, J. 2008b. Motor control of masticatory movements in the Southern hairy-nosed wombat (Lasiorhinus latifrons). *Primate craniofacial function and biology.* Springer Science & Business Media.
CROMPTON, A. W., OWERKOWICZ, T. & SKINNER, J. 2010. Masticatory motor pattern in the koala (Phascolarctos cinereus): a comparison of jaw movements in marsupial and placental herbivores. *Journal of Experimental Zoology Part A: Ecological Genetics and Physiology,* 313**,** 564-578.
DAMUTH, J. & JANIS, C. M. 2014. A comparison of observed molar wear rates in extant herbivorous mammals. *Annales Zoologici Fennici.* Finnish Zoological and Botanical Publishing Board.
DEBUYSSCHERE, M., GHEERBRANT, E. & ALLAIN, R. 2015. Earliest known European mammals: A review of the morganucodonta from saint-nicolas-de-port (upper triassic, France). *Journal of Systematic Palaeontology,* 13**,** 825-855.
DENNIS, J. C., UNGAR, P. S., TEAFORD, M. F. & GLANDER, K. E. 2004. Dental topography and molar wear in Alouatta palliata from Costa Rica. *American Journal of Physical Anthropology,* 125**,** 152-161.
DORAN, G. & ALLBROOK, D. 1973. The tongue and associated structures in two species of African pangolins, Manis gigantea and Manis tricuspis. *Journal of Mammalogy,* 54**,** 887-899.
DÖTSCH, C. 1986. Mastication in the musk shrew, Suncus murinus (Mammalia, Soricidae). *Journal of Morphology,* 189**,** 25-43.
DRUZINSKY, R. E., DOHERTY, A. H. & DE VREE, F. L. 2011. Mammalian masticatory muscles: homology, nomenclature, and diversification. *Integrative and Comparative Biology,* 51**,** 224-234.
ERCOLI, M. D., ÁLVAREZ, A., WARBURTON, N. M., JANIS, C. M., POTAPOVA, E. G., HERRING, S. W., CASSINI, G. H., TARQUINI, J. & KUZNETSOV, A. 2023. Myology of the masticatory apparatus of herbivorous mammals and a novel classification for a better understanding of herbivore diversity. *Zoological Journal of the Linnean Society,* 198**,** 1106-1155.
EVANS, A. R. & JERNVALL, J. 2009. Patterns and constraints in carnivoran and rodent dental complexity and tooth size. *Journal of Vertebrate Paleontology,* 29**,** 24A.
EVANS, A. R. & PINEDA-MUNOZ, S. 2018. Inferring Mammal Dietary Ecology from Dental Morphology. *Methods in Paleoecology: Reconstructing Cenozoic terrestrial environments and ecological communities.* Springer International Publishing.
EVANS, A. R. & SANSON, G. D. 2006. Spatial and functional modeling of carnivore and insectivore molariform teeth. *Journal of Morphology,* 267**,** 649-662.
EVANS, A. R., WILSON, G. P., FORTELIUS, M. & JERNVALL, J. 2007. High-level similarity of dentitions in carnivorans and rodents. *Nature,* 445**,** 78-81.
FABRE, A. C., BICKFORD, D., SEGALL, M. & HERREL, A. 2016. The impact of diet, habitat use, and behaviour on head shape evolution in homalopsid snakes. *Biological Journal of the Linnean Society,* 118**,** 634-647.
FABRE, A. C., PERRY, J. M., HARTSTONE-ROSE, A., LOWIE, A., BOENS, A. & DUMONT, M. 2018. Do muscles constrain skull shape evolution in Strepsirrhines? *The Anatomical Record,* 301**,** 291-310.
FASTOVSKY, D. E. 2001. Evolution of herbivory in terrestrial vertebrates: perspectives from the fossil record. *Palaios,* 16**,** 528-529.
FELSENSTEIN, J. 1985. Phylogenies and the comparative method. *The American Naturalist,* 125**,** 1-15.
FIGUEIRIDO, B. & SOIBELZON, L. H. 2010. Inferring palaeoecology in extinct tremarctine bears (Carnivora, Ursidae) using geometric morphometrics. *Lethaia,* 43**,** 209-222.
FILIPPINI, F. S., ABDALA, N. F. & CASSINI, G. H. 2022. Body mass estimation in Triassic cynodonts from Argentina based on limb variables. *Acta Palaeontologica Polonica,* 67**,** 1-15.
FLYNN, J. J., PARRISH, J. M., RAKOTOSAMIMANANA, B., RANIVOHARIMANANA, L., SIMPSON, W. F. & WYSS, A. R. 2000. New traversodontids (Synapsida: Eucynodontia) from the Triassic of Madagascar. *Journal of Vertebrate Paleontology,* 20**,** 422-427.

FORASIEPI, A. M. & SÁNCHEZ-VILLAGRA, M. R. 2014. Heterochrony, dental ontogenetic diversity, and the circumvention of constraints in marsupial mammals and extinct relatives. *Paleobiology,* 40**,** 222-237.
FORTELIUS, M. 1985. Ungulate cheek teeth: developmental, functional, and evolutionary interrelations. *Acta Zoologica Fennica,* 180**,** 1-76.
FORTELIUS, M. & SOLOUNIAS, N. 2000. Functional characterization of ungulate molars using the abrasion-attrition wear gradient: a new method for reconstructing paleodiets. *American Museum Novitates,* 2000**,** 1-36.
FRANZESE, R. & KAM, C. 2009. *Modeling and interpreting interactive hypotheses in regression analysis*, University of Michigan Press.
FREDERICH, B., ADRIAENS, D. & VANDEWALLE, P. 2008. Ontogenetic shape changes in Pomacentridae (Teleostei, Perciformes) and their relationships with feeding strategies: a geometric morphometric approach. *Biological Journal of the Linnean Society,* 95**,** 92-105.
FULWOOD, E. L., SHAN, S., WINCHESTER, J. M., GAO, T., KIRVESLAHTI, H., DAUBECHIES, I. & BOYER, D. M. 2021. Reconstructing dietary ecology of extinct strepsirrhines (Primates, Mammalia) with new approaches for characterizing and analyzing tooth shape. *Paleobiology,* 47**,** 612-631.
GARBUTT, N. 2007. *Mammals of Madagascar: a complete guide*, Yale University Press.
GAUTHIER, J., THOMAS, G., FRECKLETON, R., MEIRI, S., TOBIAS, J., RICKLEFS, R., ROSINDELL, J. 2019. *Vertlife Phylogenies.* [Online]. https://vertlife.org/data/. [Accessed 2022].
GENOVESI, P., SECCHI, M. & BOITANI, L. 1996. Diet of stone martens: an example of ecological flexibility. *Journal of Zoology,* 238**,** 545-555.
GITTLEMAN, J. L. 1985. Carnivore body size: ecological and taxonomic correlates. *Oecologia,* 67**,** 540-554.
GODFREY, L. R., WINCHESTER, J. M., KING, S. J., BOYER, D. M. & JERNVALL, J. 2012. Dental topography indicates ecological contraction of lemur communities. *American Journal of Physical Anthropology,* 148**,** 215-227.
GORNIAK, G. C. & GANS, C. 1980. Quantitative assay of electromyograms during mastication in domestic cats (Felis catus). *Journal of Morphology,* 163**,** 253-281.
GOSWAMI, A., FLYNN, J. J., RANIVOHARIMANANA, L. & WYSS, A. R. 2005. Dental microwear in Triassic amniotes: implications for paleoecology and masticatory mechanics. *Journal of Vertebrate Paleontology,* 25**,** 320-329.
GOW, C. 1978. The advent of herbivory in certain reptilian lineages during the Triassic. *Palaeontologia africana,* 21**,** 133-141.
GOW, C. 1980. The dentitions of the Tritheledontidae (Therapsida: Cynodontia). *Proceedings of the Royal Society B: Biological Sciences,* 208**,** 461-481.
GOW, C., HANCOX, P., LUCAS, S. & MORALES, M. 1993. First complete skull of the Late Triassic Scalenodontoides (Reptilia, Cynodontia) from southern Africa. *The Nonmarine Triassic. New Mexico Museum of Natural History & Science Bulletin,* 3**,** 161-168.
GRAFEN, A. 1989. The phylogenetic regression. *Philosophical Transactions of the Royal Society of London. B, Biological Sciences,* 326**,** 119-157.
GRAFEN, A. & HAILS, R. 2002. *Modern statistics for the life sciences*, Oxford University Press.
GREAVES, W. S. 1991. The orientation of the force of the jaw muscles and the length of the mandible in mammals. *Zoological Journal of the Linnean Society,* 102**,** 367-374.
GREENWALD, N. S. 1988. Patterns of tooth eruption and replacement in multituberculate mammals. *Journal of Vertebrate Paleontology,* 8**,** 265-277.
GROSSNICKLE, D. M., SMITH, S. M. & WILSON, G. P. 2019. Untangling the Multiple Ecological Radiations of Early Mammals. *Trends in ecology & evolution,* 34**,** 936-949.
HANCOX, P., NEVELING, J. & RUBIDGE, B. 2020. Biostratigraphy of the Cynognathus Assemblage Zone (Beaufort Group, Karoo Supergroup), South Africa. *South African Journal of Geology* 123**,** 217-238.

HARTSTONE-ROSE, A., HERTZIG, I. & DICKINSON, E. 2019. Bite force and masticatory muscle architecture adaptations in the dietarily diverse Musteloidea (Carnivora). *The Anatomical Record,* 302**,** 2287-2299.
HARTSTONE-ROSE, A., PERRY, J. M. & MORROW, C. J. 2012. Bite force estimation and the fiber architecture of felid masticatory muscles. *The Anatomical Record: Advances in Integrative Anatomy and Evolutionary Biology,* 295**,** 1336-1351.
HAUTIER, L., MICHAUX, J., MARIVAUX, L. & VIANEY-LIAUD, M. 2008. Evolution of the zygomasseteric construction in Rodentia, as revealed by a geometric morphometric analysis of the mandible of Graphiurus (Rodentia, Gliridae). *Zoological Journal of the Linnean Society,* 154**,** 807-821.
HEDRICK, B. P. & DUMONT, E. R. 2018. Putting the leaf-nosed bats in context: a geometric morphometric analysis of three of the largest families of bats. *Journal of Mammalogy,* 99**,** 1042-1054.
HEMAE, K. M. 1967. Masticatory function in the mammals. *Journal of dental research,* 46**,** 883-893.
HENDRICKX, C., ABDALA, F. & CHOINIERE, J. 2016. Postcanine microstructure in Cricodon metabolus, a Middle Triassic gomphodont cynodont from south-eastern Africa. *Palaeontology,* 59**,** 851-861.
HENDRICKX, C., ABDALA, F. & CHOINIERE, J. N. 2019. A proposed terminology for the dentition of gomphodont cynodonts and dental morphology in Diademodontidae and Trirachodontidae. *PeerJ,* 7**,** e6752.
HENDRICKX, C., ABDALA, F., FILIPPINI, F. S., WILLS, S., BENSON, R. & CHOINIERE, J. N. 2024. Evolution of postcanine complexity in Gomphodontia (Therapsida: Cynodontia). *The Anatomical Record*.
HENDRICKX, C., GAETANO, L. C., CHOINIERE, J. N., MOCKE, H. & ABDALA, F. 2020. A new traversodontid cynodont with a peculiar postcanine dentition from the Middle/Late Triassic of Namibia and dental evolution in basal gomphodonts. *Journal of Systematic Palaeontology,* 18**,** 1669-1706.
HERMANSON, G., BENSON, R. B., FARINA, B. M., FERREIRA, G. S., LANGER, M. C. & EVERS, S. W. 2022. Cranial ecomorphology of turtles and neck retraction as a possible trigger of ecological diversification. *Evolution,* 76**,** 2566-2586.
HERRING, S. W. 1993. Functional morphology of mammalian mastication. *American Zoologist,* 33**,** 289-299.
HERRING, S. W. & HERRING, S. E. 1974. The superficial masseter and gape in mammals. *The American Naturalist,* 108**,** 561-576.
HEYWOOD, J. 2010. Functional anatomy of bovid upper molar occlusal surfaces with respect to diet. *Journal of Zoology,* 281**,** 1-11.
HOLLIDAY, J. A. & STEPPAN, S. J. 2004. Evolution of hypercarnivory: the effect of specialization on morphological and taxonomic diversity. *Paleobiology,* 30**,** 108-128.
HOPSON, J., SCHULTZE, H. & TRUEB, L. 1991. Systematics of the nonmammalian Synapsida and implications for patterns of evolution in synapsids. *Origins of the higher groups of tetrapods: controversy and consensus.* Cornell University Press.
HOPSON, J. A. 1984. Late Triassic traversodont cynodonts from Nova Scotia and southern Africa. *Palaeontologia africana,* 25**,** 181-201.
HOPSON, J. A. & KITCHING, J. W. 2001. A probainognathian cynodont from South Africa and the phylogeny of nonmammalian cynodonts. *Bulletin of the Museum of Comparative Zoology,* 156**,** 5-35.
HOPSON, J. A. & SUES, H.-D. 2006. A traversodont cynodont from the Middle Triassic (Ladinian) of Baden-Württemberg (Germany). *Paläontologische Zeitschrift,* 80**,** 124-129.
HOSHI, H. 1971. Comparative morphology of the mammalian mandible in relation to food habit. *Okajimas folia anatomica Japonica,* 48**,** 333-345.
HUGGINS, J. A. & KENNEDY, M. L. 1989. Morphologic variation in the masked shrew (Sorex cinereus) and the smoky shrew (S. fumeus). *American Midland Naturalist***,** 11-25.

HUTTENLOCKER, A. K., SINGH, S. A., HENRICI, A. C. & SUMIDA, S. S. 2021. A Carboniferous synapsid with caniniform teeth and a reappraisal of mandibular size-shape heterodonty in the origin of mammals. *Royal Society Open Science,* 8**,** 1-10.
HUXLEY, J. S. 1924. Constant differential growth-ratios and their significance. *Nature,* 114**,** 895-896.
HUXLEY, J. S. 1950. Relative growth and form transformation. *Proceedings of the Royal Society of London. Series B-Biological Sciences,* 137**,** 465-469.
HUXLEY, J. S. & TEISSIER, G. 1936. Terminology of relative growth. *Nature,* 137**,** 780-781.
ITO, K. & ENDO, H. 2019. The effect of the masticatory muscle physiological cross-sectional area on the structure of the temporomandibular joint in Carnivora. *Journal of Veterinary Medical Science,* 81**,** 389-396.
JANIS, C. 2008. An evolutionary history of browsing and grazing ungulates. *The ecology of browsing and grazing.* Springer.
JANIS, C. M. & FORTELIUS, M. 1988. On the means whereby mammals achieve increased functional durability of their dentitions, with special reference to limiting factors. *Biological Reviews,* 63**,** 197-230.
JENKINS, F. A. 1971. *The postcranial skeleton of African cynodonts: problems in the early evolution of the mammalian postcranial skeleton,* Bulletin of the Peabody Museum of Natural History.
JENKINS, J., FARISH A & PARRINGTON, F. R. 1976. The postcranial skeletons of the Triassic mammals Eozostrodon, Megazostrodon and Erythrotherium. *Philosophical Transactions of the Royal Society of London. B, Biological Sciences,* 273**,** 387-431.
JERNVALL, J. & SELÄNNE, L. 1999. Laser confocal microscopy and geographic information systems in the study of dental morphology. *Palaeontologia electronica,* 2**,** 1-18.
JETZ, W. & FRECKLETON, R. P. 2015. Towards a general framework for predicting threat status of data-deficient species from phylogenetic, spatial and environmental information. *Philosophical Transactions of the Royal Society of London. B, Biological Sciences,* 370**,** 1-10.
JIN, C., CIOCHON, R. L., DONG, W., HUNT JR, R. M., LIU, J., JAEGER, M. & ZHU, Q. 2007. The first skull of the earliest giant panda. *Proceedings of the National Academy of Sciences,* 104**,** 10932-10937.
JONES, K. E., BIELBY, J., CARDILLO, M., FRITZ, S. A., O'DELL, J., ORME, C. D. L., SAFI, K., SECHREST, W., BOAKES, E. H. & CARBONE, C. 2009. PanTHERIA: a species-level database of life history, ecology, and geography of extant and recently extinct mammals: Ecological Archives E090-184. *Ecology,* 90**,** 2648-2648.
JONES, K. E. & SAFI, K. 2011. Ecology and evolution of mammalian biodiversity. *Philosophical Transactions of the Royal Society of London. B, Biological Sciences,* 366**,** 2451-2461.
JUN, L., SOARES, M. B. & REICHEL, M. 2008. Massetognathus (Cynodontia, Traversodontidae) from the Santa Maria Formation of Brazil. *Revista brasileira de paleontologia,* 11**,** 27-36.
KAHLKE, R.-D. & KAISER, T. M. 2011. Generalism as a subsistence strategy: advantages and limitations of the highly flexible feeding traits of Pleistocene Stephanorhinus hundsheimensis (Rhinocerotidae, Mammalia). *Quaternary Science Reviews,* 30**,** 2250-2261.
KARDONG, K. 2012. *Comparative anatomy, function, evolution. Vertebrates*, McGraw-Hill
KAY, R. F. 1978. The dental structure of mammalian folivores with special reference to Primates and Phalangeroidea (Marsupialia). *The ecology of arboreal folivores.* Smithsonian Institution Press.
KEMP, T. 1983. The relationships of mammals. *Zoological Journal of the Linnean Society,* 77**,** 353-384.
KEMP, T. S. 1979. The primitive cynodont Procynosuchus: functional anatomy of the skull and relationships. *Philosophical Transactions of the Royal Society of London. B, Biological Sciences,* 285**,** 73-122.
KEMP, T. S. 1982. *Mammal-like reptiles and the origin of mammals*, Academic Press.
KEMP, T. S. 2005. *The origin and evolution of mammals*, Oxford University Press.
KEMP, T. S. 2016. Non-mammalian synapsids: the beginning of the mammal line. *Evolution of the vertebrate ear: Evidence from the fossil record***,** 107-137.

KENDALL, D. G. 1984. Shape manifolds, procrustean metrics, and complex projective spaces. *Bulletin of the London mathematical society,* 16**,** 81-121.
KLEIBER, M. 1947. Body size and metabolic rate. *Physiological reviews,* 27**,** 511-541.
KRIWET, J., WITZMANN, F., KLUG, S. & HEIDTKE, U. H. 2008. First direct evidence of a vertebrate three-level trophic chain in the fossil record. *Proceedings of the Royal Society B: Biological Sciences,* 275**,** 181-186.
KUBO, M. O. & YAMADA, E. 2014. The inter-relationship between dietary and environmental properties and tooth wear: comparisons of mesowear, molar wear rate, and hypsodonty index of extant sika deer populations. *PLoS One,* 9**,** e90745.
LAMBERT, J. E., CHAPMAN, C. A., WRANGHAM, R. W. & CONKLIN-BRITTAIN, N. L. 2004. Hardness of cercopithecine foods: implications for the critical function of enamel thickness in exploiting fallback foods. *American Journal of Physical Anthropology,* 125**,** 363-368.
LAUTENSCHLAGER, S., GILL, P., LUO, Z. X., FAGAN, M. J. & RAYFIELD, E. J. 2017. Morphological evolution of the mammalian jaw adductor complex. *Biological Reviews,* 92**,** 1910-1940.
LEDOGAR, J. A., LUK, T. H., PERRY, J. M., NEAUX, D. & WROE, S. 2018. Biting mechanics and niche separation in a specialized clade of primate seed predators. *PLoS One,* 13**,** e0190689.
LIEM, K., BEMIS, W., WALKER, W. & GRANDE, L. 2001. *Functional Anatomy of the Vertebrates: an evolutionary perspective*, Harcourt College Publishers.
LIPARINI, A., OLIVEIRA, T. V., PRETTO, F. A., SOARES, M. B. & SCHULTZ, C. L. 2013. The lower jaw and dentition of the traversodontid Exaeretodon riograndensis Abdala, Barberena & Dornelles, from the Brazilian Triassic (Santa Maria 2 Sequence, Hyperodapedon Assemblage Zone). *Alcheringa: an Australasian Journal of Palaeontology,* 37**,** 331-337.
LIU, J. & ABDALA, F. 2014. Phylogeny and taxonomy of the Traversodontidae. *Early evolutionary history of the Synapsida.* Springer Netherlands.
LIU, J. & OLSEN, P. 2010. The phylogenetic relationships of Eucynodontia (Amniota: Synapsida). *Journal of Mammalian Evolution,* 17**,** 151-176.
LIU, J. & POWELL, J. 2009. Osteology of Andescynodon (Cynodontia: Traversodontidae) from the Middle Triassic of Argentina. *American Museum Novitates,* 2009**,** 1-19.
LUCAS, P., CORLETT, R. & LUKE, D. 1985. Plio-Pleistocene hominid diets: an approach combining masticatory and ecological analysis. *Journal of Human Evolution,* 14**,** 187-202.
LUO, Z.-X., KIELAN-JAWOROWSKA, Z. & CIFELLI, R. L. 2004. Evolution of dental replacement in mammals. *Bulletin of Carnegie Museum of Natural History,* 2004**,** 159-175.
LUO, Z. X. 2007. Transformation and diversification in early mammal evolution. *Nature,* 450**,** 1011-9.
M'KIRERA, F. & UNGAR, P. S. 2003. Occlusal relief changes with molar wear in Pan troglodytes troglodytes and Gorilla gorilla gorilla. *American Journal of Primatology: Official Journal of the American Society of Primatologists,* 60**,** 31-41.
MACHADO, F., JARDIM, L., DINNAGE, R., BRITO, D. & CARDILLO, M. 2023. Diet disparity and diversity predict extinction risk in primates. *Animal Conservation,* 26**,** 331-339.
MADDISON, W. P. 2007. Mesquite: a modular system for evolutionary analysis. Version 2.0.
MAESTRI, R., PATTERSON, B., FORNEL, R., MONTEIRO, L. & DE FREITAS, T. 2016. Diet, bite force and skull morphology in the generalist rodent morphotype. *Journal of evolutionary biology,* 29**,** 2191-2204.
MAIER, W. 1984. Tooth morphology and dietary specialization. *Food acquisition and processing in primates.* Springer US
MARCÉ-NOGUÉ, J., PÜSCHEL, T. A. & KAISER, T. M. 2017. A biomechanical approach to understand the ecomorphological relationship between primate mandibles and diet. *Scientific reports,* 7**,** 54-80.
MARSHALL, A. J., BOYKO, C. M., FEILEN, K. L., BOYKO, R. H. & LEIGHTON, M. 2009. Defining fallback foods and assessing their importance in primate ecology and evolution. *American Journal of Physical Anthropology,* 140**,** 603-614.

MARTILL, D., TAYLOR, M., DUFF, K., RIDING, J. & BOWN, P. 1994. The trophic structure of the biota of the Peterborough Member, Oxford Clay Formation (Jurassic), UK. *Journal of the Geological Society,* 151**,** 173-194.
MARTINELLI, A. & SOARES, M. B. 2016. Evolution of South American cynodonts. *Contribuciones del Museo Argentino de Ciencias Naturales "Bernardino Rivadavia"* 6**,** 183-197.
MARTINELLI, A. G., FUENTE, M. D. L. & ABDALA, F. 2009. Diademodon tetragonus Seeley, 1894 (Therapsida: Cynodontia) in the Triassic of South America and its biostratigraphic implications. *Journal of Vertebrate Paleontology,* 29**,** 852-862.
MCNAB, B. K. 1986. The influence of food habits on the energetics of eutherian mammals. *Ecological Monographs,* 56**,** 1-19.
MELO, T. P., ABDALA, F. & SOARES, M. B. 2015. The Malagasy cynodont Menadon besairiei (Cynodontia; Traversodontidae) in the Middle–Upper Triassic of Brazil. *Journal of Vertebrate Paleontology,* 35**,** e1002562.
MELSTROM, K. M. & IRMIS, R. B. 2019. Repeated Evolution of Herbivorous Crocodyliforms during the Age of Dinosaurs. *Current Biology,* 29**,** 2389-2395
MELSTROM, K. M. & WISTORT, Z. P. 2021. The application of dental complexity metrics on extant saurians. *Herpetologica,* 77**,** 279-288.
MORALES-GARCÍA, N. M., GILL, P. G., JANIS, C. M. & RAYFIELD, E. J. 2021. Jaw shape and mechanical advantage are indicative of diet in Mesozoic mammals. *Communications biology,* 4**,** 1-14.
MOTANI, R. & SCHMITZ, L. 2011. Phylogenetic versus functional signals in the evolution of form–function relationships in terrestrial vision. *Evolution,* 65**,** 2245-2257.
NAPLES, V. L. 1999. Morphology, evolution and function of feeding in the giant anteater (Myrmecophaga tridactyla). *Journal of Zoology,* 249**,** 19-41.
NAVALÓN, G., BRIGHT, J. A., MARUGÁN-LOBÓN, J. & RAYFIELD, E. J. 2019. The evolutionary relationship among beak shape, mechanical advantage, and feeding ecology in modern birds. *Evolution,* 73**,** 422-435.
NOGUEIRA, M. R., PERACCHI, A. L. & MONTEIRO, L. R. 2009. Morphological correlates of bite force and diet in the skull and mandible of phyllostomid bats. *Functional Ecology,* 23**,** 715-723.
NOWAK, R. M. 1999. *Walker's Mammals of the World*, John Hopkins University Press.
O'LEARY, M. A., BLOCH, J. I., FLYNN, J. J., GAUDIN, T. J., GIALLOMBARDO, A., GIANNINI, N. P., GOLDBERG, S. L., KRAATZ, B. P., LUO, Z.-X. & MENG, J. 2013. The placental mammal ancestor and the post–K-Pg radiation of placentals. *Science,* 339**,** 662-667.
ORKNEY, A., BJARNASON, A., TRONRUD, B. C. & BENSON, R. B. 2021. Patterns of skeletal integration in birds reveal that adaptation of element shapes enables coordinated evolution between anatomical modules. *Nature Ecology & Evolution,* 5**,** 1250-1258.
ORME, D., FRECKLETON, R., THOMAS, G., PETZOLDT, T., FRITZ, S., ISAAC, N., PEARSE, W. & ORME, M. D. 2023. Package 'caper'.
PALCI, A. & LEE, M. S. 2019. Geometric morphometrics, homology and cladistics: review and recommendations. *Cladistics,* 35**,** 230-242.
PAMPUSH, J. D., SPRADLEY, J. P., MORSE, P. E., HARRINGTON, A. R., ALLEN, K. L., BOYER, D. M. & KAY, R. F. 2016a. Wear and its effects on dental topography measures in howling monkeys (Alouatta palliata). *American Journal of Physical Anthropology,* 161**,** 705-721.
PAMPUSH, J. D., WINCHESTER, J. M., MORSE, P. E., VINING, A. Q., BOYER, D. M. & KAY, R. F. 2016b. Introducing molaR: a new R package for quantitative topographic analysis of teeth (and other topographic surfaces). *Journal of Mammalian Evolution,* 23**,** 397-412.
PARADIS, E. & SCHLIEP, K. 2019. ape 5.0: an environment for modern phylogenetics and evolutionary analyses in R. *Bioinformatics,* 35**,** 526-528.
PAVANATTO, A. E., KERBER, L. & DIAS-DA-SILVA, S. 2019. Virtual reconstruction of cranial endocasts of traversodontid cynodonts (Eucynodontia: Gomphodontia) from the upper Triassic of Southern Brazil. *Journal of morphology,* 280**,** 1267-1281.
PÉREZ-BARBERÍA, F. J. & GORDON, I. J. 1999. The functional relationship between feeding type and jaw and cranial morphology in ungulates. *Oecologia,* 118**,** 157-165.

PINEDA-MUNOZ, S., EVANS, A. R. & ALROY, J. 2016. The relationship between diet and body mass in terrestrial mammals. *Paleobiology,* 42**,** 659-669.
PINEDA-MUNOZ, S., LAZAGABASTER, I. A., ALROY, J. & EVANS, A. R. 2017. Inferring diet from dental morphology in terrestrial mammals. *Methods in Ecology and Evolution,* 8**,** 481-491.
PINEDA-MUNOZ, S., LAZAGABASTER, I. A., ALROY, J., EVANS, A. R. & COOPER, N. 2016. Inferring diet from dental morphology in terrestrial mammals. *Methods in Ecology and Evolution,* 8**,** 481-491.
POPOWICS, T. E. 2003. Postcanine dental form in the Mustelidae and Viverridae (Carnivora: Mammalia). *Journal of Morphology,* 256**,** 322-341.
POTAPOVA, E. 2020. Morphofunctional transformations of the jaw muscles in rodent evolution. *Biology Bulletin Reviews,* 10**,** 394-406.
PREVOSTI, F. J., TURAZZINI, G. F., ERCOLI, M. D. & HINGST-ZAHER, E. 2012. Mandible shape in marsupial and placental carnivorous mammals: a morphological comparative study using geometric morphometrics. *Zoological Journal of the Linnean Society,* 164**,** 836-855.
PRICE, S. A. & HOPKINS, S. S. 2015. The macroevolutionary relationship between diet and body mass across mammals. *Biological Journal of the Linnean Society,* 115**,** 173-184.
QUIROGA, J. 1980. The brain of the mammal-like reptile Probainognathus jenseni (Therapsida, Cynodontia). A correlative paleo-neoneurological approach to the neocortex at the reptile-mammal transition. *Journal fur Hirnforschung,* 21**,** 299-336.
QUIROGA, J. 1984. The endocranial cast of the advanced mammal-like reptile Therioherpeton cargnini (Therapsida-Cynodontia) from the Middle Triassic of Brazil. *Journal fur Hirnforschung,* 25**,** 285-290.
R CORE TEAM, R. 2013. R: A language and environment for statistical computing.
RADINSKY, L. B. 1981a. Evolution of skull shape in carnivores: 1. Representative modern carnivores. *Biological journal of the linnean society,* 15**,** 369-388.
RADINSKY, L. B. 1981b. Evolution of skull shape in carnivores: 2. Additional modern carnivores. *Biological Journal of the Linnean Society,* 16**,** 337-355.
RAJAK, J. 2021. A preliminary review on impact of climate change and our environment with reference to global warming. *International Journal of Environmental Sciences,* 10**,** 11-14.
RAVOSA, M. J. 1996. Jaw morphology and function in living and fossil Old World monkeys. *International Journal of Primatology,* 17**,** 909-932.
RAVOSA, M. J. 2000. Size and scaling in the mandible of living and extinct apes. *Folia Primatologica,* 71**,** 305-322.
REISZ, R. R. & SUES, H.-D. 2000. Herbivory in late Paleozoic and Triassic terrestrial vertebrates. *Evolution of herbivory in terrestrial vertebrates.* Cambridge University Press.
REUTER, D. M., HOPKINS, S. S. & PRICE, S. A. 2023. What is a mammalian omnivore? Insights into terrestrial mammalian diet diversity, body mass and evolution. *Proceedings of the Royal Society B: Biological Sciences,* 290**,** 1-11.
RICHARDSON, K. C. & WOOLLER, R. D. 1990. Adaptations of the alimentary tracts of some Australian lorikeets to a diet of pollen and nectar. *Australian journal of zoology,* 38**,** 581-586.
ROHLF, F. J. 1999. Shape statistics: Procrustes superimpositions and tangent spaces. *Journal of classification,* 16**,** 197-223.
ROHLF, F. J. & MARCUS, L. F. 1993. A revolution morphometrics. *Trends in ecology & evolution,* 8**,** 129-132.
ROHLF, F. J. & SLICE, D. 1990. Extensions of the Procrustes method for the optimal superimposition of landmarks. *Systematic zoology,* 39**,** 40-59.
ROSENBERG, H. & RICHARDSON, K. 1995. Cephalic morphology of the honey possum, Tarsipes rostratus (Marsupialia: Tarsipedidae); an obligate nectarivore. *Journal of Morphology,* 223**,** 303-323.
ROSENBERGER, A. L. 2013. Fallback foods, preferred foods, adaptive zones, and primate origins. *American Journal of Primatology,* 75**,** 883-890.

ROSENBERGER, A. L. & KINZEY, W. G. 1976. Functional patterns of molar occlusion in platyrrhine primates. *American Journal of Physical Anthropology,* 45**,** 281-297.
ROSS, C. F., IRIARTE-DIAZ, J. & NUNN, C. L. 2012. Innovative approaches to the relationship between diet and mandibular morphology in primates. *International Journal of Primatology,* 33**,** 632-660.
ROWE, T. 1988. Definition, diagnosis, and origin of Mammalia. *Journal of vertebrate Paleontology,* 8**,** 241-264.
ROWE, T. 1993. Phylogenetic systematics and the early history of mammals. *Mammal phylogeny: Mesozoic differentiation, multituberculates, monotremes, early therians, and marsupials.* Springer, New York.
RUBIDGE, B. & DAY, M. 2020. Biostratigraphy of the Eodicynodon Assemblage Zone (Beaufort Group, Karoo Supergroup), South Africa. *South African Journal of Geology* 123**,** 141-148.
RUTA, M., BOTHA-BRINK, J., MITCHELL, S. A. & BENTON, M. J. 2013. The radiation of cynodonts and the ground plan of mammalian morphological diversity. *Proceedings of the Royal Society B: Biological Sciences,* 280**,** 1-10.
SACCO, T. & VAN VALKENBURGH, B. 2006. Ecomorphological indicators of feeding behaviour in the bears (Carnivora: Ursidae). *Journal of Zoology,* 263**,** 41-54.
SALAMIN, N., WÜEST, R. O., LAVERGNE, S., THUILLER, W. & PEARMAN, P. B. 2010. Assessing rapid evolution in a changing environment. *Trends in ecology & evolution,* 25**,** 692-698.
SÁNCHEZ-VILLAGRA, M. R. & SMITH, K. K. 1997. Diversity and evolution of the marsupial mandibular angular process. *Journal of Mammalian Evolution,* 4**,** 119-144.
SANTANA, S. E., STRAIT, S. & DUMONT, E. R. 2011. The better to eat you with: functional correlates of tooth structure in bats. *Functional Ecology,* 25**,** 839-847.
SEELEY, H. G. 1895. Researches on the structure, organization, and classification of the fossil reptilia. Part IX., section 4. On the Gomphodontia. *Philosophical Transactions of the Royal Society of London. B, Biological Sciences,* 186**,** 1-57.
SELLA-TUNIS, T., POKHOJAEV, A., SARIG, R., O'HIGGINS, P. & MAY, H. 2018. Human mandibular shape is associated with masticatory muscle force. *Scientific reports,* 8**,** 1-10.
SHAN, S., KOVALSKY, S. Z., WINCHESTER, J. M., BOYER, D. M. & DAUBECHIES, I. 2019. ariaDNE: A robustly implemented algorithm for Dirichlet energy of the normal. *Methods in Ecology and Evolution,* 10**,** 541-552.
SHEINE, W. S. & KAY, R. F. 1977. An analysis of chewed food particle size and its relationship to molar structure in the primates Cheirogaleus medius and Galago senegalensis and the insectivoran Tupaia glis. *American Journal of Physical Anthropology,* 47**,** 15-20.
SHIPLEY, L. A., FORBEY, J. S. & MOORE, B. D. 2009. Revisiting the dietary niche: when is a mammalian herbivore a specialist? *Integrative and comparative biology,* 49**,** 274-290.
SHIPPS, B. K., PEECOOK, B. R. & ANGIELCZYK, K. D. 2023. The topography of diet: Orientation patch count predicts diet in turtles. *The Anatomical Record,* 306**,** 1214-1227.
SIDOR, C. A. & HOPSON, J. A. 2017. Cricodon metabolus (Cynodontia: Gomphodontia) from the Triassic Ntawere Formation of northeastern Zambia: patterns of tooth replacement and a systematic review of the Trirachodontidae. *Journal of Vertebrate Paleontology,* 37**,** 39-64.
SLICE, D. E. 2007. Geometric morphometrics. *Annual Review of Anthropology,* 36**,** 261-281.
SMITH, F. A., LYONS, S. K., ERNEST, S. M., JONES, K. E., KAUFMAN, D. M., DAYAN, T., MARQUET, P. A., BROWN, J. H. & HASKELL, J. P. 2003. Body mass of Late Quaternary mammals: ecological archives E084-094. *Ecology,* 84**,** 3403-3403.
SMITH, R. 1990. A review of stratigraphy and sedimentary environments of the Karoo Basin of South Africa. *Journal of African Earth Sciences (and the Middle East),* 10**,** 117-137.
SMITH, R. 2020. Biostratigraphy of the Cistecephalus Assemblage Zone (Beaufort Group, Karoo Supergroup), South Africa. *South African Journal of Geology,* 123**,** 181-190.
SMITH, R., RUBIDGE, B., DAY, M. & BOTHA, J. 2020. Introduction to the tetrapod biozonation of the Karoo Supergroup. *South African Journal of Geology,* 123**,** 131-140.

SMITS, P. D. & EVANS, A. R. 2012. Functional constraints on tooth morphology in carnivorous mammals. *BMC evolutionary biology,* 12**,** 1-11.
STRAIT, S. G. 1993. Molar morphology and food texture among small-bodied insectivorous mammals. *Journal of Mammalogy,* 74**,** 391-402.
STRAIT, S. G. 1997. Tooth use and the physical properties of food. *Evolutionary Anthropology: Issues, News, and Reviews,* 5**,** 199-211.
SUES, H.-D. & HOPSON, J. A. 2010. Anatomy and phylogenetic relationships of Boreogomphodon jeffersoni (Cynodontia: Gomphodontia) from the Upper Triassic of Virginia. *Journal of Vertebrate Paleontology,* 30**,** 1202-1220.
SUES, H.-D., HOPSON, J. A. & SHUBIN, N. H. 1992. Affinities of? Scalenodontoides plemmyridon Hopson, 1984 (Synapsida: Cynodontia) from the Upper Triassic of Nova Scotia. *Journal of Vertebrate Paleontology,* 12**,** 168-171.
SUES, H.-D. & OLSEN, P. E. 1990. Triassic vertebrates of Gondwanan aspect from the Richmond Basin of Virginia. *Science,* 249**,** 1020-1023.
SUES, H.-D., OLSEN, P. E. & CARTER, J. G. 1999. A late Triassic traversodont cynodont from the Newark Supergroup of North Carolina. *Journal of Vertebrate Paleontology,* 19**,** 351-354.
SUNQUIST, M., SUNQUIST, F., WILSON, D. & MITTERMEIER, R. 2009. *A Handbook of the Mammals of the World, Volume 1: Carnivores*, Lynx Edicions.
TAKAHASHI, L. & PAN, R. 1994. Mandibular morphometrics among macaques: The case of Macaca thibetana. *International journal of primatology,* 15**,** 597-621.
TAYLOR, A. B. 2006. Feeding behavior, diet, and the functional consequences of jaw form in orangutans, with implications for the evolution of Pongo. *Journal of Human Evolution,* 50**,** 377-393.
THOMAS, V. J. 2023. *Comparative Jaw Muscle Anatomy of the Numbat (Myrmecobius fasciatus) and Carnivorous Marsupials (Dasyurus Species).* Honours thesis, Murdoch University.
THOMPSON, D. A. W. 1942. On growth and form. *Dover Publications,* 1**,** 345-651.
TURNBULL, W. D. 1970. Mammalian masticatory apparatus. *Fieldiana: geology,* 18**,** 153-356.
UNGAR, P. 2004. Dental topography and diets of Australopithecus afarensis and early Homo. *Journal of human evolution,* 46**,** 605-622.
UNGAR, P. & WILLIAMSON, M. 2000. Exploring the effects of tooth wear on functional morphology: a preliminary study using dental topographic analysis. *Palaeontologia electronica,* 3**,** 1-18.
UNGAR, P. S. 2010. *Mammal teeth: origin, evolution, and diversity*, John Hopkins University Press.
UPHAM, N. S., ESSELSTYN, J. A. & JETZ, W. 2019a. Ecological causes of speciation and species richness in the mammal tree of life. *bioRxiv***,** 1-26.
UPHAM, N. S., ESSELSTYN, J. A. & JETZ, W. 2019b. Inferring the mammal tree: species-level sets of phylogenies for questions in ecology, evolution, and conservation. *PLoS biology,* 17**,** e3000494.
VAN VALKENBURGH, B. 1990. Skeletal and dental predictors of body mass in carnivores. *Body size in Mammalian Paleobiology: Estimation and biological implications.* Cambridge University Press.
VIGLIETTI, P. 2020. Biostratigraphy of the Daptocephalus Assemblage Zone (Beaufort Group, Karoo Supergroup), South Africa. *South African Journal of Geology,* 123**,** 191-206.
VIGLIETTI, P., MCPHEE, B., BORDY, E., SCISCIO, L., BARRETT, P., BENSON, R., WILLS, S., CHAPELLE, K., DOLLMAN, K. & MDEKAZI, C. 2020a. Biostratigraphy of the Massospondylus Assemblage Zone (Stormberg Group, Karoo Supergroup), South africa. *South African Journal of Geology,* 123**,** 249-262.
VIGLIETTI, P., MCPHEE, B., BORDY, E., SCISCIO, L., BARRETT, P., BENSON, R., WILLS, S., TOLCHARD, F. & CHOINIERE, J. 2020b. Biostratigraphy of the Scalenodontoides Assemblage Zone (Stormberg Group, Karoo Supergroup), South Africa. *South African Journal of Geology,* 123**,** 239-248.
VIZCAÍNO, S. F., BARGO, M. S. & CASSINI, G. H. 2006. Dental occlusal surface area in relation to body mass, food habits and other biological features in fossil xenarthrans. *Ameghiniana,* 43**,** 11-26.

VOGEL, E. R., VAN WOERDEN, J. T., LUCAS, P. W., ATMOKO, S. S. U., VAN SCHAIK, C. P. & DOMINY, N. J. 2008. Functional ecology and evolution of hominoid molar enamel thickness: Pan troglodytes schweinfurthii and Pongo pygmaeus wurmbii. *Journal of Human Evolution,* 55**,** 60-74.
VOGEL, E. R., ZULFA, A., HARDUS, M., WICH, S. A., DOMINY, N. J. & TAYLOR, A. B. 2014. Food mechanical properties, feeding ecology, and the mandibular morphology of wild orangutans. *Journal of Human Evolution,* 75**,** 110-124.
WANG, B., ZELDITCH, M., BADGLEY, C. & JIA, Z.-Y. 2021. Geometric morphometrics of mandibles for dietary differentiation of Bovidae (Mammalia: Artiodactyla). *Current Zoology,* 68**,** 237-249.
WANG, K., TIAN, S., GALINDO-GONZALEZ, J., DAVALOS, L. M., ZHANG, Y. & ZHAO, H. 2020. Molecular adaptation and convergent evolution of frugivory in Old World and neotropical fruit bats. *Molecular Ecology,* 29**,** 4366-4381.
WARBURTON, N. M. 2009. Comparative jaw muscle anatomy in kangaroos, wallabies, and rat-kangaroos (Marsupialia: Macropodoidea). *The Anatomical Record: Advances in Integrative Anatomy and Evolutionary Biology,* 292**,** 875-884.
WERDELIN, L. 1987. Jaw geometry and molar morphology in marsupial carnivores: analysis of a constraint and its macroevolutionary consequences. *Paleobiology,* 13**,** 342-350.
WEST, D. & WEST, B. J. 2012. On allometry relations. *International Journal of Modern Physics B,* 26**,** 1-57.
WEST, G. B., BROWN, J. H. & ENQUIST, B. J. 1999. A general model for the structure and allometry of plant vascular systems. *Nature,* 400**,** 664-667.
WHITE, J. M., DESANTIS, L. R., EVANS, A. R., WILSON, L. A. & MCCURRY, M. R. 2021. A panda-like diprotodontid? Assessing the diet of Hulitherium tomasettii using dental complexity (Orientation Patch Count Rotated) and dental microwear texture analysis. *Palaeogeography, Palaeoclimatology, Palaeoecology,* 583**,** 1-8.
WIGGINS, N. L., MCARTHUR, C., DAVIES, N. W. & MCLEAN, S. 2006. Behavioral responses of a generalist mammalian folivore to the physiological constraints of a chemically defended diet. *Journal of Chemical Ecology,* 32**,** 1133-1147.
WILLIAMSON, T. E., BRUSATTE, S. L. & WILSON, G. P. 2014. The origin and early evolution of metatherian mammals: the Cretaceous record. *ZooKeys,* 465**,** 1-76.
WILMAN, H., BELMAKER, J., SIMPSON, J., DE LA ROSA, C., RIVADENEIRA, M. M. & JETZ, W. 2014. EltonTraits 1.0: Species-level foraging attributes of the world's birds and mammals: Ecological Archives E095-178. *Ecology,* 95**,** 2027-2027.
WILSON, G. P., EVANS, A. R., CORFE, I. J., SMITS, P. D., FORTELIUS, M. & JERNVALL, J. 2012. Adaptive radiation of multituberculate mammals before the extinction of dinosaurs. *Nature,* 483**,** 457-60.
WINCHESTER, J. M., BOYER, D. M., ST. CLAIR, E. M., GOSSELIN-ILDARI, A. D., COOKE, S. B. & LEDOGAR, J. A. 2014. Dental topography of platyrrhines and prosimians: convergence and contrasts. *American Journal of Physical Anthropology,* 153**,** 29-44.
WOLFF-EXALTO, A. D. 1951. On differences in the lower jaw of animalivorous and herbivorous mammals. *Proceedings of the Koninklijke Nederlandse Akademie van Wetenschappen Series C Biological and Medical Sciences,* 54**,** 237-246.
WOOD, A. E. 1965. Grades and clades among rodents. *Evolution,* 19**,** 115-130.
WOODS, M., MCDONALD, R. A. & HARRIS, S. 2003. Predation of wildlife by domestic cats Felis catus in Great Britain. *Mammal review,* 33**,** 174-188.
YAMASHITA, N. 1998. Functional dental correlates of food properties in five Malagasy lemur species. *American Journal of Physical Anthropology,* 106**,** 169-188.
YAMASHITA, N. 2008. Food physical properties and their relationship to morphology: the curious case of kily. *Primate craniofacial function and biology.* Springer.
YOM-TOV, Y., MENDELSSOHN, H. & GROVES, C. P. 1995. Gazella dorcas. *Mammalian species,* 491**,** 1-6.
ZIPFEL, B., MONTGOMERY, C., NEUMANN, F. H., SCOTT, L., CHOINIERE, J. & HANCOX, J. P. 2023. Overlooked or Unimportant? An Overview of the Coprolite Collections at the University of the Witwatersrand, Johannesburg, South Africa. *Curator: The Museum Journal,* 66**,** 149-164.

ZUCCOTTI, L. F., WILLIAMSON, M. D., LIMP, W. F. & UNGAR, P. S. 1998. Modeling primate occlusal topography using geographic information systems technology. *American Journal of Physical Anthropology,* 107**,** 137-142.